BioMed Research International

Cell Biology of Pathogenic Protozoa and Their Interaction with Host Cells

Guest Editors: Marlene Benchimol, Juan C. Engel, Kevin S. W. Tan, and Wanderley de Souza

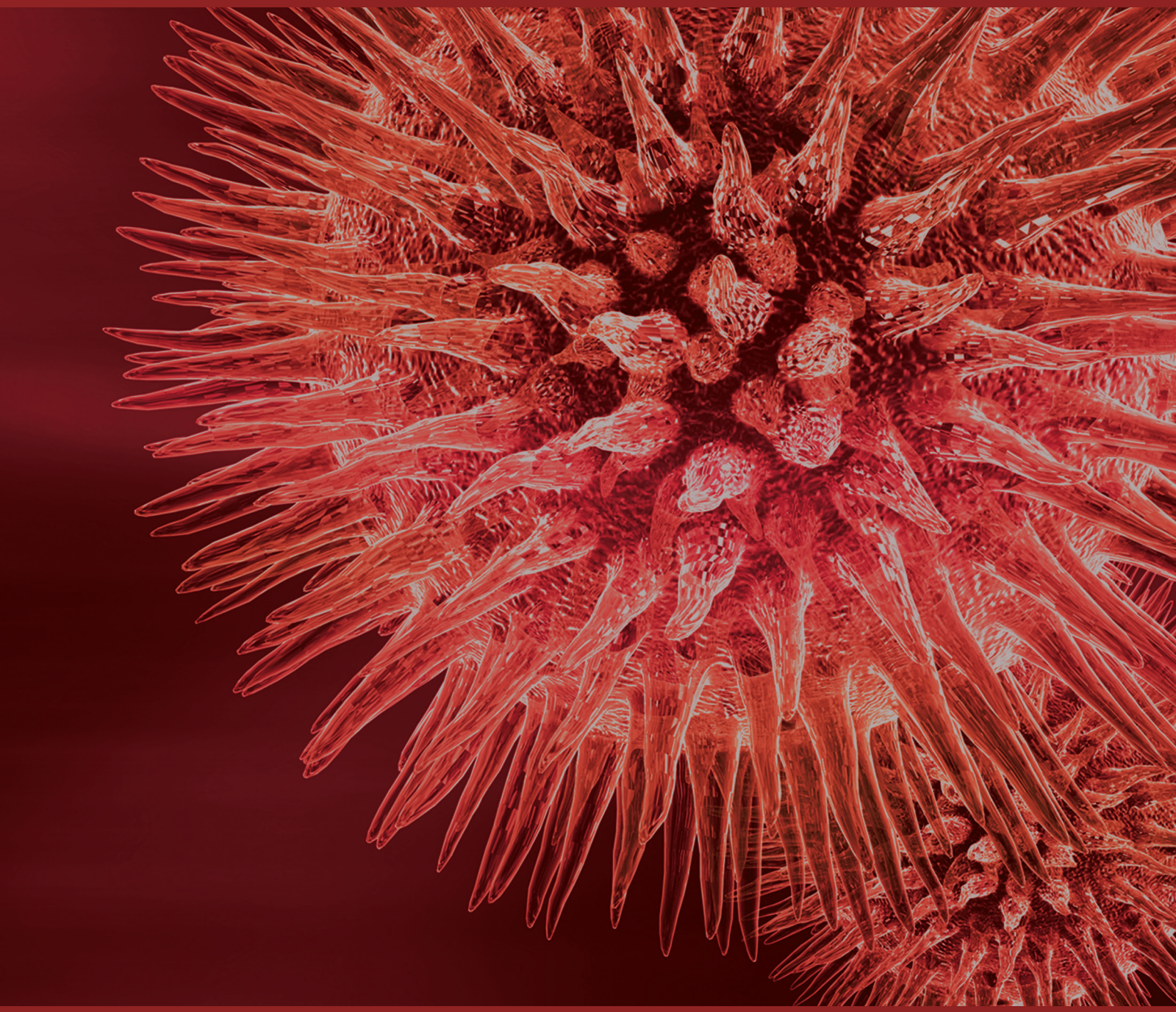

Cell Biology of Pathogenic Protozoa and Their Interaction with Host Cells

BioMed Research International

Cell Biology of Pathogenic Protozoa and Their Interaction with Host Cells

Guest Editors: Marlene Benchimol, Juan C. Engel, Kevin S. W. Tan, and Wanderley de Souza

Contents

Hindawi Publishing Corporation
BioMed Research International
Volume 2014, Article ID 143418, 2 pages
http://dx.doi.org/10.1155/2014/143418

Editorial

Cell Biology of Pathogenic Protozoa and Their Interaction with Host Cells

Marlene Benchimol,[1,2,3,4] Juan C. Engel,[5] Kevin S. W. Tan,[6] and Wanderley de Souza[2,3,4]

[1] *Universidade Santa Úrsula, Rio de Janeiro, Brazil*
[2] *Instituto de Biofísica Carlos Chagas Filho, Universidade Federal do Rio de Janeiro, Brazil*
[3] *Instituto Nacional de Metrologia e Qualidade Industrial—Inmetro, Rio de Janeiro, Brazil*
[4] *Instituto Nacional de Ciência e Tecnologia em Biologia Estrutural e Bioimagens-INBEB, Brazil*
[5] *University of California, San Francisco-Pathology, California Institute for Quantitative Biosciences (QB3), UCSF-MC 2550-Rm. 501E, 1700 4th Street San Francisco, CA 94158-2330, USA*
[6] *Laboratory of Molecular and Cellular Parasitology, Department of Microbiology, National University of Singapore, 5 Science Drive 2, Singapore 117545*

Correspondence should be addressed to Marlene Benchimol; marlenebenchimol@gmail.com

Received 14 April 2014; Accepted 14 April 2014; Published 5 June 2014

The Kingdom Protista comprises a large number of eukaryotic microorganisms which are agents of important parasitic diseases. Some of these diseases, such as Chagas disease caused by *Trypanosoma cruzi*, are mainly restricted to the Latin American regions. Others, such as toxoplasmosis caused by *Toxoplasma gondii*, are distributed throughout the world.

This special issue compiles a series of ten original contributions and two comprehensive reviews that, while not being a complete representation of the field, is an important mixture of multifaceted knowledge that we have the pleasure of sharing with the readers. These articles cover relevant aspects of the biology and interaction between host cells and species such as *Trypanosoma cruzi, Trypanosoma brucei, Toxoplasma gondii, Plasmodium falciparum, Trichomonas vaginalis, Entamoeba histolytica,* and *Blastocystis* species.

O. Sheriff et al. use *Trypanosoma brucei* as a model to analyze the dynamics of the subpellicular microtubules visualized by inducible YFP-α-tubulin expression, particularly during new flagellum/flagellum attachment zone (FAZ) biogenesis and cell growth. Cytoskeleton modifications at the posterior end of the cells were also observed using the microtubule plus-end binding protein EB1, particularly during mitosis. The results suggest an intimate connection between new microtubule formation and new FAZ assembly.

C. M. Batista et al. describe the acquisition and characterization of a monoclonal antibody that recognizes cruzipain, the major cysteine proteinase found in *Trypanosoma cruzi*, especially in the reservosome, a special organelle of the endocytic pathway of this protozoan.

S. Cheemadan et al. describe the analysis of the role of calcium signaling in the transcriptional regulation of the apicoplast genome of *Plasmodium falciparum*. The transcriptional responses of this protozoan to two calcium ionophores were analyzed, as was developmental arrest in the schizont stage. In addition, a decrease of steady state mRNA levels was observed in essentially all transcripts encoded by the apicoplast genomes of cells treated with the ionophores. In addition, the apicoplast, a nuclear encoded protein with a calcium-binding domain, was identified and localized.

J. S. Calla-Choque et al. analyze gene regulatory processes at the transcriptional and posttranscriptional levels, mediated by the iron concentration in *Trichomonas vaginalis*. A protein was identified and designated as TvACTN3, the cytoplasmic

protein that specifically binds to hairpin RNA structures from trichomonads when the parasites are grown under iron-depleted conditions. Thus, TvACTN3 could participate in the regulation of gene expression by iron in *T. vaginalis*.

C. Ximénez et al. describe the comparative analysis of the role of calreticulin (CRT) found in pathogenic *Entamoeba histolytica* and nonpathogenic *Entamoeba dispar* species that interact with human C1q, inhibiting activation of the classical complement pathway. CRT and human C1q are shown to colocalize in cytoplasmic vesicles located near the surface membrane of the parasite. The level of expression of CRT was analyzed in situ in lesions associated with amoebic liver abscess in the hamster, and the results suggested that CRT may modulate some functions during the early moments of the host-parasite relationship.

J. Pacheco-Yepez and coworkers analyze the molecular mechanisms involved in formation of amebic liver abscess induced by *Entamoeba histolytica*. Also investigated was the importance of peroxynitrite ($ONOO^-$), both as the main agent of liver abscess formation during amebic invasion and as an explanation of the superior capacity of amebas to defend themselves against this toxic agent through the peroxiredoxin and thioredoxin systems.

Z. Wu et al. describe analysis of the interaction process of *Blastocystis*, an emerging protistan parasite colonizing the human intestine, with the polarized human colonic epithelial cell line Caco-2. It was shown that the protist induces apoptosis of the epithelial cells by activating host cell caspases 3 and 9 but not 8.

K. D. Cruz et al. present experimental evidence that lipid rafts from host cells (macrophages and epithelial cells) play some role in the process of host cell invasion by the pathogenic protozoan *Toxoplasma gondii*.

M. L. Chiribao et al. report a study of the interaction of *Trypanosoma cruzi* with epithelial cells in vitro where up to 1700 significantly altered genes, regulated by the immediate infection, were identified. This indicates that host cells are reprogrammed by *T. cruzi*, which affects cellular stress responses (neutrophil chemotaxis and DNA damage response), a great number of transcription factors (including the majority of NF-B family members), and host metabolism (cholesterol, fatty acids, and phospholipids).

M. R. Garcia-Silva et al. further analyze the role played by small RNAs found in microvesicles derived from the endocytic pathway and secreted into the extracellular medium by the pathogenic protozoan *Trypanosoma cruzi*. A large set of host cell genes were reportedly expressed upon incorporation of *T. cruzi*-derived extracellular vesicles, modifying the host cell cytoskeleton, extracellular matrix, and immune response pathways.

P. Florentino et al. review, from a historical perspective, how advances in microscopic imaging contributed to understanding the *Leishmania* spp. and *Trypanosoma cruzi* host-parasite relationships.

R. F. S. Menna-Barreto and S. L. de Castro review the pivotal role played by the mitochondria of the protozoan family Trypanosomatidae on oxidative stress and bioenergetics. These metabolic processes constitute an important target for the development of new drugs against these parasites, particularly if we can better comprehend mitochondrial oxidative regulation processes.

Marlene Benchimol
Juan C. Engel
Kevin S. W. Tan
Wanderley de Souza

Hindawi Publishing Corporation
BioMed Research International
Volume 2014, Article ID 869401, 12 pages
http://dx.doi.org/10.1155/2014/869401

Research Article

Role of Calcium Signaling in the Transcriptional Regulation of the Apicoplast Genome of *Plasmodium falciparum*

Sabna Cheemadan, Ramya Ramadoss, and Zbynek Bozdech

School of Biological Sciences, Nanyang Technological University, 60 Nanyang Drive, Singapore 637551

Correspondence should be addressed to Zbynek Bozdech; zbozdech@ntu.edu.sg

Received 5 December 2013; Revised 17 February 2014; Accepted 17 February 2014; Published 27 April 2014

Academic Editor: Wanderley de Souza

Calcium is a universal second messenger that plays an important role in regulatory processes in eukaryotic cells. To understand calcium-dependent signaling in malaria parasites, we analyzed transcriptional responses of *Plasmodium falciparum* to two calcium ionophores (A23187 and ionomycin) that cause redistribution of intracellular calcium within the cytoplasm. While ionomycin induced a specific transcriptional response defined by up- or downregulation of a narrow set of genes, A23187 caused a developmental arrest in the schizont stage. In addition, we observed a dramatic decrease of mRNA levels of the transcripts encoded by the apicoplast genome during the exposure of *P. falciparum* to both calcium ionophores. Neither of the ionophores caused any disruptions to the DNA replication or the overall apicoplast morphology. This suggests that the mRNA downregulation reflects direct inhibition of the apicoplast gene transcription. Next, we identify a nuclear encoded protein with a calcium binding domain (EF-hand) that is localized to the apicoplast. Overexpression of this protein (termed PfACBP1) in *P. falciparum* cells mediates an increased resistance to the ionophores which suggests its role in calcium-dependent signaling within the apicoplast. Our data indicate that the *P. falciparum* apicoplast requires calcium-dependent signaling that involves a novel protein PfACBP1.

1. Introduction

Malaria is the most deadly parasitic disease and yet it is still one of the most common infectious diseases in the tropical and subtropical region of the planet. Approximately 2 billion people (40% of the world's population) are at risk of malaria infection in over 90 countries. Each year 300–500 million cases are being reported out of which over one million cases result in death [1]. Artemisinin-based combination therapies (ACT) are presently recommended as the first line of malaria treatment and their effectiveness underline many major accomplishments of the world wide malaria control programs over the last decade. Unfortunately, there are alarming reports of reduced sensitivity to ACTs emerging in Southeast Asia that poses a major threat for the future [2–4]. Based on the experience with previously deployed antimalaria chemotherapeutics such as chloroquine (1950s) and antifolates in (1960s), a spread of artemisinin resistance around the world could erase all advances of the malaria control programs achieved in the recent years and bring the malaria epidemics to the pre-ACT era. Hence, discovery of new malaria intervention strategies is one of the highest research priorities for the future. For this purpose, understanding of unique biological processes that are essential for malaria parasites growth and development is crucial.

Calcium signaling in *Plasmodium falciparum*, the most dangerous species of the malaria parasites, may represent one such area for drug target explorations. Previous studies established that *P. falciparum* parasites utilize calcium signaling during their life cycle progression. This is demonstrated by the wide spectrum of genes encoding calcium-dependent protein kinases and calmodulins present in the *P. falciparum* genome [5–8] but also by the tightly regulated cytoplasmic calcium concentration via intracellular calcium stores [9]. Calcium has been shown to be important for the parasite maturation [10, 11] and for the vital parasitic processes such as invasion, gliding motility [11–18], and sexual stage development [19–22]. Nonetheless, many gaps remain in the comprehensive understanding of the role of calcium signaling in *Plasmodium* parasites. In particular,

very little is known about the role of calcium signaling in transcriptional regulation of *P. falciparum*. Given that in other eukaryotic cell systems calcium-dependent transcription has a wide range of biological functions [23–28], it is reasonable to expect that in *Plasmodium*, calcium-dependent intracellular signaling is also linked with transcription, regulating multiple mechanisms important for the parasite growth, development, and adaptation to its host environment.

One of the most widely used tools for studying calcium signaling in eukaryotic cells is calcium ionophores that are able to abolish electric potential and Ca^{2+} gradients maintained at intracellular membranes, thereby mobilizing intracellular calcium stores. There are numerous examples where calcium ionophores have been used to explore calcium signaling events in eukaryotes including transcription. Genes encoding glucose-regulated proteins in hamster fibroblasts have been shown to be induced by A23187 mediated depletion of intracellular calcium stores [29]. It was also shown that an increase in the cytosolic calcium concentration induced by A23187 and ionomycin was able to trigger the commitment to differentiation and increased expression of erythroid genes in murine erythroleukemia cells [30]. Ionomycin was also shown to be able to induce calcium flux and thus expression of the T-cell CD7 gene [31]. The changes in the intracellular calcium concentration induced by calcium ionophores is also able to alter the induction of p33 gene expression by insulin [32]. There is strong experimental evidence that ionophore compounds can affect the internal calcium stores in *Plasmodium* parasites. First, calcium-imaging studies of *P. berghei* using fluorescent calcium indicators demonstrated that ionomycin increases cytoplasmic calcium concentrations from a nonacidic calcium-rich compartment and the alkalinized acidocalcisomes [33]. In *P. falciparum*, ionomycin has been shown to increase the cytoplasmic calcium concentration by releasing calcium from the intracellular calcium stores that include the parasitophorous vacuole (PV) [5, 34]. Given the high activity of the calcium ionophores in the *Plasmodium* cells [35], these compounds provide a suitable tool for studies of calcium-dependent transcriptional processes during the malaria parasite development.

In this study we analyzed the transcriptional responses of *P. falciparum* parasites to two calcium ionophores, ionomycin and A23187, in order to evaluate the effect of changing calcium distribution within the cell. We show that both inhibitors induce overlapping but not identical changes of the *P. falciparum* transcriptome ranging from up- and downregulation of many genes of a narrow set of biochemical and cellular pathways (for ionomycin) to overall developmental arrests (for A23187). Both inhibitors, however, cause a strong inhibition of transcriptional activity of essentially all genes of the apicoplast genome. Focusing on this phenomenon, we identified a nuclear encoded apicoplast targeted protein (MAL13P1.156) that carries a calcium binding (EF hand) domain. Overexpression of MAL13P1.156 confers an increase in the resistance of *P. falciparum* parasites to ionomycin, which suggests that this protein might play a role in calcium-dependent signaling pathway(s) in the apicoplast.

2. Results

2.1. Transcriptional Responses of P. falciparum to Calcium Ionophores. In the first step we wished to investigate genome-wide gene expression responses of *P. falciparum* parasites to ionomycin and A23187, two calcium ionophore compounds whose effect (presumably) leads to a release of the internal calcium stores and thus altering Ca^{2+} concentration in essentially all intracellular compartments. For this we carry out 6-hour treatments of highly synchronized *P. falciparum* culture at the schizont stage (~30 hours after invasion, hpi) with 5 μM of both ionophores (Dataset S1, available online at http://dx.doi.org/10.1155/2014/869401). Subsequent genome-wide gene expression analysis (see materials and methods) revealed that both compounds induced significant transcriptional responses (Figure 1(a)). Intriguingly, in spite of the fact that both ionomycin and A23817 have an identical activity, transport of Ca^{2+} across the membranes of eukaryotic cell compartments, the effect of these inhibitors on the *P. falciparum* transcriptome was not identical. The exposure of the *P. falciparum* parasites to A23817 led to differential expression of at least 2254 genes (1279 up- and 975 downregulated genes by >2-fold). As previously demonstrated, such broad transcriptional changes are typically not the reflections of specific transcriptional responses but rather a result of a developmental arrest [36, 37]. To test this possibility, we utilized a recently developed algorithm that allows developmental stage evaluation ("IDC aging") by assessing the correlation of the entire expression profiles in each experimental time point to the high resolution *P. falciparum* IDC transcriptome [38]. Indeed, all five time points of the A23817 treatments have mapped to the 30 hpi which corresponds to the early schizont stage that was used as a starting point of all treatment experiments (Figure 1(b)). Hence the majority of the A23817-induced differential expression corresponds to the mRNA differences between the starting/arrested parasite cultures compared to the untreated controls that progressed through the mid-to-late schizont stage normally (Figure 1(b)). In contrast to A23817, ionomycin did not arrest the *Plasmodium* schizont stage progression and the global transcriptional profiles of the five treatment time points mapped to the expected IDC timing (32–38 hpi). Instead, this compound induced a specific transcriptional response with 202 genes up- and 558 genes downregulated. Interestingly, the group of upregulated genes was statistically enriched for factors of host parasite interaction including a subgroup of the *var* gene family, the main antigenic determinants during *P. falciparum* infection. In contrast, the group of downregulated genes contained large number of factors of merozoite invasion including merozoite surface antigens, actomyosine motors, and resident proteins of invasion related organelles, rhoptry, microneme and dense granules (data not shown). In addition, 21 out of total 55 genes were predicted to play a role in the fatty acid synthesis in the apicoplast (as annotated by the Malaria Parasite Metabolic Pathway database [39]). This represents a strong statistical enrichment (P value ~ 0) and indicates a specific effect of ionomycin on the function of the apicoplast.

Corroborating this observation, both A23817 and ionomycin caused a dramatic downregulation of the vast majority

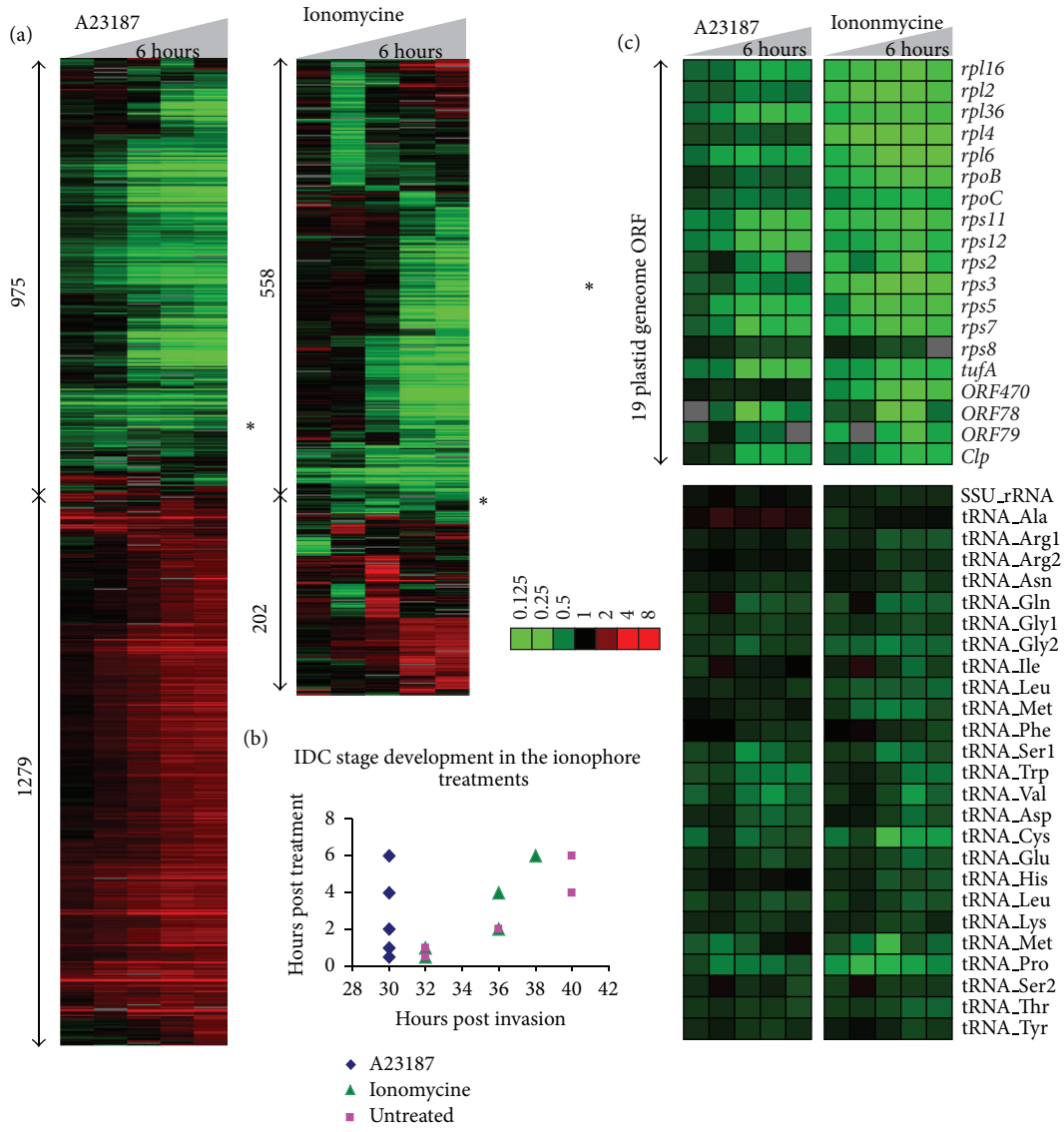

Figure 1: Transcriptional response of *P. falciparum* schizonts to calcium ionophores, ionomycin, and A23187. (a) Total 975 and 558 genes were downregulated and 1279 and 202 upregulated by >2-fold by A23187 and ionomycin, respectively. The heatmaps show relative mRNA levels in each time point compared to the corresponding time point in the untreated cells. The color code corresponds to log 2 ratios mRNA abundance between the treatment and untreated controls. The vast majority of the genes show a gradual change throughout the 6-hour treatment time courses (materials and methods) with the exception of a small gene cluster that showed much rapid decrease in mRNA abundance in both inhibitor treatments (*). (b) Pearson correlation between the treatment time points and the reference IDC transcriptome revealed that A23187 caused a developmental arrest of the *P. falciparum* development at 30 hours after invasion (hpi) (early schizont stage). In contrast, the ionomycin treated parasites exhibit expected progress through 6-hour treatment, from 32 to 38 hpi, hence indicating no developmental arrest by this inhibitor. (c) The heatmap shows relative mRNA expression level of the apicoplast genome coding genes.

of genes encoded by the plastid (apicoplast) genome. This is demonstrated by a unique narrow gene cluster with tightly correlated expression profiles (Pearson correlation > 0.93) that are characterized by a dramatic decrease of mRNA levels even in the early time points of the treatment (0.5 and 1 hour after treatment) (Figure 1(a), asterix). This is in sharp contrast with the majority of the ionophore-induced transcriptional differences that are gradual (Figure 1(a)). Visual inspections of these narrow gene clusters revealed a strong overrepresentation of plastid genome encoding genes. Total 19 out of the 29 plastid genes represented on the microarray were found downregulated as a result of both ionophore treatments (Figure 1(c)) (10 remaining ORFs showed no expression). In addition, all plastid tRNAs (25) and one rRNA genes that were detected by the microarray analysis also show decreased levels in the ionophore treatments compared to the untreated cells (Figure 1(c)). Moreover, two apicoplast encoded genes of the subunits of the putative apicoplast RNA polymerase (*rpoB* and *rpoC*) were downregulated by both ionophores. This is in contrast to the third subunit (*rpoA*)

which is encoded by the nuclear genome (PF3D7_1307600) whose expression is unaffected by neither of the inhibitors (data not shown). This suggests that the Ca-dependent regulation of the apicoplast gene transcription is independent of the nuclear genome.

Taken together, A23817 and ionomycin have a profound effect on the *P. falciparum* transcriptional cascade with the former causing a developmental arrest and the latter inducing specific transcriptional changes of the nuclear encoded genes. Besides this, both compounds have exhibited a strong inhibitory effect on the plastid transcription, downregulating essentially all genes encoded by the 35 kb DNA genome of this organelle.

2.2. Calcium Ionophores Neither Inhibit Apicoplast DNA Replication Nor Interfere with the Normal Apicoplast Development. Given the consistency of the ionophore-mediated downregulation of the apicoplast genes, we hypothesize that transcriptional regulation in the *P. falciparum* plastid is sensitive to Ca^{2+} concentration. To support this model, we wished to exclude the possibility that the decreased mRNA levels of the plastid genes are a simple reflection of discrepancies in the apicoplast development, particularly apicoplast DNA replication that is rapidly ongoing during the schizont stage. Hence we carried out comparative genomic hybridization (CGH) with total DNA isolated from schizonts treated by both calcium ionophores (Figure 2(a), Dataset S2). Even after 6 hours of treatment with both inhibitors, the apicoplast DNA content was not affected while the transcription was repeatedly downregulated as seen in the initial transcriptome analyses (Figure 2(a)). Interestingly, A23187 has much stronger effect on the mRNA level of the apicoplast genes reducing their content by median 3.24 ± 0.12 compared to ionomycin that caused reduction by 2.05 ± 0.15 after six hours of treatment.

According to previous studies on plant cells, calcium ionophores are able to inhibit protein import into the chloroplast, the orthologous endosymbiotic organelle of the apicoplast. Import of proteins with a cleavable signal peptide into the isolated intact chloroplasts can be inhibited by calcium ionophores as a consequence of emptying chloroplast calcium content [40]. In *P. falciparum*, 545 nuclear encoded proteinsare predicted to be imported into the apicoplast facilitating numerous metabolic and cellular processes associated with this compartment [41]. Inhibition of the import of these proteins will likely cause major disruptions to the apicoplast morphology as well as function. In order to investigate the effect of the ionophores on apicoplast proteins import, we utilize the acyl carrier protein (PfACP, PFB0385w) as a molecular marker of the apicoplast (Figure 2(b)). PfACP is one of the major apicoplast factors that are implicated in the type II fatty acid biosynthesis [42]. This protein carries an N-terminal signal sequence that targets its localization to the apicoplast [43]. For our study, we generate a transgenic *P. falciparum* cell line with PfACP episomal overexpression. Fluorescence microscopy analysis of the pattern of intracellular localizations of the PfACP in both ionomycin and A23187 treated cells is essentially identical to untreated cells. Similarly neither of the ionophores affected the pattern of posttranslational processing of PfACP (Figure 2(b)). The full-length apicoplast targeted proteins undergo processing by a stromal processing peptidase upon the import into the apicoplast as previously described [44]. In our results, the signal peptide cleavage is undisturbed even 6 hours after treatment (Figure 2(b)). Hence we conclude that in neither of the treatments we observe any major interference with the PfACP import into the apicoplast.

Based on previous studies of other eukaryotic systems, the ionophore-induced increases of cytosolic calcium concentrations are mediated by two possible mechanisms. These include an influx of calcium from the ambient media via native Ca^{2+} channels and a phospholipase-C (PLC) mediated calcium release from the intracellular calcium stores [45]. In the next step, we wished to test whether the ionophore effect on the apicoplast transcription is mediated by a general influx of Ca^{2+} from the extracellular medium into the parasite cytoplasm and subsequently to the apicoplast or whether it is associated with the redistribution of intracellular calcium concentration within the parasite cell. In a previous study *Trypanosoma cruzi* the causative agent of Chagas disease, it was shown that EGTA can be used to chelate the extracellular calcium, eliminating it of its influx into the ionophore treated cells and the majority of the phenotypic effect induced by the ionophores is due to redistribution of the intracellular of calcium [46]. Similar to these studies, we carried out additional transcriptome analyses where the parasites were treated with $5\,\mu$M ionomycin and at the same time the extracellular calcium was depleted by chelation with 3 mM of EGTA. As expected, we observed a similar effect of the downregulation of apicoplast gene transcription that occurs to the same degree compared to cells grown in the calcium presence (Figure 2(c), Dataset S3). These results suggest that the redistribution of the intracellular calcium such as release of the intracellular calcium stores and not the extracellular calcium influx is responsible for the observed ionophore effect on apicoplast transcription.

Taken together, these experiments show that neither of the ionophores caused dramatic disruptions of the apicoplast DNA replication or protein import. In addition, the microscopy studies did not detect any major abnormalities in the apicoplast morphology during its growth and division in the late schizont stages. Although the used techniques could not exclude subtle changes in the apicoplast morphology or protein content, these data suggest that the observed dramatic reduction of the apicoplast gene mRNA levels indeed represents a reduced transcriptional activity at the apicoplast genome. Moreover, the ionophore-induced transcriptional changes in the apicoplast are associated mainly (if not fully) with the intracellular stores of Ca^{2+}. Hence, the apicoplast transcriptional regulation is sensitive to fluctuations of Ca^{2+} concentration likely within the apicoplast itself.

2.3. Calcium Signaling in the Apicoplast. Given the potential role of calcium on transcription of the apicoplast genes,

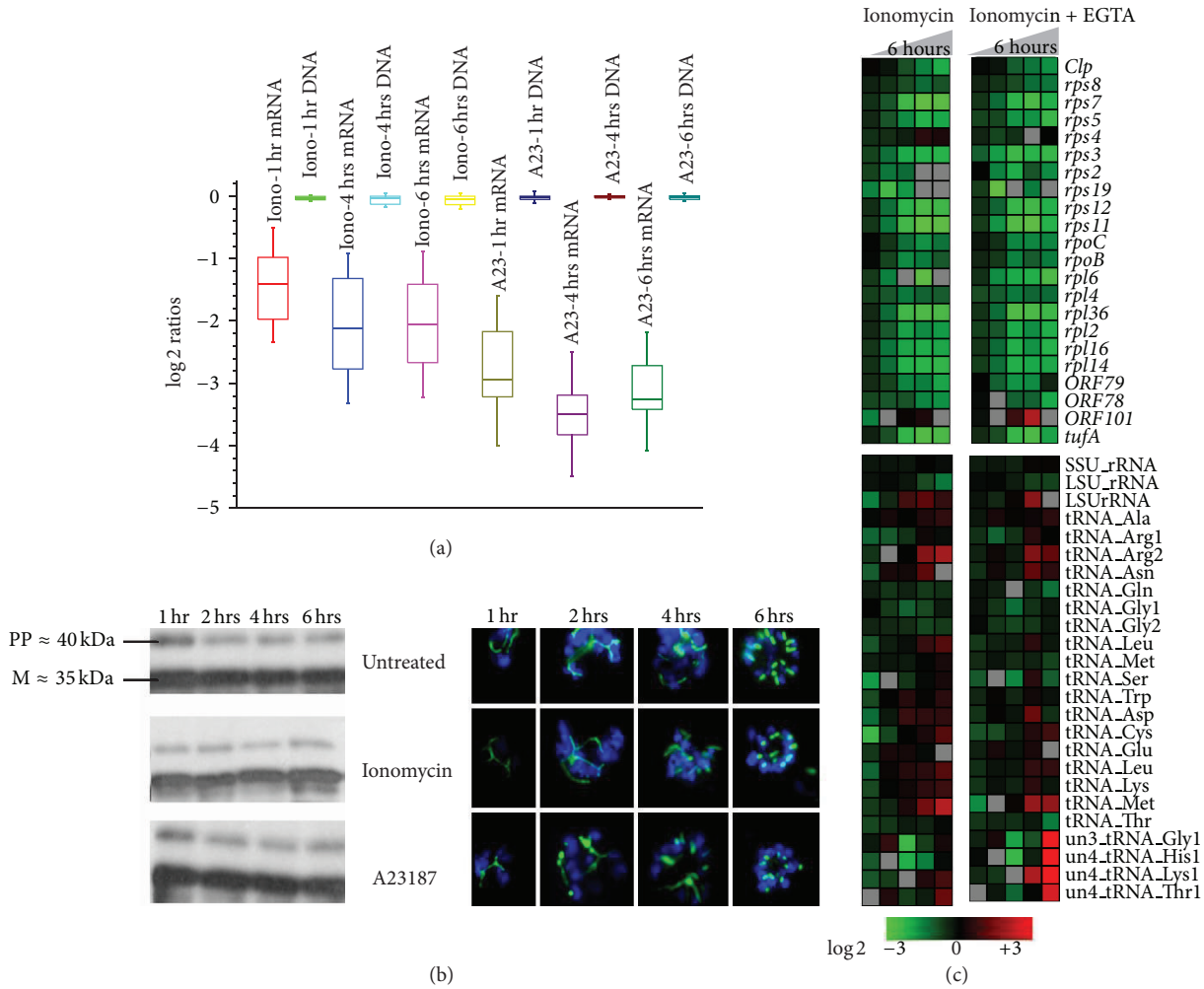

FIGURE 2: Apicoplast development and DNA replication are hardly inhibited by calcium ionophores. (a) Apicoplast DNA replication is not inhibited by calcium ionophores. Box plots for the log 2 expression ratios of averaged oligos representing all apicoplast genes (obtained from the microarray hybridization results filtered for 3-fold change in 2 time points) and log 2 ratios of the treated and untreated apicoplast DNA (obtained from a CGH experiment where the total DNA from the treated parasites was hybridized against the total DNA from the untreated parasites) have been compared. (b) Western blots show the processed band (≈35 kDa) of the ACP-GFP fusion protein (≈40 kDa) directed towards apicoplast indicating that the protein has been imported and processed without much interference even after 6 hours after treatment. Fluorescence microscopy done on ACP-GFP expressing parasites confirms the western results. (c) Relative expression of apicoplast genes in ionomycin treatment of schizonts both in presence and absence of 3 mM EGTA. (I-ionomycin, I + E-ionomycin plus EGTA).

we wished to identify a protein factor(s) that may facilitate this phenomenon. For this we carried out bioinformatics analyses of all 545 plastid targeted nuclear encoded proteins [47, 48] and identified MAL13P1.156, a calcium binding protein that contain a signal anchor with probability of 0.954 [49] and 5 of 5 positive tests for an apicoplast targeting peptide [47] at its C-terminus. A similar protein that lacks an apparent signal peptide but contains a signal anchor has been found to be targeted to the apicoplast via an independent bipartite signal targeting in *Toxoplasma gondii* [50, 51]. MAL13P1.156 is a single exon gene (1599 bp) that codes for a 64 kDa protein and contains an EF-hand domain (prediction *e*-value, $2.80E^{-13}$) at the position between 234 and 518 amino acid of the deduced polypeptide. A search of the RCSB Protein Data Bank (PDB) [52] for structurally similar proteins retrieved several sequences of calcium binding proteins with the EF-hand calcium binding domain. These include an EF-hand calcium binding protein from *Entamoeba histolytica* (*E*-value 0.002, solution NMR), CDPK3 (calcium-dependent protein kinase-3) from *Cryptosporidium parvum* (*E*-value 0.053, X-ray diffraction), myristoylated NCS1p from *Schizosaccharomyces pombe* (*E*-value 0.10, solution NMR) and CDPK-1 (calcium-dependent protein kinase-1) from *Toxoplasma gondii* (*E*-value 0.35, X-ray diffraction). Multiple alignments of the amino acids spanning the EF-hand domain (214th to 341th positions) show considerable conservation of the calcium binding domain between these structural homologues (Figure 3(e)). This suggests a putative calcium binding function of MAL13P1.156 and thus its role in calcium-dependent signaling in the apicoplast such as sensing and/or buffering free Ca^{2+} ions similar to its plant counterparts in the chloroplast [53].

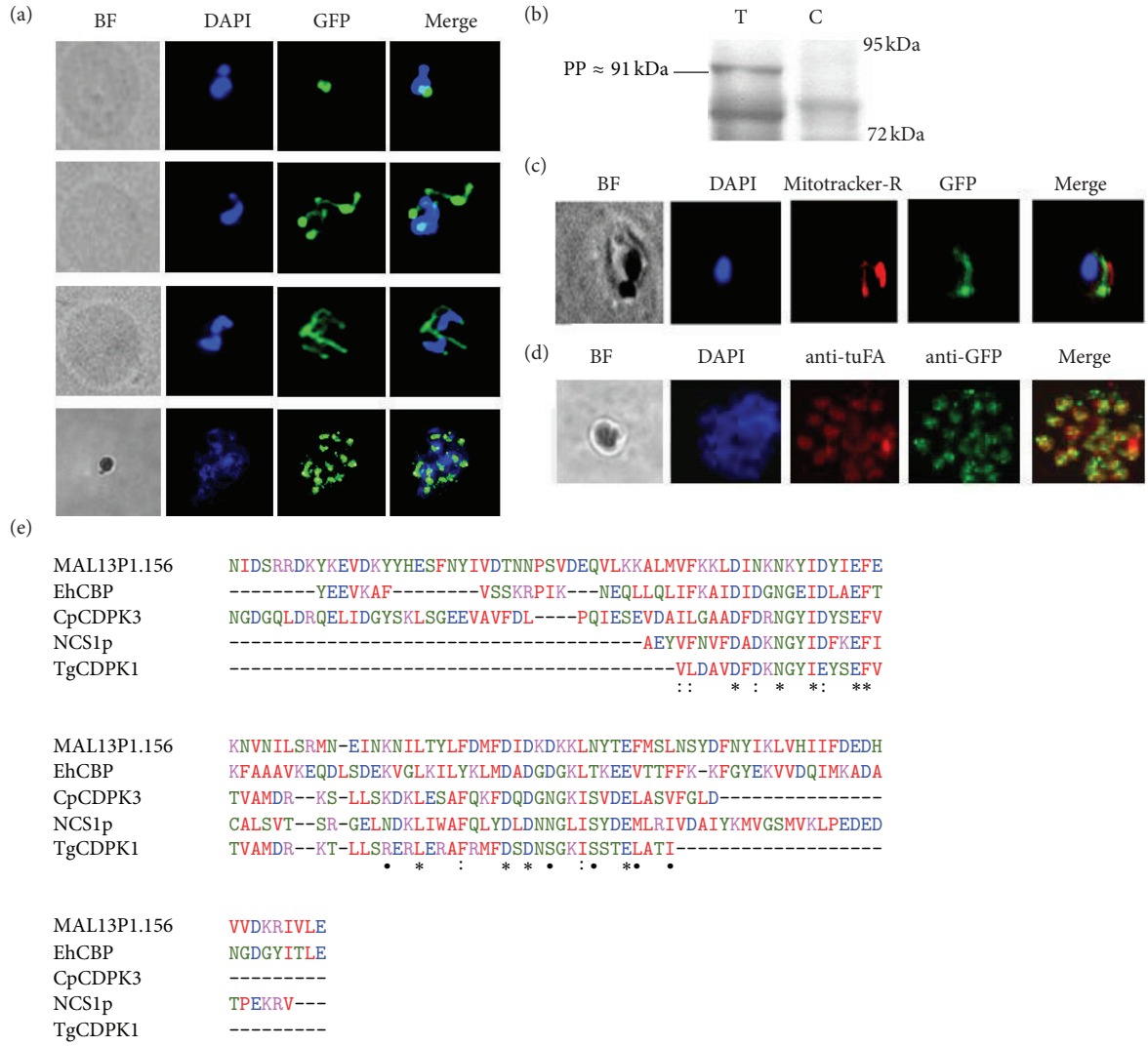

Figure 3: Identification of an apicoplast targeted protein with EF-hand domain. (a) Immunofluorescence microscopy done (anti-GFP) on parasites episomally expressing MAL13P1.156-GFP fusion shows typical apicoplast pattern. (b) Antibody against the c-terminal GFP detects MAL13P1.156 full-length protein with an apicoplast targeted protein signature (T-transfected, C-Control). (c, d) Colocalisation with Mitotracker-Red and apicoplast encoded tuF, respectively. (e) MAL13P1.156 multiple alignments with the structural homologues obtained from a sequence blast on PDB. EhCBP-*Entamoeba histolytica* calcium binding protein, CpCDPK3-*Cryptosporidium parvum* calcium-dependent protein kinase3, NCS1p-calcium binding protein NCS-1 *Schizosaccharomyces pombe*, and TgCDPK1-*Toxoplasma gondii* calcium dependent kinase1.

To investigate the biological function of MAL13P1.156, we constructed a fusion construct of this protein with a C-terminal GFP and subsequently generated a *P. falciparum* (3D7) transgenic cell line where this fusion protein is expressed episomally. Western blot analyses show a strong expression of this protein as a full-length fusion protein of 91 kDa (64 kDa full-length protein plus 27 kDa GFP) and a processed form ~72 kDa (Figure 3(b)). This proteolytic cleavage is consistent with the signal peptide processing upon import to the apicoplast. Subsequently, immunofluorescence microscopy (IFA) of the transgenic cell line using the anti-GFP antibody shows the characteristic pattern of apicoplast localization with a single small compartment in the early schizonts, elongated branched formation in the late schizonts, and finally divided punctuate formations corresponding to new apicoplast precursors in the newly formed daughter merozoites (Figure 3(a)). Finally, IFA-based colocalization studies revealed a close proximity between the MAL13P1.156 labeled compartments and mitochondria labeled by mitotracker Red (Figure 3(c)). This is consistent with physical association of apicoplast and mitochondria in *P. falciparum*. Finally there is partial but significant colocalization between MAL13P1.156 and the apicoplast marker EF-Tu (Figure 3(d)). Based on these results we conclude that MAL13P1.156 localizes to the apicoplast and hence name this protein *P. falciparum* apicoplast calcium binding protein 1 (PfACBP1).

To investigate whether PfACBP1 plays a role in intracellular calcium homeostasis of the *Plasmodium* parasites we

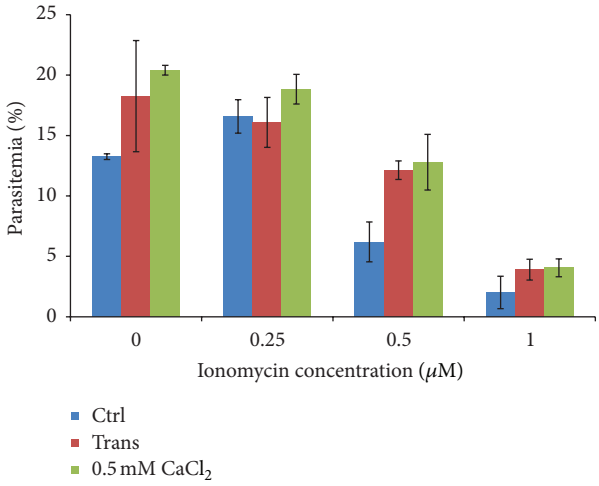

FIGURE 4: Reduced sensitivity of the transfected cells towards ionomycin. Blue-nontransfected (Ctrl), red-transfected (Trans) and green-nontransfected parasites grown in medium supplied with external calcium (500 μM). $^{*}P$ value: 0.01.

determined the sensitivity of the generated transgenic cell line to ionomycin. Here we hypothesize that MAL13P1.156 overexpressing parasites have a higher capacity to withstand ionomycin exposure and its effect as an intracellular calcium ion mobilizer that is presumably depleting the apicoplast of calcium. Overexpression of PfACBP1 would help to retain higher calcium concentration in the apicoplast via its calcium binding properties. To investigate this hypothesis, *P. falciparum* cells (mid schizont stage) were treated with 0, 0.25, 0.5 and 1 μM of Ionomycin for 12–14 hrs until next invasion and the parasite survival was monitored by Giemsa smear microscopy. At 0.5 μM of ionomycin (that roughly corresponds to the ionomycin IC50; see below), the survival of the PfACBP1 overexpressing cell line is ~2-fold higher (P value 0.01) compared to the nontransfected parasites (Figure 4). The survival rate of the transgenic cell line is comparable to the nontransfected parasites grown in the medium supplemented with 500 μM of $CaCl_2$. Here we assume that the extracellular calcium supplied in the growth medium reduces the severity of the calcium mobilization action of ionomycin (Figure 4). This increase in the resistance of the PfACBP1 overexpressing parasites suggests its role in the calcium signaling in the plastid but also the fact that the calcium depletion from the apicoplast is a part to the toxic effect of ionophores in the *P. falciparum* parasites.

3. Discussion

Here we used transcriptional profiling to analyze the mode of action of ionophores (ionomycin and A23187) in order to gain more insights into the role of Ca^{2+} signaling in *P. falciparum*. Although transcriptional profiling is known to be a powerful method to understand activities of small-molecule inhibitors in eukaryotic cells, in *P. falciparum* as well as other highly specialized pathogens, chemical or other types of external stimuli/perturbations do not always induce specific responses [37, 54, 55]. In *P. falciparum*, transcriptional responses to external perturbations range from low amplitude nonspecific changes in mRNA profiles to broad extensive transcriptional changes affecting the vast majority of the *P. falciparum* genes that are typically consistent with developmental arrests and/or induction of the sexual stages. Nonetheless, for several types of small molecule inhibitors, transcriptional responses are more specific, involving genes of direct or indirect targets [56, 57]. In this study, we used two inhibitors that are known to have similar (or overlapping) effects on calcium distribution in the eukaryotic cell. Interestingly these two inhibitors exhibit dramatically different effects on the *P. falciparum* growth. While ionomycin affected expression of a narrow group of genes, with downregulation of plastid gene expression being most pronounced, A23187 caused a broad transcriptional shift that is consistent with a developmental arrest in the schizont stage. This is surprising given that both inhibitors have similar growth inhibitory effects on the *P. falciparum* cells with IC50 (inhibition concentration by 50%) 513 and 304 nM for ionomycin and A23187, respectively (data not shown). This could be either due to a stronger effect of A23187 on calcium redistribution in the cell and subsequently a more dramatic response manifested by the developmental arrest, or alternatively this discrepancy could be caused by A23187 interacting with additional molecular targets compared to ionomycin. Although more research is required to understand the molecular mechanism(s) that underlines the developmental arrests induced by various perturbations, these data further underline the overall diversity of *P. falciparum* transcriptional responses to external stimuli and their utility for systems biology approaches using the "guilty-by-association" principle [56, 58, 59].

The main activity of calcium ionophores is to carry Ca^{2+} cations across the membranes down its concentration gradient [45]. In eukaryotic cells this causes cytoplasmic mobilizations of Ca^{2+} that are released from the intracellular calcium stores, intracellular compartments in which calcium is sequestered under normal growth concentrations. Similar to other eukaryotic cells, the main intracellular calcium stores of apicomplexan parasites include the endoplasmic reticulum (ER), nuclei, and mitochondria as well as specialized acidic compartments, acidocalcisomes [60]. In addition to these canonical calcium stores, the parasitophorous vacuole (PV) (the lumen between the parasite plasma membrane (PPM) and the parasitophorous vacuolar membrane (PVM) diving the parasite cell from the host cell cytoplasm during their intraerythrocytic development) was shown to contain high concentrations of calcium [34]. It was proposed that the high concentration of calcium in the PV, estimated at ~40 μM, creates a calcium rich microenvironment that is essential for the parasite growth in the otherwise calcium poor erythrocyte cytoplasm, >100 nM. Expectedly, ionomycin causes a rapid efflux of calcium out of the PV into the parasite cytoplasm and to the ambient media and thus diminishing the concentration gradient at the parasite plasma membrane. In addition to the PV, ionomycin can also mobilize other intracellular calcium stores in the parasites (presumably ER, mitochondria, and acidocalcisomes) raising the calcium concentration in the

parasite cytoplasm even further [34]. The rapid effect on the plastid genome transcription observed in our study suggests that the ionophores can affect the concentration of calcium diverting it from a steady state concentration that is likely essential for the proper function of this organelle. This model is supported by the fact that the ionomycin-mediated inhibition of the plastid transcription also occurs when the calcium is chelated from the ambient media (Figure 2(c)); hence, the ionophore-mediated calcium flow is directed away from the parasitized erythrocyte. Moreover, thapsigargin (THG) that increases cytoplasmic calcium by a specific release from the ER [34] has no effect on the plastid genome transcription (data not shown). Taken together these data suggest that in addition to calcisomes, ER, and mitochondria, the plastid can serves as another component of the internal calcium stores in the *Plasmodium* parasites.

There is mounting evidence that calcium signaling plays a major role in maintenance and genesis of the endosymbiotic organelles of eukaryotic cells. In the chloroplast of the plant cells, calcium is an essential signaling factor for at least three different functionalities: import of nuclear encoded proteins, vesicular transport system, and oxygenate photosynthesis (reviewed in [53]). Most of the calcium-dependent signal transduction in the chloroplast is believed to be facilitated by proteins that contain the "EF-hand" domain(s) [61]. Binding of calcium causes conformational changes to the EF-hand proteins that subsequently results in increasing binding affinity to other interacting proteins or DNA sequences. Alternatively, calcium binding could cause cross-activation of enzymatic activities of additional domains present at the polypeptide such as protein kinases in calmodulins, calcium-dependent protein kinases present in plants, and protists [62]. Here we identify a novel EF-hand protein in *P. falciparum*, PfACBP1, that is targeted to the plastid and its overexpression increases resistance of the parasite cells to ionomycin. In our bioinformatics analyses of the 545 plastid targeted proteins [47, 48], PfACBP1 showed the highest homology to the EF-hand consensus sequence which suggests its crucial role in calcium-mediated regulatory function(s) in this compartment. In future studies it will be intriguing to explore the role of PfACBP1, the highly conserved calcium binding protein, in regulation of plastid gene expression.

Until today, the plastid represents one of the most important targets for malaria chemotherapy [63]. A number of apicoplast functionalities can be targeted by specific well-established antimicrobial chemotherapeutics, some of which can be used for malaria treatment and prophylaxis. These chemotherapeutic strategies take advantage of the prokaryotic character of several basic apicoplast mechanisms including DNA replication, inhibited by fluoroquinolinone antibiotics [64]; RNA transcription inhibited by rifampicin [65]; and protein translation that can be blocked by clindamycin, azithromycin binding to 23S rRNA [66], and doxycycline and tetracycline binding to 16S rRNA [67]. All these compounds were shown to block apicoplast organellogenesis and division which leads to an absence of this compartment in the newly invaded parasite generations. Although these parasites could develop until the midstage of the (subsequent) IDC, the lack of apicoplast functionalities likely causes the ultimate cell death. Overall, this phenomenon, also known as the delayed death phenotype, is characteristic for most of these drugs with the exception of tetracycline that is believed to also affect the mitochondrion and kill the cells instantly [67]. In addition to rifampicin and other RNA synthesis blockers, doxycycline was also found to specifically and exclusively inhibit transcription of the apicoplast genome encoded genes [68]. This is somewhat surprising as the main mode of action doxycycline is blocking the apicoplast proteosynthesis. This suggests that transcriptional regulation of the apicoplast genes involves multiple components of intracellular signaling potentiality including apicoplast encoded proteins. Here we show that calcium-dependent signaling factors contribute to this regulation and that interference with these can also have toxic effect on the *Plasmodium* cells, albeit not via the delayed death mechanism.

Several biochemical pathways associated with the apicoplast are being explored as suitable drug targets for malaria chemotherapy. These include fatty acid type II (FASII) [69], nonmevalonate isoprenoid synthesis [70], apicoplast REDOX system [71], and heme synthesis [72]. Each of these pathways represents essential biological processes that take place within the endosymbiotic organelle and thus were retained through the evolution. With that, each pathway retained a certain portion of prokaryotic features that are being explored by malaria drug development efforts. The most remarkable example represents FASII that arrears to be the sole producer of fatty acids in *Plasmodium* cells as precursors of membrane synthesis and energy stores. Several inhibitors of FASII enzymes are being explored as suitable drug candidates including trichlosan (inhibitor of enoyl-ACP reductase, FabI) and thiolactomycine (inhibitor of beta-ketoacyl-ACP synthetase II and III, Fab II and III) (reviewed in [63]). Although the validity of this pathway as a drug target for blood stage parasites has been recently disputed by observations that apicoplast plays only a minor biochemical role during its asexual intraerythrocytic development [73]. FASII was found to be predominant and extremely important during the *Plasmodium* liver stage development [74]. Indeed, the *Plasmodium* liver stages appear to be highly sensitive to a FASII inhibitor hexachlorophene, as well as to rifampicin and tetracycline [74]. Given the importance of calcium-dependent signaling in the apicoplast transcription it will be interesting to explore its potential as a new target for liver stage drug development which is one of the main objectives of the future programs for malaria control and elimination proposed for the next era of malaria-related research [75].

4. Materials and Methods

4.1. Cell Culture, Drug Treatment, and DNA Microarray. All treatment experiments were carried out with the *P. falciparum* 3D7 strain. Calcium ionophore treatments were carried out as follows: highly synchronized *P. falciparum* cultures were treated with 5 μM of calcium ionophores, ionomycin and A23187 (Sigma) at the schizont stage for 30 minutes, 1 hour, 2 hours, 4 hours, and 6 hours. Total RNA from each of the time points was isolated and aminoallyl-cDNA was synthesized

using reverse transcriptase system (Fermentas). Subsequently cDNA made from the treated and untreated parasites were labeled with Cy5 (GE-Amersham). A reference pool was made by mixing equal amount of RNA from the parasites collected at 6 hours interval throughout the 48 hours life cycle and was labeled with Cy3 (GE-Amersham). The samples were then hybridized on a spotted cDNA chip platform comprising 10166 MOEs representing 5363 coding sequences [36]. The data was normalized and filtered with the condition, signal intensity > background intensity + 2 SD of background intensity using NOMAD (http://derisilab.ucsf.edu). Hierarchical clustering of the log-transformed ratios was then done using Cluster (Eisen lab) [76] and visualized using Treeview (Eisen lab) [76]. Pathway analysis was done based on the hyper geometric and binomial probability distribution and pathways which had a P value of <0.01 were considered significant. For the extracellular calcium chelation experiment, the medium was treated with 3 mM of EGTA and the ionomycin treatment was carried out later on at 5 μM concentration. Hybridization and data analysis were carried out as above.

4.2. Comparative Genomic Hybridization (CGH). Comparative genomic hybridization was carried out with total DNA isolated from the untreated parasites and the parasites treated with the calcium ionophores (ionomycin and A23187 at 5 μM concentration) at 1 hour, 4 hours, and 6 hours after treatment.

3 μg of the total DNA from each of the samples was subjected to klenow (NEB) reaction as described before [77]. Treated DNA labeled with Cy3 was then hybridized against untreated DNA labeled with Cy5. Hybridization and Data analysis were done as described above for the cDNA hybridization.

4.3. Transfection. Transfection of 3D7 parasites was performed as described before [78]. Two lines of transgenic parasites episomally expressing GFP fused to the C-terminus of acyl carrier protein (ACP) and MAL13P1.156, respectively, were developed. ACP and MAL13P1.156 were amplified from the 3D7 genomic DNA using the following primers:

ACP XhoI-Fw

5′-AGTC**CTCGAG**CACCTTATTAGAATGAAGATCTTATTACTTTG-3′

ACP-AvrII-Bw

5′-AGTC**CCTAGG**TTTTAAAGAGCTAGATGGG-3′

MAL13P1.156 XhoI-Fw

5′-AGTC**CTCGAG**ATGAAACTTTTAAATTTTCCACTGTCC-3′

MAL13P1.156 AvrII-Bw

5′-AGTC**CCTAGG**TGTGGCATATACTATGTCTGGAGCC-3′.

pARL vector [79] was modified for generating the required constructs. Stevor gene was replaced with ACP and MAL13P1.156 for generating pARL-ACP-GFP and pARL-MAL13P1.156, respectively, under the control of PfCRT promoter and hDHFR as the selectable marker.

4.4. Fluorescence Microscopy. Parasites expressing ACP-GFP episomally was used for the import inhibition experiment. Smears were made from parasites exposed to ionomycin and A23187 1 hour, 2 hours, 4 hours, and 6 hours after invasion. The smears were fixed in 4% paraformaldehyde and, after staining with DAPI, were viewed under a fluorescence microscope. For the localization and colocalization experiments, immunofluorescence assay was done using anti-GFP (mouse anti-GFP, Santacruz Biotech) and anti-tuFA (rabbit anti-tuFA, kindly given by Dr. Saman Habib, CDRI, India).

4.5. Western Blots. Proteins from the crude parasite lysates were separated on a 10% SDS polyacrylamide gel. The resolved proteins were then transferred to a nitrocellulose membrane. The blots were then probed with rabbit anti-GFP antibody which was in turn detected with anti-rabbit IgG conjugated with HRP.

4.6. Drug Assay. Nontransfectants, nontransfectants with 500 μM $CaCl_2$ in the medium, and the transfectants overexpressing MAL13P1.156 were exposed to ionomycin at 0, 0.25, 0.5, and 1 μM concentrations in the schizont stage. The newly invaded rings were counted on giemsa stained smears under a light microscope. The percentage of rings was plotted against the inhibitory concentrations.

Conflict of Interests

The authors declare that there is no conflict of interests regarding the publication of this article.

Acknowledgment

This work was supported by the Singaporean Ministry of Education, Tier 1 Grant no. RG 36/08.

References

[1] S. I. Hay, C. A. Guerra, A. J. Tatem, A. M. Noor, and R. W. Snow, "The global distribution and population at risk of malaria: past, present, and future," *The Lancet Infectious Diseases*, vol. 4, no. 6, pp. 327–336, 2004.

[2] A. M. Dondorp, F. Nosten, P. Yi et al., "Artemisinin resistance in *Plasmodium falciparum* malaria," *The New England Journal of Medicine*, vol. 361, no. 5, pp. 455–467, 2009.

[3] N. J. White, "Artemisinin resistance—the clock is ticking," *The Lancet*, vol. 376, no. 9758, pp. 2051–2052, 2010.

[4] G. Majori, "Malaria therapy in Africa with Artemisinin-based combination," *Parassitologia*, vol. 46, no. 1-2, pp. 85–87, 2004.

[5] L. M. Alleva and K. Kirk, "Calcium regulation in the intraerythrocytic malaria parasite *Plasmodium falciparum*," *Molecular and Biochemical Parasitology*, vol. 117, no. 2, pp. 121–128, 2001.

[6] P. Ward, L. Equinet, J. Packer, and C. Doerig, "Protein kinases of the human malaria parasite *Plasmodium falciparum*: the kinome of a divergent eukaryote," *BMC Genomics*, vol. 5, article 79, 2004.

[7] Y. Zhao, B. Kappes, J. Yang, and R. M. Franklin, "Molecular cloning, stage-specific expression and cellular distribution of a

putative protein kinase from *Plasmodium falciparum*," *European Journal of Biochemistry*, vol. 207, no. 1, pp. 305–313, 1992.

[8] L. Aravind, L. M. Iyer, T. E. Wellems, and L. H. Miller, "Plasmodium biology: genomic gleanings," *Cell*, vol. 115, no. 7, pp. 771–785, 2003.

[9] C. R. S. Garcia, A. R. Dluzewski, L. H. Catalani, R. Burting, J. Hoyland, and W. T. Mason, "Calcium homeostasis in intraerythrocytic malaria parasites," *European Journal of Cell Biology*, vol. 71, no. 4, pp. 409–413, 1996.

[10] D. J. Krogstad, S. P. Sutera, J. S. Marvel et al., "Calcium and the malaria parasite: parasite maturation and the loss of red cell deformability," *Blood Cells*, vol. 17, no. 1, pp. 229–241, 1991.

[11] M. Wasserman, J. P. Vernot, and P. M. Mendoza, "Role of calcium and erythrocyte cytoskeleton phosphorylation in the invasion of *Plasmodium falciparum*," *Parasitology Research*, vol. 76, no. 8, pp. 681–688, 1990.

[12] A. Vaid, D. C. Thomas, and P. Sharma, "Role of Ca^{2+}/calmodulin-PfPKB signaling pathway in erythrocyte invasion by *Plasmodium falciparum*," *Journal of Biological Chemistry*, vol. 283, no. 9, pp. 5589–5597, 2008.

[13] J. L. Green, R. R. Rees-Channer, S. A. Howell et al., "The motor complex of *Plasmodium falciparum*: phosphorylation by a calcium-dependent protein kinase," *Journal of Biological Chemistry*, vol. 283, no. 45, pp. 30980–30989, 2008.

[14] I. Siden-Kiamos, A. Ecker, S. Nybäck, C. Louis, R. E. Sinden, and O. Billker, "Plasmodium berghei calcium-dependent protein kinase 3 is required for ookinete gliding motility and mosquito midgut invasion," *Molecular Microbiology*, vol. 60, no. 6, pp. 1355–1363, 2006.

[15] T. Ishino, Y. Orito, Y. Chinzei, and M. Yuda, "A calcium-dependent protein kinase regulates Plasmodium ookinete access to the midgut epithelial cell," *Molecular Microbiology*, vol. 59, no. 4, pp. 1175–1184, 2006.

[16] A. Vaid and P. Sharma, "PfPKB, a protein kinase B-like enzyme from *Plasmodium falciparum*: II. Identification of calcium/calmodulin as its upstream activator and dissection of a novel signaling pathway," *Journal of Biological Chemistry*, vol. 281, no. 37, pp. 27126–27133, 2006.

[17] Y. Matsumoto, G. Perry, L. W. Scheibel, and M. Aikawa, "Role of calmodulin in *Plasmodium falciparum*: implications for erythrocyte invasion by the merozoite," *European Journal of Cell Biology*, vol. 45, no. 1, pp. 36–43, 1987.

[18] M. Wasserman and J. Chaparro, "Intraerythrocytic calcium chelators inhibit the invasion of *Plasmodium falciparum*," *Parasitology Research*, vol. 82, no. 2, pp. 102–107, 1996.

[19] O. Billker, S. Dechamps, R. Tewari, G. Wenig, B. Franke-Fayard, and V. Brinkmann, "Calcium and a calcium-dependent protein kinase regulate gamete formation and mosquito transmission in a malaria parasite," *Cell*, vol. 117, no. 4, pp. 503–514, 2004.

[20] F. Kawamoto, H. Fujioka, R.-I. Murakami et al., "The roles of Ca^{2+}/calmodulin- and cGMP-dependent pathways in gametogenesis of a rodent malaria parasite, Plasmodium berghei," *European Journal of Cell Biology*, vol. 60, no. 1, pp. 101–107, 1993.

[21] L. McRobert, C. J. Taylor, W. Deng et al., "Gametogenesis in malaria parasites is mediated by the cGMP-dependent protein kinase," *PLoS Biology*, vol. 6, no. 6, article e139, 2008.

[22] O. Billker, S. Lourido, and L. D. Sibley, "Calcium-dependent signaling and kinases in apicomplexan parasites," *Cell Host and Microbe*, vol. 5, no. 6, pp. 612–622, 2009.

[23] E. Borrelli, J. P. Montmayeur, N. S. Foulkes, and P. Sassone-Corsi, "Signal transduction and gene control: the cAMP pathway," *Critical reviews in oncogenesis*, vol. 3, no. 4, pp. 321–338, 1992.

[24] M. Frödin and S. Gammeltoft, "Role and regulation of 90 kDa ribosomal S6 kinase (RSK) in signal transduction," *Molecular and Cellular Endocrinology*, vol. 151, no. 1-2, pp. 65–77, 1999.

[25] G. E. Hardingham and H. Bading, "Nuclear calcium: a key regulator of gene expression," *BioMetals*, vol. 11, no. 4, pp. 345–358, 1998.

[26] A. J. Shaywitz and M. E. Greenberg, "CREB: a stimulus-induced transcription factor activated by a diverse array of extracellular signals," *Annual Review of Biochemistry*, vol. 68, pp. 821–861, 1999.

[27] M. S. Kapiloff, J. M. Mathis, C. A. Nelson, C. R. Lin, and M. G. Rosenfeld, "Calcium/calmodulin-dependent protein kinase mediates a pathway for transcriptional regulation," *Proceedings of the National Academy of Sciences of the United States of America*, vol. 88, no. 9, pp. 3710–3714, 1991.

[28] D. B. Arnold and N. Heintz, "A calcium responsive element that regulates expression of two calcium binding proteins in Purkinje cells," *Proceedings of the National Academy of Sciences of the United States of America*, vol. 94, no. 16, pp. 8842–8847, 1997.

[29] I. A. S. Drummond, A. S. Lee, E. Resendez Jr., and R. A. Steinhardt, "Depletion of intracellular calcium stores by calcium ionophore A23187 induces the genes for glucose-regulated proteins in hamster fibroblasts," *Journal of Biological Chemistry*, vol. 262, no. 26, pp. 12801–12805, 1987.

[30] J. O. Hensold, G. Dubyak, and D. E. Housman, "Calcium ionophore, A23187, induces commitment to differentiation but inhibits the subsequent expression of erythroid genes in murine erythroleukemia cells," *Blood*, vol. 77, no. 6, pp. 1362–1370, 1991.

[31] R. E. Ware, M. K. Hart, and B. F. Haynes, "Induction of T cell CD7 gene transcription by nonmitogenic ionomycin-induced transmembrane calcium flux," *Journal of Immunology*, vol. 147, no. 8, pp. 2787–2794, 1991.

[32] R. S. Weinstock, C. A. Manning, and J. L. Messina, "The regulation of p33 gene expression by insulin and calcium ionophores," *Endocrinology*, vol. 130, no. 2, pp. 616–624, 1992.

[33] N. Marchesini, S. Luo, C. O. Rodrigues, S. N. J. Moreno, and R. Docampo, "Acidocalcisomes and a vacuolar H^+-pyrophosphatase in malaria parasites," *Biochemical Journal*, vol. 347, no. 1, pp. 243–253, 2000.

[34] M. L. Gazarini, A. P. Thomas, T. Pozzan, and C. R. S. Garcia, "Calcium signaling in a low calcium environment: how the intracellular malaria parasite solves the problem," *Journal of Cell Biology*, vol. 161, no. 1, pp. 103–110, 2003.

[35] C. Gumila, M. L. Ancelin, G. Jeminet, A. M. Delort, G. Miquel, and H. J. Vial, "Differential in vitro activities of ionophore compounds against *Plasmodium falciparum* and mammalian cells," *Antimicrobial Agents and Chemotherapy*, vol. 40, no. 3, pp. 602–608, 1996.

[36] G. Hu, M. Llinás, J. Li, P. R. Preiser, and Z. Bozdech, "Selection of long oligonucleotides for gene expression microarrays using weighted rank-sum strategy," *BMC Bioinformatics*, vol. 8, article 350, 2007.

[37] K. G. le Roch, J. R. Johnson, H. Ahiboh et al., "A systematic approach to understand the mechanism of action of the bisthiazolium compound T4 on the human malaria parasite, *Plasmodium falciparum*," *BMC Genomics*, vol. 9, article 513, 2008.

[38] S. Mok, M. Imwong, M. J. Mackinnon et al., "Artemisinin resistance in *Plasmodium falciparum* is associated with an altered temporal pattern of transcription," *BMC Genomics*, vol. 12, article 391, 2011.

[39] H. Ginsburg, *Malaria Parasite Metabolic Pathways*, 2008.

[40] F. Chigri, J. Soll, and U. C. Vothknecht, "Calcium regulation of chloroplast protein import," *Plant Journal*, vol. 42, no. 6, pp. 821–831, 2005.

[41] S. A. Ralph, G. G. van Dooren, R. F. Waller et al., "Metabolic maps and functions of the *Plasmodium falciparum* apicoplast," *Nature Reviews Microbiology*, vol. 2, no. 3, pp. 203–216, 2004.

[42] N. C. Waters, K. M. Kopydlowski, T. Guszczynski et al., "Functional characterization of the acyl carrier protein (PfACP) and beta-ketoacyl ACP synthase III (PfKASIII) from *Plasmodium falciparum*," *Molecular and Biochemical Parasitology*, vol. 123, no. 2, pp. 85–94, 2002.

[43] R. F. Waller, P. J. Keeling, R. G. K. Donald et al., "Nuclear-encoded proteins target to the plastid in Toxoplasma gondii and *Plasmodium falciparum*," *Proceedings of the National Academy of Sciences of the United States of America*, vol. 95, no. 21, pp. 12352–12357, 1998.

[44] G. G. van Dooren, V. Su, M. C. D'Ombrain, and G. I. McFadden, "Processing of an apicoplast leader sequence in *Plasmodium falciparum* and the identification of a putative leader cleavage enzyme," *Journal of Biological Chemistry*, vol. 277, no. 26, pp. 23612–23619, 2002.

[45] E. N. Dedkova, A. A. Sigova, and V. P. Zinchenko, "Mechanism of action of calcium ionophores on intact cells: ionophore-resistant cells," *Membrane and Cell Biology*, vol. 13, no. 3, pp. 357–368, 2000.

[46] L. R. Garzoni, M. O. Masuda, M. M. Capella, A. G. Lopes, and M. D. N. S. Leal De Meirelles, "Characterization of $[Ca^{2+}]$i responses in primary cultures of mouse cardiomyocytes induced by Trypanosoma cruzi trypomastigotes," *Memorias do Instituto Oswaldo Cruz*, vol. 98, no. 4, pp. 487–493, 2003.

[47] B. J. Foth, S. A. Ralph, C. J. Tonkin et al., "Dissecting apicoplast targeting in the malaria parasite *Plasmodium falciparum*," *Science*, vol. 299, no. 5607, pp. 705–708, 2003.

[48] M. J. Gardner, N. Hall, E. Fung et al., "Genome sequence of the human malaria parasite *Plasmodium falciparum*," *Nature*, vol. 419, no. 6906, pp. 498–511, 2002.

[49] T. N. Petersen, S. Brunak, G. Von Heijne, and H. Nielsen, "SignalP 4.0: discriminating signal peptides from transmembrane regions," *Nature Methods*, vol. 8, no. 10, pp. 785–786, 2011.

[50] L. Lim, M. Kalanon, and G. I. McFadden, "New proteins in the apicoplast membranes: time to rethink apicoplast protein targeting," *Trends in Parasitology*, vol. 25, no. 5, pp. 197–200, 2009.

[51] A. E. DeRocher, I. Coppens, A. Karnataki et al., "A thioredoxin family protein of the apicoplast periphery identifies abundant candidate transport vesicles in Toxoplasma gondii," *Eukaryotic Cell*, vol. 7, no. 9, pp. 1518–1529, 2008.

[52] H. M. Berman, J. Westbrook, Z. Feng et al., "The Protein Data Bank," *Nucleic Acids Research*, vol. 28, no. 1, pp. 235–242, 2000.

[53] J. Bussemer, U. C. Vothknecht, and F. Chigri, "Calcium regulation in endosymbiotic organelles of plants," *Plant Signaling and Behavior*, vol. 4, no. 9, pp. 805–808, 2009.

[54] K. Ganesan, N. Ponmee, L. Jiang et al., "A genetically hard-wired metabolic transcriptome in *Plasmodium falciparum* fails to mount protective responses to lethal antifolates," *PLoS Pathogens*, vol. 4, no. 11, Article ID e1000214, 2008.

[55] A. M. Gunasekera, A. Myrick, K. L. Roch, E. Winzeler, and D. F. Wirth, "*Plasmodium falciparum*: genome wide perturbations in transcript profiles among mixed stage cultures after chloroquine treatment," *Experimental Parasitology*, vol. 117, no. 1, pp. 87–92, 2007.

[56] G. Hu, A. Cabrera, M. Kono et al., "Transcriptional profiling of growth perturbations of the human malaria parasite *Plasmodium falciparum*," *Nature Biotechnology*, vol. 28, no. 1, pp. 91–98, 2010.

[57] P. A. Tamez, S. Bhattacharjee, C. van Ooij et al., "An erythrocyte vesicle protein exported by the malaria parasite promotes tubovesicular lipid import from the host cell surface," *PLoS Pathogens*, vol. 4, no. 8, Article ID e1000118, 2008.

[58] E. A. Winzeler, "Applied systems biology and malaria," *Nature Reviews Microbiology*, vol. 4, no. 2, pp. 145–151, 2006.

[59] Y. Zhou, V. Ramachandran, K. A. Kumar et al., "Evidence-based annotation of the malaria parasite's genome using comparative expression profiling," *PLoS ONE*, vol. 3, no. 2, Article ID e1570, 2008.

[60] R. Docampo, W. de Souza, K. Miranda, P. Rohloff, and S. N. J. Moreno, "Acidocalcisomes—conserved from bacteria to man," *Nature Reviews Microbiology*, vol. 3, no. 3, pp. 251–261, 2005.

[61] A. Lewit-Bentley and S. Réty, "EF-hand calcium-binding proteins," *Current Opinion in Structural Biology*, vol. 10, no. 6, pp. 637–643, 2000.

[62] J. F. Harper and A. Harmon, "Plants, symbiosis and parasites: a calcium signalling connection," *Nature Reviews Molecular Cell Biology*, vol. 6, no. 7, pp. 555–566, 2005.

[63] R. F. Waller and G. I. McFadden, "The apicoplast: a review of the derived plastid of apicomplexan parasites," *Current Issues in Molecular Biology*, vol. 7, no. 1, pp. 57–79, 2005.

[64] A. A. Divo, A. C. Sartorelli, C. L. Patton, and F. J. Bia, "Activity of fluoroquinolone antibiotics against *Plasmodium falciparum* in vitro," *Antimicrobial Agents and Chemotherapy*, vol. 32, no. 8, pp. 1182–1186, 1988.

[65] S. Pukrittayakamee, R. Clemens, A. Chantra et al., "Therapeutic responses to antibacterial drugs in vivax malaria," *Transactions of the Royal Society of Tropical Medicine and Hygiene*, vol. 95, no. 5, pp. 524–528, 2001.

[66] E. R. Pfefferkorn and S. E. Borotz, "Comparison of mutants of Toxoplasma gondii selected for resistance to azithromycin, spiramycin, or clindamycin," *Antimicrobial Agents and Chemotherapy*, vol. 38, no. 1, pp. 31–37, 1994.

[67] A. S. Budimulja, S. Syafruddin, P. Tapchaisri, P. Wilairat, and S. Marzuki, "The sensitivity of Plasmodium protein synthesis to prokaryotic ribosomal inhibitors," *Molecular and Biochemical Parasitology*, vol. 84, no. 1, pp. 137–141, 1997.

[68] E. L. Dahl, J. L. Shock, B. R. Shenai, J. Gut, J. L. DeRisi, and P. J. Rosenthal, "Tetracyclines specifically target the apicoplast of the malaria parasite *Plasmodium falciparum*," *Antimicrobial Agents and Chemotherapy*, vol. 50, no. 9, pp. 3124–3131, 2006.

[69] R. F. Waller, S. A. Ralph, M. B. Reed et al., "A type II pathway for fatty acid biosynthesis presents drug targets in *Plasmodium falciparum*," *Antimicrobial Agents and Chemotherapy*, vol. 47, no. 1, pp. 297–301, 2003.

[70] H. Jomaa, J. Wiesner, S. Sanderbrand et al., "Inhibitors of the nonmevalonate pathway of isoprenoid biosynthesis as antimalarial drugs," *Science*, vol. 285, no. 5433, pp. 1573–1576, 1999.

[71] M. Vollmer, N. Thomsen, S. Wiek, and F. Seeber, "Apicomplexan Parasites Possess Distinct Nuclear-encoded, but Apicoplast-localized, Plant-type Ferredoxin-$NADP^+$ Reductase and Ferredoxin," *Journal of Biological Chemistry*, vol. 276, no. 8, pp. 5483–5490, 2001.

[72] N. Surolia and G. Padmanaban, "De novo biosynthesis of heme offers a new chemotherapeutic target in the human malarial parasite," *Biochemical and Biophysical Research Communications*, vol. 187, no. 2, pp. 744–750, 1992.

[73] E. Yeh and J. L. DeRisi, "Chemical rescue of malaria parasites lacking an apicoplast defines organelle function in blood-stage *Plasmodium falciparum*," *PLoS Biology*, vol. 9, no. 8, Article ID e1001138, 2011.

[74] A. S. Tarun, X. Peng, R. F. Dumpit et al., "A combined transcriptome and proteome survey of malaria parasite liver stages," *Proceedings of the National Academy of Sciences of the United States of America*, vol. 105, no. 1, pp. 305–310, 2008.

[75] The malERA Consultative Group on Drugs, "A research agenda for malaria eradication: drugs," *PLoS Medicine*, vol. 8, no. 1, p. e1000402, 2011.

[76] M. B. Eisen, P. T. Spellman, P. O. Brown, and D. Botstein, "Cluster analysis and display of genome-wide expression patterns," *Proceedings of the National Academy of Sciences of the United States of America*, vol. 95, no. 25, pp. 14863–14868, 1998.

[77] Z. Bozdech, M. Llinás, B. L. Pulliam, E. D. Wong, J. Zhu, and J. L. DeRisi, "The transcriptome of the intraerythrocytic developmental cycle of *Plasmodium falciparum*," *PLoS Biology*, vol. 1, no. 1, article E5, 2003.

[78] J. G. Waterkeyn, B. S. Crabb, and A. F. Cowman, "Transfection of the human malaria parasite *Plasmodium falciparum*," *International Journal for Parasitology*, vol. 29, no. 6, pp. 945–955, 1999.

[79] J. M. Przyborski, S. K. Miller, J. M. Pfahler et al., "Trafficking of STEVOR to the Maurer's clefts in *Plasmodium falciparum*-infected erythrocytes," *EMBO Journal*, vol. 24, no. 13, pp. 2306–2317, 2005.

Hindawi Publishing Corporation
BioMed Research International
Volume 2014, Article ID 565291, 16 pages
http://dx.doi.org/10.1155/2014/565291

Review Article

An Historical Perspective on How Advances in Microscopic Imaging Contributed to Understanding the *Leishmania* Spp. and *Trypanosoma cruzi* Host-Parasite Relationship

P. T. V. Florentino, F. Real, A. Bonfim-Melo, C. M. Orikaza, E. R. Ferreira, C. C. Pessoa, B. R. Lima, G. R. S. Sasso, and R. A. Mortara

Departamento de Microbiologia, Imunologia e Parasitologia, Escola Paulista de Medicina, UNIFESP, Rua Botucatu 862, 6th Floor, 04023-062 São Paulo, SP, Brazil

Correspondence should be addressed to R. A. Mortara; ramortara@unifesp.br

Received 3 December 2013; Accepted 10 January 2014; Published 27 April 2014

Academic Editor: Wanderley de Souza

The literature has identified complex aspects of intracellular host-parasite relationships, which require systematic, nonreductionist approaches and spatial/temporal information. Increasing and integrating temporal and spatial dimensions in host cell imaging have contributed to elucidating several conceptual gaps in the biology of intracellular parasites. To access and investigate complex and emergent dynamic events, it is mandatory to follow them in the context of living cells and organs, constructing scientific images with integrated high quality spatiotemporal data. This review discusses examples of how advances in microscopy have challenged established conceptual models of the intracellular life cycles of *Leishmania* spp. and *Trypanosoma cruzi* protozoan parasites.

1. Introduction

Leishmaniasis and Chagas disease are tropical diseases caused by protozoan parasites from the Trypanosomatidae family (*Leishmania* spp. and *Trypanosoma cruzi*, resp.). These protozoans belong to the class Kinetoplastea, a group of flagellated organisms with a peculiar organelle called a kinetoplast and a single mitochondrion [1]. These two trypanosomatids are responsible for approximately 20 million reported cases of leishmaniasis and Chagas disease and 100,000 deaths per year, primarily in tropical and subtropical areas of the globe [2]. The negative economic and social impact of these diseases, especially in Central and South America, is of great concern [3] and has stimulated scientific investments into studying their causative agents. Because the pathogenesis of *Leishmania* spp. and *T. cruzi* involves an intracellular life cycle in human and mammalian hosts, interactions between the parasite and host cells have been extensively studied *in vitro*, with particular emphasis on microscopic observations. A timeline showing important historical achievements in microscope technology and *Leishmania* spp./*T. cruzi* knowledge is presented in Figure 1.

Remarkable technological advances have increased our ability to sense or experience microscopic agents, buildingoncepts from scientific images. Researchers "embody" technology, boosting his/her experience: scientific images are obtained after technological mediation between researchers sensorial apparatus (perception) and the object of study [4]. Increased spatial resolution with the advent of electron microscopy (EM) enabled access to high quality spatial data for studying the relationship between host cells and pathogens. EM was, and still is, extremely important in determining how viruses, bacteria, fungi, and protozoan parasites (such as *Leishmania* spp. and *T. cruzi*) interact with host cells. However, the singularity of temporal data and lack of integration between high spatial resolution and access to the same individual at different time points (due to chemical fixation of samples) led to a fragmented experience of the object and, unfortunately, limitations in a full understanding of how parasites establish and propagate themselves within their hosts (Box 1).

Factual statements (singular propositions) fragmented in space and time can produce temporal, spatial, and causal gaps

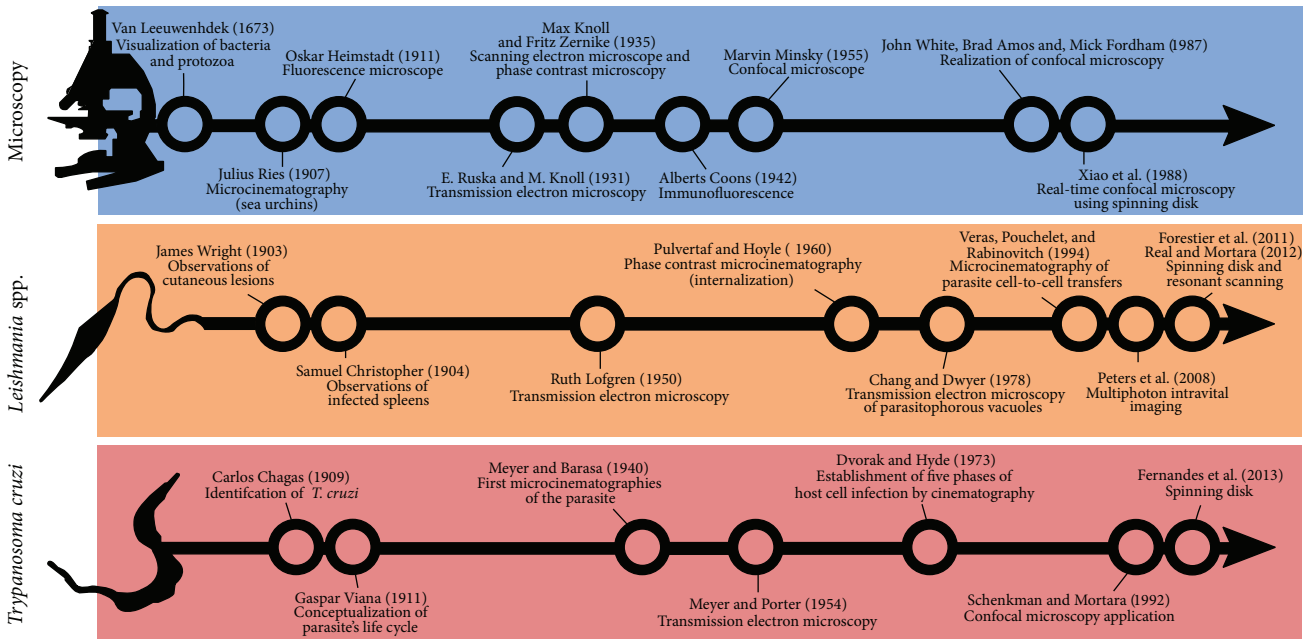

Figure 1: Timeline showing important historical achievements in microscope technology and *Leishmania* spp./*T. cruzi* knowledge. References from the timeline are shown in the text, and additional references are cited in the figure [10, 11], revised in [12, 13].

All things must pass; objects are subdued to time and space—these riddling categories have been a matter of intense philosophical and scientific debate since Aristotle (384-322 BC). A Newtonian perspective assumes that time is an independent entity that passes regardless of physical/chemical changes or an external observer. For Immanuel Kant (1724–1804), time, space, and causality are contained in the experience itself, pertaining essentially to the functioning of the mind [5]. This triad corresponds to the intrinsic properties of the intellect, which experiences not the reality of the world (confined to experimentally unreachable "things-in-themselves"), but what our senses impose relative to the world we know. To sense time and space as an experimenter is to confer to the external world (and objects of study) a "borrowed human logic, in particular a spatiotemporal pattern which is only human perception in disguise" [5]. This spatiotemporal pattern allows us to put objects of study in a causal logic, explaining past and predicting future events, and interpreting them as goal-directed, or teleological, phenomena [6].

Time and space are problematic categories to the human experience because there is a multiplicity of scales defined by different clocks (from subatomic to biological and chronological time) and spatial units in which a plethora of things of human interest are confined,spared from a direct sensorial experience. This is the case of pathogenic microorganisms, hidden from direct human experience and unknown to men until the technological advent of microscopes by Leewenhoek (1632–1723) and the conceptual revolution of the germ theory of disease suggested around the 19th century [7].

Several human pathogens were identified in the late XIX century after biomedical institutions had, as a priority, elucidated pathogen life cycles and disease etiology. Then and now, the main scientific methodological approach to obtain experimental evidence on the life cycles of pathogens has been reductionism, the division of complex systems into smaller intelligible parts. The conceptual framework of a pathogen life cycle has been constructed by a mosaic of separate observations on single factors acquired at defined time points in a defined geographical or physiological location, generally without continuous observation of the same individual (host or pathogen). Joint analysis of each factor could account for interpretation of the entire system; similarly, single spatiotemporal coordinates accessed before and after an experimental condition could explain causality. Although it is undeniable that the reductionism paradigm has been responsible for the success of modern science and technological advances in our society, it "often disregards the dynamic interaction between parts," and a complex problem "is often depicted as a collection of static components" [8]. The notion of space is also dismembered from time in reductionist approaches, and important concepts related to the disambiguation of scientific images, such as topology and interaction of objects, lack dynamic information and can produce or exacerbate "gaps in experience." Considering the unpredictability, uniqueness, and structural/dynamic complexity of organisms [6], reducing time and space in disconnected parts in order to understand biological phenomena has led to limitations in scientific investigation and inadequacy of medical conduct [8].

Box 1: A Philosophical Introduction to the Unobservable.

in experiences, which may be solved by constructing conceptual models using solid statistical historical fundamental principles. Due to partial agreement with nature, models have an important predictive power (although to a limited extent) in building an interpretative framework for other researchers until new information (obtained after technological improvements) challenges and rebuilds these frameworks [9]. The life cycles of protozoan parasites, from invasion and colonization to spreading within the host, are conceptual models based primarily on a reductionist approach that considers nonintegrated time and space observations.

Live recordings of the host-pathogen relationship have been produced as microcinematographic and video technology has progressed, but the large majority of these studies lack appropriate spatial resolution to observe detailed aspects of the interaction. Integrated or four-dimensional observation of objects approximates our experience to microscopic dynamic states, such as oscillatory or chaotic behavior, that are unreachable under the conceptual frameworks of static stability and conventional imaging technology, fixed at defined time points or contained in limited spatial/topological regions of the sample [8].

Herein we use *Leishmania* spp. and *T. cruzi* as examples of how advanced microscopic techniques are circumventing reductionism, integrating or reaching further dimensional scales, and unveiling new aspects of host cell-parasite relationships. Observations of these protozoan parasites will be discussed from a historical point of view considering breakthrough studies and acquisition of new information based on integrated spatiotemporal data.

2. Imaging *Leishmania* spp. and Host Cells

In 1881, Alphonse Laveran (1845–1922) found that a protozoan was the etiological agent that caused malaria, which encouraged researchers in the field of protozoology to describe and investigate protozoan pathogens transmitted to human hosts, especially those carried by insect vectors. This conjuncture led to the investigation of an ancient human malady described in diverse manners in antiquity and modern times [22, 23]. Discovery of the etiological agent that causes leishmaniasis, a protozoan parasite from the Trypanosomatidae family, and conceptualization of its life cycle were established from key observations in accordance with Koch's postulates and paradigms of infection and pathogenesis: identify and isolate the microorganisms, cultivate them *in vitro,* and establish a causal relationship with disease. In microscopic observations of Delhi boils, Scottish Surgeon Major David Douglas Cunningham (1843–1914) found a round-shaped parasite inhabiting cells, and Piotr Borovsky (1898), who observed similar skin lesions (Sart Sore, Turkmenistan), suggested that the intracellular bodies were protozoans. William Leishman (1865–1926) and Charles Donovan (1863–1951) found similar organisms in tissues extracted from the viscera of fatal cases of kala-azar in India. Attempting to cultivate these organisms *in vitro*, Leonard Rogers (1868–1962) and Charles Nicolle (1866–1936) extracted the round-shaped protozoans from infected tissues and cultivated them in blood agar culture media. Multiplying flagellated protozoan forms were found in the culture medium, which led to the conclusion that the parasite was a trypanosomatid. Edmond Sergent (1876–1969) and colleagues found that trypanosomatids could be digenetic parasites, transmitted from insects to mammals [24], and suggested the same life cycle for those protozoans, which were then classified as *Leishmania*. *In vitro* cultivation of these parasites allowed their inoculation into dogs, monkeys, and small rodents, which subsequently developed pathologies similar to the human disease. In 1921, it was experimentally demonstrated that *Phlebotomus*, a tiny sand fly, is the insect host for *Leishmania* and the transmitter of leishmaniasis [24, 25].

Wright (1869–1928) in 1903 [26] and Christophers (1873–1978) in 1904 [27] observed that cutaneous lesions or infected spleens presented massive infiltration of cells containing a large number of oval-shaped parasites. Christophers was the first to recognize these preferentially infected cells as macrophages, inferring that phagocytosis was responsible for the uptake of parasites by leucocytes [26, 27]. For decades, leishmaniasis was considered a disease almost exclusively of the host macrophage system [28], and phagocytosis is still considered the primary mechanism of *Leishmania* spp. internalization [29].

Pulvertaft and Hoyle [30], 56 years after Christopher's inferences, recorded the phagocytosis of *Leishmania* spp. by monocytes/macrophages. Using phase contrast live microcinematography, the authors described monocyte pseudopodia reaching and taking up leptomonad forms (now generally called promastigotes) of *L. donovani*. The promastigotes display a single flagellum in their anterior poles; Pulvertaft and Hoyle demonstrated that promastigote phagocytosis took place from the opposite pole, the posterior, within several minutes. After total engulfment, a vacuole is observed around the parasite that may be digested and disappear or, alternatively, survives and remains motile within this compartment. However, Miller and Twohy (1967) [31] and Akiyama and Haight (1971) [32] found that hamster macrophage pseudopodia initially internalized promastigotes by the flagellar anterior pole of the parasite and observed a transient vacuole around it.

Forty years later using 3D and 5D reconstruction images, Forestier and coworkers (2011) [33] observed that *L. donovani* promastigote uptake by macrophages occurs mainly by the flagellar tip and could also, in exceptional cases, occur through the posterior region and lateral portions of the body. The authors described four sequential phases of *L. donovani* promastigote establishment in host cells: (i) highly polarized attachment by the flagellar end and internalization in lysosomal compartments; (ii) reorientation; (iii) oscillating movement of the parasite to the periphery of the host cell associated with lysosome exocytosis and minor damage to the host cell; and (iv) loss of motility and final location of the parasite in parasitophorous vacuoles (PVs) near the host cell nucleus. These conclusions were only possible due to cutting-edge, high-speed live imaging under modern microscopes [34]. Courret and colleagues (2002) observed similar polarized entrance of *L. amazonensis* promastigotes into

macrophages using conventional live imaging techniques of infected samples.

The investigation of *Leishmania* internalization by macrophages largely benefited from transmission electron microscopy (TEM). Host cell pseudopodia are formed around entering parasites with concomitant microfilament aggregation; sites of close contact between parasite and host cell membranes can be visualized in detail using this technique [35]. In 1986, Wozencraft and colleagues used EM to map individual molecules involved in *Leishmania*-macrophage interactions. Using immunogold labeling, complement receptors were observed to be associated with the interface between membranes of the macrophage and the interacting *Leishmania,* but not with internalized parasites. These observations confirmed results published in the same year, demonstrating participation of this receptor in the direct binding of macrophages to *Leishmania* promastigotes [36]. It is now recognized that *Leishmania* internalization by macrophages is tightly modulated by the first and third complement receptors (CR1 and CR3) and mannose (MR) and Fc gamma receptors (FcγR) [29].

Leishmania internalization by macrophages involves accumulation of actin filaments at the internalization sites of the parasite, a feature of phagocytosis [37]. The authors of the first studies on the mobilization of host cell components towards phagocytosed parasites benefited from immunolabeling techniques associated with electron and optical microscopy. The use of antibodies conjugated to fluorophores proved to be an easy, accessible technique to study protein distribution in cell biology [38]. Regarding *Leishmania* phagocytosis, fluorescence immunolabeling of host GTPases and actin labeling enabled the observation that these molecules are colocalized during *Leishmania*-macrophage interaction [39]. Further, the authors found that different GTPases, Rac1 and RhoA, regulate internalization of opsonized and nonopsonized *Leishmania* promastigotes, respectively. Using the same immunolabeling technique, they also observed that internalization of nonopsonized amastigotes is alternatively regulated by Rac1 but, in this case, the oxidative burst triggered by host phagocytosis is restrained [40]. Thus, different receptors (for opsonized or nonopsonized parasites) trigger different GTPases that modulate host cell responses to *Leishmania*.

After internalization by host cells, *Leishmania* parasites are lodged in PVs, in which they multiply as oval-shaped amastigotes. Electron micrographs of *Leishmania* PVs acquired by Alexander and Vickerman in 1975 and Chang and Dwyer in 1978 demonstrated the phagolysosome-like nature of the vacuoles developed by this parasite [41, 42]. By loading host cell phagolysosome vesicles with electron-dense compounds, these compounds were observed inside *Leishmania* PVs, suggesting that PVs fuse with late endosomes and secondary lysosomes. In the 1990s, a series of studies from Jean-Claude Antoine demonstrated that PVs acquire early endosome markers such as Rab5 and EEA-1 that are substituted by late endosome markers, such as Rab7, and glycoproteins associated with lysosomes [43]. The resulting parasite-containing compartment is a "mature" PV presenting several phagolysosome features [34, 43–46]. PVs develop different morphologies according to *Leishmania* species: *L. mexicana* and *L. amazonensis*, for example, present a spacious PV containing several amastigotes, while most species (*L. major*, *L. donovani,* and others) present a tight-fitting PV in which PV and parasite membranes are in contact [47, 48]. PV biogenesis is still poorly understood, mainly because the majority of studies have been performed in fixed cells using endosomal/lysosomal membrane markers.

Spinning disk technology for confocal laser scanning allowed observation of PV biogenesis in live samples from the very early moments of infection at the stage of parasite phagocytosis. Multidimensional images obtained from these techniques allowed for integration of four and even five dimensions (*x, y, z,* time, fluorescence) of living cells and tissues [49]. Lippuner and colleagues [50] were some of the first researchers to record PV biogenesis in live samples using GFP-tagged Rab5 proteins on cells hosting *L. mexicana*. The authors demonstrated that the parasite inhabits PVs in which Rab5 GTPases are rapidly excluded from the vacuolar membrane (compared with latex bead phagosomes). They also documented that a parasite surface component, lipophosphoglycan (LPG), implicated in delaying PV maturation in *L. donovani* [39] accelerated the exclusion of the Rab5 marker from PVs.

Benefitting from high resolution and speed, as well as the low photocytotoxicity of the technique, Forestier and colleagues and Real and Mortara [33, 48] observed the interaction of PVs with acidified compartments of host cells. They dyed vesicles with a lysosomotropic probe (Lysotracker) over time and observed how these labeled vesicles compose PVs. These acidic vesicles were located around internalized promastigotes minutes after interaction with host cells, suggesting that recently formed PVs promptly fuse with acidic compartments [33]. The biogenesis of spacious/communal PVs formed by *L. amazonensis* versus tight-fitting PVs formed by *L. major* could also be compared using the technique. The growth of spacious PVs was accessed in terms of volumetric data in that remodeling restores PV dimensions after these large structures fuse together [48]. The fission of *L. major* PVs during parasite intracellular multiplication was also observed for the first time using GFP-tagged LAMP and Rab7 proteins and multidimensional imaging techniques. Thus, the PV membrane could be visualized during amastigote multiplication, unveiling the dynamics of PV fission [48].

However, some aspects of the *Leishmania* life cycle, such as putative host cell collapse due to parasite growth and amastigote spreading to other cells and tissues that must occur in disease persistence, are far from being elucidated and are only hypothetically mentioned in the literature. Laser scanning and/or spinning disk confocal microscopy and intravital imaging techniques are promising tools for investigating these dynamic events. It is difficult to conceive approaches to evaluate *Leishmania* egress/reinfection when only taking into account static information from fixed samples.

Considering the seminal works on leishmaniasis from the early 20th century, the preferential, almost exclusive, presence of oval-shaped parasites inside host cells was intriguing and suggested that the parasite was extremely dependent on the

intracellular environment. If few parasites could be found outside host cells, the question remained as to how they could spread to other cells and tissues and induce skin and organ lesions after an insect-vector bite.

In 1980, Dennis Snow Ridley, an expert in the pathology of leprosy, was one of the first to attempt to study *Leishmania* egress from a host cell [51]. In fixed histological samples from lesions, he observed "macrophage lysis and the presence of extracellular amastigotes in forms of disease in which parasite numbers were restricted, but not in those in which parasites were freely tolerated."

In the late 1990s, Rittig et al. [52] used time-lapse microscopy of infected human peripheral blood monocytes to properly investigate the dynamic event of *Leishmania major* egress from host cells [52, 53]. They found "numerous host cells simultaneously releasing replicated parasites" in an exocytotic-like process. Also in the 1990s, a series of unpublished cinematographic records of macrophages hosting *L. amazonensis* was made by Michel Rabinovitch and collaborators at the Institut Pasteur in Paris, France. The recordings show transference of amastigotes from macrophage-to-macrophage and infected lymphocytes being phagocytosed by macrophages, similar to Trojan horses (supplementary Video 1). These time-lapse approaches challenged the current understanding of *Leishmania* egress based on bacterial and viral conceptual intracellular cycles, which presume host cell lysis by multiplication bursts [47].

Although still hypothetical, these egress events are crucial for *Leishmania* parasites to reach the preferential intracellular niche of macrophages after their inoculation site on the mammalian host skin. From the insect blood meal to establishment inside macrophages, *Leishmania* parasites are likely transferred from cell to cell, a process that involves diversified host cell lineages. After *L. major* promastigote forms were inoculated in mice by sand flies, an intense migration of neutrophils was observed at the site of an insect blood meal 40 minutes post-inoculum [54]. The work employed multiphoton intravital microscopy (MP-IVM) on mice ear sites where infected sand flies had their blood meal. The technique allowed access to information contained in high depth tissues during transfer of parasites from insects to mice. Neutrophil-depleted mice had a decreased number of parasites after one and four weeks of *Leishmania* inoculation in their ears. This suggests that neutrophils are essential partners in establishment of the parasite in mammalian hosts in the early stages of infection. Relocation of *L. major* parasites from neutrophil to macrophage populations was inferred after six days post-inoculum, suggesting a transit of parasites between these two cell types.

Using similar microscopy techniques, dendritic cells were included as *Leishmania* host cells involved in early establishment of the parasite in mammalian organisms [55]. Injection of *L. major* promastigotes into the dermis of mice expressing fluorescent-tagged dendritic cells revealed that these cells avidly internalize parasites in the first three hours post-inoculum.

Thus, neutrophils and dendritic cells could participate in *Leishmania* pathogenesis as transient hosts until the parasite reaches its preferential niche, the macrophage. In neutrophils, *L. donovani* promastigotes are sheltered in harmless, non-degradative vacuoles until host cell apoptosis. Similar to a Trojan horse, the apoptotic neutrophil is phagocytosed by macrophages that safely transfer the parasites without exposure to the potentially hostile extracellular milieu [56]. Another interesting tactic of *Leishmania* egress and transfer between host cells is mediated by host cell extrusions. As described by Rittig and Bogdan in 2000 [53], parasites are extruded from apoptotic host cells and immediately rescued by viable neighbor macrophages (manuscript in preparation).

3. Imaging *Trypanosoma cruzi* and Host Cells

In the early 20th century in Brazil, as *Leishmania* was being characterized in Europe, Carlos Chagas (1878–1934) identified the new protozoan *Trypanosoma cruzi,* its invertebrate host, and insect vector as well as pathological aspects. In 1909, Chagas named the protozoan *Schizotrypanum cruzi* as a tribute to Oswaldo Cruz, his director at Manguinhos Institute in Rio de Janeiro, Brazil [57]. The parasite showed morphological features distinct from all *Trypanosoma* species classified at that time. The flagellated form of the protozoan, similar to *Crithidia*, was found to colonize the posterior gut of hematophagous triatomines that infested the poorly built dwellings of villagers in Lasance in the northern region of the state of Minas Gerais in Brazil. After subjecting experimental apes to infected triatomines from the genus *Corynorhinus* spp., thus applying Koch's postulates, Chagas was able to identify a flagellated form in the bloodstream of the ape completely different from that found in insects. Chagas then associated the presence of the protozoan with the pathology observed in several residents from the region and began to study three supposedly infected children [57].

Microscopic visualization of the parasite allowed its identification as a Trypanosomatid based on recognition of the blepharoplast (now called kinetoplast) present in the different developmental forms of the parasite. Based on observations and previous knowledge obtained from other protozoan parasites, such as *Plasmodium* spp., Chagas classified more than ten different evolutionary stages of *T. cruzi* in fixed and stained samples [57]. In 1911 with the support of Carlos Chagas, Gaspar Vianna conducted extensive histological analyses of organs from infected experimental animals, which led him to simplify the classification of *T. cruzi* into two main evolutionary stages: a round-shaped form without an apparent flagellum (amastigote) and a slim flagellated form (trypomastigote) [58].

At that time, animals such as monkeys and dogs were used as experimental models for *in vivo* infections [57–60]. Because these were complex models and presented a challenge for visualizing intracellular parasites, investigation into *T. cruzi* biology was primarily based on microscopic observations of the peripheral blood from infected animals and patients. Simplification of experimental models from whole animals to *T. cruzi*-infected cell cultures *in vitro* was key to studying the *T. cruzi* life cycle and its developmental forms [61, 62]. Another important step was establishment of conditions to grow the parasite *in vitro.* This allowed a better

understanding of the biology of the developmental forms found in vertebrate host cells and the invertebrate vector [63].

The first micrographic records of stained cells infected with *T. cruzi* were published in the 1930s and 1940s [59, 61], and the first microcinematographic record of the intracellular life cycle of the parasite was presented in the 1940s [64]. The pioneer recordings of Hertha Meyer by directly and continuously accessing parasites within single host mammalian cells confirmed the simplified model of the *T. cruzi* intracellular life cycle proposed by Vianna [58]. In collaboration with Keith Porter from Rockefeller University in the USA, Hertha Meyer was the first investigator to register the ultrastructure of *T. cruzi* invertebrate forms (epimastigotes) using electron microscopy [65]. Interestingly, *T. cruzi* was one of the first cells observed with this technique [66]. Current detailed knowledge of internal structures of different morphological stages of the parasite has been acquired based on comprehensive transmission electron microscopy (TEM) data and gradual improvement of the technique over the years [66]. Thus, based on these early studies, four main distinct evolutionary stages are assumed in *T. cruzi*: flagellated dividing forms (epimastigotes) found in the triatomine gut; infective slim flagellated forms (metacyclic trypomastigotes) at the rectal ampoule that, when released with the feces, may initiate host infection by infecting mammalian host cells; once free in the cytoplasm, they differentiate into multiplying intracellular round-shaped forms (amastigotes); after nine cycles of binary divisions [67], amastigotes differentiate into bloodstream trypomastigotes that burst out of infected cells, reach the circulation, and may infect other host cells or a triatomine in a future blood meal [63].

One of the first detailed time-lapse studies of the intracellular *T. cruzi* life cycle was performed in the early 1970s by Dvorak and Hyde [67]. Using microcinematographic recordings, they established a model that involves (i) an invasion (penetration) phase promoted by an infective flagellated form of the parasite; (ii) a first differentiation (reorganization) phase in which the flagellated forms turn into oval-shaped amastigote forms; (iii) a multiplication (reproduction) phase in which amastigotes multiply inside host cells; (iv) a second differentiation phase in which amastigotes differentiate back into flagellated forms; and (v) the last phase of the intracellular cycle (escape) in which the flagellated forms rupture the host cell and spread to the extracellular milieu [67]. "Continuous observations" by Dvorak and Hyde allowed a better understanding of parasite interactions with the host cell.

Possibly the most extensively studied aspect of the *T. cruzi* intracellular cycle is the internalization step, also referred to as penetration or invasion. *T. cruzi* infective forms, including metacyclic trypomastigotes (MTs), tissue culture trypomastigotes (TCTs; analogs to bloodstream trypomastigotes), and extracellular amastigotes (EAs), which are obtained by differentiating TCTs or bloodstream trypomastigotes *in vitro* and *in vivo,* respectively [68–72], invade host cells through distinct mechanisms that will be discussed in more detail.

In the late 1970s, Zanvil Cohn's group at Rockefeller University (1926–1993) showed that epimastigotes (noninfective forms) and MTs could be internalized by professional phagocytes and that only trypomastigotes could enter nonprofessional phagocytes via phagocytosis [73]. Additionally, the group observed that amastigotes released into cell culture supernatants could enter and multiply in all cell types examined. Infectivity of extracellular amastigotes was confirmed by others [69, 74–76]. Schenkman and colleagues later observed that MTs and TCTs preferentially entered polarized MDCK monolayers at the basolateral regions, whereas nonconfluent cell was mostly penetrated by TCTs at their borders [77]. Using subconfluent HeLa cells, Mortara (1991) [78] observed different patterns of parasite internalization when comparing MTs and EAs. In line with Schenkman's (1988) observations [77], MTs preferentially invaded at the edge of host cells; conversely, EAs initially bound and were then entangled by host cell microvilli at the dorsal surface of HeLa cells before internalization.

As immunofluorescence methodologies became popular in cell biology, they quickly grew to be valuable tools in studying *T. cruzi*-host cell interaction. Additionally, the advent of laser scanning confocal microscopy around the 1990s added significant improvements in both lateral and axial resolution on image acquisition compared to conventional wide field fluorescence. Protozoology also largely benefited from these techniques in that one of the first applications of confocal microscopy in studying the cell biology of parasitic infections was observation of actin redistribution in cells interacting with trypomastigotes [79]. Additionally, one of the first images combining Normarski DIC and confocal fluorescence imaging is of a HeLa cell interacting with metacyclic trypomastigotes immunostained with anti-mucin antibody 3F5 (W. Brad Amos, personal communication). The image shown in Figure 2 was that on the cover of a special issue of Memórias do Instituto Oswaldo Cruz [14].

T. cruzi developmental forms and their repertoire of distinct surface proteins trigger different signaling pathways that promote invasion. For example, MTs present an 82 kDa surface glycoprotein (GP-82) that is implicated in parasite internalization but does not trigger actin mobilization to invasion sites [80, 81]. So far, the involvement of host cell actin filaments in MTs and TCTs invasion remains controversial. Ferreira et al. observed that, during MTs host cell invasion, a surface glycoprotein GP-82 depolymerizes actin microfilaments while GP-35/50, another MTs surface molecule, induces actin recruitment [81]. Procópio and colleagues did not observe inhibitory effect of Cytochalasin D on host cell invasion of G strain MTs, concluding that actin filaments did not participate in MTs entry [80]. Regarding TCT invasion, contradictory results on involvement of host actin have also been described [79, 82–84].

By contrast, it is well established that EAs entry into host cells is highly dependent on actin mobilization [78]. EA invasion involves actin-rich cup-like structures that embrace the parasite, called the phagocytic cup (Figure 3 and supplementary Video 2) [85]. Fernandes and colleagues [86] recently demonstrated that EAs are able to trigger their own phagocytosis by HeLa cells. Using spinning-disk confocal microscopy, they observed that PVs formed by EAs remodeled their phosphoinositide content, which are important signaling components for subsequent fusion with

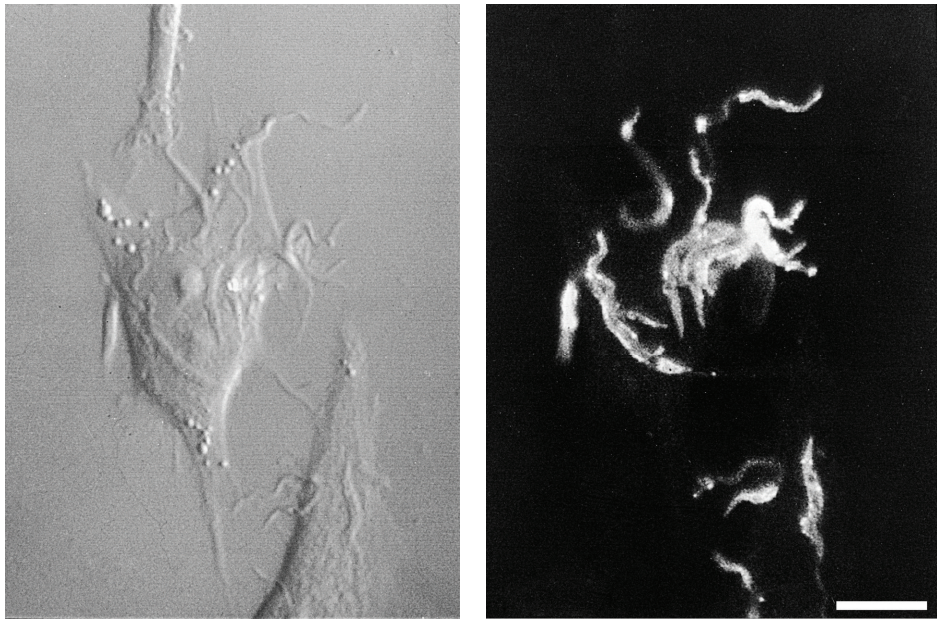

(a) (b)

Figure 2: Cover of Memórias do Instituto Oswaldo Cruz, vol. 86 (1) [14]. Likely the first DIC image obtained with a confocal microscope (W. Brad Amos, personal communication) showing HeLa cell infection by G strain metacyclic trypomastigotes. On the right, the corresponding image after immunofluorescence with monoclonal antibody anti-35/50 kDa mucin, suggesting release of the molecule in parts of internalized parasites [15].

other host cell vesicles. EA PVs first mature into a CD63-, followed by synaptotagmin VII- and then LAMP1-positive structures. These data show that EAs activate a phagocytic pathway in nonprofessional phagocytes that resembles large particle uptake by professional phagocytes [86].

Another application of immunofluorescence techniques in this area of research relates to the role of host cell lysosomes in *T. cruzi* invasion. Tardieux and colleagues [83] observed that lysosomes are recruited to TCT invasion sites, a process dependent on calcium that culminates with the formation of LAMP-positive *T. cruzi* PVs [87]. Norma Andrews' group (U. Maryland) demonstrated that TCTs induce plasma membrane lesions during the invasion process. These wounds are repaired by lysosomes that secrete sphingomyelinase, an enzyme that generates ceramide [88]. On the outer leaflet of the plasma membrane, this lipid induces inward budding that could drive parasite internalization. Using live imaging techniques, the authors confirmed previous TEM observations, showing the dynamics of lysosome mobilization towards cell periphery during interaction with trypomastigotes [89].

Based on the observation of PIP-3 recruitment by TCTs at early steps of interaction with mammalian cells, a lysosome-independent pathway for trypomastigote entry has also been described [90]. Although most of the results in this work consist of very compelling evidence, it is worth mentioning that Figure 2 (related to the attached supplementary video 1) clearly shows moving parasites from as early as 3 min (possibly under the cells). What is then referred to as the "second parasite" also appears moving in the field (possibly already inside the cell) and the so-called recruitment of Akt-PH-GFP for this parasite, that begins at around 13 minutes, is undoubtedly arising from the protrusion of the trypomastigote, actively moving from *inside* the cell. The implication of this observation is that these trypomastigotes most likely had invaded the imaged cell *before* this period. Considering the theme of this review, this might possibly be regarded as a misinterpretation of a rather compelling live image of *T. cruzi* trypomastigotes interacting with host cells. Recently, Barrias et al. [91] provided evidence suggesting that *T. cruzi* trypomastigotes may also subvert the macropinocytic pathway to enter host cells.

Interestingly, they also reported intracellular trypomastigotes protruding from within the host cell after 15 minutes of infection. Although the authors focused their observations on parasite entry, it appeared that parasites could also attempt to escape or egress from the host cell [89]. Similar behavior of internalized TCTs pushing out from infected cells had already been described by Dvorak and Hyde in their pioneering studies [67]. In 1992, Schenkman and Mortara [79] observed membrane protrusions and actin recruitment that were associated with TCT invasion sites in HeLa cells. At that time, fixed samples were visualized by confocal, transmission, and scanning electron microscopy (SEM). Static images were interpreted as depicting events associated with parasite entry. In light of observations made by Hyde and Dvorak and Fernandes et al. [16, 67], formation of pseudopodia described by Schenkman and Mortara [79] in fixed samples processed 30 minutes after cell invasion was most certainly related to protrusion of already-internalized parasites rather than internalization, as interpreted at the time. Integration of temporal information with spatial data invites careful contemplation of host-parasite interaction

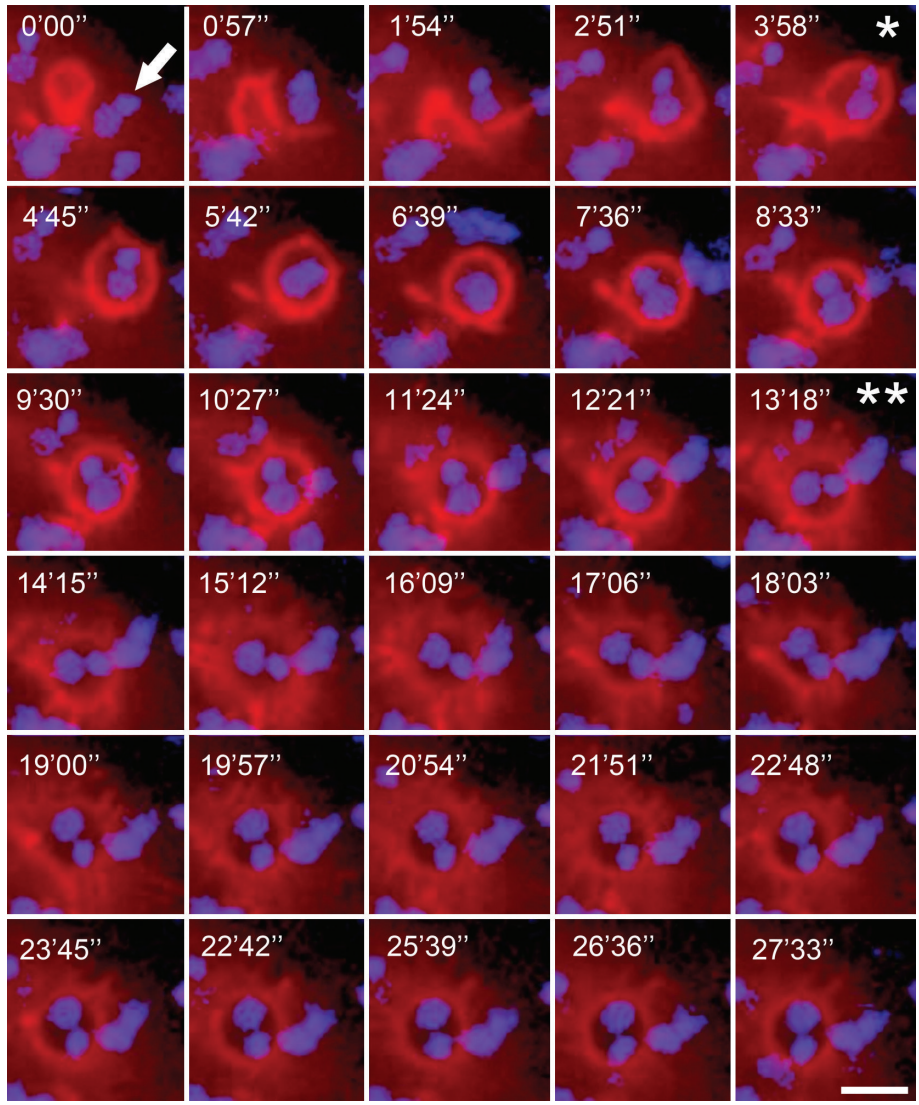

Figure 3: Actin recruitment by EAs in the phagocytic cup (Supplementary Video 2 available online at http://dx.doi.org/10.1155/2014/565291). HeLa cells transfected with fluorescent actin marker were incubated with EAs (arrow) and observed by time-lapse confocal microscopy (Leica SP5 TS) for 30 minutes at one frame per 57 seconds. Total EA internalization occurred within approximately 4 minutes (∗), but actin mobilization diffused approximately 9 minutes after total EA internalization (∗∗) 13 minutes after recording initiation. Actin is shown in red (Life-actin, ibidi); EA nucleus and kinetoplast are shown in blue (Hoescht 33258). Scale bar, 5 μm.

micrographs from fixed samples. In particular, considering *T. cruzi* trypomastigotes inside host cells and exposition of parasite flagella after host cell membrane damage [67, 89], static images published years ago could be ambiguously interpreted as both invasion and exit processes.

After internalization, a poorly understood aspect of the *T. cruzi* intracellular life cycle is formation and escape from PVs. Ultrastructural studies demonstrated that, shortly after invasion (around 60 minutes), *T. cruzi* trypomastigotes are lodged in a vacuole surrounded by a thin membrane, and "at later times, all the parasites were seen free in the cytoplasm" [73]. This transient PV is able to fuse with host cell lysosomes in phagocytic and nonphagocytic cells, which is clearly observed by confocal and electron microscopy [73, 89, 90, 92–96]. The precise mechanisms by which parasites escape from PVs into the cell cytoplasm have not been fully disclosed, but *T. cruzi* trypomastigotes and amastigotes have been shown to secrete a membrane pore-forming protein, TC-TOX, which is active at pH 5.5 and could be implicated in PV rupture [97–99]. The question remains as to whether *T. cruzi* differentiates into amastigotes inside or outside the PV. de Carvalho and de Souza [95] suggested that trypomastigotes were able to disrupt PVs before differentiation into amastigotes, which is a feature of phagolysosomes in an acidic milieu. Indeed, it is possible to observe small pores in PV membranes that developed after 1 hour and 30 minutes of trypomastigotes infection in macrophages using TEM [95]. Using multidimensional live imaging of HeLa cells transfected with RFP-tagged Rab7 and infected with metacyclic forms of *T. cruzi* expressing GFP, we observed initial morphological changes of MT into round-shaped forms followed by dissolution of RFP-Rab7 around the parasite (Figure 4 and supplementary Video

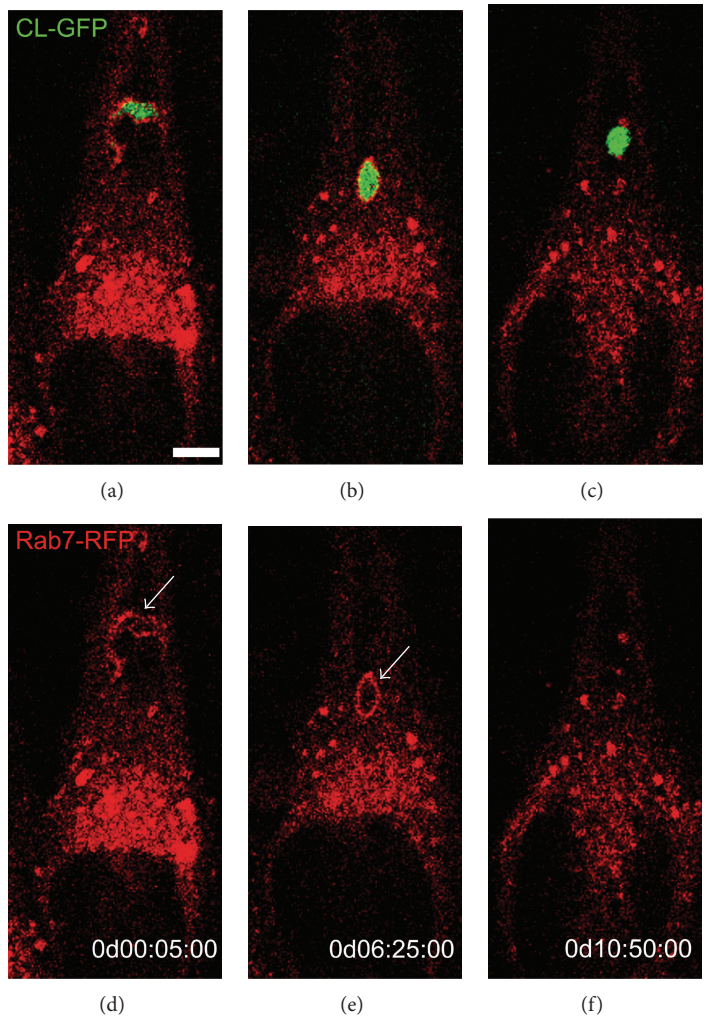

Figure 4: *T. cruzi* metacyclic trypomastigote forms begin to differentiate into amastigote-like forms inside the parasitophorous vacuole (supplementary Video 3). HeLa cells transfected with Rab7-Red fluorescent protein (RFP) were infected with metacyclic trypomastigotes (MTs) from a CL strain transfected with green fluorescent protein (GFP). Time-lapse images show the parasite internalized inside the parasitophorous vacuole (PV) labeled with Rab7-RFP (white arrow) after one hour. MTs differentiated into round-shaped forms, followed by loss of Rab-7 staining, suggesting parasite escape from the PV. Time-lapse acquisition is displayed as days : hours : minutes : seconds (dd : hh : mm : ss). Scale bar, 5 μm. Images acquired with a confocal microscope (Leica SP5 TS).

3). In contrast to previous investigations, the data suggest that MT begins to differentiate into an amastigote form before escape to the host cell cytosol. Further experiments using multidimensional images and appropriate markers of *T. cruzi* differentiation will potentially reveal if differentiation into amastigotes takes place in PVs or in the cytosol and provide important information for future studies on drug delivery.

Egress from host cells is also poorly understood. Although host cell egress was highlighted in Hertha Meyer's recordings in the 1940s, there are few studies on the subject. Edgar Rowland's group was one of the first to systematically investigate *T. cruzi* egress using an interesting experimental approach: culture medium with serum obtained from chronically infected mice showed inhibition of parasite egress and a decrease in intracellular replication in fibroblasts [100, 101]. This inhibitory effect was also observed in serum obtained from chronic chagasic patients [102]. It is possible to hypothesize that antibodies (anti-egressins) are reaching intracellular parasites and, according to the authors, promoting intracellular agglutination of *T. cruzi* forms to block egress. At a later phase of the *T. cruzi* intracellular life cycle, the plasma membrane of infected host cells is weakened, leading to higher permeability to molecules, including antibodies [103]. *T. cruzi* egress from host cells has also been investigated by our group. The precise moment of trypomastigote exit from a host cell was captured using field-emission scanning electron microscopy (FE-SEM) (Figure 5(a)). FE-SEM is a valuable microscopy tool to analyze biological surfaces with higher spatial resolution than SEM [104]. Various morphological and parasite-host cell interaction-related processes have been highlighted using conventional or FE-SEM, including the flagellar attachment zone [105], colonization forms in the

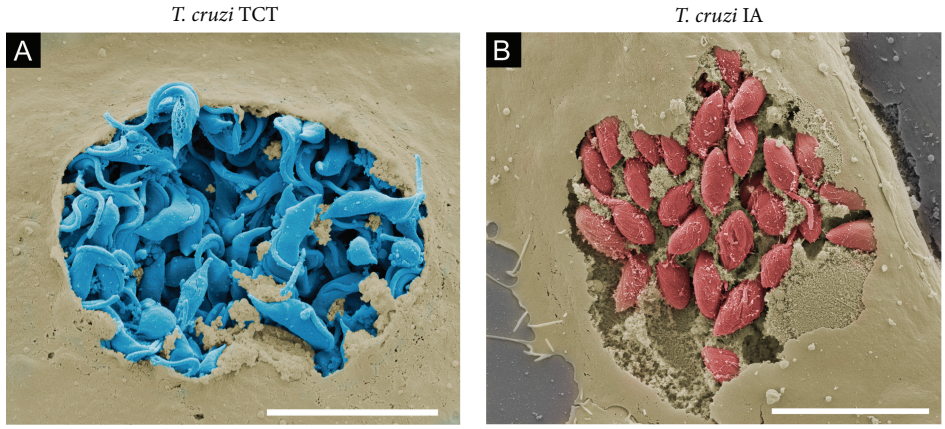

Figure 5: Visualization of the *T. cruzi* intracellular life cycle using field-emission scanning electron microscopy. (a) Tissue cultured trypomastigotes (TCTs) (blue) egress from Vero cells (light brown). (b) Intracellular amastigotes (red) of *T. cruzi* hosted by Vero cells (light brown). Infected cells were fixed with 4% paraformaldehyde and then subjected to electron scanning processing. Briefly, samples were dehydrated in an ethanol series, subjected to critical-point drying from CO_2 and gold sputtering. In (b), samples processed as in (a) were fractured by adhesive tape and then gold sputtered. Scale bars, 10 μm.

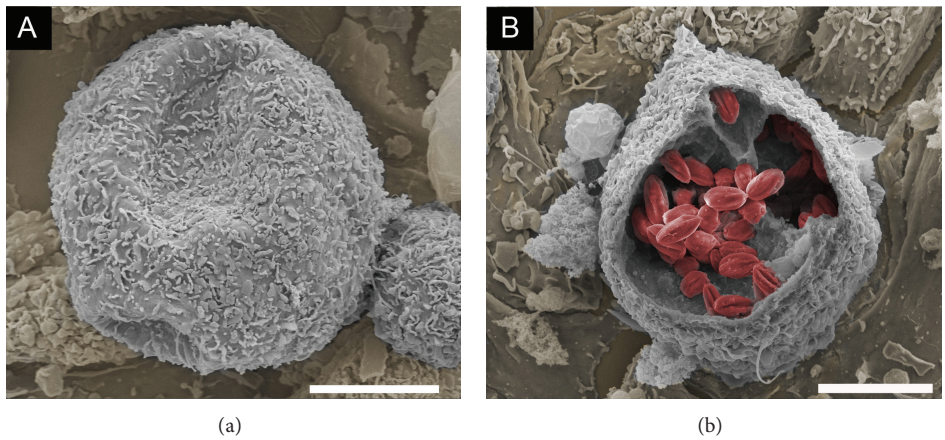

Figure 6: Visualization of bone marrow-derived macrophages infected with *L. amazonensis* using field-emission scanning electron microscopy. In (a), intact cell (light grey) and, in (b), *L. amazonensis* amastigotes (red) within spacious PVs were exposed through fracture by Scotch tape, followed by gold sputtering. The samples were processed as described in the legend of Figure 5. Scale bar, 10 μm.

insect vector and its excretion [106, 107], stimuli to differentiate its life cycle form and invasion [108–110], and cytoskeleton organization during infection [89, 111]. One of our aims using this technique was to try and observe intracellular parasites in host cells and entire organs using the ingenious "scotch tape technique," which fractures the cell monolayer and tissue samples [112, 113]. This approach allowed us to observe intracellular amastigotes of *T. cruzi* in the cytoplasm of Vero cells (Figure 5(b)) as well as intracellular amastigotes of *L. amazonensis* located in large vacuoles of macrophages derived from mouse bone marrow (Figure 6(b)).

Several protocols have been used to visualize host cytoskeleton interaction with parasites using EM. Fernandes and colleagues [89] treated infected cells with a membrane extraction solution containing Triton X-100, taxol, and phalloidin to stabilize microtubules and microfilaments [17]. This strategy enabled the authors to visualize the initial invasion profile using TEM (to generate a three-dimensional projection) in which the posterior end of trypomastigotes penetrates underneath HeLa cells, resulting in actin filament enrichment at the undulated cell cortex [86]. We used the same approach to visualize intracellular amastigotes in the host cell cytoplasm. As shown in Figure 7, we observed intracellular amastigotes of *T. cruzi* (Figure 7(a)) and *L. amazonensis* (Figure 7(b)) hosted by cells in which the cytoskeleton network was preserved. In these images, amastigotes were also subjected to membrane extraction to observe internal structures of the parasites.

Our group has focused efforts on the observation of intracellular parasites in infected hearts of mice at the SEM level. Detailed information from infected cardiac tissue is relevant for elucidating *T. cruzi* pathogenesis due to heart tissue damage caused by the parasite and/or autoimmune effects, which are poorly understood and controversial [114].

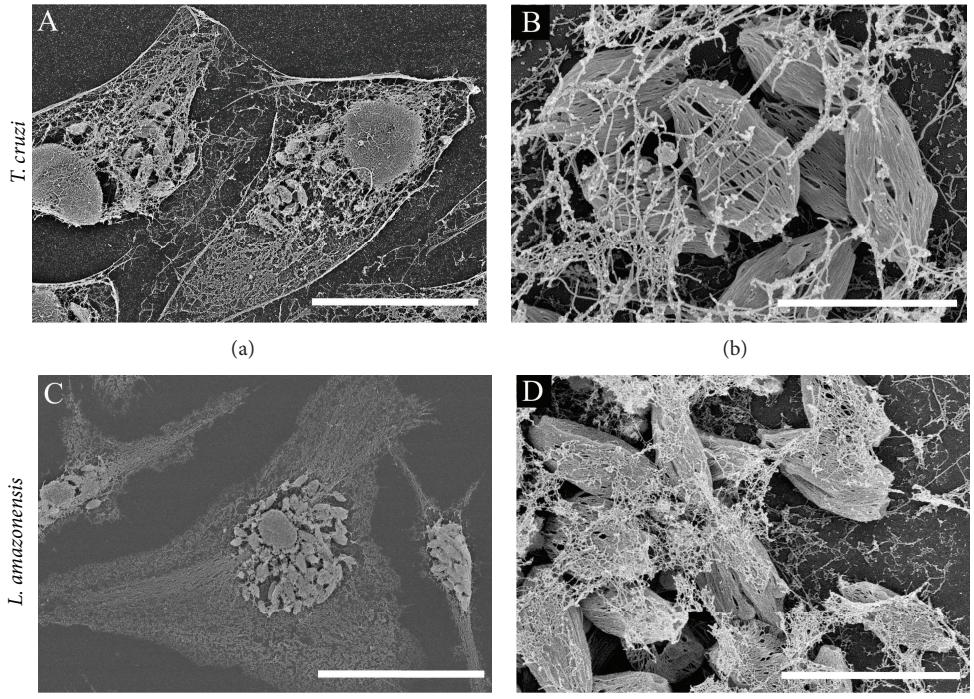

Figure 7: Visualization of host cell cytoskeleton networks and intracellular amastigotes of *T. cruzi* (a, b) and *L. amazonensis* (c, d) with host cell cytoskeleton networks. Infected HeLa cells (a, b) and mouse bone marrow macrophages (c, d) were treated with a membrane extraction solution containing Triton X-100, taxol, and phalloidin (to stabilize microtubules and microfilaments) [16, 17]. Cytoskeletons of infected cells were visualized by field emission scanning electron microscopy after processing and gold coating. Scale bars: (a) 20 μm; (b) 3 μm; (c) 30 μm; (d) 5 μm.

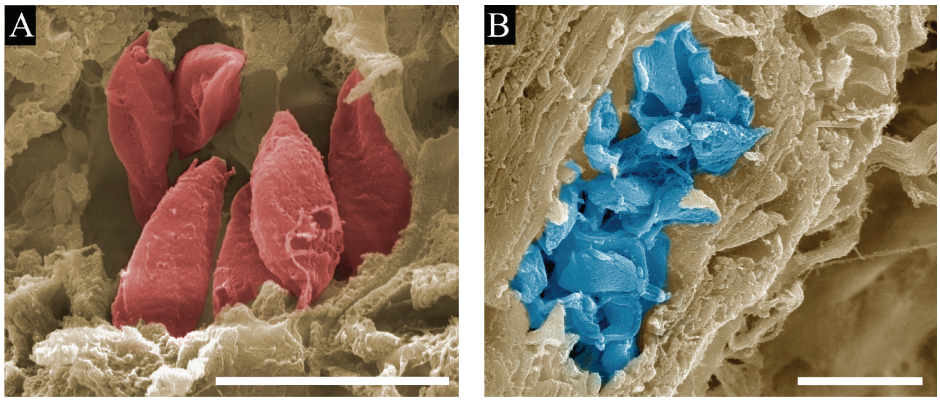

Figure 8: Field-emission scanning electron microscopy of mouse hearts infected with *T. cruzi*. Thick paraffin embedded sections of mouse hearts infected with Y strain metacyclic trypomastigotes were deparaffinized and processed for field emission scanning electron microscopy [18–21]. Briefly, paraffin was removed by melting the sections block and then deparaffinized with xylol and ethanol. Next, heart muscle sections cut with a razor blade were dehydrated in an ethanol series, subjected to critical-point drying, and gold sputtered. (a) Amastigotes (red), scale bar, 4 μm; (b) trypomastigotes (blue), scale bar, 10 μm.

Pathological investigations on fatal cases of Chagas disease performed by Gaspar Vianna in association with the German pathologist Hermann Dürk in 1917 defined acute and chronic phases of the disease, with the latter phase associated with cardiac involvement [115]. The association between *T. cruzi* infection and cardiac failure in chronic patients was a well-established concept by the 1960s [116]. Common techniques for SEM visualization of internal structures, such as cryofracturing, freeze fracturing or microdissection, either are not precise enough for observing localized histological events or require specialized trained personnel in addition to high financial and equipment costs necessary to perform these procedures. Other researchers have performed SEM in paraffin-histological sections within their respective fields

of research [18–21], but an image of *T. cruzi*-infected tissue from thick sections (>40 μm) has not been produced. In thick paraffin histological sections submitted for SEM processing, we observed *T. cruzi* amastigote and trypomastigote nests within heart muscle fibers (Figures 8(a) and 8(b)). This simple, cost-effective, and rapid approach was applied after conventional formaldehyde fixation and paraffin embedding, followed by deparaffination with xylol, dehydration with ethanol, critical-point drying, and sputter-coating with gold for SEM. Mice hearts were stored in paraffin blocks for several years before they were processed using SEM, highlighting the good condition of the tissue and its structures despite a long period of time in storage. A related and relevant issue that deserves more in-depth study is understanding how circulating parasites reach this organ. Intravital imaging techniques of whole animals and multiphoton confocal microscopy of infected tissues should allow for fluorescent-tagged *T. cruzi* tracking in what could become a challenging and encouraging perspective for future investigations.

4. Concluding Remarks

Innovative techniques consistently improve our interpretations of biological processes and their mechanisms in biomedical research. In this review, we presented examples of advances in microscopy that contributed to building concepts regarding host-parasite interactions of the human kinetoplastid parasites *Leishmania* spp. and *T. cruzi*. There are several other cases of conceptual breakthroughs that we did not cover in this review on microscopy, including newly developed techniques that could certainly lead to important changes in how we conceptualize similar intracellular parasites. Namely, electron tomography in cryopreserved samples allows for 3D reconstruction of infected cells and parasites bypassing cumbersome serial slicing; superresolution microscopes (PALM/STORM and STED) increase optical resolution to tens of nanometers and allow for live imaging; bioluminescent parasites could be tracked in whole organisms using *in vivo* bioluminescent imaging systems [117, 118]; and use of reporters, probes, or other microcopy techniques (FRAP, FRET and FLIM) improves microscopic observations regarding biochemical/molecular mechanisms of host/pathogen interactions. We can rely on history to repeat itself in that further studies using these cutting-edge microscopic technologies will change our perception of *Leishmania* spp. and *T. cruzi* intracellular parasitism and contribute to the development of novel and more efficient strategies of chemotherapy and vaccination.

Disclosure

The authors agree that the first two authors should be regarded as joint first authors.

Conflict of Interests

The authors declare that there is no conflict of interests regarding the publication of this paper.

Acknowledgments

The authors would like to thank Maria Cecília Fernandes, Mauro Cortez, and Leonardo Rodrigues de Andrade for their help with *T. cruzi* and *L. major* cytoskeleton imaging (Figure 7); Michel Rabinovith, Patrícia Sampaio Tavares Veras, and Marcel Pouchelet for the use of the video of *Leishmania* cell-to-cell transfer captured at the Institute Pasteur; and André Aguillera for his skillful help with FE-SEM imaging. They also thank Fundação de Amparo à Pesquisa do Estado de São Paulo (FAPESP), Conselho Nacional de Desenvolvimento Científico e Tecnológico (CNPq), and Coordenação de Aperfeiçoamento de Pessoal de Nível Superior (Capes) for financial support through grants and fellowships.

References

[1] D. Moreira, P. López-García, and K. Vickerman, "An updated view of kinetoplastid phylogeny using environmental sequences and a closer outgroup: proposal for a new classification of the class Kinetoplastea," *International Journal of Systematic and Evolutionary Microbiology*, vol. 54, no. 5, pp. 1861–1875, 2004.

[2] K. Stuart, R. Brun, S. Croft et al., "Kinetoplastids: related protozoan pathogens, different diseases," *Journal of Clinical Investigation*, vol. 118, no. 4, pp. 1301–1310, 2008.

[3] W. de Souza, T. M. U. de Carvalho, and E. S. Barrias, "Review on *Trypanosoma cruzi*: host cell interaction," *International Journal of Cell Biology*, vol. 2010, Article ID 295394, 18 pages, 2010.

[4] R. Rosenberger, "A case study in the applied philosophy of imaging: the synaptic vesicle debate," *Science Technology and Human Values*, vol. 36, no. 1, pp. 6–32, 2011.

[5] H. Boxenbaum, "Time concepts in physics, biology, and pharmacokinetics," *Journal of Pharmaceutical Sciences*, vol. 75, no. 11, pp. 1053–1062, 1986.

[6] E. Mayr, "Cause and effect in biology—kinds of causes, predictability, and teleology are viewed by a practicing biologist," *Science*, vol. 134, p. 1501, 1961.

[7] M. Egaña Aranguren, K. Wolstencroft, U. Sattler et al., "Using OWL to model biological knowledge," *International Journal of Human Computer Studies*, vol. 65, no. 7, pp. 583–594, 2007.

[8] A. C. Ahn, M. Tewari, C.-S. Poon, and R. S. Phillips, "The limits of reductionism in medicine: could systems biology offer an alternative?" *PLoS Medicine*, vol. 3, no. 6, pp. 709–713, 2006.

[9] R. Sattler, *Biophilosophy: Analytic and Holistic Perspectives*, Springer, Berlin, Germany, 1986.

[10] "Milestones in light microscopy," *Nature Cell Biology*, vol. 11, pp. 1165–1165, 2009.

[11] G. Q. Xiao, T. R. Corle, and G. S. Kino, "Real-time confocal scanning optical microscope," *Applied Physics Letters*, vol. 53, no. 8, pp. 716–718, 1988.

[12] H. Landecker, "Seeing things: from microcinematography to live cell imaging," *Nature Methods*, vol. 6, no. 10, pp. 707–709, 2009.

[13] R. Lofgren, "The structure of *Leishmania* tropica as revealed by phase and electron microscopy," *Journal of Bacteriology*, vol. 60, pp. 617–625, 1950.

[14] R. A. Mortara, "Differential interference contrast and confocal fluorescence photomicrograph showing the distribution of the 35/50 kDa surface glycoconjugate of *Trypanosoma cruzi*

trypomastigotes during invasion of HeLa cells," *Memórias do Instituto Oswaldo Cruz*, vol. 86, supplement 1, p. 1, 1991.

[15] S. Schenkman, M. A. J. Ferguson, N. Heise, M. L. Cardoso de Almeida, R. A. Mortara, and N. Yoshida, "Mucin-like glycoproteins linked to the membrane by glycosylphosphatidylinositol anchor are the major acceptors of sialic acid in a reaction catalyzed by trans-sialidase in metacyclic forms of *Trypanosoma cruzi*," *Molecular and Biochemical Parasitology*, vol. 59, no. 2, pp. 293–304, 1993.

[16] M. C. Fernandes, L. R. de Andrade, N. W. Andrews, and R. A. Mortara, "*Trypanosoma cruzi* trypomastigotes induce cytoskeleton modifications during hela cell invasion," *Memórias do Instituto Oswaldo Cruz*, vol. 106, no. 8, pp. 1014–1016, 2011.

[17] C. Sant'Anna, L. Campanati, C. Gadelha et al., "Improvement on the visualization of cytoskeletal structures of protozoan parasites using high-resolution field emission scanning electron microscopy (FESEM)," *Histochemistry and Cell Biology*, vol. 124, no. 1, pp. 87–95, 2005.

[18] D. A. Gaudet and E. G. Kokko, "Application of scanning electron microscopy to paraffin-embedded plant tissues to study invasive process of plant-pathogenic fungi," *Phytopathology*, vol. 74, p. 3, 1984.

[19] H. D. Geissinger, "Correlated light optical and scanning electron microscopy of Gram smears of bacteria and paraffin sections of cardiac muscle," *Journal of Microscopy*, vol. 93, no. 2, pp. 109–117, 1971.

[20] W. P. Wergin, R. W. Yaklich, S. Roy et al., "Imaging thin and thick sections of biological tissue with the secondary electron detector in a field-emission scanning electron microscope," *Scanning*, vol. 19, no. 6, pp. 386–395, 1997.

[21] S. D. Russell and C. P. Daghlian, "Scanning electron microscopic observations on deembedded biological tissue sections: comparison of different fixatives and embedding materials," *Journal of Electron Microscopy Technique*, vol. 2, no. 5, pp. 489–495, 1985.

[22] R. Lainson and J. J. Shaw, *Evolution, Classification and Geographical Distribution*, W. Peters, R. Killick-Kendrick, Eds., Academic Press, San Diego, Calif, USA, 1987.

[23] A. J. Altamirano-Enciso, M. C. A. Marzochi, J. S. Moreira, A. O. Schubach, and K. B. F. Marzochi, "On the origin and spread of cutaneous and mucosal leishmaniasis, based on pre- and post- colombian historical source," *História Ciências Saúde, Manguinhos*,, vol. 10, no. 3, pp. 852–882, 2003.

[24] J.-P. Dedet, "Edmond Sergent's discoveries on the vectorial transmission of agents of human and animal infectious diseases," *Bulletin de la Societé de Pathologie Exotique*, vol. 100, no. 2, pp. 147–150, 2007.

[25] J. Théodoridès, "Historical note on the discovery of the transmission of cutaneous leishmaniasis by phlebotomes," *Bulletin de la Societé de Pathologie Exotique*, vol. 90, no. 3, pp. 177–178, 1997.

[26] J. H. Wright, "Protozoa in a case of tropical ulcer ("Delhi Sore")," *Journal of Medical Research*, vol. 10, pp. 472–482, 1903.

[27] S. R. Christophers, "On a parasite found in persons suffering from enlargement of the spleen in India," Second Report, Office of the Superintendent of Government Printing, Calcutta, India, 1904.

[28] D. Heyneman, "Immunology of leishmaniasis," *Bulletin of the World Health Organization*, vol. 44, no. 4, pp. 499–514, 1971.

[29] N. Ueno and M. E. Wilson, "Receptor-mediated phagocytosis of *Leishmania*: implications for intracellular survival," *Trends in Parasitology*, vol. 28, pp. 335–344, 2012.

[30] R. J. V. Pulvertaft and G. F. Hoyle, "Stages in the life-cycle of *Leishmania donovani*," *Transactions of the Royal Society of Tropical Medicine and Hygiene*, vol. 54, no. 2, pp. 191–196, 1960.

[31] H. C. Miller and D. W. Twohy, "Infection of macrophages in culture by leptomonads of *Leishmania donovani*," *The Journal of Protozoology*, vol. 14, no. 4, pp. 781–789, 1967.

[32] H. J. Akiyama and R. D. Haight, "Interaction of *Leishmania donovani* and hamster peritoneal macrophages. A phase-contrast microscopical study," *American Journal of Tropical Medicine and Hygiene*, vol. 20, no. 4, pp. 539–545, 1971.

[33] C.-L. Forestier, C. MacHu, C. Loussert, P. Pescher, and G. F. Späth, "Imaging host cell-*Leishmania* interaction dynamics implicates parasite motility, lysosome recruitment, and host cell wounding in the infection process," *Cell Host and Microbe*, vol. 9, no. 4, pp. 319–330, 2011.

[34] N. Courret, C. Fréhel, N. Gouhier et al., "Biogenesis of *Leishmania*-harbouring parasitophorus vacuoles following phagocytosis of the metacyclic promastigote or amastigote stages of the parasites," *Journal of Cell Science*, vol. 115, no. 11, pp. 2303–2316, 2002.

[35] M. Aikawa, L. D. Hendricks, Y. Ito, and M. Jagusiak, "Interactions between macrophagelike cells and *Leishmania braziliensis in vitro*," *American Journal of Pathology*, vol. 108, no. 1, pp. 50–59, 1982.

[36] J. M. Blackwell and J. E. Plant, "Expression of the natural resistance gene (Lsh) in wild mice infected experimentally with *Leishmania donovani* or *Salmonella typhimurium*," *Current topics in Microbiology and Immunology*, vol. 127, pp. 323–330, 1986.

[37] D. C. Love, M. M. Kane, and D. M. Mosser, "*Leishmania amazonensis*: the phagocytosis of amastigotes by macrophages," *Experimental Parasitology*, vol. 88, no. 3, pp. 161–171, 1998.

[38] D. Coling and B. Kachar, "Theory and application of fluorescence microscopy," *Current Protocols in Neuroscience*, vol. 2, Unit 2.1, 2001.

[39] R. Lodge and A. Descoteaux, "*Leishmania donovani* promastigotes induce periphagosomal F-actin accumulation through retention of the GTPase Cdc42," *Cellular Microbiology*, vol. 7, no. 11, pp. 1647–1658, 2005.

[40] R. Lodge and A. Descoteaux, "Phagocytosis of *Leishmania donovani* amastigotes is Rac1 dependent and occurs in the absence of NADPH oxidase activation," *European Journal of Immunology*, vol. 36, no. 10, pp. 2735–2744, 2006.

[41] J. Alexander and K. Vickerman, "Fusion of host cell secondary lysosomes with the parasitophorous vacuoles of *Leishmania mexicana* infected macrophages," *The Journal of Protozoology*, vol. 22, no. 4, pp. 502–508, 1975.

[42] K. P. Chang and D. M. Dwyer, "*Leishmania donovani*. Hamster macrophage interactions *in vitro*: cell entry, intracellular survival, and multiplication of amastigotes," *Journal of Experimental Medicine*, vol. 147, no. 2, pp. 515–530, 1978.

[43] J.-C. Antoine, E. Prina, T. Lang, and N. Courret, "The biogenesis and properties of the parasitophorous vacuoles that harbour *Leishmania* in murine macrophages," *Trends in Microbiology*, vol. 6, no. 10, pp. 392–401, 1998.

[44] E. Prina and J. Antoine Cl., "Localization and activity of various lysosomal proteases in rat macrophages infected with *Leishmania amazonensis*," *Pathologie Biologie*, vol. 38, no. 10, pp. 1020–1022, 1990.

[45] J.-C. Antoine, E. Prina, C. Jouanne, and P. Bongrand, "Parasitophorous vacuoles of *Leishmania amazonensis*-infected

macrophages maintain an acidic pH," *Infection and Immunity*, vol. 58, no. 3, pp. 779–787, 1990.

[46] T. Lang, C. de Chastellier, C. Frehel et al., "Distribution of MHC class I and of MHC class II molecules in macrophages infected with *Leishmania amazonensis*," *Journal of Cell Science*, vol. 107, no. 1, pp. 69–82, 1994.

[47] E. Handman and D. V. Bullen, "Interaction of *Leishmania* with the host macrophage," *Trends in Parasitology*, vol. 18, pp. 332–334, 2002.

[48] F. Real and R. A. Mortara, "The diverse and dynamic nature of *Leishmania* parasitophorous vacuoles studied by multidimensional imaging," *PLoS Neglected Tropical Diseases*, vol. 6, no. 2, Article ID e1518, 2012.

[49] T. Lang, H. Lecoeur, and E. Prina, "Imaging *Leishmania* development in their host cells," *Trends in Parasitology*, vol. 25, no. 10, pp. 464–473, 2009.

[50] C. Lippuner, D. Paape, A. Paterou et al., "Real-time imaging of *Leishmania mexicana*-infected early phagosomes: a study using primary macrophages generated from green fluorescent protein-Rab5 transgenic mice," *FASEB Journal*, vol. 23, no. 2, pp. 483–491, 2009.

[51] D. S. Ridley, "A histological classification of cutaneous leishmaniasis and its geographical expression," *Transactions of the Royal Society of Tropical Medicine and Hygiene*, vol. 74, no. 4, pp. 515–521, 1980.

[52] M. G. Rittig, K. Schröppel, K.-H. Seack et al., "Coiling phagocytosis of trypanosomatids and fungal cells," *Infection and Immunity*, vol. 66, no. 9, pp. 4331–4339, 1998.

[53] M. G. Rittig and C. Bogdan, "*Leishmania*-host-cell interaction: complexities and alternative views," *Parasitology Today*, vol. 16, no. 7, pp. 292–297, 2000.

[54] N. C. Peters, J. G. Egen, N. Secundino et al., "In vivo imaging reveals an essential role for neutrophils in leishmaniasis transmitted by sand flies," *Science*, vol. 321, no. 5891, pp. 970–974, 2008.

[55] L. G. Ng, A. Hsu, M. A. Mandell et al., "Migratory dermal dendritic cells act as rapid sensors of protozoan parasites," *PLoS Pathogens*, vol. 4, no. 11, Article ID e1000222, 2008.

[56] P. Gueirard, A. Laplante, C. Rondeau, G. Milon, and M. Desjardins, "Trafficking of *Leishmania donovani* promastigotes in non-lytic compartments in neutrophils enables the subsequent transfer of parasites to macrophages," *Cellular Microbiology*, vol. 10, no. 1, pp. 100–111, 2008.

[57] C. Chagas, "Nova tripanozomiaze humana: estudos sobre a morfolojia e o ciclo evolutivo do*Schizotrypanum cruzi* n. gen., n. sp., ajente etiolojico de nova entidade morbida do homem," *Memórias do Instituto Oswaldo Cruz*, vol. 1, pp. 159–218, 1909.

[58] G. Vianna, "Contribuição para o estudo da anatomia patolójica da "Moléstia de Carlos Chagas" (Esquizotripanose humana ou tireoidite parasitária)," *Memórias do Instituto Oswaldo Cruz*, vol. 3, pp. 276–293, 1911.

[59] E. Dias, "Estudos sobre o *Schizotrypanum cruzi*," *Memórias Do Instituto Oswaldo Cruz*, vol. 28, pp. 1–110, 1934.

[60] E. Villela and C. M. Torres, "Histopathology of the central nervous system in experimental paralysis caused by *Schizotrypanum cruzi*," *Memórias do Instituto Oswaldo Cruz*, vol. 19, pp. 199–221, 1926.

[61] C. Romaña and H. Meyer, "Estudo do ciclo evolutivo do, "*Schizotrypanum cruzi*" em cultura de tecidos de embrião de galinha," *Memórias do Instituto Oswaldo Cruz*, vol. 37, pp. 19–27, 1942.

[62] C. A. Kofoid, F. D. Wood, and E. C. E. McNeil, *The Cycle of Trypanosoma Cruzi in Tissue Culture of Embryonic Heart Muscle*, University of California Press, Berkeley, Calif, USA, 1935.

[63] Z. Brener, "Biology of *Trypanosoma cruzi*," *Annual Review of Microbiology*, vol. 27, pp. 347–382, 1973.

[64] H. Meyer and A. Barasa, "Life cycle of *Schizotrypanum cruzi* in tissue cultures," http://www.itarget.com.br/newclients/sbpz.org.br/2011/extra/download/cruzi1.mpg.

[65] H. Meyer and K. R. Porter, "A study of *Trypanosoma cruzi* with the electron microscope," *Parasitology*, vol. 44, no. 1-2, pp. 16–23, 1954.

[66] W. de Souza, "Electron microscopy of trypanosomes—a historical view," *Memórias do Instituto Oswaldo Cruz*, vol. 103, no. 4, pp. 313–325, 2008.

[67] J. A. Dvorak and T. P. Hyde, "*Trypanosoma cruzi*: interaction with vertebrate cells *in vitro*. I. Individual interactions at the cellular and subcellular levels," *Experimental Parasitology*, vol. 34, no. 2, pp. 268–283, 1973.

[68] E. R. Ferreira, A. Bonfim-Melo, R. A. Mortara, and D. Bahia, "*Trypanosoma cruzi* extracellular amastigotes and host cell signaling: more pieces to the puzzle," *Frontiers in Immunology*, vol. 3, p. 363, 2012.

[69] V. Ley, N. W. Andrews, E. S. Robbins, and V. Nussenzweig, "Amastigotes of *Trypanosoma cruzi* sustain an infective cycle in mammalian cells," *Journal of Experimental Medicine*, vol. 168, no. 2, pp. 649–659, 1988.

[70] F. M. Lima, P. Oliveira, R. A. Mortara, J. F. Silveira, and D. Bahia, "The challenge of Chagas' disease: has the human pathogen, *Trypanosoma cruzi*, learned how to modulate signaling events to subvert host cells?" *New Biotechnology*, vol. 27, no. 6, pp. 837–843, 2010.

[71] R. A. Mortara, W. K. Andreoli, N. N. Tantwaki et al., "Mammalian cell invasion and intracellular trafficking by *Trypanosoma cruzi* infective forms," *Anais da Academia Brasileira de Ciencias*, vol. 77, no. 1, pp. 77–94, 2005.

[72] S. Tomlinson, F. Vandekerckhove, U. Frevert, and V. Nussenzweig, "The induction of *Trypanosoma cruzi* trypomastigote to amastigote transformation by low pH," *Parasitology*, vol. 110, no. 5, pp. 547–554, 1995.

[73] N. Nogueira and Z. Cohn, "*Trypanosoma cruzi*: mechanism of entry and intracellular fate in mammalian cells," *Journal of Experimental Medicine*, vol. 143, no. 6, pp. 1402–1420, 1976.

[74] K. Behbehani, "Developmental cycles of *Trypanosoma (Schizotrypanum) cruzi* (Chagas, 1909) in mouse peritoneal macrophages *in vitro*," *Parasitology*, vol. 66, no. 2, pp. 343–353, 1973.

[75] L. Hudson, D. Snary, and S. J. Morgan, "*Trypanosoma cruzi*: continuous cultivation with murine cell lines," *Parasitology*, vol. 88, pp. 283–294, 1984.

[76] S. Chia-Tung Pan, "*Trypanosoma cruzi*: *in vitro* interactions between cultured amastigotes and human skin-muscle cells," *Experimental Parasitology*, vol. 45, no. 2, pp. 274–286, 1978.

[77] S. Schenkman, N. W. Andrews, V. Nussenzweig, and E. S. Robbins, "*Trypanosoma cruzi* invade a mammalian epithelial cell in a polarized manner," *Cell*, vol. 55, no. 1, pp. 157–165, 1988.

[78] R. A. Mortara, "*Trypanosoma cruzi*: amastigotes and trypomastigotes interact with different structures on the surface of HeLa cells," *Experimental Parasitology*, vol. 73, no. 1, pp. 1–14, 1991.

[79] S. Schenkman and R. A. Mortara, "HeLa cells extend and internalize pseudopodia during active invasion by *Trypanosoma cruzi* trypomastigotes," *Journal of Cell Science*, vol. 101, no. 4, pp. 895–905, 1992.

[80] D. O. Procópio, S. da Silva, C. C. Cunningham, and R. A. Mortara, "*Trypanosoma cruzi*: effect of protein kinase inhibitors and cytoskeletal protein organization and expression on host cell invasion by amastigotes and metacyclic trypomastigotes," *Experimental Parasitology*, vol. 90, no. 1, pp. 1–13, 1998.

[81] D. Ferreira, M. Cortez, V. D. Atayde, and N. Yoshida, "Actin cytoskeleton-dependent and -independent host cell invasion by *Trypanosoma cruzi* is mediated by distinct parasite surface molecules," *Infection and Immunity*, vol. 74, no. 10, pp. 5522–5528, 2006.

[82] S. Schenkman, E. S. Robbins, and V. Nussenzweig, "Attachment of *Trypanosoma cruzi* to mammalian cells requires parasite energy, and invasion can be independent of the target cell cytoskeleton," *Infection and Immunity*, vol. 59, no. 2, pp. 645–654, 1991.

[83] I. Tardieux, P. Webster, J. Ravesloot et al., "Lysosome recruitment and fusion are early events required for trypanosome invasion of mammalian cells," *Cell*, vol. 71, no. 7, pp. 1117–1130, 1992.

[84] C. T. Fonseca Rosestolato, J. da Matta Furniel Dutra, W. de Souza, and T. M. Ulisses de Carvalho, "Participation of host cell actin filaments during interaction of trypomastigote forms of *Trypanosoma cruzi* with host cells," *Cell Structure and Function*, vol. 27, no. 2, pp. 91–98, 2002.

[85] D. O. Procópio, H. C. Barros, and R. A. Mortara, "Actin-rich structures formed during the invasion of cultured cells by infective forms of *Trypanosoma cruzi*," *European Journal of Cell Biology*, vol. 78, no. 12, pp. 911–924, 1999.

[86] M. C. Fernandes, A. R. Flannery, N. Andrews, and R. A. Mortara, "Extracellular amastigotes of *Trypanosoma cruzi* are potent inducers of phagocytosis in mammalian cells," *Cellular Microbiology*, vol. 15, pp. 977–991, 2013.

[87] B. A. Burleigh and A. M. Woolsey, "Cell signalling and *Trypanosoma cruzi* invasion," *Cellular Microbiology*, vol. 4, no. 11, pp. 701–711, 2002.

[88] C. Tam, V. Idone, C. Devlin et al., "Exocytosis of acid sphingomyelinase by wounded cells promotes endocytosis and plasma membrane repair," *Journal of Cell Biology*, vol. 189, no. 6, pp. 1027–1038, 2010.

[89] M. C. Fernandes, M. Cortez, A. R. Flannery, C. Tam, R. A. Mortara, and N. W. Andrews, "*Trypanosoma cruzi* subverts the sphingomyelinase-mediated plasma membrane repair pathway for cell invasion," *Journal of Experimental Medicine*, vol. 208, no. 5, pp. 909–921, 2011.

[90] A. M. Woolsey, L. Sunwoo, C. A. Petersen, S. M. Brachmann, L. C. Cantley, and B. A. Burleigh, "Novel Pl 3-kinase-dependent mechanisms of trypanosome invasion and vacuole maturation," *Journal of Cell Science*, vol. 116, no. 17, pp. 3611–3622, 2003.

[91] E. S. Barrias, L. C. Reignault, W. de Souza, and T. M. Carvalho, "*Trypanosoma cruzi* uses macropinocytosis as an additional entry pathway into mammalian host cell," *Microbes and Infection*, vol. 14, pp. 1340–1351, 2012.

[92] L. O. Andrade and N. W. Andrews, "Lysosomal fusion is essential for the retention of *Trypanosoma cruzi* inside host cells," *Journal of Experimental Medicine*, vol. 200, no. 9, pp. 1135–1143, 2004.

[93] K. L. Caradonna and B. A. Burleigh, "Mechanisms of host cell invasion by *Trypanosoma cruzi*," *Advances in Parasitology*, vol. 76, pp. 33–61, 2011.

[94] H. Tanowitz, M. Wittner, Y. Kress, and B. Bloom, "Studies of *in vitro* infection by *Trypanosoma cruzi*. I. Ultrastructural studies on the invasion of macrophages and L cells," *American Journal of Tropical Medicine and Hygiene*, vol. 24, no. 1, pp. 25–33, 1975.

[95] T. M. Ulisses de Carvalho and W. de Souza, "Early events related with the behaviour of *Trypanosoma cruzi* within an endocytic vacuole in mouse peritoneal macrophages," *Cell Structure and Function*, vol. 14, no. 4, pp. 383–392, 1989.

[96] T. C. de Araújo-Jorge, "The biology of *Trypanosoma cruzi*-macrophage interaction," *Memórias do Instituto Oswaldo Cruz*, vol. 84, no. 4, pp. 441–462, 1989.

[97] S. S. C. Rubin-de-Celis, H. Uemura, N. Yoshida, and S. Schenkman, "Expression of trypomastigote trans-sialidase in metacyclic forms of *Trypanosoma cruzi* increases parasite escape from its parasitophorous vacuole," *Cellular Microbiology*, vol. 8, no. 12, pp. 1888–1898, 2006.

[98] N. W. Andrews and M. B. Whitlow, "Secretion of *Trypanosoma cruzi* of a hemolysin active at low pH," *Molecular and Biochemical Parasitology*, vol. 33, no. 3, pp. 249–256, 1989.

[99] N. W. Andrews, C. K. Abrams, S. L. Slatin, and G. Griffiths, "A *T. cruzi*-secreted protein immunologically related to the complement component C9: evidence for membrane pore-forming activity at low pH," *Cell*, vol. 61, no. 7, pp. 1277–1287, 1990.

[100] D. Moore-Lai and E. Rowland, "Discovery and characterization of an antibody, anti-egressin, that is able to inhibit *Trypanosoma cruzi* egress *in vitro*," *Journal of Parasitology*, vol. 90, no. 3, pp. 524–530, 2004.

[101] J. L. Wendelken and E. C. Rowland, "Agglutination of *Trypanosoma cruzi* in infected cells treated with serum from chronically infected mice," *Journal of Parasitology*, vol. 95, no. 2, pp. 337–344, 2009.

[102] J. Costales and E. C. Rowland, "Human chagasic serum contains antibodies capable of inhibiting *Trypanosoma cruzi* egress from tissue culture cells," *Journal of Parasitology*, vol. 91, no. 4, pp. 950–953, 2005.

[103] J. Costales and E. C. Rowland, "A role for protease activity and host-cell permeability during the process of *Trypanosoma cruzi* egress from infected cells," *Journal of Parasitology*, vol. 93, no. 6, pp. 1350–1359, 2007.

[104] W. Coene, G. Janssen, M. Op de Beeck, and D. van Dyck, "Phase retrieval through focus variation for ultra-resolution in field-emission transmission electron microscopy," *Physical Review Letters*, vol. 69, no. 26, pp. 3743–3746, 1992.

[105] G. M. Rocha, B. A. Brandão, R. A. Mortara, M. Attias, W. de Souza, and T. M. U. Carvalho, "The flagellar attachment zone of *Trypanosoma cruzi* epimastigote forms," *Journal of Structural Biology*, vol. 154, no. 1, pp. 89–99, 2006.

[106] R. Zeledón, R. Bolaños, M. R. Espejo Navarro, and M. Rojas, "Morphological evidence by scanning electron microscopy of excretion of metacyclic forms of *Trypanosoma cruzi* in vector's urine," *Memorias do Instituto Oswaldo Cruz*, vol. 83, no. 3, pp. 361–365, 1988.

[107] C. A. Boker and G. A. Schaub, "Scanning electron microscopic studies of *Trypanosoma cruzi* in the rectum of its vector *Triatoma infestans*," *Zeitschrift fur Parasitenkunde*, vol. 70, no. 4, pp. 459–469, 1984.

[108] M. C. Bonaldo, T. Souto-Padron, W. de Souza, and S. Goldenberg, "Cell-substrate adhesion during *Trypanosoma cruzi*

differentiation," *Journal of Cell Biology*, vol. 106, no. 4, pp. 1349–1358, 1988.

[109] E. S. Barrias, J. M. F. Dutra, W. de Souza, and T. M. U. Carvalho, "Participation of macrophage membrane rafts in *Trypanosoma cruzi* invasion process," *Biochemical and Biophysical Research Communications*, vol. 363, no. 3, pp. 828–834, 2007.

[110] R. A. Mortara, L. M. S. Minelli, F. Vandekerckhove, V. Nussenzweig, and F. Juarez Ramalho-Pinto, "Phosphatidylinositol-specific phospholipase C (PI-PLC) cleavage of GPI-anchored surface molecules of *Trypanosoma cruzi* triggers *in vitro* morphological reorganization of trypomastigotes," *Journal of Eukaryotic Microbiology*, vol. 48, no. 1, pp. 27–37, 2001.

[111] G. M. Rocha, K. Miranda, G. Weissmüller, P. M. Bisch, and W. de Souza, "Ultrastructure of *Trypanosoma cruzi* revisited by atomic force microscopy," *Microscopy Research and Technique*, vol. 71, no. 2, pp. 133–139, 2008.

[112] R. C. Magno, L. Lemgruber, R. C. Vommaro, W. de Souza, and M. Attias, "Intravacuolar network may act as a mechanical support for *Toxoplasma gondii* inside the parasitophorous vacuole," *Microscopy Research and Technique*, vol. 67, no. 1, pp. 45–52, 2005.

[113] P. R. Flood, "Dry-fracturing techniques for the study of soft internal biological tissues in the scanning electron microscope," *Scanning Electron Microscopy*, vol. 2, pp. 287–294, 1975.

[114] F. E. G. Cox, "History of human parasitology," *Clinical Microbiology Reviews*, vol. 15, no. 4, pp. 595–612, 2002.

[115] M. Perleth, "The discovery of Chagas' disease and the formation of the early Chagas' disease concept," *History and philosophy of the life sciences*, vol. 19, no. 2, pp. 211–236, 1997.

[116] F. Köberle, "Chagas' disease and chagas' syndromes: the pathology of American trypanosomiasis," *Advances in Parasitology*, vol. 6, pp. 63–116, 1968.

[117] E. de la Llave, H. Lecoeur, A. Besse, G. Milon, E. Prina, and T. Lang, "A combined luciferase imaging and reverse transcription polymerase chain reaction assay for the study of *Leishmania* amastigote burden and correlated mouse tissue transcript fluctuations," *Cellular Microbiology*, vol. 13, no. 1, pp. 81–91, 2011.

[118] S. Goyard, P. L. Dutra, P. Deolindo, D. Autheman, S. D'Archivio, and P. Minoprio, "*In vivo* imaging of trypanosomes for a better assessment of host-parasite relationships and drug efficacy," *Parasitology International*, vol. 63, pp. 260–268, 2013.

Hindawi Publishing Corporation
BioMed Research International
Volume 2014, Article ID 127453, 10 pages
http://dx.doi.org/10.1155/2014/127453

Research Article

Entamoeba histolytica and *E. dispar* Calreticulin: Inhibition of Classical Complement Pathway and Differences in the Level of Expression in Amoebic Liver Abscess

Cecilia Ximénez,[1] Enrique González,[1] Miriam E. Nieves,[1] Angélica Silva-Olivares,[2] Mineko Shibayama,[2] Silvia Galindo-Gómez,[2] Jaime Escobar-Herrera,[3] Ma del Carmen García de León,[1] Patricia Morán,[1] Alicia Valadez,[1] Liliana Rojas,[1] Eric G. Hernández,[1] Oswaldo Partida,[1] and René Cerritos[1]

[1] *Departamento de Medicina Experimental, Facultad de Medicina, UNAM, Dr. Balmis 148, Colonia Doctores, 06726 México, DF, Mexico*
[2] *Departamento de Infectómica y Patogénesis Molecular, CINVESTAV, 07360 México, DF, Mexico*
[3] *Departamento de Biología Celular, CINVESTAV, 07360 México, DF, Mexico*

Correspondence should be addressed to Cecilia Ximénez; cximenez@unam.mx

Received 4 December 2013; Revised 19 February 2014; Accepted 7 March 2014; Published 22 April 2014

Academic Editor: Marlene Benchimol

The role of calreticulin (CRT) in host-parasite interactions has recently become an important area of research. Information about the functions of calreticulin and its relevance to the physiology of *Entamoeba* parasites is limited. The present work demonstrates that CRT of both pathogenic *E. histolytica* and nonpathogenic *E. dispar* species specifically interacted with human C1q inhibiting the activation of the classical complement pathway. Using recombinant *Eh*CRT protein, we demonstrate that CRT interaction site and human C1q is located at the N-terminal region of *Eh*CRT. The immunofluorescence and confocal microscopy experiments show that CRT and human C1q colocalize in the cytoplasmic vesicles and near to the surface membrane of previously permeabilized trophozoites or are incubated with normal human serum which is known to destroy trophozoites. In the presence of peripheral mononuclear blood cells, the distribution of *Eh*CRT and C1q is clearly over the surface membrane of trophozoites. Nevertheless, the level of expression of CRT *in situ* in lesions of amoebic liver abscess (ALA) in the hamster model is different in both *Entamoeba* species; this molecule is expressed in higher levels in *E. histolytica* than in *E. dispar*. This result suggests that *Eh*CRT may modulate some functions during the early moments of the host-parasite relationship.

1. Introduction

Calreticulin (CRT) is a highly conserved multifunctional protein that was originally identified as a major calcium-binding protein of the endoplasmic reticulum [1]. CRT has been detected in every eukaryotic cell, with the exception of erythrocytes. All CRT proteins contain three structural domains: a globular N-terminal domain, a proline-rich P domain, and an acidic C-terminal domain. The N-terminal domain is involved in protein-protein interactions, RNA-binding, and autoantibody binding. The P domain binds Ca^{2+} with high affinity and low capacity, while the C-terminal domain, which is the least conserved domain among CRTs, binds Ca^{2+} with low affinity [1, 2].

The role of CRT in host-parasite interactions has recently become an important area of research. CRT genes from a number of parasites (*Trypanosoma*, *Leishmania*, *Entamoeba*, *Onchocerca*, *Schistosoma*, and *Haemonchus*) have been cloned and sequenced, revealing approximately 50% identity with CRT human gene [3–8].

Although the functions of CRT are conserved in vertebrates, some CRT functions differ among parasites [9, 10]; parasite CRTs bind host C1q and inhibit C1q-dependent complement activation. *Haemonchus contortus* CRT binds host

C-reactive protein and C1q; this interaction may inhibit the activation of the classical complement pathway [11]. The ectoparasite *Amblyomma americanum* secretes CRT during feeding, suggesting that the anticoagulant ability of CRT may prevent blood clotting and permit the parasite to feed on the host or induce host antiparasite responses [12]. The presence of CRT in the penetration gland cells of *Schistosoma* suggests that this molecule may be important for the host skin penetration [13].

Among protozoan parasites, the binding and inhibition of human C1q by CRT have been demonstrated in both *Trypanosoma cruzi* and *T. carassii*. *T. cruzi* and *T. carassii* CRT (*Tc*CRT) bind human or fish C1q, respectively, and specifically inhibit the classical complement pathway. This suggests an evolutive conserved interaction between CRT and C1q [14, 15].

Previously, we reported the presence of CRT in *E. histolytica* (*Eh*CRT). This protein induces an important immunogenic response in the human host. More than 90% of patients with amoebic liver abscess (ALA) develop high levels of serum antibodies against *Eh*CRT [16]. We also reported the cloning of CRT gene in *E. histolytica* and the preparation of monospecific antibodies against recombinant CRT (r*Eh*CRT); the immunohistochemical assays on trophozoites show that *Eh*CRT is located in the cytoplasmic vesicles and in vesicles in close contact with the inner cytoplasmic membrane. In histopathological studies, on sections of experimental ALA in hamsters, *Eh*CRT was clearly detected into the trophozoites and seems to be neither exposed in the surface of trophozoites nor exported into the hepatic tissue [8]. The binding of C1q to CRT in the surface of *E. histolytica* trophozoites has been recently reported after its activation in cell-to-cell interaction with Jurkat cells; authors mention that during erytrophagocytosis the CRT is located in the surface of trophozoites and in the phagocytic cups [17]. CRT in the surface of apoptotic human cells seems to function as a receptor for C1q allowing the phagocytosis of damaged cells. More so, the overexpression of crt gene is related to the presence of apoptosis inductors [18].

In mammals, translocation of CRT from the RE to the membrane can be mediated by the vesicular transportation from the RE to the Golgi, mediated by the SNARE-dependent fusion of exocytic vesicles with plasma membrane. Other possible mechanisms of translocation of CRT to the plasma membrane could be mediated by the ERP57 chaperone protein, albeit this mechanism is not yet totally demonstrated [19].

One of the indicators of virulence of *E. histolytica* trophozoites that has been cited over the years [20, 21] is resistance to the lytic action of human serum. The referred capacity of CRT to bind host C1q observed in some parasites has been considered as an evasion mechanism of the host immune response, impairing the lytic action of complement. In the case of *E. histolytica*, it is possible that resistance of virulent trophozoites to the lyses of human serum could be mediated by the C1q binding capacity of *Eh*CRT.

In the present work, we tested the human C1q binding capacity of recombinant *Eh*CRT and native CRT in an ELISA system in both pathogenic *E. histolytica* and nonpathogenic *E. dispar* species. We also demonstrated that CRT and C1q colocalize in the cytoplasmic vesicles and those near the surface membrane of previously permeabilized trophozoites. Besides, we tested the capacity of recombinant *Eh*CRT to bind human C1q and, as a consequence, be able to inhibit the classical complement pathway *in vitro*. Results suggest a clear amoebicidal activity of human serum against trophozoites that can be inhibited indistinguishably in presence of recombinant or native *Eh*CRT; the interaction of CRT-C1q evaluated was equal for both species of *Entamoebas*.

2. Material and Methods

2.1. Production of Recombinant EhCRT. Full-length r*Eh*CRT and N- and C-terminal-domain proteins were expressed and purified as previously described [8, 22]. Briefly, the plasmid pBluescript-KS+ (pbKS+) was used to clone PCR products. We obtained three clones, which we refer to as pb-*Eh*CRT, pb-*Eh*CRT-N, and pb-*Eh*CRT-C. These recombinant plasmids were subcloned into the prokaryotic expression vector pProEX HT-b (Gibco Life Technologies, Grand Island, NY, USA) to express the CRT constructed in fusion with a six-histidine tag on the NH_2 end. Competent *Escherichia coli* BL21 cells were transformed with one of the recombinant plasmids. The expression of recombinant proteins r*Eh*CRT, r*Eh*CRT-N, and r*Eh*CRT-C was induced with a final concentration of 1 mM isopropyl-β-D-thiogalactoside (IPTG). The QIAexpressionist system (Qiagen, Valencia, CA, USA) was used to purify recombinant proteins.

The cells were harvested by centrifugation at 3000 ×g for 12 min, and the bacterial pellet was resuspended in 5 mL of lysis buffer (8 M urea, 0.1 M NaH_2PO_4, and 0.1 M Tris-HCl, pH 8.0). The lysate was added to a 50% suspension of Ni-NTA agarose (Qiagen). The mixture was filtered through a filtration column (Qiagen), and the recombinant proteins were eluted with 8 M urea buffer, pH 4.5. The selected fractions were dialysed against 19 mM phosphate-buffered saline (PBS) to eliminate the urea.

2.2. Purification of Native EhCRT and EdCRT. Specific anti-r*Eh*CRT IgG antibodies were obtained previously [8] and were used to purify native *Eh*CRT and *Ed*CRT by affinity chromatography. 20 mg of IgG anti-r*Eh*CRT was bound to a Sepharose 4B column (Sigma Chemical Co., St Louis, MO, USA). A membrane-enriched *E. histolytica* or *E. dispar* extract was obtained as previously reported [23]. A 10 mg quantity of the respective antigen was applied to the column and incubated for 1 h. The column was washed with PBS, pH 7.5. This bound protein was eluted with 0.5 M glycine, pH 4.5, and 1 mL fractions were collected into 100 μL of 1.0 M Tris-HCl, pH 8.5, to neutralize the acidity of the elution buffer to preserve activity. Protein concentrations were determined using a Bradford Assay kit (Bio-Rad, Hercules, CA, USA).

2.3. Isolation of Human Lymphocytes. Peripheral mononuclear blood cell (PMBC) was isolated from fresh human blood obtained in heparinized tubes from human volunteers. Whole blood was centrifuged by gradient of Ficoll-Hypaque

(Gibco BRL); the PMBC was separated and washed three times with PBS and used immediately for assays of interaction with trophozoites of *E. histolytica* or *E. dispar* (1 : 6 ameba/lymphocytes).

2.4. Interaction of EhCRT or EdCRT with Human C1q. Microtiter plates (EIA/RIA strip, Costar, Cambridge, MA, USA) were coated overnight at room temperature (RT) with 50 μL of 0–200 μM of full-length recombinant r*Eh*CRT, r*Eh*CRT-N, or r*Eh*CRT-C or native n*Eh*CRT or n*Ed*CRT suspended in 0.1 M Na_2CO_3, pH 9.6. Each step was followed by three washes with 0.5% Tween 20/PBS. Nonspecific binding sites were blocked with 3% PBS/BSA, for 2 h at 37°C. After washing, 50 μL of a 1 : 10 dilution of NHS in PBS was added to each well and incubated for 2 h at 37°C. The plates were washed as before, and 50 μL of mouse anti-human C1q (1 : 500) (Santa Cruz Biotechnology, Santa Cruz, CA, USA) was added to each well and incubated for 2 h at 37°C. The plates were washed again as before, and the antigen-antibody reaction was detected by incubation with HRP-conjugated goat anti-mouse IgG (1 : 1000) for 2 h at 37°C. The reaction was developed by the addition of 200 μL of *ortho*-phenylenediamine phosphate (OPD) (10 mg/mL), and the absorbance was measured at 490 nm in a microplate reader (ELx800, BioTek Instruments, Winooski, VT, USA).

2.5. Inhibition of C1q-Dependent Haemolytic Assays. For classical pathway complement activation, sheep red blood cells (SRBCs) were sensitized with rabbit anti-SRBC (1 : 400) (antibody ab50676, Abcam, Cambridge, MA, USA). A 500 μL aliquot of 10^7 antibody-sensitized erythrocytes (EAs) was incubated with normal human serum (NHS) diluted 1 : 10 in isotonic veronal-buffered saline containing 0.1 mM $CaCl_2$, 0.5 mM $MgCl_2$, 0.1% gelatine, and 1% glucose (GVB^{++}) in a final volume of 1000 μL as a positive control. To assess the inhibition of complement activation, the NHS (1 : 10) was preincubated with 2 μg of native n*Eh*CRT or n*Ed*CRT, then added to EAs, and incubated for 1 h at 37°C. After the addition of 1 mL of cold GVB^{++}, intact cells were centrifuged at 400 ×g for 15 min. Haemoglobin in the supernatant was measured at 550 nm with a DU-650 Spectrophotometer Beckman (Beckman, Danvers, MA, USA). Total haemolysis (100%) was measured by treating EAs with water. Background spontaneous haemolysis (0%) was determined by incubating EAs without serum. Haemolytic activity is expressed as a percentage of total haemolysis.

In a similar assay, 10^7 EAs were incubated with C1q-depleted human serum (Calbiochem, a division of Merck KGaA, Darmstadt, Germany) and then added to 2 μg of human C1q (Sigma). Haemolysis was calculated as before. To overcome the inhibitory effect of *Eh*CRT on the classical complement pathway, we used IgG anti-*Eh*CRT produced in mice.

2.6. Amoebicidal Activity of Human Serum. Axenic trophozoites of *E. histolytica*, *E. dispar*, or a virulent strain of *E. histolytica*, newly recovered from hamster livers [22], were harvested by centrifugation at 500 ×g for 10 min, washed twice with PBS, counted, adjusted to a cell density of 2×10^5, and incubated with TYIS-33 medium [24] added with (10, 20, 40, and 60%) NHS. The mixtures were incubated at 37°C for 15, 30, and 60 min; viability of trophozoites was estimated through the 2% trypan blue exclusion technique [25]; live trophozoites were counted in a haemocytometer. Cell counts were expressed as a percentage of dead cells. Heat-inactivated human serum was used as a negative control. To evaluate the inhibition of lyses due to interaction of *Eh*CRT with the human C1q, 10 μg of r*Eh*CRT was added to NHS incubating during 10 min; thereafter, the mixture was added to the trophozoites suspension. Lyses percentage was defined as the decrease in viable trophozoites in the presence of NHS compared with the heat-inactivated human serum control. Values were calculated as follows: (number of viable cell in control − number of viable cell in the presence of NHS)/viable cell in control) × 100. Results are the mean of three independent experiments with each *E. dispar* or *E. histolytica* species or virulent strain of *E. histolytica*.

2.7. Human C1q and EhCRT/EdCRT Colocalization. Trophozoites of *E. histolytica* or *E. dispar* were grown under axenic conditions using TYIS-33 or TYIS-2 [24], respectively, for 48 h. After incubation, the trophozoites were allowed to adhere to sterile glass cover slips for 2 h at 37°C and then fixed with 3.5% paraformaldehyde/PBS. Thereafter, cells were permeabilized or not with 0.1% (v/v) Triton X-100 and blocked with 3% BSA. Trophozoites were then incubated with 4 μg of C1q for 30 min. The slides were washed several times with PBS and incubated for 1 hr with specific rabbit anti-*Eh*CRT (1 : 40 dilution) and mouse anti-human C1q antibodies (1 : 40). Thereafter, a mixture of secondary antibodies was used to reveal the antigen-antibody reactions (Alexa Fluor Cy5 goat anti-rabbit IgG and Alexa Fluor 488 goat anti-mouse IgG, both 1 : 100) (Molecular Probes, Invitrogen, Eugene, OR, USA).

In a similar assay, trophozoites were incubated with NHS (1 : 10) or human peripheral mononuclear blood cells (PMBC) (1 : 6, trophozoites/lymphocytes ratio) for 60 min before incubation with 4 μg of C1q and finally processed for immunohistochemical assay as previously described [5]. Samples were examined by confocal microscopy (DM1RE-2, Leica Mikrosysteme, Wetzlar, Germany) using appropriate fluorescence emission filters. Images (z-series) were acquired with image-processing software (Leica, LCS Lite Profile Pro) using 0.5 μm steps. The images correspond to the maximum-intensity projection of the z-series.

2.8. Experimental Amoebic Liver Abscess. Experimental acute ALA was produced in 100 g hamsters following a technique described by Tsutsumi et al. (1984) [26]. Briefly, 2.5×10^5 or 2×10^6 axenic trophozoites of *EhVIR* (newly recovered from hamster liver) or *E. dispar*, respectively, were inoculated into the portal vein of anesthetized hamsters. After 5, 15, and 30 min and 1, 3, and 9 hours, animals (5 hamsters at a time) were euthanized by an anaesthesia overdose. The liver was removed and fixed in 4% paraformaldehyde in PBS, followed by dehydration and paraffin embedding. Serial

sections of 6 μm thickness were obtained and deparaffinized from tissue blocks; lesions and trophozoites were identified by hematoxylin/eosin stain. The sliced sections were used for immunohistochemical and reverse transcriptase real-time PCR (qRT-PCR) assays.

The institutional committee previously approved protocols for animal care. The institution fulfils all the technical specifications for the production, care, and use of laboratory animals and is certified by a National Law (NOM-062-ZOO-1999). All hamsters were handled according to the guidelines of the 2000 AVMA Panel of Euthanasia.

2.9. Immunochemical Detection of EhCRT and C1q in Amoebic Liver Abscess Lesions. Selected samples were blocked with 3% PBS/BSA solution and reacted with specific mouse anti-*Eh*CRT antibody diluted 1 : 50 and in another slice with mouse anti-human C1q antibody (1 : 20); thereafter, slices were incubated at 4°C overnight. Antigen-antibody reaction was detected using 1 : 500 dilution of goat anti-mouse IgG antibody coupled to alkaline phosphatase (Zymed Laboratories, San Francisco, CA, USA); NBT/BCIP substrate (Roche Diagnostics GmbH; Mannheim, Germany) was used as the chromogen. Monoclonal mouse IgG_1 antibody against *Aspergillus niger* glucose oxidase was used as the negative control (clone DAK-GO1, code number X09931, Dako, Glostrup, Denmark). To avoid cross-reaction with CRT from hamster hepatic tissue, anti-*Eh*CRT antibodies were adsorbed with a lyophilized extract of hamster liver. The samples were counterstained with aqueous eosin.

2.10. Relative mRNA Quantification of EdCRT and EhCRT by qRT-PCR. The detection of CRT mRNA was carried out using a two-step *in situ* RT-PCR procedure as previously reported with some modifications [5]. Previously selected hamster liver tissue sections (3 sections after intraportal inoculation) were pretreated with 0.5 μg/μL proteinase K (Sigma Aldrich, St. Louis, MO, USA) and with 1 U/sample of DNase I, RNase-free (Roche Diagnostics GmbH, Mannheim, Germany). After washing with DEPC-treated water, reverse transcription was performed using SuperScript II reverse transcriptase following the manufacturer's specifications (Invitrogen, Carlsbad, CA, USA). Slides were incubated at 42°C for 2 h in a sealed humidified chamber.

The relative quantification (RQ) of the investigated samples by real-time PCR was performed using the previously synthesized cDNA in the *in situ* RT assays. For this purpose, a 7300 Applied Biosystems apparatus (Applied Biosystems, Carlsbad, CA, USA) and the Quantitect SYBR green PCR kit were used (Qiagen, Valencia, CA, USA).

qPCR was performed for 60 cycles of a 3-step PCR, including 10 seconds of denaturation at 95°C, a 30 sec primer-dependent annealing phase at 58°C, and a 10 sec template-dependent elongation at 72°C. The amplification of each template was performed in duplicate in one PCR run. The differential expression of the investigated genes was calculated as the normalized ratio to *Eh*β-actin.

Results of the threshold cycle (Ct indicates number of cycles to which the amplified product is detected) dates were exported to an Excel sheet to calculate gene expression levels (RQ) using $2^{-\Delta\Delta Ct}$ method described by Livak and Schmittgen (2001) [27].

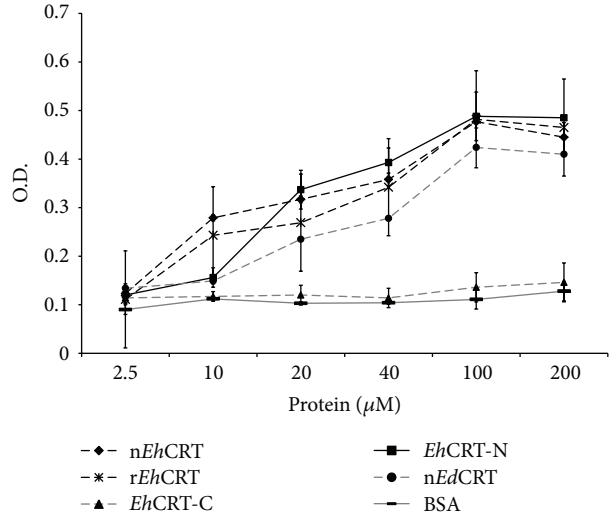

Figure 1: *Eh*CRT/*Ed*CRT interaction with human C1q (ELISA). Microtiter wells were coated with 2.5 to 200 μM of the *Eh*CRT or *Ed*CRT and incubated with 1 : 10 diluted normal human serum supplemented with 4 μg of human C1q; the interaction of *Eh*CRT-C1q was revealed using an anti-human C1q monoclonal antibody produced in mice and then an anti-mouse IgG produced in goat conjugated to peroxidase. Values are the mean of three different assays performed in triplicate ± SD.

2.11. Statistical Analysis. All values are expressed as the mean ± SD of at least three independent experiments. Statistical significance was determined with unpaired Student's *t*-test between each condition used (control against problem), and for comparisons of multiple groups with one-way analysis of variance (ANOVA), differences were considered statistically significant when P values were <0.05.

3. Results

3.1. CRT Binds Human C1q. To assess the interaction between *Eh*CRT and human C1q, a direct binding ELISA was conducted. Figure 1 shows data of the interaction assay between r*Eh*CRT (full-length molecule, N-terminal binding domain, or C-terminal binding domain), n*Eh*CRT or n*Ed*CRT, and human C1q. Differences observed in binding between the native *Eh*CRT or *Ed*CRT and the full-length r*Eh*CRT or r*Eh*CRT-N were not statistically significant. The interaction was dose dependent and saturable; the maximum absorbance was obtained when 100 μM of CRT was used; the OD remained constant in the presence of larger quantities of CRT. In contrast, the r*Eh*CRT-C-terminal protein did not bind to human C1q.

3.2. C1q-Dependent Haemolytic Assays. The ability of *Eh*CRT to inhibit the activation of the classical complement pathway

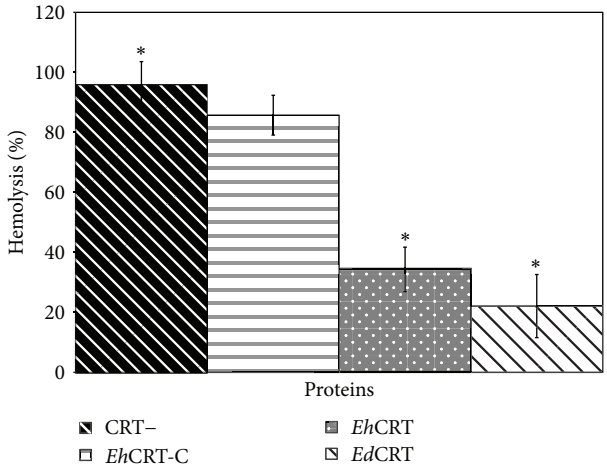

Figure 2: *Eh*CRT inhibits classical pathway-mediated hemolysis. Different proteins of (CRT+) *Eh*CRT or *Ed*CRT; (CRT−) BSA or *Eh*CRT-C was added to 1 : 10 dilution of NHS (as source of C1q), incubated 30 min at 37°C, and then added to 10^8 cell/mL of EA; the mixtures were incubated for 60 min at 37° C. After centrifugation, the OD (550 nm) of the supernatants was measured. The percentage of lyses was calculated using as reference the 100% lyses of erythrocytes in water. Values are the mean of three independent experiments ± SD. Differences between groups ∗ were compared through ANOVA test detecting statistical significance ($P = 0.05$).

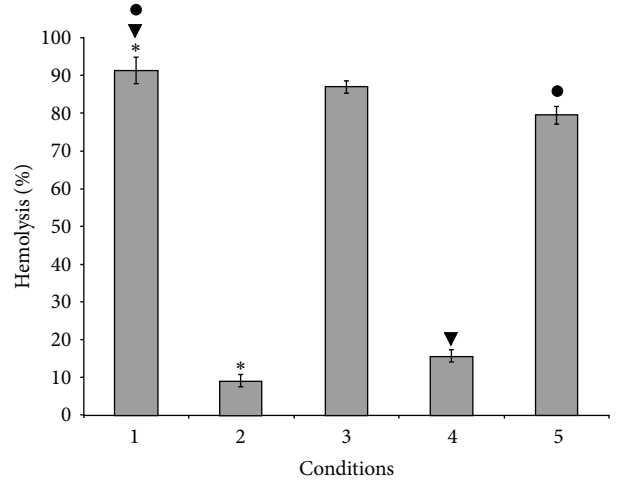

Figure 3: *Eh*CRT-human C1q on the activation of classical complement pathway: hemolysis assay. 1: corresponding to NHS (positive control); 2: human C1q-depleted serum (NHSC1q$^-$); 3: (NHSC1q$^-$) + C1q; 4: (NHSC1q$^-$) + C1q + *Eh*CRT; 5: (NHSC1q$^-$) + C1q + *Eh*CRT + IgG anti-*Eh*CRT. Assays were performed in triplicate; values are the mean of three different experiments ± SD. Differences between groups ∗, ●, and ▼ were compared through ANOVA test. Statistical significance ($P = 0.012$).

by binding to C1q was tested in a simple assay of inhibition of the haemolysis of SRBCs previously sensitized with antibody (EAs). Human serum was used as the source of C1q. The optimal dilution of the human serum was determined previously by a complement titration curve (data not shown); the optimal dilution of serum was 1 : 10. Figure 2 shows the values of inhibition of the activation of the classical complement pathway assays, in the presence of different concentrations of n*Eh*CRT or n*Ed*CRT. Both proteins inhibited the lysis of EAs in a dose-dependent manner as shown by the decrease in haemolytic activity (34–22% of baseline). By contrast, in the control assay (without CRT−) or in case we use the recombinant protein *Eh*CRT-C, there was no significant decrease in haemolytic activity (95–86% of baseline) due to the absence of C1q binding site.

To confirm that this activity is the result of the interaction of human C1q with *Eh*CRT or *Ed*CRT, we used C1q-depleted human serum; when this serum was added to human C1q in the presence of *Eh*CRT, haemolysis was inhibited. Moreover, when *Eh*CRT was pretreated with anti-CRT antibodies, *Eh*CRT could not bind to C1q, and the activation of the classical complement pathway was restored (Figure 3).

3.3. Amoebicidal Activity of Normal Human Serum. To test that human serum is indeed harmful to trophozoites through the action of serum complement, we previously titre the NHS; 40% of NHS was the optimal concentration to obtain reproducible results; proper time for interaction with trophozoites was 60 min. In these conditions, axenic *E. histolytica*

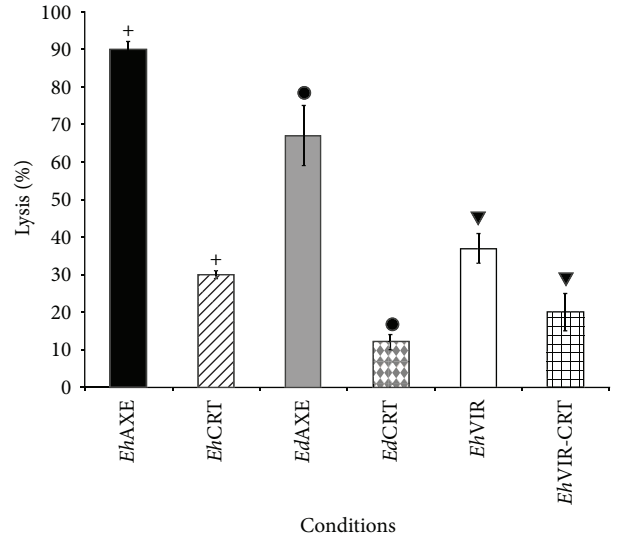

Figure 4: Amoebicidal activity of human serum. Trophozoites of *E. histolytica* and *E. dispar* were harvested by ice bath and then centrifuged at 500 g for 10 min, washed, counted, adjusted to a cell density of 2×10^5, and incubated with TYIS-33 medium added with 40% NHS at different times; viability was assessed by trypan blue exclusion technique. To estimate the inhibition of lyses due to interaction of *Eh*CRT-C1q, 10 μg of r*Eh*CRT was added to NHS incubating during 10 min, and the mixture was then added to trophozoites suspension. The percent of lyses was defined as the decrease of trophozoites viability in the presence of NHS compared with the heat-inactivated human serum control. Differences between groups +, ●, and ▼ were compared through Student's t-test detecting statistical significance ($P < 0.05$).

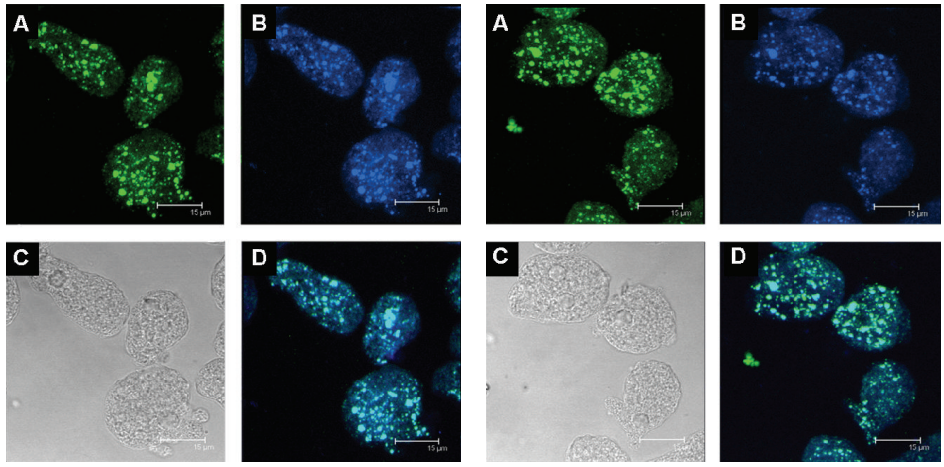

(a) (b)

Figure 5: Confocal microscopy assay: colocation of *Eh*CRT or *Ed*CRT and human C1q. Panels (a) and (b) represent different patterns of immunodetection when using *E. histolytica* or *E. dispar* trophozoites, respectively; A: rabbit anti-*Eh*CRT and Alexa Fluor 350-conjugated secondary antibody; B: trophozoites reacted with mouse anti-human C1q and with anti-mouse Alexa Fluor 488; C: representing the differential interference contrast (DIC); D: colocation of *Eh*CRT with the C1q human protein (Channel Mergin). The micrographs showed the maximal projection of the z-series. Scale bar represents 15 μm.

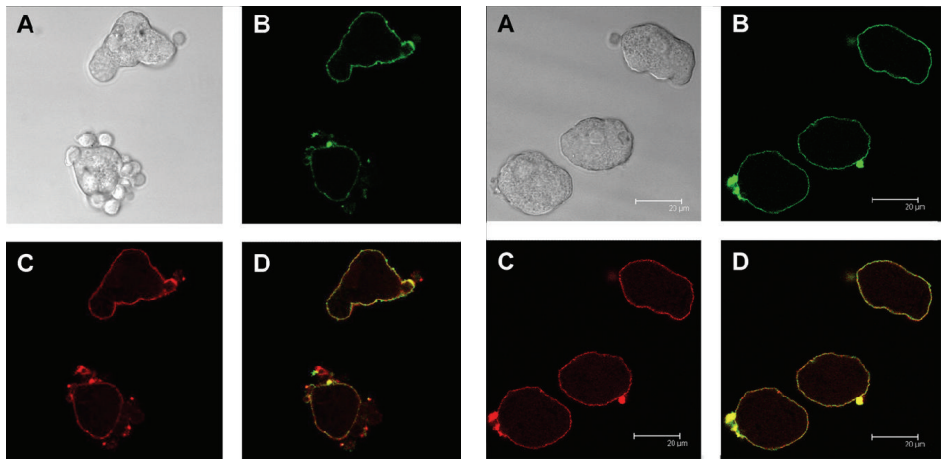

(a) (b)

Figure 6: Colocalization of *Eh*CRT or *Ed*CRT and human C1q after interaction with PMBC. C1q and *Eh*CRT or *Ed*CRT colocalization by confocal microscopy of (a) *E. histolytica;* (b) *E. dispar* trophozoites. Trophozoites were grown under axenic conditions and incubated during 30 min with PMBC; thereafter, C1q was added and incubated for 30 min. Then, the mixture was added with specific primary antibodies, anti-rabbit *Eh*CRT IgG and mouse anti-human C1q IgG, respectively. The reaction was revealed with Alexa Fluor 555 goat anti-rabbit IgG and Alexa Fluor 488 goat anti-mouse IgG. The micrographs show the maximal projection of the z-series. Scale bar represents 20 μm. A: phase contrast microscopy; B: *Eh*CRT (red); C: C1q (green); D: merge.

HM1:IMSS (nonvirulent) and axenic *E. dispar* SAW760 strain are both susceptible to lysis by complement; however, *E. dispar* SAW760 is more susceptible than the virulent strain of *E. histolytica;* this strain showed a clear resistance to lyses (37%) ($P < 0.005$). The resistance of trophozoites to the lyses mediated by the r*Eh*CRT-C1q binding is shown in Figure 4. Moreover, there is a clear reduction in the values of lyses of trophozoites in the presence of r*Eh*CRT preincubated with NHS (40%). Differences with respect to controls (NHS without r*Eh*CRT) were statistically significant ($P < 0.004$).

3.4. Human C1q and EhCRT/EdCRT Colocalization. To evaluate the interaction of *Eh*CRT/*Ed*CRT in trophozoites with human C1q, a colocalization assay was performed directly on trophozoites of both *E. histolytica* and *E. dispar* species by confocal microscopy. Both proteins clearly colocalized in previously permeabilized trophozoites; the fluorescent signal was detected in the cytoplasmic vesicles but was more concentrated near the cytoplasmic membrane (Figure 5); apparently, there are no differences in distribution of fluorescence in trophozoites between the two species. However, in

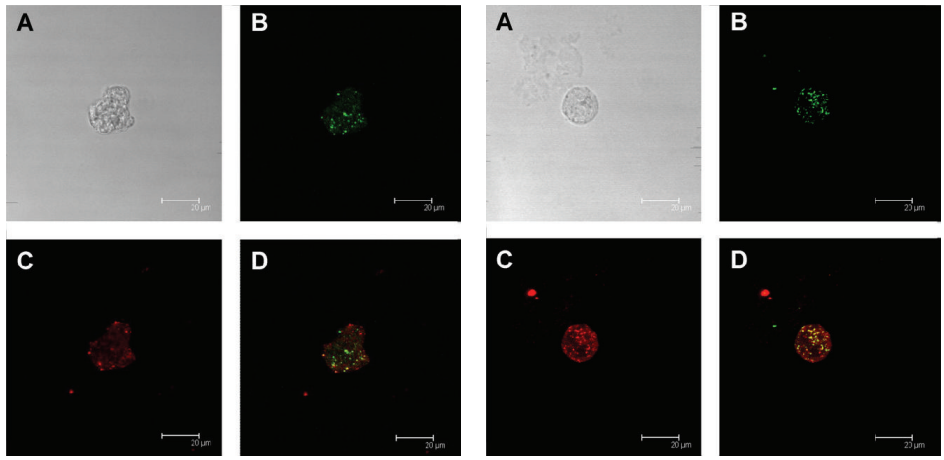

(a) (b)

Figure 7: Colocalization of *Eh*CRT or *Ed*CRT and human C1q after interaction with NHS: human C1q and *Eh*CRT or *Ed*CRT colocalization estimated by confocal microscopy of (a) *E. histolytica*; (b) *E. dispar* trophozoites. Trophozoites were grown under axenic conditions and were allowed to adhere to sterile glass cover slips. Trophozoites were incubated with normal human serum (NHS) (source of C1q) and then fixed with 3.5% paraformaldehyde/PBS; thereafter, trophozoites were incubated with specific primary antibodies, rabbit anti-*Eh*CRT IgG and mouse anti-human C1q IgG, respectively. The reaction was revealed with Alexa Fluor 555 goat anti-rabbit IgG and Alexa Fluor 488 goat anti-mouse IgG. The micrographs show the maximal projection of the z-series. Scale bar represents 20 μm. A: phase contrast microscopy; B: *Eh*CRT (red); C: C1q (green); D: merge.

nonpermeabilized trophozoites activated with peripheral mononuclear blood cells, the immunolocalization of CRT/C1q was detected on the surface membrane of trophozoites (Figure 6). Furthermore, when the trophozoites were incubated with NHS, the colocalization of both proteins was detected mainly in the cytoplasmic vesicles (Figure 7); this could be due to the destruction of trophozoites membranes induced by NHS.

3.5. Immunochemical Detection of EhCRT and C1q in Amoebic Liver Abscess Lesions. Representative sections of hepatic tissue obtained at 30 min and 3 h after the intraportal inoculation of *E. histolytica* virulent trophozoites or *E. dispar* are shown in Figures 8(a) and 8(b), respectively. The immunodetection of CRT and C1q in the trophozoites established in the hepatic tissue is evident and displays a similar distribution on trophozoites as observed in the confocal microscopy assays (Figure 5). The immunohistochemical signals, both anti-*Eh*CRT and anti-C1q, were displayed in different size cytoplasmic vesicles. In some trophozoites, signals are apparently located on the cell surface membrane in both *Entamoebas*. It is clear that trophozoites apparently do not secrete or export the CRT protein into the hepatic tissue. The negative control and secondary antibody did not show background reactivity. These assays can be found in the Supplementary Material available online at http://dx.doi.org/10.1155/2014/127453.

3.6. Relative mRNA Quantification of EdCRT and EhCRT by qRT-PCR. The relative quantification (RQ) of *Eh*CRT or *Ed*CRT mRNA expression is shown in Figure 9. The values correspond to the relative expression of cDNA into ALA specimens assayed by qPCR. The *Ed*CRT was expressed for a short period of time after inoculation (15 min RQ = 1.5) but it started to decline quickly for the remaining time resulting in lower levels than baseline. In contrast, *Eh*CRT increases at 30 min (RQ = 2) reaching a peak after 60 min (RQ = 5) between 3 h (RQ = 4.5); however, it decreased to values close to baseline thereafter. The level of expression of *Eh*CRT in comparison with *Ed*CRT was statistically significant ($P = 0.04$).

4. Discussion

E. histolytica and *E. dispar* are parasites whose natural host is the human being; their target organ is the large bowel. Therefore, they are in intimate contact with the local immune system. In human populations, the infection can be persistent or recurrent, self-limited, and usually asymptomatic (90% of cases), suggesting a balanced host-parasite interaction and some kind of immune response evasion mechanism. *E. histolytica* and *E. dispar* activate both classical and alternative pathways of serum complement [28, 29]. This activity is part of the immunological mechanisms induced by these protozoa during the early phases of host-parasite relationship. These mechanisms are among the main resistance mechanisms of hosts against parasite infection, but parasites have evolved alternative methods to evade immune attack and survive in the tissues of their host. One of these alternatives is the expression of an interesting and complex protein, calreticulin. This ubiquitous endoplasmic reticulum-associated protein has a large spectrum of functions, including the capacity to bind C1q, which is the first component of the classical serum complement pathway. CRT-C1q binding inhibits the activation of the complement cascade in different hosts; this mechanism has been considered an evasion mechanism of

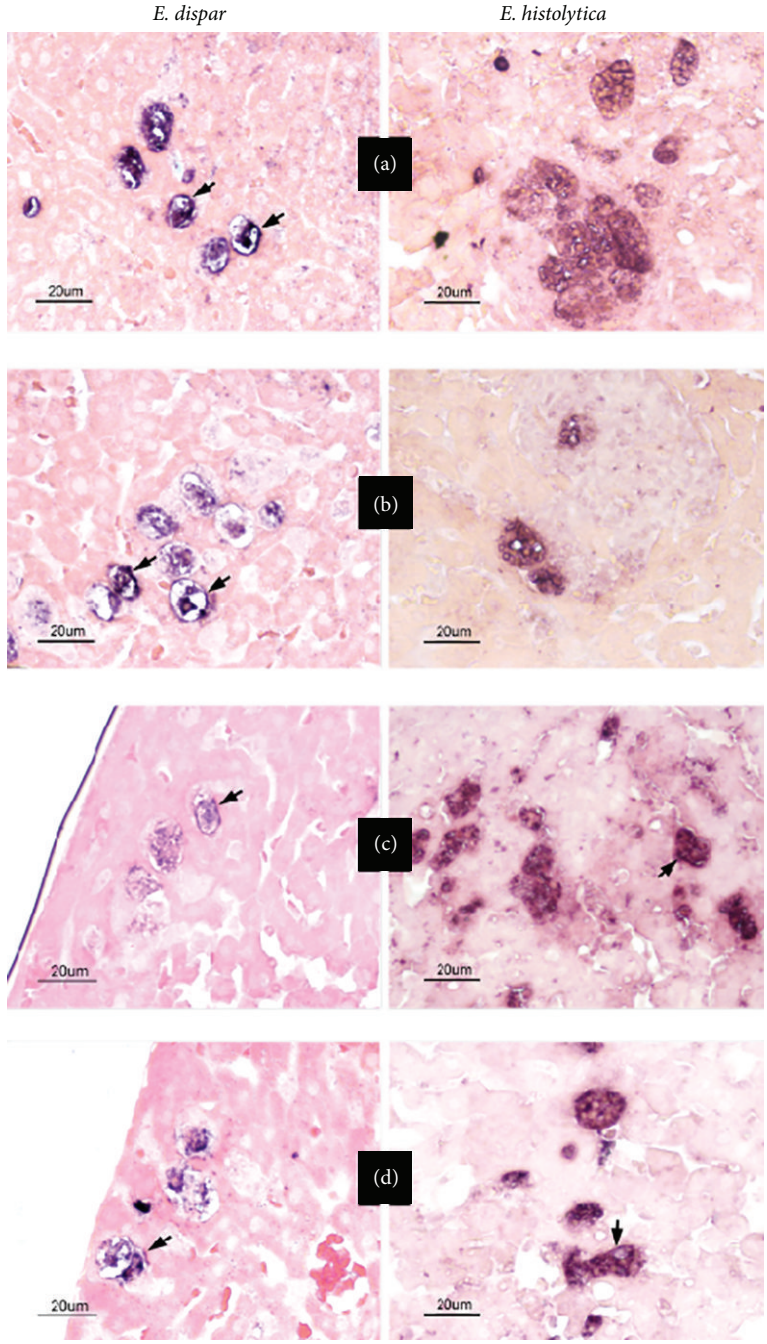

Figure 8: Immunohistochemical staining of *Eh*CRT or *Ed*CRT and C1q *in situ*. Representative images of immunohistochemical detection of CRT and C1q in amoebic liver abscess sections of livers from hamsters inoculated with *E. histolytica* HM1:IMSS virulent trophozoites and *E. dispar* SAW760 trophozoites and sacrificed at different times after inoculation for 30 min (a, b) and 3 h (c, d) (representative times). (a and c) Tissue section stained with mouse IgG against *Eh*CRT and (b and d) section stained with mouse IgG against C1q. Scale bar represents 20 μm. The control assays of negative and secondary antibody were unstained; they are included as Supplementary Material.

the immune response developed by a number of parasites [9, 10].

This evasion mechanism has been described in schistosomiasis, oncocercosis, trypanosomiasis [3, 5, 14], and now in amoebiasis. The interaction of CRT from *T. cruzi* (*Tc*CRT) with human C1q is one of the most studied systems. In this protozoan, CRT not only allows the evasion of the immune response but also modulates it. Furthermore, the presence of CRT on the surface of the parasite increases its infectivity by binding to C1q promoting the early phagocytosis of the parasite [30, 31].

In contrast to *T. cruzi*, in our *in vitro* assays, *E. histolytica* and *E. dispar* trophozoites do not express CRT on the external surface and do not export CRT into tissues in the *in vivo*

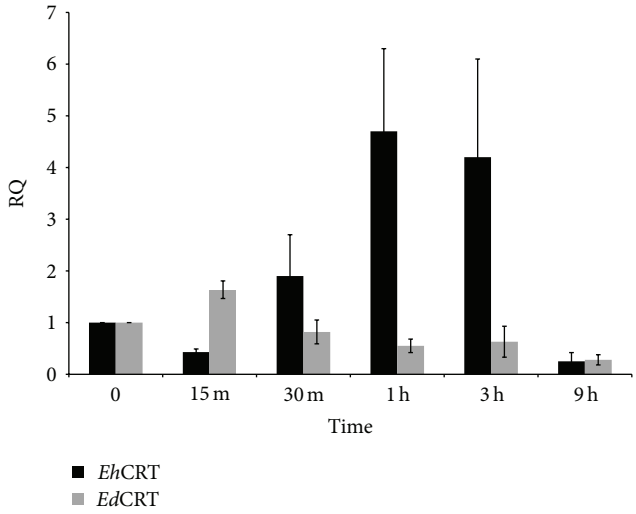

Figure 9: Relative quantification (RQ) of expression of mRNA for *Eh*CRT and *Ed*CRT. Reverse transcription real-time PCR was used to independently measure mRNA expression of *Ed*CRT and *Eh*CRT in trophozoites present in tissue sections of liver in hamsters after different times of postinoculation. The values represent the mean of three independent experiments. Differences between *E. histolytica* and *E. dispar* were compared through Student's *t*-test detecting statistical significance $^{*}(P = 0.005)$.

model of amoebic liver abscess in hamsters [5]. Recently, the presence of CRT was reported in cytoplasmic membranes of trophozoites previously activated with Jurkat cells [17] or concanavalin A-activated trophozoites [32]. In the present study, we demonstrate that trophozoites activated by human PBMC also show the presence of CRT in the surface membrane (Figure 6). In the *in vivo* experiment of amoebic liver abscess in hamsters, the localization of CRT was also observed on the surface of trophozoites (Figure 8).

*Eh*CRT is highly immunogenic in humans, mice, and rabbits, suggesting that, in natural or experimental infection with *E. histolytica*, *Eh*CRT is in some way exposed to the host immunocompetent cells. The mechanism of this interaction may be time dependent and may occur via surface expression and/or by exposure to apoptotic or dead trophozoites as was previously reported [16].

In human trypanosomiasis, the role of *Tc*CRT as an immune evasion mechanism is easily understood because CRT is located on the surface of the trypomastigote in blood during the acute phase of infection and accessible to C1q. The role of *Entamoeba* CRT in pathogenicity is less clear. In intestinal amoebiasis, trophozoites are not totally exposed to complement system; apparently, the complement system only crosses to the mucosa membrane in conditions of disease as cancer, inflammatory bowel diseases, or autoimmune inflammatory intestinal diseases [33]. In amoebiasis infection, only in the case of invasive intestinal amoebiasis trophozoites are exposed to serum complement system. In the case of ALA, the trophozoites are indeed exposed to complement system. In this sense, trophozoites that express CRT on the surface membrane can bind C1q, induce the inhibition of the classical pathway of complement, and be protected from the lyses. This can be the case of our *in vivo* experimental model. During phagocytosis, C1q facilitates the binding to apoptotic epithelial cells by *E. histolytica* trophozoites [34]. Moreover, *Eh*CRT has been detected in the uropods induced in trophozoites by concanavalin A [32, 35], which may function as another mechanism by which *Eh*CRT/*Ed*CRT is exposed to the host immune system. However, capping formation in animal models and in human amoebic invasive lesions has not been observed. Draws attention the over expression of *Eh*crt gene in *E. histolytica* during first hours of host-parasite interaction in contrast with the *E dispar* specie, which do not over express this gene. This may suggest that over expression of crt gen could be a regulatory mechanisms that may allow the adaptation and survival of the parasite in the host tissues, as has been described in other parasites [31]. These are more suitable for the hostile environment in the liver. Besides, we cannot discard the possible selective pressure of serum complement over the infective trophozoites allowing the survival of complement resistant trophozoites in infected tissues. Finally, these trophozoites will be responsible for amoebic abscess development.

Conflict of Interests

The authors declare that there is no conflict of interests regarding the publication of this paper.

Acknowledgments

The authors are very grateful to Dr. Marco Antonio Santillán for his generous gift of SRBCs and to Mario Nequiz-Avendaño for the *Entamoeba histolytica* HM1:IMSS axenic culture. The authors are also highly grateful with Dr. Adolfo Martinez-Palomo and Technician Lizbeth Salazar Villatoro for providing them with the axenic culture of *E. dispar* SAW760 strain. The authors are indebted to Marco Gudiño and Mrs. Ma Lourdes Alonso De la Rosa for art design and to Mrs. Ma Elena Ortiz for secretarial assistance.

References

[1] M. Michalak, E. F. Corbett, N. Mesaeli, K. Nakamura, and M. Opas, "Calreticulin: one protein, one gene, many functions," *Biochemical Journal*, vol. 344, no. 2, pp. 281–292, 1999.

[2] L. I. Gold, P. Eggleton, M. T. Sweetwyne et al., "Calreticulin: non-endoplasmic reticulum functions in physiology and disease," *The FASEB Journal*, vol. 24, no. 3, pp. 665–683, 2010.

[3] K. Marcelain, A. Colombo, M. C. Molina et al., "Development of an immunoenzymatic assay for the detection of human antibodies against *Trypanosoma cruzi* calreticulin, an immunodominant antigen," *Acta Tropica*, vol. 75, no. 3, pp. 291–300, 2000.

[4] M. Joshi, G. P. Pogue, R. C. Duncan et al., "Isolation and characterization of *Leishmania donovani* calreticulin gene and its conservation of the RNA binding activity," *Molecular and Biochemical Parasitology*, vol. 81, no. 1, pp. 53–64, 1996.

[5] E. González, M. C. García de Leon, I. Meza et al., "*Tripanozoma cruzi* calreticulin: an endoplasmic reticulum protein expressed

by trophozoites into experimentally induced amoebic liver abscesses," *Parasitology Research*, vol. 108, no. 2, pp. 439–449, 2011.

[6] L. A. Rokeach, P. A. Zimmerman, and T. R. Unnasch, "Epitopes of the *Onchocerca* volvulus RAL1 antigen, a member of the calreticulin family of proteins, recognized by sera from patients with onchocerciasis," *Infection and Immunity*, vol. 62, no. 9, pp. 3696–3704, 1994.

[7] N. El Gengehi, R. El Ridi, N. Abdel Tawab, M. El Demellawy, and B. L. Mangold, "A *Schistosoma mansoni* 62-kDa band is identified as an irradiated vaccine T-cell antigen and characterized as calreticulin," *The Journal of Parasitology*, vol. 86, no. 5, pp. 993–1000, 2000.

[8] S. Suchitra and P. Joshi, "Characterization of *Haemonchus contortus* calreticulin suggests its role in feeding and immune evasion by the parasite," *Biochimica et Biophysica Acta*, vol. 1722, no. 3, pp. 293–303, 2005.

[9] H. L. Nakhasi, G. P. Pogue, R. C. Duncan et al., "Implications of Calreticulin function in parasite biology," *Parasitology Today*, vol. 14, no. 4, pp. 157–160, 1998.

[10] V. Ferreira, M. C. Molina, C. Valck et al., "Role of calreticulin from parasites in its interaction with vertebrate hosts," *Molecular Immunology*, vol. 40, no. 17, pp. 1279–1291, 2004.

[11] S. Naresha, A. Suryawanshi, M. Agarwal, B. P. Singh, and P. Joshi, "Mapping the complement C1q binding site in Haemonchus contortus calreticulin," *Molecular and Biochemical Parasitology*, vol. 166, no. 1, pp. 42–46, 2009.

[12] D. C. Jaworski, F. A. Simmen, W. Lamoreaux, L. B. Coons, M. T. Muller, and G. R. Needham, "A secreted calreticulin protein in ixodid tick (*Ambylomma americanum*) saliva," *Journal of Insect Physiology*, vol. 41, no. 4, pp. 369–375, 1995.

[13] J. Khalife, J. L. Liu, R. Pierce, E. Porchet, C. Godin, and A. Capron, "Characterization and localization of *Schistosoma mansoni* calreticulin Sm58," *Parasitology*, vol. 108, no. 5, pp. 527–532, 1994.

[14] V. Ferreira, C. Valck, G. Sánchez et al., "The classical activation pathway of human complement system is specifically inhibited by calreticulin from *Tripanosoma cruzi*," *Journal of Immunology*, vol. 172, no. 5, pp. 3042–3050, 2004.

[15] A. Oladiran and M. Belosevic, "*Trypanosoma carassii* calreticulin binds host complement component C1q and inhibits classical complement pathway-mediated lysis," *Developmental and Comparative Immunology*, vol. 34, no. 4, pp. 396–405, 2010.

[16] E. Gonzalez, G. Rico, G. Mendoza et al., "Calreticulin–like molecule in trophozoites of *Entamoeba histolytica* HM1:IMSS," *American Journal of Tropical Medicine and Hygiene*, vol. 67, no. 6, pp. 636–639, 2002.

[17] A. . Vaithilingam, J. E. Teixeira, P. J. Miller, B. T. Heron, and C. D. Huston, "*Entamoeba histolytica* cell surface calreticulin binds human C1q and functions in amebic phagocytosis of host cells," *Infection and Immunity*, vol. 80, no. 6, pp. 2008–2018, 2012.

[18] C. A. Ogden, A. deCathelineau, P. R. Hoffmann et al., "C1q and mannose binding lectin engagement of cell surface calreticulin and CD91 initiates macropinocytosis and uptake of apoptotic cells," *Journal of Experimental Medicine*, vol. 194, no. 6, pp. 781–795, 2001.

[19] T. Panaretakis, N. Joza, N. Modjtahedi et al., "The co-translocation of ERp57 and calreticulin determines the immunogenicity of cell death," *Cell Death and Differentiation*, vol. 15, no. 9, pp. 1499–1509, 2008.

[20] S. L. Reed, J. G. Curd, and I. Gigli, "Activation of complement by pathogenic and nonpathogenic *Entamoeba histolytica*," *Journal of Immunology*, vol. 136, no. 6, pp. 2265–2270, 1986.

[21] L. L. Braga, H. Ninomiya, J. J. McCoy et al., "Inhibition of the complement membrane attack complex by the galactose-specific adhesin of *Entamoeba histolytica*," *Journal of Clinical Investigation*, vol. 90, no. 3, pp. 1131–1137, 1992.

[22] E. González, N. Villegas-Sepúlveda, R. Bonilla et al., "Cloning and expression of *Entamoeba histolytica* calreticulin gene," in *Proceedings of the 5th International Congress on Tropical Medicine and International Health, MEDIMOND S.r.l. International Proceedings*, pp. 43–49, 2007.

[23] C. Ximénez, O. Leyva, P. Morán et al., "*Entamoeba histolytica*: antibody response to recent and past invasive events," *Annals of Tropical Medicine and Parasitology*, vol. 87, no. 1, pp. 31–39, 1993.

[24] L. S. Diamond, D. R. Harlow, and C. C. Cunnick, "A new medium for the axenic cultivation of *Entamoeba histolytica* and other *Entamoeba*," *Transactions of the Royal Society of Tropical Medicine and Hygiene*, vol. 72, no. 4, pp. 431–432, 1978.

[25] J. E. . Colingan, A. M. Kruisbeek, D. H. Margulies, E. M. Shevach, and W. Strober, "Trypan blue exclusion test of cell viability," in *Current Protocols in Immunology*, John Wiley and Sons, 1997.

[26] V. Tsutsumi, R. Mena-Lopez, F. Anaya-Velazquez, and A. Martinez-Palomo, "Cellular bases of experimental amebic liver abscess formation," *American Journal of Pathology*, vol. 117, no. 1, pp. 81–91, 1984.

[27] K. J. Livak and T. D. Schmittgen, "Analysis of relative gene expression data using real-time quantitative PCR and the 2-ΔΔCT method," *Methods*, vol. 25, no. 4, pp. 402–408, 2001.

[28] J. Calderon and R. D. Schreiber, "Activation of the alternative and classical complement pathways by *Entamoeba histolytica*," *Infection and Immunity*, vol. 50, no. 2, pp. 560–565, 1985.

[29] B. Walderich, A. Weber, and J. Knobloch, "Sensitivity of *Entamoeba histolytica* and *E. dispar* patient isolates to human complement," *Parasite Immunology*, vol. 19, no. 6, pp. 265–271, 1997.

[30] G. Ramírez, C. Valck, V. P. Ferreira, N. López, and A. Ferreira, "Extracellular Trypanosoma cruzi calreticulin in the host-parasite interplay," *Trends in Parasitology*, vol. 27, no. 3, pp. 115–122, 2011.

[31] G. Ramírez, C. Valck, M. C. Molina et al., "*Entamoeba histolytica* calreticulin: a novel virulence factor that binds complement C1 on the parasite surface and promotes infectivity," *Immunobiology*, vol. 216, no. 1-2, pp. 265–273, 2011.

[32] F. Girard-Misguich, M. Sachse, J. Santi-Rocca, and N. Guillén, "The endoplasmic reticulum chaperone calreticulin is recruited to the uropod during capping of surface receptors in *Entamoeba histolytica*," *Molecular and Biochemical Parasitology*, vol. 157, no. 2, pp. 236–240, 2008.

[33] D. J. B. Marks, C. R. Seymour, G. W. Sewell et al., "Inflammatory bowel diseases in patients with adaptive and complement immunodeficiency disorders," *Inflammatory Bowel Diseases*, vol. 16, no. 11, pp. 1984–1992, 2010.

[34] J. E. Teixeira, B. T. Heron, and C. D. Huston, "C1q- and collectin-dependent phagocytosis of apoptotic host cells by the intestinal protozoan *Entamoeba histolytica*," *Journal of Infectious Diseases*, vol. 198, no. 7, pp. 1062–1070, 2008.

[35] J. Marquay Markiewicz, S. Syan, C.-C. Hon, C. Weber, D. Faust, and N. Guillen, "A proteomic and cellular analysis of uropods in the pathogen *Entamoeba histolytica*," *PLoS Neglected Tropical Diseases*, vol. 5, no. 4, p. e1002, 2011.

Hindawi Publishing Corporation
BioMed Research International
Volume 2014, Article ID 324230, 17 pages
http://dx.doi.org/10.1155/2014/324230

Review Article

Peroxynitrite and Peroxiredoxin in the Pathogenesis of Experimental Amebic Liver Abscess

Judith Pacheco-Yepez,[1] Rosa Adriana Jarillo-Luna,[2] Manuel Gutierrez-Meza,[1] Edgar Abarca-Rojano,[1] Bruce Allan Larsen,[3] and Rafael Campos-Rodriguez[3]

[1] *Sección de Estudios de Posgrado e Investigación, Escuela Superior de Medicina, IPN, Plan de San Luis y Díaz Mirón s/n, 11340 México, DF, Mexico*
[2] *Departamento de Morfología, Escuela Superior de Medicina, IPN, Plan de San Luis y Díaz Mirón s/n, 11340 México, DF, Mexico*
[3] *Departamento de Bioquimica, Escuela Superior de Medicina, IPN, Plan de San Luis y Díaz Mirón s/n, 11340 México, DF, Mexico*

Correspondence should be addressed to Rafael Campos-Rodriguez; citlicampos@gmail.com

Received 5 November 2013; Accepted 12 March 2014; Published 15 April 2014

Academic Editor: Marlene Benchimol

The molecular mechanisms by which *Entamoeba histolytica* causes amebic liver abscess (ALA) are still not fully understood. Amebic mechanisms of adherence and cytotoxic activity are pivotal for amebic survival but apparently do not directly cause liver abscess. Abundant evidence indicates that chronic inflammation (resulting from an inadequate immune response) is probably the main cause of ALA. Reports referring to inflammatory mechanisms of liver damage mention a repertoire of toxic molecules by the immune response (especially nitric oxide and reactive oxygen intermediates) and cytotoxic substances released by neutrophils and macrophages after being lysed by amoebas (e.g., defensins, complement, and proteases). Nevertheless, recent evidence downplays these mechanisms in abscess formation and emphasizes the importance of peroxynitrite ($ONOO^-$). It seems that the defense mechanism of amoebas against $ONOO^-$, namely, the amebic thioredoxin system (including peroxiredoxin), is superior to that of mammals. The aim of the present text is to define the importance of $ONOO^-$ as the main agent of liver abscess formation during amebic invasion, and to explain the superior capacity of amoebas to defend themselves against this toxic agent through the peroxiredoxin and thioredoxin system.

1. Introduction

Amoebiasis is a result of infection with the enteropathogen protozoan *Entamoeba histolytica* (*E. histolytica*). Once the amoeba has established itself in the host, its dissemination to the liver and the formation of abscesses in this organ lead to high morbidity and mortality.

Patients with amebic liver abscess (ALA) arrive to the hospital in the chronic phase of this pathogenesis, when the abscess has already formed. Therefore, observations in patients of the first phase of ALA, involving the inflammatory reaction of the immune response, have been sporadic (when patients arrive for other reasons and inflammation is found). In order to understand the first phase of ALA in humans, animal models have been employed. These models have proven useful even though there are important differences between hamsters and humans in the chronic phase of ALA [1, 2].

The molecular mechanisms by which *E. histolytica* causes ALA are still not fully understood. Based on evidence from the hamster model of amoebiasis, it seems that an inadequate immune response in individuals susceptible to amoebiasis fails to impede an amebic invasion, thus leading to uncontrolled inflammation. Chronic inflammation is accompanied by the production of several toxic molecules, including nitric oxide (NO) and reactive oxygen intermediates (ROIs), such as the superoxide anion (O_2^-). Recently it has become clear that these molecules are substrates for synthesis of a highly oxidizing agent known as peroxynitrite ($ONOO^-$). Furthermore, reports have pointed out that *E. histolytica* has very effective defense mechanisms against the formation of $ONOO^-$, as well as for its interception and inactivation.

The principal mechanism for $ONOO^-$ interception seems to be the thioredoxin system. The aim of present text is to define the importance of $ONOO^-$ as the main agent of liver abscess formation during amebic invasion and to explain the apparently superior capacity of the amoeba to defend itself against this toxic agent through the peroxiredoxin and thioredoxin system.

2. Adhesion and Cytotoxic Activity of Amoebas during Amoebiasis and ALA

There is still sharp controversy among scientists today regarding the molecular mechanisms of amoebiasis and amebic liver invasion caused by the pathogen *E. histolytica*. Some researchers pose that the direct damage to liver tissue by amoebas (through mechanisms of adherence and toxicity) causes the formation of liver abscess during amoebiasis. Other researchers assert that the importance of amebic mechanisms in the initial stage of amoebiasis is to allow the pathogens to survive and multiply in microenvironments, thus provoking the chronic inflammatory response that provides the principal mechanisms of damage to liver tissue, eventually resulting in ALA. To a great extent, the controversy hinges on an ambiguous use of language on both sides of the question.

Adherence of amoebas to the colonic epithelium and other host cells is unquestionably of fundamental importance in amoebiasis during the initial stages of the pathogenesis, which include the initial infection and extraintestinal invasion. That is, adherence is essential for the amoeba to invade the host and establishes itself in microenvironments in which it can survive. The virulence factor of adherence is to a great extent mediated by the N-acetyl-D-galactosamine inhibitable (Gal/GalNAc) lectin [3, 4], the 220 kDa lectin [5], and other adhesins such as the 112 kDa adhesin [6]. There are reports of reduced amebic adherence to human erythrocytes, neutrophils, colonic mucins, and epithelia when amebic lectins are inhibited [5–7]. Recently it was shown that EhCPADH, a complex formed by a cysteine proteinase and an adhesin, mediates adherence, phagocytosis, and cytolysis. Immunization with a recombinant polypeptide, EhADH243, induces protection in hamsters against development of ALA [8]. It has also been demonstrated that the recombinant enzyme rEhCP112 digested gelatin, collagen type I, fibronectin, hemoglobin, and Madin-Darby canine kidney (MDCK) cell monolayers; the EhCP112 enzyme is secreted by the trophozoites [9].

The Gal/GalNAc lectin is a virulence factor required for trophozoite adherence to target cells, as shown by inhibition of this lectin with galactose [10, 11]; cell killing occurs in the typical Gal/GalNAc manner. It has been shown that peroxiredoxin (Prx) interacts with Gal/GalNAc lectin and that the lectin-peroxiredoxin complex is located at the amoeba-host cell contact sites. Therefore, the recruitment of Prx probably protects the trophozoites against the ROS generated by host cells (phagocytic and epithelial), which would facilitate the invasion [12, 13].

Molecular mechanisms of pathogenicity that allow *E. histolytica* trophozoites to survive and proliferate within a wide variety of host environments are related not only to adherence but also to cytotoxic activity. Trophozoites can damage host cells through direct contact or close proximity, as well as through phagocytic activity towards dead and dying host cells in a receptor-mediated fashion [14]. Of the molecules secreted by amoebas, cysteine proteases are particularly important [15–20]. They are responsible for a cytolytic effect on host cells [7], the modulation of the cell-mediated immune response, and the proteolysis of the host extracellular matrix [16, 21–25]. Previous works show that when mutated, cysteine proteinase 5 (CP5) has a reduced activity and the trophozoite has a reduced ability to generate ALA [26].

Extensive tissue damage has been attributed to the cysteine proteinases of *E. histolytica* because they are (i) secreted in large quantities and can cleave extracellular matrix proteins, thus facilitating amebic invasion; (ii) secreted in higher quantities by virulent than nonvirulent trophozoites; and (iii) found to participate in the inflammation of the gut and ALA [15–20, 27]. However, cysteine proteases are dispensable for phagocytosis and cytopathogenicity [28, 29]. Their main physiological role could be the digestion of host cells, as they are required for rosette formation, hemolysis, and digestion of erythrocytes.

Another molecule that could participate in the damage of host cell is the cyclooxygenase- (COX-) like enzyme in *E. histolytica*, responsible for the biosynthesis of prostaglandin E_2 (PGE_2). The production of PGE_2 by the COX-like enzyme in amebic liver granuloma can downregulate effector and accessory cell functions of infiltrate immune cells [30].

Although the aforementioned processes are fundamental in the initial stages of amoebiasis, they seem to be quite secondary as mechanisms of necrosis leading to hepatic abscesses in the latter stages of this disorder. Adhesion is important for the survival of amoebas and the establishment of prolonged contact of amoebas and toxic molecules with host endothelial cells. However, neither adhesion nor these toxic molecules seem to be responsible for the host tissue damage that directly results in amebic colitis and ALA. These disorders occur during the latter stages of amoebiasis, when the majority of host cells in contact with amoebas appear not to be damaged [31–33]. It seems likely that damage to host cells at this time is carried out in function of the inflammatory process [31].

The proposal that host cell damage results mainly from a chronic inflammatory response is corroborated by a number of different studies. Some recent reports [34, 35] are revealing in this sense, as they analyze the pathogenesis of ALA in hamsters inoculated with engineered HGL-2 trophozoites defective in Gal/GalNAc function. The authors show that HGL-2 amoebas infect hamster liver despite lacking this important adhesion molecule, although the pattern of infection is different from that produced by wild-type *E. histolytica*. HGL-2 amoebas cause a large number of inflammatory foci with a disorganized structure, and these foci are located in the vicinity of blood vessels. Despite their reduced capacity for adhering to the host endothelium and penetrating liver

tissue [34], these defective trophozoites are able to provoke ALA [35].

In histopathological terms, the chronic phase of ALA in humans corresponds to lytic or liquefactive necrosis, whereas in rodent models there is granulomatous inflammation [1, 2, 36–38]. Hence, hepatic damage in hamsters is caused by apoptosis and necrosis rather than the lytic necrosis found in humans [39–41]. However, hamster models have provided important insights into the possible mechanisms of the inflammatory response to amebic invasion in the acute phase [1, 2].

In a hamster model and at thirty minutes following inoculation, *E. histolytica* amoebas were found in the portal vein (resulting in slightly dilated sinusoids), in the lumen of small branches of the portal vein, and in the central veins [2]. After one hour trophozoites were located in the sinusoids throughout the hepatic lobules [2]. At three hours after inoculation, polymorphonuclear leukocytes (PMNs) surrounded the amoebas with one or several layers of cells and thus impeded them from making direct contact with hepatocytes. Nonetheless, lysis continued. Under these conditions, the leukocytes that managed to make direct contact with amoebas were undamaged [2]. Afterwards, there was a continual increase in the quantity of PMNs and the lysis of leukocytes in liver sections during the development of ALA. The massive destruction of leukocytes favored greater necrosis and hemorrhaging of parenchymal tissue and the formation of ischemic areas. Whereas few amoebas were found in necrotic areas at this stage, there are many in the periphery of the lesion, where mononuclear cells (histiocytes with an epithelioid appearance) started to form a palisade that separated parenchymatous cells from the necrotic area.

Since studies with hamster models demonstrate that ALAs generally develop in the absence of direct contact with amoebas, it is necessary to explore the possible mechanisms that could account for their formation. The mechanisms of chronic inflammation seem to be a likely candidate [2, 42, 43]. Of course, it is the adhesion of amoebas and their capacity to evade the host immune defenses that provoke a continuous inflammatory response [31, 44–46].

3. Chronic Inflammation as the Possible Cause of ALA

3.1. Nitric Oxide and the Pathogenesis of ALA. Some research groups have long suspected that chronic inflammation is the cause of ALA. Until recently, the mechanisms of chronic inflammation considered as the cause of abscess formation were mainly the amebicidal effects of NO, ROIs, cytokines, and cysteine proteinases [45, 47–51].

In this sense, it has been emphasized that greater quantities of NO are found in the serum of hamsters with liver abscesses than in healthy animals [52, 53]. Some reports have shown that the amebicidal activity of activated macrophages is mainly associated with NO synthesis [54–56]. Nevertheless, the amoebas continue to survive and proliferate.

Some studies have reported that reactive oxygen species (ROS) and NO produced by activated neutrophils or macrophages lead to the lysing of *E. histolytica* [56–60]. *In vitro* studies used a high concentration of NO (1 mM) [48, 54, 61, 62], whereas *in vivo* the concentration of NO in inflamed tissues is approximately 1 μM [60, 63]. During the development of ALA, there is evidence of trophozoite resistance to high concentrations of NO *in vitro* [48] and *in vivo* [52, 53]. Despite the relatively high iNOS mRNA expression and NO production, *E. histolytica* continues to show an invasive capacity *in vivo*. Hence, the percentages of amoebas that remain viable represent a sufficient number to sustain an amebic invasion.

Two hypotheses can be formulated based on the apparent lack of effectiveness of NO as an amebicidal agent *in vivo*: (i) that NO is not really toxic enough to carry out an effective amebicidal function or (ii) that virulent amoebas have an adequate defense mechanism against NO activity. Regarding the latter conclusion, several studies indicate that the capacity of *E. histolytica* to resist the destructive action of NO and ROIs, whether *in vivo* or *in vitro*, probably owes itself to the expression by this *Entamoeba* species of high levels of antioxidant proteins, such as Prx, flavoprotein A, superoxide dismutase (SOD), and rubrerythrin [64–67].

3.2. The Possible Role of Peroxynitrite in Inflammation and ALA. It is now known that there are molecules of the inflammatory response much more detrimental than NO. In fact, NO is a precursor of one of these molecules. During the inflammatory process, NO and the O_2^- are produced simultaneously, and they react at diffusion-controlled rates to produce the $ONOO^-$ anion [63, 68]. The reaction is as follows:

$$NO + O_2^- \longrightarrow ONOO^- \quad (1)$$

Unlike NO and O_2^-, $ONOO^-$ is not a free radical, but it is a highly oxidizing agent. The coupling of NO with O_2^- to yield $ONOO^-$ in biological systems is currently accepted as the main biological source of $ONOO^-$, which is extremely reactive with biological molecules and highly toxic to cells.

There is no direct *in vivo* evidence of $ONOO^-$, probably due to its high reactivity [69, 70]. However, nitrate and nitrite, the products of spontaneous decomposition of this molecule, have been detected in the serum of hamsters with ALA [52, 53].

The two substrates of $ONOO^-$, NO and the O_2^-, seem to be abundantly produced in inflammatory sites during the host response to amebic invasion [31, 52, 53, 71]. For instance, O_2^- is produced by the reaction of NADPH oxidase (or xanthine oxidase) and dioxygen (O_2) (Figure 1) via electron leakage in the mitochondrial respiratory chain and at the endoplasmic reticulum [70]. The levels of O_2^- can undergo a 3- to 4-fold increase during the inflammatory response when the NADPH oxidase complex expressed in phagocytic cells and endothelial cells is activated and reacts in the oxygenated environment to generate O_2^- (Figure 1) [68, 72, 73].

To some extent, *in vitro* and *in vivo* reports are contradictory. On the one hand, *in vitro* studies report that macrophages isolated from ALA in gerbils are deficient in their capacity to produce NO as a result of the modulation

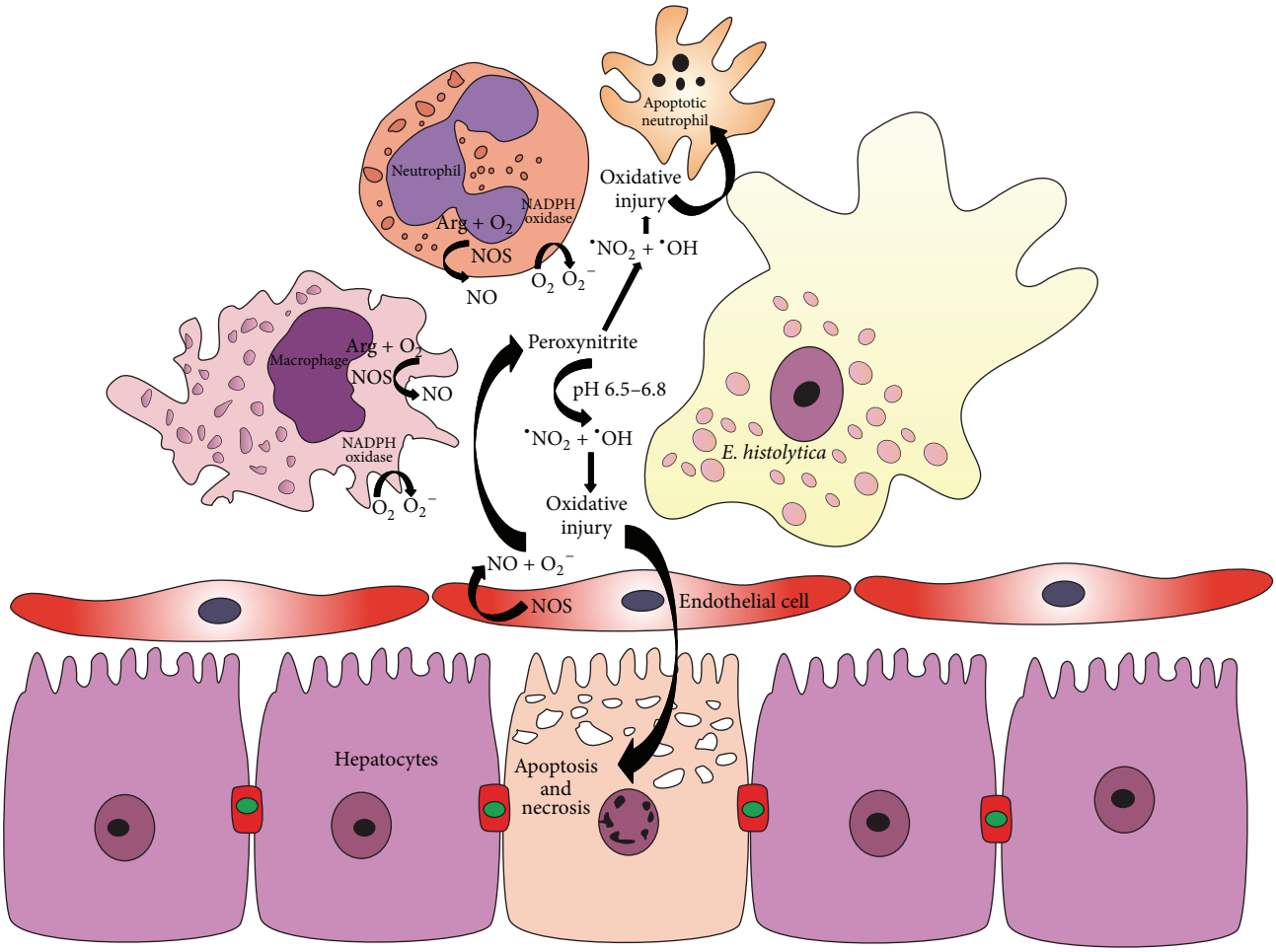

Figure 1: Hypothetical model of the generation of $ONOO^-$ in ALA. Under inflammatory conditions the two substrates of $ONOO^-$, nitric oxide (NO) and the superoxide anion (O_2^-), are produced simultaneously. This allows for the production of large quantities of $ONOO^-$, which is a highly oxidizing agent. Indeed, the products of spontaneous decomposition of $ONOO^-$, nitrate and nitrite, are found at higher than normal levels in inflamed tissue. The superoxide anion is produced by NADPH oxidase expressed in activated neutrophils, macrophages, and endothelial cells. NO is produced by NOS found in inflammatory cells or in the vascular endothelium. The protonated form of $ONOO^-$ is disintegrated to form free nitrogen dioxide ($^{\bullet}NO_2$) and the hydroxyl radical ($^{\bullet}OH$). Under conditions of hepatic hypoxia, low concentrations of L-arginine and oxygen enhance arginase activity that hydrolyzes L-arginine, thus competing with the substrate for NOS enzymes. This leads to the uncoupling of NOS, simultaneously producing O_2^- and NO, and thus resulting in additional $ONOO^-$ generation. $ONOO^-$ reacts directly with thiol groups of host cells. High levels of $ONOO^-$ lead to the development of ALA by inducing apoptosis and necrosis in hepatic cells.

of iNOS mRNA [74]. On the other hand, there are studies using a hamster model that report the *in vivo* production of NO in the zone of liver abscess, mediated by iNOS mRNA expression [53]. The deficient capacity of macrophages isolated from ALA for developing a respiratory burst does not denote the absence of the O_2^- anion, because the production of this anion does not depend solely on this mechanism.

The production of NO requires the presence of a nitric oxide synthase (NOS), a family of enzymes that includes iNOS, eNOS, and nNOS. iNOS can be found in the inflammatory cells, while eNOS is present in the vascular endothelium [63, 75]. In sites of inflammation, the cytokine-induced activity of iNOS increases. The iNOS-mediated formation of O_2 via a novel pathway in L-Arg depletes murine macrophages, and the O_2 formed in this way interacts with NO to form $ONOO^-$, which then enhances macrophage immune function. However, the overproduction of these oxidants could also trigger cell death (Figure 1) [76].

Both NADPH oxidase and NOS are found in phagocytes and activated NOS is found in endothelial cells (Figure 1) [69]. Although NO is a relatively stable and highly diffusible free radical, O_2^- is very short lived and has restricted diffusion across biomembranes. Thus, the presence of O_2^- would seem to be the limiting factor for the synthesis of $ONOO^-$. Nutrient deprivation, ischemia, and cytokines (e.g., TNFα and IL-1) under the hypoxic conditions of inflammation all increase the activity of endothelial NADPH oxidase and the consequent production of O_2^- [72].

Under some inflammatory conditions the production of NO and O_2^- is strongly activated, which could lead to

a 1,000-fold increase in the production of each. This in turn would cause a 1,000,000-fold increase in the formation of $ONOO^-$ [63, 69, 70]. High levels of $ONOO^-$ lead to the dysfunction of critical cellular processes, the disruption of cell signaling pathways, and the induction of cell death through both apoptosis and necrosis [63]. Thus, $ONOO^-$ is thought to be the potential cause of a number of inflammatory diseases [68] and could possibly lead to the development of ALA.

The production of $ONOO^-$ is increased by two mechanisms under conditions of ischemia or hypoxia. Firstly, hypoxia in the liver leads to low concentrations of L-arginine and oxygen (hypoxia and anoxia), which enhance macrophage arginase activity [77–80]. Arginase, the principal enzyme of the urea cycle, hydrolyzes L-arginine to urea and L-ornithine. On the other hand, L-arginine and a cofactor (tetrahydrobiopterin, BH4) are substrates for NOS enzymes. Thus, arginase competes with NOS enzymes for their common substrate (L-arginine), leading to the uncoupling of all three isoforms of NOS [80].

Secondly, hypoxia induces production of the hypoxia inducible factor, which also promotes the uncoupling of NOS [81–83] as well as the activation of arginase-2 [84]. This uncoupling simultaneously produces O_2^- and NO [85], leading to additional $ONOO^-$ generation [69, 70, 76, 86]. Indeed, more $ONOO^-$ is formed in hypoxic regions of the liver where the pH is low, leading to the production of hydroxyl-like free radical species in the absence of oxygen [87].

$ONOO^-$ is capable of reacting directly or indirectly with biological tissues. It reacts directly with thiol groups, the preferential targets for $ONOO^-$ reactivity *in vivo* [70], causing oxidative damage to iron-sulfur centers and the active site of -SH groups in tyrosine phosphatases, lipids, and CO_2. On the other hand, $ONOO^-$ can act indirectly by decomposing into highly reactive radicals. The $ONOO^-$ ion is more stable than its protonated form (ONOOH, pKa 6.5 to 6.8), which decomposes rapidly via homolysis of the O–O bond to form free nitrogen dioxide ($^\bullet NO_2$) and the hydroxyl ($^\bullet OH$) radical (Figure 3). The latter radical has a highly oxidizing effect on many biomolecules, including tyrosine residues, thiols, DNA, and unsaturated fatty-acid-containing phospholipids [68, 88].

Compared to the reactivity of the $^\bullet NO_2$ and $^\bullet OH$ radicals, the reactions of $ONOO^-$ are relatively slow. Thus, $ONOO^-$ should certainly be more selective for its target molecules and better able to react relatively far from its site of formation [70]. When generated from a cellular source, $ONOO^-$ could influence surrounding target cells within one to two cellular layers (~5–20 μm) [69].

By reacting with lipids, DNA, and proteins via direct oxidative reactions or via indirect radical-mediated mechanisms, $ONOO^-$ can trigger cellular responses ranging from subtle modulations of cell signaling to overwhelming oxidative injury that commits cells to necrosis or apoptosis [69]. When damage mediated by $ONOO^-$ induces cell necrosis, the release of the intracellular content of cells (e.g., HMGB1: high mobility group protein B1) into the extracellular space can trigger an additional inflammatory response, representing a positive-feedback cycle of further $ONOO^-$ generation [69].

DNA damage induced by $ONOO^-$, leading to the activation of poly (ADP-ribose) polymerase (PARP), can also increase the inflammatory response. It has been shown that PARP coactivates many inflammatory cascades and increases tissue infiltration by activated phagocytes in experimental models of inflammation, circulatory shock, and ischemia-reperfusion [63, 89]. Through these mechanisms, $ONOO^-$ amplifies neutrophil-dependent responses (adhesion, migration, and activation of neutrophils) under inflammatory conditions, and thus contributes to the detrimental effects of inflammation in arthritis, colitis, and other inflammatory diseases [63, 70].

4. Defense Mechanisms against $ONOO^-$

In mammalian tissue, peroxides like H_2O_2 and $ONOO^-$ are produced as a result of normal cellular processes, including metabolism and inflammation. As a result, host tissue and amoebas must have defense mechanisms against these molecules. To be able to provoke an uncontrolled inflammatory response, the trophozoite defense system against $ONOO^-$ would have to be better than that of the host. Biological protection against $ONOO^-$ is organized in two main categories: prevention and interception [90, 91].

4.1. Prevention of $ONOO^-$ Formation. One defense mechanism by amoebas and mammalian tissue against $ONOO^-$ is the prevention of its formation through the inhibition of its precursors, NO and O_2^- [92]. The steady state concentrations of O_2^- are normally kept relatively low, in the nanomolar to picomolar range. The main route of O_2^- consumption in biological systems is its reaction with superoxide dismutase (SOD) to form hydrogen peroxide (H_2O_2) and dioxygen. On the other hand, NO is scavenged by hemoglobin, decreasing its levels in the blood [93]. NO readily reacts with oxyhemoglobin or oxymyoglobin to give nitrate (NO_3^-) and oxidized hemoproteins (methemoglobin and metmyoglobin) as follows:

$$\mathrm{Hb\,(Fe-O_2)} + \mathrm{NO} \longrightarrow \mathrm{metHb\,(Fe\ III)} + \mathrm{NO_3^-} \quad (2)$$

Due to the high concentrations of oxyhemoglobin in the body, this molecule may provide the primary metabolic as well as detoxification mechanism for NO *in vivo* [93–95]. Thus, red blood cell-encapsulated hemoglobin can react very quickly with NO and scavenge virtually all the molecules produced by endothelial and inflammatory cells [94, 95]. However, the inactivation of NO by Hb and by self-oxidation could be less efficient in a hypoxic environment, as this reaction requires oxygen.

One generally recognized mechanism for the inactivation of NO is its reaction with O_2 [93]. Since NO and O_2 are much more soluble in lipid layers than aqueous fractions, biological membranes may act as a "lens" that can focus and magnify the self-oxidation of NO [96, 97].

E. histolytica has developed some mechanisms to avoid NO production. For example, soluble amoeba proteins suppress INFγ induced amebicidal activity, thus affecting the expression of the mRNA iNOS gene and consequently NO

production [74]. Moreover, there is evidence that the monocyte locomotion inhibitory factor of *E. histolytica* inhibits the *in vitro* NO production normally induced by cytokines in human leukocytes [98]. It has also been reported that *E. histolytica* arginase inhibits NO production by consuming L-arginine, the substrate of iNOS in activated macrophages. All of these amebic mechanisms should certainly contribute to the survival *E. histolytica* [99].

4.2. Interception or Inactivation of $ONOO^-$. Due to a direct reaction with low-molecular weight compounds (e.g., carbon dioxide, thiols, ascorbate, selenocompounds, and synthetic metalloporphyrins) and other proteins (e.g., certain peroxidases, hemoglobin, albumin, and selenoproteins), $ONOO^-$ is decomposed into nontoxic products. Efficient $ONOO^-$ scavengers include selenium compounds, particularly 2-phenyl-1, 2 benzisoselenazol-3(2H)-one (ebselen), selenomethionine, and selenocysteine, as well as selenium-containing proteins, such as glutathione peroxidase and thioredoxin-reductase [70, 90]. Additionally, (−)-epicatechin and other flavonoids can contribute to the cellular defense against $ONOO^-$ [91]. Considering their approximate concentrations *in vivo* and their reaction rate constants in relation to $ONOO^-$, the best of these low-weight molecules for the interception of $ONOO^-$ would seem to be CO_2, hemoglobin, and glutathione [90].

5. The Thioredoxin System

The principal mechanism for interception of $ONOO^-$ is probably the thioredoxin system, which is comprised of thioredoxin (Trx) and thioredoxin reductase (TrxR). This system together with peroxiredoxin (Prx) mediates the NADPH-dependent reduction of H_2O_2 and tert-butyl hydroperoxide in *Entamoeba* species [100]. For Trx to carry out most of its functions, the disulfide active site in this protein must be reduced in the following manner:

$$\text{Oxidized Trx} + \text{TrxR (with NADPH)} \longrightarrow \text{Dithiol Trx} \quad (3)$$

Once Trx accepts electrons from TrxR, it can reduce Prx. Another NADH enzyme, flavin oxidoreductase, also carries out this function [100]. The resulting form of Prx can protect against oxidative stress by decomposing H_2O_2 into water (H_2O) and probably $ONOO^-$ into nitrite [101].

5.1. TrxR. The different functions of Trx are entirely dependent upon the activity of TrxR [102], and the latter has two major forms in nature. Whereas the larger form of TrxR has a selenoprotein (~Mr = 55 kDa) and corresponds to mammals, the relatively small nonselenoprotein form of TrxR is found in bacteria, plants, archaea, and most unicellular eukaryotes [102, 103].

Homodimeric mammalian TrxR consists of two subunits in a head-to-tail arrangement. Both subunits are absolutely required for normal catalysis during the catalytic cycle [102]. The C-terminal -Gly-Cys-Sec-Gly-COOH motif of the human selenoprotein (about 16 amino acids long) is found in all mammalian TrxR, and the Cys-Sec dyad of this motif has been identified as a reversible selenenylsulfide/selenothiol, constituting the active site of the enzyme [102]. The electrons from NADPH reduce a redox active disulfide and transfer them to the C-terminal active site of a selenothiol located in the sequence Gly-Cys-Sec-Gly, which is conserved in all isoforms of TrxR. From this site electrons are transferred to Trx, allowing the latter to carry out its functions, such as the reduction of protein disulfides or other substrates [104].

For example, the two major forms of human Trx, cytosolic Trx1 (the TXN1 gene product) and mitochondrial Trx2 (the TXN2 gene product), are reduced by TrxR and NADPH [101, 102]. As a result, these two forms of Trx can provide electrons to proteins such as ribonucleotide reductase (formation of deoxyribonucleotides from ribonucleotides). In this way Trx reacts with ribonucleotide precursors to synthesize deoxyribonucleotides, peroxiredoxins, and methionine sulfoxide reductases [102].

As can be appreciated, the Trx-reducing activity of mammalian TrxR is totally selenium dependent [102], and aberrations in selenium metabolism must have a direct impact on the functions and levels of different selenoproteins, as well as on many cellular systems that are linked to Trx activity.

5.2. The Amebic Trx System. Previous works reported the molecular cloning, expression, purification, and functional characterization of two genes from *E. histolytica* that encode for TrxR and Trx (EhTrxR and EhTrx). It turns out that EhTrxR belongs to the low-molecular-weight family of TrxRs, which have a redox active site containing two key cysteine residues without a selenoprotein [100]. This is a homodimeric covalent protein that catalyzes the NAD(P)H-dependent reduction of thioredoxins (Figure 2) and S-nitrosothiols [92].

Unlike the TrxR of *E. histolytica*, that of mammals is dependent on selenoproteins. On the other hand, both mammalian TrxR and EhTrxR reduce the corresponding form of Trx by using NADPH [100]. The resulting form of Trx reduces Prx, which in turn can reduce H_2O_2 to H_2O and probably ONOOH to nitrite (Figure 2), thus acting as an antioxidant system [100].

EhTrxR, EhTrx, and Prx have been immunolocalized under the plasma membrane in *E. histolytica*. Contrarily, mammalian TrxR, Trx, and Prx have not been found under the membrane (see Section 5.3.4) [64, 105]. This cellular location in *E. histolytica* favors the potential *in vivo* functionality of the ROS detoxification system. On the one hand, one amebic mechanism of resistance to lipid peroxidation is the composition of the amebic membrane, which has a high concentration of saturated lipids [106]. On the other hand, the EhTrx system could offer an alternative protective mechanism against lipid peroxidation, thus maintaining intracellular proteins and DNA safe from highly toxic reactive oxygen and nitrogen species. In such a case, this would represent a key mechanism in relation to the virulence of *E. histolytica* when exposed to highly toxic ROIs [105] and should be pivotal to amebic survival during extraintestinal infection [92].

5.3. Peroxiredoxin. Peroxiredoxins (Prxs) are a family of antioxidant enzymes that are principally reduced by

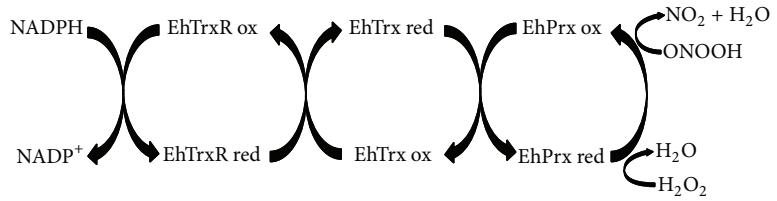

Figure 2: *E. histolytica* thioredoxin system. The *Entamoeba* thioredoxin system is comprised of thioredoxin (Trx) and thioredoxin reductase (TrxR), coupled with peroxiredoxin (Prx) and NADPH. Trx has to be reduced to fulfill its functions, and this reduction is carried out through catalyzation by TrxR using NADPH as a cofactor. Once Trx accepts electrons from TrxR, it can reduce peroxiredoxin (Prx). The resulting form of Prx can protect against oxidative stress by decomposing H_2O_2 into H_2O. Based on the figure by Arias et al. [105].

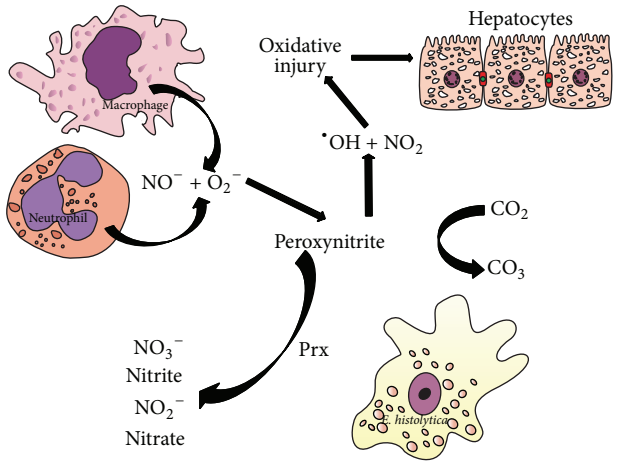

Figure 3: Amebic peroxiredoxin in ALA. During the development of ALA, activated phagocytes produce increased levels of superoxide (O_2^-) and NO, thus generating the $ONOO^-$ anion, which in turn causes oxidative damage to hepatocytes. $ONOO^-$ can decompose into nitrogen dioxide ($^{\bullet}NO_2$) and the highly oxidizing hydroxyl radical ($^{\bullet}OH$). The $ONOO^-$ anion can be intercepted by direct reaction with carbon dioxide, decomposing it into nontoxic products. The Prx enzymes of parasites (e.g., *E. histolytica*) and other bacteria are involved in protection of these organisms by the reduction of host-produced hydrogen peroxides and $ONOO^-$.

Trx [107]. Once reduced, Prx can in turn reduce H_2O_2 and perhaps $ONOO^-$ to harmless forms. These peroxide-eliminating enzymes are truly ubiquitous, existing in yeast, plant, and animal cells, including protozoa, helminths, parasites, and most (if not all) eubacteria and archaea [108]. Prxs are preferentially expressed under conditions of stress induced by elevated levels of reactive oxygen species (ROS) and reactive nitrogen species.

5.3.1. Mammalian Prx. There are at least five subfamilies of mammalian Prx enzymes, which are categorized on the basis of their protein sequence and cellular location. Although located primarily in the cytosol, Prx is also found within mitochondria, chloroplasts, and peroxisomes, associated with nuclei and membranes [108, 109]. The two categories of Prx consist of 1-Cys and 2-Cys. Each form has a distinct number of cysteinyl residues involved in catalysis [108, 109].

5.3.2. Amebic Prx. Although parasites are in an anaerobic environment during colonization of the colon, when invading tissue they are exposed to aerobic conditions. Several studies have identified H_2O_2 as lethal to *Entamoeba* species [57, 58, 64, 110]. Thus, in the oxygen-rich microenvironment that exists at the site of hepatic lesions, the capacity of Prx to prevent the deleterious production of H_2O_2 in the host must certainly play an important role in the survival of parasites [65, 111–113].

E. histolytica Prx (EhPrx) can degrade H_2O_2 [111, 114] as well as alkyl and aryl hydroperoxides [64]. It may also degrade $ONOO^-$ to nitrite. Like mammalian Prx, the peroxidase activity of EhPrx depends on Trx and TrxR activity [115]. EhPrx removes H_2O_2 *in vitro* in the presence of NADPH, EhTrxR, and EhTrx (Figure 2). This capacity of Prx has been confirmed in both native and recombinant proteins [111, 114, 115].

Virulent *E. histolytica* is reportedly more resistant to H_2O_2 than *E. dispar* and the nonvirulent strains of *E. histolytica* [64, 116, 117]. There are reports of an increase in protein and gene expression of Prx by *E. histolytica* in an oxygen-rich environment [65, 112]. By employing a fluorometric stopped-flow assay, the H_2O_2 detoxification activity of EhPrx and Prx of *E. dispar* was found to be similar [64]. Thus, it seems that the principal difference between EhPrx and the Prx of *E. dispar* is the location of this antioxidant. Accordingly, the ability of *E. dispar* to become virulent under certain conditions may be due in part to the possible change of location of Prx in distinct environments [114]. Trophozoites deficient in Prx are more sensitive than the wild type to an oxygenated environment and to H_2O_2 in axenic culture [118].

Logically, the size of liver abscesses is lower in hamsters inoculated with Prx-downregulated *E. histolytica* trophozoites compared to normal HM1:IMSS (6–9 versus 20–25 mm) [118]. Similarly, overexpression of Prx in *E. histolytica* Rahman rendered the transgenic trophozoites more resistant to killing by H_2O_2 (5 mM) *in vitro* [116] and Rahman trophozoites expressing higher levels of Prx have been associated, based on histological analysis of human colonic xenografts, with higher levels of intestinal inflammation and more severe disease [116].

Trophozoites cultured axenically are less virulent, both in the hamster model of ALA and in the mouse model of amebic colitis [119, 120]. RNA from such low virulence

trophozoites was compared with the transcripts of amoebas whose virulence was maintained by passing them through hamster liver abscesses. Among the upregulated transcripts found in the virulent amoebas were those involved in both oxidative and stress defense, including three Prx transcripts [121]. Hence, Prx levels of *E. histolytica* HM1:IMSS trophozoites may increase in response to the presence of host inflammatory cells [116].

Moreover, immunization of gerbils and hamsters with recombinant Prx results in partial protection against ALA formation and/or a reduction in the size of the abscesses [122–124]. Thus a strengthened immune response against amebic Prx may protect hamsters against the development of ALA [123].

The evidence regarding the activity and location of EhPrx, together with the resistance provided by Prx to the toxic effects of H_2O_2, clearly suggests the importance of this antioxidant enzyme for the survival and virulence of *E. histolytica* trophozoites [116, 118].

5.3.3. Prx Structure and Action Mechanisms. EhPrx has a 52% identity with the human PrxII-2 Cys, the main difference being the extended cysteine-rich N-terminal region in the amebic version, probably contributing to its enzymatic activity [111]. Several authors have demonstrated that peroxiredoxin forms a 60 kDa dimer through disulfide bonds [113, 124] and forms an oligomer or oligomers with high-molecular mass on the cell surface (>200 kDa) [112]. Thus, EhPrx is typically found as an obligate homodimer (2-Cys Prxs) with identical active sites [108].

Furthermore, EhPrx can form a high-molecular mass oligomer on the cell surface [111, 112] because it contains two conserved sequence motifs (region I, sequence PLDWTF, and region II, sequence DSVYCHQAWCEA) that are necessary for decamer formation in 2-Cys Prxs [108, 125]. This decameric structure (ring-like higher oligomers or toroids) is comprised of five dimers (that may or may not be functionally active) linked end-on through predominantly hydrophobic interactions [109, 126].

EhPrx retains arginine 163 and the two conserved cysteine residues (VCP motifs, Cys 87 and 208) that are required for its catalytic activity [108, 109, 115]. The structure and sequence of the peroxidatic active site is highly conserved among Prx classes (1-Cys, typical 2-Cys, and atypical 2-Cys Prxs). The features of typical 2-Cys Prx are highly conserved across all kingdoms, with 30% or greater sequence identity. The most conserved regions include (i) the peroxidative cysteine (generally near residue 50) within the DFTFVCPTEI motif in mammals and the DWTFVCPTEI motif in *E. histolytica* and (ii) the resolving cysteine (near residue 170) within the VCP motif [108]. Therefore, the catalytic activity of the Prx of *Entamoeba* spp. must be similar to other typical Cys-2 Prx.

Various studies have demonstrated that Prx, whether of mammalian, bacterial, or parasitic origin, can reduce $ONOO^-$ to nitrite *in vitro* [69, 127–130]. One study confirmed a protective role of Prx against $ONOO^-$ *in vivo* (Figure 3) [101].

5.3.4. Location of Prx. Mammalian Prx is mainly located in the cytosol, membrane, and mitochondria [108]. Contrarily, EhPrx has been detected not only in the nucleus and cytoplasm [131] but also on the peripheral membrane [12, 132, 133]. EhPrx probably forms a high-molecular-mass oligomer (>200 kDa) on the cell surface [111, 112]. Indeed, peroxiredoxin (29 kDa) is the major thiol-containing surface protein of *E. histolytica* and has both peroxidase and antioxidant activities [64, 132].

Prx interacts with galactose and the GalNAc lectin, which are both found at sites of amoeba-host cell contact. The recruitment of Prx at this site probably protects trophozoites against the ROIs generated by host phagocytic and epithelial cells [12, 13]. The membrane location of EhPrx suggests an important role for the Trx-dependent metabolic pathway as a redox interchanger, which could be critical for the maintenance and virulence of the parasite when exposed to highly toxic ROIs [105]. In this location the system protects the membrane against lipid peroxidation and may participate in the protection of hemoglobin and other intracellular proteins against free radical damage by stimulating potassium efflux.

The enzymatic activity, quantity, and location of EhPrx probably account for the greater resistance of this amebic strain to oxidants like H_2O_2. Hence, the Trx-Prx system of *E. histolytica* seems to help it survive and proliferate in a highly oxygenated environment, leading to greater invasiveness [114] and virulence.

6. Other Defense Mechanisms of *E. histolytica* during Amebic Invasion

6.1. Flavodiiron Proteins. Flavodiiron proteins are enzymes found in strict and facultative anaerobic bacteria and archaea, as well as a limited number of eukaryotes such as the pathogenic protozoa *Trichomonas vaginalis*, *Entamoeba*, and *Giardia intestinalis* [66, 134–138]. Due to the role of flavodiiron proteins in the catalysis or reduction of O_2 to H_2O and NO to N_2O, they have been proposed as a protective mechanism against nitrosative stress or oxygen toxicity in anaerobes [137, 139, 140]. *E. histolytica* has four copies of flavoprotein A [66], suggesting that this enzyme plays a significant role in these two mechanisms. However, the substrate preferences (O_2 or NO) of the *E. histolytica* flavodiiron proteins and their role during infection have not been determined [141].

6.2. Erythrophagocytosis. Phagocytosis is considered a virulence sign in *E. histolytica* [14, 142–145]. Recent data suggest that transmembrane kinases (TMK) have a role in phagocytosis of human erythrocytes [146]. Erythrophagocytosis may be important for the survival, growth, and proliferation of *E. histolytica* in an aerobic or even microaerobic environment [147, 148]. *E. histolytica* trophozoites preferentially interact with red blood cells, meaning that the phagocytic activity of erythrocytes by *E. histolytica* trophozoites should certainly have a very important function in amoebiasis. Indeed, the phagocytic capacity of trophozoites has been taken as a

qualitative marker of pathogenicity [142, 145, 149]. Erythrophagocytosis may help the amoeba to scavenge NO and other reactive oxygen and nitrogen intermediates and thus help the parasite to survive in the oxygen-rich environment of oxidative stress [147].

Hemoglobin and Prx are two major proteins present in erythrocytes. For example, Prx2 is an abundant erythrocyte protein [109, 147]. Therefore, the process of erythrophagocytosis may serve two important functions in the amebic trophozoites that would contribute to parasite virulence. Firstly, erythrocytes rich in hemoglobin (Hb) may help trophozoites to scavenge NO, which readily reacts with oxyhemoglobin and oxymyoglobin to give nitrate (NO_3^-) and the oxidized hemoproteins, methemoglobin, and metmyoglobin. The reaction with hemoglobin is the primary detoxification mechanism for NO [93–95]. Secondly, erythrocytes *rich* in Prx may help amoebas to scavenge $ONOO^-$. Hb and Prx-2 of the erythrocytes are extremely efficient at scavenging H_2O_2, NO, and $ONOO^-$.

These mechanisms are probably pivotal for parasite survival under the nitrogen and oxygen-rich environment of inflammation (Figure 3) [148]. Also, phagocytosis of bacteria containing Prx could increase the pathogenicity of *E. histolytica* in the host intestine and possibly also act as a stimulus to induce the invasive behavior of trophozoites [150]. *E. histolytica* might have a mechanism of incorporating Prx similar to that of *Plasmodium falciparum*, which imports Prx-2 from human erythrocytes into its cytosol. This Prx-2 exists in a functional form and a significant concentration [151].

7. An Overview of the Prx Model of Amoebiasis

Abundant evidence in the literature suggests that inflammation and inflammatory mediators are the cause of tissue damage in ALA (see Sections 3.1 and 3.2), as few trophozoites are present in the extensive areas of apoptosis and necrosis [152]. Furthermore, in the absence of inflammatory cells, virulent *E. histolytica* trophozoites lead to little or no abscess formation in hamsters [44, 153].

N-Acetylcysteine (NAC) also inhibits tissue damage in the latter stages of ALA in hamster. In the liver of hamsters treated with NAC, there are many clusters of well-preserved amoebas in close contact with hepatocytes, sparse inflammatory infiltrate, and minimal or no tissue damage [42]. The inhibitory effect of NAC on tissue damage during late stages of EALAH was explained [42] as the inhibition of leukocyte-endothelium adhesion molecules and reduced migration of leukocytes, leading to an inhibitory effect of NAC on NO production and ROS activity, and consequently a reduction of the toxic effect on cells. According to Olivos-García et al. [42] "*ROS and NOS (NO and $ONOO^-$) may be the principal molecules responsible for tissue destruction during the late stages of ALA*" [42]. However, NAC also reduces $ONOO^-$ mediated toxicity in various pathophysiological conditions [69, 154, 155]. Hence, the point of view in the aforementioned quote is perhaps better explained by the Prx model, which holds that the inhibition of the synthesis of $ONOO^-$ would not only maintain amoebas alive but also reduce both inflammatory infiltrate and tissue damage.

7.1. Initial Phase: Acute Inflammation. It is well known that some individuals are susceptible to *E. histolytica* trophozoites while others are resistant [31, 156]. In susceptible individuals, trophozoites invade the intestine, survive the host immune response, and arrive to the liver through the blood flow. Their presence in the sinusoids is associated with an influx of host immune cells. We propose that the key to susceptibility is the incapacity of the immune response to eliminate the amoebas before the latter are able to establish colonies and provoke a chronic inflammatory response.

During this initial stage of amoebiasis in hamsters, the two major components of the inflammatory response are PMNs and mononuclear cells (MO), both involved in cellular infiltration [1, 2]. PMNs cause the formation of numerous inflammatory foci that produce large amounts of NO and O_2^-, which in turn lead to the production of $ONOO^-$ (Figure 4). This highly reactive oxidizing agent probably lyses neutrophils, endothelial cells, hepatocytes, and other parenchymal cells. Lysed neutrophils release proteolytic enzymes, adding to the assortment of toxic compounds that cause damage to endothelial, parenchymal, and inflammatory cells (Figure 4) [1, 2]. It has been proposed that with inflammation there is massive trophozoite death [157], which does indeed seem to be the case for individuals resistant to *E. histolytica*. However, for susceptible individuals, it seems more likely that amoebas take advantage of the inflammatory environment in the first stage of the pathogenesis by ingesting nutrients from dead inflammatory cells.

7.2. Chronic Phase: Uncontrolled Inflammation. Amoebic lesions in hamsters are formed by necrosis and apoptosis of hepatocytes [1, 2, 37, 39, 40, 152, 157]. The evidence outlined in the present review seems to indicate that these abscesses are not formed principally through direct contact between amoebas and host cells but instead by the uncontrolled inflammatory response produced when susceptible individuals are unable to eliminate amoebas.

Under conditions of uncontrolled inflammation, there is an ever greater quantity of amoebas, amebic molecules (cysteine proteinases, LPFG, Gal/GalNAc-specific lectin, and prostaglandin E2), and cytokines (IL-1a, IL-6, IL-8, and TNF-a) that induce the production of adhesion molecules (e.g., ICAM-1 and E-selectin), which in turn attract macrophages and lymphocytes [31]. These cells together with Kupffer cells produce large amounts of cytokines, which further amplify the inflammatory response [31, 158–160]. The abundant number of monocytes, macrophages, and Kupffer cells, as well as activated endothelial cells and host mitochondria, produce ever greater quantities of NO and O_2^-, which probably lead to the formation of large amounts of the $ONOO^-$ anion (Figure 4).

The Prx model proposes that diffusible molecules, such as $ONOO^-$ and TNF-α, are able to commit cells to necrosis or apoptosis in the liver (Figure 4) [68, 69]. Corroborating this idea, one study reported that inflammation is induced

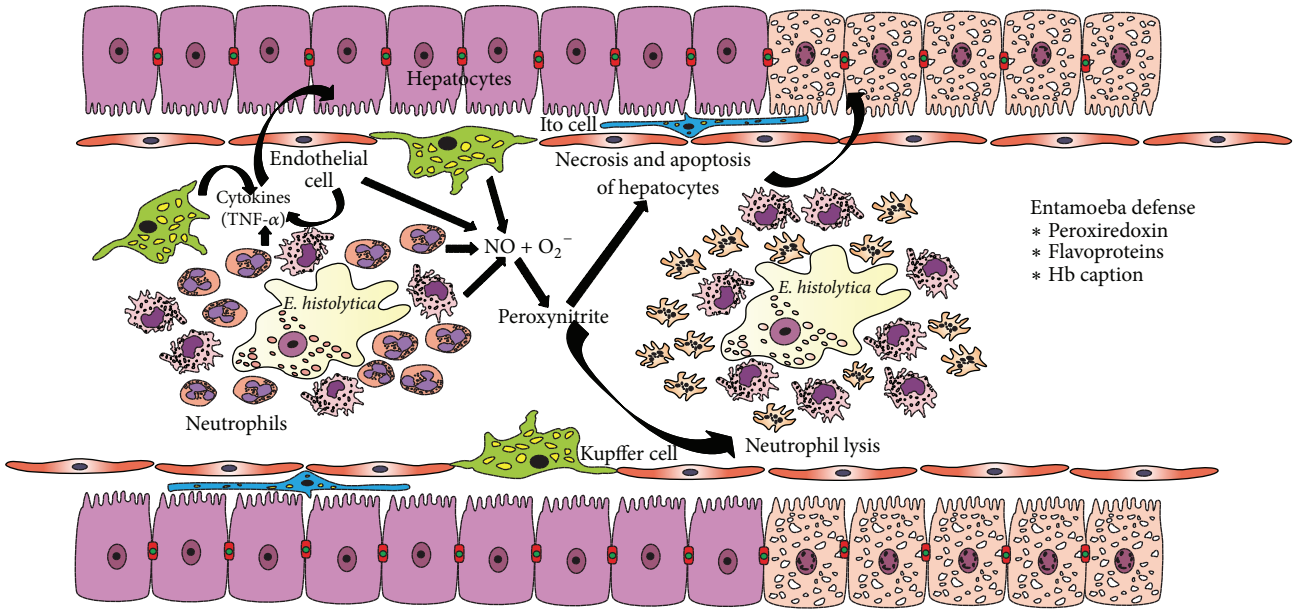

Figure 4: Role of $ONOO^-$ and *E. histolytica* Prx in the pathogenesis of ALA. The early stages of ALA are characterized by an acute and chronic host inflammatory response, where an abundant number of monocytes, macrophages, Kupffer cells and activated endothelial cells produce large amounts of nitric oxide and the superoxide anion. Moreover, these molecules may be released after immune cells are lysed. Therefore, there is probably a high concentration of $ONOO^-$ at inflammatory sites, which in turn would promote necrosis and/or apoptosis of hepatocytes. Amebic flavoproteins and Prx play a protective role against the oxidative and nitrosative attack of phagocytic cells and against the H_2O_2 produced by the amebic metabolism.

when parasites or immune cells secrete or release diffusible products after cell death [51]. $ONOO^-$ interacts with lipids, DNA, and proteins via direct oxidative reactions or indirect, radical-mediated mechanisms. Among the latter mechanisms, nitrogen dioxide ($^{\bullet}NO_2$) and hydroxyl radicals ($^{\bullet}OH$) are of particular importance (Figure 3).

The continuous, prolonged, and uncontrolled inflammatory response seems to be responsible for the production of large granulomas or "abscesses" in hamsters, which are characteristic of the chronic phase of ALA in experimental animal models [31]. At 3-4 days after inoculation of axenic amoebas, the chronic granulomatous reaction in the liver is formed by typical multiple granulomas, which have a central necrosis limited peripherally by a palisade of epithelioid cells and more externally by connective fibers. Amoebas are recognizable between the necrosis and epithelioid cells [1, 2].

With chronic inflammation and necrosis comes ischemia of the lesions [31, 153, 161]. Consequently, there is reduced availability of the host molecules that could counteract $ONOO^-$ (e.g., carbon dioxide, hemoglobin, and albumin) [69, 70]. Indeed, it has been shown that in ischemic tissues there is a greater $ONOO^-$ concentration [87].

7.3. Defense against $ONOO^-$: Amoebas versus Host Cells. To be able to provoke an uncontrolled inflammatory response, the *E. histolytica* defense system against $ONOO^-$ would have to be better than that of the host. According to evidence in the literature, there are four important factors in this sense.

Firstly, since Prx-2 is an abundant erythrocyte protein [109, 147], *E. histolytica* trophozoites may ingest high quantities of Prx through erythrocyte phagocytosis, as occurs with agents of other parasitic diseases [151]. This would not be the case for host cells. Hence, the quantity of this enzyme in amoebas is probably greater than in mammals. Moreover, erythrocytes, which are rich in hemoglobin (Hb), may help the amoeba to scavenge NO.

Secondly, in *E. histolytica* Prx has a prominent surface and subcortical distribution [12, 131–133], which probably makes these trophozoites more capable of surviving the attack of $ONOO^-$ produced externally. Contrarily, Prx is mainly located in the cytosol and mitochondria of hamsters.

Thirdly, the structure of mammalian cells leaves them more susceptible to an $ONOO^-$ attack. That is, mitochondria are found in mammalian cells but not in trophozoites, and mitochondria play an essential role in the mechanisms of cell death (by apoptosis and necrosis) triggered by $ONOO^-$ [63].

Fourthly, the effectiveness of Prx in mammals is completely selenium dependent, and plasma selenium concentration and the synthesis of selenoproteins (probably including TrxR) seem to be markedly reduced during inflammation, evidenced by a severe drop in the concentration of these proteins in the liver during sepsis or sepsis-like illness [162, 163]. In addition, if indeed selenium inhibits the activation of NF-kappaB, as has been reported [164], the deficit of selenium would tend to feed uncontrolled inflammation, which would further reduce the levels of selenium in liver and serum.

Most ingested selenium enters specific selenium metabolism pathways in the liver, thus providing the raw material for the synthesis of selenoproteins. One such protein produced in the liver is selenoprotein P

(SelP), whose main function is the transport of selenium to remote tissues. Additionally, locally expressed SelP may have other functions, as demonstrated in the brain [163, 165]. One of these functions is the chelation of heavy metals, presumably by forming nontoxic selenium-metal complexes, thus preventing cell toxicity and protecting against $ONOO^-$ mediated oxidation and nitration [165]. A recent report indicated that SelP protects mice against trypanosomiasis [166]. Therefore the reduction of selenium metabolism and selenoprotein synthesis by hepatic damage should certainly diminish the synthesis and activity of mammalian TrxR in hepatocytes and inflammatory cells.

The apparent importance of the scarcity of selenium in the liver during the pathogenesis of ALA is further supported by the effect of supplementation with selenium during chronic inflammation. The consequence is the restoration of depleted hepatic and serum selenium levels caused by an increase in selenoprotein biosynthesis, leading to the suppression of CRP production and an attenuation of the inflammatory process [164]. However, selenium supplementation can also produce undesirable effects, such as increasing susceptibility to infection by reducing inflammation, or inducing sexually dimorphic effects [167]. The relationship between selenium, selenoprotein synthesis, and host-pathogen interactions is an important issue and warrants further investigation [168].

Hence, EhPrx is considered to be an important protective mechanism against two elements: (i) the oxidative attack by host phagocytic cells activated during the amebic invasion and (ii) the H_2O_2 produced by amebic metabolism [114]. Ample evidence indicates that the protection afforded by Prx against $ONOO^-$ is essential not only for the survival but also for the pathogenicity of trophozoites.

8. Drug Design

The Trx system provides interesting drug design targets. The structural and mechanistic differences, between human and *P. falciparum* TrxR and more generally between the mammalian and the bacterial TrxR, should make this protein a new drug design target for antibacterial agents [103, 165, 169]. Additionally, the stimulation of host or the inhibition of amebic Prx might be a useful strategy for the treatment of amoebic liver abscess.

This area of research is only beginning to be explored. Recently it has been reported that auranofin, a gold-containing drug that inhibits TrxR, has a higher amebicidal activity than metronidazole *in vitro*. In a hamster model of amebic liver abscess, orally administered auranofin markedly decreased the number of parasites, the detrimental host inflammatory response, and hepatic damage. However, many trophozoites are resistant to auranofin [170].

Selenocysteine 496 of human TrxR is a major target of the antirheumatic gold-containing drug auranofin. Although auranofin is a potent inhibitor of mammalian TrxR *in vitro*, it is practically ineffective *in vivo* [171–173].

9. Perspective

Amoebiasis caused by *E. histolytica* is an important public health problem in emerging countries. It is generally the poorest who have the greatest exposure to this amebic species and at the same time the greatest susceptibility. Therefore, it is important to understand the pathogenic mechanisms of this disease in order to define molecular targets and design economical drugs to act against such targets.

The hypothesis of the "uncontrolled inflammatory response" as the main cause of amoebiasis has been evolving for approximately three decades. The understanding of the mechanisms of chronic inflammation and their possible relation to amebic colitis and ALA may be reaching the proper depth of understanding in order to be able to finally produce novel therapies. Intervention in the Trx system of the host or parasite could possibly provide the long-sought solution to this public health problem. In relation to *E. histolytica* trophozoites, the surface and subcortical distribution of Prx, which provides this amebic species with many advantages in terms of survival and virulence, might also provide an easily accessible drug target.

Conflict of Interests

Authors have no affiliations or financial involvement with any organization or entity that has a financial interest in or conflict of interests with the subject matter or materials discussed in the paper.

Acknowledgment

This work was supported in part by grants from SEPI-IPN. Judith Pacheco-Yepez, Rosa Adriana Jarillo-Luna, Edgar Abarca-Rojano, and Rafael Campos-Rodriguez are fellows of COFAA-IPN and EDI-IPN.

References

[1] V. Tsutsumi and A. Martinez-Palomo, "Inflammatory reaction in experimental hepatic amebiasis. An ultrastructural study," *American Journal of Pathology*, vol. 130, no. 1, pp. 112–119, 1988.

[2] V. Tsutsumi, R. Mena-Lopez, F. Anaya-Velazquez, and A. Martinez-Palomo, "Cellular bases of experimental amebic liver abscess formation," *American Journal of Pathology*, vol. 117, no. 1, pp. 81–91, 1984.

[3] K. Chadee, W. A. Petri Jr., D. J. Innes, and J. I. Ravdin, "Rat and human colonic mucins bind to and inhibit adherence lectin of *Entamoeba histolytica*," *The Journal of Clinical Investigation*, vol. 80, no. 5, pp. 1245–1254, 1987.

[4] J. I. Ravdin, C. F. Murphy, R. A. Salata, R. L. Guerrant, and E. L. Hewlett, "N-acetyl-d-galactosamine-inhibitable adherence lectin of *Entamoeba histolytica*. I. Partial purification and relation to amoebic virulence in vitro," *Journal of Infectious Diseases*, vol. 151, no. 5, pp. 804–815, 1985.

[5] I. Meza, F. Cazares, J. L. Rosales-Encina, P. Talamas-Rohana, and M. Rojkind, "Use of antibodies to characterize a 220-kilodalton surface protein from *Entamoeba histolytica*," *Journal of Infectious Diseases*, vol. 156, no. 5, pp. 798–805, 1987.

[6] G. García-Rivera, M. A. Rodríguez, R. Ocádiz et al., "*Entamoeba histolytica*: a novel cysteine protease and an adhesin form the 112 kDa surface protein," *Molecular Microbiology*, vol. 33, no. 3, pp. 556–568, 1999.

[7] W. A. Petri Jr. and J. I. Ravdin, "Cytopathogenicity of *Entamoeba histolytica*: the role of amebic adherence and contact-dependent cytolysis in pathogenesis," *European Journal of Epidemiology*, vol. 3, no. 2, pp. 123–136, 1987.

[8] C. Martínez-López, E. Orozco, T. Sánchez, R. M. García-Pérez, F. Hernández-Hernández, and M. A. Rodríguez, "The EhADH112 recombinant polypeptide inhibits cell destruction and liver abscess formation by *Entamoeba histolytica* trophozoites," *Cellular Microbiology*, vol. 6, no. 4, pp. 367–376, 2004.

[9] R. Ocádiz, E. Orozco, E. Carrillo et al., "EhCP112 is an *Entamoeba histolytica* secreted cysteine protease that may be involved in the parasite-virulence," *Cellular Microbiology*, vol. 7, no. 2, pp. 221–232, 2005.

[10] W. A. Petri Jr., "Pathogenesis of amebiasis," *Current Opinion in Microbiology*, vol. 5, no. 4, pp. 443–447, 2002.

[11] M. Espinosa-Cantellano and A. Martínez-Palomo, "Pathogenesis of intestinal amebiasis: from molecules to disease," *Clinical Microbiology Reviews*, vol. 13, no. 2, pp. 318–331, 2000.

[12] M. A. Hughes, C. W. Lee, C. F. Holm et al., "Identification of *Entamoeba histolytica* thiol-specific antioxidant as a GalNAc lectin-associated protein," *Molecular and Biochemical Parasitology*, vol. 127, no. 2, pp. 113–120, 2003.

[13] C. A. Gilchrist and W. A. Petri Jr., "Using differential gene expression to study *Entamoeba histolytica* pathogenesis," *Trends in Parasitology*, vol. 25, no. 3, pp. 124–131, 2009.

[14] N. C. V. Christy and W. A. Petri Jr., "Mechanisms of adherence, cytotoxicity and phagocytosis modulate the pathogenesis of *Entamoeba histolytica*," *Future Microbiology*, vol. 6, no. 12, pp. 1501–1519, 2011.

[15] W. E. Keene, M. E. Hidalgo, E. Orozco, and J. H. McKerrow, "*Entamoeba histolytica*: correlation of the cytopathic effect of virulent trophozoites with secretion of a cysteine proteinase," *Experimental Parasitology*, vol. 71, no. 2, pp. 199–206, 1990.

[16] J. Matthiesen, A. K. Bar, A. K. Bartels et al., "Overexpression of specific cysteine peptidases confers pathogenicity to a non-pathogenic *Entamoeba histolytica* clone," *mBio*, vol. 4, no. 2, 2013.

[17] S. L. Stanley Jr., T. Zhang, D. Rubin, and E. Li, "Role of the *Entamoeba histolytica* cysteine proteinase in amebic liver abscess formation in severe combined immunodeficient mice," *Infection and Immunity*, vol. 63, no. 4, pp. 1587–1590, 1995.

[18] S. Ankri, T. Stolarsky, R. Bracha, F. Padilla-Vaca, and D. Mirelman, "Antisense inhibition of expression of cysteine proteinases affects *Entamoeba histolytica*-induced formation of liver abscess in hamsters," *Infection and Immunity*, vol. 67, no. 1, pp. 421–422, 1999.

[19] M. Tillack, N. Nowak, H. Lotter et al., "Increased expression of the major cysteine proteinases by stable episomal transfection underlines the important role of EhCP5 for the pathogenicity of *Entamoeba histolytica*," *Molecular and Biochemical Parasitology*, vol. 149, no. 1, pp. 58–64, 2006.

[20] D. Bansal, P. Ave, S. Kerneis et al., "An ex-vivo human intestinal model to study *Entamoeba histolytica* pathogenesis," *PLoS Neglected Tropical Diseases*, vol. 3, no. 11, article e551, 2009.

[21] R. D. Horstmann, M. Leippe, and E. Tannich, "Host tissue destruction by *Entamoeba histolytica*: molecules mediating adhesion, cytolysis, and proteolysis," *Memorias do Instituto Oswaldo Cruz*, vol. 87, supplement 5, pp. 57–60, 1992.

[22] X. Que and S. L. Reed, "Cysteine proteinases and the pathogenesis of amebiasis," *Clinical Microbiology Reviews*, vol. 13, no. 2, pp. 196–206, 2000.

[23] S. Pertuz Belloso, P. Ostoa Saloma, I. Benitez, G. Soldevila, A. Olivos, and E. García-Zepeda, "*Entamoeba histolytica* cysteine protease 2 (EhCP2) modulates leucocyte migration by proteolytic cleavage of chemokines," *Parasite Immunology*, vol. 26, no. 5, pp. 237–241, 2004.

[24] X. Que, S.-H. Kim, M. Sajid et al., "A surface amebic cysteine proteinase inactivates interleukin-18," *Infection and Immunity*, vol. 71, no. 3, pp. 1274–1280, 2003.

[25] Z. Zhang, L. Wang, K. B. Seydel et al., "*Entamoeba histolytica* cysteine proteinases with interleukin-1 beta converting enzyme (ICE) activity cause intestinal inflammation and tissue damage in amoebiasis," *Molecular Microbiology*, vol. 37, no. 3, pp. 542–548, 2000.

[26] C. A. Gilchrist and W. A. Petri Jr., "Virulence factors of *Entamoeba histolytica*," *Current Opinion in Microbiology*, vol. 2, no. 4, pp. 433–437, 1999.

[27] Y. Hou, L. Mortimer, and K. Chadee, "*Entamoeba histolytica* cysteine proteinase 5 binds integrin on colonic cells and stimulates NFκB-mediated pro-inflammatory responses," *The Journal of Biological Chemistry*, vol. 285, no. 46, pp. 35497–35504, 2010.

[28] H. Irmer, M. Tillack, L. Biller et al., "Major cysteine peptidases of *Entamoeba histolytica* are required for aggregation and digestion of erythrocytes but are dispensable for phagocytosis and cytopathogenicity," *Molecular Microbiology*, vol. 72, no. 3, pp. 658–667, 2009.

[29] A. Olivos-García, E. Tello, M. Nequiz-Avendaño et al., "Cysteine proteinase activity is required for survival of the parasite in experimental acute amoebic liver abscesses in hamsters," *Parasitology*, vol. 129, no. 1, pp. 19–25, 2004.

[30] I. Dey, K. Keller, A. Belley, and K. Chadee, "Identification and characterization of a cyclooxygenase-like enzyme from *Entamoeba histolytica*," *Proceedings of the National Academy of Sciences of the United States of America*, vol. 100, no. 23, pp. 13561–13566, 2003.

[31] R. Campos-Rodríguez, R. A. Jarillo-Luna, B. A. Larsen, V. Rivera-Aguilar, and J. Ventura-Juárez, "Invasive amebiasis: a microcirculatory disorder?" *Medical Hypotheses*, vol. 73, no. 5, pp. 687–697, 2009.

[32] J. L. Griffin, "Human amebic dysentery. Electron microscopy of *Entamoeba histolytica* contacting, ingesting, and digesting inflammatory cells," *American Journal of Tropical Medicine and Hygiene*, vol. 21, no. 6, pp. 895–906, 1972.

[33] F. Pittman, J. C. Pittman, and W. K. el-Hashimi, "Human amebiasis. Light and electron microscopy findings in colonic mucosal biopsies from patients with acute amebic colitis," in *Proceedings of the International Conference on Amebiasis*, B. Sepulveda and L. S. Diamond, Eds., pp. 398–417, Mexico City, Mexico, 1976.

[34] S. Blazquez, M.-C. Rigothier, M. Huerre, and N. Guillén, "Initiation of inflammation and cell death during liver abscess formation by *Entamoeba histolytica* depends on activity of the galactose/N-acetyl-d-galactosamine lectin," *International Journal for Parasitology*, vol. 37, no. 3-4, pp. 425–433, 2007.

[35] P. Tavares, M.-C. Rigothier, H. Khun, P. Roux, M. Huerre, and N. Guillén, "Roles of cell adhesion and cytoskeleton activity in *Entamoeba histolytica* pathogenesis: a delicate balance," *Infection and Immunity*, vol. 73, no. 3, pp. 1771–1778, 2005.

[36] J. Aguirre-García, "Histopathological peculiarities of the amebic lesion," *Archivos de Investigacion Medica*, vol. 1, supplement, pp. 147–156, 1970.

[37] K. Chadee and E. Meerovitch, "The pathogenesis of experimentally induced amebic liver abscess in the gerbil (Meriones unguiculatus)," *American Journal of Pathology*, vol. 117, no. 1, pp. 71–80, 1984.

[38] W. B. Lushbaugh, A. B. Kairalla, A. F. Hofbauer, and F. E. Pittman, "Sequential histopathology of cavitary liver abscess formation induced by axenically grown *Entamoeba histolytica*," *Archivos de Investigacion Medica*, vol. 11, no. 1, pp. 163–168, 1980.

[39] O. Berninghausen and M. Leippe, "Necrosis versus apoptosis as the mechanism of target cell death induced by *Entamoeba histolytica*," *Infection and Immunity*, vol. 65, no. 9, pp. 3615–3621, 1997.

[40] K. B. Seydel and S. L. Stanley Jr., "*Entamoeba histolytica* induces host cell death in amebic liver abscess by a non-fas-dependent, non-tumor necrosis factor alpha-dependent pathway of apoptosis," *Infection and Immunity*, vol. 66, no. 6, pp. 2980–2983, 1998.

[41] C. Velazquez, M. Shibayama-Salas, J. Aguirre-Garcia, V. Tsutsumi, and J. Calderon, "Role of neutrophils in innate resistance to *Entamoeba histolytica* liver infection in mice," *Parasite Immunology*, vol. 20, no. 6, pp. 255–262, 1998.

[42] A. Olivos-García, J. C. Carrero, E. Ramos et al., "Late experimental amebic liver abscess in hamster is inhibited by cyclosporine and N-acetylcysteine," *Experimental and Molecular Pathology*, vol. 82, no. 3, pp. 310–315, 2007.

[43] R. Perez-Tamayo, R. D. Martinez, I. Montfort, I. Becker, E. Tello, and R. Perez-Montfort, "Pathogenesis of acute experimental amebic liver abscess in hamsters," *Journal of Parasitology*, vol. 77, no. 6, pp. 982–988, 1991.

[44] R. Pérez-Tamayo, I. Montfort, A. O. García, E. Ramos, and C. B. Ostria, "Pathogenesis of acute experimental liver amebiasis," *Archives of Medical Research*, vol. 37, no. 2, pp. 203–209, 2006.

[45] R. B. I. Pérez-Tamayo, I. Montfort, and R. Pérez-Montfort, "Pathobiology of amebiasis," in *Amebiasis: Infection and Disease by Entamoeba Histolytica*, R. R. Krestchmer, Ed., pp. 123–157, CRC Press, Boca Raton, Fla, USA, 1990.

[46] S. L. Stanley Jr., "Pathophysiology of amoebiasis," *Trends in Parasitology*, vol. 17, no. 6, pp. 280–285, 2001.

[47] A. Olivos-García, E. Saavedra, E. Ramos-Martínez, M. Nequiz, and R. Pérez-Tamayo, "Molecular nature of virulence in *Entamoeba histolytica*," *Infection, Genetics and Evolution*, vol. 9, no. 6, pp. 1033–1037, 2009.

[48] E. Ramos, A. Olivos-García, M. Nequiz et al., "*Entamoeba histolytica*: apoptosis induced in vitro by nitric oxide species," *Experimental Parasitology*, vol. 116, no. 3, pp. 257–265, 2007.

[49] L. Mortimer and K. Chadee, "The immunopathogenesis of *Entamoeba histolytica*," *Experimental Parasitology*, vol. 126, no. 3, pp. 366–380, 2010.

[50] K. S. Ralston and W. A. Petri Jr., "Tissue destruction and invasion by *Entamoeba histolytica*," *Trends in Parasitology*, vol. 27, no. 6, pp. 254–263, 2011.

[51] J. Santi-Rocca, M.-C. Rigothier, and N. Guillén, "Host-microbe interactions and defense mechanisms in the development of amoebic liver abscesses," *Clinical Microbiology Reviews*, vol. 22, no. 1, pp. 65–75, 2009.

[52] J. Pacheco-Yépez, R. Campos-Rodríguez, M. Shibayama, J. Ventura-Juárez, J. Serrano-Luna, and V. Tsutsumi, "*Entamoeba histolytica*: production of nitric oxide and in situ activity of NADPH diaphorase in amebic liver abscess of hamsters," *Parasitology Research*, vol. 87, no. 1, pp. 49–56, 2001.

[53] J. Ramírez-Emiliano, A. González-Hernández, and S. Arias-Negrete, "Expression of inducible nitric oxide synthase mRNA and nitric oxide production during the development of liver abscess in hamster inoculated with *Entamoeba histolytica*," *Current Microbiology*, vol. 50, no. 6, pp. 299–308, 2005.

[54] J. Y. Lin and K. Chadee, "Macrophage cytotoxicity against *Entamoeba histolytica* trophozoites is mediated by nitric oxide from L-arginine," *Journal of Immunology*, vol. 148, no. 12, pp. 3999–4005, 1992.

[55] J.-Y. Lin, R. Seguin, K. Keller, and K. Chadee, "Tumor necrosis factor alpha augments nitric oxide-dependent macrophage cytotoxicity against *Entamoeba histolytica* by enhanced expression of the nitric oxide synthase gene," *Infection and Immunity*, vol. 62, no. 5, pp. 1534–1541, 1994.

[56] R. A. Jarillo-Luna, R. Campos-Rodríguez, and V. Tsutsumi, "*Entamoeba histolytica*: immunohistochemical study of hepatic amoebiasis in mouse. Neutrophils and nitric oxide as possible factors of resistance," *Experimental Parasitology*, vol. 101, no. 1, pp. 40–56, 2002.

[57] E. Ghadirian, S. D. Somerfield, and P. A. L. Kongshavn, "Susceptibility of *Entamoeba histolytica* to oxidants," *Infection and Immunity*, vol. 51, no. 1, pp. 263–267, 1986.

[58] H. W. Murray, S. B. Aley, and W. A. Scott, "Susceptibility of *Entamoeba histolytica* to oxygen intermediates," *Molecular and Biochemical Parasitology*, vol. 3, no. 6, pp. 381–391, 1981.

[59] R. A. Salata, R. D. Pearson, and J. I. Ravdin, "Interaction of human leukocytes and *Entamoeba histolytica*: killing of virulent amebae by the activated macrophage," *The Journal of Clinical Investigation*, vol. 76, no. 2, pp. 491–499, 1985.

[60] K. B. Seydel, S. J. Smith, and S. L. Stanley Jr., "Innate immunity to amebic liver abscess is dependent on gamma interferon and nitric oxide in a murine model of disease," *Infection and Immunity*, vol. 68, no. 1, pp. 400–402, 2000.

[61] R. Siman-Tov and S. Ankri, "Nitric oxide inhibits cysteine proteinases and alcohol dehydrogenase 2 of *Entamoeba histolytica*," *Parasitology Research*, vol. 89, no. 2, pp. 146–149, 2003.

[62] J. Santi-Rocca, S. Smith, C. Weber et al., "Endoplasmic reticulum stress-sensing mechanism is activated in *Entamoeba histolytica* upon treatment with nitric oxide," *PLoS ONE*, vol. 7, no. 2, Article ID e31777, 2012.

[63] P. Pacher, J. S. Beckman, and L. Liaudet, "Nitric oxide and peroxynitrite in health and disease," *Physiological Reviews*, vol. 87, no. 1, pp. 315–424, 2007.

[64] M.-H. Choi, D. Sajed, L. Poole et al., "An unusual surface peroxiredoxin protects invasive *Entamoeba histolytica* from oxidant attack," *Molecular and Biochemical Parasitology*, vol. 143, no. 1, pp. 80–89, 2005.

[65] M. A. Akbar, N. S. Chatterjee, P. Sen et al., "Genes induced by a high-oxygen environment in *Entamoeba histolytica*," *Molecular and Biochemical Parasitology*, vol. 133, no. 2, pp. 187–196, 2004.

[66] B. Loftus, I. Anderson, R. Davies et al., "The genome of the protist parasite *Entamoeba histolytica*," *Nature*, vol. 433, no. 7028, pp. 865–868, 2005.

[67] R. C. MacFarlane and U. Singh, "Identification of differentially expressed genes in virulent and nonvirulent Entamoeba species: potential implications for amebic pathogenesis," *Infection and Immunity*, vol. 74, no. 1, pp. 340–351, 2006.

[68] S. Goldstein and G. Merényi, "The chemistry of peroxynitrite: implications for biological activity," *Methods in Enzymology*, vol. 436, pp. 49–61, 2008.

[69] C. Szabó, H. Ischiropoulos, and R. Radi, "Peroxynitrite: biochemistry, pathophysiology and development of therapeutics," *Nature Reviews Drug Discovery*, vol. 6, no. 8, pp. 662–680, 2007.

[70] R. Radi, A. Denicola, B. Alvarez, G. Ferrer-Sueta, and H. Rubbo, "The biological chemistry of peroxynitrite," in *Nitric Oxide: Biology and Pathobiology*, L. J. Ignarro, Ed., pp. 57–82, Academic Press, San Diego, Calif, USA, 2000.

[71] M. E. Quintanar-Quintanar, A. Jarillo-Luna, V. Rivera-Aguilar et al., "Immunosuppressive treatment inhibits the development of amebic liver abscesses in hamsters," *Medical Science Monitor*, vol. 10, no. 9, pp. BR317–BR324, 2004.

[72] J.-M. Li and A. M. Shah, "Endothelial cell superoxide generation: regulation and relevance for cardiovascular pathophysiology," *American Journal of Physiology—Regulatory Integrative and Comparative Physiology*, vol. 287, no. 5, pp. R1014–R1030, 2004.

[73] W. Dröge, "Free radicals in the physiological control of cell function," *Physiological Reviews*, vol. 82, no. 1, pp. 47–95, 2002.

[74] W. Wang, K. Keller, and K. Chadee, "*Entamoeba histolytica* modulates the nitric oxide synthase gene and nitric oxide production by macrophages for cytotoxicity against amoebae and tumour cells," *Immunology*, vol. 83, no. 4, pp. 601–610, 1994.

[75] S. Moncada, "Nitric oxide: discovery and impact on clinical medicine," *Journal of the Royal Society of Medicine*, vol. 92, no. 4, pp. 164–169, 1999.

[76] Y. Xia and J. L. Zweier, "Superoxide and peroxynitrite generation from inducible nitric oxide synthase in macrophages," *Proceedings of the National Academy of Sciences of the United States of America*, vol. 94, no. 13, pp. 6954–6958, 1997.

[77] J. E. Albina, M. D. Caldwell, W. L. Henry Jr., and C. D. Mills, "Regulation of macrophage functions by L-arginine," *Journal of Experimental Medicine*, vol. 169, no. 3, pp. 1021–1029, 1989.

[78] J. E. Albina, W. L. Henry Jr., B. Mastrofrancesco, B.-A. Martin, and J. S. Reichner, "Macrophage activation by culture in an anoxic environment," *Journal of Immunology*, vol. 155, no. 9, pp. 4391–4396, 1995.

[79] J. E. Albina, C. D. Mills, W. L. Henry Jr., and M. D. Caldwell, "Regulation of macrophage physiology by L-arginine: role of the oxidative L-arginine deiminase pathway," *Journal of Immunology*, vol. 143, no. 11, pp. 3641–3646, 1989.

[80] J. E. Albina, C. D. Mills, W. L. Henry Jr., and M. D. Caldwell, "Temporal expression of different pathways of l-arginine metabolism in healing wounds," *Journal of Immunology*, vol. 144, no. 10, pp. 3877–3880, 1990.

[81] M. A. Robinson, J. E. Baumgardner, V. P. Good, and C. M. Otto, "Physiological and hypoxic O_2 tensions rapidly regulate NO production by stimulated macrophages," *American Journal of Physiology—Cell Physiology*, vol. 294, no. 4, pp. C1079–C1087, 2008.

[82] C. Peyssonnaux, V. Datta, T. Cramer et al., "HIF-1α expression regulates the bactericidal capacity of phagocytes," *The Journal of Clinical Investigation*, vol. 115, no. 7, pp. 1806–1815, 2005.

[83] V. Nizet and R. S. Johnson, "Interdependence of hypoxic and innate immune responses," *Nature Reviews Immunology*, vol. 9, no. 9, pp. 609–617, 2009.

[84] K. Krotova, J. M. Patel, E. R. Block, and S. Zharikov, "Hypoxic upregulation of arginase II in human lung endothelial cells," *American Journal of Physiology—Cell Physiology*, vol. 299, no. 6, pp. C1541–C1548, 2010.

[85] W. Durante, F. K. Johnson, and R. A. Johnson, "Arginase: a critical regulator of nitric oxide synthesis and vascular function," *Clinical and Experimental Pharmacology and Physiology*, vol. 34, no. 9, pp. 906–911, 2007.

[86] Y. Xia, V. L. Dawson, T. M. Dawson, S. H. Snyder, and J. L. Zweier, "Nitric oxide synthase generates superoxide and nitric oxide in arginine-depleted cells leading to peroxynitrite-mediated cellular injury," *Proceedings of the National Academy of Sciences of the United States of America*, vol. 93, no. 13, pp. 6770–6774, 1996.

[87] G. E. Arteel, M. B. Kadiiska, I. Rusyn et al., "Oxidative stress occurs in perfused rat liver at low oxygen tension by mechanisms involving peroxynitrite," *Molecular Pharmacology*, vol. 55, no. 4, pp. 708–715, 1999.

[88] C. Szabó, "Pathopysiological roles of nitric oxide in inflammation," in *Nitric Oxide: Biology and Pathobiology*, L. J. Ignarro, Ed., pp. 841–872, Academic Press, San Diego, Calif, USA, 2000.

[89] Y. Gao, "The multiple actions of NO," *Pflugers Archiv—European Journal of Physiology*, vol. 459, no. 6, pp. 829–839, 2010.

[90] G. E. Arteel, K. Briviba, and H. Sies, "Protection against peroxynitrite," *FEBS Letters*, vol. 445, no. 2-3, pp. 226–230, 1999.

[91] L.-O. Klotz and H. Sies, "Defenses against peroxynitrite: selenocompounds and flavonoids," *Toxicology Letters*, vol. 140-141, pp. 125–132, 2003.

[92] D. G. Arias, E. L. Regner, A. A. Iglesias, and S. A. Guerrero, "*Entamoeba histolytica* thioredoxin reductase: molecular and functional characterization of its atypical properties," *Biochimica et Biophysica Acta*, vol. 1820, pp. 1859–1866, 2012.

[93] L. Ignarro, "Introduction and overview," in *Nitric Oxide: Biology and Pathobiology*, L. Ignarro, Ed., pp. 3–19, Academic Press, San Diego, Calif, USA, 2000.

[94] J. R. Lancaster Jr., "Simulation of the diffusion and reaction of endogenously produced nitric oxide," *Proceedings of the National Academy of Sciences of the United States of America*, vol. 91, no. 17, pp. 8137–8141, 1994.

[95] X. Liu, Q. Yan, K. L. Baskerville, and J. L. Zweier, "Estimation of nitric oxide concentration in blood for different rates of generation: evidence that intravascular nitric oxide levels are too low to exert physiological effects," *The Journal of Biological Chemistry*, vol. 282, no. 12, pp. 8831–8836, 2007.

[96] X. Liu, M. J. S. Miller, M. S. Joshi, D. D. Thomas, and J. R. Lancaster Jr., "Accelerated reaction of nitric oxide with O_2 within the hydrophobic interior of biological membranes," *Proceedings of the National Academy of Sciences of the United States of America*, vol. 95, no. 5, pp. 2175–2179, 1998.

[97] K. L. Davis, E. Martin, I. V. Turko, and F. Murad, "Novel effects of nitric oxide," *Annual Review of Pharmacology and Toxicology*, vol. 41, pp. 203–236, 2001.

[98] G. Rico, E. Leandro, S. Rojas, J. A. Giménez, and R. R. Kretschmer, "The monocyte locomotion inhibitory factor produced by *Entamoeba histolytica* inhibits induced nitric oxide production in human leukocytes," *Parasitology Research*, vol. 90, no. 4, pp. 264–267, 2003.

[99] K. Elnekave, R. Siman-Tov, and S. Ankri, "Consumption of L-arginine mediated by *Entamoeba histolytica* L-arginase (EhArg) inhibits amoebicidal activity and nitric oxide production by activated macrophages," *Parasite Immunology*, vol. 25, no. 11-12, pp. 597–608, 2003.

[100] D. G. Arias, C. E. Gutierrez, A. A. Iglesias, and S. A. Guerrero, "Thioredoxin-linked metabolism in *Entamoeba histolytica*," *Free Radical Biology and Medicine*, vol. 42, no. 10, pp. 1496–1505, 2007.

[101] S. G. Rhee, H. Z. Chae, and K. Kim, "Peroxiredoxins: a historical overview and speculative preview of novel mechanisms and emerging concepts in cell signaling," *Free Radical Biology and Medicine*, vol. 38, no. 12, pp. 1543–1552, 2005.

[102] E. S. J. Arnér, "Focus on mammalian thioredoxin reductases—important selenoproteins with versatile functions," *Biochimica et Biophysica Acta*, vol. 1790, no. 6, pp. 495–526, 2009.

[103] C. H. Williams Jr., L. D. Arscott, S. Müller et al., "Thioredoxin reductase: two modes of catalysis have evolved," *European Journal of Biochemistry*, vol. 267, no. 20, pp. 6110–6117, 2000.

[104] A. Holmgren and J. Lu, "Thioredoxin and thioredoxin reductase: current research with special reference to human disease," *Biochemical and Biophysical Research Communications*, vol. 396, no. 1, pp. 120–124, 2010.

[105] D. G. Arias, P. G. Carranza, H. D. Lujan, A. A. Iglesias, and S. A. Guerrero, "Immunolocalization and enzymatic functional characterization of the thioredoxin system in *Entamoeba histolytica*," *Free Radical Biology and Medicine*, vol. 45, no. 1, pp. 32–39, 2008.

[106] M. K. Sawyer, J. M. Bischoff, M. A. Guidry, and R. E. Reeves, "Lipids from *Entamoeba histolytica*," *Experimental Parasitology*, vol. 20, no. 3, pp. 295–302, 1967.

[107] H. Z. Chae, S. J. Chung, and S. G. Rhee, "Thioredoxin-dependent peroxide reductase from yeast," *The Journal of Biological Chemistry*, vol. 269, no. 44, pp. 27670–27678, 1994.

[108] Z. A. Wood, E. Schröder, J. Robin Harris, and L. B. Poole, "Structure, mechanism and regulation of peroxiredoxins," *Trends in Biochemical Sciences*, vol. 28, no. 1, pp. 32–40, 2003.

[109] E. Schroder, J. A. Littlechild, A. A. Lebedev, N. Errington, A. A. Vagin, and M. N. Isupov, "Crystal structure of decameric 2-cys peroxiredoxin from human erythrocytes at 1.7 a resolution," *Structure*, vol. 8, pp. 605–615, 2000.

[110] A. S. Ghosh, S. Dutta, and S. Raha, "Hydrogen peroxide-induced apoptosis-like cell death in *Entamoeba histolytica*," *Parasitology International*, vol. 59, no. 2, pp. 166–172, 2010.

[111] I. Bruchhaus, S. Richter, and E. Tannich, "Removal of hydrogen peroxide by the 29 kDa protein of *Entamoeba histolytica*," *Biochemical Journal*, vol. 326, part 3, pp. 785–789, 1997.

[112] B. M. Flores, M. A. Batzer, M. A. Stein, C. Petersen, D. L. Diedrich, and B. E. Torian, "Structural analysis and demonstration of the 29 kDa antigen of pathogenic *Entamoeba histolytica* as the major accessible free thiol-containing surface protein," *Molecular Microbiology*, vol. 7, no. 5, pp. 755–763, 1993.

[113] B. M. Flores, S. L. Reed, J. I. Ravdin, and B. E. Torian, "Serologic reactivity to purified recombinant and native 29-kilodalton peripheral membrane protein of pathogenic *Entamoeba histolytica*," *Journal of Clinical Microbiology*, vol. 31, no. 6, pp. 1403–1407, 1993.

[114] X.-J. Cheng, E. Yoshihara, T. Takeuchi, and H. Tachibana, "Molecular characterization of peroxiredoxin from Entamoeba moshkovskii and a comparison with *Entamoeba histolytica*," *Molecular and Biochemical Parasitology*, vol. 138, no. 2, pp. 195–203, 2004.

[115] L. B. Poole, H. Z. Chae, B. M. Flores, S. L. Reed, S. G. Rhee, and B. E. Torian, "Peroxidase activity of a TSA-like antioxidant protein from a pathogenic amoeba," *Free Radical Biology and Medicine*, vol. 23, no. 6, pp. 955–959, 1997.

[116] P. H. Davis, X. Zhang, J. Guo, R. R. Townsend, and S. L. Stanley Jr., "Comparative proteomic analysis of two *Entamoeba histolytica* strains with different virulence phenotypes identifies peroxiredoxin as an important component of amoebic virulence," *Molecular Microbiology*, vol. 61, no. 6, pp. 1523–1532, 2006.

[117] E. Ramos-Martínez, A. Olivos-García, E. Saavedra et al., "*Entamoeba histolytica*: oxygen resistance and virulence," *International Journal for Parasitology*, vol. 39, no. 6, pp. 693–702, 2009.

[118] A. Sen, N. S. Chatterjee, M. A. Akbar, N. Nandi, and P. Das, "The 29-kilodalton thiol-dependent peroxidase of *Entamoeba histolytica* is a factor involved in pathogenesis and survival of the parasite during oxidative stress," *Eukaryotic Cell*, vol. 6, no. 4, pp. 664–673, 2007.

[119] I. Bruchhaus, T. Roeder, H. Lotter, M. Schwerdtfeger, and E. Tannich, "Differential gene expression in *Entamoeba histolytica* isolated from amoebic liver abscess," *Molecular Microbiology*, vol. 44, no. 4, pp. 1063–1072, 2002.

[120] E. R. Houpt, D. J. Glembocki, T. G. Obrig et al., "The mouse model of amebic colitis reveals mouse strain susceptibility to infection and exacerbation of disease by $CD4^+$ T cells," *Journal of Immunology*, vol. 169, no. 8, pp. 4496–4503, 2002.

[121] J. Santi-Rocca, C. Weber, G. Guigon, O. Sismeiro, J.-Y. Coppée, and N. Guillén, "The lysine- and glutamic acid-rich protein KERP1 plays a role in *Entamoeba histolytica* liver abscess pathogenesis," *Cellular Microbiology*, vol. 10, no. 1, pp. 202–217, 2008.

[122] B. Jiménez-Delgadillo, P. P. Chaudhuri, L. Baylón-Pacheco, A. López-Monteon, P. Talamás-Rohana, and J. L. Rosales-Encina, "*Entamoeba histolytica*: cDNAs cloned as 30 kDa collagen-binding proteins (CBP) belong to an antioxidant molecule family. Protection of hamsters from amoebic liver abscess by immunization with recombinant CBP," *Experimental Parasitology*, vol. 108, no. 1-2, pp. 7–17, 2004.

[123] M. C. González-Vázquez, A. Carabarin-Lima, L. Baylón-Pacheco, P. Talamás-Rohana, and J. L. Rosales-Encina, "Obtaining of three recombinant antigens of *Entamoeba histolytica* and evaluation of their immunogenic ability without adjuvant in a hamster model of immunoprotection," *Acta Tropica*, vol. 122, no. 2, pp. 169–176, 2012.

[124] C.-J. G. Soong, B. E. Torian, M. D. Abd-Alla, T. F. H. G. Jackson, V. Gatharim, and J. I. Ravdin, "Protection of gerbils from amebic liver abscess by immunization with recombinant *Entamoeba histolytica* 29-kilodalton antigen," *Infection and Immunity*, vol. 63, no. 2, pp. 472–477, 1995.

[125] Z. A. Wood, L. B. Poole, R. R. Hantgan, and P. A. Karplus, "Dimers to doughnuts: redox-sensitive oligomerization of 2-cysteine peroxiredoxins," *Biochemistry*, vol. 41, no. 17, pp. 5493–5504, 2002.

[126] J. R. Harris, E. Schröder, M. N. Isupov et al., "Comparison of the decameric structure of peroxiredoxin-II by transmission electron microscopy and X-ray crystallography," *Biochimica et Biophysica Acta*, vol. 1547, no. 2, pp. 221–234, 2001.

[127] R. Bryk, P. Griffin, and C. Nathan, "Peroxynitrite reductase activity of bacterial peroxiredoxins," *Nature*, vol. 407, no. 6801, pp. 211–215, 2000.

[128] M. Trujillo, H. Budde, M. D. Piñeyro et al., "Trypanosoma brucei and Trypanosoma cruzi tryparedoxin peroxidases catalytically detoxify peroxynitrite via oxidation of fast reacting thiols," *The Journal of Biological Chemistry*, vol. 279, no. 33, pp. 34175–34182, 2004.

[129] M. Trujillo, G. Ferrer-Sueta, and R. Radi, "Kinetic studies on peroxynitrite reduction by peroxiredoxins," *Methods in Enzymology*, vol. 441, pp. 173–196, 2008.

[130] M. Dubuisson, D. Vander Stricht, A. Clippe et al., "Human peroxiredoxin 5 is a peroxynitrite reductase," *FEBS Letters*, vol. 571, no. 1–3, pp. 161–165, 2004.

[131] H. Tachibana, S. Kobayashi, Y. Kato, K. Nagakura, Y. Kaneda, and T. Takeuchi, "Identification of a pathogenic isolate-specific 30,000-M(r) antigen of *Entamoeba histolytica* by using a monoclonal antibody," *Infection and Immunity*, vol. 58, no. 4, pp. 955–960, 1990.

[132] B. E. Torian, B. M. Flores, V. L. Stroeher, F. S. Hagen, and W. E. Stamm, "cDNA sequence analysis of a 29-kDa cysteine-rich surface antigen of pathogenic *Entamoeba histolytica*," *Proceedings of the National Academy of Sciences of the United States of America*, vol. 87, no. 16, pp. 6358–6362, 1990.

[133] S. L. Reed, B. M. Flores, M. A. Batzer et al., "Molecular and cellular characterization of the 29-kilodalton peripheral membrane protein of *Entamoeba histolytica*: differentiation between pathogenic and nonpathogenic isolates," *Infection and Immunity*, vol. 60, no. 2, pp. 542–549, 1992.

[134] J. O. Andersson, R. P. Hirt, P. G. Foster, and A. J. Roger, "Evolution of four gene families with patchy phylogenetic distributions: influx of genes into protist genomes," *BMC Evolutionary Biology*, vol. 6, article 27, 2006.

[135] A. di Matteo, F. M. Scandurra, F. Testa et al., "The O_2-scavenging flavodiiron protein in the human parasite Giardia intestinalis," *The Journal of Biological Chemistry*, vol. 283, no. 7, pp. 4061–4068, 2008.

[136] P. Sarti, P. L. Fiori, E. Forte et al., "Trichomonas vaginalis degrades nitric oxide and expresses a flavorubredoxin-like protein: a new pathogenic mechanism?" *Cellular and Molecular Life Sciences*, vol. 61, no. 5, pp. 618–623, 2004.

[137] J. B. Vicente, F. Testa, D. Mastronicola et al., "Redox properties of the oxygen-detoxifying flavodiiron protein from the human parasite Giardia intestinalis," *Archives of Biochemistry and Biophysics*, vol. 488, no. 1, pp. 9–13, 2009.

[138] T. Smutná, V. L. Gonçalves, L. M. Saraiva, J. Tachezy, M. Teixeira, and I. Hrdý, "Flavodiiron protein from Trichomonas vaginalis hydrogenosomes: the terminal oxygen reductase," *Eukaryotic Cell*, vol. 8, no. 1, pp. 47–55, 2009.

[139] J. B. Vicente, M. A. Carrondo, M. Teixeira, and C. Frazão, "Structural studies on flavodiiron proteins," *Methods in Enzymology*, vol. 437, pp. 3–19, 2008.

[140] C. M. Gomes, A. Giuffrè, E. Forte et al., "A novel type of nitric-oxide reductase: Escherichia coli flavorubredoxin," *The Journal of Biological Chemistry*, vol. 277, no. 28, pp. 25273–25276, 2002.

[141] J. B. Vicente, V. Tran, L. Pinto, M. Teixeira, and U. Singh, "A detoxifying oxygen reductase in the anaerobic protozoan *Entamoeba histolytica*," *Eukaryotic Cell*, vol. 11, pp. 1112–1118, 2012.

[142] V. Tsutsumi, A. Ramirez-Rosales, H. Lanz-Mendoza et al., "*Entamoeba histolytica*: erythrophagocytosis, collagenolysis, and liver abscess production as virulence markers," *Transactions of the Royal Society of Tropical Medicine and Hygiene*, vol. 86, no. 2, pp. 170–172, 1992.

[143] K. K. Hirata, X. Que, S. G. Melendez-Lopez et al., "A phagocytosis mutant of *Entamoeba histolytica* is less virulent due to deficient proteinase expression and release," *Experimental Parasitology*, vol. 115, no. 2, pp. 192–199, 2007.

[144] R. M. Mukherjee, K. C. Bhol, S. Mehra, T. K. Maitra, and K. N. Jalan, "Study of *Entamoeba histolytica* isolates from Calcutta with special reference to their zymodeme, animal pathogenicity and erythrophagocytosis," *Journal of Diarrhoeal Diseases Research*, vol. 9, no. 1, pp. 11–15, 1991.

[145] E. Orozco, G. Guarneros, A. Martinez-Palomo, and T. Sanchez, "*Entamoeba histolytica*. Phagocytosis as a virulence factor," *Journal of Experimental Medicine*, vol. 158, no. 5, pp. 1511–1521, 1983.

[146] L. A. Baxt and U. Singh, "New insights into *Entamoeba histolytica* pathogenesis," *Current Opinion in Infectious Diseases*, vol. 21, no. 5, pp. 489–494, 2008.

[147] B. L. Tekwani and R. K. Mehlotra, "Molecular basis of defence against oxidative stress in *Entamoeba histolytica* and Giardia lamblia," *Microbes and Infection*, vol. 1, no. 5, pp. 385–394, 1999.

[148] R. Bracha and D. Mirelman, "Virulence of *Entamoeba histolytica* trophozoites. Effects of bacteria, microaerobic conditions, and metronidazole," *Journal of Experimental Medicine*, vol. 160, no. 2, pp. 353–368, 1984.

[149] D. Trissl, A. Martinez-Palomo, and M. de la Torre, "Surface properties of Entamoeba: increased rates of human erythrocyte phagocytosis in pathogenic strains," *Journal of Experimental Medicine*, vol. 148, no. 5, pp. 1137–1145, 1978.

[150] J. M. Galván-Moroyoqui, M. del Carmen Domínguez-Robles, E. Franco, and I. Meza, "The interplay between Entamoeba and enteropathogenic bacteria modulates epithelial cell damage," *PLoS Neglected Tropical Diseases*, vol. 2, no. 7, article e266, 2008.

[151] S. Koncarevic, P. Rohrbach, M. Deponte et al., "The malarial parasite Plasmodium falciparum imports the human protein peroxiredoxin 2 for peroxide detoxification," *Proceedings of the National Academy of Sciences of the United States of America*, vol. 106, no. 32, pp. 13323–13328, 2009.

[152] L. C. Pelosof, P. H. Davis, Z. Zhang, X. Zhang, and S. L. Stanley Jr., "Co-ordinate but disproportionate activation of apoptotic, regenerative and inflammatory pathways characterizes the liver response to acute amebic infection," *Cellular Microbiology*, vol. 8, no. 3, pp. 508–522, 2006.

[153] A. Olivos-García, M. Nequiz-Avendaño, E. Tello et al., "Inflammation, complement, ischemia and amoebic survival in acute experimental amoebic liver abscesses in hamsters," *Experimental and Molecular Pathology*, vol. 77, no. 1, pp. 66–71, 2004.

[154] A. Cabassi, E. C. Dumont, H. Girouard et al., "Effects of chronic N-acetylcysteine treatment on the actions of peroxynitrite on aortic vascular reactivity in hypertensive rats," *Journal of Hypertension*, vol. 19, no. 7, pp. 1233–1244, 2001.

[155] M. Zafarullah, W. Q. Li, J. Sylvester, and M. Ahmad, "Molecular mechanisms of N-acetylcysteine actions," *Cellular and Molecular Life Sciences*, vol. 60, no. 1, pp. 6–20, 2003.

[156] R. Campos-Rodríguezp and A. Jarillo-Luna, "The pathogenicity of *Entamoeba histolytica* is related to the capacity of evading innate immunity," *Parasite Immunology*, vol. 27, no. 1-2, pp. 1–8, 2005.

[157] M.-C. Rigothier, H. Khun, P. Tavares, A. Cardona, M. Huerre, and N. Guillén, "Fate of *Entamoeba histolytica* during establishment of amoebic liver abscess analyzed by quantitative radioimaging and histology," *Infection and Immunity*, vol. 70, no. 6, pp. 3208–3215, 2002.

[158] E. Helk, H. Bernin, T. Ernst et al., "Tnfalpha-mediated liver destruction by kupffer cells and ly6chi monocytes during *Entamoeba histolytica* infection," *PLoS Pathogens*, vol. 9, Article ID e1003096, 2013.

[159] C. Maldonado-Bernal, C. J. Kirschning, Y. Rosenstein et al., "The innate immune response to *Entamoeba histolytica* lipopeptidophosphoglycan is mediated by toll-like receptors 2 and 4," *Parasite Immunology*, vol. 27, no. 4, pp. 127–137, 2005.

[160] M. Sharma, H. Vohra, and D. Bhasin, "Enhanced pro-inflammatory chemokine/cytokine response triggered by pathogenic *Entamoeba histolytica*: basis of invasive disease," *Parasitology*, vol. 131, no. 6, pp. 783–796, 2005.

[161] R. Perez-Tamayo, I. Montfort, E. Tello, and A. Olivos, "Ischemia in experimental acute amebic liver abscess in hamsters," *International Journal for Parasitology*, vol. 22, no. 1, pp. 125–129, 1992.

[162] X. Forceville, D. Vitoux, R. Gauzit, A. Combes, P. Lahilaire, and P. Chappuis, "Selenium, systemic immune response syndrome, sepsis, and outcome in critically ill patients," *Critical Care Medicine*, vol. 26, no. 9, pp. 1536–1544, 1998.

[163] R. F. Burk and K. E. Hill, "Selenoprotein P: an extracellular protein with unique physical characteristics and a role in selenium homeostasis," *Annual Review of Nutrition*, vol. 25, pp. 215–235, 2005.

[164] L. H. Duntas, "Selenium and inflammation: underlying anti-inflammatory mechanisms," *Hormone and Metabolic Research*, vol. 41, no. 6, pp. 443–447, 2009.

[165] L. V. Papp, J. Lu, A. Holmgren, and K. K. Khanna, "From selenium to selenoproteins: synthesis, identity, and their role in human health," *Antioxidants and Redox Signaling*, vol. 9, no. 7, pp. 775–806, 2007.

[166] T. Bosschaerts, M. Guilliams, W. Noel et al., "Alternatively activated myeloid cells limit pathogenicity associated with African trypanosomiasis through the IL-10 inducible gene selenoprotein P," *Journal of Immunology*, vol. 180, no. 9, pp. 6168–6175, 2008.

[167] Z. Huang, A. H. Rose, and P. R. Hoffmann, "The role of selenium in inflammation and immunity: from molecular mechanisms to therapeutic opportunities," *Antioxidants and Redox Signaling*, vol. 16, no. 7, pp. 705–743, 2012.

[168] K. Renko, P. J. Hofmann, M. Stoedter et al., "Down-regulation of the hepatic selenoprotein biosynthesis machinery impairs selenium metabolism during the acute phase response in mice," *The FASEB Journal*, vol. 23, no. 6, pp. 1758–1765, 2009.

[169] K. Becker, S. Gromer, R. H. Schirmer, and S. Müller, "Thioredoxin reductase as a pathophysiological factor and drug target," *European Journal of Biochemistry*, vol. 267, no. 20, pp. 6118–6125, 2000.

[170] A. Debnath, D. Parsonage, R. M. Andrade et al., "A high-throughput drug screen for *Entamoeba histolytica* identifies a new lead and target," *Nature Medicine*, vol. 18, no. 6, pp. 956–960, 2012.

[171] O. Rackham, A.-M. J. Shearwood, R. Thyer et al., "Substrate and inhibitor specificities differ between human cytosolic and mitochondrial thioredoxin reductases: implications for development of specific inhibitors," *Free Radical Biology and Medicine*, vol. 50, no. 6, pp. 689–699, 2011.

[172] A. Bindoli, M. P. Rigobello, G. Scutari, C. Gabbiani, A. Casini, and L. Messori, "Thioredoxin reductase: a target for gold compounds acting as potential anticancer drugs," *Coordination Chemistry Reviews*, vol. 253, no. 11-12, pp. 1692–1707, 2009.

[173] C. F. Shaw III, "Gold-based therapeutic agents," *Chemical Reviews*, vol. 99, no. 9, pp. 2589–2600, 1999.

Hindawi Publishing Corporation
BioMed Research International
Volume 2014, Article ID 209163, 11 pages
http://dx.doi.org/10.1155/2014/209163

Research Article

Strain-Dependent Induction of Human Enterocyte Apoptosis by *Blastocystis* Disrupts Epithelial Barrier and ZO-1 Organization in a Caspase 3- and 9-Dependent Manner

Zhaona Wu, Haris Mirza, Joshua D. W. Teo, and Kevin S. W. Tan

Laboratory of Molecular and Cellular Parasitology, Department of Microbiology, Yong Loo Lin School of Medicine, National University of Singapore, 5 Science, Drive 2, Singapore 117596

Correspondence should be addressed to Kevin S. W. Tan; kevin_tan@nuhs.edu.sg

Received 21 November 2013; Accepted 4 March 2014; Published 14 April 2014

Academic Editor: Marlene Benchimol

Blastocystis is an emerging protistan parasite colonizing the human intestine. It is frequently reported to cause general intestinal symptoms of vomiting, diarrhea, and abdominal pain. We recently demonstrated that *Blastocystis* rearranged cytoskeletal proteins and induced intestinal epithelial barrier compromise. The effect of *Blastocystis* on enterocyte apoptosis is unknown, and a possible link between microbially induced enterocyte apoptosis and increased epithelial permeability has yet to be determined. The aim of this study is to assess if *Blastocystis* induces human enterocyte apoptosis and whether this effect influences human intestinal epithelial barrier function. Monolayers of polarized human colonic epithelial cell-line Caco-2 were incubated with *Blastocystis* subtype 7 and subtype 4. Assays for both early and late markers of apoptosis, phosphatidylserine externalization, and nuclear fragmentation, respectively, showed that *Blastocystis* ST-7, but not ST-4, significantly increased apoptosis in enterocytes, suggesting that *Blastocystis* exhibits host specificity and strain-to-strain variation in pathogenicity. ST-7 also activated Caco-2 caspases 3 and 9 but not 8. ST-7 induced changes in epithelial resistance, permeability, and tight junction (ZO-1) localization. Pretreatment of Caco-2 monolayers with a pan-caspase inhibitor z-VAD-fmk significantly inhibited these changes. This suggests a role for enterocyte apoptosis in *Blastocystis*-mediated epithelial barrier compromise in the human intestine.

1. Introduction

Blastocystis is an anaerobic protistan parasite of the gut [1–3]. It is a species complex comprising of 17 subtypes out of which at least 9 are known to infect humans [4]. Other common hosts are rats, pigs, and chickens [1]. It is one of the most common parasites found in humans [3] with prevalence ranging from 10% in developed countries to 50% in developing countries [3]. Infection with the parasite is associated with common intestinal symptoms of mucous and watery diarrhea, bloating, abdominal pain, and vomiting [3]. It has a higher prevalence in impoverished children [5] and patients immunocompromised due to HIV infection [6] or malignancy [7], suggesting opportunistic pathobiology [3]. It is often associated with irritable bowel syndrome [8–11] and urticaria [12, 13]. It is also considered one of the causes of traveler's diarrhea [14]. Chronic and recurrent infections are common despite prolonged antimicrobial treatment [13, 15]. Recent studies suggest that in some cases the parasite is also capable of epithelial invasion [16–19].

Despite being discovered more than 100 years ago [20, 21] as well as the recent advances in our understanding of this organism regarding its potential virulence factors and host responses [15, 22], its pathogenic potential remains controversial [4], owing to frequent reports of asymptomatic carriage, nonresponsiveness to chemotherapy, coinfections with other known pathogens, and high degree of genetic and pathobiological diversity within and across subtypes [23]. Strain-to-strain variation in virulence of the parasite has been reported in clinical and animal infection studies [8, 24, 25]. We recently reported that a subtype-7 (ST-7) isolate of *Blastocystis* recovered from a symptomatic patient exhibits higher cysteine protease and arginase activity (potential parasite virulence factors) compared to ST-4 isolates [15, 26].

ST-7 strain also exhibited higher immune evasion potential in inducing degradation of secretory IgAs and downregulation of epithelial antiparasitic nitric oxide production [15, 27]. However, direct evidence of comparative study in pathogenic effects of different *Blastocystis* strains on the host cells with a well-recognized host-pathogen interaction mode is still limited.

Modulation of intestinal epithelial barrier function is one of the major mechanisms employed by pathogens to induce host pathology [28]. Organisms ranging from viruses [29] to bacteria [30] as well as parasites such as *Giardia* [31] and *Entamoeba* [32] are known to compromise epithelial barrier function. Compromise of epithelium's barrier function exposes subepithelial tissue to toxic luminal contents [33], which could lead to dire consequences for the host. Interestingly, various luminal parasites sabotage this gate function by utilizing the apoptotic machinery of the host cell [34, 35]. Apoptosis or programmed cell death is a mechanism of clearing up unwanted cells by the body while simultaneously limiting overt immune response [36]. *Entamoeba* induces enterocyte apoptosis to facilitate the parasite infection of gut [37] while *Giardia* induces epithelial barrier compromise by activating caspase 3-mediated enterocyte programmed cell death [38]. There is ample evidence suggesting that *Blastocystis* causes intestinal epithelial barrier compromise in vitro and in vivo [22, 25, 39]. Rodent *Blastocystis* has been shown to induce caspase-mediated apoptosis, with no effect on the barrier function of rat intestinal epithelium [39]. An association of parasite-induced apoptosis with disruption of epithelial barrier function, as observed in *Giardia* and *Entamoeba* infections, is not known in human intestinal epithelium.

By using a human intestinal Caco-2 cell line that has been well established as an in vitro model system to study *Blastocystis*-host interaction [4, 15, 22], we report for the first time that *Blastocystis* subtype 7 (ST-7; isolate B), recovered from a symptomatic patient, induces breakdown of epithelial barrier function and caspase-3- and 9-mediated apoptosis and rearrangement of the tight junction associated protein ZO-1. In contrast, a subtype recovered from a rat (ST-4; isolate WR-1), previously reported to induce rat epithelial injury [39], did not cause any pathology in human epithelium. In this study, caspase inhibition in human gut epithelium prevented the effect of parasite on barrier dysfunction. This contrasts with the previous study involving rat epithelial cells, in which caspase inhibition did not rescue cells from barrier compromise [39].

2. Materials and Methods

2.1. Culture of Caco-2 Colonic Epithelial Cell Line. All *Blastocystis*-host interaction experiments were performed using Caco-2 human colonic cell line (ATCC). Caco-2 stock cultures were maintained in T-75 flasks in a humidified incubator with 5% CO_2 at 37°C. Cell cultures were grown in Dulbecco's modified Eagle's medium (HyClone) supplemented with 10% heat-inactivated fetal bovine serum (HyClone) and 1% each of sodium pyruvate, MEM, and antibiotic "Penstrep" (Gibco). Culture health was evaluated using the Trypan blue assay and only cultures with >95% viability were used for the experiments. Cells were trypsinized with 0.25% trypsin-EDTA. Cell cultures for western blotting experiments were grown on standard cell-culture 6-well plates (Corning). For confocal imaging, cells were cultured on poly-L-lysine treated 12 mm glass coverslips, placed in standard 6-well culture plates (Corning). Cell cultures for annexin-V-FITC apoptosis assay were grown on standard 24-well cell-culture plates (Corning). For transepithelial resistance (TER) and permeability experiments, cells were grown on Millipore transwell filters with PET membranes of 3 μm pore size placed in 24-well tissue culture plates. In order to synchronize cells before experiments, all cultures were serum-starved overnight in antibiotic free and serum free DMEM. For caspase inhibition experiments, cell cultures were pretreated with 40 μM broad-spectrum caspase inhibitor, z-VAD-fmk (Sigma) for 4 h. Cytochalasin D (Sigma) was used as a positive control for epithelial resistance and permeability experiments at a concentration of 1 μg/mL. Staurosporine was used as a positive control for apoptosis and ZO-1 rearrangement experiments at a concentration of 0.5 μM.

2.2. Parasite Culture and Lysate. Two axenized *Blastocystis* isolates belonging to different subtypes (ST) were used in this study. Isolate B, belonging to ST-7, was isolated from a symptomatic patient at the Singapore General Hospital [26], while isolate WR-1, belonging to ST-4, was isolated from a Wistar rat during an animal survey [26]. Both ST-7 and ST-4 represent zoonotic subtypes. They are frequently isolated from stool samples. ST-7 is often associated with intestinal symptoms and has been known to induce epithelial barrier disruption [8, 22]. Other than humans, common hosts for ST-7 and ST-4 isolates are birds and rats, respectively [40].

Parasite cultures were maintained in prereduced Iscove's modified Dulbecco's medium (IMDM) supplemented with 10% heat-inactivated horse serum. Cultures were kept under anaerobic conditions in an Anaerojar (Oxoid) with gas pack (Oxoid) at 37°C. Only log-phase cultures were harvested for lysate preparation. The cultures were washed twice in sterile PBS. Parasitic lysates were prepared by three freeze-thaw cycles in liquid nitrogen and 37°C water bath. Unless otherwise indicated, monolayers in all experiments were incubated with 10^8 parasite/mL lysate.

2.3. Epithelial Resistance. Transepithelial resistance (TER) across Caco-2 monolayer was measured using Millipore-ERS-2 Volt-Ohm-Meter. Caco-2 monolayers were grown on Millipore transwell system as described above and TER was measured every alternate day until it peaked (~ day 21; 1000 Ω/cm^2). *Blastocystis* ST-7 and *Blastocystis* ST-4 were coincubated with epithelium for 3, 6, 12, and 24 h. For dose-dependent experiments, monolayers were coincubated with 0.25 to 2×10^8 parasites/mL for 24 h. After incubation, monolayers were carefully washed twice with Hank's balanced salt solution (HBBS). 200 μL of warm media was added to the apical compartment before taking TER measurements.

All measurements were done at 37°C to minimize reading fluctuations.

2.4. Epithelial Permeability. Caco-2 monolayers were cultured on a transwell system as described earlier till they reach confluency and tight junction maturation on day 21. After confirmation of maturation by TER measurement, monolayers were coincubated with parasites for 24 h. Following coincubation, epithelial and basolateral compartments were washed twice, followed by addition of 400 μL of warm HBSS at the basolateral compartments and 200 μL of 100 μg/mL FITC-conjugated Dextran 4000 solution in HBSS to apical compartments. After 3 h, Dextran-FITC flux across monolayers was measured by transferring 300 μL of basolateral HBSS to a 96-well plate (corning) and measuring fluorescence using an ELISA reader (Tecan Infinite M200) at excitation and emission wavelengths of 492 and 518, respectively.

2.5. Flow Cytometry. Annexin-V binding assay was used to observe early apoptotic changes in Caco-2 cells. Caco-2 monolayers were grown in 24-well culture plates and coincubated with *Blastocystis* ST-7 or ST-4 for 3 h. Monolayers were then washed with PBS twice and then were trypsinized with 0.25% trypsin-EDTA, resuspended, and collected. Annexin-V-FITC apoptosis detection kit (BioVision) was used according to manufacturer's instructions. Propidium iodide (PI) was used to exclude necrotic cells. After cell staining, samples were analyzed using a flow cytometer (DakoCytomation; Cyan LX) at 488 nm excitation wavelength, with a 515 nm band-pass filter for fluorescein detection and a 600 nm filter for PI detection. The lower right quadrant was defined to represent the apoptotic cells showing annexin-V-FITC-positive and PI-negative staining.

2.6. Immunohistochemistry and Confocal Microscopy. Monolayers were incubated with *Blastocystis* for 6 h for immunohistochemical detection of ZO-1 rearrangements in Caco-2 cells. After coincubation, monolayers were washed twice and fixed with 2% (w/v) formaldehyde in PBS. Cells were then washed and incubated overnight with 1000 × dilution of primary antibody against ZO-1 tight junction protein (Sigma; 1 : 1000 in PBS) at 4°C. Monolayers were washed twice with PBS and incubated for 1 h with Cy3-tagged secondary antibody, followed by another round of washing. For DNA staining assay, monolayers were treated with parasites for 24 h, washed, and fixed as described above. After fixation, monolayers were washed and incubated with 10 μg/mL of cell-permeable DNA-stain Hoechst (Invitrogen) for 10 min and washed again. All monolayers were mounted on a glass slide using fluorescence mounting media (VECTASHIELD) before being observed under a confocal microscope (Olympus BX60; Olympus, Japan). The ImageJ software was used for image analysis.

2.7. Western Blots. For western blot analysis, Caco-2 monolayers were grown on 6-well cell-culture plates (corning) until 100% confluency. Monolayers were then incubated with 1 × 10^8 parasites/mL for 6 and 12 h, respectively, washed with PBS twice, and then scraped and collected. Monolayers were then incubated with RIPA lysis buffer supplemented with protease and phosphatase inhibitors (Pierce). Lysed samples were centrifuged at 21,000 rpm at 4°C for 30 minutes. Protein concentration of the supernatant was determined with the D_C Protein Assay (Bio-Rad Laboratories). SDS-PAGE gels (12% and 15% Tris-HCL Ready-Gels; Bio-Rad Laboratories) were used to separate total proteins. Proteins were then transferred using a polyvinylidene difluoride (PVDF) membrane (Immobilon-P; Millipore). 5% of nonfat dry milk in % TBS-T was then used to block the membranes. After blocking, membranes were incubated with primary antibodies against, caspase 3, caspase 8, caspase 9, or ZO-1 (1 : 1000; Sigma) overnight at 4°C. After incubation with primary antibodies, membranes were washed and incubated with HRP-tagged secondary antibodies. Bands were detected using Amersham ECL Plus western blotting detection system (GE Healthcare). Autoradiographic films (Kodak) were then exposed to the membranes and developed on *X-ray* film processor SRX-101A (Konica Minolta).

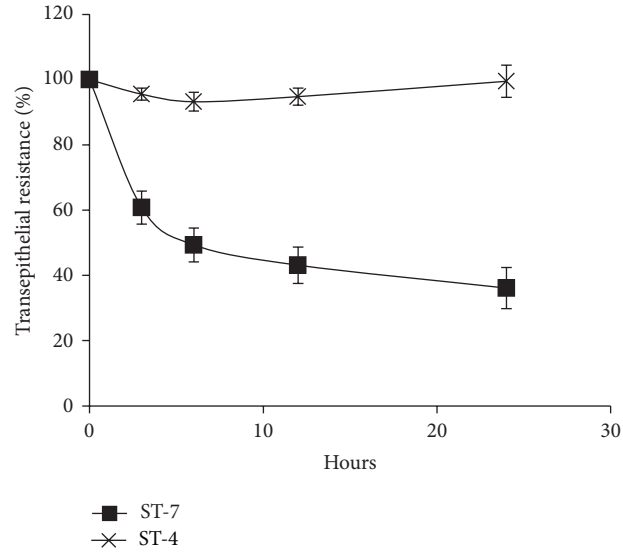

Figure 1: Time-dependent effect of *Blastocystis* ST-7 and ST-4 on the transepithelial resistance (TER) of Caco-2 cell monolayers. Confluent monolayers of Caco-2 cells were coincubated with ST-7 and ST-4 for the indicated times. TER was then measured as described in Section 2. ST-7 treated monolayers, compared to ST-4 and negative control, showed a significant drop in TER after 3, 6, 12, and 24 h (P value < 0.01). Values are means ± standard error (error bars) (n = 6).

2.8. Statistical Analysis. The ANOVA test was used to confirm the statistical significance of our results.

3. Results

3.1. Blastocystis ST-7 Decreases Transepithelial Resistance (TER) and Increases Permeability to FITC-Conjugated Dextran in Caco-2 Monolayers. Blastocystis ST-7, but not ST-4, induced a time-dependent drop in Caco-2 TER (Figure 1).

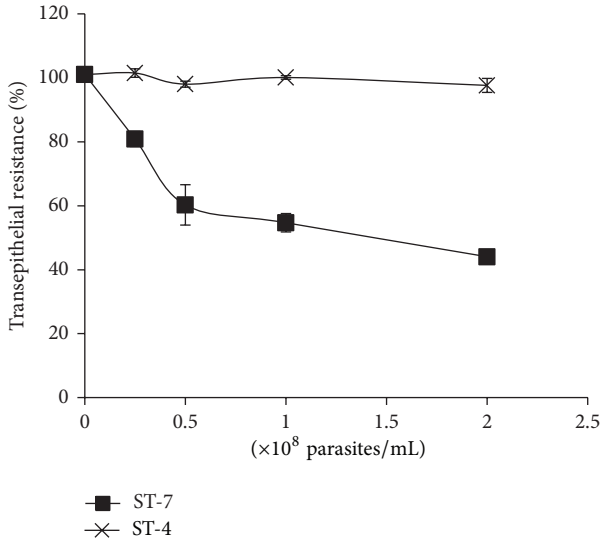

Figure 2: Dose-dependent effect of *Blastocystis* ST-4 and ST-7 on transepithelial resistant (TER) of Caco-2 cell monolayers. Confluent monolayers were coincubated with varying doses of ST-4 and ST-7 for 24 h. Compared to negative control, *Blastocystis* ST-7 induced a significant drop in Caco-2 TER at 0.25, 0.5, 1, and 2×10^8 parasite/mL (P value < 0.01). Values are mean ± standard error (error bars) (n = 6).

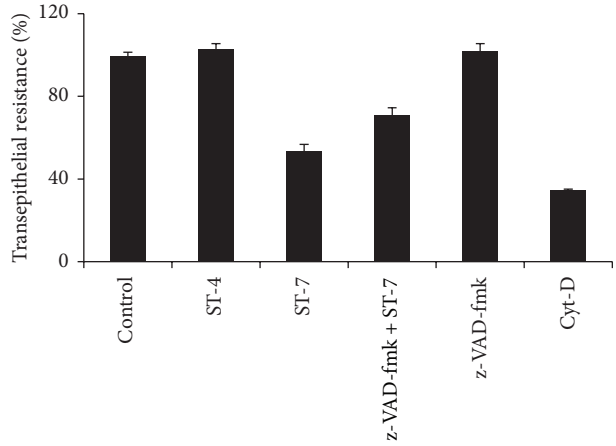

Figure 3: Effects of caspase inhibition on *Blastocystis* ST-7-induced decrease in transepithelial resistance (TER) of Caco-2 monolayers. Confluent monolayers of Caco-2 cells were coincubated for 24 h with ST-7 after pretreatment of cells with broad-spectrum caspase inhibitor z-VAD-fmk. Thereafter, TER was measured as described in Section 2. Pretreatment of Caco-2 cells with caspase inhibitor considerably rescued these cells from *Blastocystis* ST-7-induced effect (P value < 0.01). Cytochalasin D (Cyt-D) was used as a positive control in decreasing TER. Values are means ± standard error (error bars) (n = 6).

A significant drop in Caco-2 TER was observed as early as after 3 h of coincubation (P value < 0.01). ST-7 also exhibited a dose-dependent effect on TER (Figure 2). The minimum dose of 0.25×10^8/mL of ST-7 induced a significant drop in epithelial resistance (Figure 2). In order to confirm the parasite-mediated epithelial dysfunction suggested by drop in TER, we measured the flux of Dextran-FITC probe across Caco-2 monolayers (Figure 4). As expected, a significant increase in epithelial permeability was observed when 10^8 parasite/mL of ST-7 was coincubated with Caco-2 for 24 h (P value < 0.01) (Figure 4). On the other hand ST-4 did not cause a significant change in TER (Figures 1, 2, and 3) neither at the highest parasite dose (2×10^8) (Figure 2) nor after the longest coincubation period (24 h) (Figure 1). ST-4 did not induce increase in epithelial permeability to FITC-conjugated Dextran either (Figure 4). This suggests a strain-dependent variation in parasite-mediated Caco-2 barrier disruption.

3.2. *Blastocystis* ST-7 Induces Early and Late Apoptotic Changes in Caco-2 Cells

(i) PS-Flipping Indicated by Annexin-FITC Binding. One of the early indicators of apoptosis is the flipping of phosphatidylserine (PS) molecules from the inner to outer leaflet of the plasma membrane. A 35- to 36-kDa molecule, annexin-V, binds to PS with high specificity in the presence of calcium. Viable, apoptotic, and necrotic cells can be distinguished when FITC conjugated-annexin-V is used in conjunction

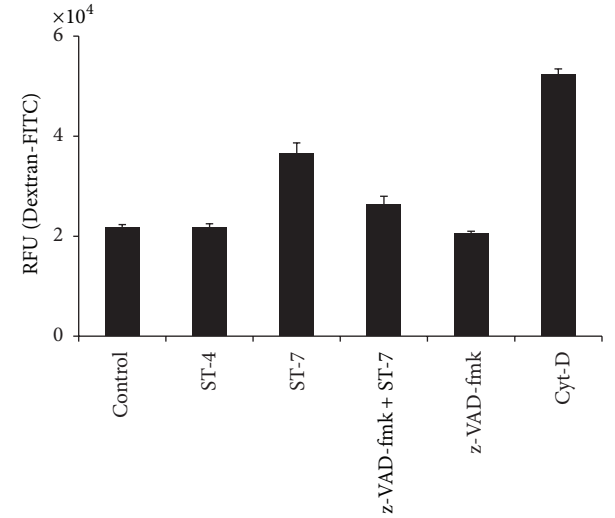

Figure 4: Flux measurement with FITC-conjugated Dextran. Confluent monolayers of Caco-2 cells were coincubated for 24 h with *Blastocystis* ST-4 or ST-7. Some monolayers were coincubated with ST-7 after pretreatment of cells with the broad-spectrum caspase inhibitor Z-VAD-fmk. Permeability was determined by measurement of Dextran-FITC fluxes across the monolayer as described in Section 2. A significant increase in the epithelial permeability can be noticed after incubation with ST-7, compared to negative control and ST-4 coincubation (P value < 0.01). Pretreatment of Caco-2 cells with caspase inhibitor significantly rescued these cells from *Blastocystis*-induced effect on permeability. Cytochalasin D (Cyt-D) was used as a positive control in inducing permeability increase. Values are means ± standard error (error bars) (n = 6).

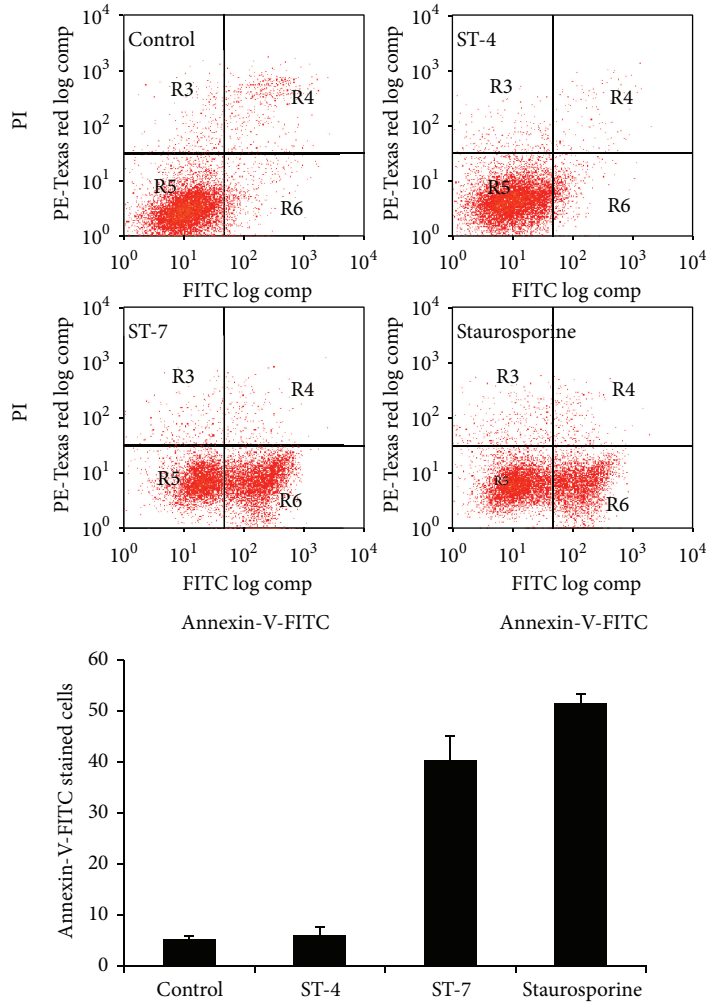

Figure 5: Flow cytometry analysis of annexin-V-FITC and propidium iodide staining. Representative dot plots of Caco-2 cells preincubated with culture media as negative control, *Blastocystis* ST-7, ST-4, and 0.5 μM staurosporine as positive control. 2×10^4 cells were analysed in each sample. Values represent mean ± standard error (error bars; $n = 3$). Caco-2 cells interacting with ST-7 exhibited significantly higher percentage of annexin-V^+ and PI^- cells (lower right quadrant) compared to cells coincubated with ST-4 or culture media only (P value < 0.01). Values are means ± standard error (error bars) ($n = 6$).

with PI. The lower right quadrants of the dot plots represent the apoptotic cell population, positive for annexin binding but PI negative (Figure 5). Upper quadrants represent necrotic cells due to permeability to PI (Figure 5). After interaction with *Blastocystis* ST-7, Caco-2 cells exhibited a significant rise in percentage of apoptotic cells compared to negative control and those interacting with ST-4 (P value < 0.01) (Figure 5). These findings are in agreement with a strain-dependent pathogenicity of the parasite.

(ii) Nuclear Fragmentation Indicated by Hoechst Staining [41]. One of the most distinctive features of apoptosis is morphological change in the nucleus, easily observed under florescence microscopy (Figure 6). After 24 h interaction with *Blastocystis* ST-7, nuclei of the Caco-2 cells exhibited nuclear condensation and fragmentation (Figure 6) typical of apoptotic cells. Significantly higher number of apoptotic cells was observed in membranes interacting with ST-7 compared to those with ST-4 (P value < 0.01) and negative control (P value < 0.01) (Figure 6).

3.3. Blastocystis ST-7 Induces Caspases 3 and 9 Activation in Caco-2 Cells. Caspases are proenzymes, which are activated by cleavage into active fragments in apoptotic cells. In this study, western blot analysis revealed that *Blastocystis* ST-7 coincubation with Caco-2, resulted in cleavage of Caco-2 caspases 3 and 9 (Figure 7). No cleavage of caspase 8 was observed even after 12 h interaction with ST-7 (Figure 7) suggesting that *Blastocystis* ST-7 induces Caco-2 programmed cell death by activation of the intrinsic apoptotic pathway. ST-4, as expected, did not activate any of the three caspases tested in this study (Figure 7).

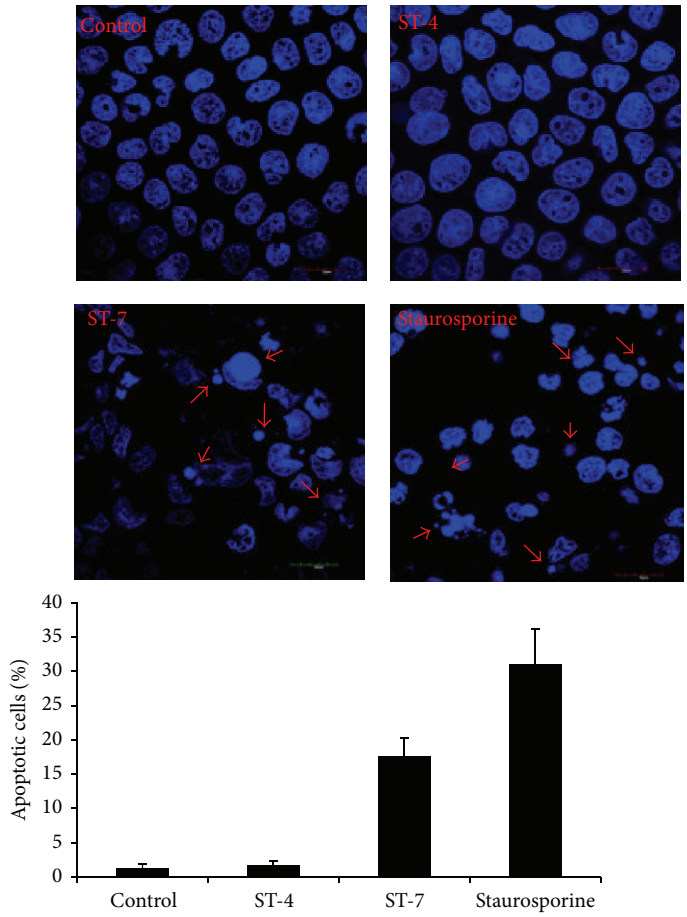

FIGURE 6: Representative fluorescence micrographs showing apoptosis of Caco-2 cells after DAPI staining. Cells were grown on glass coverslips and incubated for 24 h with culture media, ST-4, ST-7, or 0.5 μM staurosporine as positive control. Cells coincubated with ST-7 and staurosporine exhibit nuclear fragmentation and condensation (arrow) typical of apoptotic cells. Histogram represents percentage of apoptotic cells after DAPI fluorescence assay. Caco-2 monolayers coincubated with ST-7 exhibited significantly higher percentage of apoptosis (P value < 0.05) compared to ST-4 and negative control. Values are means ± standard error ($n = 6$ per group). For each sample, ~100 cells were counted at 1000x magnification.

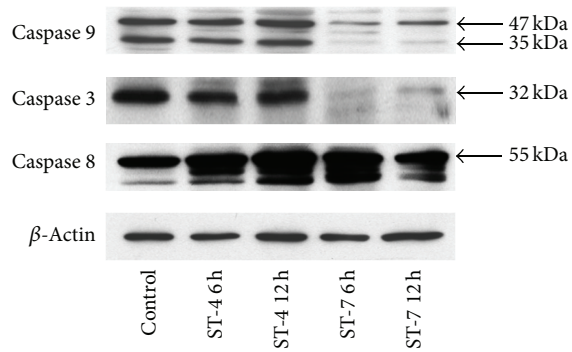

FIGURE 7: Western blot analysis of caspase activation (cleavage) in Caco-2 cells. Caco-2 cells were grown on cell-culture plates and harvested after coincubation with *Blastocystis* ST-4 and ST-7 for 6 and 12 h, as described in Section 2. Interaction with ST-7 resulted in loss of caspase 3 and caspase 9 bands suggesting activation, while caspase 8 remained unchanged. ST-4 did not cause any cleavage of caspases in Caco-2.

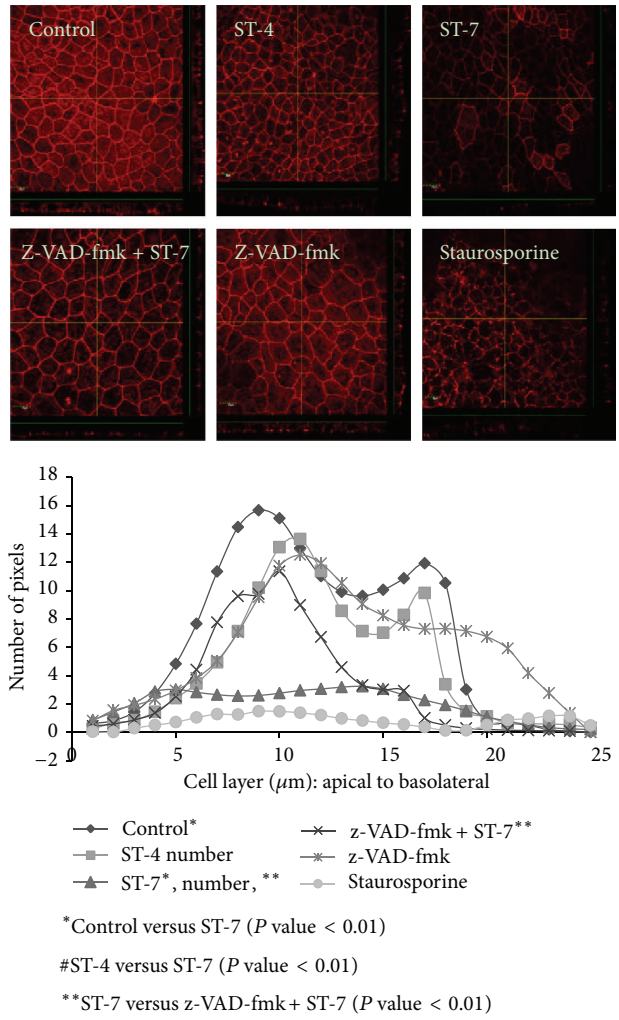

Figure 8: (a) Representative confocal micrographs illustrating ZO-1 distribution in Caco-2 monolayers. Monolayers were grown to confluence on poly-L-lysine treated coverslips. Caco-2 cells were then coincubated for 6 h with either *Blastocystis* ST-4 or ST-7. Some monolayers were treated with broad-spectrum caspase inhibitor z-VAD-fmk before coincubation with ST-7. Normal culture media and 0.5 μM staurosporine were used as negative and positive controls, respectively. Compared to negative control, ST-7 treatment resulted in obvious reduction in ZO-1 apical localization in Caco-2 cell line. ST-4 did not alter ZO-1 integrity. Pretreatment with z-VAD-fmk rescued ST-7-induced ZO-1 changes in the epithelium. (b) Quantification of ZO-1 staining is shown as graphs. Each cell layer (1–25) corresponds to series of images from Z-stack sections taken at 1 μm thickness through the cell monolayer shown in Figure 8. *X*-axis illustrates cell layers from apical to basolateral. *Y*-axis illustrates the number of pixels present over the entire area of image. Monolayers interacting with ST-7 and treated with staurosporine resulted in marked reduction in number of pixels in cell layers representing apical region, compared to ST-4 treated epithelium and normal control. Pretreatment of epithelium with broad-spectrum caspase inhibitor, z-VAD-fmk, resulted in inhibition of ST-7-induced ZO-1 changes in the monolayer. Results shown are mean of 4 separate Z-stacks for each treatment. (magnification: 600x).

3.4. Blastocystis ST-7 Induces Caspase-Dependent ZO-1 Rearrangement in Caco-2. Compromise of epithelial barrier function, as observed in this study, is often associated with alterations of tight junction proteins. In this study, we observed that *Blastocystis* ST-7 induced an alteration in tight junction protein complex in conjunction with epithelial barrier dysfunction (Figures 8 and 9). Confocal micrographs suggest that exposure of Caco-2 monolayer to ST-7 induced a significant drop in anti-ZO-1 antibody binding to the apical junctional ring of epithelium (P value < 0.01) (Figure 8). ST-4 and negative control, on the other hand, had no effect on epithelial ZO-1 (Figure 8). Furthermore, western blot analysis showed that interaction with ST-7 resulted in a loss of Caco-2 ZO-1 band at 250 kDA (Figure 9). Interaction with ST-4 and negative control had no effect on ZO-1 distribution in Caco-2 (Figures 8 and 9). Interestingly, inhibition of host caspases by z-VAD-fmk prevented ST-7-induced ZO-1 changes (Figures 8 and 9).

3.5. Inhibition of Caco-2 Caspases Prevented Blastocystis ST-7-Induced Epithelial Barrier Dysfunction. It has been reported previously that host epithelial dysfunction induced by luminal parasites is caused by increased apoptosis in enterocytes. In this study, we observed that inhibition of host caspases by

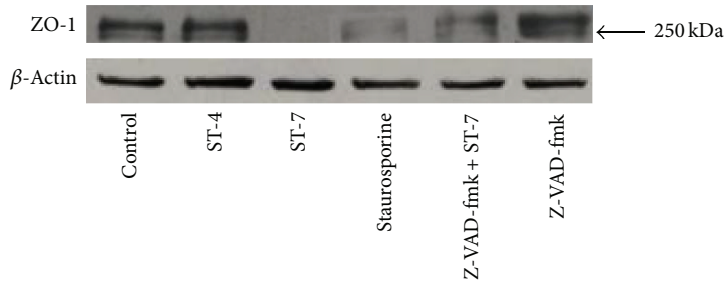

Figure 9: Western blot analysis of ZO-1 integrity in Caco-2 epithelium. Monolayers were grown on cell-culture plates and harvested after coincubation with *Blastocystis* ST-4, ST-7, normal growth media, and 0.5 μM staurosporine. Monolayers were also treated with broad-spectrum caspase inhibitor z-VAD-fmk before incubation with ST-7. After coincubation with ST-7 and staurosporine for 6 h, loss of ZO-1 band was observed. The ZO-1 band remained unchanged in untreated Caco-2 cells and those interacting with ST-4. Caspase inhibition resulted in rescue of ST-7-induced loss of ZO-1.

broad-spectrum caspase inhibitor, z-VAD-fmk, significantly prevented ST-7-induced TER drop (P value < 0.01) (Figure 3) and inhibited parasite-induced increase in permeability (P value < 0.01) (Figure 4) of Caco-2 monolayers. These findings (Figures 3 and 4), in conjunction with inhibition of ST-7-induced ZO-1 alteration (Figures 8 and 9) by z-VAD-fmk, suggested a role of parasite-induced apoptosis in epithelial barrier dysfunction.

4. Discussion

In this study, using two clinically relevant *Blastocystis* isolates, we reported that a *Blastocystis* ST-7 isolate recovered from a human patient-induced epithelial barrier dysfunction in Caco-2 human epithelial cell-line, while a ST-4 isolate recovered from rat host did not induce enterocyte pathology. The intestinal epithelium serves as the body's first line of defense against luminal contents comprising of a diverse flora including pathogenic and nonpathogenic prokaryotes and eukaryotes [33]. Intestinal epithelial cells or enterocytes regulate the back and forth flow of contents between the gut lumen and subepithelial tissue [33]. Dysfunction of this barrier is the cause of a wide range of human diseases [28]. *Blastocystis*-induced compromise of human epithelial barrier, observed in our study, reinforces its status as a human pathogen.

We are also reporting for the first time that *Blastocystis* causes apoptosis in human epithelial cells. Apoptosis is a preprogrammed mechanism of clearing up unwanted cells by the body [42] without overtly stimulating a host immune response [36]. Cells undergo apoptosis even under physiological conditions, but several pathogens including parasites have evolved mechanisms to disrupt this machinery, by either upregulating [38, 43] or downregulating [44] it for their survival in the host. *Blastocystis* ST-7 induced both early and late hallmarks of apoptosis, that is, PS-externalization and nuclear fragmentation, respectively, in human enterocytes. Increased enterocyte apoptosis in some cases is also proposed to be a host response to infection by increasing the cell turnover in order to rid the body of the infected cells [45]. Mucosal sloughing reported during *Blastocystis* infections [46] might be a result of this increased turnover. Anti-inflammatory effects of apoptosis are also well recognized [47]. The relatively moderate level of apoptosis induced by *Blastocystis* in intestinal epithelium is similar to the programmed cell death of enterocytes when exposed to *Cryptosporidium* [48] and *Giardia* [38]. It is suggested that upregulation of host cell apoptosis might be a reason for lack of overt host inflammatory response during parasitic infections [38, 48] and might assist them in colonizing the hostile host environment. Although further investigation is needed in this area, the absence of obvious gut inflammatory changes in *Blastocystis*-infected hosts might be due to the ability of the parasite to downregulate host inflammatory response by induction of enterocyte apoptosis.

This is also the first study reporting that *Blastocystis* induces epithelial apoptosis by activation of the intrinsic pathway. Caspase 3 activation lies at the center of the caspase-mediated apoptosis [42]. It is preceded by activation of either intrinsic pathway, involving mitochondrial injury and caspase 9 activation, or extrinsic pathway due to Fas/FasL receptor-mediated caspase 8 activation. Parasites have evolved complex mechanisms to activate epithelial caspase 3. *Giardia* activates extrinsic as well as intrinsic apoptotic pathways [49]. *Entamoeba* on the other hand does not require either caspase 8 or caspase 9 for enterocyte caspase 3 activation [50]. In an earlier study, we reported that *Blastocystis* ST-4 induced rat epithelial apoptosis by caspase 3 activation [39]. There is no data available suggesting a similar outcome in human epithelium. Upstream pathways involved in caspase 3 activation by the parasite are not known either. In this study, the rodent strain had no effect on Caco-2 cell line, but ST-7, isolated from human host, induced caspase 3 activation. *Blastocystis* unlike *Giardia* or *Entamoeba* only activated caspase 9. A recent study suggested the involvement of Rho kinases in selective activation of caspase 9, leading to apoptosis [51]. A role of Rho kinase has been suggested in *Blastocystis*-induced breakdown of host epithelial barrier function and cytoskeletal rearrangement [22]. Although more data is required, selective activation of caspase 9 by *Blastocystis* in this study might be a result of epithelial Rho kinase modulation by the parasite. Further understanding of the unique cellular mechanisms employed by *Blastocystis* to induce host cell apoptosis might help us

to develop targeted therapeutics to prevent parasite-induced host pathology.

Tight junctions are key regulators of epithelial barrier function [33, 52]. ZO-1 is an important component of apical junctional complex, anchoring tight junctions to actin cytoskeleton [33]. Our data shows that *Blastocystis* ST-7 induces rearrangement of ZO-1 in intestinal epithelium. Several parasites are known to cause ZO-1 alterations by a wide array of mechanisms [33, 53, 54]. *Acanthamoeba* activates Rho/Rho-kinase pathway [53], whereas *Giardia* utilizes myosin light chain kinase [54] and caspases [38] to induce changes in ZO-1 organization. Apoptosis also plays a diverse role in the modulation of epithelial barrier function and tight junction reorganization. On one hand, enterocyte apoptosis ensures that epithelial barrier remains sealed [52], while in other cases induction of apoptosis is employed by pathogens to increase epithelial permeability [38] and cause host pathology [37]. Inhibition of host caspases resulted in prevention of *Giardia*-induced modulation of epithelial permeability and ZO-1 organization [38] while, inhibition of caspase-mediated apoptosis in enteropathogenic *E. coli* (EPEC) infections did not prevent the epithelial ZO-1 alterations [55]. In a recent study with rodent epithelium, pretreatment of host epithelium with pan-caspase inhibitor z-VAD-fmk did not rescue *Blastocystis* ST-4-induced epithelial barrier dysfunction [39]. In the current study, z-VAD-fmk treatment of epithelium significantly inhibited *Blastocystis* ST-7-induced epithelial barrier compromise. Parasite-induced ZO-1 alteration was also prevented significantly by host caspase inhibition, reiterating that role of enterocyte apoptosis in parasite- induced epithelial barrier dysfunction. Interestingly, changes in ZO-1 were also shown to be prevented by Rho kinase [22], again raising the question of the role of Rho kinase in caspase-mediated apoptosis.

We also observed for the first time a strain-dependent variation in *Blastocystis*-induced epithelial barrier compromise. *Blastocystis* ST-4 did not induce an increase in epithelial permeability, enterocyte apoptosis, or ZO-1 rearrangement in Caco-2 cells. We have also similarly observed that ST-7 and not ST-4 induced apoptosis in HT-29 cells, another transformed human intestinal epithelial cell line (results not shown). Several studies have suggested strain-dependent differences in *Blastocystis* virulence [8, 25]. Strain-to-strain variation in virulence is not unique to *Blastocystis* and it has been observed in intestinal parasites such as *Giardia*, *Cryptosporidium,* and *Entamoeba* [38, 56, 57], providing a plausible explanation for the large number of asymptomatic carriers of these pathogens [58, 59]. This might also explain frequent reports of asymptomatic *Blastocystis* carriers. In a recent study [26], we reported that *Blastocystis* exhibits a strain-dependent variation in the activity of cysteine proteases, potential parasite virulence factors [22, 27]. ST-7 of the parasite, reported to have higher cysteine protease activity [26], caused epithelial barrier dysfunction in the current study, while ST-4 with comparatively lower cysteine protease activity [26] did not. Although more data is needed, these findings suggest a possible association between parasite cysteine protease activity and its ability to induce epithelial barrier dysfunction. Interestingly, ST-4 caused epithelial barrier dysfunction in rat epithelium [39], suggesting that this strain exhibits host specificity in its ability to induce epithelial barrier compromise, as observed in *Cryptosporidium* infections [56]. Although human ST-4 infections are commonly associated with intestinal symptoms, its inability to induce epithelial barrier compromise in this study suggests that ST-4 might induce human pathology by some other mechanisms [60, 61].

To conclude, this is the first study to show that *Blastocystis* ST-7, a parasite subtype recovered from a human patient, induced enterocyte-apoptosis by activating caspases 3 and 9, suggesting the involvement of the intrinsic apoptotic pathway in pathogenesis. We also showed that this cytopathic human isolate of *Blastocystis* (ST-7) caused rearrangement of ZO-1 protein. Inhibition of host caspases prevented parasite-induced epithelial barrier dysfunction as well as ZO-1 rearrangement, suggesting the role of caspase-dependent enterocyte apoptosis in host epithelial barrier dysfunction induced by *Blastocystis*. Furthermore, the inability of rodent subtype ST-4 to induce any changes in Caco-2 provides evidence of host specificity and strain dependency in *Blastocystis*-induced human epithelial pathology. The strain-to-strain variation in parasite virulence is a plausible explanation for the large number asymptomatic human carriers of *Blastocystis*.

Conflict of Interests

The authors declare that there is no conflict of interests regarding the publication of this paper.

Authors' Contribution

Zhaona Wu and Haris Mirza contributed equally to the paper.

References

[1] K. S. Tan, "New insights on classification, identification, and clinical relevance of Blastocystis spp.," *Clinical Microbiology Reviews*, vol. 21, no. 4, pp. 639–665, 2008.

[2] C. Noël, F. Dufernez, D. Gerbod et al., "Molecular phylogenies of *Blastocystis* isolates from different hosts: implications for genetic diversity, identification of species, and zoonosis," *Journal of Clinical Microbiology*, vol. 43, no. 1, pp. 348–355, 2005.

[3] K. S. Tan, H. Mirza, J. D. W. Teo, B. Wu, and P. A. MacAry, "Current views on the clinical relevance of *Blastocystis* spp.," *Current Infectious Disease Reports*, vol. 12, no. 1, pp. 28–35, 2010.

[4] P. D. Scanlan and C. R. Stensvold, "*Blastocystis*: getting to grips with our guileful guest," *Trends in Parasitology*, vol. 29, no. 11, pp. 523–529, 2013.

[5] V. Mehraj, J. Hatcher, S. Akhtar, G. Rafique, and M. A. Beg, "Prevalence and factors associated with intestinal parasitic infection among children in an urban slum of Karachi," *PLoS ONE*, vol. 3, no. 11, Article ID e3680, 2008.

[6] A. Kurniawan, T. Karyadi, S. W. Dwintasari et al., "Intestinal parasitic infections in HIV/AIDS patients presenting with diarrhoea in Jakarta, Indonesia," *Transactions of the Royal Society of Tropical Medicine and Hygiene*, vol. 103, no. 9, pp. 892–898, 2009.

[7] Y. Taşova, B. Şahin, S. Koltaş, and S. Paydaş, "Clinical significance and frequency of *Blastocystis* hominis in Turkish patients with hematological malignancy," *Acta Medica Okayama*, vol. 54, no. 3, pp. 133–136, 2000.

[8] C. R. Stensvold, H. C. Lewis, A. M. Hammerum et al., "*Blastocystis*: unravelling potential risk factors and clinical significance of a common but neglected parasite," *Epidemiology and Infection*, vol. 137, no. 11, pp. 1655–1663, 2009.

[9] J. Yakoob, W. Jafri, M. A. Beg et al., "*Blastocystis* hominis and Dientamoeba fragilis in patients fulfilling irritable bowel syndrome criteria," *Parasitology Research*, vol. 107, no. 3, pp. 679–684, 2010.

[10] M. E. Ramirez-Miranda, R. Hernandez-Castellanos, E. Lopez-Escamilla et al., "Parasites in Mexican patients with irritable bowel syndrome: a case-control study," *Parasites and Vectors*, vol. 3, no. 1, p. 96, 2010.

[11] P. Poirier, I. Wawrzyniak, C. P. Vivares, F. Delbac, and H. El Alaoui, "New insights into *Blastocystis* spp.: a potential link with irritable bowel syndrome," *PLoS Pathog*, vol. 8, Article ID e1002545, 2012.

[12] D. M. Hameed, O. M. Hassanin, and N. M. Zuel-Fakkar, "Association of *Blastocystis* hominis genetic subtypes with urticaria," *Parasitology Research*, vol. 108, no. 3, pp. 553–560, 2011.

[13] C. Vogelberg, C. R. Stensvold, S. Monecke et al., "*Blastocystis* sp. subtype 2 detection during recurrence of gastrointestinal and urticarial symptoms," *Parasitology International*, vol. 59, no. 3, pp. 469–471, 2010.

[14] M. R. Sohail and P. R. Fischer, "*Blastocystis* hominis and travelers," *Travel Medicine and Infectious Disease*, vol. 3, no. 1, pp. 33–38, 2005.

[15] H. Mirza, Z. Wu, F. Kidwai, and K. S. W. Tan, "A metronidazole-resistant isolate of *Blastocystis* spp. Is susceptible to nitric oxide and downregulates intestinal epithelial inducible nitric oxide synthase by a novel parasite survival mechanism," *Infection and Immunity*, vol. 79, no. 12, pp. 5019–5026, 2011.

[16] S. Chandramathi, K. Suresh, and U. R. Kuppusamy, "Elevated levels of urinary hyaluronidase in humans infected with intestinal parasites," *Annals of Tropical Medicine and Parasitology*, vol. 104, no. 5, pp. 449–452, 2010.

[17] S. Chandramathi, K. G. Suresh, A. A. Mahmood, and U. R. Kuppusamy, "Urinary hyaluronidase activity in rats infected with *Blastocystis* hominis-evidence for invasion?" *Parasitology Research*, vol. 106, no. 6, pp. 1459–1463, 2010.

[18] K.-C. Hu, C.-C. Lin, T.-E. Wang, C.-Y. Liu, M.-J. Chen, and W.-H. Chang, "Amoebic liver abscess or is it?" *Gut*, vol. 57, no. 5, pp. 627–683, 2008.

[19] W. D. Patino, D. Cavuoti, S. K. Banerjee, K. Swartz, R. Ashfaq, and T. Gokaslan, "Cytologic diagnosis of *Blastocystis* hominis in peritoneal fluid: a case report," *Acta Cytologica*, vol. 52, no. 6, pp. 718–720, 2008.

[20] A. Alexeieff, "Sur la nature des formations dites, 'Kystes de Trichomonas intestinalis'," *Comptes Rendus des Séances et Mémoires de la Société de Biologie*, vol. 71, pp. 296–298, 1911.

[21] E. Brumpt, "*Blastocystis* hominis n sp. et formes voisines," *Bulletin de la Société de Pathologie Exotique*, vol. 5, pp. 725–730, 1912.

[22] H. Mirza, Z. Wu, J. D. Teo, and K. S. Tan, "Statin pleiotropy prevents rho kinase-mediated intestinal epithelial barrier compromise induced by *Blastocystis* cysteine proteases," *Cellular Microbiology*, vol. 14, no. 9, pp. 1474–1484, 2012.

[23] H. Mirza and K. S. Tan, "Clinical aspects of *Blastocystis* infections: advancements amidst controversies," in *Blastocystis: Pathogen or Passenger?* H. Mehlhorn, K. S. Tan, and H. Yoshikawa, Eds., pp. 65–84, Springer, Berlin, Germany, 2012.

[24] A. Iguchi, A. Ebisu, S. Nagata et al., "Infectivity of different genotypes of human *Blastocystis* hominis isolates in chickens and rats," *Parasitology International*, vol. 56, no. 2, pp. 107–112, 2007.

[25] E. Hussein, A. Hussein, M. Eida, and M. Atwa, "Pathophysiological variability of different genotypes of human *Blastocystis* hominis Egyptian isolates in experimentally infected rats," *Parasitology Research*, vol. 102, no. 5, pp. 853–860, 2008.

[26] H. Mirza and K. S. Tan, "*Blastocystis* exhibits inter- and intra-subtype variation in cysteine protease activity," *Parasitology Research*, vol. 104, no. 2, pp. 355–361, 2009.

[27] M. Puthia, A. Vaithilingam, J. Lu, and K. S. W. Tan, "Degradation of human secretory immunoglobulin a by *Blastocystis*," *Parasitology Research*, vol. 97, no. 5, pp. 386–389, 2005.

[28] J. R. O'Hara and A. G. Buret, "Mechanisms of intestinal tight junctional disruption during infection," *Frontiers in Bioscience*, vol. 13, no. 18, pp. 7008–7021, 2008.

[29] H. J. Epple, T. Schneider, H. Troeger et al., "Impairment of the intestinal barrier is evident in untreated but absent in suppressively treated HIV-infected patients," *Gut*, vol. 58, no. 2, pp. 220–227, 2009.

[30] T. Matysiak-Budnik, B. Coffin, A. Lavergne-Slove, J. Sabate, F. Mégraud, and M. Heyman, "Helicobacter pylori increases the epithelial permeability to a food antigen in human gastric biopsies," *American Journal of Gastroenterology*, vol. 99, no. 2, pp. 225–232, 2004.

[31] H. Troeger, H. Epple, T. Schneider et al., "Effect of chronic Giardia lamblia infection on epithelial transport and barrier function in human duodenum," *Gut*, vol. 56, no. 3, pp. 328–335, 2007.

[32] S. Rawal, S. Majumdar, and H. Vohra, "Activation of MAPK kinase pathway by Gal/GalNAc adherence lectin of E. histolytica: gateway to host response," *Molecular and Cellular Biochemistry*, vol. 268, no. 1-2, pp. 93–101, 2005.

[33] J. R. Turner, "Intestinal mucosal barrier function in health and disease," *Nature Reviews Immunology*, vol. 9, no. 11, pp. 799–809, 2009.

[34] H. L. Nielsen, H. Nielsen, T. Ejlertsen et al., "Oral and fecal Campylobacter concisus strains perturb barrier function by apoptosis induction in HT-29/B6 intestinal epithelial cells," *PLoS ONE*, vol. 6, no. 8, Article ID e23858, 2011.

[35] A. C. Chin, D. A. Teoh, K. G.-E. Scott, J. B. Meddings, W. K. Macnaughton, and A. G. Buret, "Strain-dependent induction of enterocyte apoptosis by Giardia lamblia disrupts epithelial barrier function in a caspase-3-dependent manner," *Infection and Immunity*, vol. 70, no. 7, pp. 3673–3680, 2002.

[36] Y. Gao, J. M. Herndon, H. Zhang, T. S. Griffith, and T. A. Ferguson, "Antiinflammatory effects of CD95 ligand (FasL)-induced apoptosis," *Journal of Experimental Medicine*, vol. 188, no. 5, pp. 887–896, 1998.

[37] S. M. Becker, K. Cho, X. Guo et al., "Epithelial cell apoptosis facilitates Entamoeba histolytica infection in the gut," *American Journal of Pathology*, vol. 176, no. 3, pp. 1316–1322, 2010.

[38] A. Chin, D. Teoh, K. Scott, J. B. Meddings, W. K. Macnaughton, and A. G. Buret, "Strain-dependent induction of enterocyte apoptosis by Giardia lamblia disrupts epithelial barrier function in a caspase-3-dependent manner," *Infection and Immunity*, vol. 70, no. 7, pp. 3673–3680, 2002.

[39] M. K. Puthia, S. W. S. Sio, J. Lu, and K. S. W. Tan, "*Blastocystis* ratti induces contact-independent apoptosis, F-actin rearrangement, and barrier function disruption in IEC-6 cells," *Infection and Immunity*, vol. 74, no. 7, pp. 4114–4123, 2006.

[40] C. R. Stensvold, H. V. Smith, R. Nagel, K. E. P. Olsen, and R. J. Traub, "Eradication of *Blastocystis* carriage with antimicrobials: reality or delusion?" *Journal of Clinical Gastroenterology*, vol. 44, no. 2, pp. 85–90, 2010.

[41] A. M. Petersen, C. R. Stensvold, H. Mirsepasi et al., "Active ulcerative colitis associated with low prevalence of *Blastocystis* and Dientamoeba fragilis infection," *Scandinavian Journal of Gastroenterology*, vol. 48, no. 5, pp. 638–639, 2013.

[42] J. Savill, "Recognition and phagocytosis of cells undergoing apoptosis," *British Medical Bulletin*, vol. 53, no. 3, pp. 491–508, 1997.

[43] C. D. Huston, D. R. Boettner, V. Miller-Sims, and W. A. Petri Jr., "Apoptotic killing and phagocytosis of host cells by the parasite Entamoeba histolytica," *Infection and Immunity*, vol. 71, no. 2, pp. 964–972, 2003.

[44] T. Yamada, T. Tomita, L. M. Weiss, and A. Orlofsky, "Toxoplasma gondii inhibits granzyme B-mediated apoptosis by the inhibition of granzyme B function in host cells," *International Journal for Parasitology*, vol. 41, no. 6, pp. 595–607, 2011.

[45] L. J. Cliffe, N. E. Humphreys, T. E. Lane, C. S. Potten, C. Booth, and R. K. Grencis, "Immunology-accelerated intestinal epithelial cell turnover: a new mechanism of parasite expulsion," *Science*, vol. 308, no. 5727, pp. 1463–1465, 2005.

[46] K. T. Moe, M. Singh, J. Howe et al., "Experimental *Blastocystis* hominis infection in laboratory mice," *Parasitology Research*, vol. 83, no. 4, pp. 319–325, 1997.

[47] C. Haslett, "Granulocyte apoptosis and inflammatory disease," *British Medical Bulletin*, vol. 53, no. 3, pp. 669–683, 1997.

[48] D. F. Mccole, L. Eckmann, F. Laurent, and M. F. Kagnoff, "Intestinal epithelial cell apoptosis following Cryptosporidium parrum infection," *Infection and Immunity*, vol. 68, no. 3, pp. 1710–1713, 2000.

[49] M. A. Panaro, A. Cianciulli, V. Mitolo et al., "Caspase-dependent apoptosis of the HCT-8 epithelial cell line induced by the parasite Giardia intestinalis," *FEMS Immunology and Medical Microbiology*, vol. 51, no. 2, pp. 302–309, 2007.

[50] C. D. Huston, E. R. Houpt, B. J. Mann, C. S. Hahn, and W. A. Petri Jr., "Caspase 3-dependent killing of host cells by the parasite Entamoeba histolytica," *Cellular Microbiology*, vol. 2, no. 6, pp. 617–625, 2000.

[51] D. P. Del Re, S. Miyamoto, and J. H. Brown, "RhoA/Rho kinase up-regulate Bax to activate a mitochondrial death pathway and induce cardiomyocyte apoptosis," *Journal of Biological Chemistry*, vol. 282, no. 11, pp. 8069–8078, 2007.

[52] A. M. Marchiando, L. Shen, W. V. Graham et al., "The epithelial barrier is maintained by in vivo tight junction expansion during pathologic intestinal epithelial shedding," *Gastroenterology*, vol. 140, no. 4, pp. e1201–e1218, 2011.

[53] N. A. Khan and R. Siddiqui, "Acanthamoeba affects the integrity of human brain microvascular endothelial cells and degrades the tight junction proteins," *International Journal for Parasitology*, vol. 39, no. 14, pp. 1611–1616, 2009.

[54] K. G. Scott, J. B. Meddings, D. R. Kirk, S. P. LeesMiller, and A. G. Buret, "Intestinal infection with Giardia spp. reduces epithelial barrier function in a myosin light chain kinase-dependent fashion," *Gastroenterology*, vol. 123, no. 4, pp. 1179–1190, 2002.

[55] A. Buret, M. E. Olson, D. Grant Gall, and J. A. Hardin, "Effects of orally administered epidermal growth factor on enteropathogenic Escherichia coli infection in rabbits," *Infection and Immunity*, vol. 66, no. 10, pp. 4917–4923, 1998.

[56] A. Hashim, G. Mulcahy, B. Bourke, and M. Clyne, "Interaction of Cryptosporidium hominis and Cryptosporidium parvum with primary human and bovine intestinal cells," *Infection and Immunity*, vol. 74, no. 1, pp. 99–107, 2006.

[57] P. Davis, J. Schulze, and S. L. Stanley Jr., "Transcriptomic comparison of two Entamoeba histolytica strains with defined virulence phenotypes identifies new virulence factor candidates and key differences in the expression patterns of cysteine proteases, lectin light chains, and calmodulin," *Molecular and Biochemical Parasitology*, vol. 151, no. 1, pp. 118–128, 2007.

[58] J. Yakoob, Z. Abbas, M. A. Beg et al., "Prevalences of Giardia lamblia and Cryptosporidium parvum infection in adults presenting with chronic diarrhoea," *Annals of Tropical Medicine and Parasitology*, vol. 104, no. 6, pp. 505–510, 2010.

[59] R. Haque, D. Mondal, P. Duggal et al., "Entamoeba histolytica infection in children and protection from subsequent amebiasis," *Infection and Immunity*, vol. 74, no. 2, pp. 904–909, 2006.

[60] M. K. Puthia, A. Vaithilingam, J. Lu, and K. S. W. Tan, "Degradation of human secretory immunoglobulin a by *Blastocystis*," *Parasitology Research*, vol. 97, no. 5, pp. 386–389, 2005.

[61] M. K. Puthia, J. Lu, and K. S. W. Tan, "*Blastocystis* ratti contains cysteine proteases that mediate interleukin-8 response from human intestinal epithelial cells in an NF-kappaB-dependent manner," *Eukaryotic Cell*, vol. 7, no. 3, pp. 435–443, 2008.

Hindawi Publishing Corporation
BioMed Research International
Volume 2014, Article ID 439501, 12 pages
http://dx.doi.org/10.1155/2014/439501

Research Article

Early *Trypanosoma cruzi* Infection Reprograms Human Epithelial Cells

María Laura Chiribao,[1,2] Gabriela Libisch,[1] Adriana Parodi-Talice,[1,3] and Carlos Robello[1,2]

[1] *Unidad de Biología Molecular, Montevideo 11400, Institut Pasteur de Montevideo, Uruguay*
[2] *Departamento de Bioquímica, Facultad de Medicina, Universidad de la República, Montevideo 11300, Uruguay*
[3] *Sección Genética, Facultad de Ciencias, Universidad de la República, Montevideo 11400, Uruguay*

Correspondence should be addressed to Carlos Robello; robello@pasteur.edu.uy

Received 6 December 2013; Revised 27 February 2014; Accepted 27 February 2014; Published 9 April 2014

Academic Editor: Wanderley de Souza

Trypanosoma cruzi, the causative agent of Chagas disease, has the peculiarity, when compared with other intracellular parasites, that it is able to invade almost any type of cell. This property makes Chagas a complex parasitic disease in terms of prophylaxis and therapeutics. The identification of key host cellular factors that play a role in the *T. cruzi* invasion is important for the understanding of disease pathogenesis. In Chagas disease, most of the focus is on the response of macrophages and cardiomyocytes, since they are responsible for host defenses and cardiac lesions, respectively. In the present work, we studied the early response to infection of *T. cruzi* in human epithelial cells, which constitute the first barrier for establishment of infection. These studies identified up to 1700 significantly altered genes regulated by the immediate infection. The global analysis indicates that cells are literally reprogrammed by *T. cruzi*, which affects cellular stress responses (neutrophil chemotaxis, DNA damage response), a great number of transcription factors (including the majority of NFκB family members), and host metabolism (cholesterol, fatty acids, and phospholipids). These results raise the possibility that early host cell reprogramming is exploited by the parasite to establish the initial infection and posterior systemic dissemination.

1. Introduction

Trypanosoma cruzi, the causative agent of Chagas disease, has the peculiarity, when compared with other intracellular parasites, to invade almost any type of cell. In *T. cruzi*, pathogen-associated molecular patterns involve a great number of surface molecules that induce changes in cell signaling of host cells [1]. The early cell infection by cell-derived trypomastigotes involves adhesion, penetration, and transit through host cell parasitophorous vacuoles in order to establish an intracellular infection. In this sense, trypomastigotes must interact through their surface with host-surface molecules in order to generate signaling and/or metabolic changes that favor infection. As an obligate intracellular protozoan parasite, *T. cruzi* has evolved several mechanisms for recognition, adhesion, and penetration. Particularly, the presence of hundreds of copies of several gene families coding for surface glycoproteins [2] and the simultaneous expression of several genes of each family [3] are probably responsible for this pathogen's ability to infect a wide range of cell types. However, little is known about the specific responses of each different cell type. Most of the focus has been placed on the study of macrophages and cardiomyocytes, since they are responsible for host defenses and antigen presenting or cardiac lesions in Chagas disease, respectively [4, 5]. However, when these parasites enter their host through a skin lesion, by contact with mucous tissue or by ingestion, the establishment of the infection depends on its ability to rapidly invade epithelial cells that constitute the first barrier against infections. The epithelium provides both a physical barrier and a variety of antimicrobial factors to avoid microbial entry [6]. In this sense, parasites must be able not only to invade epithelial cells, but also to insure dissemination and the establishment of a future chronic infection.

The study of gene expression profiles during infection constitutes a very powerful tool in order to compare global

responses of several kinds of cells, allowing the identification of new genes and/or pathways implicated in the establishment of the infection and pathogenesis. Although several reports have been published with these approaches, a high variability in parasite strains, host cells, mammal species, and times of infection generate a complex picture and few general conclusions. Cardiac cells have been the most studied using mice models [7–9], revealing hundreds of differentially expressed genes in infected cells. The response of mice macrophages has also been studied at 24 hours postinfection, comparing different stimuli and cytokine profiles [10]. Recently, Caradonna et al. analyzed the medium and late responses (18 hs and 72 hs, resp.) to *T. cruzi* in HeLa cells, through a different approach (genome-wide RNAi screen [11]) showing the relevance of host metabolism on intracellular *T. cruzi* growth. In this work, we focused our study on the early response of human cells to *Trypanosoma cruzi* infection. It is important to note that previous reports show that the early response of human cells to *T. cruzi* involves minimal modulation of gene expression, particularly in HeLa cells, where few changes were described in the early infection [12, 13]. Epithelial cells were used as a model since, as described above, they constitute the first barrier against infection. As expected, strong changes in gene expression profiling were found immediately after parasites contacted host cells, involving reprogramming of gene expression in the first 6 hours of infection.

2. Materials and Methods

2.1. Cell Cultures, Parasites, and Infection Assays. HeLa human cell line was grown in Dulbecco's Modified Eagle's Medium (DMEM) (Gibco) supplemented with 10% heat inactivated fetal bovine serum (FBS) (Gibco) at 37°C in a 5% CO_2 atmosphere. Dm28C *T. cruzi* strain was used throughout this work [14].

For infection assays, cell-derived trypomastigotes were incubated with semiconfluent HeLa cells (10 : 1 parasite : cell ratio) during 4 hours at 37°C in DMEM supplemented with 2% FBS. After interaction period, parasites were removed, and cells were washed with PBS twice and incubated with DMEM with 2% SBF. Cell samples were taken at 0, 3, and 6 hours after the interaction period henceforth named t_0, t_3, and t_6, respectively.

2.2. RNA Extraction and Microarray Procedures. Total RNA was isolated with phenol/chloroform as described by the manufacturer (Tri Reagent, Sigma-Aldrich, USA). Processed samples were quantified in a spectrophotometer (NanoDrop 1000 and Thermo Scientific), exhibiting a high content of total RNA and a good quality without degradation, according to the RIN (RNA integrity number) values obtained from a Bioanalyzer 2100 (Agilent Technologies), which were all above 8. Microarray analysis was performed using a 4 × 44 K Human Genome Oligo Microarray (G4112F, Agilent), in a One-color design. A 200 ng aliquot of total RNA was reverse-transcribed into cDNA, and this was transcribed into cRNA and labeled using the Low Input Quick Amp Labeling Kit, One-color (Agilent Technologies). The labeled cRNA was purified with Illustra RNAspin mini Isolation kit (GE Healthcare, USA). The quality of each cRNA sample was verified by total yield and specificity calculated based on NanoDrop ND-1000 spectrophotometer measurements (NanoDrop Technologies, USA).

After that, we proceeded with the hybridization, washing, assembling of the chips, and scanning, according to the protocol specified by Agilent. The glass slides were scanned using an Agilent microarray scanner G2565BA and default settings for all parameters. The labeled samples were placed in human hybridizing chips for 17 h at 60°C with a 10 rpm rotation. Successive washings were done with different washing, stabilization, and drying solutions according to Agilent's Low Input Quick Amp Labeling Kit protocol. We used Agilent Feature Extraction (version 9.5.1) for quality control, data filtering, and data normalization. The software also converts the scanned images in quantitative data for further analysis. The software automatically finds and places microarray grids, rejects outlier pixels, accurately determines feature intensities and calculates log ratios (Agilent's processed signal value), flags outlier pixels, and calculates statistical confidences. It also performs dye normalization within arrays using Lowess normalization. Three biological replicates were performed to each condition.

Microarray experiments were statistically compared using GeneSpring software 12.0 GX. Genes significantly up- and downregulated were identified by the ANOVA-test with a P value of 0.05 and a Benjamini-Hochberg false discovery rate correction for multiple testing.

2.3. Real-Time RT-PCR. The RNA samples used in the microarray experiment were used to validate some of the differentially expressed genes, through real-time PCR. For each sample, cDNA was synthesized by reverse transcription using the SuperScript II Reverse Transcriptase (Invitrogen) with Oligo(dT) primers and 500 ng of total RNA added as a template. The primer sequences and expected product length of amplicons are listed in Supplementary Table 1 (see Table S1 in Supplementary Material available online at http://dx.doi.org/10.1155/2014/439501). Almost all the primers used span an exon-exon junction to avoid DNA amplification (Supplementary Table 1). Real-time reactions were performed using 5 μL Sybr Green (KAPA SYBR FAST Universal 2X qPCR Master Mix, Kapa Biosystems), 200 nM of forward and reverse primers, and 1 μL of a 1/5 dilution cDNA, in a final volume of 10 μL. Samples were analyzed in duplicate in an Eco real-time PCR System (Illumina). Standard amplification conditions were 3 min at 95°C and 40 cycles of 15 s at 95°C, 30 s at 58°C, and 30 s at 72°C. After each PCR reaction, the corresponding dissociation curves were analyzed to ensure that the desired amplicon was being detected and to discard contaminating DNA or primer dimers.

The threshold cycle (CT) value for each gene was normalized to GAPDH, calculating the ΔCt for each gene in all samples (3 replicates of control and infected cells at t_0). The comparative CT method (ΔΔCt method) was used to determine the relative quantity of the target genes, and the fold change in expression was calculated as 2-ΔΔCt.2,5.

2.4. Western Blot. Lysates of control and infected HeLa cells were obtained by washing and resuspending monolayers directly in Cell Lysis Buffer (Promega). After centrifugation at 12000 g for 10 minutes, protein extracts were resolved by SDS-PAGE in a 12% polyacrylamide gel under reducing conditions and electrotransferred to Amersham Hybond ECL Nitrocellulose membranes (GE Healthcare). Membranes were blocked in 5% skimmed milk and 0.1% Tween 20 in PBS for 1 hour at 22°C. After washing with 0.1% Tween PBS, blots were incubated with an appropriate dilution of primary antibody, overnight at 4°C, in 1% Bovine Serum Albumin (BSA) (Sigma) and 0.1% Tween 20 in PBS. After three washes, a dilution of peroxidase conjugated anti-mouse antibody (DAKO) was applied at room temperature for 1 hour. The signal was developed with Super Signal West Pico Chemiluminiscent Substrate (Thermo Scientific).

2.5. Red Nile Staining. For Red Nile staining assay, cells were seeded in 12-well plates with coverslips and infected with trypomastigotes for 4 hours. After 0, 3, and 6 hours (t_0, t_3, and t_6), cells were fixed with 4% paraformaldehyde for 20 minutes at room temperature. After fixation, coverslips were incubated with 0.1 M glycine for 10 minutes and permeabilized with 0.5% Triton-X100 for 5 minutes at room temperature. For neutral lipid staining, cells were incubated for 10 minutes at 37°C with 500 nM Red Nile (Sigma) and rinsed with PBS. Coverslips were mounted with Fluoroshield with DAPI (Sigma) and visualized in a LeicaTCSSP5 Confocal Microscope.

3. Results

3.1. Trypanosoma cruzi Early Infection Remodels HeLa Cell Gene Expression. The effect of *T. cruzi* early infection on host gene expression was investigated on infected HeLa cells at 0, 3, and 6 h postinteraction period (t_0, t_3, and t_6), representing the initial events of penetration, intravacuolar stage, and the release of parasites to the cytosol, respectively, as previously described [9]. Total RNA extracted from infected and noninfected cells was labeled and hybridized to a Human GE 4 × 44 K Microarray (Agilent), which allows the evaluation of the gene expression profile of 19,596 different human genes. Genes showing at least a 2-fold change in their expression and a 95% probability of being differentially expressed ($P < 0.05$) were considered to be significantly regulated by the infection. The total number of significant differentially expressed genes is shown in Figure 1: more than a thousand genes are upregulated in the early response to infection, whereas less than 400 genes were downregulated, when comparing control versus *T. cruzi* infected cells. Major changes were observed at 3 hr postinfection, with a total of 1700 differentially expressed genes. During the course of the early response to the infection most of the upregulated genes (946) changed at t_0 and remained in this condition in all further times (Figure 2(a)). In contrast, only 28 genes remained downregulated during the 6-hour period (Figure 2(b)). A selection of 300 upregulated and 100 downregulated genes is presented in Supplementary Table 2.

3.2. Gene Ontology (GO) and Pathway Analysis. GO and pathway analysis were performed using GeneSpring (Agilent Technologies), comparing each time point with control cells, indicating that a wide range of biological processes was altered immediately after infection, the most relevant ones being immune response, cellular defense mechanisms, proliferation/differentiation, metabolism, and cell signaling (Figure 3(a)). However, at each stage of the early infection the most affected pathways differ significantly when comparing each condition with the previous one (Figure 3(b)). Hence the major expression changes in the proinflammatory response take place at t_0 (e.g., Toll-like receptor pathway and TNF-α and TGF-β signaling), and the remodeling of metabolism is maximal at t_3 (e.g., folate metabolism and lipid metabolism), whereas at t_6 the highest changes tend towards transport processes and stress response other than immune responses (e.g., DNA damage response and signaling by G protein receptors). An overview of the most affected pathways is shown in Figure 4. Representative genes of the affected pathways were further evaluated by real-time PCR (Figure 5), confirming these results.

As previously reported [7, 9, 12, 15], infection of mammalian cells (other than epithelial ones) by *T. cruzi* elicits a strong response whose major contribution is due to interrelated inflammatory, apoptotic, stress, and proliferative responses. In the present model of early response of epithelial cells we found that more than 50% of the affected pathways were related to these processes, mainly at t_0 (Figures 3 and 4). The intensity of this response is more evident when only those genes that are upregulated more than 10 times with respect to the control are grouped (Table 1).

3.3. The Predominance of Neutrophil Chemotactic Factors. With respect to inflammation related genes, most of them are presented in Table 1: namely, they are highly overexpressed and, as expected, major changes occur in cytokines and chemokines. Remarkably, the most upregulated chemokines have similar functions: recruitment of professional phagocytic cells (CXCL1, CXCL2, and IL-8), particularly neutrophils. Besides, the common receptor for some of them (CXCR2) is also overexpressed. It is worth mentioning that IL-8 is a chemotactic factor rather than a classical cytokine (currently named CXCL8) and was discovered as "neutrophil chemotactic factor" [16].

3.4. Regulation of Genes Controlling Cell Survival. Concerning programmed cell death, the predominance of a high number of genes related to inhibition of apoptosis is notorious. In particular, the antiapoptotic genes BIRC3 at t_0 and BCL2A1 at t_3 reach a maximum of 23-fold and 27-fold increase on their expression, respectively, and they remain highly overexpressed along the early response. The proliferative response is more relevant at t_0 and the main pathways involved are TNF-like weak inducer of apoptosis (TWEAK) signaling pathway, which relates the inflammatory and proliferative responses through NFκB signaling. The Wnt signaling pathway is also significantly altered during early infection (Supplementary Table 3). It is noteworthy

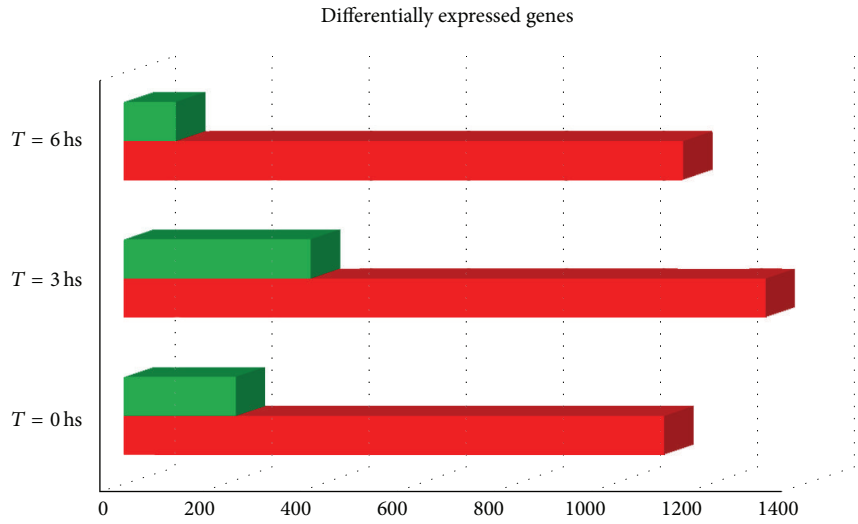

	$T = 0$ hs	$T = 3$ hs	$T = 6$ hs
Downregulated	231	384	108
Upregulated	1108	1316	1147

FIGURE 1: Differential gene expression in *T. cruzi* infected HeLa cells at t_0, t_3, and t_6 compared to noninfected control cells (≥2-fold, $P \leq 0.05$). Red bars indicate upregulated genes and green bars indicate downregulated genes. Inset table shows number of differentially expressed genes for each condition.

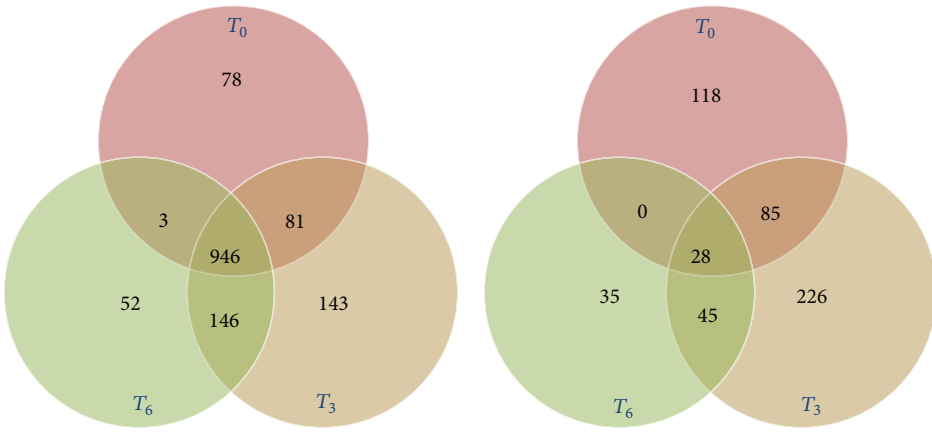

Time	Upregulated	Downregulated
0 hs versus control	1108	231
3 hs versus 0 hs	289	271
6 hs versus 3 hs	52	35

(c)

FIGURE 2: Venn diagrams comparing (a) upregulated and (b) downregulated genes (fold change ≥ 2, $P \leq 0.05$) with respect to control cells; (c) number of genes up- or downregulated, comparing one condition to the previous one (t_0 versus C, t_3 versus t_0, and t_6 versus t_3) using fold change ≥ 2 and $P \leq 0.05$.

that, among the proliferative response related genes, there is a synergism with the highly induced chemokines: the colony stimulating factor 3, specific for neutrophils, is seven-fold upregulated immediately after infection (Supplementary Table 2).

3.5. Transcription Factors in the Early Response to Infection. Many of the differentially regulated genes following infection were transcription factors whose function affects the expression of many genes (see specific heat map in Figure 3). In Supplementary Table 4 a list of the up- and downregulated

Table 1: Overexpressed genes with fold change ≥10 at any time postinfection ($P \leq 0.05$).

Gene ID	Description	FC-t_0	FC-t_3	FC-t_6
Immune response				
CCL20	Chemokine (C-C motif) ligand 20	85,2	93,3	14,5
CCL8	Chemokine (C-C motif) ligand 8	39,9	23,1	3,1
CD96	CD96 molecule	27,4	24,4	24,2
CXCL1	Chemokine (C-X-C motif) ligand 1	20,0	18,9	7,6
CXCL2	Chemokine (C-X-C motif) ligand 2	49,8	12,3	6,2
CXCL3	Chemokine (C-X-C motif) ligand 3	64,9	12,7	4,1
EREG	Epiregulin	9,2	13,8	4,1
IL1A	Interleukin 1, alpha	18,0	6,3	2,3
IL6	Interleukin 6	27,3	6,9	2,6
IL8	Interleukin 8	326,9	67,9	16,6
OLR1	Oxidized low density lipoprotein (lectin-like) receptor 1	16,2	24,9	14,7
PTX3	Pentraxin 3, long	13,8	13,1	9,3
Apoptosis inhibition				
BCL2A1	BCL2-related protein A1	16,4	27,4	8,2
BIRC3	Baculoviral IAP repeat containing 3	23,6	7,2	2,8
Transcription				
LMO2	LIM domain only 2 (rhombotin-like 1)	11,6	12,4	4,6
MYCL1	V-myc myelocytomatosis viral oncogene homolog 1	2,2	5,5	10,7
RELB	V-rel reticuloendotheliosis viral oncogene homolog B	11,0	9,3	5,0
Signalling				
RGR	Retinal G protein coupled receptor	20,7	24,1	20,4
PRKG1	Human mRNA for type I beta cGMP-dependent protein kinase	22,2	27,7	24,0
Binding				
MUC4	Mucin 4, cell surface associated	1,9	10,7	4,5
SDC4	Syndecan 4	11,4	7,7	2,5
STATH	Statherin	10,7	13,2	10,9
Transport				
SLC9A6	Solute carrier family 9 (sodium/hydrogen exchanger), member 6	12,7	13,7	11,3
Fatty acid synthesis				
ELOVL7	ELOVL fatty acid elongase 7	10,8	10,3	5,1
Stress response				
SOD2	Superoxide dismutase 2, mitochondrial	15,2	3,3	3,2
Other				
TCL6	T-cell leukemia/lymphoma 6 (nonprotein coding)	28,4	28,3	26,1
TNIP3	TNFAIP3 interacting protein 3	19,4	28,9	10,6
WFDC10A	WAP four-disulfide core domain 10A	3,2	10,0	10,1
NCRNA00246A	nonprotein coding RNA 246A	10,0	11,9	11,3
LOC283174	Hypothetical LOC283174	44,3	39,9	40,4
FLJ44715	cDNA FLJ44715 fis	18,8	21,0	19,6
A1BG	cDNA FLJ31639 fis	29,1	39,1	30,8
ART3	ADP-ribosyltransferase 3	2,2	5,8	12,5

transcription factors is presented: as can be seen, several members of the NFκB family (Table 2) change their expression, suggesting activation by different pathways. Particularly RELB, related to the noncanonical pathway, is among the most upregulated genes. Several members of adaptor-related protein complex 1 (AP-1) family proteins were also upregulated, such as JUN, JUND, ATF2, FOSL1, and FOSL2. These transcription factors regulate a variety of activities including proliferation, apoptosis, and inflammation in response to different stress signals including microbial infections [17]. Another remark is that 15% of the downregulated genes are transcription factors.

3.6. Induction of DNA Damage Response Related Genes. The expression of genes involved in DNA damage response (DDR) pathways was significantly regulated by infection.

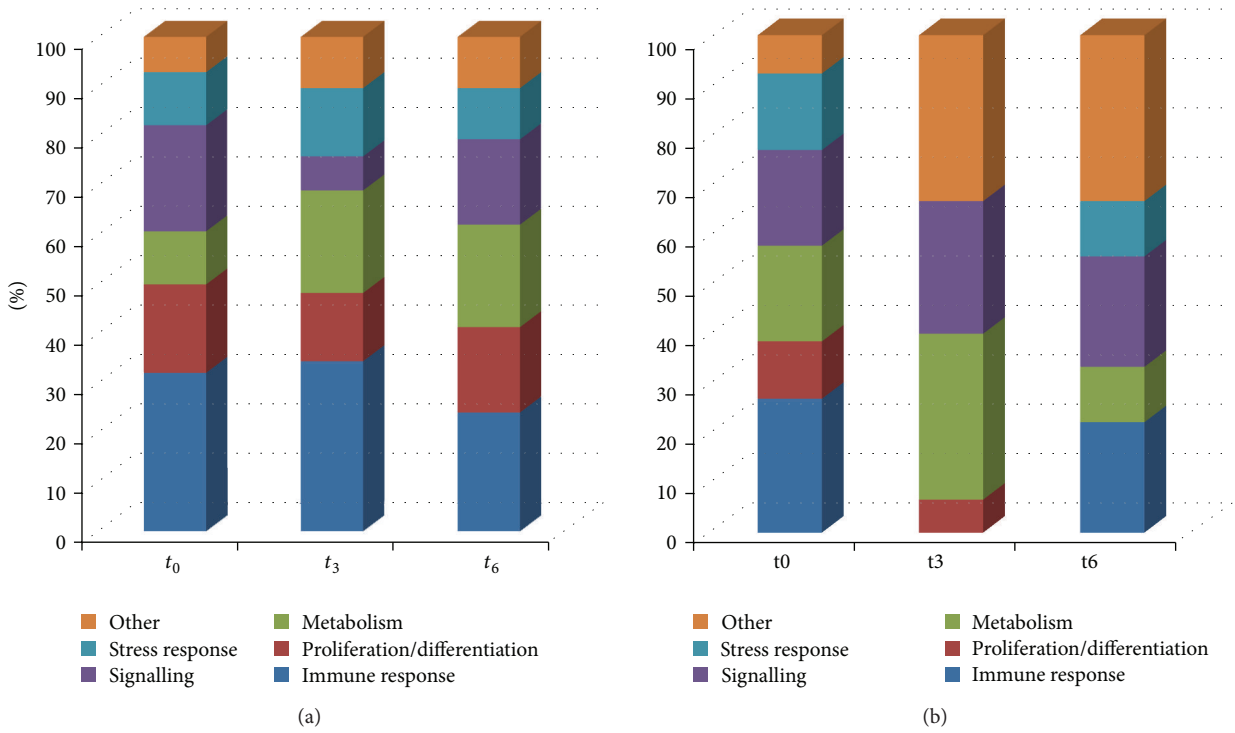

Figure 3: Cellular processes predicted to be modulated during *T. cruzi* infection. (a) Pathways analysis with upregulated genes from t_0, t_3, and t_6; (b) pathways analysis with upregulated genes comparing t_0 versus C, t_3 versus t_0, and t_6 versus t_3, showing characteristic pathways altered at each time point.

Table 2: Members of NFκB family differentially expressed during infection with *T. cruzi*.

Gene	FC-t_0	FC-t_3	FC-t_6
NKFB1	4,0	2,2	1,4
NFKB2	4,1	3,7	2,2
REL	2,5	1,3	–1,0
RELB	11,0	9,3	5
NFKBIA	4,2	1,3	1,5
NFKBIE	3,2	1,7	1,8
NFKBIZ	4,2	1,2	1,8

DDR is a highly coordinated cellular system able to sense and counteract DNA damage caused by a variety of environmental and endogenous genotoxic insults [18]. Among all the genes related to DDR transduction pathways, we grouped those involved in DNA repair mechanisms and those related to cell cycle regulation (Figure 6). Among DNA repair-related genes, there are several encoding for enzymes involved in DNA metabolism that were induced upon infection such as polymerase (DNA directed) kappa (POLK), polymerase (DNA directed) beta (POLB), RecQ protein-like (DNA helicase Q1-like) (RECQL), and single-strand-selective monofunctional uracil-DNA glycosylase 1 (SMUG1). We also detected differentially expressed genes that participate in recruitment of mediators or effectors of DNA repair such as promyelocytic leukemia (PML), DOT1-like histone H3K79 methyltransferase (DOT1L) and ring finger protein 8, and E3 ubiquitin protein ligase (RNF8). Several genes involved in cell cycle control were found to be modulated after infection. Among these, p15 (CDKN2B) and p21 (CDKN1A), which are cyclin-dependent kinase inhibitors implicated in the suppression of cell proliferation under several stresses, were upregulated upon infection.

3.7. Trypanosoma cruzi Alters Host Cell Lipid Metabolism. A group of host genes significantly regulated by *T. cruzi* were those involved in host lipid metabolism: cholesterol, fatty acids, and phospholipids (Figure 7(a)). Concerning cholesterol metabolism, the most remarkable changes occur in cholesterol transport related genes: low density lipoprotein receptor (rLDL) and oxidized low density lipoprotein receptor (OLR1), responsible for the entry of cholesterol and oxidized cholesterol, respectively, are overexpressed immediately after infection. In particular, OLR1 gene expression is highly upregulated, not only at the transcriptional level (Table 1) but also at the translational level (Figure 7(b)). ABCA1, which mediates the cholesterol flux and has been described to be overexpressed in cells that accumulate cholesterol [19], is also upregulated upon infection. Several genes from fatty acid metabolism are affected, in particular members of the acyl-CoA synthetase family (ACSL6, ACSM5, and AMAC1; Figure 7(a)) and fatty acids transport (SLC27A1) that participate in fatty acid activation and uptake [20]. One of the most overexpressed genes (Table 1) is a very long

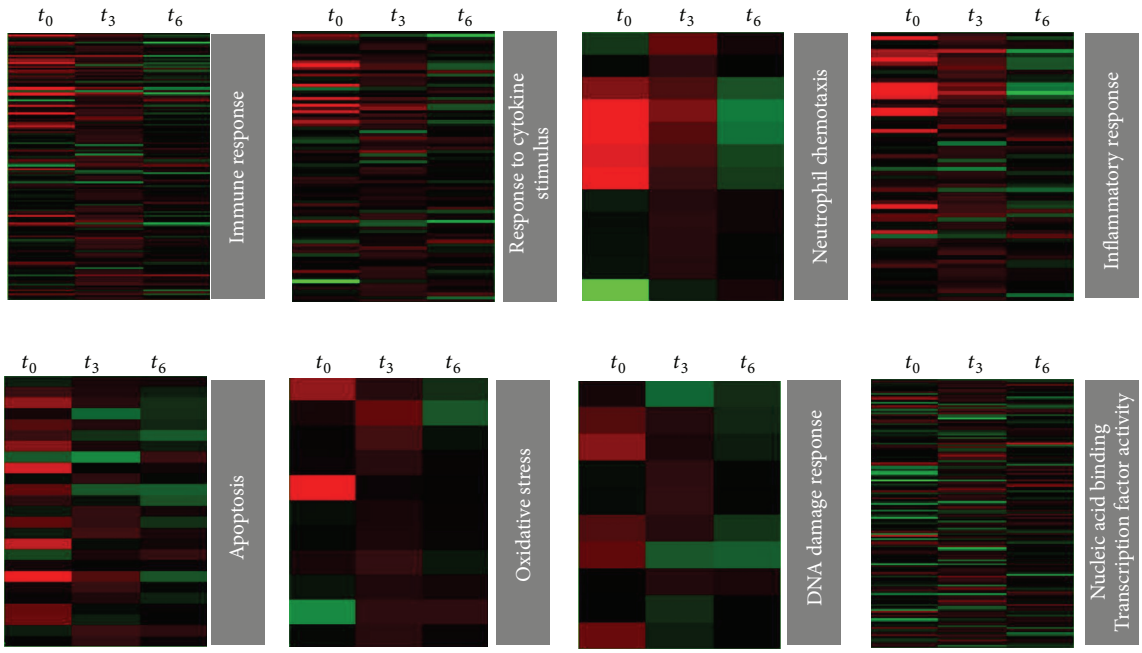

FIGURE 4: Heat maps of some representative biological processes altered during *T. cruzi* infection. Genes regulated by *T. cruzi* involved in immune response/inflammation (top) and genes involved in stress response and transcription factor activity (down) are represented.

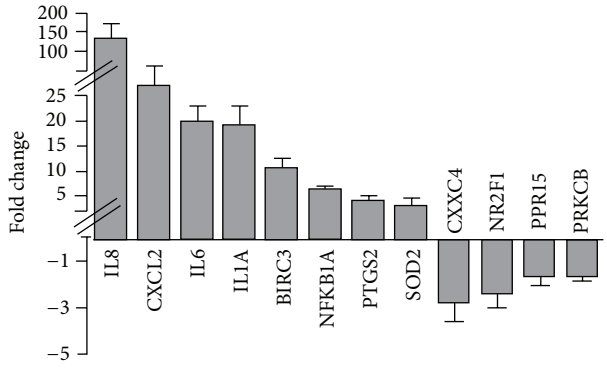

FIGURE 5: Quantitation of selected genes by real-time PCR. Mean relative fold changes of upregulated and down-egulated genes analyzed by qPCR in 3 biological replicates of infected HeLa cells at t_0 relative to that in control cells. Error bar represents SD of replicates. The cross-bars in the y-axis indicate changes in the scale used.

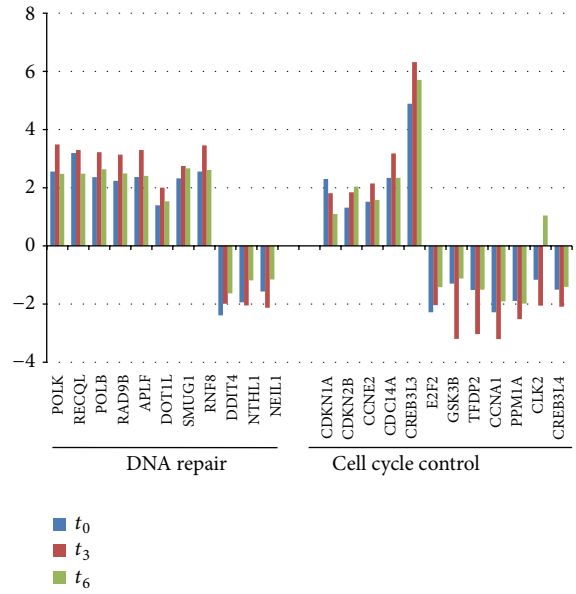

FIGURE 6: Temporal regulation of host genes related to cell cycle control and DNA repair on infected cells.

chain fatty acid, elongase 7 (ELOVL7), which elongates fatty acids of 16 to 24 carbons, with the highest activities towards C18-CoAs [21, 22]. Very long fatty acids are essential precursors of signaling molecules related to the arachidonic acid and prostaglandin metabolisms, the limiting pathway being catalyzed by prostaglandin-endoperoxide synthase 2 (PTGS2). Consistently, we found that this gene is rapidly overexpressed both at the transcriptional and translational levels (Figure 7(b) and Supplementary Table 2). These changes were so drastic in host cells to the extent that, six hours after penetration, a significant accumulation of lipid bodies was found [23] (Figure 7(c)).

4. Discussion

The ability of *Trypanosoma cruzi* to invade almost any kind of nonimmune cell makes Chagas a complex parasitic disease in terms of prophylaxis and therapeutics. Since the parasite cannot go through the skin, penetration is possible through the site of the insect bite (mainly after scratching the skin) or by invading mucous tissues (this would include cases of

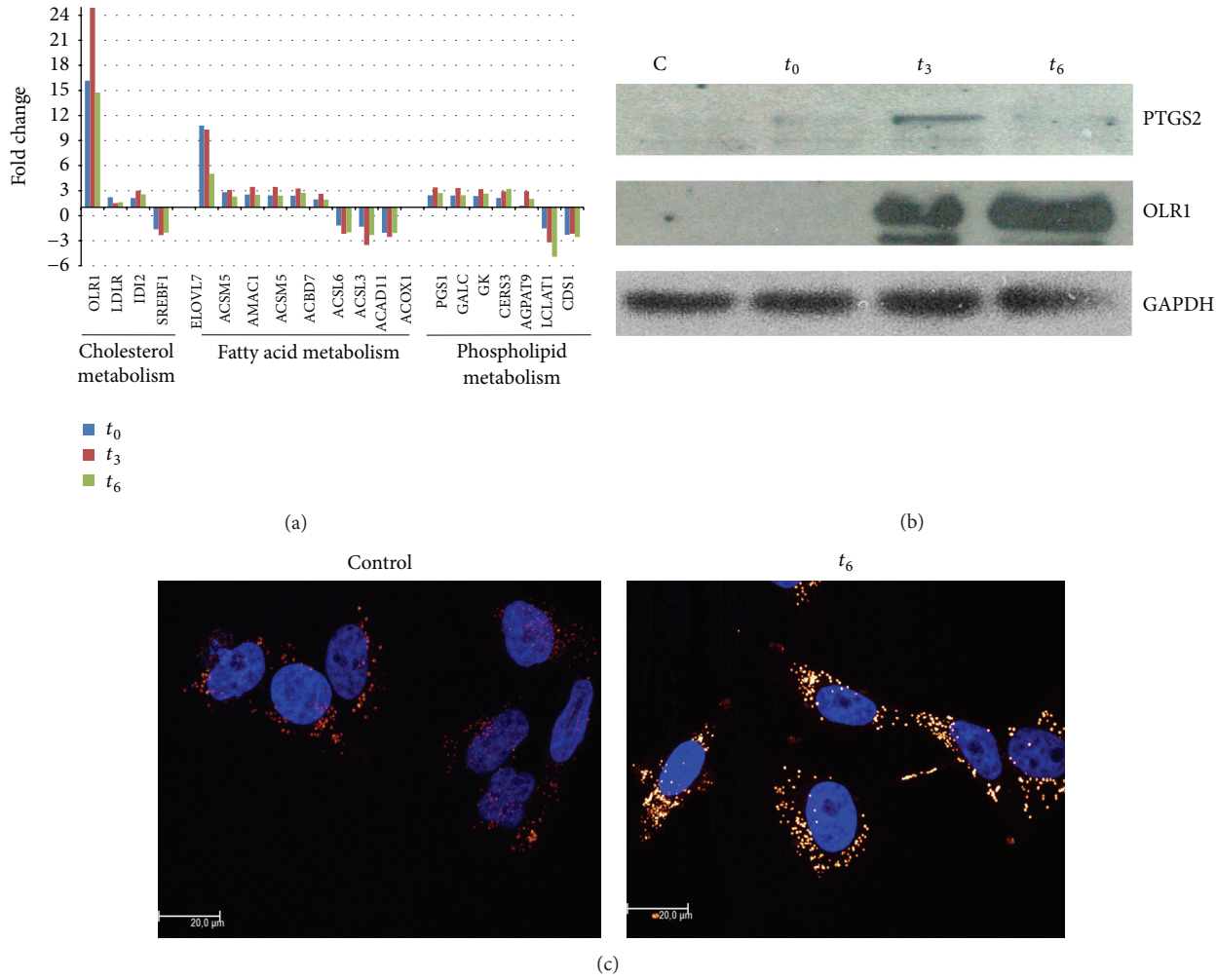

FIGURE 7: (a) Temporal regulation of host genes related to lipid metabolism after infection with *T. cruzi*. (b) Western blot analysis showing overexpression of PTGS2 and OLR1 proteins and normalization with GADPH. (c) Red Nile staining of control and infected cells at t_6.

oral infection). In any case, the common physical barrier is constituted by epithelial cells, and the early infection will be relevant for the establishment of a chronic disease. Some reports about transcriptomics of the human cell response in epithelium and fibroblasts showed minimal alterations at the level of gene expression. De Avalos et al. [13] described that only 6 genes were downregulated, whereas no genes were induced in the fibroblast early response to *T. cruzi* infection. On the other hand, in epithelial cells only 41 genes were found to be induced after infection [12]. However, in a more recent work in mice cardiomyocytes [9] the authors made a very complete characterization of the cell response and showed that hundreds of genes changed, a result that is expected for such a complex intracellular parasite. In that context we decided to evaluate the early response to *T. cruzi* by analyzing three time points (t_0, t_3, and t_6), in order to get a general view of the response during adhesion/penetration, the intravacuolar stage, and the early cytosolic stage, respectively. The results of this study demonstrated that immediately after contact with human epithelial cells, *T. cruzi* triggers a strong response, where more than 1300 genes were upregulated and almost 400 genes were downregulated. Most of the regulated genes are involved either in cellular defense, metabolism, or response to stress, including DNA damage response. Some genes of our interest were further evaluated by real-time PCR, and two inflammation related genes were studied at protein level, showing that mRNA upregulation was correlated with protein induction. The major response was achieved at t_0, and most genes (946) were maintained upregulated during early infection, whereas only 28 of the downregulated genes were common to the three studied time points.

4.1. Cellular Defense Mechanisms. In this work, a number of genes involved in cellular defense mechanisms were found differentially expressed, particularly genes related to inflammation and immune response. This response is characteristic in Chagas disease, and the fact that about 30% of the altered genes belong to this category is not surprising. However, the pattern of chemical mediators differed substantially from previous gene profiling studies involving *T. cruzi*. The majority of the most highly expressed chemokines function as chemotactic factors for neutrophils. Particularly, the most

upregulated gene is IL-8 (327- and 157-fold at t_0 in microarray experiment and RT-PCR, resp.). As was previously described, this molecule is a potent neutrophil chemotactic factor, belonging to the CXC chemokine subfamily, which signals through CXCR1 and CXCR2 G-coupled proteins. The two major effects of IL-8 are chemotaxis of neutrophils and neovascularization. Moreover, it enhances the proliferation and survival of endothelial cells and angiogenesis [24]. This property has been related to the ability of cancer cells to survive and migrate from the primary site [25]. Although this proinflammatory response clearly reflects defense mechanisms against the parasite, we cannot discard that it can be exploited by the parasite as a strategy for survival and dissemination: vascularization and recruitment of cells that can be infected by *T. cruzi*. This strategy for dissemination by PMN attraction and infection has been reported for *Leishmania* infection, mainly through overexpression of IL-8 [26], and also for many intracellular pathogens that can survive in the hostile neutrophil-filled environment, and this enables the subsequent infection of macrophages [27]. CXCR2, the major receptor for IL-8, is also clearly overexpressed, indicating that this chemokine also acts on HeLa cells. Interestingly, IL-8 binding to CXCR2 triggers the rise of intracellular calcium from intracellular stores [28], which may in turn contribute to infection.

An important feature in the infection by *T. cruzi* is the oxidant stress response that is very relevant for the parasite's pathogenesis. Although the oxidative stress generated after the infection is a hallmark of professional phagocytic cells, it has been demonstrated that oxidative stress in nonphagocytic cells is generated by many mechanisms, including dysfunction of mitochondria in infected mice [29] and cardiomyocytes [30] and cytokines signaling like TNF [5], and also by the action of lipoxygenase, cyclooxygenase, and cytochrome P450-dependent oxygenases during arachidonic acid metabolism [31]. In infected epithelial cells we found many enzymes involved in arachidonic acid metabolism and many p450-dependent oxygenases as well as TNF alpha-signaling pathway activity, which suggests that many sources of ROS are active in these cells. Consistent with this idea, many antioxidant enzymes that are known to be upregulated after oxidative stress, particularly mitochondrial superoxide dismutase (SOD2), glutamate-cysteine ligase (GCLC) and hemoxygenase 1 (HMOX1), metallothioneins (MTX), gluthathione peroxidase (GPX2), and thioredoxin reductase 1 (TXNRD1), are induced after infection in epithelial cells [32]. It has been proved that exposure to TNF leads to an acute GSH depletion in epithelial cells due to its oxidation to GSSG. The reduction of GSH is sensed by stressed cells mainly through redox-sensitive transcription factors (AP-1 and NfκB), causing phosphorylation and degradation of IκB, which is a critical step for NfκB activation [33, 34]. On the other hand, the activation of NFκB regulates the expression of many proinflammatory cytokines like IL-8, IL-6, and TNF α, as well as antioxidant enzymes [35]. Due to the interconnection among inflammation and oxidative stress, it seems that the appropriate balance between proinflammatory and prooxidant and antioxidant and anti-inflammatory mediators could be responsible for the overall response in Chagas disease infection [36, 37]. As in infected cardiomyocytes [38], this balance could also determine the activation of DDR seen in infected epithelial cells and also the resolution of these pathways leading either to senescence, DNA repair, or apoptosis.

4.2. Trypanosoma cruzi Early Infection Regulates Genes Involved in Metabolism. Genes involved in cellular metabolism were found to be regulated during early *T. cruzi* infection. This is a common observation in host-pathogen interactions, although in the case of *T. cruzi*, metabolism remodeling has been widely associated with the generation of ATP by host cells [11]. In this study, a strong component of lipid metabolism was found, mainly affecting genes related to cholesterol, fatty acid, and phospholipid metabolism. Remarkably, OLR1 is one of the most upregulated genes and its expression at the translational level indicates that the expression of the receptor peaks at 3 hours after invasion. In *T. cruzi*, it was previously reported that infection enhances LDL receptor expression, which is used by the parasite to enter host cells [39]. We also found upregulation of this receptor gene but at a lower level, whereas OLR1 is more than 15-fold overexpressed along the experiment when compared to noninfected cells. It has been demonstrated that *Chlamydia pneumoniae* induces overexpression of OLR1, which in turn serves as a gateway for *Chlamydia pneumoniae* invasion [40–42]. The finding of a strong upregulation of OLR1 deserves further studies in order to evaluate whether it can constitute a new strategy of *T. cruzi* invasion. Finally, since OLR1 is a relevant factor in the development of atherosclerotic lesions, this strong upregulation during *T. cruzi* infection can explain, at least in part, the major susceptibility to atherosclerosis in *T. cruzi* infected mice [43].

Concerning fatty acid metabolism, it was recently described that, during the medium and late *T. cruzi* infection of HeLa cells, perturbations in host fatty acid metabolism alter intracellular parasite growth rates [11]. In particular, Caradonna et al. showed that the genes coding for proteins involved in activation/transport of VLCFAs (SLC27A2) and β-oxidation (ACAA1 and IDH1) in peroxisomes directly affect intracellular amastigotes growth. Interestingly, here we found that SLC27A1 gene is overexpressed in infected cells. SLC27A1 codes for a long chain fatty acid (LCFA) transporter, located in the plasma membrane. Taken together, these results allow us to hypothesize that both events are connected: during the early infection parasites favor LCFA cell uptake and elongation of LCFA to VLCFA through ELOV7 overexpression. These VLCFAs will be used in peroxisomes for β-oxidation during the medium and late infection [44]. However, it should be remarked that energy production is not the most important role of VLCFAs: they are relevant for many physiological processes like membrane composition maintenance, inflammatory responses, and neutrophil migration, as well as in the synthesis of signaling molecules like eicosanoids, sphingosine 1-phosphate, and precursors of prostaglandins biosynthesis [21, 22, 45]. In this sense, the induction of PTGE2 in the early infection suggests a coordinated function with ELOVL7. Which is the relative relevance of the different roles of VLCFAs with respect to the

parasite survival and establishment of the infection remains to be elucidated.

Finally, several genes coding for phospholipid metabolism related enzymes were regulated under infection, such as CER3, which is essential for epidermal lipid homeostasis [46], AGPAT9, and PGS1, while LCLAT1 and CDS1 were downregulated, suggesting the relevance of phospholipid metabolism in signaling and membrane homeostasis during *T. cruzi* early infection. All of these results led us to evaluate the presence of lipid bodies in the immediate response of HeLa cells to *T. cruzi*. Lipid bodies constitute lipid rich organelles involved in cell metabolism and signaling and also a nutrient source for intracellular pathogens [47]. They are highly regulated in macrophages derived from mice infected with *T. cruzi* leading to foamy cell formation and, in some cases, to atherosclerotic lesions [48]. In this work we demonstrate the formation of lipid accumulation immediately after infection, indicating that this is a more general parasite strategy, not only confined to macrophages.

4.3. Trypanosoma cruzi Early Infection Induces DNA Damage Response. DDR is a signaling network triggered upon DNA lesions, which coordinates several programs, including DNA repair, cell cycle checkpoints, senescence, or apoptosis [18]. The DDR components in the transduction pathway are sensors of damage, signal transducers, and effectors. DNA damage leads to activation of ataxia-telangiectasia mutated (ATM) and ATM- and Rad3-related (ATR) signaling pathways, depending on the nature of the damage. These kinases, in turn, phosphorylate multiple substrates to activate cell cycle regulators and stimulate DNA repair by inducing DNA-repair proteins transcriptionally or posttranscriptionally. In this study, host genes involved in DDR were found to be significantly regulated upon infection with *T. cruzi*. Among them, several genes encoding for enzymes involved in DNA metabolism were induced upon infection, such as DNA polymerases POLK and POLB, DNA helicase RECQL, and DNA glycosylase SMUG1 involved in various types of DNA repair, including mismatch repair, base excision repair, and direct repair. In addition to DNA repair-related genes, we also detected differentially expressed genes that participate in the recruitment of mediators or effectors of DNA repair, such as PML, DOT1L, and RNF8. Interestingly, PML (promyelocytic leukemia protein), involved in chromatin metabolism and DNA repair, has been associated with response to viral infection [49].

On the other hand, a group of DDR related genes which contribute to cell cycle arrest were altered in the early infection (Figure 6). It is remarkable that p21 (CDKN1A) is upregulated in the early infection, suggesting that *T. cruzi* infection triggers a transient cell cycle arrest which may allow the cell to repair the damage. In addition to CDKN1A, other genes detected as differentially expressed have been involved in cell cycle progression regulation at G1, such as CDKN2B, CCNE2, CLK2, GSK3B, PPP2R5C, E2F2, PPM1A, TFDP2, CCNA1, and DCD14A. The rapid induction of DDR leads to the need to develop further studies to confirm whether DNA damage occurs immediately after infection. Besides, taking into account that DDR involves not only gene expression changes, but also posttranslational modifications, mainly due to the kinase activities of ATM and ATR, a profound evaluation of this response should be performed.

5. Conclusions

In summary, we have demonstrated that the early response to *T. cruzi* infection has a widespread effect on the expression of host genes involved in cellular defense mechanisms, stress responses, and metabolism. The importance of these findings is also relevant by comparing our findings to those previously reported in HeLa cells. The gene expression patterns identified may also provide insights into some of the strategies of initial infection, particularly dissemination: we postulate similar mechanisms of metastatic cancer cells mediated by interleukin 8. Finally, we show activation of DNA damage response, which deserves further studies.

Conflict of Interests

The authors declare that there is no conflict of interests regarding the publication of this paper.

Acknowledgments

The authors acknowledge Gonzalo Greif (IPM) for reanalyzing the results with MeV v4.8, Pilar Zorrila and Alejandra García (IPM) for technical assistance in microarray and real-time PCR experiments, and Fernando Hernandez (IVIC, Venezuela) for technical assistance in cell cultures. This work was supported by research funds from the Institut Pasteur de Montevideo and fellowships (María Laura Chiribao and Gabriela Libisch) from the Agencia Nacional de Investigación e Innovación (ANII). Adriana Parodi-Talice and Carlos Robello are researchers from the Sistema Nacional de Investigadores (ANII), Montevideo, Uruguay.

References

[1] F. Y. Maeda, C. Cortez, R. M. Alves, and N. Yoshida, "Mammalian cell invasion by closely related *Trypanosoma* species *T. dionisii* and *T. cruzi*," *Acta Tropica*, vol. 121, no. 2, pp. 141–147, 2012.

[2] N. M. El-Sayed et al., "The genome sequence of *Trypanosoma cruzi*, etiologic agent of Chagas disease," *Science*, vol. 309, no. 5733, pp. 409–415, 2005.

[3] J. A. Atwood III, D. B. Weatherly, T. A. Minning et al., "Microbiology: the *Trypanosoma cruzi* proteome," *Science*, vol. 309, no. 5733, pp. 473–476, 2005.

[4] K. L. Caradonna and B. A. Burleigh, "Mechanisms of host cell invasion by *Trypanosoma cruzi*," *Advances in Parasitology*, vol. 76, pp. 33–61, 2011.

[5] C. L. Epting, B. M. Coates, and D. M. Engman, "Molecular mechanisms of host cell invasion by *Trypanosoma cruzi*," *Experimental Parasitology*, vol. 126, no. 3, pp. 283–291, 2010.

[6] W. E. Paul, *Fundamental Immunology*, 6th edition, 2008.

[7] N. Garg, V. L. Popov, and J. Papaconstantinou, "Profiling gene transcription reveals a deficiency of mitochondrial oxidative phosphorylation in *Trypanosoma cruzi*-infected murine hearts: implications in chagasic myocarditis development," *Biochimica*

et Biophysica Acta: Molecular Basis of Disease, vol. 1638, no. 2, pp. 106–120, 2003.

[8] R. C. D. S. Goldenberg, D. A. Iacobas, S. Iacobas et al., "Transcriptomic alterations in *Trypanosoma cruzi*-infected cardiac myocytes," *Microbes and Infection*, vol. 11, no. 14-15, pp. 1140–1149, 2009.

[9] P. A. Manque, C. Probst, M. C. S. Pereira et al., "*Trypanosoma cruzi* infection induces a global host cell response in Cardiomyocytes," *Infection and Immunity*, vol. 79, no. 5, pp. 1855–1862, 2011.

[10] S. Zhang, C. C. Kim, S. Batra, J. H. McKerrow, and P. Loke, "Delineation of diverse macrophage activation programs in response to intracellular parasites and cytokines," *PLoS Neglected Tropical Diseases*, vol. 4, no. 3, article e648, 2010.

[11] K. L. Caradonna et al., "Host metabolism regulates intracellular growth of *Trypanosoma cruzi*," *Cell Host & Microbe*, vol. 13, no. 1, pp. 108–117, 2013.

[12] T. Shigihara, M. Hashimoto, N. Shindo, and T. Aoki, "Transcriptome profile of *Trypanosoma cruzi*-infected cells: simultaneous up- and down-regulation of proliferation inhibitors and promoters," *Parasitology Research*, vol. 102, no. 4, pp. 715–722, 2008.

[13] S. V. De Avalos, I. J. Blader, M. Fisher, J. C. Boothroyd, and B. A. Burleigh, "Immediate/early response to *Trypanosoma cruzi* infection involves minimal modulation of host cell transcription," *The Journal of Biological Chemistry*, vol. 277, no. 1, pp. 639–644, 2002.

[14] V. T. Contreras, T. C. Araujo-Jorge, M. C. Bonaldo et al., "Biological aspects of the Dm 28c clone of *Trypanosoma cruzi* after metacyclogenesis in chemically defined media," *Memorias do Instituto Oswaldo Cruz*, vol. 83, no. 1, pp. 123–133, 1988.

[15] J. A. Costales, J. P. Daily, and B. A. Burleigh, "Cytokine-dependent and-independent gene expression changes and cell cycle block revealed in *Trypanosoma cruzi*-infected host cells by comparative mRNA profiling," *BMC Genomics*, vol. 10, article 252, 2009.

[16] K. Matsushima, K. Morishita, T. Yoshimura et al., "Molecular cloning of a human monocyte-derived neutrophil chemotactic factor (MDNCF) and the induction of MDNCF mRNA by interleukin 1 and tumor necrosis factor," *Journal of Experimental Medicine*, vol. 167, no. 6, pp. 1883–1893, 1988.

[17] R. Wisdom, "Ap-1: one switch for many signals," *Experimental Cell Research*, vol. 253, no. 1, pp. 180–185, 1999.

[18] S. P. Jackson and J. Bartek, "The DNA-damage response in human biology and disease," *Nature*, vol. 461, no. 7267, pp. 1071–1078, 2009.

[19] C. Cavelier, I. Lorenzi, L. Rohrer, and A. von Eckardstein, "Lipid efflux by the ATP-binding cassette transporters ABCA1 and ABCG1," *Biochimica et Biophysica Acta: Molecular and Cell Biology of Lipids*, vol. 1761, no. 7, pp. 655–666, 2006.

[20] M. Digel, R. Ehehalt, W. Stremmel, and J. Füllekrug, "Acyl-CoA synthetases: fatty acid uptake and metabolic channeling," *Molecular and Cellular Biochemistry*, vol. 326, no. 1-2, pp. 23–28, 2009.

[21] A. Kihara, "Very long-chain fatty acids: elongation, physiology and related disorders," *The Journal of Biochemistry*, vol. 152, no. 5, pp. 387–395, 2012.

[22] T. Naganuma, Y. Sato, T. Sassa, Y. Ohno, and A. Kihara, "Biochemical characterization of the very long-chain fatty acid elongase ELOVL7," *FEBS Letters*, vol. 585, no. 20, pp. 3337–3341, 2011.

[23] H. D'Avila, C. G. Freire-de-Lima, N. R. Roque et al., "Host cell lipid bodies triggered by *Trypanosoma cruzi* infection and enhanced by the uptake of apoptotic cells are associated with prostaglandin E2 generation and increased parasite growth," *Journal of Infectious Diseases*, vol. 204, no. 6, pp. 951–961, 2011.

[24] Y. M. Zhu and P. J. Woll, "Mitogenic effects of interleukin-8/CXCL8 on cancer cells," *Future Oncology*, vol. 1, no. 5, pp. 699–704, 2005.

[25] D. Gales, C. Clark, U. Manne, and T. Samuel, "The chemokine CXCL8 in carcinogenesis and drug response," *ISRN Oncology*, vol. 2013, Article ID 859154, 8 pages, 2013.

[26] G. Van Zandbergen, N. Hermann, H. Laufs, W. Solbach, and T. Laskay, "Leishmania promastigotes release a granulocyte chemotactic factor and induce interleukin-8 release but inhibit gamma interferon-inducible protein 10 production by neutrophil granulocytes," *Infection and Immunity*, vol. 70, no. 8, pp. 4177–4184, 2002.

[27] T. Laskay, G. van Zandbergen, and W. Solbach, "Neutrophil granulocytes as host cells and transport vehicles for intracellular pathogens: apoptosis as infection-promoting factor," *Immunobiology*, vol. 213, no. 3-4, pp. 183–191, 2008.

[28] M. Veenstra and R. M. Ransohoff, "Chemokine receptor CXCR2: physiology regulator and neuroinflammation controller?" *Journal of Neuroimmunology*, vol. 246, no. 1-2, pp. 1–9, 2012.

[29] J.-J. Wen, M. Dhiman, E. B. Whorton, and N. J. Garg, "Tissue-specific oxidative imbalance and mitochondrial dysfunction during *Trypanosoma cruzi* infection in mice," *Microbes and Infection*, vol. 10, no. 10-11, pp. 1201–1209, 2008.

[30] J.-J. Wen, G. Vyatkina, and N. Garg, "Oxidative damage during chagasic cardiomyopathy development: role of mitochondrial oxidant release and inefficient antioxidant defense," *Free Radical Biology and Medicine*, vol. 37, no. 11, pp. 1821–1833, 2004.

[31] S. Gupta, M. Dhiman, J.-J. Wen, and N. J. Garg, "ROS Signalling of inflammatory cytokines during *Trypanosoma cruzi* infection," *Advances in Parasitology*, vol. 76, pp. 153–170, 2011.

[32] I. Rahman and W. MacNee, "Regulation of redox glutathione levels and gene transcription in lung inflammation: therapeutic approaches," *Free Radical Biology and Medicine*, vol. 28, no. 9, pp. 1405–1420, 2000.

[33] A. Bowie and L. A. J. O'Neill, "Oxidative stress and nuclear factor-κB activation: a reassessment of the evidence in the light of recent discoveries," *Biochemical Pharmacology*, vol. 59, no. 1, pp. 13–23, 2000.

[34] M. E. Ginn-Pease and R. L. Whisler, "Optimal NFκB mediated transcriptional responses in Jurkat T cells exposed to oxidative stress are dependent on intracellular glutathione and costimulatory signals," *Biochemical and Biophysical Research Communications*, vol. 226, no. 3, pp. 695–702, 1996.

[35] N. D. Perkins, "Integrating cell-signalling pathways with NF-kappaB and IKK function," *Nature Reviews Molecular Cell Biology*, vol. 8, no. 1, pp. 49–62, 2007.

[36] F. S. Machado, H. B. Tanowitz, and A. L. Ribeiro, "Pathogenesis of chagas cardiomyopathy: role of inflammation and oxidative stress," *Journal of the American Heart Association*, vol. 2, no. 5, Article ID e000539, 2013.

[37] M. A. Zacks, J.-J. Wen, G. Vyatkina, V. Bhatia, and N. Garg, "An overview of chagasic cardiomyopathy: pathogenic importance of oxidative stress," *Anais da Academia Brasileira de Ciencias*, vol. 77, no. 4, pp. 695–715, 2005.

[38] X. Ba, S. Gupta, M. Davidson, and N. J. Garg, "*Trypanosoma cruzi* induces the reactive oxygen species-PARP-1-RelA pathway for up-regulation of cytokine expression in cardiomyocytes," *The Journal of Biological Chemistry*, vol. 285, no. 15, pp. 11596–11606, 2010.

[39] F. Nagajyothi, L. M. Weiss, D. L. Silver et al., "*Trypanosoma cruzi* utilizes the host low Density Lipoprotein receptor in invasion," *PLoS Neglected Tropical Diseases*, vol. 5, no. 2, article e953, 2011.

[40] L. A. Campbell, A. W. Lee, M. E. Rosenfeld, and C. C. Kuo, "Chlamydia pneumoniae induces expression of pro-atherogenic factors through activation of the lectin-like oxidized LDL receptor-1," *Pathogens and Disease*, 2013.

[41] L. A. Campbell, M. Puolakkainen, A. Lee, M. E. Rosenfeld, H. J. Garrigues, and C.-C. Kuo, "Chlamydia pneumoniae binds to the lectin-like oxidized LDL receptor for infection of endothelial cells," *Microbes and Infection*, vol. 14, no. 1, pp. 43–49, 2012.

[42] T. Yoshida, N. Koide, I. Mori, H. Ito, and T. Yokochi, "Chlamydia pneumoniae infection enhances lectin-like oxidized low-density lipoprotein receptor (LOX-1) expression on human endothelial cells," *FEMS Microbiology Letters*, vol. 260, no. 1, pp. 17–22, 2006.

[43] D. Sunnemark, R. A. Harris, J. Frostegård, and A. Örn, "Induction of early atherosclerosis in CBA/J mice by combination of *Trypanosoma cruzi* infection and a high cholesterol diet," *Atherosclerosis*, vol. 153, no. 2, pp. 273–282, 2000.

[44] C. M. Anderson and A. Stahl, "SLC27 fatty acid transport proteins," *Molecular Aspects of Medicine*, vol. 34, no. 2-3, pp. 516–528, 2013.

[45] K. Tamura, A. Makino, F. Hullin-Matsuda et al., "Novel lipogenic enzyme ELOVL7 is involved in prostate cancer growth through saturated long-chain fatty acid metabolism," *Cancer Research*, vol. 69, no. 20, pp. 8133–8140, 2009.

[46] F. P. Radner et al., "Mutations in *CERS3* cause autosomal recessive congenital ichthyosis in humans," *PLoS Genet*, vol. 9, no. 6, Article ID e1003536, 2013.

[47] M. Stehr, A. A. Elamin, and M. Singh, "Cytosolic lipid inclusions formed during infection by viral and bacterial pathogens," *Microbes and Infection*, vol. 14, no. 13, pp. 1227–1237, 2012.

[48] N. Kume and T. Kita, "Roles of lectin-like oxidized LDL receptor-1 and its soluble forms in atherogenesis," *Current Opinion in Lipidology*, vol. 12, no. 4, pp. 419–423, 2001.

[49] R. D. Everett, "Interactions between DNA viruses, ND10 and the DNA damage response," *Cellular Microbiology*, vol. 8, no. 3, pp. 365–374, 2006.

Hindawi Publishing Corporation
BioMed Research International
Volume 2014, Article ID 305239, 11 pages
http://dx.doi.org/10.1155/2014/305239

Research Article

Gene Expression Changes Induced by *Trypanosoma cruzi* Shed Microvesicles in Mammalian Host Cells: Relevance of tRNA-Derived Halves

Maria R. Garcia-Silva,[1] Florencia Cabrera-Cabrera,[1] Roberta Ferreira Cura das Neves,[2] Thaís Souto-Padrón,[2] Wanderley de Souza,[3] and Alfonso Cayota[1,4]

[1] *Functional Genomics Unit, Institut Pasteur de Montevideo, Mataojo 2020, 11400 Montevideo, Uruguay*
[2] *Laboratório de Biologia Celular e Ultraestrutura, Instituto de Microbiologia Paulo de Góes, Universidade Federal do Rio de Janeiro, Cidade Universitária, Ilha do Fundão, 21941-590 Rio de Janeiro, RJ, Brazil*
[3] *Laboratório de Ultraestrutura Celular Hertha Meyer, Instituto de Biofísica Carlos Chagas Filho, Universidade Federal do Rio de Janeiro, Avenue Carlos Chagas Filho 373, 21941-902 Rio de Janeiro, RJ, Brazil*
[4] *Department of Medicine, Faculty of Medicine, Avenida Italia s/n, 11600 Montevideo, Uruguay*

Correspondence should be addressed to Alfonso Cayota; cayota@pasteur.edu.uy

Received 5 December 2013; Accepted 1 March 2014; Published 9 April 2014

Academic Editor: Marlene Benchimol

At present, noncoding small RNAs are recognized as key players in novel forms of posttranscriptional gene regulation in most eukaryotes. However, canonical small RNA pathways seem to be lost or excessively simplified in some unicellular organisms including *Trypanosoma cruzi* which lack functional RNAi pathways. Recently, we reported the presence of alternate small RNA pathways in *T. cruzi* mainly represented by homogeneous populations of tRNA- and rRNA-derived small RNAs, which are secreted to the extracellular medium included in extracellular vesicles. Extracellular vesicle cargo could be delivered to other parasites and to mammalian susceptible cells promoting metacyclogenesis and conferring susceptibility to infection, respectively. Here we analyzed the changes in gene expression of host HeLa cells induced by extracellular vesicles from *T. cruzi*. As assessed by microarray assays a large set of genes in HeLa cells were differentially expressed upon incorporation of *T. cruzi*-derived extracellular vesicles. The elicited response modified mainly host cell cytoskeleton, extracellular matrix, and immune responses pathways. Some genes were also modified by the most abundant tRNA-derived small RNAs included in extracellular vesicles. These data suggest that microvesicles secreted by *T. cruzi* could be relevant players in early events of the *T. cruzi* host cell interplay.

1. Introduction

Trypanosoma cruzi, the causative agent of Chagas' disease, is a protozoan parasitewith a complex life cycle, which includes intracellular and extracellular forms that alternate between invertebrate insect vectors belonging to the subfamily Triatominae and mammalian hosts including humans [1, 2]. To cope with these changing environments, *T. cruzi* must undergo rapid and significant changes in gene expression which are achieved essentially at the posttranscriptional level by mechanisms that remain to be completely elucidated [3].

Even though small regulatory RNAs (i.e., microRNAs, siRNAs and piRNAs) have recently emerged as key players in novel forms of posttranscriptional gene regulation in most eukaryotes [4], there is no experimental evidence indicating the presence of canonical machineries associated with small RNA-mediated pathways in *T. cruzi* and other unicellular organisms including *S. cerevisiae*, *L. major*, and *P. falciparum* [5].

In a recent work aimed to identify the presence of alternative small RNA pathways which could contribute to the posttranscriptional control in *T. cruzi*, we reported the presence of homogeneous population of small RNAs derived from mature tRNAs representing from 25 to 30% of the small RNA population [6]. Shortly after, the specific production by

T. cruzi of different populations of small RNAs derived not only from tRNAs but also from rRNAs and sn/snoRNAs was also reported [7, 8].

More recently, we reported that vesicles carrying small tRNAs and the trypanosomatid's Argonaut protein TcPIWI-tryp [9] were actively secreted to the extracellular medium and acted as vehicles for the transfer of these molecules to other parasites and to mammalian susceptible cells but not to nonsusceptible ones. These data suggested that extracellular vesicles (EVs) shed by *T. cruzi* were not only associated with life cycle transition of epimastigotes toward the infective trypomastigote form, but also associated with infection susceptibility of mammalian cells.

It is now accepted that secreted exosomes and shed microvesicles/ectosomes [10] serve as a means for the delivery of genetic information (e.g., miRNAs and mRNAs) and proteins between cells. Interestingly, these exosomal mRNAs and microRNAs were completely functional in recipient cells, thus playing pivotal roles in cell-to-cell communication [11]. It was therefore possible to speculate that *T. cruzi* extracellular vesicles and their cargo could represent a route of intercellular communication delivering "molecular messages" to others cells aimed to induce coordinated responses to assure parasite survival through both the emergence of infective forms and the establishment of a cellular environment able to facilitate infection. In this respect, it was recently reported that *T. cruzi* trypomastigotes invade 5-fold as much susceptible cells when these are preincubated with purified parasite extracellular vesicles [12]. These results suggest that secreted vesicles from *T. cruzi* and their cargo could act as virulence factors by promoting metacyclogenesis and enhancing host cell susceptibility or both.

In order to gain insight on host-pathogen signaling we analyzed the effects induced by *T. cruzi* shed vesicles and their associated small tRNAs cargo on gene expression of susceptible HeLa cells. By using a microarray approach we report that a large set of genes were differentially expressed upon incorporation of *T. cruzi* shed extracellular vesicles in HeLa cells. The elicited response modified mainly host cell cytoskeleton, extracellular matrix, and immune responses pathways. Furthermore, some of the differently expressed genes were also modified when cells were transformed with specific tsRNAs contained in EVs. Taken together, our data provide significant new insight into the early events of the *T. cruzi*-host cell interplay even before contact between the parasite and host cells is established and in the maintenance of the infection which could conduct us to rethink some concepts in host-pathogen biology.

2. Material and Methods

2.1. T. cruzi Epimastigotes and HeLa Cell Line Culture. *T. cruzi* epimastigotes from the Dm28c clone [13] were maintained in exponential growth phase in axenic culture in Liver Infusion Tryptose (LIT) medium supplemented with 10% fetal bovine serum (FBS) at 28°C, with passages every 4 days. Cells from the HeLa cell line were grown in RPMI medium supplemented with 10% FBS and antibiotics (penicillin 100 U/mL and streptomicyn 100 mg/mL) at 37°C, 5% CO_2 with passages every 3 days.

2.2. T. cruzi Microvesicles Purification. Epimastigotes submitted to nutritional stress for 48 h in FBS free RPMI were used as a source of EVs. This nutrient starvation has been recognized as an important condition inducing the emergence of a significant fraction of infective trypomastigote-like parasites [9]. The supernatants of $1 \cdot 10^{11}$ parasites cultured for 48 hours in FBS free RPMI medium were collected and centrifuged at 2000 g for 15 min to eliminate remnant cells. The 2000 g supernatants were collected and centrifuged at 15,000 g at 4°C for 30 min to remove cell debris and eventual apoptotic blebs. The 15,000 g supernatant was ultracentrifuged at 110,000 g at 4°C for 70 min to pellet small extracellular vesicles. The pellet was washed twice in PBS and further ultracentrifuged at 110,000 g for 1 h. Isolation procedures were evaluated by transmission electron microscopy and quantification of EVs was done by determining the total protein concentration by the Bradford protein quantification assay (Pierce). By these procedures the total protein yield of the small vesicular fraction was about 1.2 μg per $1 \cdot 10^{10}$ parasites.

2.3. Optimization of EVs-Cells Incubation Conditions. For the determination of the incubation time, $0.5 \cdot 10^6$ cells were incubated with 300 ng of the *T. cruzi* EVs preparation for 5 minutes, 30 minutes, 2 h, and 24 h. Following incubation, cells were washed twice with PBS, stained with DAPI, and analyzed by fluorescence microscopy. For the determination of the EVs-per-cell ratio, 0.5×10^6 HeLa cells were grown over cover slips in 6 well plates and incubated with 0, 40, 80, 160, 320, and 600 ng of EVs, for 2 hours at 37°C and 5% CO_2. Cells were then subjected to FISH assays as previously described [6] for the detection of certain small RNAs known to be present in *T. cruzi*'s EVs. Briefly, cells were washed twice in PBS and then fixed with 4% paraformaldehyde in PBS for 10 min at room temperature, washed twice with PBS, and further incubated in 25 mM NH_4Cl for 10 min. After washing twice in PBS cells were permeabilized with 0.2% Triton X-100 in PBS for 5 min. Slides were then blocked and prehybridized for 2 h at room temperature in bovine serum albumin 2%, 5X Denhardt, 4X SSC, and 35% formamide (hybridization solution). Hybridization was performed overnight in a humid chamber at 37°C in the presence of 100 nM of the indicated oligonucleotide conjugated to Cy3. After hybridization slides were washed twice in 2X SSC-50% formamide, twice in 2X SSC, once in 1X SSC, incubated with SSC 1X—DAPI (1 mg/mL), and finally washed with 0.5X SSC and 0,1X SSC. For signal amplification, cells were then incubated with an anti-Cy3 antibody (Invitrogen) and revealed with an anti-mouse-TRITC antibody (Invitrogen).

2.4. sRNA Transfection of HeLa Cells. HeLa cells were transfected using $tsRNA^{Leu}$ and $tsRNA^{Thr}$ synthetic oligoribonucleotides and their corresponding scrambled sequences as controls. Synthetic oligoribonucleotides were chemically modified to avoid degradation by ribonucleases with terminal

phosphorothioate bonds and 2′O-methyl ribonucleotides (IDT Inc.) and were labeled with either Cy3 or FAM. Lipofectamine 2000 (Invitrogen) was used as transfection agent (2 μL/mL in Opti-MEM medium) and probes were used at a final concentration of 20 nM.

2.5. Microarray Assays

2.5.1. Sample Collection and RNA Isolation and Processing. For EVs-treated cells, HeLa cells were incubated with *T. cruzi*'s EVs for 2 hours at 37°C and 5% CO_2. Following this incubation, culture medium containing any remaining EVs was removed, cells were washed with PBS, and fresh culture medium was added. Cells were harvested for RNA extraction at 6, 24, or 72 hours after incubation with EVs. Control cells were incubated with EVs-free medium. Each condition was done in triplicate.

For tsRNA/lipofectamine transfected cells, HeLa cells were transfected with $tsRNA^{Thr}$-FAM or $tsRNA^{Leu}$-Cy3 and their respective scramble controls ($tsRNA^{Thr}$Scr-FAM, or $tsRNA^{Leu}$Scr-Cy3) and harvested 24 hours after transfection for RNA extraction. Control cells were treated only with lipofectamine. Cells transfected with either $tsRNA^{Thr}$-FAM or $tsRNA^{Leu}$-Cy3 were included in triplicate, whereas $tsRNA^{Thr}$Scr-FAM, $tsRNA^{Leu}$Scr-Cy3 and control cells were included in duplicate.

For RNA extraction, cells were harvested, washed twice with PBS, and extracted with TRIzol (Invitrogen) following the manufacturer's protocol and further purified with the Illustra RNAspin Mini Isolation kit (GE Healthcare). Both the integrity and quality of the obtained RNA samples were assayed with the RNA 6000 Nano LabChip in the 2100 Bioanalyzer System (Agilent Technologies). Amplification and labeling of the samples were carried out using the Quick Amp Labeling Kit-one color (Agilent Technologies) following the manufacturer's instructions. All samples were labeled with Cy3. Amplified and labeled RNA samples were purified using the RNAeasy mini kit (QIAGEN) and analyzed on a NanoDrop 1000 Spectrophotometer (Thermo Scientific) for quantification and labeling efficiency.

2.5.2. Hybridization, Washing, Scanning of Microarray Chips, and Data Analysis. Hybridization and washing were done using the Gene Expression Hybridization kit (Agilent Technologies) and the Gene Expression Wash Buffer kit (Agilent Technologies), respectively, following the supplier's instructions. Scanning and primary quality controls were carried out in a High-Resolution C scanner (Agilent Technologies).

The obtained results were analyzed with the GeneSpring Multi-Omics Analysis software, version 12.1 (Agilent Technologies). Fluorescence intensity values were log-transformed and normalized, and differentially expressed genes were determined using an ANOVA test (P value $\leq$ 0.05). Differentially expressed genes were then filtered by fold change (specified in the text) and utilized for pathway analysis using the GeneSpring software or the online available tool DAVID [14, 15].

2.6. Real-Time PCR (qPCR). For validation of the microarray results, 1 μg of RNA was retrotranscribed using Invitrogen's Super Script II Reverse Transcriptase and an oligo-dT primer. GAPDH was used for data normalization. Assays were performed in an Illumina Eco Real-Time PCR System using Roche's FastStart Universal SYBR Green Master. The $2^{-\Delta\Delta Ct}$ method and a t-test were used to determine significant differences. The sequences and properties of all the oligonucleotides used throughout this work are summarized in (Supplementary Table 1; see Supplementary Material available online at http://dx.doi.org/10.1155/2014/305239).

3. Results and Discussion

3.1. Monitoring and Kinetics of Uptake of EVs Cargo by HeLa Cells. A series of assays was carried out in order to determine the optimum conditions under which the interaction between *T. cruzi* shed EVs and HeLa cells was successful in terms of fusion and EVs cargo delivery. As shown in Figure 1(a), we purified a fraction of EVs shed by epimastigotes submitted to nutritional stress that will be used along the experiments. It is known that epimastigote starvation reproduces the biological environment found in the most posterior portion of the digestive tract of the invertebrate host where metacyclogenesis takes place as an adaptive response to nutritional stress.

For determination of incubation times, HeLa cells at $0.5 \cdot 10^6/mL^{-1}$ were incubated in the presence of 300 ng of EVs preparation for different times (Figure 1(b)) and analyzed by FISH for the presence of *T. cruzi* specific intracellular 5′ halves $tRNA^{Glu}$, which was used as a tracer molecule of EVs cargo. Results clearly showed that EVs cargo was incorporated by HeLa cells as early as 30 minutes with a diffuse cytoplasmic pattern which adopted a granular disposition beyond 2 h (Figure 1(b)). According to these results an incubation time of 2 h was then selected as representative for further assays.

To determine the best EVs/host cell ratio to employ in our assays, the same amount of HeLa cells was treated for 2 hr with different amounts of EVs ranging from 0 to 600 ng of the EVs preparation. Cells were then subjected to $tRNA^{Glu}$—derived 5′ halves visualization by FISH. As depicted in Figure 1(c) the treatment with 160 ng was identified as an intermediate condition, where cells did not appear oversaturated. Once we selected an incubation condition of 2 h long with 160 ng of purified *T. cruzi* shed EVs, viability assays excluded deleterious effects on cell performance under culture in these conditions (results not shown). It is important to note that the treatment conditions selected here do not necessarily represent the actual conditions that take place during natural infection and to the best of our knowledge information regarding the amount of EVs produced by parasites during the course of infection remains to be elucidated.

3.2. A Microarray-Based Kinetic Analysis Revealed That HeLa Cells Respond to T. cruzi EVs with Significant Changes in Gene Expression Patterns Lasting for at Least 72 h. Changes in gene expression profiles of EVs-treated cells were analyzed by triplicate using an Agilent's microarrays platform at three

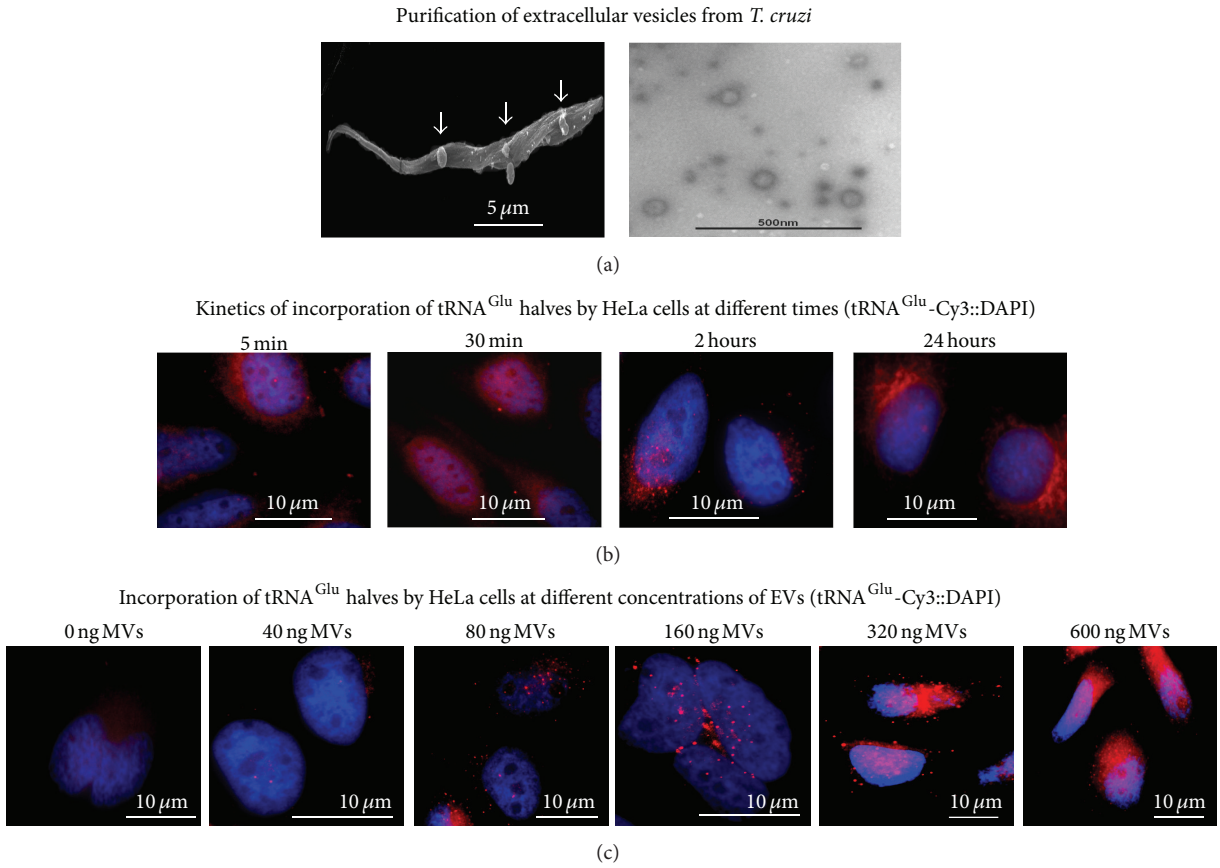

Figure 1: Production of extracellular vesicles by *T. cruzi* and time-course analysis of the uptake of EVs cargo by HeLa cells. (a) Left: scanning electron microscopy of *T. cruzi* epimastigotes showing a parasite with vesicles emerging from the flagellum and the cell body. Right: representative micrograph of purified EVs fraction assessed by transmission electron microscopy. ((b)-(c)) FISH for 5′ halves of $tRNA^{Glu}$ to monitor the incorporation of EVs cargo by HeLa cells exposed to 300 ng of EVs fraction at different times (b) and HeLa cells exposed to different concentrations of EVs ranging from 0 to 600 ng for two hours.

different time points. A total of 743 unique transcripts differentially expressed with a fold change ≥3 and a significance level of ≤0.05 were identified and selected for further analysis (Supplementary Table 2). A graphical view and clusterization analysis (Figure 2) revealed that intact EVs elicit a response in host cells that is more marked at 6 hrs after treatment, is maintained after 24 hrs, but decays towards 72 hrs, where most cellular modified mRNAs returned to basal levels. As depicted in Figure 3(a), the number of total genes differentially expressed at each time point was 605, 351, and 49 at 6 h, 24 h, and 72 h, respectively. A complete picture of the modified genes at different time points is displayed in Figure 3(b) which shows that nearly 40% of the affected genes after 6 hrs were also modified after 24 hrs, whereas only 2.5% remained changed after 72 hrs. The same analysis but now performed separately for up- and downregulated genes revealed a similar behavior (Figures 3(c) and 3(d)). The obtained results seem to indicate that *T. cruzi* shed EVs trigger an important change in the host's cellular gene expression profile.

Recently, Trocoli-Torrecilhas and coworkers described that the treatment of mice with trypomastigote-derived EVs prior to infection caused premature death with an intense inflammatory response while favoring heart parasitism [12]. Later, cells treated with trypomastigote-derived EVs were found to be 5 times more infected by *T. cruzi* than untreated ones [16]. These findings strongly suggest that EVs could play a relevant role during infection. In addition, the uptake of these EVs and their cargo by other parasites as well as mammalian host cells was also described [9]. EVs uptake by other parasites was reported to trigger life cycle transitions and to be involved in promoting susceptibility to infection of host cells [17, 18]. Altogether, evidence gathered so far provide support to the notion that *T. cruzi* secreted EVs in early times may be "preparing" host cells for invasion, through either the interaction with the cell surface or their internalization [16]. Taking into account that the interaction between EVs and host cells would take place previously to direct interaction with parasites themselves, it is possible that the changes that they bring about will take place rather quickly. In addition, if EVs role is that of facilitating parasite entry into the cell, it may not be necessary for the effect of EVs to be sustained over time, since once the infection has been achieved, the parasites themselves represent stimuli enough to continue

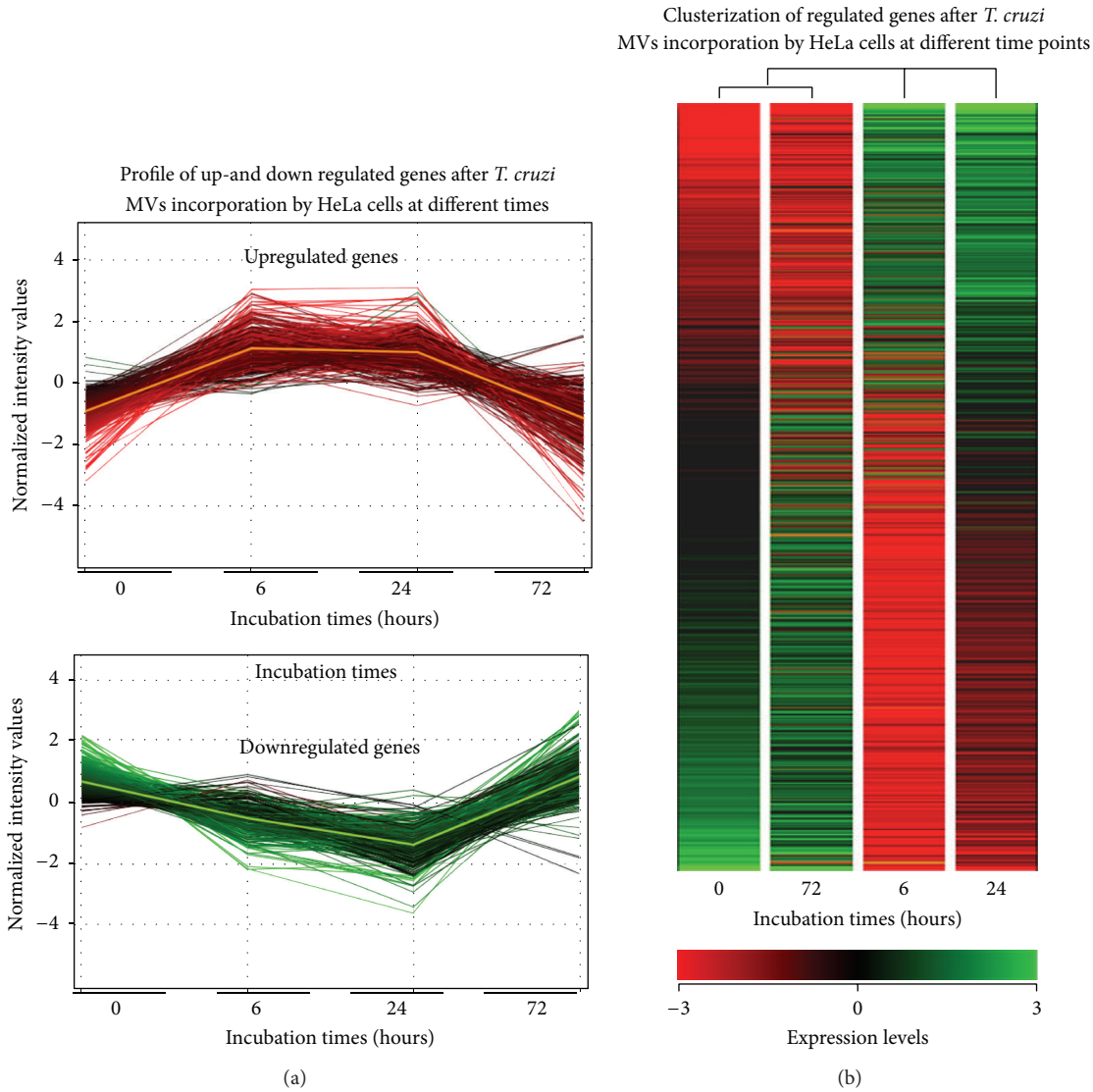

Figure 2: Profile of transcriptomic changes in HeLa cells cocultured with EVs secreted by *T. cruzi*. HeLa cells were exposed to 160 ng of EVs fraction for two hours and analyzed at different time points. (a) Profile of upregulated (upper panel) and downregulated (bottom panel) genes at different times. (b) Cluster analysis of HeLa regulated genes (FC ≥ 3) at different time points (red: underexpressed; green: overexpressed). Experiments were performed by duplicate on three independent samples.

with the infection process. In the subsequent period of times studied, for example, 24 hours, the changes observed in the host cell could be due to modifications needed to maintain a productive infection once the parasite entered the cell. This could be achieved by modifications in the gene expression of the infected cell itself, as we have seen in the present work, or could be through changes in neighboring cells which enable a proparasitic environment. Of note, in our experimental setting, parasites are absent throughout the entire assay which allows a complete recovery by 72 h.

3.3. EVs Secreted by T. cruzi Induce a Broad Response Modifying Host Cell Cytoskeleton, Extracellular Matrix, and Immune Responses Pathways. Differentially expressed genes were grouped into functionally related groups of genes using the GeneSpring software and the public bioinformatic resource DAVID. Several pathways were identified as affected by EVs treatment, particularly after 6 or 24 hrs (Figure 4(a)). Some of these pathways were of particular interest in light of the infection-favoring role of EVs derived from stressed epimastigotes [9]. That is the case of the Rho GTPases signaling pathway affected both at 6 and 24 hrs after treatment. Genes belonging to this pathway were modified in a way that would keep this signaling pathway inactive (Figure 4(b)). This family of proteins coordinates and regulates aspects related to cell morphology and motility, through rearrangement of the cytoskeleton. When active, this pathway induces actin polymerization [19]. In fact, the regulation of actin cytoskeleton is one of the pathways identified as affected by EVs treatment at the same time

Number of genes differently expressed at different times versus control cells (0 hours)

	Total	Total (FC ≥ 3)	6 hours (FC ≥ 3)	24 hours (FC ≥ 3)	72 hours (FC ≥ 3)
Number of modified genes	5580	743	605	351	49

(a)

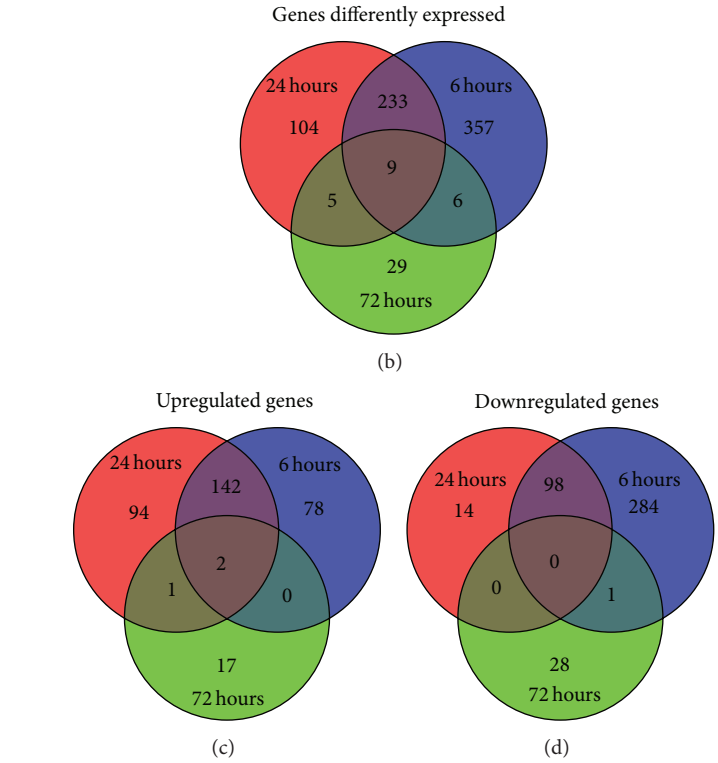

Figure 3: Temporal changes of gene expression in HeLa cells induced by extracellular vesicles secreted by *T. cruzi*. HeLa cells were exposed to 160 ng of EVs fraction for two hours and analyzed at 6, 24, and 72 hours. (a) Table showing the number of differentially expressed genes at different time points. (b) Venn diagrams showing shared and exclusive differentially expressed genes with fold change (FC) ≥ 3. (c) Venn diagrams showing shared and exclusive upregulated genes with FC ≥ 3. (d) Venn diagrams showing shared and exclusive downregulated genes with FC ≥ 3. Experiments were performed by duplicate on three independent samples.

points. Cytoskeleton reorganization has been recognized as one of the main processes that takes place during parasite entry, with actin depolymerization most likely facilitating entry but not retention of parasites within the cell [20, 21]. In this context, EV-triggered depolymerization of cortical actin cytoskeleton in the early stages of interaction would facilitate the initial entry of parasites. Recent work by Mott and coworkers [22] evaluated how host cell mechanics in terms of cytoskeleton remodeling and stiffness were affected by *T. cruzi* trypomastigotes infection and by exposure to shed components present in conditioned medium. Nevertheless, further experiments on EVs-treated cells are necessary to assess whether predicted depolymerization actually takes place at the time points evaluated here.

Matrix metalloproteinases (MMP) are responsible for extracellular matrix (ECM) remodeling. Analysis with both DAVID and GeneSpring revealed that MMPs were altered after 24 h of treatment with EVs. Surprisingly, both MMP and 2 MMP inhibitors (TIMPs) were found to be upregulated (Figure 4(b)). The parasite is known to secrete proteases capable of degrading the ECM, therefore collaborating with the invasion process [23, 24]. In addition, host MMPs have been implicated in the process of tissue damage during infection [25, 26]. One can speculate that EVs stimulate the expression of MMP in order to facilitate ECM degradation before the parasites own proteases, therefore favoring the invasion process. The coexpression of TIMPs may represent the cells response to an unexpected increase in the corresponding MMP activity.

Despite the fact that *T. cruzi*'s EVs seem to aid in the establishment of an infection-favorable cellular environment by eliciting changes in gene expression in response to foreign molecules. In this sense, the NOD-like receptor signaling pathway was found to be activated 6 and 24 hrs after treatment. As depicted in Figure 4(b), mRNAs encoding proteins involved in signal transduction as well as the pathway final products (IL-6, IL-18, CCL2, and CXCL2) were found to be upregulated. It seems likely that cells are able to perceive

Pathways affected by co-incubation of HeLa cells and *T. cruzi*'s EVs.

Pathway	Tool	Condition
NOD-like receptors	GeneSpring/DAVID	6 and 24 hours
Actin cytoskeleton regulation	GeneSpring	6 and 24 hours
IL-1 signaling	GeneSpring	6 hours
Rho GTPases signaling	DAVID	6 and 24 hours
Matrix metalloproteinases	GeneSpring/DAVID	24 hours
Complement and coagulation cascades	GeneSpring/DAVID	6 hours

(a)

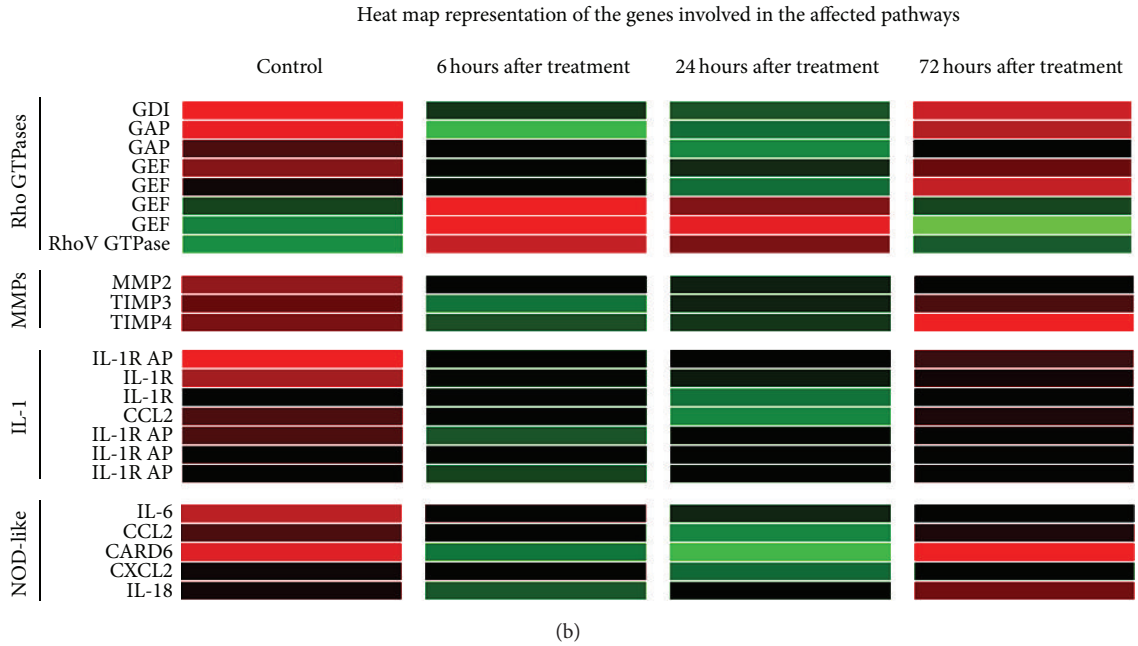

(b)

Figure 4: Pathways affected by EVs treatment. HeLa cells were exposed to 160 ng of EVs fraction for two hours and analyzed at 6, 24, and 72 hours. (a) Table showing the cellular pathways affected by EVs treatment. The corresponding time points and the analysis tool used are included. (b) Heat map representation of the modified genes involved in these pathways (indicated at the left of the figure) for each time point (indicated at the top). For the Rho GTPase pathway the role of the modified genes is expressed as GDI (guanine nucleotide dissociation inhibitor), GAP (GTPase-activating protein), or GEF (guanine nucleotide exchange factor). MMP: matrix metalloproteinase; TIMP: tissue inhibitor of metalloproteinases; IL-1R: interleukin 1 receptor; IL-1R AP: interleukin 1 receptor adaptor protein; CCL2: CC-chemokine ligand 2; CXCL2: CXC-chemokine ligand 2; IL-6: interleukin 6; IL-18: interleukin 18; CARD6: caspase recruitment domain family, member 6. Red: underexpressed; green: overexpressed. Experiments were performed by duplicate on three independent samples.

the presence of strange molecules within the cytoplasm and respond to these signals by producing proinflammatory cytokines and interleukins. Tightly related to the NOD-like signaling pathway is that of IL-1, which was found to be altered 24 h after incubation with EVs. As depicted in Figure 4(b), both the receptor and coreceptor of both types of IL-1 were found to be upregulated as is the proinflammatory cytokine CCL2, a final product of this pathway.

By using a microarray-based approach Manque and collaborators [27] demonstrated that the expression profile of murine cardiomyocytes was greatly affected during the early stages of invasion and infection by *T. cruzi* trypomastigotes. Similar to what we found with EVs incubation, cytoskeleton and ECM remodeling were some of the processes the authors found to be affected, as well as the expression of proinflammatory cytokines and other genes involved in the immune response.

3.4. HeLa Cells Respond to T. cruzi tsRNAs with Changes in the Expression Levels of Specific Genes. Deep sequencing of small RNAs included in EVs from stressed epimastigotes revealed that small RNAs derived from rRNA and tRNA represented about 45% for each. Of note, more than 80% of tsRNAs derived from a restricted group of 4 tRNAs (Leu, Thr, Glu, and Arg) [9]. In order to evaluate their potential effect on host cells, HeLa cells were transfected with Cy3 or FAM-labeled synthetic $tsRNA^{Thr}$, $tsRNA^{Leu}$, and their corresponding scrambled sequences as controls. Transfection

Genes modified by synthetic stRNA-Thr (fold change ≥ 3)

Gene name	Gene symbol	Fold change (24 hours)	Fold change with EVs (time point in hours)
Bromodomain and WD repeat domain containing 1	BRWD1	−4.68	—
Vacuolar protein sorting 8 homolog (S. cerevisiae)	VPS8	−3.98	—
Major facilitator superfamily domain containing 8	MFSD8	−3.65	—
Serine/arginine repetitive matrix 4	SRRM4	−3.50	—
LON peptidase N-terminal domain and ring finger 2	LONRF2	−3.48	—
Hydroxyprostaglandin dehydrogenase 15-(NAD)	HPGD	−3.38	1.8 (6) 3,7 (24)
Remodeling and spacing factor 1	RSF1	−3.26	—
Myeloid/lymphoid (trithorax homolog, Drosophila)	MLLT10	−3.07	—
Hook homolog 1 (Drosophila)	HOOK1	−3.07	3.5 (6) 4.5 (24) 1.7 (72)
Required for meiotic nuclear division 5 homolog A	RMND5A	−3.06	—
Tribbles homolog 1 (Drosophila)	TRIB1	3.04	—
Early growth response 1	EGR1	3.05	—
Activating transcription factor 3	ATF3	3.28	−1.9 (6) 1.2 (24) −1.7 (72)
Chemokine (C-X-C motif) ligand 1	CXCL1	3.41	—
Nuclear receptor subfamily 4, group A, member 1	NR4A1	3.50	—
Chemokine (C-X-C motif) ligand 2	CXCL2	3.66	1.2 (6) 3.2 (24) 1.9 (72)
Hypothetical protein LOC100293390	LOC100293390	3.83	—
Guanylate binding protein 5	GBP5	3.83	—
Dual specificity phosphatase 6	DUSP6	4.08	−1.2 (6) 2.9 (24) 3.0 (72)
Early growth response 2	EGR2	4.16	—

(a)

Genes modified by synthetic stRNA-Leu (fold change ≥ 3)

Gene name	Gene symbol	Fold change (24 hours)	Fold change with EVs (time point in hours)
Copine IV	CPNE4	3.00	—
Sprouty homolog 4 (Drosophila)	SPRY4	3.29	—
General transcription factor IIA	GTF2A1	3.36	—

(b)

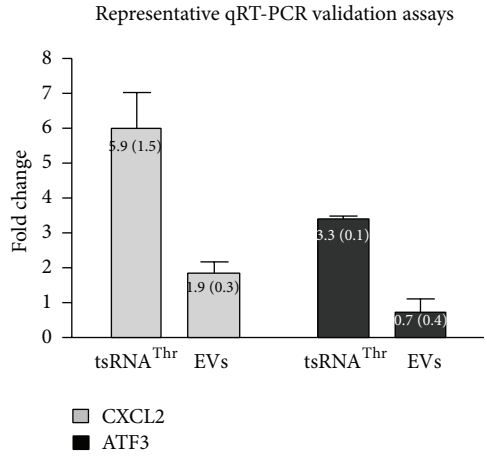

(c)

Figure 5: Genes affected by transfection with tsRNA^{Thr} or tsRNA^{Leu}. (a) Tables showing the name, gene symbol, and fold change for each of the twenty transcripts whose expression was modified upon transfection with tsRNA^{Thr} and the 3 transcripts modified after transfection with tsRNA^{Leu}. (b) Genes which were also modified by EVs are highlighted in grey with the respective fold change.(c) Representative quantitative RT-PCR assays for the CXCL2 and ATF3 genes. Numbers in graphics represent the mean value with their respective SD in brackets. In all cases experiments were performed by duplicate on three independent samples.

efficiency was estimated by fluorescence microscopy, being more than 90% in all experiments. Cell viability was not affected as determined by crystal violet assays (data not shown). A list of genes modified upon transfection with tsRNA^{Thr}, tsRNA^{Leu} was obtained by subtracting genes non-specifically affected by lipofectamine or the corresponding scrambled counterpart. As depicted in Figure 5, transfection of HeLa cells with tsRNA^{Thr} induced significant changes in the level of 20 transcripts at 24 h with a fold change ≥ 3. For tsRNA^{Leu} we only could identify the modulation of 3 transcripts when using a fold change ≥ 3. Further analysis of individual transcripts modified by these tsRNAs revealed that

only some of them were also affected by incubation with EVs at any time regardless of their fold change. Indeed, five genes differentially expressed after tsRNA^{Thr} transfection were also affected by EVs treatment (HPGD, HOOK1, ATF3, CXCL2 y DUSP6 in Figure 5). In this respect, the possibility exists that the effect induced by individual components of complex structures as EVs could be masked or modulated by whole changes induced by EVs containing a diversity of different molecules derived from lipids, proteins, and nucleic acids. In agreement with this idea, it can be noted that some of the genes that were upregulated by EVs treatment (e.g., HPGD and HOOK1) were significantly downregulated by treatment with tsRNA^{Thr}. Conversely, the ATF3 transcript which was downregulated by EVs underwent an opposite response showing a significant upregulation upon transfection of tsRNA^{Thr}. Of note, in the cases of transcripts modified by both EVs and tsRNA^{Thr}, the fold change observed was more important for the single small tRNA. It should be also taken into account that the tsRNA concentrations used here do not necessary mimic those found within EVs or in cells after their entry. Finally, the tsRNA entry pathway may not be the same when delivered by EVs or by transfection agents such as lipofectamine. Thus, their intracellular distribution may vary in each case, affecting in turn their access to different cellular compartments, which could explain the observed differences.

Some transcripts specifically modified by both EVs and tsRNA^{Thr} were reported to be relevant in host-parasite biology. The ATF3 gene encodes a cAMP-dependent transcription factor, whose expression is induced by stress signals such as cytokines, lack of nutrients, and bacterial infection. ATF3 is capable of both activating and repressing transcription of target genes involved in cell defense mechanisms and immune response against pathogens [28, 29]. The CXCL2 is a member of the CXC family of chemokines, recognized as key mediators of inflammatory processes [30, 31]. Analysis of these two genes revealed the existence of some evidence of coexpression between ATF3 and CXCL2 which is consistent with their role in immune responses. Finally, DUSP6 is a dual-specificity phosphatase, which belongs to the MAPK phosphatase family, with specificity for extracellular-signal regulated kinases (ERKs), whose activity was associated with adhesion, cell growth, proliferation, cytoskeleton regulation, and survival pathways [32–34].

Transcripts specifically modified by individual tsRNAs derived from threonine and leucine were confirmed by qRT-PCR. A representative experiment for CXCL2 and ATF3 is depicted in Figure 5(c). In all cases, the fold change values obtained by qRT-PCR were significantly higher than values obtained by microarrays quantification.

The verification of CXCL2 and ATF3 overexpression after tsRNA^{Thr} transfection provides evidence that supports the notion that tRNA-derived small RNAs are capable of modulating gene expression. This does not imply that the tsRNA^{Thr} cargo of EVs is solely responsible for the overexpression of these genes, but it does mean that it is capable of doing so. Additional studies should be performed in order to verify if the changes in gene expression observed are due to the direct interaction between tsRNA and mRNA or if it is a "secondary" effect, mediated by other elements present in host cells.

Due to the fact that, like other small RNAs, tsRNAs have been proposed to act as regulators of mRNA levels and stability, we performed a bioinformatic analysis of putative "seeds" or complementary binding sequences for the *T. cruzi*-derived tsRNA^{Thr} in modified transcripts of HeLa cells. This analysis revealed that ATF3, CXCL2, and DUSP6 have putative binding sites for the tsRNA^{Thr} (Supplementary Figure 1). This could imply that these mRNAs have the potential to be direct targets of tsRNA^{Thr}. Despite some experimental evidence suggesting [35, 36] that tsRNA was able to regulate gene expression through translation initiation inhibition and possibly direct the specific degradation of mRNAs, this mechanism of action remains to be experimentally validated. It is also possible that the tsRNA^{Thr}-mediated upregulation of certain transcripts could be a downstream effect of tsRNAs on other direct targets. Alternatively, binding of tsRNA with its target mRNA could take place and induce upregulation, as it has been reported for certain miRNAs under particular cellular conditions [37]. In this respect, bioinformatic search for possible binding sites on target mRNAs (including 5′ and 3′ UTR sequences) in combination with reporter assays should be conducted to validate any mechanism of action involving direct interaction of tsRNAs with their putative mRNA targets. It is also possible that tsRNAs action could be mediated through RNA binding proteins or other potential molecules.

4. Conclusions

In this work we reported that extracellular vesicles secreted by *T. cruzi* epimastigotes undergoing nutritional stress are able to induce epigenetic changes in mammalian cells susceptible to infection. Additionally, several transcripts modified by EVs were also found to change upon transfection of HeLa cells with two of the most abundant tRNA-derived small RNAs included in EVs. These data suggest that *T. cruzi* secreted vesicles could have a high impact in host cells responses against pathogens and that tRNA-derived halves could be one of the molecules inducing these changes. Taken together, these results highlight the relevance of extracellular vesicles and their cargo in early steps of host-pathogen interactions.

Conflict of Interests

The authors declare that there is no conflict of interests regarding the publication of this paper.

Authors' Contribution

Maria R. Garcia-Silva and Florencia Cabrera-Cabrera contributed equally to this work.

References

[1] M. P. Barrett, R. J. S. Burchmore, A. Stich et al., "The trypanosomiases," *The Lancet*, vol. 362, no. 9394, pp. 1469–1480, 2003.

[2] R. C. B. Q. Figueiredo, D. S. Rosa, and M. J. Soares, "Differentiation of *Trypanosoma cruzi* epimastigotes: metacyclogenesis and adhesion to substrate are triggered by nutritional stress," *Journal of Parasitology*, vol. 86, no. 6, pp. 1213–1218, 2000.

[3] C. Clayton and M. Shapira, "Post-transcriptional regulation of gene expression in trypanosomes and leishmanias," *Molecular and Biochemical Parasitology*, vol. 156, no. 2, pp. 93–101, 2007.

[4] M. Ghildiyal and P. D. Zamore, "Small silencing RNAs: an expanding universe," *Nature Reviews Genetics*, vol. 10, no. 2, pp. 94–108, 2009.

[5] H. Cerutti and J. A. Casas-Mollano, "On the origin and functions of RNA-mediated silencing: from protists to man," *Current Genetics*, vol. 50, no. 2, pp. 81–99, 2006.

[6] M. R. Garcia-Silva, M. Frugier, J. P. Tosar et al., "A population of tRNA-derived small RNAs is actively produced in *Trypanosoma cruzi* and recruited to specific cytoplasmic granules," *Molecular and Biochemical Parasitology*, vol. 171, no. 2, pp. 64–73, 2010.

[7] O. Franzén, E. Arner, M. Ferella et al., "The short non-coding transcriptome of the protozoan parasite *Trypanosoma cruzi*," *PLoS Neglected Tropical Diseases*, vol. 5, no. 8, Article ID e1283, 2011.

[8] L. Reifur, M. R. Garcia-Silva, S. B. Poubel et al., "Distinct subcellular localization of tRNA-derived fragments in the infective metacyclic forms of *Trypanosoma cruzi*," *Memórias do Instituto Oswaldo Cruz*, vol. 107, pp. 816–819, 2012.

[9] M. R. Garcia-Silva, R. F. Cura das Neves, F. Cabrera-Cabrera et al., "Extracellular vesicles shed by *Trypanosoma cruzi* are linked to small RNA pathways, life cycle regulation, and susceptibility to infection of mammalian cells," *Parasitology Research*, vol. 113, no. 1, pp. 285–304, 2014.

[10] E. Cocucci, G. Racchetti, and J. Meldolesi, "Shedding microvesicles: artefacts no more," *Trends in Cell Biology*, vol. 19, no. 2, pp. 43–51, 2009.

[11] H. Valadi, K. Ekström, A. Bossios, M. Sjöstrand, J. J. Lee, and J. O. Lötvall, "Exosome-mediated transfer of mRNAs and microRNAs is a novel mechanism of genetic exchange between cells," *Nature Cell Biology*, vol. 9, no. 6, pp. 654–659, 2007.

[12] A. C. Trocoli Torrecilhas, R. R. Tonelli, W. R. Pavanelli et al., "*Trypanosoma cruzi*: parasite shed vesicles increase heart parasitism and generate an intense inflammatory response," *Microbes and Infection*, vol. 11, no. 1, pp. 29–39, 2009.

[13] V. T. Contreras, T. C. Araujo-Jorge, M. C. Bonaldo et al., "Biological aspects of the Dm 28c clone of *Trypanosoma cruzi* after metacyclogenesis in chemically defined media," *Memorias do Instituto Oswaldo Cruz*, vol. 83, no. 1, pp. 123–133, 1988.

[14] W. da Huang, B. T. Sherman, and R. A. Lempicki, "Systematic and integrative analysis of large gene lists using DAVID bioinformatics resources," *Nature Protocols*, vol. 4, no. 1, pp. 44–57, 2009.

[15] W. da Huang, B. T. Sherman, and R. A. Lempicki, "Bioinformatics enrichment tools: paths toward the comprehensive functional analysis of large gene lists," *Nucleic Acids Research*, vol. 37, no. 1, pp. 1–13, 2009.

[16] A. C. Torrecilhas, R. I. Schumacher, M. J. Alves, and W. Colli, "Vesicles as carriers of virulence factors in parasitic protozoan diseases," *Microbes and Infection*, vol. 14, no. 15, pp. 1465–1474, 2012.

[17] J. M. Inal, E. A. Ansa-Addo, and S. Lange, "Interplay of host-pathogen microvesicles and their role in infectious disease," *Biochemical Society Transactions*, vol. 41, pp. 258–262, 2013.

[18] P. Deolindo, I. Evans-Osses, and M. I. Ramirez, "Microvesicles and exosomes as vehicles between protozoan and host cell communication," *Biochemical Society Transactions*, vol. 41, pp. 252–257, 2013.

[19] A. B. Jaffe and A. Hall, "Rho GTPases: biochemistry and biology," *Annual Review of Cell and Developmental Biology*, vol. 21, pp. 247–269, 2005.

[20] C. L. Epting, B. M. Coates, and D. M. Engman, "Molecular mechanisms of host cell invasion by *Trypanosoma cruzi*," *Experimental Parasitology*, vol. 126, pp. 283–291, 2011.

[21] N. Yoshida, "Molecular basis of mammalian cell invasion by *Trypanosoma cruzi*," *Anais da Academia Brasileira de Ciencias*, vol. 78, no. 1, pp. 87–111, 2006.

[22] A. Mott, G. Lenormand, J. Costales, J. J. Fredberg, and B. A. Burleigh, "Modulation of host cell mechanics by *Trypanosoma cruzi*," *Journal of Cellular Physiology*, vol. 218, no. 2, pp. 315–322, 2009.

[23] M. J. M. Alves and W. Colli, "*Trypanosoma cruzi*: adhesion to the host cell and intracellular survival," *IUBMB Life*, vol. 59, no. 4-5, pp. 274–279, 2007.

[24] F. Y. Maeda, C. Cortez, and N. Yoshida, "Cell signaling during *Trypanosoma cruzi* invasion," *Frontiers in Immunology*, vol. 3, article 361, 2012.

[25] C. Castillo, R. Lopez-Munoz, J. Duaso et al., "Role of matrix metalloproteinases 2 and 9 in *ex vivoTrypanosoma cruzi* infection of human placental chorionic villi," *Placenta*, vol. 33, pp. 991–997, 2012.

[26] N. Geurts, G. Opdenakker, and P. E. van den Steen, "Matrix metalloproteinases as therapeutic targets in protozoan parasitic infections," *Pharmacology and Therapeutics*, vol. 133, no. 3, pp. 257–279, 2012.

[27] P. A. Manque, C. M. Probst, M. C. S. Pereira et al., "*Trypanosoma cruzi* infection induces a global host cell response in cardiomyocytes," *Infection and Immunity*, vol. 79, no. 5, pp. 1855–1862, 2011.

[28] J. Rynes, C. D. Donohoe, P. Frommolt, S. Brodesser, M. Jindra, and M. Uhlirova, "Activating transcription factor 3 regulates immune and metabolic homeostasis," *Molecular and Cellular Biology*, vol. 32, pp. 3949–3962, 2012.

[29] M. R. Thompson, D. Xu, and B. R. G. Williams, "ATF3 transcription factor and its emerging roles in immunity and cancer," *Journal of Molecular Medicine*, vol. 87, no. 11, pp. 1053–1060, 2009.

[30] J. B. da Silva, E. Carvalho, A. E. Covarrubias et al., "Induction of TNF-alfa and CXCL-2 mRNAs in different organs of mice infected with pathogenic Leptospira," *Microbial Pathogenesis*, vol. 52, no. 4, pp. 206–216, 2012.

[31] J. Ha, Y. Lee, and H.-H. Kim, "CXCL2 mediates lipopolysaccharide-induced osteoclastogenesis in RANKL-primed precursors," *Cytokine*, vol. 55, no. 1, pp. 48–55, 2011.

[32] C. J. Caunt and S. M. Keyse, "Dual-specificity MAP kinase phosphatases (MKPs): shaping the outcome of MAP kinase signalling," *FEBS Journal*, vol. 280, pp. 489–504, 2013.

[33] R. J. Dickinson and S. M. Keyse, "Diverse physiological functions for dual-specificity MAP kinase phosphatases," *Journal of Cell Science*, vol. 119, no. 22, pp. 4607–4615, 2006.

[34] K. I. Patterson, T. Brummer, P. M. O'Brien, and R. J. Daly, "Dual-specificity phosphatases: critical regulators with diverse cellular targets," *Biochemical Journal*, vol. 418, no. 3, pp. 475–489, 2009.

[35] S. Yamasaki, P. Ivanov, G.-F. Hu, and P. Anderson, "Angiogenin cleaves tRNA and promotes stress-induced translational repression," *Journal of Cell Biology*, vol. 185, no. 1, pp. 35–42, 2009.

[36] P. Ivanov, M. M. Emara, J. Villen, S. P. Gygi, and P. Anderson, "Angiogenin-induced tRNA fragments inhibit translation initiation," *Molecular Cell*, vol. 43, no. 4, pp. 613–623, 2011.

[37] S. Vasudevan, "Posttranscriptional upregulation by microRNAs," *Wiley Interdisciplinary Reviews: RNA*, vol. 3, pp. 311–330, 2012.

Hindawi Publishing Corporation
BioMed Research International
Volume 2014, Article ID 614014, 14 pages
http://dx.doi.org/10.1155/2014/614014

Review Article

The Double-Edged Sword in Pathogenic Trypanosomatids: The Pivotal Role of Mitochondria in Oxidative Stress and Bioenergetics

Rubem Figueiredo Sadok Menna-Barreto and Solange Lisboa de Castro

Laboratório de Biologia Celular, Instituto Oswaldo Cruz, Fundação Oswaldo Cruz, Avenida Brasil 4365, 21040-360 Manguinhos, RJ, Brazil

Correspondence should be addressed to Rubem Figueiredo Sadok Menna-Barreto; rubemsadok@gmail.com

Received 3 December 2013; Accepted 17 February 2014; Published 31 March 2014

Academic Editor: Wanderley de Souza

The pathogenic trypanosomatids *Trypanosoma brucei*, *Trypanosoma cruzi*, and *Leishmania* spp. are the causative agents of African trypanosomiasis, Chagas disease, and leishmaniasis, respectively. These diseases are considered to be neglected tropical illnesses that persist under conditions of poverty and are concentrated in impoverished populations in the developing world. Novel efficient and nontoxic drugs are urgently needed as substitutes for the currently limited chemotherapy. Trypanosomatids display a single mitochondrion with several peculiar features, such as the presence of different energetic and antioxidant enzymes and a specific arrangement of mitochondrial DNA (kinetoplast DNA). Due to mitochondrial differences between mammals and trypanosomatids, this organelle is an excellent candidate for drug intervention. Additionally, during trypanosomatids' life cycle, the shape and functional plasticity of their single mitochondrion undergo profound alterations, reflecting adaptation to different environments. In an uncoupling situation, the organelle produces high amounts of reactive oxygen species. However, these species role in parasite biology is still controversial, involving parasite death, cell signalling, or even proliferation. Novel perspectives on trypanosomatid-targeting chemotherapy could be developed based on better comprehension of mitochondrial oxidative regulation processes.

1. Trypanosomatids and Diseases

Among trypanosomatids, there are several pathogenic species: *Trypanosoma brucei*, the causative agent of African trypanosomiasis; *Trypanosoma cruzi,* of Chagas disease; and *Leishmania* spp., of leishmaniasis. These diseases, with high morbidity and mortality rates, affect millions of impoverished populations in the developing world, display a limited response to chemotherapy, and are classified as neglected tropical diseases by the World Health Organization [1].

Trypanosomatids exhibit the most typical eukaryotic organelles such as plasma membrane, endoplasmic reticulum, and Golgi; however, some particular structures are also presented. Immediately below the plasma membrane, there is a structural cage of stable microtubules called subpellicular microtubules. The flagellum originated from a flagellar pocket presenting a typical axoneme and a paraflagellar rod, structures involved in the flagellum beating. The nucleus is single maintaining the integrity of its envelope during the whole mitosis [2]. Glycosomes are peroxisomes-like organelles exclusive of trypanosomatids, where it was also compartmentalized part of glycolytic pathway as well as lipids and amino acids oxidation enzymes [3]. Another peculiar structure is acidocalcisome, acidic electron-dense organelle involved in polyphosphate and pyrophosphate metabolism that also works as ions storage [4]. As it will be described in item Section 3.1, the mitochondrial morphology in trypanosomatids is unique presenting a characteristic architecture. These protozoa belong to the earliest diverging branches of the eukaryotic evolutionary tree which have mitochondria, fact that reflects in the mitochondrial organization. The topology of DNA network together with the functionality of the maxicircles and minicircles led to peculiar events in this

organelle biogenesis, despite the similarities between mitochondrial genome of trypanosomatids and other eukaryotes. Some mitochondrial genes named cryptogenes presented unusual structure, being the transcripts remodeling by an RNA editing process [5].

Human African trypanosomiasis (HAT) or sleeping sickness is caused by *T. brucei* and can be fatal if not treated. In 2009, after continued control efforts, the number of reported cases dropped below 10,000 for the first time in 50 years; presently, the estimated number of cases is currently 30,000, and 70 million people are at risk of HAT [6]. This disease is transmitted by the bite of certain species of the genus *Glossina* (tsetse flies), found only in sub-Saharan Africa. HAT occurs in two clinical forms: chronic caused by *T. brucei gambiense* (mostly in West and Central Africa) that accounts for more than 98% of reported cases and acute caused by *T. brucei rhodesiense* (mainly in East and South Central Africa). The acute disease (stage 1) is characterized by the presence of the parasites in the vasculature and lymphatic systems. Without treatment, the parasites penetrate the blood-brain barrier and invade the central nervous system initiating chronic stage (stage 2) that manifests as mental disturbances, anxiety, hallucinations, slurred speech, seizures, and difficulty in walking and talking [7]. These problems can develop over many years in the gambiense form and over several months in the rhodesiense form. The type of chemotherapeutic treatment depends on the stage of the disease, that is, on the degree of central nervous system involvement and the consequent pharmacological need to breach the blood-brain barrier reaching the parasite [8]. The drugs used in the first stage are of lower toxicity and are easier to administer, with pentamidine for infections by *T. b. gambiense* and suramin for *T. b. rhodesiense*. In this case, *T. b. rhodesiense* infections are treated with melarsoprol, while *T. b. gambiense* infections are treated with either eflornithine or a nifurtimox/eflornithine combination therapy (NECT). However, none of these treatments are ideal. Melarsoprol is extremely toxic and has increasing treatment failures. Eflornithine is expensive, is laborious to administer, and lacks efficacy against *T. b. rhodesiense*. The development of NECT reduced the i.v. infusions of eflornithine but it is not ideal, since parenteral administration is still required and patients must be hospitalized for the duration of treatment.

Chagas disease is caused by the protozoan *T. cruzi* and affects approximately eight million individuals in Latin America, of whom 30–40% either have or will develop cardiomyopathy, digestive megasyndromes, or both [9]. Although vectorial (*Triatoma infestans*) and transfusional transmissions have steadily declined [10], this disease can also be orally transmitted through the ingestion of contaminated food or liquids. More recently, a major concern has been the emergence of Chagas disease in nonendemic areas, such as North America and Europe, due to the immigration of infected individuals [11]. Chagas disease is characterised by two clinical phases: a short, acute phase defined by patent parasitaemia and a long, progressive chronic phase [12]. The available chemotherapy for this illness includes two nitroheterocyclic agents, nifurtimox and benznidazole, which are effective against acute infections but show poor activity in the late chronic phase, with severe collateral effects and limited efficacy against different parasitic isolates. These drawbacks justify the urgent need to identify better drugs to treat chagasic patients [13].

Leishmaniasis, which is caused by different species of *Leishmania* with an estimated 12 million cases worldwide, being the infection caused by the bite of infected female sandflies of the genera *Phlebotomus* (Europe, Asia, Africa) and *Lutzomyia* (America) [14]. In VL, *Leishmania donovani* and *Leishmania infantum* (equivalent to *Leishmania chagasi* in South America), being different pathologies associated with these species. *L. donovani* causes distinct pathologies in India and Sudan as well as some strains of *L. infantum* can cause CL. The post-treatment some *L. donovani*-infected patients develop into the diffuse cutaneous form (DCL) named post-kala-azar dermal leishmaniasis (PKDL) [15]. CL also presents in patients in many different forms, though most patients have limited self-cured cutaneous lesions. Over 15 species of *Leishmania* cause CL in humans, with species such as *Leishmania major*, *Leishmania tropica,* and *Leishmania aethiopica* in the Old World and *Leishmania mexicana*, *Leishmania amazonensis*, *Leishmania braziliensis*, *Leishmania panamensis,* and *Leishmania guyanensis* in the New World. Pentostam and Glucantime are first-line drugs for both VL and CL; however, they present several limitations, including severe side effects, the need for daily parenteral administration, and the development of drug resistance. Amphotericin B, normally considered a second-line drug, has been the first line in Bihar (India) for VL following the loss of effectiveness of antimonial drugs. The Amphotericin B formulation AmBisome, the aminoglycoside paromomycin, and the phospholipid analogue miltefosine (oral administration) have been registered for the treatment of VL. On the other hand, for CL, besides antimonials, there are limited proven treatments, that is, pentamidine, amphotericin B, and miltefosine to specific types in South America and paromomycin, only as topical formulation [16, 17].

2. Mitochondria in Higher Eukaryotes

The mitochondrion is a membrane-bound organelle responsible for energy production is involved in growth, differentiation, calcium homeostasis, redox balance, the stress response, and death [18, 19]. The compartmentalised organisation of the mitochondrion in inner and outer membranes, intermembrane space, and the matrix provides an optimal microenvironment for many other biosynthetic and catabolic pathways, such as β-oxidation, heme biosynthesis, steroidogenesis, gluconeogenesis, and amino acid metabolism [20].

Mitochondrial shape and positioning in cells are tightly regulated by fission and fusion events, and an imbalance between these events can lead to shifts in the morphology and viability of the organelle [21]. Fission is required for organelle biogenesis and for the removal of aged or damaged mitochondria through autophagy (mitophagy), allowing organelle content to be degraded or recycled. Fusion is a two-step process in which the outer and inner membranes fuse by separate events. In mammals, outer membrane fusion is

controlled by the GTPase mitofusin (Mfn 1 and 2), whereas inner membrane fusion is controlled by optic atrophy OPA 1, a dynamin-like protein responsible for the maintenance of crista morphology [21].

The mitochondrial precursor proteins are synthesised in the cytosol by free ribosomes and must be imported into the organelle by translocases present in the outer and inner mitochondrial membranes [22]. Signal peptides and specific chaperones direct these precursors to the target compartment. The translocase of the outer membrane (TOM) complex is responsible for the first recognition, and the translocase of the inner membrane (TIM) complex is involved in the import of the cleavable preproteins into the organelle matrix. Additionally, OXA complex helps TOM in the insertion of inner membrane proteins and sorting and assembly machinery (SAM) complex is involved in the assembly of β-barrel proteins into the outer mitochondrial membrane [23].

In response to changes in the intracellular environment by different stress signals, such as a loss of growth factors, hypoxia, oxidative stress, and DNA damage, mitochondria become producers of excessive reactive oxygen species (ROS) and release prodeath proteins, resulting in disrupted ATP synthesis and the activation of cell death pathways [24]. The switch to apoptotic cell death is mediated by cysteine proteases named caspases, which cleave strategic substrates. Another important step in the apoptotic pathway is the permeabilisation of the outer mitochondrial membrane, leading the release of proapoptotic proteins. During stress, both autophagy and apoptosis are activated, and enhanced mitophagy is an early response that promotes survival by removing damaged mitochondria. With increased mitochondrial injury, apoptosis becomes dominant, and inactivation of critical proteins of the autophagic pathway leads to cell death [25].

3. Mitochondria in Trypanosomatids

3.1. Ultrastructural Architecture and Mitochondrial Dynamics. The most remarkable morphological difference between the mitochondria of higher eukaryotes and trypanosomatids is the number and relative volume of the organelles. Thousands of mitochondria can be detected in mammalian cells, representing nearly 20% of the total cellular volume, whereas only a single and ramified organelle is observed in the parasites [26]. This peculiar ultrastructural characteristic was confirmed in all *T. cruzi* developmental forms by 3D reconstruction [27, 28], and the hypothesis was extended to other pathogenic trypanosomatids.

The mitochondrial distribution varies according to the parasite and its developmental form. Generally, the organelle is elongated close to the subpellicular microtubules and the plasma membrane surrounding the entire cell and is dilated only in a disk-shaped structure called the kinetoplast (Figure 1). The ultrastructural aspect of the kinetoplast network in *T. cruzi* trypomastigotes is rounded, differing from all other species and developmental stages that present a bar shape in ultrathin sections. The morphology of the cristae and matrix is also variable, being irregularly distributed in most of the species [29, 30]. The relative volume of the entire organelle directly depends on nutrient availability, reaching 12% of the protozoan volume [30]. As occurred in other eukaryotes, the mitochondrion of trypanosomatids is very dynamic, changing its shape and function in response to the host environment, and changes in bioenergetics metabolism affect the organelle morphology [21]. As described above for other eukaryotic cells, this mitochondrial remodelling is orchestrated by fission and fusion processes and/or autophagy [31]. Despite the morphological evidence reported, the molecular mechanisms involved in the mitophagic process in protozoa are unknown [32]. However, the presence of a dynamin-like protein (DLP) has been detected in *T. brucei* and *L. major* and is related to the fission step, as in mammals [21], and to subsequent organelle segregation during mitosis [33]. To ensure correct segregation, the kDNA network is physically connected to basal bodies through a cluster of filaments that cross the kinetoplast outer and inner membranes [5]. Furthermore, BLAST analysis indicates that DLP is highly conserved in pathogenic trypanosomatids (data not shown). To date, Mtn, the main mitochondrial fusion component, has not been detected in this protozoan family, reinforcing the 3D models of a single organelle proposed by Paulin [27].

In all eukaryotes, including trypanosomatids, a large proportion of mitochondrial proteins are encoded in nuclear genes. However, after transcription, these molecules have to be translocated by the TOM, TIM, SAM, and OXA complexes from the cytosol to the organelle [34], although such complexes are poorly characterised in protists. In trypanosomatids, these translocases were first assessed in *T. brucei*, in which the essential complex TOM40 is replaced by an archaic translocase named pATOM36, responsible for at least part of the import of mitochondrial matrix proteins [35]. Moreover, tbTIM50 and tbTIM17 were described recently [36], but the exact molecular mechanisms involved in mitochondrial protein import in trypanosomatids are still unknown. Interestingly, several pieces of evidence, including data on characterisation of the mitochondria protein-import machinery, suggest that trypanosomatids are among the earliest diverging eukaryotes to have mitochondria [37].

3.2. Molecular Structure and Function of the kDNA Network. The most peculiar characteristic of trypanosomatids is DNA organisation in the kinetoplast. In these protozoa, the mitochondrial genome consists of a complex network of interlocked DNA rings subdivided into two classes: maxicircles and minicircles, representing approximately 30% of the total cellular genome [5, 30]. The kDNA composition varies depending on the species. Approximately, several thousand minicircles and a few dozen maxicircles can be observed per organelle, with only 10% of the entire network mass composed of maxicircles [5, 38].

Maxicircles correspond to mitochondrial DNA in other eukaryotes and encode several genes of respiratory chain complexes, such as cytochrome oxidase, NADH dehydrogenase, and ATP synthase subunits. However, the primary transcripts of these genes need to be processed by inserting

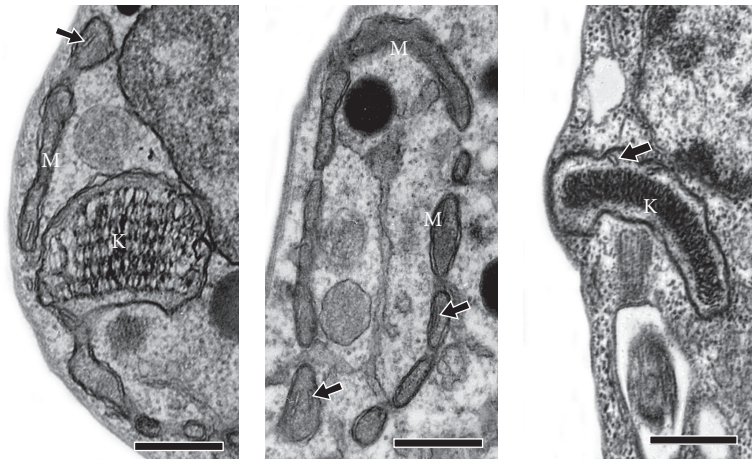

Figure 1: Ultrastructural analysis of the trypanosomatid mitochondrion. *T. cruzi* bloodstream trypomastigote (a) and epimastigotes (b and c). The organelle presents an elongated aspect (M), showing rare cristae (arrows). Differences in kinetoplast morphology (K) can also be observed. Bars: 400 nm.

or removing uridylate residues to create functional mRNAs [39, 40]. Maxicircle transcripts have to be edited to create functional open reading frames. This editing process depends on the templates encoded by minicircles known as guide RNAs, which are responsible for nearly 60% of mRNA synthesised *de novo* [41]. The great variety of guide RNAs necessary to extensively edit maxicircle transcripts is a reasonable explanation for the large number of minicircle copies in comparison with the maxicircle repertoire in the kDNA network [42].

Despite the high heterogeneity of the minicircle population, a conserved region has been identified, to which the origins of replication are localised. Replication specifically occurs in the nuclear S phase, involving the participation of crucial proteins that support the process, such as polymerases, ligases, and topoisomerases [43]. In the early steps, minicircles are released from the network by topoisomerase II and replicate as free molecules. The minicircles are then closed covalently, forming a network again, but a continuous gap or nick can be observed until the replication of all molecules [41]. Another characteristic of minicircles is bent DNA structures consisting of multiple adenines sequences (5–26 bp) that participate in network organisation [39, 44].

3.3. Role in Bioenergetics. Trypanosomatid bioenergetics present remarkable differences from mammalian cells, such as the compartmentalisation of several steps of glycolysis into an organelle named the glycosome and mitochondrial ETC differences, accounting for the great majority of reports on *T. brucei* [45]. Due to their complex life cycles, trypanosomatids adapt to the environment in different hosts, reflecting the functional plasticity of the mitochondrion observed between the parasitic forms [3, 41, 46, 47].

As in higher eukaryotes, mitochondrial respiration occurs via the electron transport chain, which is composed of four integral enzyme complexes in the mitochondrial inner membrane: NADH-ubiquinone oxidoreductase (complex I), succinate-ubiquinone oxidoreductase (complex II), ubiquinolcytochrome c oxidoreductase (complex III or cytochrome bc1), and cytochrome oxidase (complex IV or cytochrome a3), with ubiquinone (coenzyme Q) and cytochrome c functioning as electron carriers between these complexes. Complexes I, III, and IV function as H+ pumps that generate a proton electrochemical gradient that drives ATP synthesis via the reversible mitochondrial ATP synthase (complex V), which couples the processes of respiration and phosphorylation [29, 48, 49].

T. brucei bloodstream forms are essentially glycolytic, living in an environment that presents high glucose levels. In this life stage, many tricarboxylic acid (TCA) cycle enzymes and cytochromes are not expressed in the mitochondrion, affecting energy production [45, 50]. However, F_0-F_1 ATP synthase and consequently the mitochondrial membrane potential (MMP) are still preserved, suggesting basal uncoupled activity in the organelle [51]. The mitochondrion of insect forms is much more functional, perhaps due to the large amounts of ETC substrates in the tsetse fly midgut [46]. This hypothesis also fits *T. cruzi* very well. Our group showed that epimastigotes' ETC is much more efficient than that of bloodstream trypomastigotes, confirming the functional adaptation of the parasite to the host substrates' availability [47].

Among the ETC substrates, succinate plays an essential role in trypanosomatids [52, 53]. In one of the most remarkable mitochondrial studies in these protozoa, Vercesi and colleagues [54] detailed the kinetics of succinate-sensitive oxygen uptake in digitonin-permeabilised *T. cruzi* epimastigotes and also described ETC stages 3 and 4. The oxidation of succinate by complex II leads to the transfer of electrons to complex III via ubiquinone, as occurred in higher eukaryotes. The activity of complexes II–IV was demonstrated in late 1970s in these protozoa, but the presence of functional complex I is still controversial [55, 56].

Curiously, rotenone-independent oxygen uptake has been described in these protozoa, with phenotypic effects observed only at high concentrations of this inhibitor [57]. Although the occurrence of NADH oxidation in *T. brucei* mitochondria is well known, no experimental data have confirmed its participation in respiration processes, even after the prediction of 19 complex I subunits in these parasites, including subunits that are involved in redox reactions [56]. In *T. cruzi* and *L. donovani*, oxygraphic studies revealed that pharmacological inhibition or the presence of natural subunit deletions does not affect oxygen consumption [52, 58]. All of these data indicate important differences in complex I subunits between trypanosomatids and other eukaryotes [56].

Interestingly, KCN, a complex IV inhibitor, does not completely abolish the respiratory rates of *T. brucei*, *T. cruzi,* and *L. donovani*, indicating the existence of a terminal oxidase that is an alternative to cytochrome oxidase. In *T. brucei*, this alternative oxidase (AOX) has been well characterised, with its three-dimensional structure being solved by X-ray crystallography [59]. AOX is a diiron protein that catalyses the four-electron reduction of oxygen to water by ubiquinol. AOX plays a critical role in the bloodstream forms of African trypanosomes, and its expression and amino acid sequence are identical in HAT-causing and non-human infective trypanosomes [60]. In trypanosomatids, the activity of salicylhydroxamic acid, an AOX inhibitor, was observed in both *T. brucei* and *T. cruzi*, suggesting a role in the organisms' energetic metabolism [3, 60]. In contrast, no effect of this inhibitor was detected in cyanide-insensitive *L. donovani* respiration, reinforcing the idea that the exact participation of AOX remains unclear and must be further investigated in trypanosomatids [61].

3.4. Role in Oxidative Stress. The single mitochondrion is one of the major sources of ROS in trypanosomatids, even under physiological conditions. Interestingly, these reactive species could play different roles in the parasites, involving signalling or cytotoxicity, and the cellular strategy for scavenging these species is crucial for protozoan survival [62–64]. Inside the parasites' organelle, the main site of ROS generation is the ETC complexes, except for *T. brucei* bloodstream forms. During mitochondrial respiration, part of the oxygen is reduced to superoxide anions and subsequently to hydrogen peroxide and hydroxyl radicals [65]. These species can cross the mitochondrial membranes and spread through the cytosol and other organelles, culminating in interference in biosynthetic pathways and deleterious consequences [62].

Complex I presents low NADH dehydrogenase activity, justifying the limited generation of superoxide observed in *T. brucei* procyclics and *T. cruzi* epimastigotes [58, 66]. The production of superoxide by rotenone-treated *L. donovani* promastigotes reinforces the necessity of further studies on the biological function of complex I in these parasites. Additionally, the involvement of complex II in ROS generation has been described in parasites treated with the specific inhibitor thenoyltrifluoroacetone [67]. However, there is no doubt that the most prominent ROS source in trypanosomatids is complex III [62, 66, 67]. Additionally, complex IV is not an electron leakage point in the ETC in trypanosomatids or even in higher eukaryotes. Treatment with salicylhydroxamic acid (SHAM) impairs complex IV, compromising electron flow and favouring electron escape from oxygen [62]. Our group reported that *T. cruzi* trypomastigotes present high activity for complexes II-III and low activity for complex IV, which correlates with the high ROS amounts detected in bloodstream forms in comparison with epimastigotes [47]. It was proposed that the AOX described in *T. brucei*, coexisting with complex IV, could play a role in ROS scavenging by the removal of excess reducing equivalents. The inhibition of this oxidase by SHAM confirmed this hypothesis, leading to an increase in ROS production within the protozoan mitochondrion [68].

To control the ROS concentration, pathogenic trypanosomatids present mitochondrial antioxidant defences. However, several differences can be observed in relation to mammals. Among the peculiarities of the protozoan antioxidant repertoire, the presence of an iron-superoxide dismutase and a selenium-independent glutathione peroxidase stands out, as these features are described in *T. brucei*, *T. cruzi,* and several species of *Leishmania* [61]. Surprisingly, the role of iron-superoxide dismutases is distinct among trypanosomatids. In *T. brucei*, these enzymes are not essential for the survival of bloodstream trypomastigotes, most likely due to the low ROS amounts produced by the rudimentary mitochondrion of this parasitic form [69]. In contrast, *T. cruzi* metacyclic trypomastigotes and *L. donovani* amastigotes express iron-superoxide dismutase isoforms in high amounts, indicating a possible relationship between the protozoan antioxidant system and host susceptibility to the infection [70, 71]. Moreover, thiol-based redox metabolism in these parasites involves a dithiol named trypanothione, formed by the conjugation of two glutathione molecules and one spermidine, and its corresponding reductase, a mitochondrial isoform already described in *T. cruzi* [64]. Peroxiredoxins, and especially tryparedoxin peroxidase, are also crucial to hydrogen peroxide detoxification, together with trypanothione reductase and tryparedoxin [72]. Interestingly, an increase in the expression of cytosolic and mitochondrial isoforms of tryparedoxin peroxidase in benznidazole-resistant *T. cruzi* was previously reported, reinforcing the importance of the antioxidant system for the infection outcome [73].

Depending on their concentration, ROS can act as signalling molecules. The detoxification of these species by pathogenic trypanosomatids represents a crucial step in the success of the host-parasite interaction because ROS production is one of the mammalian mechanisms used to control the infection [74]. Recently, Piacenza and coworkers [75] demonstrated mitochondrial redox homeostasis in *T. cruzi* and found that its modulation by antioxidant defences (cytosolic and mitochondrial peroxiredoxins and trypanothione synthetase) contributes to the parasite's virulence, facilitating progression of the infection to the chronic phase. Additionally, Nogueira and colleagues (2011) reported that heme-induced ROS formation favours epimastigote proliferation through the activation of calmodulin kinase II and that this phenotype is regulated by treatment with exogenous

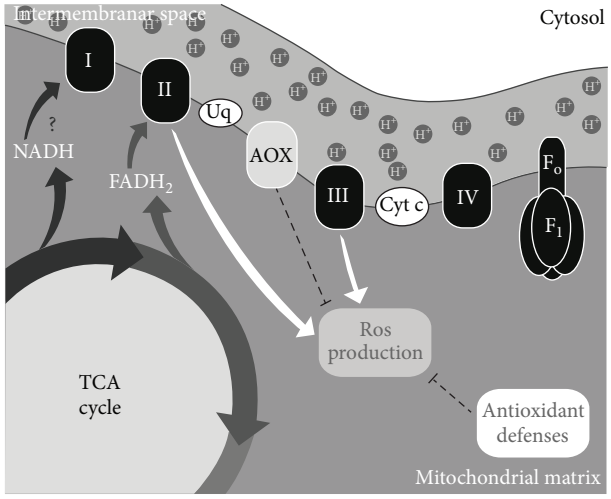

Figure 2: Mechanistic overview of oxidative stress in the trypanosomatid mitochondrion. Complexes II and III are the main sources of ROS, and complex I is not functional in these protozoa. AOX and antioxidant enzymes scavenge these reactive species within the organelle. White arrows: ROS generation and dashed lines: ROS scavenger.

antioxidants [76]. This finding indicates that an oxidative stress stimulus is necessary for cell cycle maintenance, at least in *T. cruzi*, and is fundamental to better comprehension of the regulation processes involved. Figure 2 summarises mitochondrial ROS production in trypanosomatids.

3.5. Role in Cell Death. The existence of programmed cell death (PCD) in unicellular organisms has been a much-debated subject in the last two decades, as the precise molecular mechanisms that trigger death in protozoan parasites are still poorly comprehended. Despite the absence of strong evidence, an altruistic hypothesis has been proposed for trypanosomatids and other protists [32]. In fact, certain typical apoptotic hallmarks have been found, especially in pathogenic trypanosomatids. However, due to the lack of certain crucial molecular events, the existence of PCD in protozoa is still unconfirmed, so the term "apoptosis-like" is more suitable [32, 77].

Among PCD features, the proteolytic activity of caspases should be highlighted. These proteases have very specific substrates, and their cleavage represents a key step in the execution of apoptosis [78]. However, the orthologues of caspases that are present in pathogenic trypanosomatids, named metacaspases, demonstrate no involvement in cell death [79, 80]. In *Leishmania*, metacaspases are mitochondrial, but proteolysis has not been observed in parasites under oxidative stress [79]. In *T. cruzi*, the overexpression of metacaspase-3 and metacaspase-5 indicates their participation in cell cycle regulation and metacyclogenesis [81]. More investigation is necessary to clarify the exact role of metacaspases in unicellular organisms.

Most of the reports examining cell death in protozoa have evaluated the involved pathways under nonphysiological conditions (physical or chemical stresses). The mitochondrion plays a central role in this process, and alterations such as mitochondrial swelling and membrane depolarisation are the most recurrent signs of cell death [29, 77, 82–84].

As already discussed, the high ROS amounts produced by ETC impairment lead to severe deleterious effects in trypanosomatids. In this scenario, *T. cruzi* incubation in the presence of human sera induces important mitochondrial dysfunction and parasite death, a phenotype reverted by iron superoxide dismutase [85]. Similar results were observed in *T. brucei* and *L. donovani* after treatment with ROS inducers. Apoptotic-like features, including a loss of the MMP, were detected, and this phenotype was prevented by pretreatment with the ROS scavengers glutathione and *N*-acetylcysteine [67, 86]. Moreover, *T. brucei* AOX overexpression reduces ROS generation and consequently prevents the appearance of cell death phenotypes [68, 87].

3.6. Proteomic Analysis. Due to the posttranscriptional gene regulation of trypanosomatids, high-throughput proteomics have become essential for protein expression analysis and the validation of genomic annotations [88]. Nontranslated mRNA detection in *T. cruzi* also confirmed the limitation of RNA-based techniques in evaluating the protozoan's gene expression [89]. The proteomic map of pathogenic trypanosomatids has been assessed for the identification of virulence factors and stage-specific proteins and even for the characterisation of immunogenic molecule candidates for vaccines or diagnosis. In the last decade, subcellular proteomic studies have investigated enriched fractions of different organelles from these parasites, including the mitochondrion [88, 90]. This approach increases the number of proteins identifications in the desired fraction, increasing the coverage of the desired organellar content [91].

Different proteomic strategies have been employed in the investigation of the mitochondrial protein profile in trypanosomatids [90]. Mass spectrometry analysis of the mRNA editing mechanism presented in the mitochondria of *T. brucei* described 16 proteins involved in this process. The evaluation of mitochondrion-enriched fractions of *T. brucei* also led to the identification of several mitochondrial proteins, and especially ETC multiprotein complexes, including a unique oxidoreductase complex present only in kinetoplastids [92, 93]. Subsequently, many other proteins related to the TCA cycle, β-oxidation, and amino acid proteolysis were identified in procyclic but not in bloodstream trypomastigotes, reinforcing *T. brucei* mitochondrial plasticity [94]. In 2009, a shotgun approach was used to assess both the soluble and the hydrophobic proteomic content of the *T. brucei* mitochondrion [95]. This study led to the identification of 1,000 mitochondrial proteins, nearly 25% of which needed to have their function and localisation confirmed to exclude purification artefacts. More recently, label-free quantitative mass spectrometry was employed for the characterisation of *T. brucei* mitochondrial outer membrane [40]. Interestingly, 82 proteins were identified, of which approximately 36% are specific to trypanosomatids, but, to date, these proteins have unknown function. Knockdown assays of three of the

proteins demonstrated their participation in the regulation of mitochondrial shape [40]. Additionally, proteomic characterisation of mitochondrial ribosomes was performed for procyclic forms of *T. brucei*, and more than 130 proteins were identified to be associated with the ribosomal structure by liquid chromatography and tandem mass spectrometry (LC-MS/MS) [96].

In *T. cruzi*, the specific mitochondrial protein profile has not yet been investigated. Atwood and colleagues (2005) [71] performed one of the most complete studies on this parasite's proteomics, describing the protein content of different developmental stages. Using a shotgun approach, 2,784 proteins were identified, with 838 detected in all parasitic forms, and a hypothetical annotation was presented for a substantial proportion. Among these identifications, several mitochondrial molecules, such as antioxidant enzymes and chaperones, were described, and their expression in the different parasitic forms evidenced adaptations to host environments. A large subcellular study by Ferella and coworkers [91] reported the expression of nearly all enzymes from the TCA cycle and succinate dehydrogenase subunits in the mitochondrion-enriched fraction. It is important to mention that the described mitochondrial proteins were not identified in a large-scale study by the Atwood III group [71], reinforcing the necessity of subfractionation to increase the number of identifications in specific organelles. In parallel, differential proteomic analyses of parasites treated with drugs were performed and indicated remarkable alterations in the mitochondrial protein content, confirming previous ultrastructural evidence [82, 97, 98]. Mass spectrometry was employed to investigate the drug resistance-related pathways in the parasite, revealing many mitochondrial proteins, such as chaperones, proteases, and antioxidant enzymes, are highly expressed in the resistant phenotype [99]. Recently, our group suggested that the mitochondrial isoform of the gluconeogenesis-related enzyme phosphoenolpyruvate carboxykinase (gi | 1709734) is a promising drug target based on proteomic analysis. The sequence differences between the parasitic and the human enzymes and their substrate specificity indicate that this molecule is a good candidate for drug intervention [100].

The profile of mitochondrial proteins in parasites of the genus *Leishmania* was first assessed in 2006. A two-dimensional electrophoretic analysis of mitochondrion-enriched fractions from *L. infantum* revealed several well-known mitochondrial proteins, and especially chaperones, whose localisation was confirmed by GFP-protein detection by fluorescence microscopy [90, 101]. In *L. donovani*, isobaric tagging for relative and absolute protein quantitation followed by an LC-MS/MS approach supported the hypothesis that changes in energetic metabolism are directly involved in parasite differentiation, as mitochondrial proteins related to the TCA cycle and oxidative phosphorylation are modulated during the parasite's life cycle [102]. The supplementary data in Supplementary Material available online at http://dx.doi.org/10.1155/2014/614014 summarize the proteomic findings in the mitochondrial profile of pathogenic trypanosomatids.

3.7. The Organelle as a Drug Target. The identification of a drug target in a pathogen requires that the target be either absent or at least substantially different in the host. Using metabolic systems that are very different from those of the host, parasites can adapt to the low oxygen tension present within the host animal. Most parasites do not use the oxygen available within the host to generate ATP but rather employ anaerobic metabolic pathways. Phylogenetically, trypanosomatids branch out relatively early relative to the higher eukaryotes. These organisms' cellular organisation is significantly different from that of the mammalian cells, and, thus, the existence of biochemical pathways unique to these pathogens is expected [103].

The fact that kinetoplastids have a single mitochondrion, rudimentary antioxidant defences, and a set of alternative oxidases indicates that this organelle is a potential candidate for drug intervention. In addition, several metabolic pathways are common to all pathogenic trypanosomatids, so, in principle, finding a single drug that is useful against all trypanosomatid diseases is a reasonable expectation. However, to date, this has not been the case, most likely due to the diversity of surroundings inside the parasite's hosts. African trypanosomes live in the bloodstream and cerebrospinal fluid, *T. cruzi* lives in the cytosol of various cell types, and *Leishmania* spp. lives within the phagolysosomes of macrophages.

The mitochondrion represents the most recurrent target, and the intensity of the alterations in this organelle is time dependent and varies with the compound employed [30, 104, 105]. Numerous articles point to the mitochondrion as a drug target in trypanosomatids, primarily based on transmission electron microscopy analysis and MMP evaluation using flow cytometry [29, 83, 106, 107]. As an example, the ultrastructural effect of a naphthoquinone on *T. cruzi* mitochondria can be observed in Figure 3. It is important to keep in mind, however, that induced mitochondrial alterations may be due to either a primary effect directly acting on this organelle or secondary lesions caused by a loss of cellular viability triggered by another cell component or metabolic pathway. Several other classes of compounds also interfere with the ultrastructure and physiology of the mitochondria of trypanosomatids such as sterol biosynthesis inhibitors (SBIs). Trypanosomatids have a strict requirement for specific endogenous ergosterol and analogs and cannot use the supply of cholesterol present in the mammalian host. One of the characteristic ultrastructural effects of SBIs on trypanosomatids is a marked swelling of their single giant mitochondrion, correlated with the depletion of the endogenous parasite sterols, which can lead to cell lysis [108–112]. Epimastigotes of *T. cruzi* treated with ketoconazole plus the lysophospholipid analogue edelfosine presented also severe mitochondrial swelling, with a decrease in electron density of its matrix and appearance of concentric membranar structures inside the organelle [113]. The group of Urbina has shown that *T. cruzi* mitochondrial membranes, in contrast to those of vertebrate cells, are indeed rich in specific parasite's sterols, which are probably required for their energy transducing activities [114, 115].

Figure 3: Common drug effects on the pathogenic trypanosomatid mitochondrion. Treatment with a naphthoquinone leads to mitochondrial swelling (asterisk) and the appearance of concentric membranar structures inside the organelle (arrows). K: typical morphology of the kDNA network. Bar: 200 nm.

The mitochondrial metabolism of *Leishmania* spp. amastigotes and promastigotes, *T. cruzi* trypomastigotes and epimastigotes, and *T. brucei* procyclic forms is similar [53]. The inhibition of certain potential targets is associated with triggering apoptosis-like effects by MMP impairment and/or ROS production. The mitochondrial targeting of drugs may rely on free-radical production and/or calcium homeostasis [116].

Different potential targets can be identified in trypanosomatid mitochondria due to their unique characteristics in comparison with their mammalian counterpart: kDNA, topoisomerases, ETC and related enzymes, and RNA editing [30, 105].

Several drugs induce kDNA disorganisation such as diaminobenzidine, geranylgeraniol and vinblastine induce mitochondrial swelling and irregularly shaped kDNA [107, 117]. In trypanosomatids, growing evidence supports kDNA as the primary target of aromatic diamidines [118]. Ultrastructural and flow cytometric studies have shown that aromatic diamidines and reversed amidines target the *T. cruzi* mitochondrion-kinetoplast complex by interference with the MMP [119, 120]. In *T. brucei*, bloodstream forms exhibit a partial or even complete loss of kDNA, termed dyskinetoplastidy (Dk) and akinetoplastidy (Ak), respectively, which can be induced in the laboratory by DNA-binding drugs such as acriflavine or ethidium bromide [121]. In nature, most *T. brucei* strains contain a kinetoplast, and RNAi assays show that knockdown of kDNA replication and editing proteins is lethal to bloodstream forms [121], suggesting that the kinetoplast is a valid drug target. Moreover, Jensen and Englund [122] reported that minicircle replication is the most vulnerable target of ethidium bromide, which is still used to treat trypanosomiasis in African cattle [123]. Because the kinetoplast has no counterpart in other eukaryotes, complex kDNA replication and segregation present a potential drug target.

DNA topoisomerases are a well-studied mitochondrial target. These enzymes are involved in essential processes, such as DNA replication, transcription, recombination, and repair, and have been used as chemotherapeutic targets in bacterial diseases. DNA topoisomerases are broadly classified as type I, which cleaved single-stranded DNA, and type II, which acted on double-stranded DNA [124]. Two classes of drugs target topoisomerases: poisons (class I) which stabilise the DNA-enzyme complex, resulting in DNA breakdown, and catalytic inhibitors (class II) which compete with ATP for binding to the catalytic site interfering with the enzyme's function [117, 125]. Topoisomerase I purified from *T. cruzi* and *L. donovani* was found to be independent of ATP [126, 127]. In *T. brucei*, this enzyme is composed of two subunits encoded by two genes: one for the DNA-binding domain and a second for the C-terminal catalytic domain [128]. Topoisomerase II genes have been described in *T. brucei*, *T. cruzi*, *L. donovani,* and *L. infantum* [129, 130]. Interestingly, topoisomerase II from *T. brucei* and *L. donovani* exhibits both ATP-dependent and ATP-independent activities. The treatment of *T. brucei*, *T. cruzi,* and *L. donovani* with camptothecin (an inhibitor of eukaryotic DNA topoisomerase I) induces both nuclear and mitochondrial DNA cleavage and covalent linkage to the protein, which is consistent with the existence of drug-sensitive topoisomerase I activity in both compartments [131]. In contrast to other eukaryotic topoisomerases, *L. donovani* topoisomerase is distinct from that of other eukaryotes with respect to its biological properties and sensitivity to drugs [127, 132]. *L. donovani* promastigotes and amastigotes present different sensibility to topoisomerase I inhibitors [133–136]. In *T. cruzi*, topoisomerase II is highly expressed in the replicative forms of the parasite, accounting for the trypanocidal effect of the specific inhibitors clorobiocin, novobiocin, ofloxacin, and nalidixic acid [137–139]. Ultrastructural alterations were also observed in *L. amazonensis* promastigotes treated with these inhibitors [138].

The ETC in trypanosomatids has peculiarities that make its components a promising target, given that MMP maintenance is vital for cell survival. Studies have shown that the loss of MMP induced by drugs is associated with pathogenic trypanosomatid death [67, 83, 140, 141]. Most of the studies on ETC as a drug target in trypanosomatids have been performed with *L. donovani* promastigotes. Pentamidine also induced a rapid collapse of the mitochondrial inner membrane potential of *L. donovani* promastigotes [142]. The association of resistance to pentamidine with mitochondrial alterations was based on studies with its fluorescent analogue DB99 in which drug accumulation in the kinetoplast was observed with wild-type *L. donovani* but not with a resistant strain [143]. Mehta and Saha [67] observed that concurrent inhibition of respiratory chain complex II with pentamidine administration increases the cytotoxicity of the drug. Inhibitors of respiratory chain complexes I (rotenone), II (-noyltrifluoroacetone (TTFA)), and III (antimycin A) resulted in MMP dissipation, ROS production, and the induction of apoptosis-like effects. Additionally, 4,4′-bis((tri-n-pentylphosphonium)methyl)benzophenone dibromide and sitamaquine also target complex II, causing dramatic mitochondrial compromise, including organelle swelling, a decrease in cytoplasmic ATP, ROS production, inhibition

of the oxygen consumption rate, and impairment of the cell cycle in *L. donovani* [144, 145]. Meanwhile, tafenoquine (a primaquine analogue) and miltefosine (a lysophospholipid analogue) inhibit complexes III and IV, respectively, leading to a similar phenotype [146, 147].

Because AOX does not exist in hosts, this enzyme has been proposed as an innovative target for antitrypanosomatid drug development, and related attempts have been reported in the literature [148]. Ascofuranone, an antibiotic isolated from the fungus *Ascochyta viciae*, has been reported as effective against African trypanosomes *in vitro*, and ubiquinol oxidase was identified as the drug's molecular target [148, 149]. It was reported that treatment with ascofuranone led to the appearance of PCD-like features in *T. b. rhodesiense* bloodstream forms [87].

Mitochondrial RNA editing is a vital and unique process that occurs in the mitochondria of trypanosomatids. This specificity makes RNA editing a potential target for new antiparasitic drugs. In *T. brucei*, an RNA editing process has been described. The mRNAs encoding the cytochrome system are mainly edited in the procyclic forms, whereas the mRNAs encoding the NADH dehydrogenase complex are edited in the bloodstream forms [150]. This differential RNA editing observed in the parasite has been less studied in other trypanosomatids. Kim et al. [151] examined the differential expression of subunit II of cytochrome oxidase, but, in contrast to *T. brucei*, no differences were observed in the mRNA levels of this enzyme in either *T. cruzi* insects or mammalian stages. Furthermore, the contribution of the RNA editing process to mitochondrial functional plasticity cannot be excluded. Presently, this possibility should be considered as a hypothesis, and additional studies are needed for confirmation [152]. In this context, Liang and Connell [153] employed high-throughput screening to identify specific inhibitors of RNA editing. Five compounds were identified (GW5074, mitoxantrone, NF 023, protoporphyrin IX, and D-sphingosine), which proved to be inhibitors of insertional editing. More specifically, GW5074 and protoporphyrin IX inhibited the editing process at the level of endonuclease cleavage, which begins the editing process [153]. Recently, another potential target in the RNA editing process was proposed, and inhibition of the RNA ligase KREL1 was described in *T. brucei* [154].

4. Conclusions

In the last decade, the mechanisms of action of numerous drugs have been found to be involved directly or indirectly in mitochondrial metabolism, leading this organelle to become a promising target in the treatment of different diseases. In pathogenic trypanosomatids, the presence of a single mitochondrion, together with its peculiarities, such as the existence of AOX and unique antioxidant defences, attributes a crucial role to the organelle in the development of novel active compounds. Moreover, the morphological and functional plasticity of the mitochondrion during these parasites' life cycles also represent a fundamental step in protozoan adaptations to the host environment. Variation in the efficiency of the respiratory machinery could compromise the redox balance and culminate in ROS generation. Despite their well-known cytotoxic effect, the role of ROS in these protozoa is complex. Depending on the concentration, these reactive species lead to the parasites' death or participate in their cell signalling and proliferation. Thus, better comprehension of oxidative regulation could support new perspectives on trypanosomatid-targeting chemotherapy.

Conflict of Interests

The authors declare that there is no conflict of interests regarding the publication of this paper.

Authors' Contribution

The authors contributed equally to the paper.

Acknowledgments

The authors are grateful to Marcelle Caminha for her essential compilation work, summarised in Supplementary Table 1. The present study was supported by Grants from Fundação Carlos Chagas Filho de Amparo a Pesquisa do Estado do Rio de Janeiro (FAPERJ), Conselho Nacional de Desenvolvimento Científico e Tecnológico (CNPq), and Papes/Fundação Oswaldo Cruz (Fiocruz).

References

[1] WHO, "Neglected tropical diseases," 2013, http://www.who.int/neglected_diseases/en/.

[2] W. de Souza, "Special organelles of some pathogenic protozoa," *Parasitology Research*, vol. 88, no. 12, pp. 1013–1025, 2002.

[3] V. Hannaert, F. Bringaud, F. R. Opperdoes, and P. A. M. Michels, "Evolution of energy metabolism and its compartmentation in Kinetoplastida," *Kinetoplastid Biology and Disease*, vol. 2, article 11, 2003.

[4] R. Docampo, W. de Souza, K. Miranda, P. Rohloff, and S. N. J. Moreno, "Acidocalcisomes—conserved from bacteria to man," *Nature Reviews Microbiology*, vol. 3, no. 3, pp. 251–261, 2005.

[5] A. Schneider, "Unique aspects of mitochondrial biogenesis in trypanosomatids," *International Journal for Parasitology*, vol. 31, no. 13, pp. 1403–1415, 2001.

[6] WHO, 2013, http://www.who.int/trypanosomiasis_african/en/.

[7] P. G. Kennedy, "Clinical features, diagnosis, and treatment of human African trypanosomiasis (sleeping sickness)," *Lancet Neurology*, vol. 12, no. 2, pp. 186–194, 2013.

[8] R. Brun, R. Don, R. T. Jacobs, M. Z. Wang, and M. P. Barrett, "Development of novel drugs for human African trypanosomiasis," *Future Microbiology*, vol. 6, no. 6, pp. 677–691, 2011.

[9] A. Rassi Júnior, A. Rassi, and J. M. Rezende, "American trypanosomiasis (Chagas disease)," *Infectious Disease Clinics in North America*, vol. 26, no. 2, pp. 275–291, 2012.

[10] C. J. Schofield, J. Jannin, and R. Salvatella, "The future of Chagas disease control," *Trends in Parasitology*, vol. 22, no. 12, pp. 583–588, 2006.

[11] G. A. Schmunis and Z. E. Yadon, "Chagas disease: a Latin American health problem becoming a world health problem," *Acta Tropica*, vol. 115, no. 1-2, pp. 14–21, 2010.

[12] A. Rassi Jr., A. Rassi, and J. A. Marin-Neto, "Chagas disease," *The Lancet*, vol. 375, no. 9723, pp. 1388–1402, 2010.

[13] M. D. N. C. Soeiro and S. L. de Castro, "Screening of potential anti-*Trypanosoma cruzi* candidates: *in vitro* and *in vivo* studies," *Open Medicinal Chemistry Journal*, vol. 5, no. 1, pp. 21–30, 2011.

[14] WHO, "Global report for research on infectious diseases of poverty," 2012, http://whqlibdoc.who.int/publications/2012/9789241564489_eng.pdf.

[15] M. P. Barrett and S. L. Croft, "Management of trypanosomiasis and leishmaniasis," *British Medical Bulletin*, vol. 104, pp. 175–196, 2012.

[16] S. L. Croft and P. Olliaro, "Leishmaniasis chemotherapy-challenges and opportunities," *Clinical Microbiology and Infection*, vol. 17, no. 10, pp. 1478–1483, 2011.

[17] S. Sundar and A. Singh, "What steps can be taken to counter the increasing failure of miltefosine to treat visceral leishmaniasis?" *Expert Review of Anti-Infective Therapy*, vol. 11, no. 2, pp. 117–119, 2013.

[18] M. R. Duchen, "Mitochondria and calcium: from cell signalling to cell death," *Journal of Physiology*, vol. 529, no. 1, pp. 57–68, 2000.

[19] P. Kakkar and B. K. Singh, "Mitochondria: a hub of redox activities and cellular distress control," *Molecular and Cellular Biochemistry*, vol. 305, no. 1-2, pp. 235–253, 2007.

[20] L. Galluzzi, O. Kepp, C. Trojel-Hansen, and G. Kroemer, "Mitochondrial control of cellular life, stress, and death," *Circulation Research*, vol. 111, no. 9, pp. 1198–1207, 2012.

[21] L. D. Osellame, T. S. Blacker, and M. R. Duchen, "Cellular and molecular mechanisms of mitochondrial function," *Best Practice & Research Clinical Endocrinology & Metabolism*, vol. 26, no. 6, pp. 711–723, 2012.

[22] M. F. Bauer, S. Hofmann, W. Neupert, and M. Brunner, "Protein translocation into mitochondria: the role of TIM complexes," *Trends in Cell Biology*, vol. 10, no. 1, pp. 25–31, 2000.

[23] B. Alberts, A. Johnson, J. Lewis et al., *Molecular Biology of the Cell*, Garland Science, New York, NY, USA, 5th edition, 2007.

[24] L. Ravagnan, T. Roumier, and G. Kroemer, "Mitochondria, the killer organelles and their weapons," *Journal of Cellular Physiology*, vol. 192, no. 2, pp. 131–137, 2002.

[25] A. Kubli and B. Å. Gustafsson, "Mitochondria and mitophagy: the yin and yang of cell death control," *Circulation Researchno*, vol. 111, no. 9, pp. 1208–1221, 2012.

[26] L. Simpson, "The kinetoplast of the hernoflagellates," *International Review of Cytology*, vol. 32, pp. 139–207, 1972.

[27] J. J. Paulin, "The chondriome of selected trypanosomatids. A three-dimensional study based on serial thick sections and high voltage electron microscopy," *Journal of Cell Biology*, vol. 66, no. 2, pp. 404–413, 1975.

[28] L. B. Newberry and J. J. Paulin, "Reconstruction of the chondriome of the amastigote from *Trypanosoma cruzi*," *Journal of Parasitology*, vol. 75, no. 4, pp. 649–652, 1989.

[29] W. de Souza, M. Attias, and J. C. F. Rodrigues, "Particularities of mitochondrial structure in parasitic protists (Apicomplexa and Kinetoplastida)," *The International Journal of Biochemistry & Cell Biology*, vol. 41, no. 10, pp. 2069–2080, 2009.

[30] L. M. Fidalgo and L. Gille, "Mitochondria and trypanosomatids: targets and drugs," *Pharmaceutical Research*, vol. 28, no. 11, pp. 2758–2770, 2011.

[31] L. Griparic and A. M. van der Bliek, "The many shapes of mitochondrial membranes," *Traffic*, vol. 2, no. 4, pp. 235–244, 2001.

[32] M. Duszenko, M. L. Ginger, A. Brennand et al., "Autophagy in protists," *Autophagy*, vol. 7, no. 2, pp. 127–158, 2011.

[33] G. W. Morgan, D. Goulding, and M. C. Field, "The single dynamin-like protein of Trypanosoma brucei regulates mitochondrial division and is not required for endocytosis," *The Journal of Biological Chemistry*, vol. 279, no. 11, pp. 10692–10701, 2004.

[34] A. Schneider, D. Bursać, and T. Lithgow, "The direct route: a simplified pathway for protein import into the mitochondrion of trypanosomes," *Trends in Cell Biology*, vol. 18, no. 1, pp. 12–18, 2008.

[35] M. Pusnik, J. Mani, O. Schmidt et al., "An essential novel component of the noncanonical mitochondrial outer membrane protein import system of trypanosomatids," *Molecular Biology of the Cell*, vol. 23, no. 17, pp. 3420–3428, 2012.

[36] M. R. Duncan, M. Fullerton, and M. Chaudhuri, "Tim50 in *Trypanosoma brucei* possesses a dual specificity phosphatase activity and is critical for mitochondrial protein import," *The Journal of Biological Chemistry*, vol. 288, no. 5, pp. 3184–3197, 2013.

[37] M. Pusnik, O. Schmidt, A. J. Perry et al., "Mitochondrial preprotein translocase of trypanosomatids has a bacterial origin," *Current Biology*, vol. 21, no. 20, pp. 1738–1743, 2011.

[38] T. A. Shapiro and P. T. Englund, "The structure and replication of kinetoplast DNA," *Annual Review of Microbiology*, vol. 49, pp. 117–143, 1995.

[39] R. E. Jensen and A. E. Johnson, "Opening the door to mitochondrial protein import," *Nature Structural Biology*, vol. 8, no. 12, pp. 1008–1010, 2001.

[40] M. Niemann, S. Wiese, J. Mani et al., "Mitochondrial outer membrane proteome of *Trypanosoma brucei* reveals novel factors required to maintain mitochondrial morphology," *Molecular and Cellular Proteomics*, vol. 12, no. 2, pp. 515–528, 2013.

[41] B. Liu, Y. Liu, S. A. Motyka, E. E. C. Agbo, and P. T. Englund, "Fellowship of the rings: the replication of kinetoplast DNA," *Trends in Parasitology*, vol. 21, no. 8, pp. 363–369, 2005.

[42] M. Hong and L. Simpson, "Genomic organization of *Trypanosoma brucei* kinetoplast DNA minicircles," *Protist*, vol. 154, no. 2, pp. 265–279, 2003.

[43] R. Woodward and K. Gull, "Timing of nuclear and kinetoplast DNA replication and early morphological events in the cell cycle of *Trypanosoma brucei*," *Journal of Cell Science*, vol. 95, no. 1, pp. 49–57, 1990.

[44] J. C. Hines and D. S. Ray, "Structure of discontinuities in kinetoplast DNA-associated minicircles during S phase in *Crithidia fasciculata*," *Nucleic Acids Research*, vol. 36, no. 2, pp. 444–450, 2008.

[45] C. E. Clayton and P. Michels, "Metabolic compartmentation in African trypanosomes," *Parasitology Today*, vol. 12, no. 12, pp. 465–471, 1996.

[46] A. G. Tielens and J. J. Van Hellemond, "Differences in energy metabolism between Trypanosomatidae," *Parasitology Today*, vol. 14, no. 7, pp. 265–271, 1998.

[47] R. L. S. Gonçalves, R. F. S. Menna Barreto, C. R. Polycarpo, F. R. Gadelha, S. L. Castro, and M. F. Oliveira, "A comparative assessment of mitochondrial function in epimastigotes and bloodstream trypomastigotes of *Trypanosoma cruzi*," *Journal of Bioenergetics and Biomembranes*, vol. 43, no. 6, pp. 651–661, 2011.

[48] B. Chance and G. R. Williams, "The respiratory chain and oxidative phosphorylation," *Advances in Enzymology and Related Subjects of Biochemistry*, vol. 17, pp. 65–134, 1956.

[49] H. Schägger, "Respiratory chain supercomplexes," *IUBMB Life*, vol. 52, no. 3–5, pp. 119–128, 2001.

[50] J. W. Priest and S. L. Hajduk, "Developmental regulation of *Trypanosoma brucei* cytochrome c reductase during bloodstream to procyclic differentiation," *Molecular and Biochemical Parasitology*, vol. 65, no. 2, pp. 291–304, 1994.

[51] D. P. Nolan and H. P. Voorheis, "The mitochondrion in bloodstream forms of *Trypanosoma brucei* is energized by the electrogenic pumping of protons catalysed by the F1F0-ATPase," *European Journal of Biochemistry*, vol. 209, no. 1, pp. 207–216, 1992.

[52] A. Denicola-Seoane, H. Rubbo, E. Prodanov, and J. F. Turrens, "Succinate-dependent metabolism in *Trypanosoma cruzi* epimastigotes," *Molecular and Biochemical Parasitology*, vol. 54, no. 1, pp. 43–50, 1992.

[53] A. G. M. Tielens and J. J. van Hellemond, "Surprising variety in energy metabolism within Trypanosomatidae," *Trends in Parasitology*, vol. 25, no. 10, pp. 482–490, 2009.

[54] A. E. Vercesi, C. F. Bernardes, M. E. Hoffmann, F. R. Gadelha, and R. Docampo, "Digitonin permeabilization does not affect mitochondrial function and allows the determination of the mitochondrial membrane potential of *Trypanosoma cruzi in situ*," *The Journal of Biological Chemistry*, vol. 266, no. 22, pp. 14431–14434, 1991.

[55] G. C. Hill, "Electron transport systems in kinetoplastida," *Biochimica et Biophysica Acta*, vol. 456, no. 2, pp. 149–193, 1976.

[56] F. R. Opperdoes and P. A. M. Michels, "Complex I of Trypanosomatidae: does it exist?" *Trends in Parasitology*, vol. 24, no. 7, pp. 310–317, 2008.

[57] F. R. Hernandez and J. F. Turrens, "Rotenone at high concentrations inhibits NADH-fumarate reductase and the mitochondrial respiratory chain of *Trypanosoma brucei* and *T. cruzi*," *Molecular and Biochemical Parasitology*, vol. 93, no. 1, pp. 135–137, 1998.

[58] J. César Carranza, A. J. Kowaltowski, M. A. G. Mendonça, T. C. De Oliveira, F. R. Gadelha, and B. Zingales, "Mitochondrial bioenergetics and redox state are unaltered in *Trypanosoma cruzi* isolates with compromised mitochondrial complex i subunit genes," *Journal of Bioenergetics and Biomembranes*, vol. 41, no. 3, pp. 299–308, 2009.

[59] T. Shiba, Y. Kido, K. Sakamoto et al., "Structure of the trypanosome cyanide-insensitive alternative oxidase," *Proceedings of the National Academy of Sciences USA*, vol. 110, no. 12, pp. 4580–4585, 2013.

[60] M. Chaudhuri, R. D. Ott, and G. C. Hill, "Trypanosome alternative oxidase: from molecule to function," *Trends in Parasitology*, vol. 22, no. 10, pp. 484–491, 2006.

[61] K. R. Santhamma and A. Bhaduri, "Characterization of the respiratory chain of *Leishmania donovani* promastigotes," *Molecular and Biochemical Parasitology*, vol. 75, no. 1, pp. 43–53, 1995.

[62] M. Tomás and H. Castro, "Redox metabolism in mitochondria of trypanosomatids," *Antioxidants & Redox Signaling*, vol. 19, no. 7, pp. 696–707, 2013.

[63] A. Boveris and A. O. M. Stoppani, "Hydrogen peroxide generation in *Trypanosoma cruzi*," *Experientia*, vol. 33, no. 10, pp. 1306–1308, 1977.

[64] P. S. Brookes, A.-L. Levonen, S. Shiva, P. Sarti, and V. M. Darley-Usmar, "Mitochondria: regulators of signal transduction by reactive oxygen and nitrogen species," *Free Radical Biology & Medicine*, vol. 33, no. 6, pp. 755–764, 2002.

[65] J. F. Turrens, "Oxidative stress and antioxidant defenses: a target for the treatment of diseases caused by parasitic protozoa," *Molecular Aspects of Medicine*, vol. 25, no. 1-2, pp. 211–220, 2004.

[66] J. Fang and D. S. Beattie, "Rotenone-insensitive NADH dehydrogenase is a potential source of superoxide in procyclic *Trypanosoma brucei* mitochondria," *Molecular and Biochemical Parasitology*, vol. 123, no. 2, pp. 135–142, 2002.

[67] A. Mehta and C. Shaha, "Apoptotic death in *Leishmania donovani* promastigotes in response to respiratory chain inhibition: complex II inhibition results in increased pentamidine cytotoxicity," *The Journal of Biological Chemistry*, vol. 279, no. 12, pp. 11798–11813, 2004.

[68] J. Fang and D. S. Beattie, "Alternative oxidase present in procyclic *Trypanosoma brucei* may act to lower the mitochondrial production of superoxide," *Archives of Biochemistry and Biophysics*, vol. 414, no. 2, pp. 294–302, 2003.

[69] S. R. Wilkinson, S. R. Prathalingam, M. C. Taylor, A. Ahmed, D. Horn, and J. M. Kelly, "Functional characterisation of the iron superoxide dismutase gene repertoire in *Trypanosoma brucei*," *Free Radical Biology & Medicine*, vol. 40, no. 2, pp. 198–209, 2006.

[70] S. Ghosh, S. Goswami, and S. Adhya, "Role of superoxide dismutase in survival of *Leishmania* within the macrophage," *Biochemical Journal*, vol. 369, no. 3, pp. 447–452, 2003.

[71] J. A. Atwood III, D. B. Weatherly, T. A. Minning et al., "The *Trypanosoma cruzi* proteome," *Science*, vol. 309, no. 5733, pp. 473–476, 2005.

[72] L. R. Krauth-Siegel, M. A. Comini, and T. Schlecker, "The trypanothione system," *Subcellular Biochemistry*, vol. 44, pp. 231–251, 2007.

[73] F. B. Nogueira, J. C. Ruiz, C. Robello, A. J. Romanha, and S. M. F. Murta, "Molecular characterization of cytosolic and mitochondrial tryparedoxin peroxidase in *Trypanosoma cruzi* populations susceptible and resistant to benznidazole," *Parasitology Research*, vol. 104, no. 4, pp. 835–844, 2009.

[74] R. D. Pearson and R. T. Steigbigel, "Phagocytosis and killing of the protozoan *Leishmania donovani* by human polymorphonuclear leukocytes," *Journal of Immunology*, vol. 127, no. 4, pp. 1438–1443, 1981.

[75] L. Piacenza, G. Peluffo, M. N. Alvarez, A. Martínez, and R. Radi, "*Trypanosoma cruzi* antioxidant enzymes as virulence factors in Chagas disease," *Antioxidants & Redox Signaling*, vol. 19, no. 7, pp. 723–734, 2013.

[76] N. P. D. A. Nogueira, C. F. de Souza, F. M. D. S. Saraiva et al., "Heme-induced ROS in *Trypanosoma cruzi* activates CaMKII-like that triggers epimastigote proliferation. One helpful effect of ROS," *PloS One*, vol. 6, no. 10, Article ID e25935, 2011.

[77] J. C. F. Rodrigues, S. H. Seabra, and W. de Souza, "Apoptosis-like death in parasitic protozoa," *Brazilian Journal of Morphological Sciences*, vol. 23, no. 1, pp. 87–98, 2006.

[78] U. Fischer, R. U. Jänicke, and K. Schulze-Osthoff, "Many cuts to ruin: a comprehensive update of caspase substrates," *Cell Death & Differentiation*, vol. 10, no. 1, pp. 76–100, 2003.

[79] B. Meslin, H. Zalila, N. Fasel, S. Picot, and A.-L. Bienvenu, "Are protozoan metacaspases potential parasite killers?" *Parasites and Vectors*, vol. 4, no. 1, article 26, 2011.

[80] W. R. Proto, G. H. Coombs, and J. C. Mottram, "Cell death in parasitic protozoa: regulated or incidental?" *Nature Reviews Microbiology*, vol. 11, no. 1, pp. 58–66, 2013.

[81] M. Laverrière, J. J. Cazzulo, and V. E. Alvarez, "Antagonic activities of *Trypanosoma cruzi* metacaspases affect the balance between cell proliferation, death and differentiation," *Cell Death & Differentiation*, vol. 19, no. 8, pp. 1358–1369, 2012.

[82] R. F. S. Menna-Barreto, J. R. Corrêa, A. V. Pinto, M. J. Soares, and S. L. De Castro, "Mitochondrial disruption and DNA fragmentation in *Trypanosoma cruzi* induced by naphthoimidazoles synthesized from β-lapachone," *Parasitology Research*, vol. 101, no. 4, pp. 895–905, 2007.

[83] R. F. S. Menna-Barreto, K. Salomão, A. P. Dantas et al., "Different cell death pathways induced by drugs in *Trypanosoma cruzi*: an ultrastructural study," *Micron*, vol. 40, no. 2, pp. 157–168, 2009.

[84] R. F. S. Menna-Barreto, J. R. Corrêa, C. M. Cascabulho et al., "Naphthoimidazoles promote different death phenotypes in *Trypanosoma cruzi*," *Parasitology*, vol. 136, no. 5, pp. 499–510, 2009.

[85] L. Piacenza, F. Irigoín, M. N. Alvarez et al., "Mitochondrial superoxide radicals mediate programmed cell death in *Trypanosoma cruzi*: cytoprotective action of mitochondrial iron superoxide dismutase overexpression," *Biochemical Journal*, vol. 403, no. 2, pp. 323–334, 2007.

[86] G. Sudhandiran and C. Shaha, "Antimonial-induced increase in intracellular Ca^{2+} through non-selective cation channels in the host and the parasite is responsible for apoptosis of intracellular *Leishmania donovani* amastigotes," *The Journal of Biological Chemistry*, vol. 278, no. 27, pp. 25120–25132, 2003.

[87] A. Tsuda, W. H. Witola, K. Ohashi, and M. Onuma, "Expression of alternative oxidase inhibits programmed cell death-like phenomenon in bloodstream form of *Trypanosoma brucei* rhodesiense," *Parasitology International*, vol. 54, no. 4, pp. 243–251, 2005.

[88] R. F. Menna-Barreto and J. Perales, "The expected outcome of the *Trypanosoma cruzi* proteomic map: a review of its potential biological applications for drug target discovery," *Subcellular Biochemistry*, vol. 74, pp. 305–322, 2014.

[89] F. B. Holetz, L. R. Alves, C. M. Probst et al., "Protein and mRNA content of TcDHH1-containing mRNPs in *Trypanosoma cruzi*," *The FEBS Journal*, vol. 277, no. 16, pp. 3415–3426, 2010.

[90] P. Cuervo, G. B. Domont, and J. B. De Jesus, "Proteomics of trypanosomatids of human medical importance," *Journal of Proteomics*, vol. 73, no. 5, pp. 845–867, 2010.

[91] M. Ferella, D. Nilsson, H. Darban et al., "Proteomics in *Trypanosoma cruzi*-localization of novel proteins to various organelles," *Proteomics*, vol. 8, no. 13, pp. 2735–2749, 2008.

[92] A. K. Panigrahi, T. E. Allen, K. Stuart, P. A. Haynes, and S. P. Gygi, "Mass spectrometric analysis of the editosome and other multiprotein complexes in *Trypanosoma brucei*," *Journal of the American Society for Mass Spectrometry*, vol. 14, no. 7, pp. 728–735, 2003.

[93] A. K. Panigrahi, Y. Ogata, A. Zíková et al., "A comprehensive analysis of *Trypanosoma brucei* mitochondrial proteome," *Proteomics*, vol. 9, no. 2, pp. 434–450, 2009.

[94] D. Vertommen, J. Van Roy, J.-P. Szikora, M. H. Rider, P. A. M. Michels, and F. R. Opperdoes, "Differential expression of glycosomal and mitochondrial proteins in the two major life-cycle stages of *Trypanosoma brucei*," *Molecular and Biochemical Parasitology*, vol. 158, no. 2, pp. 189–201, 2008.

[95] A. K. Panigrahi, A. Zíková, R. A. Dalley et al., "Mitochondrial complexes in *Trypanosoma brucei*: a novel complex and a unique oxidoreductase complex," *Molecular and Cellular Proteomics*, vol. 7, no. 3, pp. 534–545, 2008.

[96] A. Zíková, A. K. Panigrahi, R. A. Dalley et al., "*Trypanosoma brucei* mitochondrial ribosomes: affinity purification and component identification by mass spectrometry," *Molecular and Cellular Proteomics*, vol. 7, no. 11, pp. 1286–1296, 2008.

[97] R. F. S. Menna-Barreto, A. Henriques-Pons, A. V. Pinto, J. A. Morgado-Diaz, M. J. Soares, and S. L. De Castro, "Effect of a β-lapachone-derived naphthoimidazole on *Trypanosoma cruzi*: identification of target organelles," *Journal of Antimicrobial Chemotherapy*, vol. 56, no. 6, pp. 1034–1041, 2005.

[98] R. F. S. Menna-Barreto, D. G. Beghini, A. T. S. Ferreira, A. V. Pinto, S. L. De Castro, and J. Perales, "A proteomic analysis of the mechanism of action of naphthoimidazoles in *Trypanosoma cruzi* epimastigotes *in vitro*," *Journal of Proteomics*, vol. 73, no. 12, pp. 2306–2315, 2010.

[99] H. M. Andrade, S. M. F. Murta, A. Chapeaurouge, J. Perales, P. Nirdé, and A. J. Romanha, "Proteomic analysis of *Trypanosoma cruzi* resistance to benznidazole," *Journal of Proteome Research*, vol. 7, no. 6, pp. 2357–2367, 2008.

[100] D. G. Beghini, A. T. S. Ferreira, V. C. de Almeida et al., "New insights in *Trypanosoma cruzi* proteomic map: further post-translational modifications and potential drug targets in Y strain epimastigotes," *Journal of Integrated Omics*, vol. 2, pp. 106–113, 2012.

[101] M. Hide, A. S. Ritleng, J. P. Brizard, A. Monte-Allegre, and D. Sereno, "*Leishmania infantum*: tuning digitonin fractionation for comparative proteomic of the mitochondrial protein content," *Parasitology Research*, vol. 103, no. 4, pp. 989–992, 2008.

[102] D. Rosenzweig, D. Smith, F. Opperdoes, S. Stern, R. W. Olafson, and D. Zilberstein, "Retooling *Leishmania* metabolism: from sand fly gut to human macrophage," *The FASEB Journal*, vol. 22, no. 2, pp. 590–602, 2008.

[103] M. P. Barrett, J. C. Mottram, and G. H. Coombs, "Recent advances in identifying and validating drug targets in trypanosomes and leishmanias," *Trends in Microbiology*, vol. 7, no. 2, pp. 82–88, 1999.

[104] T. M. Silva, E. F. Peloso, S. C. Vitor, L. H. G. Ribeiro, and F. R. Gadelha, "O_2 consumption rates along the growth curve: new insights into *Trypanosoma cruzi* mitochondrial respiratory chain," *Journal of Bioenergetics and Biomembranes*, vol. 43, no. 4, pp. 409–417, 2011.

[105] N. Sen and H. K. Majumder, "Mitochondrion of protozoan parasite emerges as potent therapeutic target: exciting drugs are on the horizon," *Current Pharmaceutical Design*, vol. 14, no. 9, pp. 839–846, 2008.

[106] J. C. F. Rodrigues and W. de Souza, "Ultrastructural alterations in organelles of parasitic protozoa induced by different classes of metabolic inhibitos," *Current Pharmaceutical Design*, vol. 14, no. 9, pp. 925–938, 2008.

[107] M. A. Vannier-Santos and S. L. De Castro, "Electron microscopy in antiparasitic chemotherapy: a (close) view to a kill," *Current Drug Targets*, vol. 10, no. 3, pp. 246–260, 2009.

[108] K. Lazardi, J. A. Urbina, and W. de Souza, "Ultrastructural alterations induced by two ergosterol biosynthesis inhibitors, ketoconazole and terbinafine, on epimastigotes and amastigotes of *Trypanosoma (Schizotrypanum) cruzi*," *Antimicrobial Agents and Chemotherapy*, vol. 34, no. 11, pp. 2097–2105, 1990.

[109] M. A. Vannier-Santos, J. A. Urbina, A. Martiny, A. Neves, and W. de Souza, "Alterations induced by the antifungal compounds ketoconazole and terbinafine in *Leishmania*," *The Journal of Eukaryotic Microbiology*, vol. 42, no. 4, pp. 337–346, 1995.

[110] J. C. F. Rodrigues, C. F. Bernardes, G. Visbal, J. A. Urbina, A. E. Vercesi, and W. de Souza, "Sterol methenyl transferase

inhibitors alter the ultrastructure and function of the *Leishmania amazonensis* mitochondrion leading to potent growth inhibition," *Protist*, vol. 158, no. 4, pp. 447–456, 2007.

[111] S. T. Macedo-Silva, J. A. Urbina, W. de Souza, and J. C. Rodrigues, "*In vitro* activity of the antifungal azoles itraconazole and posaconazole against *Leishmania amazonensis*," *PLoS One*, vol. 8, no. 12, Article ID e83247, 2013.

[112] G. Pérez-Moreno, M. Sealey-Cardona, C. Rodrigues-Poveda et al., "Endogenous sterol biosynthesis is important for mitochondrial function and cell morphology in procyclic forms of *Trypanosoma brucei*," *International Journal of Parasitology*, vol. 42, no. 11, pp. 975–989, 2012.

[113] R. M. Santa-Rita, R. Lira, H. S. Barbosa, J. A. Urbina, and S. L. de Castro, "Anti-proliferative synergy of lysophospholipid analogues and ketoconazole against *Trypanosoma cruzi* (Kinetoplastida: Trypanosomatidae): cellular and ultrastructural analysis," *Journal of Antimicrobial Chemotherapy*, vol. 55, no. 5, pp. 780–784, 2005.

[114] C. O. Rodrigues, R. Catisti, S. A. Uyemura et al., "The sterol composition of *Trypanosoma cruzi* changes after growth in different culture media and results in different sensitivity to digitonin-permeabilization," *Journal of Eukaryotic Microbiology*, vol. 48, no. 5, pp. 588–594, 2001.

[115] J. A. Urbina, "Ergosterol biosynthesis and drug development for Chagas disease," *Memorias do Instituto Oswaldo Cruz*, vol. 104, no. 1, pp. 311–318, 2009.

[116] R. Docampo, F. R. Gadelha, S. N. Moreno, G. Benaim, M. E. Hoffmann, and A. E. Vercesi, "Disruption of Ca^{2+} homeostasis in *Trypanosoma cruzi* by crystal violet," *The Journal of Eukaryotic Microbiology*, vol. 40, no. 3, pp. 311–316, 1993.

[117] M. C. M. Motta, "Kinetoplast as a potential chemotherapeutic target of trypanosomatids," *Current Pharmaceutical Design*, vol. 14, no. 9, pp. 847–854, 2008.

[118] M. N. Soeiro, S. L. de Castro, E. M. de Souza, D. G. Batista, C. F. Silva, and D. W. Boykin, "Diamidine activity against trypanosomes: the state of the art," *Current Molecular Pharmacology*, vol. 1, no. 2, pp. 151–161, 2008.

[119] C. F. Silva, M. B. Meuser, E. M. de Souza et al., "Cellular effects of reversed amidines on *Trypanosoma cruzi*," *Antimicrobial Agents and Chemotherapy*, vol. 51, no. 11, pp. 3803–3809, 2007.

[120] D. D. G. J. Batista, M. M. Batista, G. M. De Oliveira et al., "Arylimidamide DB766, a potential chemotherapeutic candidate for Chagas' disease treatment," *Antimicrobial Agents and Chemotherapy*, vol. 54, no. 7, pp. 2940–2952, 2010.

[121] A. Schnaufer, G. J. Domingo, and K. Stuart, "Natural and induced dyskinetoplastic trypanosomatids: how to live without mitochondrial DNA," *International Journal for Parasitology*, vol. 32, no. 9, pp. 1071–1084, 2002.

[122] R. E. Jensen and P. T. Englund, "Network news: the replication of kinetoplast DNA," *Annual Review of Microbiology*, vol. 66, pp. 473–491, 2012.

[123] A. Roy Chowdhury, R. Bakshi, J. Wang et al., "The killing of African trypanosomes by ethidium bromide," *PLoS Pathogens*, vol. 6, no. 12, Article ID e1001226, 2010.

[124] T. A. Shapiro and A. F. Showalter, "*In vivo* inhibition of trypanosome mitochondrial topoisomerase II: effects on kinetoplast DNA maxicircles," *Molecular and Cellular Biology*, vol. 14, no. 9, pp. 5891–5897, 1994.

[125] R. Díaz-González, Y. Pérez-Pertejo, C. F. Prada, C. Fernández-Rubio, R. Balaña-Fouce, and R. M. Reguera, "Novel findings on trypanosomatid chemotherapy using DNA topoisomerase inhibitors," *Mini Reviews in Medicinal Chemistry*, vol. 9, no. 6, pp. 674–676, 2009.

[126] G. F. Riou, M. Gabillot, S. Douc-Rasy, A. Kayser, and M. Barrois, "A type I DNA topoisomerase from *Trypanosoma cruzi*," *European Journal of Biochemistry*, vol. 134, no. 3, pp. 479–484, 1983.

[127] A. Das, A. Dasgupta, T. Sengupta, and H. K. Majumder, "Topoisomerases of kinetoplastid parasites as potential chemotherapeutic targets," *Trends in Parasitology*, vol. 20, no. 8, pp. 381–387, 2004.

[128] A. L. Bodley, A. K. Chakraborty, S. Xie, C. Burri, and T. A. Shapiro, "An unusual type IB topoisomerase from African trypanosomes," *Proceedings of the National Academy of Sciences of the United States of America*, vol. 100, no. 13, pp. 7539–7544, 2003.

[129] S. P. Fragoso and S. Goldenberg, "Cloning and characterization of the gene encoding *Trypanosoma cruzi* DNA topoisomerase II," *Molecular and Biochemical Parasitology*, vol. 55, no. 1-2, pp. 127–134, 1992.

[130] T. Hanke, M. J. Ramiro, S. Trigueros, J. Roca, and V. Larraga, "Cloning, functional analysis and post-transcriptional regulation of a type II DNA topoisomerase from *Leishmania infantum*. A new potential target for anti-parasite drugs," *Nucleic Acids Research*, vol. 31, no. 16, pp. 4917–4928, 2003.

[131] A. L. Bodley and T. A. Shapiro, "Molecular and cytotoxic effects of camptothecin, a topoisomerase I inhibitor, on trypanosomes and *Leishmania*," *Proceedings of the National Academy of Sciences of the United States of America*, vol. 92, no. 9, pp. 3726–3730, 1995.

[132] B. B. Das, T. Sengupta, A. Ganguly, and H. K. Majumder, "Topoisomerases of kinetoplastid parasites: why so fascinating?" *Molecular Microbiology*, vol. 62, no. 4, pp. 917–927, 2006.

[133] N. Sen, B. B. Das, A. Ganguly, T. Mukherjee, S. Bandyopadhyay, and H. K. Majumder, "Camptothecin-induced imbalance in intracellular cation homeostasis regulates programmed cell death in unicellular hemoflagellate *Leishmania donovani*," *The Journal of Biological Chemistry*, vol. 279, no. 50, pp. 52366–52375, 2004.

[134] N. Sen, B. Banerjee, B. B. Das et al., "Apoptosis is induced in leishmanial cells by a novel protein kinase inhibitor withaferin A and is facilitated by apoptotic topoisomerase I-DNA complex," *Cell Death & Differentiation*, vol. 14, no. 2, pp. 358–367, 2007.

[135] A. Roy, A. Ganguly, S. BoseDasgupta et al., "Mitochondria-dependent reactive oxygen species-mediated programmed cell death induced by 3,3′-diindolylmethane through inhibition of F0F1-ATP synthase in unicellular protozoan parasite Leishmania donovani," *Molecular Pharmacology*, vol. 74, no. 5, pp. 1292–1307, 2008.

[136] S. Chowdhury, T. Mukherjee, R. Mukhopadhyay et al., "The lignan niranthin poisons *Leishmania donovani* topoisomerase IB and favours a Th1 immune response in mice," *EMBO Molecular Medicine*, vol. 4, no. 10, pp. 1126–1143, 2012.

[137] M. Gonzales-Perdomo, S. L. De Castro, M. N. S. L. Meirelles, and S. Goldenberg, "*Trypanosoma cruzi* proliferation and differentiation are blocked by topoisomerase II inhibitors," *Antimicrobial Agents and Chemotherapy*, vol. 34, no. 9, pp. 1707–1714, 1990.

[138] D. P. Cavalcanti, S. P. Fragoso, S. Goldenberg, W. de Souza, and M. C. M. Motta, "The effect of topoisomerase II inhibitors on the kinetoplast ultrastructure," *Parasitology Research*, vol. 94, no. 6, pp. 439–448, 2004.

[139] A. A. Zuma, D. P. Cavalcanti, M. C. P. Maia, W. de Souza, and M. C. M. Motta, "Effect of topoisomerase inhibitors and DNA-binding drugs on the cell proliferation and ultrastructure of *Trypanosoma cruzi*," *International Journal of Antimicrobial Agents*, vol. 37, no. 5, pp. 449–456, 2011.

[140] J. C. F. Rodrigues, C. F. Bernardes, G. Visbal, J. A. Urbina, A. E. Vercesi, and W. de Souza, "Sterol methenyl transferase inhibitors alter the ultrastructure and function of the *Leishmania amazonensis* mitochondrion leading to potent growth inhibition," *Protist*, vol. 158, no. 4, pp. 447–456, 2007.

[141] P. Mukherjee, S. B. Majee, S. Ghosh, and B. Hazra, "Apoptosis-like death in *Leishmania donovani* promastigotes induced by diospyrin and its ethanolamine derivative," *International Journal of Antimicrobial Agents*, vol. 34, no. 6, pp. 596–601, 2009.

[142] A. E. Vercesi and R. Docampo, "Ca^{2+} transport by digitonin-permeabilized Leishmania donovani. Effects of Ca^{2+}, pentamidine and WR-6026 on mitochondrial membrane potential *in situ*," *Biochemical Journal*, vol. 284, no. 2, pp. 463–467, 1992.

[143] A. Mukherjee, P. K. Padmanabhan, M. H. Sahani, M. P. Barrett, and R. Madhubala, "Roles for mitochondria in pentamidine susceptibility and resistance in *Leishmania donovani*," *Molecular and Biochemical Parasitology*, vol. 145, no. 1, pp. 1–10, 2006.

[144] J. Román Luque-Ortega, P. Reuther, L. Rivas, and C. Dardonville, "New benzophenone-derived bisphosphonium salts as leishmanicidal leads targeting mitochondria through inhibition of respiratory complex II," *Journal of Medicinal Chemistry*, vol. 53, no. 4, pp. 1788–1798, 2010.

[145] L. Carvalho, J. R. Luque-Ortega, C. López-Martín, S. Castanys, L. Rivas, and F. Gamarro, "The 8-aminoquinoline analogue sitamaquine causes oxidative stress in *Leishmania donovani* promastigotes by targeting succinate dehydrogenase," *Antimicrobial Agents and Chemotherapy*, vol. 55, no. 9, pp. 4204–4210, 2011.

[146] J. R. Luque-Ortega and L. Rivas, "Miltefosine (hexadecylphosphocholine) inhibits cytochrome c oxidase in *Leishmania donovani* promastigotes," *Antimicrobial Agents and Chemotherapy*, vol. 51, no. 4, pp. 1327–1332, 2007.

[147] L. Carvalho, J. R. Luque-Ortega, J. I. Manzano, S. Castanys, L. Rivas, and F. Gamarro, "Tafenoquine, an antiplasmodial 8-aminoquinoline, targets *Leishmania* respiratory complex III and induces apoptosis," *Antimicrobial Agents and Chemotherapy*, vol. 54, no. 12, pp. 5344–5351, 2010.

[148] C. Nihei, Y. Fukai, and K. Kita, "Trypanosome alternative oxidase as a target of chemotherapy," *Biochimica et Biophysica Acta—Molecular Basis of Disease*, vol. 1587, no. 2-3, pp. 234–239, 2002.

[149] Y. Yabu, T. Suzuki, C.-I. Nihei et al., "Chemotherapeutic efficacy of ascofuranone in *Trypanosoma vivax*-infected mice without glycerol," *Parasitology International*, vol. 55, no. 1, pp. 39–43, 2006.

[150] K. Stuart and A. K. Panigrahi, "RNA editing: complexity and complications," *Molecular Microbiology*, vol. 45, no. 3, pp. 591–596, 2002.

[151] K. S. Kim, S. M. R. Teixeira, L. V. Kirchhoff, and J. E. Donelson, "Transcription and editing of cytochrome oxidase II RNAs in *Trypanosoma cruzi*," *The Journal of Biological Chemistry*, vol. 269, no. 2, pp. 1206–1211, 1994.

[152] L. S. Paes, B. S. Mantilla, M. J. Barisón, C. Wrenger, and A. M. Silber, "The uniqueness of the trypanosoma cruzi mitochondrion: opportunities to target new drugs against chagaś disease," *Current Pharmaceutical Design*, vol. 17, no. 20, pp. 2074–2099, 2011.

[153] S. Liang and G. J. Connell, "Identification of specific inhibitors for a trypanosomatid RNA editing reaction," *RNA*, vol. 16, no. 12, pp. 2435–2441, 2010.

[154] J. D. Durrant, L. Hall, R. V. Swift, M. Landon, A. Schnaufer, and R. E. Amaro, "Novel naphthalene-based inhibitors of *Trypanosoma brucei* RNA editing ligase 1," *PLoS Neglected Tropical Diseases*, vol. 4, no. 8, article e803, 2010.

Hindawi Publishing Corporation
BioMed Research International
Volume 2014, Article ID 893272, 12 pages
http://dx.doi.org/10.1155/2014/893272

Research Article

Tracking the Biogenesis and Inheritance of Subpellicular Microtubule in *Trypanosoma brucei* with Inducible YFP-α-Tubulin

Omar Sheriff,[1] Li-Fern Lim,[1] and Cynthia Y. He[1,2]

[1] *Department of Biological Sciences, National University of Singapore, Singapore 117543*
[2] *Centre for BioImaging Sciences, National University of Singapore, Singapore 117546*

Correspondence should be addressed to Cynthia Y. He; dbshyc@nus.edu.sg

Received 27 December 2013; Accepted 19 February 2014; Published 30 March 2014

Academic Editor: Wanderley de Souza

The microtubule cytoskeleton forms the most prominent structural system in *Trypanosoma brucei*, undergoing extensive modifications during the cell cycle. Visualization of tyrosinated microtubules leads to a semiconservative mode of inheritance, whereas recent studies employing microtubule plus end tracking proteins have hinted at an asymmetric pattern of cytoskeletal inheritance. To further the knowledge of microtubule synthesis and inheritance during *T. brucei* cell cycle, the dynamics of the microtubule cytoskeleton was visualized by inducible YFP-α-tubulin expression. During new flagellum/flagellum attachment zone (FAZ) biogenesis and cell growth, YFP-α-tubulin was incorporated mainly between the old and new flagellum/FAZ complexes. Cytoskeletal modifications at the posterior end of the cells were observed with EB1, a microtubule plus end binding protein, particularly during mitosis. Additionally, the newly formed microtubules segregated asymmetrically, with the daughter cell inheriting the new flagellum/FAZ complex retaining most of the new microtubules. Together, our results suggest an intimate connection between new microtubule formation and new FAZ assembly, consequently leading to asymmetric microtubule inheritance and cell division.

1. Introduction

Trypanosomes are early divergent unicellular protists with a digenic lifecycle successively proliferating in an insect vector and a mammalian host, with several transitional forms. The *Trypanosoma brucei* cell division cycle has been subject to careful investigation. One fascinating feature of *T. brucei* division is the biogenesis and inheritance of a subpellicular microtubule cytoskeleton, which provides the structural basis for the highly organized and polarized *T. brucei* cell body and accurate temporal and spatial duplication of subcellular organelles [1, 2].

The subpellicular microtubule network comprises longitudinal arrays of α/β-tubulin heterodimers cross-linked to each other as well as to the plasma membrane via various microtubule-associated proteins [3–5]. The microtubule cytoskeleton follows a helical pattern along the long axis of the cell body and once formed remains extremely stable, without apparent disassembly at any time of the cell cycle [6, 7]. The microtubules in the array originate from microtubule organizing centres (MTOC) occupying various niches, each with the potential to be regulated independently [8, 9]. While most of the subpellicular microtubules originate from the anterior region of the cell body and extend posteriorly with their plus ends congregated at the posterior tip of the cell, four specialized microtubules known as the microtubule quartet (MtQ) are nucleated close to the basal body/probasal body complex that also nucleates the flagellum axoneme, extending anteriorly and ending at the anterior tip of the cell [1, 10]. The MtQ is closely associated with an electron-dense filamentous structure, together forming the flagellum attachment zone (FAZ).

During the cell cycle, a new FAZ is assembled together with the new flagellum, posterior to the existing flagellum/FAZ. As the new flagellum/FAZ elongates coordinately, the cell body extends longitudinally, accommodating duplication and segregation of intracellular organelles such as the kinetoplast (condensed mitochondria DNA) and the nucleus. Once

the new flagellum/FAZ reaches the same length as the old structures, cell division initiates at the anterior tip of the cell body that is possibly defined by the distal tip of the new FAZ. Cell division then proceeds posteriorly following a helical path between the old and new flagellum/FAZ, and cleaves the cell into two daughters [1, 11, 12]. One daughter inherits the old flagellum/FAZ and the other inherits the newly formed flagellum/FAZ.

The FAZ is tightly linked to subpellicular microtubule biogenesis and organization. Inhibition of FAZ assembly by RNAi depletion of an integral FAZ component CC2D inhibits subpellicular microtubule synthesis, generating a new daughter cell possessing a new flagellum with a shorter cell body [12]. Recent efforts in characterizing the stages of cytokinesis [13] have revealed penetration of microtubules between the new and the old FAZ, in addition to extensive microtubule modifications at the posterior ends of both the daughter cells. However, the construction of the subpellicular microtubule cytoskeleton during cell cycle progression has not been observed directly. Studies on microtubule dynamics have relied heavily on YL1/2, a monoclonal antibody directed against the tyrosinated C-terminal end of α-tubulin [14]. Since this tyrosine is subjected to removal by a carboxypeptidase upon incorporation of α/β-tubulin dimers into the microtubule, YL1/2 has been used as a marker for newly formed microtubules [14]. Based on YL1/2 labelling pattern, a semiconservative model has been proposed for subpellicular microtubule duplication in *T. brucei*. The increase in cell size during duplication is therefore deduced to be brought about by intercalation and posterior extension of new microtubules into the existing subpellicular corset [15]. However, the regulation of tyrosination cycles and its effect on microtubule dynamics is not thoroughly understood [16], and the YL1/2 antibody is known to cross-react with another protein, *Tb*RP2 [17]. A new, improved method to monitor microtubule synthesis directly in *T. brucei* is therefore needed.

In this study, we utilize a tetracycline inducible YFP-α-tubulin expression system to follow new microtubule synthesis during the cell cycle of the procyclic (an insect-stage) *T. brucei*. A polyclonal antibody against microtubule "plus" end binding protein, EB1, was also used to monitor microtubule dynamics at the posterior end of the cell. Together, the results suggest that new microtubule synthesis during cell duplication occurs mainly in the region between the old and the new FAZ. At cell division, the more posterior daughter cell inherited more of the newly formed microtubules. Consistent with previous observations, segregation of the duplicated microtubule array was correlated with remodelling at the plus ends.

2. Materials and Methods

2.1. Cell Lines. YTat1.1 procyclic form *T. brucei rhodesiense* was cultured in Cunningham medium containing 15% heat inactivated fetal bovine serum (BD Biosciences) at 28°C [18]. These were used to create a cell line stably expressing YFP-EB1. Other studies, including inducible YFP-α-tubulin expression, endogenous replacements of EB1, and inducible RNA interference, were carried out in procyclic 29.13 *T. brucei brucei* cells [19] that were maintained in Cunningham medium containing 15% heat inactivated, tetracycline-free bovine serum (clonetech), 15 μg/ml G418, and 50 μg/ml hygromycin at 28°C. Cell proliferation was measured and growth curve was generated as reported earlier [20].

2.2. Plasmids Construction and Transfection. For stable protein expression in *T. brucei*, the full-length coding sequence of *T. brucei* EB1 (Tb09.160.1440) or GCP2 (Tb927.10.9770) was amplified from genomic DNA by PCR and inserted after the C terminus of the Yellow Fluorescence Protein (YFP) reporter cloned in the pXS2 vector to obtain YFP-EB1 and YFP-GCP2 [2, 21]. Ty1-tagged EB1 (Ty1-EB1) was also generated using the pXS2 vector. YFP tagged EB1 was used to replace one endogenous allele and was stably expressed using a modified pCR4Blunt-TOPO vector [22]. To do this, a 500 bp 5′-UTR fragment immediately upstream of EB1 start codon was cloned between PacI and HindIII sites. A 500 bp fragment of EB1 coding sequence immediately downstream of the start codon was cloned into BamHI and NsiI sites. The plasmid was then linearized with PacI and NsiI double digestion before transfection. pLEW100 was used for tetracycline inducible expression of YFP-α-tubulin (Tb927.1.2340) [19]. For *T. brucei* GCP2 RNAi, an automated, web-based program was used to search for suitable RNAi target [23] (http://trypanofan.path.cam.ac.uk/software/RNAit.html). A 508 bp fragment specific to the GCP2 coding sequence (nucleotide 1470–1977) was amplified and cloned into the p2T7 vector [24]. For stable transfections, 15 μg of linearized plasmid was transfected into YTat1.1 or 29.13 cells by electroporation (1500 V, 25 μF). Stable, clonal cell lines were generated by serial dilution with medium containing appropriate antibiotics.

2.3. Immunofluorescence Assays. *T. brucei* cells were washed and resuspended in phosphate buffered saline (PBS, pH 7.4) and settled on cover slips to allow cells to attach to the glass surface. Cells were then fixed and permeabilized with methanol at −20°C. Alternatively, cells were extracted with droplets of freshly prepared PEM buffer (100 mM PIPES, 1 mM EGTA, 0.1 mM $CaCl_2$, 1 mM $MgSO_4$, pH6.9) containing 1% Nonidet P-40 for 5 min at room temperature, and then fixed with 4% formaldehyde. The fixed samples were blocked with 3% BSA in PBS and then probed with appropriate antibodies: anti-CC2D [12] or monoclonal L3B2 antibody [25] for FAZ, anti-PAR [26] or anti-PFR1 [27] for the paraflagellar rod along the flagellum, and YL1/2 [14] for tyrosinated α-tubulin and the basal bodies (AbCam). The kinetoplast and the nucleus were stained with DAPI (2 μg/ml). Images were acquired using Observer Z1 (Zeiss) equipped with a 63X NA1.4 objective and a CoolSNAP HQ2 CCD camera (Photometrics) and processed with ImageJ and Adobe Photoshop. To image the subpellicular microtubules and the FAZ, serial z-stack images were acquired at 0.5 μm interval throughout the entire cell.

2.4. Anti-EB1 Antibody. His-tagged EB1 (His-EB1) was generated by cloning the full-length *T. brucei* EB1 coding sequence inframe into the expression vector pET30a+ (Novagen).

His-EB1 recombinant protein was then expressed in BL21 *E. coli* and affinity-purified using HIS-Select nickel affinity gel (Sigma). The pooled fractions containing His-EB1 were then exchanged into a gel filtration buffer (25 mM Tris pH7.4, 500 mM NaCl) by running the fractions through a Superdex 200 gel filtration column (GE Healthcare). Purity of the purified His-EB1 was assessed using sodium dodecyl sulphate polyacrylamide gel electrophoresis (SDS-PAGE); most His-EB1 protein was recovered in the soluble fraction (data not shown). Purified His-EB1 protein was used for polyclonal antibody production in rabbits, and the affinity-purified immune serum of one rabbit was used in all subsequent experiments.

2.5. Cell Motility Assay. TbGCP2-RNAi cells were diluted using fresh culture medium to approximately 10^5 cells/ml. 10 μl of diluted cell culture was loaded onto a hemocytometer and visualized using a 20X NA0.4 objective within 30 minutes of removal from the 28°C incubator. Images were captured every ~0.5 second for a total of 60 seconds using a high-speed HSM camera (Zeiss). The movement of individual cells was traced using ImageJ software with MtrackJ plugin [28]. The mean velocity of individual cells was calculated based on the total moving distance in 60 seconds.

3. Results

3.1. Expression and Incorporation of YFP-α-Tubulin into Microtubules. In the *T. brucei* genome, the tubulin genes are clustered as 13–18 tandem repeats of identical α/β-tubulin gene pairs [29, 30] which are highly conserved across the eukaryotes [31]. Epitope tagging of tubulins has been challenging, as GFP fusions at C-terminus of tubulin genes have failed to complement their corresponding null mutants in *Saccharomyces cerevisiae* [32]. Moreover, β-tubulin contains a GTP hydrolysis site and its overexpression or the addition of tags has been reported to be lethal in *S. cerevisiae* [33, 34]. Most in vivo studies of the microtubule cytoskeleton have been performed by expressing tagged α-tubulin at reduced levels in the presence of endogenous tubulin [32, 35, 36]. Tag locations and expression systems vary depending on the organisms [36]. In *T. brucei*, transient expression of β-tubulin with an internal or C-terminal Ty1 tag was successful [37], though stable expression or integration of tagged-β-tubulin into the microtubule has not been reported. The C-terminus of *T. brucei* α-tubulin is subject to the tyrosination cycle [38]; therefore, *T. brucei* α-tubulin coding sequence was amplified and fused to the C-terminus of a YFP reporter. To monitor new microtubule synthesis and inheritance, recombinant YFP-α-tubulin was expressed from a pLew100 vector under the tight regulation of a tetracycline inducible promoter [19]. A similar approach was previously used to study flagellum assembly dynamics in *T. brucei* [39].

The inducible expression of YFP-α-tubulin protein was monitored by immunoblots with a monoclonal antibody directed against α-tubulin (Figure 1(a)). In addition to the endogenous α-tubulin at ~50 kDa and a 75 kDa band corresponding to the YFP-α-tubulin fusion appeared 2 hours after induction, and the intensity increased over time. Continuous

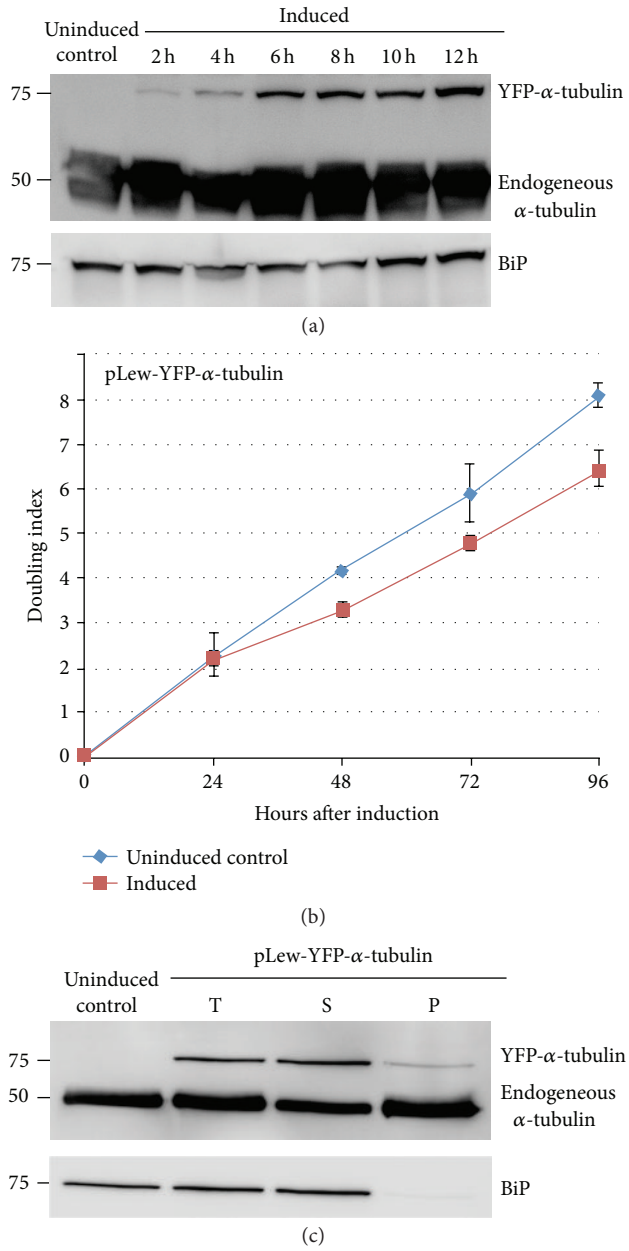

Figure 1: Inducible expression of YFP-α-tubulin in *T. brucei*. Cells stably transfected with pLew-YFP-α-tubulin were cultivated in the absence or presence of tetracycline to induce YFP-α-tubulin expression. Samples were taken at various time points for immunoblots (a), growth curve analyses (b), and cell fractionation studies (c). YFP-α-tubulin was detected as early as 2 hours after induction. Continuous induction led to slightly increased YFP-α-tubulin level and had little effect on parasite proliferation. Immunoblots of detergent extracted YFP-α-tubulin cells indicated that only a small amount of YFP-α-tubulin was incorporated into the detergent insoluble cytoskeleton (P). T: total cells; S: detergent soluble fraction.

expression of YFP-α-tubulin caused no measurable change in doubling time at 24 hours after induction and only a moderate increase in doubling time at later time points (12.3 ± 1.3 hours for uninduced control and 15.0 ± 0.5 hours for induced population) (Figure 1(b)). Induced cells expressing

YFP-α-tubulin continued to proliferate weeks after induction (data not shown), possibly due to the low expression levels of YFP-α-tubulin compared to endogenous α-tubulin (Figure 1(a)).

Since the microtubule cytoskeleton of *T. brucei* is resistant to detergent extractions [6], the incorporation of YFP-α-tubulin into the microtubule array was verified by immunoblots performed on detergent extracted fractions of control and cells induced for YFP-α-tubulin expression for 24 hours (Figure 1(c)). YFP-α-tubulin was mostly present in the detergent-soluble fraction and only a small portion was incorporated into the detergent-resistant cytoskeleton fraction. Efficient detergent extraction was verified by the immunolabelling of BiP, an ER luminal protein mostly found in detergent soluble fractions (Figure 1(c)).

3.2. Cell Cycle-Dependent Incorporation of New Microtubules. The establishment of a cell line expressing YFP-α-tubulin under the control of an inducible promoter provided an ability to monitor the formation of new microtubules in an asynchronous population of cells at various cell cycle stages. Cells induced for YFP-α-tubulin expression for 8 hours were extracted with 1% NP-40 in PEM buffer, fixed with 4% formaldehyde, and probed with anti-GFP antibody that cross-reacted with YFP.

Cells in the early stage of the cell cycle with a single flagellum showed incorporation of YFP-α-tubulin at the posterior region of the parasite and weak, speckled labelling in the rest of the cell. This labelling pattern was similar to that of YL1/2, which labeled the basal bodies in addition to the posterior region of the cells (Figures 2(a) and 2(b)). As these cells were likely to be in the late duplication stage at the time YFP-α-tubulin was expressed, the YFP-α-tubulin and YL1/2 staining patterns suggested low microtubule polymerization activity in late and early cell cycle stages in the cell, except for the posterior region.

As cell cycle progressed, basal bodies duplicated and new flagellum/FAZ emerged. YFP-α-tubulin labelling, which was mostly restricted to the posterior region in the earlier stage, now spread toward the anterior part of the cell body (Figures 2(c)–2(f)). Interestingly, YFP-α-tubulin staining was more intense on one side of the cell body, along the new FAZ (Figures 2(e) and 2(f)). At this stage, YL1/2 labelling on the duplicated basal bodies and posterior region remained strong. In many cells, YL1/2 also appeared to stain the growing new flagellum and its close proximity as reported previously [13, 40] (Figures 2(c) and 2(d)).

As the new flagellum/FAZ complex continued to elongate, basal bodies and associated kinetoplast and flagellum/FAZ segregated (Figure 3). Nuclear division could also be observed in some cells (Figure 3(a)), where YFP-α-tubulin was present on the intranuclear mitotic spindle. The increased separation of new and old flagellum/FAZ complexes allowed better visualization of newly synthesized, YFP-α-tubulin labeled microtubule in the subpellicular array. Remarkably, strong YFP-α-tubulin staining in a striated pattern was found along the new FAZ, particularly in the region between the old and the new FAZ (Figures 3(c) and 3(d)), suggesting active microtubule polymerization in this region. The YL1/2 antibody, similar to the earlier stage, stained the posterior region, the basal bodies, and the elongating new flagellum but not the intranuclear spindle (Figures 3(a) and 3(b)).

In cells at later stages of mitosis and those entering cytokinesis, the preferred incorporation of YFP-α-tubulin in the region along the new FAZ became even more pronounced (Figure 4). As the formation of the two daughter cells became more evident, the asymmetric segregation of the microtubules also became clear. Whereas the daughter cell inheriting the new flagellum-FAZ complex retained most of the YFP tagged microtubules; the other daughter that inherited the old flagellum/FAZ contained less YFP-labelled microtubules. This asymmetric microtubule biogenesis and inheritance, though could be observed by YL1/2 staining in some cells (Figure 4(b)), was not consistently observed as with YFP-α-tubulin [13].

Immunofluorescence of YFP-α-tubulin was also performed in cells induced for YFP-α tubulin expression for 24 hours (data not shown). In these cells, YFP-α-tubulin was found throughout the cell at all cell cycle stages, similar to that of anti-α-tubulin antibody. This confirmed the incorporation of YFP-α-tubulin into the entire cytoskeleton of *T. brucei* at later time points after induction.

3.3. Cellular Localization of T. brucei EB1, a Microtubule Plus End Binding Protein. The presence of strong YL1/2 and YFP-α-tubulin labelling in the posterior region at all cell cycle stage suggested microtubule dynamics at the plus end, which was then monitored by labelling of EB1, a microtubule plus end tracking protein. *T. brucei* genome encodes a single homologue (Tb09.160.1440) of EB1, which contains an N-terminal calponin homology (CH) domain (amino acids 19–147, with an E-value of 3.5×10^{-20}), and a C-terminal EB1-like homology (EBH) domain (amino acids 489–534; with an E-value of 3.2×10^{-14}). Both CH and EBH domains have also been identified in other EB1 proteins [41–43].

In order to establish *T. brucei* EB1's localization within the cell, YFP- or Ty1-tagged EB1 was stably expressed in *T. brucei* cells and produced similar labelling patterns (Figures 5(a) and 5(b)). In most of the cells, specific localization of YFP-EB1 was observed at the posterior tip of the cell, widely accepted to be where the plus ends of the unidirectional corset microtubules converge (Figure 5(c)) [1]. Interestingly, the EB1 labelling pattern varied with cell cycle stages (see Figure S1 in Supplementary Material available online at http://dx.doi.org/10.1155/2014/893272) As new flagellum/FAZ initiated and elongated, YFP-EB1 at the posterior end of the subpellicular array elongated, forming a line that appeared to stretch between the posterior tips of the two daughter cells (Figure S1(d)). The line appeared to lengthen in tandem with the division of nuclei and segregation of the daughter cells. As cell division further progressed, specific YFP-EB1 localization reappeared at the posterior tips of the new daughter cells (Figure S1(e)). It should be noted that a low level YFP-EB1 fluorescence was also observed in the cell body throughout the cell cycle, such a pattern has been previously described for γ-tubulin as well [8] (Figure S1). This may represent YFP-EB1 association with subpellicular microtubules other than the plus ends.

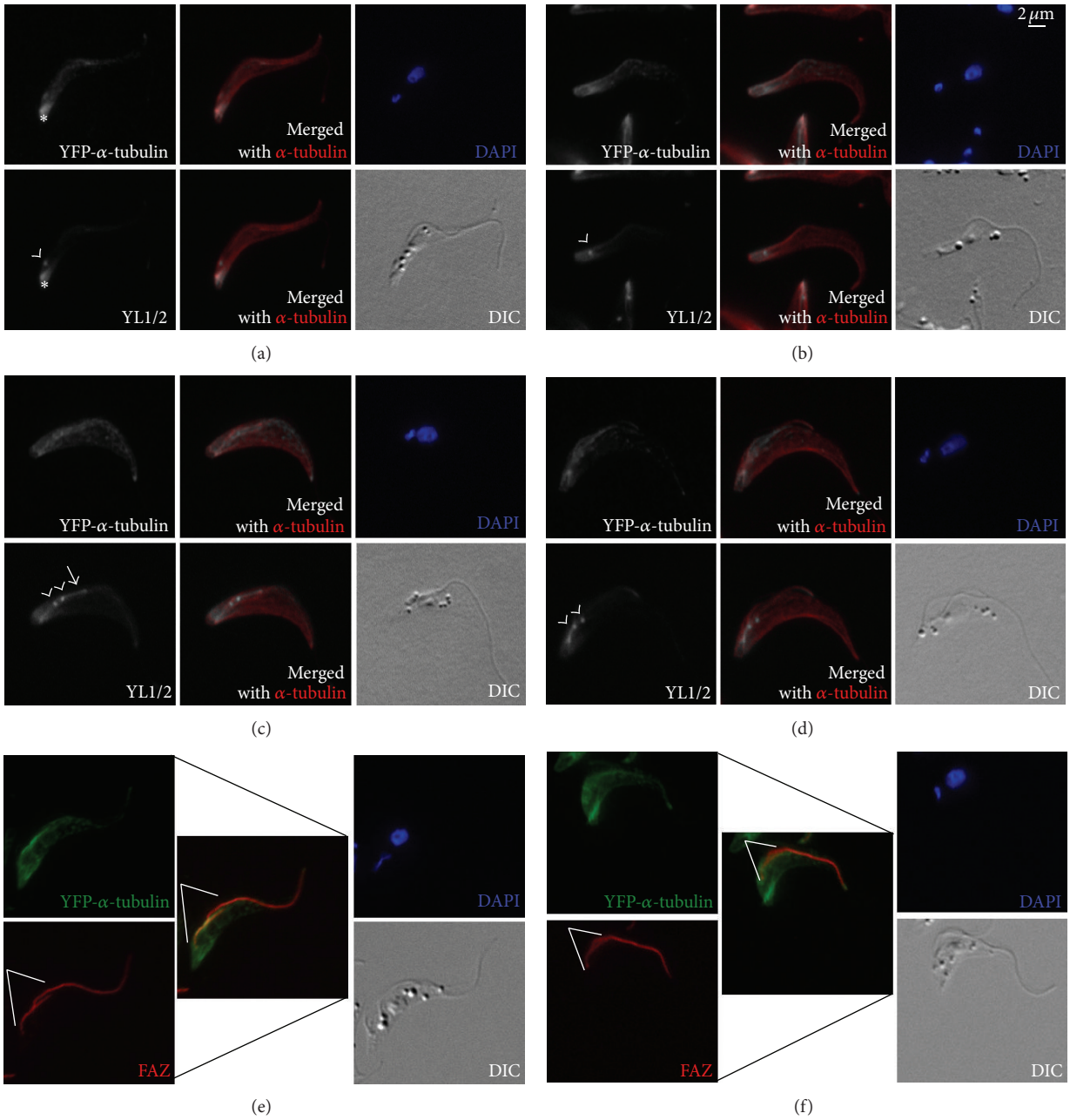

FIGURE 2: Incorporation of inducible YFP-α-tubulin in early cell cycle stages. pLew-YFP-α-tubulin cells were induced for 8 hours, extracted with 1% NP-40, and fixed for staining with anti-GFP (for YFP-α-tubulin), α-tubulin, YL1/2, FAZ and DAPI. In the early cell cycle stage, neither the kinetoplast (small blue dot) nor the nucleus (large blue dot) had duplicated. Basal bodies duplication is one of the earliest events of the cell cycle. * marks the posterior tip of the parasite cell; arrowheads: basal bodies; white lines: new FAZ; arrow: flagellum.

3.4. Characterization of a Polyclonal Anti-EB1 Antibody. An effect of the GFP tag on the functions of EB1 has been previously reported [44]. To confirm the YFP-EB1 localization, a polyclonal anti-EB1 antibody was raised against purified His-EB1. Affinity-purified anti-EB1 recognized a single band at approximately 57 kDa that corresponded to the expected size of *T. brucei* EB1 in wild type parasite cell lysates. Anti-EB1 also reacted to an additional band at approximately 84 kDa, which corresponded to the expected size of YFP-tagged EB1, in YFP-EB1 cell lysates (Figure S2).

Immunofluorescence staining using the anti-EB1 antibody (Figures 5(d) and 5(e)) revealed a pattern that was mostly consistent with the staining pattern of YFP-EB1. Again, anti-EB1 labeled the posterior tip of the parasite cells during early stages of the cell cycle (Figure 5(d)). As mitosis began and daughter cells formed, the posterior, EB1-containing dot elongated, forming a punctate line joining the posterior ends of the dividing daughters. During cytokinesis, specific anti-EB1 labelling reappeared at the posterior tips of both daughter cells.

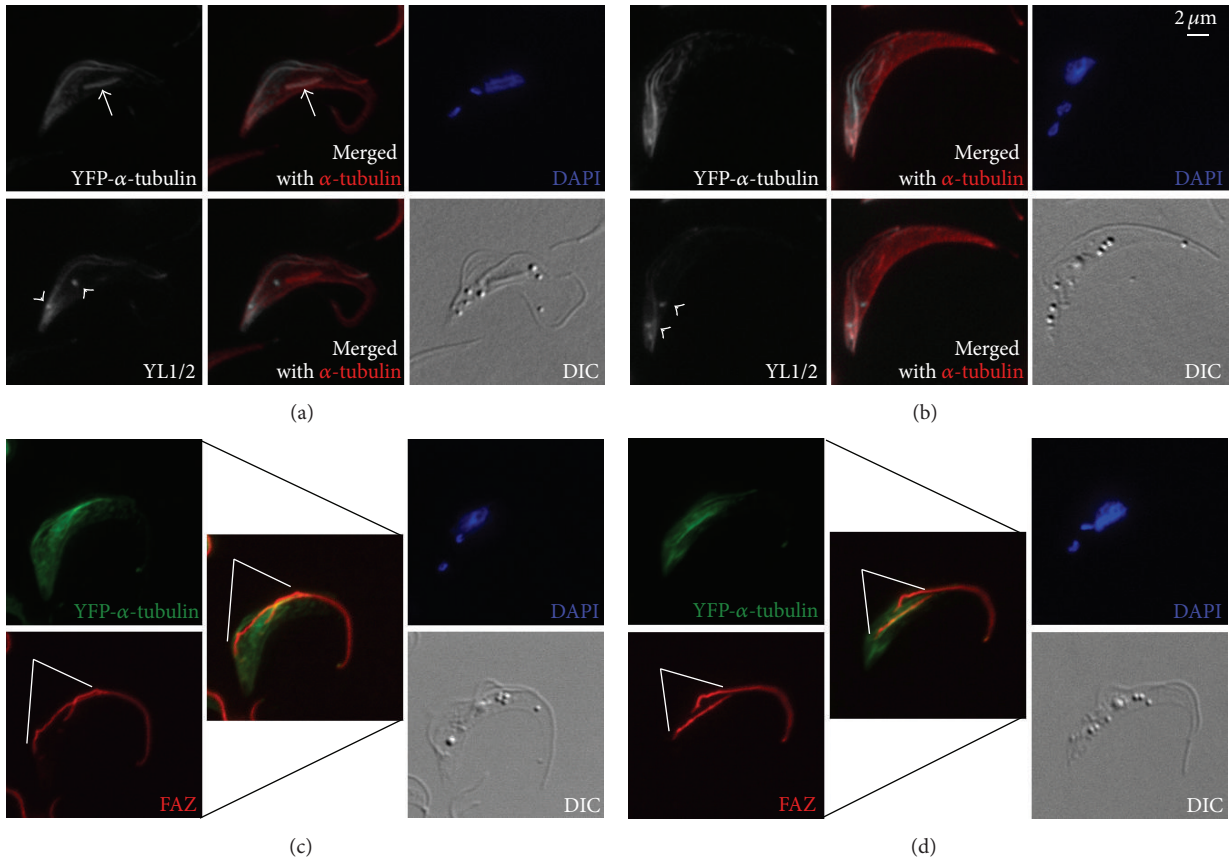

FIGURE 3: YFP-α-tubulin is incorporated primarily in the region between the old and new FAZ in duplicating cells. In the duplicating cells, kinetoplast has duplicated and segregated before the nucleus. Mitotic cells containing an intranuclear spindle can also be observed. Samples were processed as in Figure 2. Arrowheads: basal bodies; white lines: new FAZ; arrow: intranuclear spindle.

Similar to YFP-EB1 labelling, anti-EB1 also showed weak staining in the cell body at all times of the cell cycle. Besides, a weak but consistent staining along the FAZ, particularly the new FAZ, was also observed. The FAZ staining by anti-EB1 was likely nonspecific, as FAZ labelling was rarely observed in YFP-EB1 cells (Figures S1, 5(a), and 5(c)). Furthermore EB1-RNAi cells that showed reduced anti-EB1 labelling at the posterior tip still retained the FAZ labelling (data not shown).

3.5. Role of Microtubule Synthesis on Flagella-FAZ Assembly. By examining the incorporation of inducible YFP-α-tubulin into the cytoskeleton, we were able to track new microtubule polymerization and inheritance in *T. brucei*, particularly in duplicating cells. Asymmetric new microtubule synthesis and inheritance was observed and the more posterior daughter cell (that inherited the new flagellum/FAZ complex) retained more newly synthesized microtubules than the other daughter cell.

To further understand how new microtubule synthesis affects *T. brucei* cell cycle progression, particularly the formation of the more posterior daughter cell, Tb927.10.9770, a putative γ-tubulin complex 2 protein (GCP2) based on the presence of the characteristic Grip1/2 motifs, was depleted by inducible RNAi [45]. GCP2, GCP3, and γ-tubulin form the γ-tubulin small complex (γTuSC), important for microtubule nucleation, plus end catastrophe and minus end shrinkage [46, 47].

In *T. brucei*, GCP2-RNAi caused a reduction in cell motility and cell proliferation and led to eventual cell death, 96 hours after induction (Figures 6(a) and 6(b)). Microscopic examination of the DNA contents in the GCP2-RNAi population revealed a significant increase of 1K2N cells at 48 hours after induction ($P < 0.001$). At the same time, multinucleated cells also accumulated ($P < 0.001$), suggesting an inhibition of kinetoplast segregation and cell division in GCP2-RNAi cells. Motility tracking indicated a reduction in directional motility and velocity 48 hours after induction ($P < 0.001$) (Figures 6(c) and 6(d)), further supporting an effect of GCP2-RNAi in microtubule-related functions.

In *T. brucei*, both kinetoplast segregation and cell division are microtubule-driven processes that are tightly linked to proper FAZ assembly [1, 12, 48–50] and flagellum motility [51–53]. Cells undergoing new flagellum/FAZ assembly were therefore measured for new flagellum and FAZ length in control and GCP2-RNAi populations. In control cells, new FAZ elongation coordinated with the new flagellum ($R^2 = 0.87$), just as previously observed [25]. Upon GCP2-RNAi, this coordinated assembly was disrupted ($R^2 = 0.35$ at 48 h after induction) (Figure 6(e)), with the formation of FAZ trailing behind that of the flagellum (Figure 6(f)). This result suggests

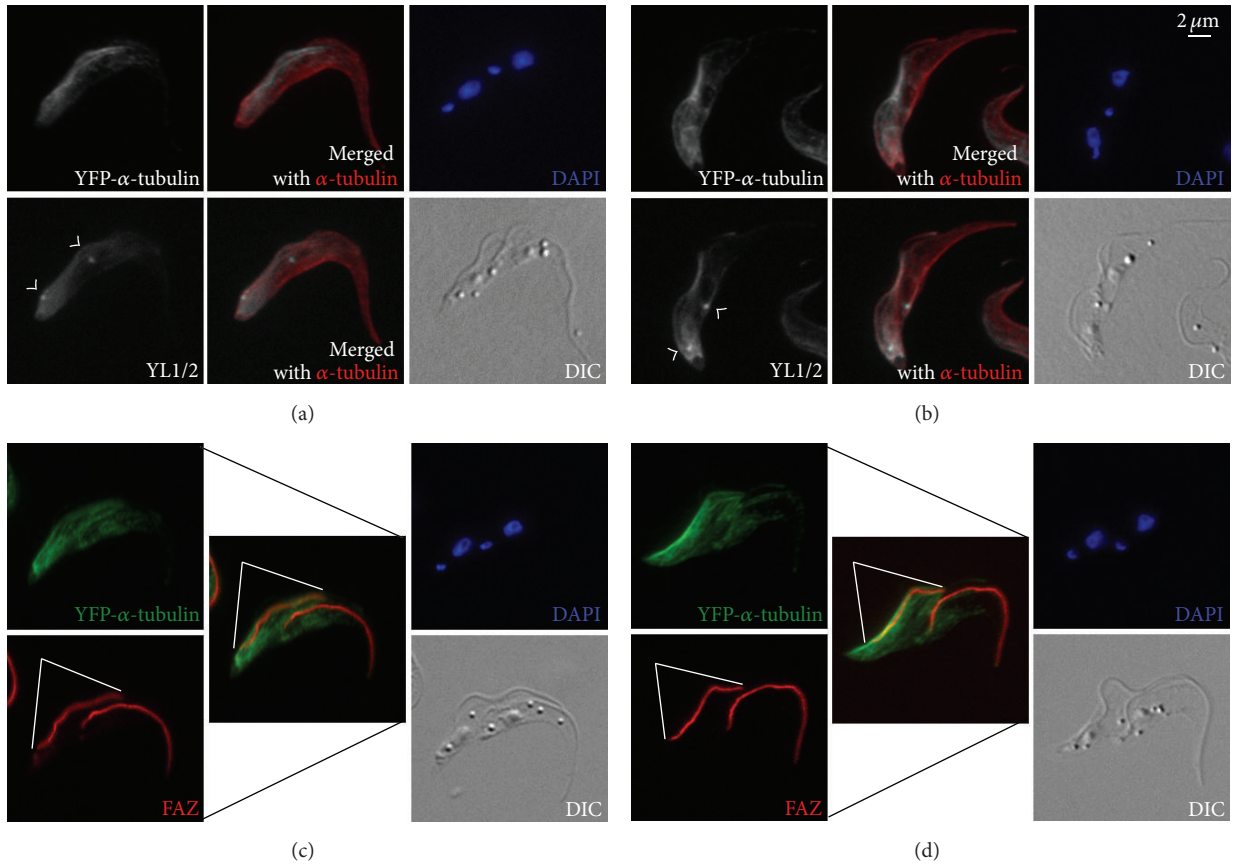

Figure 4: Asymmetric inheritance of newly formed subpellicular microtubules in *T. brucei* cell division. In these postmitotic cells, both kinetoplasts and nuclei have been duplicated and segregated. The partitioning of intracellular organelles and the cytoskeleton network into the daughter cells become evident. Samples were processed as in Figure 2. Arrowheads: basal bodies; white lines: new FAZ.

an effect of new microtubule polymerization on new FAZ assembly.

4. Discussion

By inducible expression of YFP-tagged α-tubulin,the biogenesis and inheritance of subpellicular microtubules during *T. brucei* cell cycle was monitored. Unlike YL1/2, which reacts to tyrosinated α-tubulin and therefore has been used as a probe for microtubule polymerization activities, inducible expression of YFP-α-tubulin allowed not only specific labelling of newly synthesized microtubules, but also tracking of their incorporation into the existing cytoskeletal network during cell growth and their inheritance at cell division.

Cellular distribution of inducible YFP-α-tubulin indicated that new microtubule incorporation occurred primarily in a region along the new FAZ and between the new and the old FAZs during cell growth. Similar staining was previously reported also for YL1/2, and these observations are consistent with EM observation of new subpellicular microtubules added into the region between the old and the new FAZs [13]. The addition of new microtubules in this region likely mediates the segregation of the basal bodies as wells as other cellular organelles [1, 50] and facilitates the formation of the membrane fold in preparation for cell division [13].

These observations also pointed towards a tight link between new microtubule synthesis and new FAZ formation. FAZ has been previously shown to play a direct role on cell morphology [12]. Cells depleted of an integral FAZ component CC2D could not form a new FAZ. Microtubule polymerization and organization in the region between the old and the new FAZs was also affected and thus generating daughter cells of shorter length [12]. The link between new FAZ assembly and new microtubule formation was further confirmed by GCP2 depletion. It is not clear, however, how new FAZ assembly is coordinated with new microtubule synthesis. One integral component of FAZ is the MtQ, which may be crucial in linking microtubule synthesis to FAZ assembly. One study [8] suggested tight association of γ-tubulin along the flagellum, in detergent-resistant manner. Whether γ-tubulin or GCP2 may have a structural role in FAZ assembly, as well as function in new microtubule nucleation, remains to be investigated. Additionally, the lagging behind of the FAZ formation with regard to that of the flagellum could be compounded by the motility defect observed in the GCP2 depleted cells. Impaired motility has been identified to be responsible for disruption of basal body migration and its proximal organelles such as the flagellum pocket and the collar [54, 55].

Distribution of YFP-α-tubulin in dividing *T. brucei* indicated a distinct, asymmetric inheritance of subpellicular

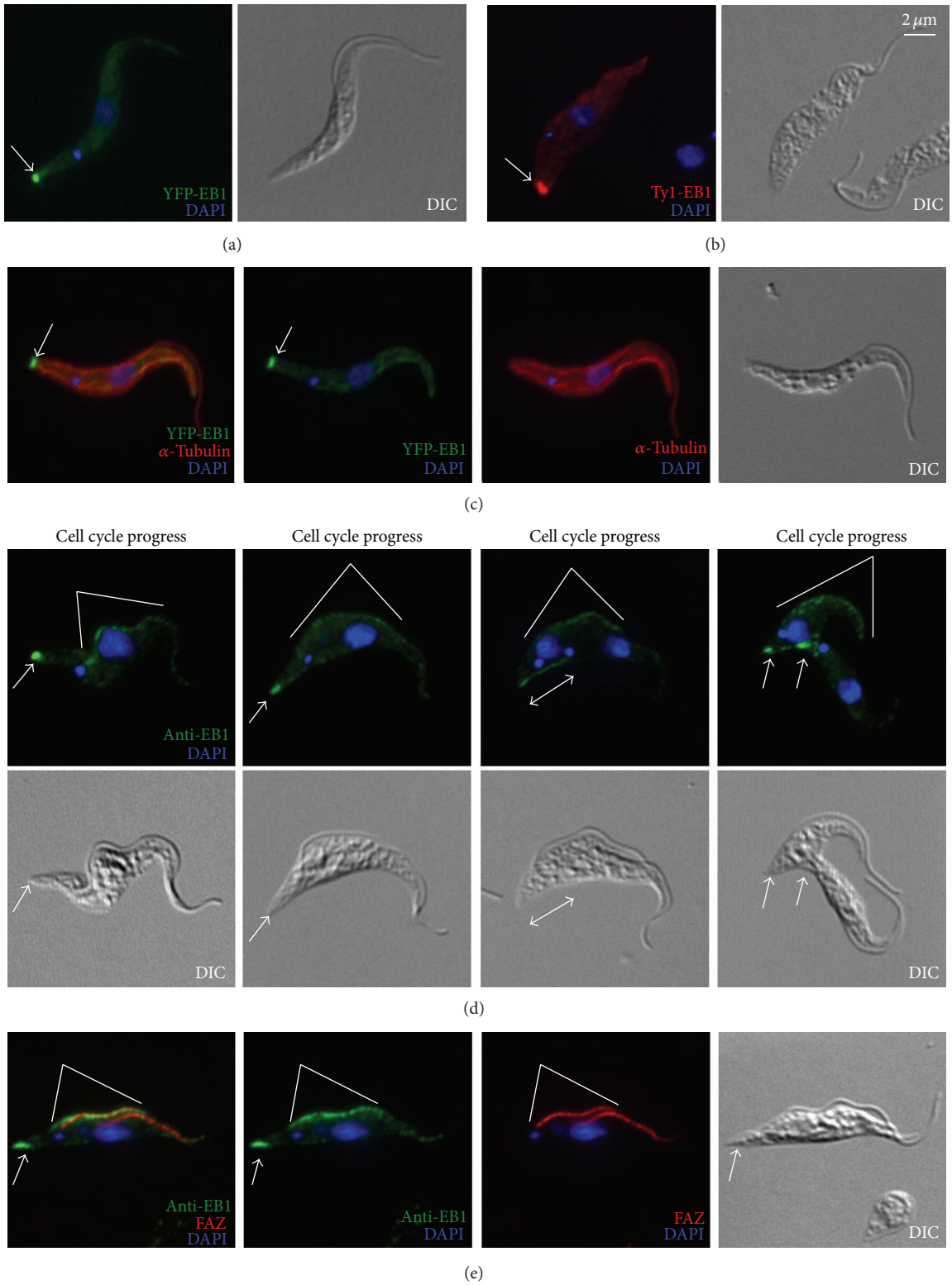

Figure 5: Subpellicular microtubule plus end dynamics revealed by EB1. Cells stably expressing YFP-EB1 (a) or Ty1-EB1 (b) were fixed with cold methanol and labeled with DAPI for DNA. YFP-EB1 cells were also immunolabeled with anti-α-tubulin which revealed the total microtubule profile in a parasite cell (c). A polyclonal anti-EB1 was used to label microtubule plus ends throughout the cell cycle (d). Cells double labeled for anti-EB1 and FAZ revealed a possible nonspecific labelling of anti-EB1 along the FAZ region (e). Arrows, EB1 staining at the posterior tip of the cell; double headed arrow: elongated EB1 pattern during mitosis; white lines: possible nonspecific EB1 labelling near FAZ.

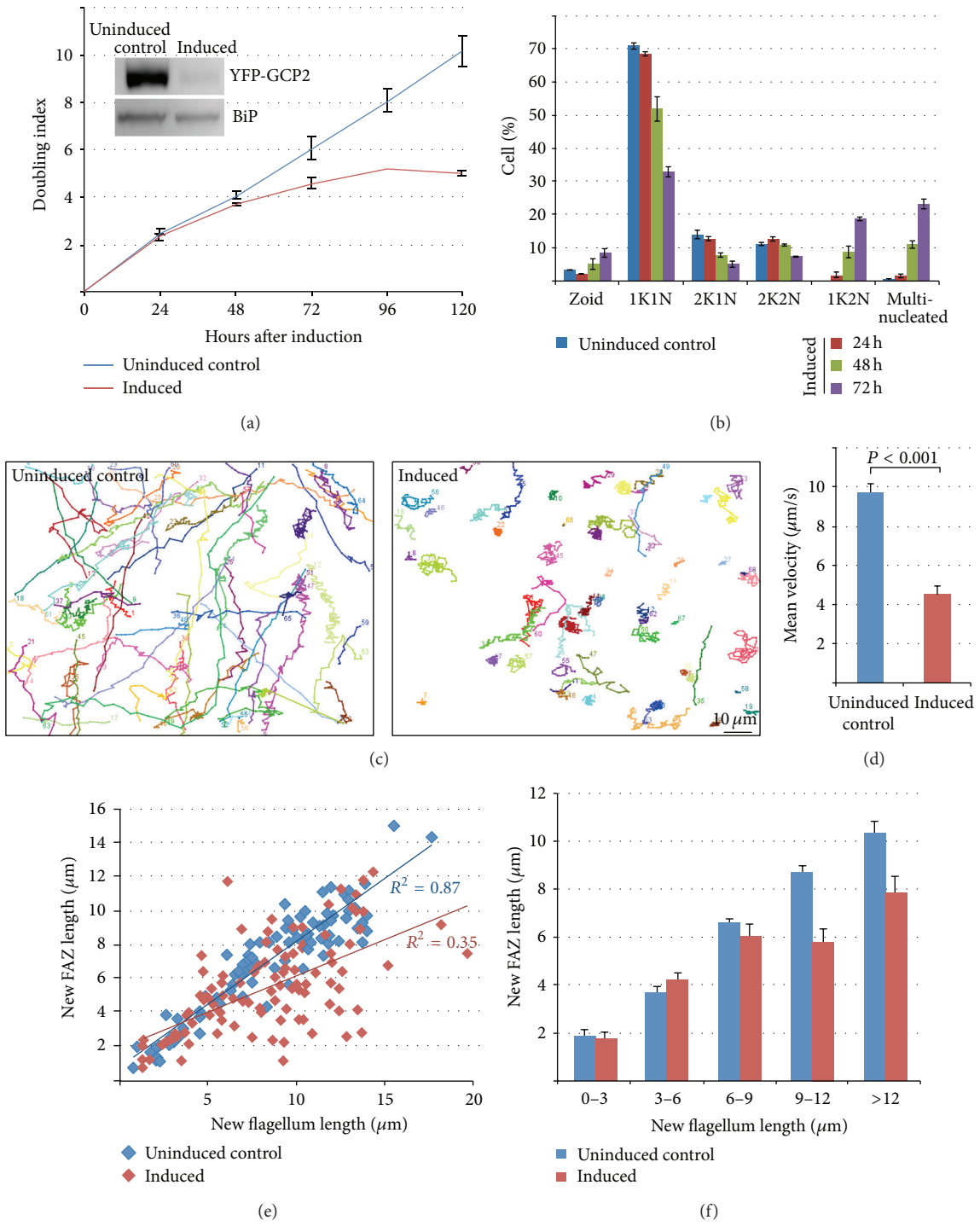

Figure 6: GCP2-RNAi affects new FAZ extension. Cells with a stably integrated GCP2-RNAi construct were grown with tetracycline to induce RNAi or without as control. To monitor the efficiency of RNAi, GCP2-RNAi cells were transfected to allow transient transfection of YFP-GCP2 (a). Samples were then taken every 24 hours after induction for growth assay ((a); results shown as mean ± SD, $n = 3$) and immunoblotting with anti-YFP and anti-BiP (inset). For quantitation of cell cycle effects (b), 400 cells were scored for their DNA contents in each of 3 independent experiments and the results shown as mean ± SD. For motility assays ((c), (d)), uninduced control and cells induced for GCP2-RNAi for 48 hours were diluted in fresh medium, imaged at 2 frames/second for 1 minute, and the movement of individual cells tracked (c) and velocity calculated (d). The 2D-tracks of ~60 cells from three independent experiments were generated by in silico tracking on movies. The velocity results are shown as mean velocity ± SEM of 3 independent experiments with 20–25 cells per experiment. The effect of GCP2 depletion on the new FAZ and flagella elongation was monitored in >100 biflagellated cells in control or cells induced for GCP-RNAi for 48 hours ((e), (f)). The length of new FAZ was plotted against corresponding new flagellum length for each cell measured (e). Alternatively, cells were grouped based on new flagellum length range and FAZ length (shown as mean length ± SEM) was plotted against the flagellum length range (f).

microtubules, with the more posterior daughter cell inheriting most of the newly formed microtubules. This asymmetric inheritance was never observed with YL1/2, possibly due to extensive microtubule plus end remodelling in both daughter cells prior to cell division as previously observed using YFP-XMAP215 as a marker for microtubule plus ends [13]. Using YFP fusion or antibodies to *T. brucei* EB1, a microtubule plus end tracking protein, dynamic microtubule remodeling in the posterior region of both daughter cells was confirmed, particularly during mitosis and cell division stages. The anti-EB1 antibody thus provided a useful tool for monitoring microtubule dynamics in *T. brucei* cells.

5. Conclusion

In this current study, we extended the study of subpellicular microtubule biogenesis and inheritance in *T. brucei* by tracking the incorporation of inducible YFP-α-tubulin during cell cycle progression. Our results showed that new microtubule synthesis was correlated with new FAZ assembly. Newly formed microtubules were incorporated into the microtubule array primarily in the region between the new and old FAZ. Most of the newly synthesized microtubules were inherited by the more posterior daughter cell that also retained the newly assembled flagellum/FAZ. Polarized new microtubule biogenesis, together with active microtubule plus end remodeling in both daughter cells, led to asymmetric inheritance of subpellicular microtubules in *T. brucei* cell division.

Conflict of Interests

The authors declare that there is no conflict of interests regarding the publication of this paper.

Acknowledgments

This work was funded by the Singapore National Research Foundation and Singapore Ministry of Education. The authors wish to thank Chao Wang and Adam Yuan at the Protein Expression Facility at the Singapore Mechanobiology Institute for technical assistance in protein expression and purification.

References

[1] D. R. Robinson, T. Sherwin, A. Ploubidou, E. H. Byard, and K. Gull, "Microtubule polarity and dynamics in the control of organelle positioning, segregation, and cytokinesis in the trypanosome cell cycle," *Journal of Cell Biology*, vol. 128, no. 6, pp. 1163–1172, 1995.

[2] C. Y. He, H. H. Ho, J. Malsam et al., "Golgi duplication in *Trypanosoma brucei*," *Journal of Cell Biology*, vol. 165, no. 3, pp. 313–321, 2004.

[3] N. Balaban and R. Goldman, "Isolation and characterization of a unique 15 kilodalton trypanosome subpellicular microtubule-associated protein," *Cell Motility and the Cytoskeleton*, vol. 21, no. 2, pp. 138–146, 1992.

[4] A. Woods, A. J. Baines, and K. Gull, "A high molecular mass phosphoprotein defined by a novel monoclonal antibody is closely associated with the intermicrotubule cross bridges in the *Trypanosoma brucei* cytoskeleton," *Journal of Cell Science*, vol. 103, part 3, pp. 665–675, 1992.

[5] E. Detmer, A. Hemphill, N. Müller, and T. Seebeck, "The *Trypanosoma brucei* autoantigen 1/6 is an internally repetitive cytoskeletal protein," *European Journal of Cell Biology*, vol. 72, no. 4, pp. 378–384, 1997.

[6] T. Sherwin and K. Gull, "The cell division cycle of *Trypanosoma brucei* brucei: timing of event markers and cytoskeletal modulations," *Philosophical transactions of the Royal Society of London. B: Biological sciences*, vol. 323, no. 1218, pp. 573–588, 1989.

[7] A. Hemphill, D. Lawson, and T. Seebeck, "The cytoskeletal architecture of *Trypanosoma brucei*," *Journal of Parasitology*, vol. 77, no. 4, pp. 603–612, 1991.

[8] V. Scott, T. Sherwin, and K. Gull, "γ-Tubulin in trypanosomes: molecular characterisation and localisation to multiple and diverse microtubule organising centres," *Journal of Cell Science*, vol. 110, part 2, pp. 157–168, 1997.

[9] P. G. McKean, A. Baines, S. Vaughan, and K. Gull, "γ-Tubulin functions in the nucleation of a discrete subset of microtubules in the eukaryotic flagellum," *Current Biology*, vol. 13, no. 7, pp. 598–602, 2003.

[10] K. Gull, "The cytoskeleton of trypanosomatid parasites," *Annual Review of Microbiology*, vol. 53, pp. 629–655, 1999.

[11] H. Farr and K. Gull, "Cytokinesis in trypanosomes," *Cytoskeleton*, vol. 69, pp. 931–941, 2012.

[12] Q. Zhou, B. Liu, Y. Sun, and C. Y. He, "A coiled-coil- and C2-domain-containing protein is required for FAZ assembly and cell morphology in *Trypanosoma brucei*," *Journal of Cell Science*, vol. 124, no. 22, pp. 3848–3858, 2011.

[13] R. J. Wheeler, N. Scheumann, B. Wickstead, K. Gull, and S. Vaughan, "Cytokinesis in *Trypanosoma brucei* differs between bloodstream and tsetse trypomastigote forms: implications for microtubule-based morphogenesis and mutant analysis," *Molecular Microbiology*, vol. 90, no. 6, pp. 1339–1355, 2013.

[14] J. V. Kilmartin, B. Wright, and C. Milstein, "Rat monoclonal antitubulin antibodies derived by using a new nonsecreting rat cell line," *Journal of Cell Biology*, vol. 93, no. 3, pp. 576–582, 1982.

[15] T. Sherwin and K. Gull, "Visualization of detyrosination along single microtubules reveals novel mechanisms of assembly during cytoskeletal duplication in trypanosomes," *Cell*, vol. 57, no. 2, pp. 211–221, 1989.

[16] K. R. Matthews, T. Sherwin, and K. Gull, "Mitochondrial genome repositioning during the differentiation of the African trypanosome between life cycle forms is microtubule mediated," *Journal of Cell Science*, vol. 108, no. 6, pp. 2231–2239, 1995.

[17] J. Andre, L. Kerry, X. Qi et al., "An alternative model for the role of RP2 in flagellum assembly in the African trypanosome," *The Journal of Biological Chemistry*, vol. 289, pp. 464–475, 2013.

[18] L. Ruben, C. Egwuagu, and C. L. Patton, "African trypanosomes contain calmodulin which is distinct from host calmodulin," *Biochimica et Biophysica Acta—General Subjects*, vol. 758, no. 2, pp. 104–113, 1983.

[19] E. Wirtz, S. Leal, C. Ochatt, and G. A. M. Cross, "A tightly regulated inducible expression system for conditional gene knockouts and dominant-negative genetics in *Trypanosoma brucei*," *Molecular and Biochemical Parasitology*, vol. 99, no. 1, pp. 89–101, 1999.

[20] Q. Zhou, L. Gheiratmand, Y. Chen et al., "A comparative proteomic analysis reveals a new bi-lobe protein required for bi-lobe duplication and cell division in *Trypanosoma brucei*," *PloS One*, vol. 5, no. 3, article e9660, 2010.

[21] J. D. Bangs, E. M. Brouch, D. M. Ransom, and J. L. Roggy, "A soluble secretory reporter system in *Trypanosoma brucei*. Studies on endoplasmic reticulum targeting," *The Journal of Biological Chemistry*, vol. 271, no. 31, pp. 18387–18393, 1996.

[22] B. Morriswood, C. Y. He, M. Sealey-Cardona, J. Yelinek, M. Pypaert, and G. Warren, "The bilobe structure of *Trypanosoma brucei* contains a MORN-repeat protein," *Molecular and Biochemical Parasitology*, vol. 167, no. 2, pp. 95–103, 2009.

[23] S. Redmond, J. Vadivelu, and M. C. Field, "RNAit: an automated web-based tool for the selection of RNAi targets in *Trypanosoma brucei*," *Molecular and Biochemical Parasitology*, vol. 128, no. 1, pp. 115–118, 2003.

[24] B. Wickstead, K. Ersfeld, and K. Gull, "Targeting of a tetracycline-inducible expression system to the transcriptionally silent minichromosomes of *Trypanosoma brucei*," *Molecular and Biochemical Parasitology*, vol. 125, no. 1-2, pp. 211–216, 2002.

[25] L. Kohl, T. Sherwin, and K. Gull, "Assembly of the paraflagellar rod and the flagellum attachment zone complex during the *Trypanosoma brucei* cell cycle," *Journal of Eukaryotic Microbiology*, vol. 46, no. 2, pp. 105–109, 1999.

[26] R. Ismach, C. M. Cianci, J. P. Caulfield, P. J. Langer, A. Hein, and D. McMahon-Pratt, "Flagellar membrane and paraxial rod proteins of Leishmania: characterization employing monoclonal antibodies," *Journal of Protozoology*, vol. 36, no. 6, pp. 617–624, 1989.

[27] L. Gheiratmand, A. Brasseur, Q. Zhou, and C. Y. He, "Biochemical characterization of the bi-lobe reveals a continuous structural network linking the bi-lobe to other single-copied organelles in *Trypanosoma brucei*," *The Journal of Biological Chemistry*, vol. 288, pp. 3489–3499, 2013.

[28] E. Meijering, O. Dzyubachyk, and I. Smal, "Methods for cell and particle tracking," *Methods in Enzymology*, vol. 504, pp. 183–200, 2012.

[29] T. Seebeck, P. A. Whittaker, M. A. Imboden, N. Hardman, and R. Braun, "Tubulin genes of *Trypanosoma brucei*: a tightly clustered family of alternating genes," *Proceedings of the National Academy of Sciences of the United States of America*, vol. 80, no. 15, pp. 4634–4638, 1983.

[30] S. Sather and N. Agabian, "A 5′ spliced leader is added in trans to both α- and β-tubulin transcripts in *Trypanosoma brucei*," *Proceedings of the National Academy of Sciences of the United States of America*, vol. 82, no. 17, pp. 5695–5699, 1985.

[31] B. E. Kimmel, S. Samson, J. Wu, R. Hirschberg, and L. R. Yarbrough, "Tubulin genes of the African trypanosome *Trypanosoma brucei* rhodesiense: nucleotide sequence of a 3.7-kb fragment containing genes for alpha and beta tubulins," *Gene*, vol. 35, no. 3, pp. 237–248, 1985.

[32] J. L. Carminati and T. Stearns, "Microtubules orient the mitotic spindle in yeast through dynein- dependent interactions with the cell cortex," *Journal of Cell Biology*, vol. 138, no. 3, pp. 629–641, 1997.

[33] B. Weinstein and F. Solomon, "Phenotypic consequences of tubulin overproduction in *Saccharomyces cerevisiae*: differences between alpha-tubulin and beta-tubulin," *Molecular and Cellular Biology*, vol. 10, no. 10, pp. 5295–5304, 1990.

[34] M. Andresen, R. Schmitz-Salue, and S. Jakobs, "Short tetracysteine tags to β-tubulin demonstrate the significance of small labels for live cell imaging," *Molecular Biology of the Cell*, vol. 15, no. 12, pp. 5616–5622, 2004.

[35] N. M. Rusan, C. J. Fagerstrom, A.-M. C. Yvon, and P. Wadsworth, "Cell cycle-dependent changes in microtubule dynamics in living cells expressing green fluorescent protein-α tubulin," *Molecular Biology of the Cell*, vol. 12, no. 4, pp. 971–980, 2001.

[36] H. V. Goodson, J. S. Dzurisin, and P. Wadsworth, "Methods for expressing and analyzing GFP-tubulin and GFP-microtubule-associated proteins," *Cold Spring Harbor Protocols*, vol. 5, no. 9, 2010.

[37] P. Bastin, A. Bagherzadeh, K. R. Matthews, and K. Gull, "A novel epitope tag system to study protein targeting and organelle biogenesis in *Trypanosoma brucei*," *Molecular and Biochemical Parasitology*, vol. 77, no. 2, pp. 235–239, 1996.

[38] A. Schneider, U. Plessmann, and K. Weber, "Subpellicular and flagellar microtubules of *Trypanosoma brucei* are extensively glutamylated," *Journal of Cell Science*, vol. 110, part 4, pp. 431–437, 1997.

[39] P. Bastin, T. H. MacRae, S. B. Francis, K. R. Matthews, and K. Gull, "Flagellar morphogenesis: protein targeting and assembly in the paraflagellar rod of trypanosomes," *Molecular and Cellular Biology*, vol. 19, no. 12, pp. 8191–8200, 1999.

[40] R. Sasse and K. Gull, "Tubulin post-translational modifications and the construction of microtubular organelles in *Trypanosoma brucei*," *Journal of Cell Science*, vol. 90, part 4, pp. 577–589, 1988.

[41] W. Bu and L.-K. Su, "Characterization of functional domains of human EB1 family proteins," *The Journal of Biological Chemistry*, vol. 278, no. 50, pp. 49721–49731, 2003.

[42] S. Honnappa, C. M. John, D. Kostrewa, F. K. Winkler, and M. O. Steinmetz, "Structural insights into the EB1-APC interaction," *EMBO Journal*, vol. 24, no. 2, pp. 261–269, 2005.

[43] S. Honnappa, S. M. Gouveia, A. Weisbrich et al., "An EB1-binding motif acts as a microtubule tip localization signal," *Cell*, vol. 138, no. 2, pp. 366–376, 2009.

[44] S. B. Skube, J. M. Chaverri, and H. V. Goodson, "Effect of GFP tags on the localization of EB1 and EB1 fragments in vivo," *Cytoskeleton*, vol. 67, no. 1, pp. 1–12, 2010.

[45] R. N. Gunawardane, O. C. Martin, K. Cao et al., "Characterization and reconstitution of Drosophila γ-tubulin ring complex subunits," *Journal of Cell Biology*, vol. 151, no. 7, pp. 1513–1524, 2000.

[46] S. Zimmerman and F. Chang, "Effects of γ-tubulin complex proteins on microtubule nucleation and catastrophe in fission yeast," *Molecular Biology of the Cell*, vol. 16, no. 6, pp. 2719–2733, 2005.

[47] L. Cuschieri, R. Miller, and J. Vogel, "γ-Tubulin is required for proper recruitment and assembly of Kar9-Bim1 complexes in budding yeast," *Molecular Biology of the Cell*, vol. 17, no. 10, pp. 4420–4434, 2006.

[48] S. Y. Sun, C. Wang, Y. A. Yuan, and C. Y. He, "An intracellular membrane junction consisting of flagellum adhesion glycoproteins links flagellum biogenesis to cell morphogenesis in *Trypanosoma brucei*," *Journal of Cell Science*, vol. 126, part 2, pp. 520–531, 2013.

[49] D. J. Lacount, B. Barrett, and J. E. Donelson, "*Trypanosoma brucei* FLA1 is required for flagellum attachment and cytokinesis," *The Journal of Biological Chemistry*, vol. 277, no. 20, pp. 17580–17588, 2002.

[50] D. R. Robinson and K. Gull, "Basal body movements as a mechanism for mitochondrial genome segregation in the trypanosome cell cycle," *Nature*, vol. 352, no. 6337, pp. 731–733, 1991.

[51] S. Absalon, L. Kohl, C. Branche et al., "Basal body positioning is controlled by flagellum formation in *Trypanosoma brucei*," *PLoS ONE*, vol. 2, no. 5, article e437, 2007.

[52] H. R. Dawe, H. Farr, N. Portman, M. K. Shaw, and K. Gull, "The Parkin co-regulated gene product, PACRG, is an evolutionarily conserved axonemal protein that functions in outer-doublet microtubule morphogenesis," *Journal of Cell Science*, vol. 118, no. 23, pp. 5421–5430, 2005.

[53] R. Broadhead, H. R. Dawe, H. Farr et al., "Flagellar motility is required for the viability of the bloodstream trypanosome," *Nature*, vol. 440, no. 7081, pp. 224–227, 2006.

[54] S. Absalon, T. Blisnick, M. Bonhivers et al., "Flagellum elongation is required for correct structure, orientation and function of the flagellar pocket in *Trypanosoma brucei*," *Journal of Cell Science*, vol. 121, no. 22, pp. 3704–3716, 2008.

[55] S. Lacomble, S. Vaughan, C. Gadelha et al., "Three-dimensional cellular architecture of the flagellar pocket and associated cytoskeleton in trypanosomes revealed by electron microscope tomography," *Journal of Cell Science*, vol. 122, no. 8, pp. 1081–1090, 2009.

Hindawi Publishing Corporation
BioMed Research International
Volume 2014, Article ID 687835, 9 pages
http://dx.doi.org/10.1155/2014/687835

Research Article

Disruption of Lipid Rafts Interferes with the Interaction of *Toxoplasma gondii* with Macrophages and Epithelial Cells

Karla Dias Cruz,[1] Thayana Araújo Cruz,[1] Gabriela Veras de Moraes,[1] Tatiana Christina Paredes-Santos,[1] Marcia Attias,[1] and Wanderley de Souza[1,2]

[1] *Laboratório de Ultraestrutura Celular Hertha Meyer, Instituto de Biofísica Carlos Chagas Filho, Universidade Federal do Rio de Janeiro, 21941-902 Rio de Janeiro, RJ, Brazil*
[2] *Instituto Nacional de Metrologia e Qualidade Industrial-Inmetro, 25250-020 Duque de Caxias, RJ, Brazil*

Correspondence should be addressed to Marcia Attias; mattias@biof.ufrj.br

Received 10 September 2013; Revised 26 December 2013; Accepted 8 January 2014; Published 9 March 2014

Academic Editor: Marlene Benchimol

The intracellular parasite *Toxoplasma gondii* can penetrate any warm-blooded animal cell. Conserved molecular assemblies of host cell plasma membranes should be involved in the parasite-host cell recognition. Lipid rafts are well-conserved membrane microdomains that contain high concentrations of cholesterol, sphingolipids, glycosylphosphatidylinositol, GPI-anchored proteins, and dually acylated proteins such as members of the Src family of tyrosine kinases. Disturbing lipid rafts of mouse peritoneal macrophages and epithelial cells of the lineage LLC-MK2 with methyl-beta cyclodextrin (MβCD) and filipin, which interfere with cholesterol or lidocaine, significantly inhibited internalization of *T. gondii* in both cell types, although adhesion remained unaffected in macrophages and decreased only in LLC-MK2 cells. Scanning and transmission electron microscopy confirmed these observations. Results are discussed in terms of the original role of macrophages as professional phagocytes versus the LLC-MK2 cell lineage originated from kidney epithelial cells.

1. Introduction

Toxoplasma gondii, one of the most widely distributed pathogenic protozoa, is highly competent at invading a variety of cell types from different animals (Reviews in [1, 2]). Studies conducted by several groups over the last twenty years have provided a substantial amount of information on the roles of the proteins that the parasite secretes once it attaches to the host cell surface. These proteins trigger a series of events that culminate in the penetration of the host cell by the parasite through a typical endocytic process that includes the formation of a vacuole known as the parasitophorous vacuole (PV) [3–6]. Several proteins present in the micronemes and rhoptries and two major secretory organelles found in the apical portion of the protozoan, have been shown to play important roles in the interaction process [7, 8]. However, relatively little is known about the role of the host cell surface components during the parasite-host interaction [9–12]. Because *T. gondii* is able to penetrate all of the host cells tested, it is highly likely that molecular assemblies that are conserved in different cell types are involved in the parasite-host cell interaction process. One of these well-conserved machineries is the so-called "lipid rafts," which are membrane microdomains that contain high concentrations of cholesterol, sphingolipids, glycosylphosphatidylinositol, GPI-anchored proteins, dually acylated proteins such as members of the Src family of tyrosine kinases, and so forth (reviews in [13–15]). Previous studies have shown that disturbing host cell lipid rafts by using drugs that interfere with cholesterol, such as methyl-beta cyclodextrin (MβCD) and filipin, or lidocaine, which does not interfere with cholesterol, significantly inhibited the infection of the cells by the protozoa *Leishmania donovani* [16], *Leishmania chagasi* [17], *Trypanosoma cruzi* [18, 19], and *Plasmodium falciparum* [20]. In the case of *T. gondii*, Coppens and Joiner [21] showed that depletion of the host

cell membrane cholesterol using lovastatin or MβCD reduced parasite internalization and increased the number of parasites attached to the host cell surface.

To determine the role of membrane lipid microdomains in the interactions between protozoa and host cells, we used professional phagocytic cells (macrophages) and an epithelial cell line (LLC-MK2) in conjunction with several compounds that interfere with lipid microdomains to analyze the effect of these compounds on parasite-host interactions. The cells were visualized by electron microscopy, and the obtained results are reported here.

2. Materials and Methods

2.1. Chemicals. Methyl-β-cyclodextrin (MβCD), filipin III, β subunit of the cholera toxin (CTB), and lidocaine were obtained from Sigma-Aldrich Chemical Laboratory, USA. Stock solutions of MβCD, CTB, and lidocaine were diluted in water and filipin was diluted in dimethylsulfoxide (DMSO).

2.2. Parasites. The RH strain of *Toxoplasma gondii* was maintained by intraperitoneal passage into mice as described elsewhere [22].

2.3. Host Cells. The epithelial cell line LLC-MK_2 (ATTC) and mouse peritoneal macrophages were used in this study. The cells were cultured in RPMI 1640 (Gibco) medium supplemented with 10% fetal bovine serum and maintained at 37°C in a 5% CO_2 atmosphere. The macrophages were prepared and maintained as described previously [19].

2.4. Host Cell-Parasite Interaction. The interaction experiments were carried out with cells plated on 13 mm glass slides. Either the cells or the parasites were incubated in the presence of the various compounds tested, as indicated in the Results section. The parasite-to-host cell ratio was adjusted to 50 : 1. After the cells were allowed to interact, the host cells were washed to remove the unattached parasites and were then fixed in freshly prepared 4% formaldehyde in 0.1 M phosphate buffer, pH 7.2. After fixation, the cells were washed and stained with Giemsa, and the coverslips were dehydrated in acetone-xylol and mounted on glass slides with Entellan mounting media for subsequent observation with a light microscope (Carl Zeiss Microscopy GmbH, Jena, Germany). The adhesion and internalization indices were determined as described previously [23]. At least three independent experiments in duplicate were performed, and at least 600 cells were analyzed on each coverslip. The data obtained in the control experiments were normalized to 100. Graphic and statistical analyses, including Student's t-test and one-way ANOVA, were conducted with Prisma Graph Pad software (GraphPad Software).

2.5. Cell Viability Assay. After incubation with one of the drugs, the cells were rinsed in PBS and incubated in the presence of 0.2% Trypan blue for 5 minutes. The percentage of labeled cells (only dead cells are labeled) was determined by microscopic examination of at least 300 cells in at least three independent experiments.

2.6. Fluorescence Microscopy. To examine the localization of the GM1 ganglioside, the cells were washed in RPMI 1640 medium (GIBCO, Life Technologies Corporation) and incubated in the presence of 50 μg/mL of the β subunit of cholera toxin (Sigma-Aldrich, USA) for 45 minutes. Subsequently, the cells were washed with PBS, pH 8.0, and incubated in the presence of 5 μg/mL DAPI (Sigma-Aldrich, USA) to label the cell nuclei. After incubation, the cells were washed, mounted on glass slides with 0.2 M N-propyl gallate in 90% glycerol, and observed using a Zeiss Axioplan fluorescence microscope (Carl Zeiss Microscopy GmbH, Jena, Germany).

2.7. Scanning Electron Microscopy. After interacting with the parasites, the host cells mounted on coverslips were fixed in a solution containing 2.5% glutaraldehyde in 0.1 M cacodylate buffer, pH 7.2, for 1 hour, washed in buffer, and postfixed for 30 minutes in the dark in a solution containing 1% osmium tetroxide and 0.8% potassium ferrocyanide in the same buffer. The cells were washed again in buffer, dehydrated in ethanol, and submitted to critical point drying in CO_2 using CPD 30 Baltec equipment. The samples were then coated with a 0.2 nm thick layer of gold and examined in a Jeol JSM 6340 field emission scanning electron microscope operating at 3–5 kV.

2.8. Transmission Electron Microscopy. After interacting with the parasites, the host cells were fixed for 1 hour at 4°C in a solution containing 2.5% glutaraldehyde and 1.4% freshly prepared formaldehyde in 0.1 M cacodylate buffer, pH 7.2. Then, the cells were washed in buffer and postfixed for 40 minutes in the dark in a solution containing 1% osmium tetroxide and 0.8% potassium ferrocyanide in 0.1 M cacodylate buffer, pH 7.2. The cells were then washed in buffer, dehydrated in acetone, and embedded in an Epoxy resin. Thin sections were obtained using an ultramicrotome. The sections were stained with uranyl acetate and lead citrate and examined using a transmission electron microscope (Zeiss 900 or Jeol 1200) operating at 80 kV.

3. Results

3.1. MβCD Treatment of the Host Cell Interferes with the Interaction Process. We used MβCD, a cyclodextrin that is a glucose oligomer that interacts with membranes and sequesters lipophilic molecules within its hydrophobic nucleus [13]. Treatment of LLC-MK2 cells with MβCD followed by incubation with *T. gondii* significantly decreased ($P < 0.0001$) both the adhesion and the internalization indices (Figure 1(a)). Inhibition was evident even at a concentration of 5 mM MβCD, reaching values as high as 70%. Inhibition did not increase when higher concentrations of MβCD were used. In macrophages, only a slight inhibition of the adhesion index was observed. However, internalization was drastically reduced by up to 95% by treatment with 5 mM MβCD (Figure 1(b)). Notably, treatment of both cells types with

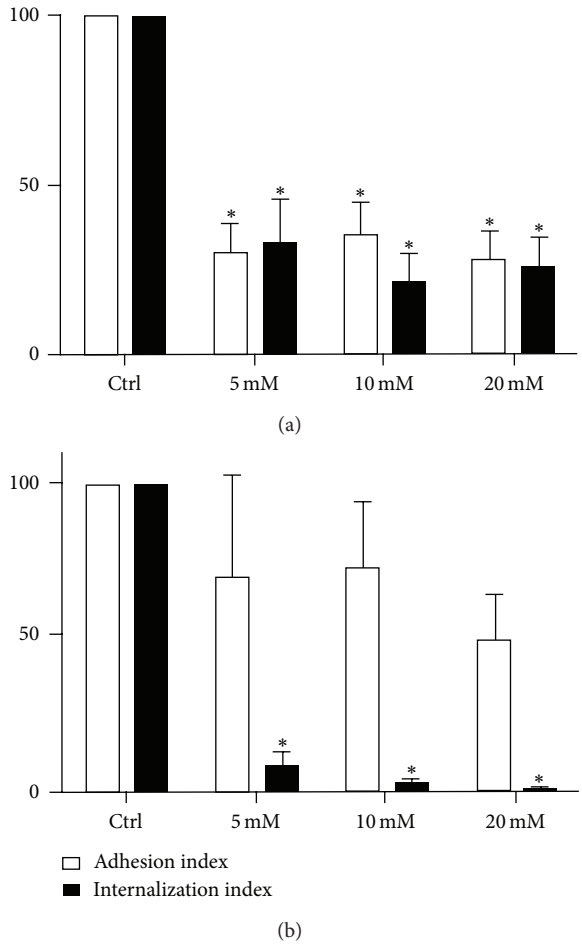

Figure 1: *T. gondii* adhesion and internalization percentages with LLC-MK2 cells (a) and murine macrophages (b) that were treated with MβCD (5, 10, and 20 mM) for 30 min before the addition of *T. gondii* tachyzoites. The host cells were pretreated and washed before interacting for 10 minutes with the parasites (50 : 1). The data shown are the means ± SE of duplicated points from three independent experiments. The control values were set at 100. In LLC-MK2 cells, both adhesion and internalization were inhibited. However, only internalization was affected in macrophages.

MβCD at the concentrations used did not significantly interfere with cell viability, as determined using Trypan blue (data not shown). Scanning electron microscopy of MβCD-treated macrophages revealed that the cells became more retracted and rounded. Some cells detached from the glass surface such that the number of cells per square micrometer was significantly decreased, as shown in Figure 2. However, the detached cells were still viable (data not shown). The parasites attached to untreated macrophages triggered endocytic processes, and membrane projections were observed surrounding the parasites during the process of internalization (Figure 3(a)). In contrast, no surface membrane projections were observed surrounding the parasites attached to the surface of MβCD-treated macrophages (Figure 3(b)). Transmission electron microscopy observations confirmed that parasites were internalized by untreated host cells (Figure 4(a)) but they remained attached to the surface of MβCD-treated cells (Figure 4(b)).

We also analyzed the reversibility of the MβCD treatment. For this experiment, the cells were initially treated with MβCD for 30 minutes. Subsequently, some cultures were washed and incubated in fresh medium for 2 hours before interaction with the parasites. No reversibility was observed with the LLC-MK2 cells (Figure 5(a)). However, a significant reversible effect on the internalization of the parasites by macrophages was achieved (Figure 5(b)), but this effect was less evident for the adhesion index. Scanning electron microscopy showed that the recovered macrophages possessed surface projections that covered the attached parasites, similar to what was observed in the control (not shown).

3.2. Filipin Treatment of Host Cells Interferes with Their Interaction with T. gondii. Filipin is a polyenic antibiotic that binds to cholesterol and thus interferes with the fluidity of cell membranes. Therefore, we decided to analyze its effect on the *T. gondii*-host cell interaction. Incubation of the LLLC-MK2 cells in the presence of 1 or 3 nM but not 6 nM filipin slightly decreased the adhesion of the parasites to the cells (Figure 6(a)) but did not interfere with internalization. In macrophages (Figure 6(b)), filipin inhibited both adhesion and internalization. At a filipin concentration of 6 nM, internalization was inhibited by 85%. In the tested conditions, the treated cells remained viable (data not shown). Scanning and transmission electron microscopy confirmed these observations (data not shown).

3.3. Treatment of the Host Cells with the B Subunit of the Cholera Toxin Inhibits Parasite-Host Cell Interaction. We also analyzed the influence of the GM1 ganglioside on the interaction process. For this experiment, the cells were treated for 30 min at 4°C with the β subunit of cholera toxin (CTB) and then allowed to interact with parasites at 37°C. Treatment with CTB greatly inhibited the adhesion to and invasion of LLC-MK2 cells and reached inhibition values of 80% (Figure 7(a)). The macrophages treated with CTB also showed altered adhesion and internalization indices (Figure 7(b)). Treatment of the cells with CTB did not affect their viability (data not shown).

3.4. Treatment with Lidocaine Interferes with T. gondii-Host Cell Interaction. We used lidocaine in our experiments because it is able to penetrate the membrane lipid bilayer and can disrupt the lipid rafts [24]. We selected concentrations of lidocaine ranging from 57.5 to 230 μM and incubated the cells with the lidocaine for 20 minutes at 37°C. After incubation, the cells were washed in media and allowed to interact with the parasites. We observed that the lidocaine treatment markedly inhibited the adhesion and internalization of the parasites incubated with LLC-MK2 cells by up to 90% (Figure 8(a)). The same treatment interfered to a lesser extent with parasite adhesion to the macrophages, but it significantly inhibited internalization (Figure 8(b)). Cell viability tests indicated that the cells remained viable after incubation with lidocaine (data not shown).

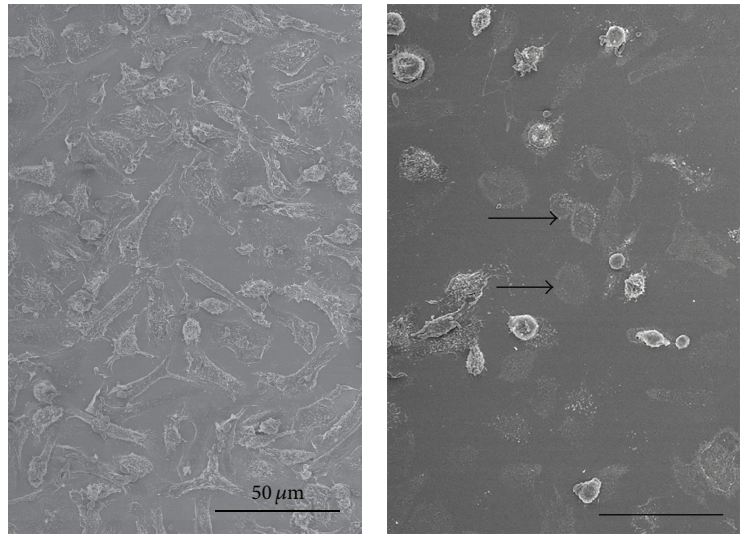

(a) (b)

Figure 2: Scanning electron microscopy images of control macrophages (a) evenly spread over the glass surface. (b) Treatment with 20 mM MβCD caused the macrophages to detach from the glass, leaving a print in the coverslip (arrows). Macrophages that resisted the treatment were more spherical, suggesting a retraction of filopodia and adhesion points. Bar: 50 μm.

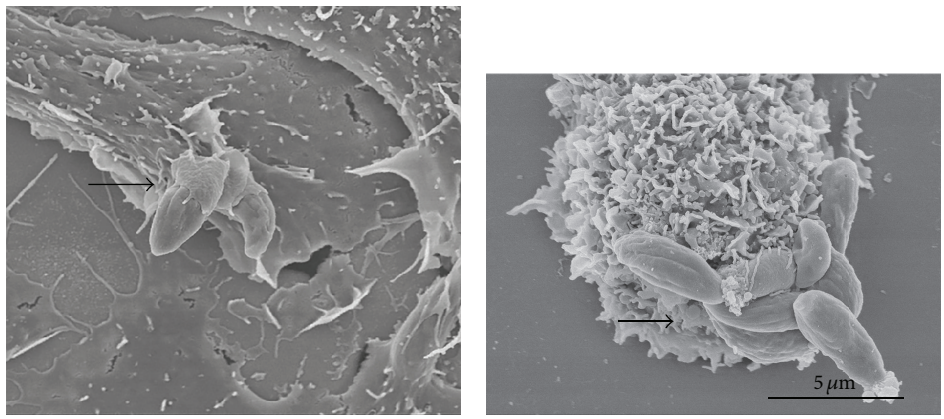

(a) (b)

Figure 3: Scanning electron microscopy images of untreated macrophages (a) and two parasites partially covered by membrane projections, indicating that they are undergoing internalization (arrow). (b) Eight parasites (arrow) can be seen adhered to this macrophage that was previously treated with 20 mM MβCD.

3.5. Effect of Pretreating T. gondii with MβCD, Filipin, CTB, or Lidocaine on the Interaction with Host Cells. Experiments were performed to determine if the same compounds tested in the host cells also affected membrane domains on the surface of *T. gondii*. Table 1 summarizes the observations made from these experiments. It is important to note that the effects observed from treating the parasites were not as clear as those obtained following treatment of the host cells. In most of the experiments, we observed a reduction in the internalization index with a much slighter effect on the adhesion index.

4. Discussion

The concept that the cell membrane is more mosaic than fluid with nonrandom distribution of lipids was a major step in understanding the behavior of cells, particularly cell interaction with pathogens (review in [25]). In basal conditions, lipid rafts are small regions of the membranes. However, they can form larger clusters in response to certain stimuli [26, 27]. Data obtained by several groups in the last decade have established that the interaction of intracellular pathogenic protozoa with host cells involves two well-defined

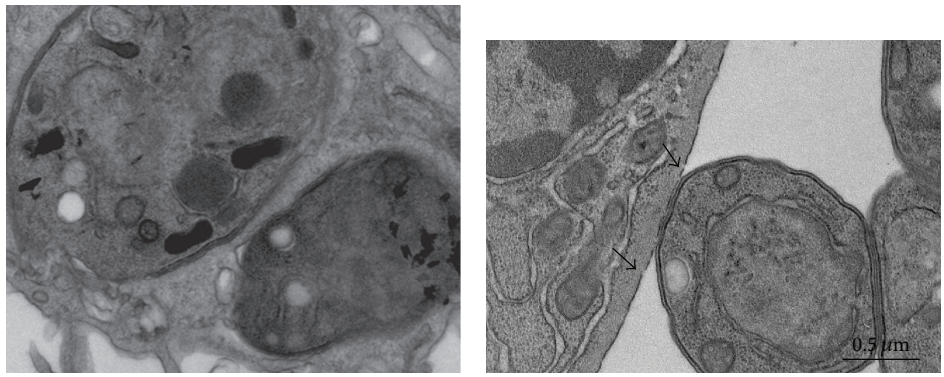

(a) (b)

Figure 4: Transmission electron microscopy images of a control (untreated) macrophage (a) containing two parasites. (b) A single parasite is seen adhered to the surface of a cell that had been pretreated with 20 mM MβCD. The plasma membrane shows a dotted pattern (arrowheads).

Table 1: Effect of drugs that interfere with lipid rafts on *Toxoplasma gondii* adhesion and internalization of host cells.

Cell type	Macrophages		LLC-MK2	
Treatment	Adhesion	Internalization	Adhesion	Internalization
MβCD	Nonaffected	Decreased	Decreased	Decreased
Filipin	Nonaffected	Decreased	Nonaffected	Nonaffected
CTB	Nonaffected	Decreased	Decreased	Decreased
Lidocaine	Nonaffected	Decreased	Decreased	Decreased

steps: adhesion and internalization (reviews in [24, 28–30]). Adhesion can occur even at low temperatures or when the host cell cytoskeleton is blocked by the use of drugs, and the participation of molecules that are exposed on the surface of both interacting cells is very important to this process [31]. The internalization process involves cell signaling events followed by endocytosis [29], and the composition of the plasma membrane and the mobility of membrane-associated molecules, which depends on the fluidity of the lipid bilayer and association with cytoskeletal components, play an important role.

It is well established that lipid rafts in the membrane of the host cell are involved in the internalization of pathogenic protozoa such as *Leishmania* [16], *Trypanosoma cruzi* [18, 19], *Plasmodium falciparum* [20], and *Toxoplasma gondii* [21]. The moving junction, a specialized contact area established by *Plasmodium* during invasion of an erythrocyte [32] and between *Toxoplasma* and any host cell it invades [33], selects host cell rafts and proteins that will be part of the parasitophorous vacuole membrane [34]. However, caveolin I, a typical raft-associated protein, is excluded from the parasitophorous vacuole of *T. gondii* [33], as well as flotillin-2 [35]. In this study with *T. gondii*, we further analyzed the role of membrane lipid domains, including lipid rafts, in the interaction process using LLC-MK2 cells and murine macrophages and treatment with several inhibitors. Our results were visualized by electron microscopy to obtain a more detailed view of the parasite-host cell interface.

We used MβCD, filipin, the β subunit of cholera toxin, and lidocaine to interfere with the membrane of the host cell. These various treatments affected both the shape of the cells and their ability to adhere to the glass coverslips. However, cell viability was not significantly altered, as assessed using the Trypan blue test.

MβCD is a glucose oligomer that sequesters lipophilic molecules in hydrophobic nuclear membranes [13], and it has been widely used to deplete cholesterol from membranes and prevent endocytic processes. Treatment of host cells with MβCD has been shown to decrease the internalization of *Leishmania* [16], *T. cruzi* [18, 19], and *T. gondii* [21]. In *Plasmodium*, depletion of cholesterol from the membranes of infected erythrocytes caused precocious liberation of parasites, which were noninfective [34]. Red blood cells depleted from cholesterol also prevent invasion by *Plasmodium falciparum* [36]. Our observations confirm the results previously described for these protozoa, but we also were able to show that the effects of the treatment varied according to the host cell used. Indeed, MβCD treatment only slightly interfered with the adhesion of *T. gondii* to macrophages; however, it inhibited adhesion to LLC-MK2 cells by 75%. A similar effect was reported for fibroblasts and CHO cells [21]. Notably, in the case of *T. gondii*, MβCD interfered acutely with parasite internalization at concentrations as low as 5 mM, while similar effects on *T. cruzi* were obtained with 20 mM [19]. In malaria parasites, also apicomplexans, erythrocyte lipid rafts are recruited to the site of invasion and can be remodeled by *Plasmodium* to establish blood stage infection [37].

We used scanning and transmission electron microscopy to analyze the interaction process in untreated control cells and drug-treated cells. Our observations show clearly that host cells treated with MβCD or with the other tested

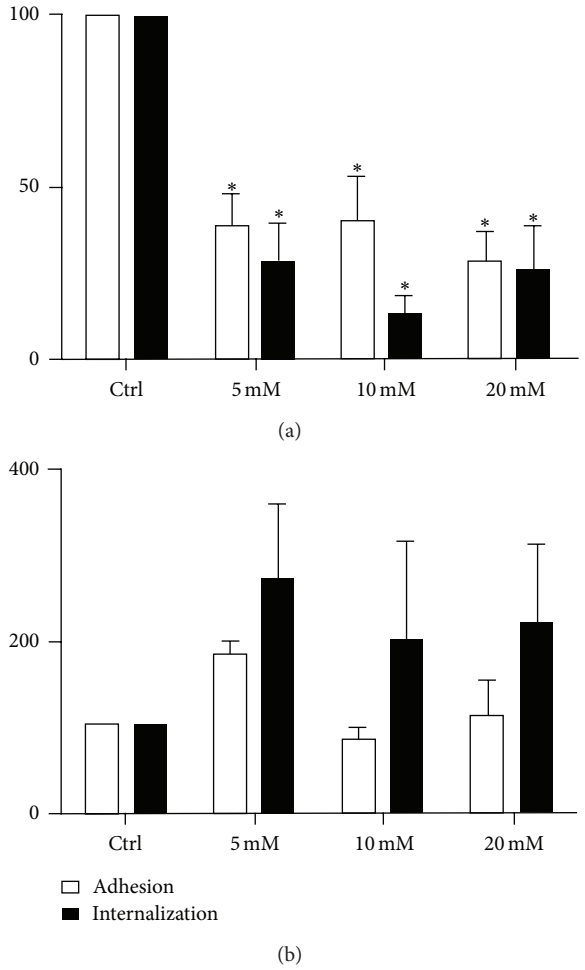

Figure 5: Reversibility of the effect of MβCD. Estimation of adhesion and internalization percentage of *T. gondii* with LLC-MK2 cells (a) and murine macrophages (b) treated with MβCD (5, 10, and 20 mM) for 30 min and then incubated for 2 hours with 20% FCS in RPMI medium before the *T. gondii* tachyzoites were added for 10 minutes (50 : 1). The data shown are the means ± SE of duplicated points from three independent experiments. $^{*}P < 0.05$. The results were normalized. Reversibility was observed only in macrophages.

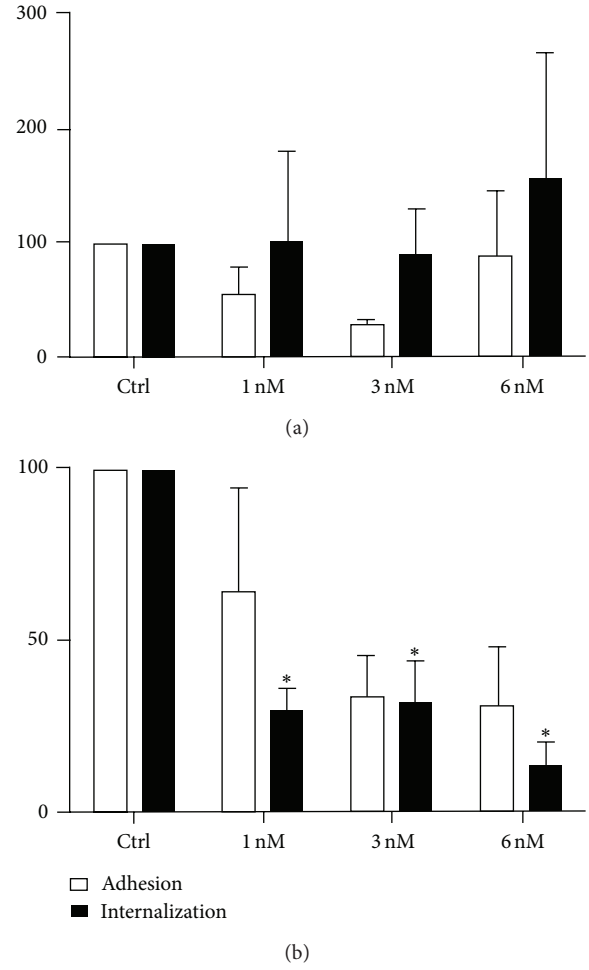

Figure 6: Adhesion and internalization percentages with (a) LLC-MK2 cells and (b) murine macrophages after filipin treatment (1, 3, and 6 nM) for 30 min before the addition of the parasites (50 : 1) for 10 minutes. At 6 nM filipin, the adhesion of the parasites to the LLC-MK2 cells was slightly decreased, and internalization was significantly inhibited. In macrophages, internalization was inhibited by 85%. The data shown are the means ± SE of duplicated points from three independent experiments. $^{*}P < 0.05$. The results were normalized.

drugs had parasites which adhered to the cell surface, but, unlike the untreated cells, no host cell surface projections surrounded the parasites. Therefore, interfering with the plasma membrane lipids of the host cell blocks the formation of surface projections.

Filipin is another compound that has been used to interfere with membrane cholesterol. Unlike MβCD, this polyenic antibiotic does not extract cholesterol but instead binds to it and forms filipin-sterol complexes that drastically decrease the fluidity of the plasma membrane [30]. Filipin inhibited the internalization of *T. gondii* by macrophages by up to 85%, but it did not have a significant effect on the interaction of the parasite with LLC-MK2 cells. We previously reported that filipin had a discrete effect on both the adhesion and internalization of *T. cruzi* [19].

We also tested the effect of lidocaine on host-parasite interactions. Lidocaine is a local anesthetic that disrupts lipid rafts without altering membrane cholesterol [38] and has been shown to inhibit the infection of erythrocytes by *Plasmodium falciparum* by 90% [39]. Treatment of host cell with lidocaine markedly inhibited both the adhesion and internalization of *T. gondii* by LLC-MK2 cells but only decreased internalization in macrophages.

Previous studies have shown that treating host cells with the β subunit of cholera toxin, which is produced by the bacterium *Vibrio cholera* and binds to the GM1 ganglioside, a well-known marker of lipid rafts [17], markedly blocked the internalization of *T. cruzi* by macrophages [19]. A similar effect was observed both for the adhesion and internalization steps in the interaction of *T. gondii* with LLC-MK2 cells and for its internalization into macrophages. Surprisingly, it had

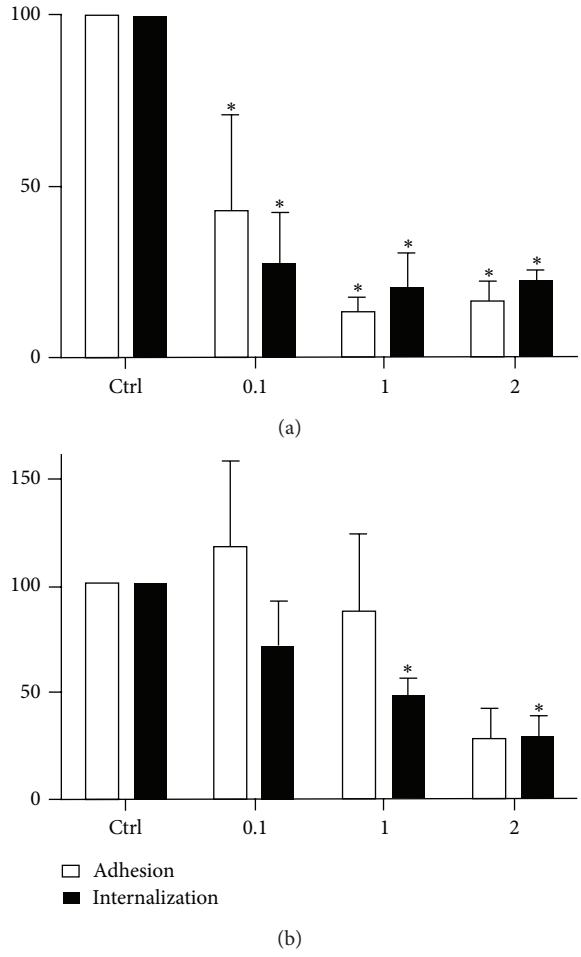

Figure 7: Adhesion and internalization indices of *T. gondii* in LLC-MK2 cells (a) and murine macrophages (b) after treatment with cholera toxin-B (CTB) (0.1, 1, and 2 μg/mL) for 20 minutes at 4°C before the addition of parasites (50 : 1) at 37°C for 10 minutes. The cells were then fixed and stained. In LLC-MK2 cells, adhesion and internalization were reduced at all concentrations tested, and in macrophages, a significant reduction in internalization was observed at the higher concentrations. Parasite loads were quantified microscopically, and the data shown are the means ± SE of duplicated points from three independent experiments. $^{*}P < 0.05$. The results were normalized.

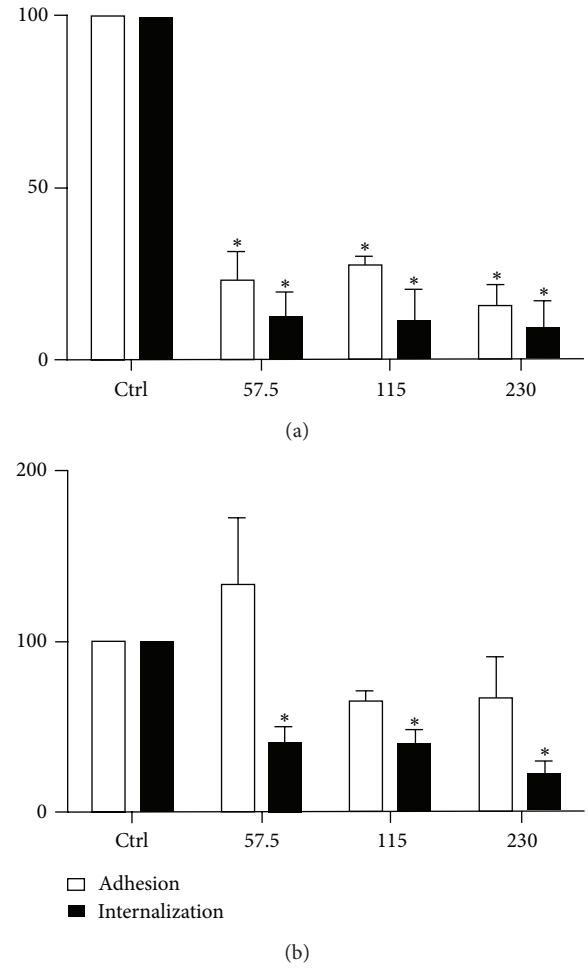

Figure 8: Estimation of the adhesion and internalization indices of *T. gondii* in LLC-MK2 cells (a) and murine macrophages (b) pretreated with lidocaine (57.5 μM, 115 μM, and 230 μM) for 20 minutes before the addition of parasites at 37°C for 10 minutes. In LLC-MK2 cells, both adhesion and internalization were reduced at all concentrations. In macrophages, a significant reduction was observed only for internalization. The parasite loads were quantified microscopically. The data shown are the means ± SE of duplicated points from three independent experiments. $^{*}P < 0.05$. The results were normalized.

only a small effect on the attachment of *T. gondii* to macrophage surfaces.

Taken together, the available data clearly show that the organization of the lipid rafts in the host cell plasma membrane is essential for the initiation of the endocytosis that leads to the internalization of *T. gondii*, even when cholesterol is present in the plasma membrane. The differences observed between adhesion and internalization indices between macrophages and LLC-MK2 cells could be explained by the very nature of these cell types. Macrophages are professional phagocytes and internalization was not blocked as efficiently as for LLC-MK2 cells. That could be due to the fact that the observed internalization was the result of phagocytosis, rather than active invasion by the parasites. Adhesion indices on the other hand were reduced in both cell types, indicating that raft disruption impairs this key step in parasite active invasion of host cells.

We also carried out experiments to determine whether treating the parasite with the same compounds discussed above also interfered with the interaction process. We observed decreased internalization in most of the experiments, but they had a high standard deviation that was most likely due to the heterogeneity of the parasites used, which were obtained from the peritoneum of experimentally infected mice. Furthermore, the very intense and continuous secretion of micronemes constantly renews the outer membrane of the parasite. These observations suggest that the organization of the lipid bilayer of the parasite also plays a role in the process of adhesion to and internalization by host cells.

Previous studies have suggested that an interchange of surface components of the two cells involved in the interaction process occurs [40].

Conflict of Interests

The authors declare that there is no conflict of interests regarding the publication of this paper.

Acknowledgments

This work was supported by grants to the authors from Conselho Nacional de Desenvolvimento Científico e Tecnológico-CNPq, Fundação Carlos Chagas Filho de Amparo à Pesquisa do Estado do Rio de Janeiro-FAPERJ, and Coordenação de Aperfeiçoamento de Pessoal de Nível Superior-CAPES.

References

[1] D. Hill and J. P. Dubey, "*Toxoplasma gondii*: transmission, diagnosis, and prevention," *Clinical Microbiology and Infection*, vol. 8, no. 10, pp. 634–640, 2002.

[2] J. L. Jones and J. P. Dubey, "Foodborne toxoplasmosis," *Clinical Infectious Diseases*, vol. 55, no. 6, pp. 845–851, 2012.

[3] T. C. Jones and J. G. Hirsch, "The interaction between *Toxoplasma gondii* and mammalian cells. II. The absence of lysosomal fusion with phagocytic vacuoles containing living parasites," *Journal of Experimental Medicine*, vol. 136, no. 5, pp. 1173–1194, 1972.

[4] T. C. Jones, S. Yeh, and J. G. Hirsch, "The interaction between *Toxoplasma gondii* and mammalian cells. I. Mechanism of entry and intracellular fate of the parasite," *Journal of Experimental Medicine*, vol. 136, no. 5, pp. 1157–1172, 1972.

[5] A. P. Sinai and K. A. Joiner, "Safe haven: the cell biology of nonfusogenic pathogen vacuoles," *Annual Review of Microbiology*, vol. 51, pp. 415–462, 1997.

[6] K. A. Joiner, D. Bermudes, A. Sinai, H. Qi, V. Polotsky, and C. J. M. Beckers, "Structure and function of the *Toxoplasma gondii* vacuole," *Annals of the New York Academy of Sciences*, vol. 797, pp. 1–7, 1996.

[7] V. B. Carruthers and L. D. Sibley, "Sequential protein secretion front three distinct organelles of *Toxoplasma gondii* accompanies invasion of human fibroblasts," *European Journal of Cell Biology*, vol. 73, no. 2, pp. 114–123, 1997.

[8] V. Carruthers and J. C. Boothroyd, "Pulling together: an integrated model of *Toxoplasma cell* invasion," *Current Opinion in Microbiology*, vol. 10, no. 1, pp. 83–89, 2007.

[9] E. Suss-Toby, J. Zimmerberg, and G. E. Ward, "Toxoplasma invasion: the parasitophorous vacuole is formed from host cell plasma membrane and pinches off via a fission pore," *Proceedings of the National Academy of Sciences of the United States of America*, vol. 93, no. 16, pp. 8413–8418, 1996.

[10] C. Pacheco-Soares and W. De Souza, "Redistribution of parasite and host cell membrane components during *Toxoplasma gondii* invasion," *Cell Structure and Function*, vol. 23, no. 3, pp. 159–168, 1998.

[11] C. Pacheco-Soares and W. De Souza, "Labeled probes inserted in the macrophage membrane are transferred to the parasite surface and internalized during cell invasion by *Toxoplasma gondii*," *Parasitology Research*, vol. 86, no. 1, pp. 11–17, 2000.

[12] I. Coppens, "Contribution of host lipids to *Toxoplasma* pathogenesis," *Cellular Microbiology*, vol. 8, no. 1, pp. 1–9, 2006.

[13] F. G. Van Der Goot and T. Harder, "Raft membrane domains: from a liquid-ordered membrane phase to a site of pathogen attack," *Seminars in Immunology*, vol. 13, no. 2, pp. 89–97, 2001.

[14] A. M. Goldston, R. R. Powell, and L. A. Temesvari, "Sink or swim: lipid rafts in parasite pathogenesis," *Trends in Parasitology*, vol. 28, no. 10, pp. 417–426, 2012.

[15] F. S. MacHado, N. E. Rodriguez, D. Adesse et al., "Recent developments in the interactions between caveolin and pathogens," *Advances in Experimental Medicine and Biology*, vol. 729, pp. 65–82, 2012.

[16] T. J. Pucadyil, P. Tewary, R. Madhubala, and A. Chattopadhyay, "Cholesterol is required for *Leishmania donovani* infection: implications in leishmaniasis," *Molecular and Biochemical Parasitology*, vol. 133, no. 2, pp. 145–152, 2004.

[17] N. E. Rodríguez, U. Gaur, and M. E. Wilson, "Role of caveolae in *Leishmania chagasi* phagocytosis and intracellular survival in macrophages," *Cellular Microbiology*, vol. 8, no. 7, pp. 1106–1120, 2006.

[18] M. C. Fernandes, M. Cortez, K. A. Geraldo Yoneyama, A. H. Straus, N. Yoshida, and R. A. Mortara, "Novel strategy in *Trypanosoma cruzi* cell invasion: implication of cholesterol and host cell microdomains," *International Journal for Parasitology*, vol. 37, no. 13, pp. 1431–1441, 2007.

[19] E. S. Barrias, J. M. F. Dutra, W. D. Souza, and T. M. U. Carvalho, "Participation of macrophage membrane rafts in *Trypanosoma cruzi* invasion process," *Biochemical and Biophysical Research Communications*, vol. 363, no. 3, pp. 828–834, 2007.

[20] N. L. Hiller, T. Akompong, J. S. Morrow, A. A. Holder, and K. Haldar, "Identification of a stomatin orthologue in vacuoles induced in human erythrocytes by malaria parasites. A role for microbial raft proteins in apicomplexan vacuole biogenesis," *Journal of Biological Chemistry*, vol. 278, no. 48, pp. 48413–48421, 2003.

[21] I. Coppens and K. A. Joiner, "Host but not parasite cholesterol controls *Toxoplasma cell* entry by modulating organelle discharge," *Molecular Biology of the Cell*, vol. 14, no. 9, pp. 3804–3820, 2003.

[22] T. C. Paredes-Santos, W. de Souza, and M. Attias, "Dynamics and 3D organization of secretory organelles of *Toxoplasma gondii*," *Journal of Structural Biology*, vol. 177, no. 2, pp. 420–430, 2012.

[23] L. A. Caldas, M. Attias, and W. De Souza, "Dynamin inhibitor impairs *Toxoplasma gondii* invasion," *FEMS Microbiology Letters*, vol. 301, no. 1, pp. 103–108, 2009.

[24] L. David Sibley, "Invasion and intracellular survival by protozoan parasites," *Immunological Reviews*, vol. 240, no. 1, pp. 72–91, 2011.

[25] F. S. Vieira, G. Corrêa, M. Einicker-Lamas, and R. Coutinho-Silva, "Host-cell lipid rafts: a safe door for micro-organisms?" *Biology of the Cell*, vol. 102, no. 7, pp. 391–407, 2010.

[26] P. Liu and R. G. W. Anderson, "Compartmentalized production of ceramide at the cell surface," *Journal of Biological Chemistry*, vol. 270, no. 45, pp. 27179–27185, 1995.

[27] C. R. Bollinger, V. Teichgräber, and E. Gulbins, "Ceramide-enriched membrane domains," *Biochimica et Biophysica Acta*, vol. 30, pp. 284–294, 2005.

[28] W. de Souza and T. M. U. de Carvalho, "Active penetration of *Trypanosoma cruzi* into host cells: historical considerations and current concepts," *Frontiers in Immunology*, vol. 4, no. 2, 2013.

[29] N. Yoshida, K. M. Tyler, and M. S. Llewellyn, "Invasion mechanisms among emerging food-borne protozoan parasites," *Trends in Parasitology*, vol. 27, no. 10, pp. 459–466, 2011.

[30] S. Besteiro, J.-F. Dubremetz, and M. Lebrun, "The moving junction of apicomplexan parasites: a key structure for invasion," *Cellular Microbiology*, vol. 13, no. 6, pp. 797–805, 2011.

[31] B. Cowper, S. Matthews, and F. Tomley, "The molecular basis for the distinct host and tissue tropisms of coccidian parasites," *Molecular and Biochemical Parasitology*, vol. 186, no. 1, pp. 1–10, 2012.

[32] M. Aikawa, L. H. Miller, J. Johnson, and J. Rabbege, "Erythrocyte entry by malarial parasites. A moving junction between erythrocyte and parasite," *Journal of Cell Biology*, vol. 77, no. 1, pp. 72–82, 1978.

[33] D. G. Mordue, N. Desai, M. Dustin, and L. D. Sibley, "Invasion by *Toxoplasma gondii* establishes a moving junction that selectively excludes host cell plasma membrane proteins on the basis of their membrane anchoring," *Journal of Experimental Medicine*, vol. 190, no. 12, pp. 1783–1792, 1999.

[34] S. Lauer, J. VanWye, T. Harrison et al., "Vacuolar uptake of host components, and a role for cholesterol and sphingomyelin in malarial infection," *EMBO Journal*, vol. 19, no. 14, pp. 3556–3564, 2000.

[35] A. J. Charron and L. D. Sibley, "Molecular partitioning during host cell penetration by *Toxoplasma gondii*," *Traffic*, vol. 5, no. 11, pp. 855–867, 2004.

[36] B. U. Samuel, N. Mohandas, T. Harrison et al., "The role of cholesterol and glycosylphosphatidylinositol-anchored proteins of erythrocyte rafts in regulating raft protein content and malarial infection," *Journal of Biological Chemistry*, vol. 276, no. 31, pp. 29319–29329, 2001.

[37] S. C. Murphy, S. Fernandez-Pol, P. H. Chung et al., "Cytoplasmic remodeling of erythrocyte raft lipids during infection by the human malaria parasite *Plasmodium falciparum*," *Blood*, vol. 110, no. 6, pp. 2132–2139, 2007.

[38] G. Gimpl and K. Gehrig-Burger, "Cholesterol reporter molecules," *Bioscience Reports*, vol. 27, no. 6, pp. 335–358, 2007.

[39] K. Kamata, S. Manno, M. Ozaki, and Y. Takakuwa, "Functional evidence for presence of lipid rafts in erythrocyte membranes: Gsα in rafts is essential for signal transduction," *American Journal of Hematology*, vol. 83, no. 5, pp. 371–375, 2008.

[40] I. Koshino and Y. Takakuwa, "Disruption of lipid rafts by lidocaine inhibits erythrocyte invasion by *Plasmodium falciparum*," *Experimental Parasitology*, vol. 123, no. 4, pp. 381–383, 2009.

Hindawi Publishing Corporation
BioMed Research International
Volume 2014, Article ID 424767, 20 pages
http://dx.doi.org/10.1155/2014/424767

Research Article

α-Actinin TvACTN3 of *Trichomonas vaginalis* Is an RNA-Binding Protein That Could Participate in Its Posttranscriptional Iron Regulatory Mechanism

Jaeson Santos Calla-Choque, Elisa Elvira Figueroa-Angulo, Leticia Ávila-González, and Rossana Arroyo

Departamento de Infectómica y Patogénesis Molecular, Centro de Investigación y de Estudios Avanzados del IPN (CINVESTAV-IPN), 07360 México, DF, Mexico

Correspondence should be addressed to Rossana Arroyo; rarroyo@cinvestav.mx

Received 9 September 2013; Accepted 24 November 2013; Published 2 March 2014

Academic Editor: Wanderley De Souza

Trichomonas vaginalis is a sexually transmitted flagellated protist parasite responsible for trichomoniasis. This parasite is dependent on high levels of iron, favoring its growth and multiplication. Iron also differentially regulates some trichomonad virulence properties by unknown mechanisms. However, there is evidence to support the existence of gene regulatory mechanisms at the transcriptional and posttranscriptional levels that are mediated by iron concentration in *T. vaginalis*. Thus, the goal of this study was to identify an RNA-binding protein in *T. vaginalis* that interacts with the tvcp4 RNA stem-loop structure, which may participate in a posttranscriptional iron regulatory mechanism mediated by RNA-protein interactions. We performed RNA electrophoretic mobility shift assay (REMSA) and supershift, UV cross-linking, Northwestern blot, and western blot (WB) assays using cytoplasmic protein extracts from *T. vaginalis* with the tvcp4 RNA hairpin structure as a probe. We identified a 135-kDa protein isolated by the UV cross-linking assays as α-actinin 3 (TvACTN3) by MALDI-TOF-MS that was confirmed by LS-MS/MS and *de novo* sequencing. TvACTN3 is a cytoplasmic protein that specifically binds to hairpin RNA structures from trichomonads and humans when the parasites are grown under iron-depleted conditions. Thus, TvACTN3 could participate in the regulation of gene expression by iron in *T. vaginalis* through a parallel posttranscriptional mechanism similar to that of the IRE/IRP system.

1. Introduction

Cellular iron is an essential cofactor for many biochemical activities, including oxygen transport, cellular respiration, and DNA synthesis. Thus, iron deficiency can cause cell growth arrest and death. However, iron overload is also potentially toxic; under aerobic conditions, it catalyzes the formation of reactive oxygen species and generates highly reactive radicals through the Fenton reaction [1]. The dual role of this element has led to the evolution of an elegant regulatory system that maintains iron homeostasis and contributes to its systemic balance [2–4].

In vertebrates, cellular iron homeostasis is maintained by the coordinated expression of proteins involved in iron uptake, storage, utilization, and export, which are regulated at the posttranscriptional level. This mechanism is based on the interactions of cytoplasmic iron regulatory proteins (IRPs) with conserved RNA stem-loop structures known as iron-responsive elements (IREs), which are located in the untranslated regions (UTRs) of specific mRNAs [4–7], under iron-limited conditions. Depending on the location of the RNA hairpin structures at the 5′- or 3′-UTRs of mRNA, the regulatory outcomes of these interactions are (a) the translation inhibition of 5′-UTR IRE-containing mRNAs and (b) the protection and stability of 3′-UTR IRE-containing mRNAs [3].

The IRE/IRP interaction in the 5′-UTR modulates the expression of mRNAs encoding H- and L-ferritin (IRE-fer),

ALAS2, m-aconitase, ferroportin, HIF-2α, β-APP, and α-synuclein, which control iron storage, erythroid iron utilization, energy homeostasis, iron efflux, hypoxic responses, and neurological pathways. Conversely, the IRE/IRP interaction in the 3′-UTR stabilizes mRNAs encoding TfR1, DMT1, Cdc14A, and MRCKα, which are involved in iron uptake, iron transport, the cell cycle, and cytoskeletal remodeling [7].

There are two cytoplasmic iron regulatory proteins in vertebrates, namely, IRP-1 and IRP-2. IRP-1 (97 kDa) and IRP-2 (105 kDa) share ~57% sequence identity with one another and ~31% sequence identity with mitochondrial aconitase, but only IRP-1 has retained its cytoplasmic aconitase activity [7]. Although IRP-1 and IRP-2 are similar in sequence and structure, their actions are significantly different. IRP-1 contains a [4Fe-4S] cluster, and high iron concentrations prevent IRE-protein interactions [8]. *In vitro* studies have revealed that the iron-sulfur cluster can be disassembled in the presence of oxidizing (NO and H_2O_2) and reducing agents, such as β-mercaptoethanol, resulting in greater IRE affinity at high iron concentrations [9, 10]. At low iron concentrations, the iron-sulfur cluster is labile and disassembled, and the RNA binding site is exposed at the IRP, enabling RNA-protein interactions [10]. By contrast, IRP-2 binding to IRE structure is not regulated by the assembly and disassembly of an iron-sulfur cluster.

Trichomonas vaginalis is a flagellated protist parasite responsible for trichomoniasis, one of the most common nonviral sexually transmitted infections in humans. This protist is dependent on high levels of iron, favoring its growth and multiplication in culture and in the human vagina, where the iron concentration is constantly changing throughout the menstrual cycle. Iron also differentially regulates some trichomonad virulence properties by unknown mechanisms [11, 12]. Knowledge of iron gene expression regulation in *T. vaginalis* is still very limited.

There is evidence to support the existence of gene regulatory mechanisms at the transcriptional and posttranscriptional levels that are mediated by iron concentration in *T. vaginalis*. An iron-responsive promoter and the regulatory proteins that interact with it are involved in the positive transcriptional regulation of ap65-1 gene expression by iron [13], but this system is specific to this particular gene. Moreover, an atypical IRE hairpin structure has been reported in the mRNA of cysteine proteinase 4 (TvCP4) that is upregulated by iron at the posttranscriptional level. This atypical IRE structure specifically interacts with human IRP-1 and also appears to interact with trichomonad cytoplasmic proteins from parasites grown under iron-restricted conditions [11]. However, the specificity and identity of these proteins are unknown because *T. vaginalis* lacks aconitase activity and genes encoding IRP-like proteins. Interestingly, these trichomonad cytoplasmic proteins also specifically interact with human IRE-fer. Taken together, these data suggest the existence of a posttranscriptional iron regulatory mechanism in *T. vaginalis* that is parallel to the typical IRE/IRP system [11, 12].

Therefore, the goal of this work was to identify at least one of the cytoplasmic RNA-binding proteins of *T. vaginalis* that interacts with these IRE structures to provide insight into the posttranscriptional iron regulatory mechanism of this early-evolved protist parasite. Using RNA electrophoretic mobility shift assay (REMSA) and supershift, UV cross-linking, and Northwestern blot (NWB) assays in concert with mass spectrometry (MS) analysis, we identified and characterized the 135-kDa cytoplasmic protein α-actinin (TvACTN3), which has the ability to bind to RNA and could participate in the posttranscriptional iron regulatory mechanism of *T. vaginalis*.

2. Materials and Methods

2.1. Parasite and HeLa Cell Cultures. *T. vaginalis* parasites from a fresh clinical CNCD 147 isolate were cultured in trypticase-yeast extract-maltose (TYM) medium [14] supplemented with 10% (v/v) heat-inactivated horse serum (HIHS) and incubated at 37°C for 24 h. Regular TYM-HIHS medium contains 20 μM iron [14, 15]. Parasites in the logarithmic phase of growth were also cultured in iron-depleted or iron-rich conditions (0 or 250 μM iron, resp.), and the culture medium was supplemented with 150 μM 2,2′-dipyridyl (Sigma-Aldrich, Co., St. Louis, MO, USA) or 250 μM ferrous ammonium sulfate (J. T. Baker, USA) solutions, respectively, 24 h prior to parasite inoculation [11, 15]. HeLa cells were grown in Dulbecco's modified Eagle medium (DMEM) (Invitrogen-Gibco, Carlsbad, CA, USA), supplemented with 10% HIHS at 37°C for 48 h in a 5% CO_2 atmosphere to obtain confluent cell monolayers [16].

2.2. Parasite Cell Fractionation. Parasite cell fractionation was performed by combining previously described methods [17] with a few modifications. In brief, *T. vaginalis* parasites (5×10^8 with a cell density of 1.5×10^6 parasites/mL) cultured under different iron conditions were harvested at 750 ×g for 5 min at 4°C and washed twice with ice-cold PBS, pH 7.0. The parasite pellet was resuspended in 1 mL of extraction buffer (EB) (10 mM HEPES (pH 7.6), 3 mM $MgCl_2$, 40 mM KCl, 5% glycerol, and 0.5% Nonidet P-40; Sigma) containing protease inhibitors (7.5 mM TLCK and 1.6 mM leupeptin; Sigma), vortexed, and incubated for 20 min on ice. The parasite lysate was centrifuged for 10 min at 1,000 ×g. The pellet (P1: nucleus and cell debris) was discarded. The supernatant (SN1) was centrifuged for 10 min at 10,000 ×g, and the new supernatant (SN2: cytoplasmic extracts) was stored at −70°C for up to two weeks until use in REMSA and supershift, UV cross-linking, and NWB assays. The pellet (P2: membrane extracts) was resuspended in 750 μL buffer R (20 mM HEPES (pH 7.6), 2 mM $MgCl_2$, 1 mM EDTA) and stored at −70°C until use.

2.3. Cytoplasmic Extracts from HeLa Cells. HeLa cell cytoplasmic extracts were prepared as previously described [11]. In brief, HeLa cells (40×10^6 with a cell density of 1.5×10^6 cells/mL) were detached with 0.05 M EDTA, for 5 min at 25°C, centrifuged at 2,500 ×g for 5 min at 4°C and washed twice with ice-cold PBS. The cell pellet was resuspended in lysis buffer A (10 mM HEPES (pH 7.9), 15 mM $MgCl_2$, and 10 mM KCl), homogenized in a Dounce homogenizer (10–20 strokes), and centrifuged at 10,000 ×g for 30 min at 4°C.

The supernatants were diluted to a final protein concentration of 10 mg/mL and stored at −70°C until use.

2.4. In Vitro Transcription of RNA Sequences. The DNA used for *in vitro* transcription included the following: the plasmid pSPT-fer (kindly donated by Dr. Lukas Kühn), which contains the human ferritin H-chain IRE (IRE-fer) region was linearized with *Bam*HI [18], and two tvcp4 amplicons, namely, (i) amplicon 31 from −3 to 28 nt (including the IRE-tvcp4 sequence) and (ii) amplicon 97 from 12 to 107 nt (a *deletion mutant* that disrupts IRE-tvcp4) [11]. The amplicons were produced by PCR with the primers sense (31), antisense (31), sense (97), and antisense (97) (Table 1). The PCR sense primers contained a bacteriophage T7 promoter sequence (underline nt) and an additional GG sequence to enhance transcription. The purified PCR products (Qiaquick kit, Qiagen Mexico, S. de R.L. de C.V. Mexico) were used as templates for RNA synthesis using an *in vitro* transcription kit (Ambion, Inc. Austin, TX, USA). The transcription reaction was conducted according to the manufacturer's recommendations. Following transcription, the DNA templates were removed by treatment with DNase I (Ambion), and unincorporated nucleotides were removed by precipitation with 5 μg glycogen, 100 mM ammonium acetate salts, and two volumes of absolute ethanol. To synthesize radiolabeled RNA transcripts, 20 μCi [α^{32}P] UTP (800 Ci/mmol; Dupont Mexico, S.A. de C.V., Mexico) was included in the transcription reaction. The IRE-fer transcript encoding the canonical IRE was used as the positive control where indicated. An unrelated RNA transcript was used as a negative control [19]. To obtain the RNA secondary structure, transcripts were incubated at 70°C for 15 min and cooled down at room temperature for 20 min.

2.5. RNA Electrophoretic Mobility Shift Assay (REMSA) and Supershift Assay. REMSA assays were performed to detect RNA-protein interactions as reported by Leibold and Munro [20] with some modifications. In brief, 200,000 cpm (10–15 ng) of ^{32}P-UTP-labeled RNAs was incubated for 20 min at 4°C with 20 μg cytoplasmic HeLa cell extracts or 50 μg *T. vaginalis* cytoplasmic extracts from parasites grown in iron-rich and iron-depleted conditions in interaction buffer (10 mM HEPES (pH 7.6), 3 mM $MgCl_2$, 40 mM KCl, 5% glycerol in DEPC water) in the presence of 20 U RNasin (Roche), 4 μg tRNA, and 2% β-mercaptoethanol (only for assessing interactions in the HeLa cytoplasmic extract). After incubation, 20 U RNase T1 and 10 μg RNase A were added to the mixture and incubated for 30 min at 25°C. Then, heparin (5 μg) was added and incubated for 10 min at 4°C. The RNA-protein complexes (RPCs) were resolved on 6% nondenaturing polyacrylamide gels and visualized by autoradiography [18]. To assess specificity, competition REMSAs were performed by adding 50 and 100-fold molar excesses of unlabeled RNA, followed by incubation for 30 min at 4°C. For the supershift assays, 1-2 μL (1 μg/μL) commercial polyclonal antibody against recombinant α-actinin from chicken (α-chACTN, PA1-28036, Thermo Scientific), a monoclonal antibody against recombinant α-actinin from bovine ([BM 75.2], Abcam), 5–15 μL rabbit α-TvACTN3r serum, or 10 μL control rabbit against *T. vaginalis* triosephosphate isomerase 2r (α-TvTIM2r) serum [21] (as an unrelated antibody) was added, along with the cytoplasmic extracts from trichomonads grown in iron-depleted conditions, before adding the RNA probes. These experiments were independently performed at least three times, with similar results.

2.6. UV Cross-Linking Assay. Trichomonad cytoplasmic extracts and the recombinant proteins TvACTN3r, the TvACTN3 domains (DIr, DIIr, and DIIIr), hIRP-1r (used as a positive control), and BSA (1 μg) (used as a negative control) were incubated with 200,000 cpm (10–15 ng) ^{32}P-labeled RNA probes for 30 min at 4°C in 25 μL reaction buffer (10 mM HEPES-KOH [pH 7.4], 3 mM $MgCl_2$, 5% (v/v) glycerol, 100 mM KCl, 20 U RNasin, and 5 μg yeast tRNA; Invitrogen). After RNA-binding, the reaction mixture was placed on ice and irradiated with a UV-lamp (UVP; 800,000 μJ/cm^2) for 15 min. Unprotected RNA was digested for 30 min at 25°C with RNase A (10 μg) and RNase T1 (20 U). RPCs were resolved on 10% SDS-PAGE gels. The gels were stained with Coomassie Brilliant Blue (CBB) and dried, and radioactive bands were visualized by autoradiography in a FLA 5000 phosphoimager (Fujifilm, Co, Tokyo Japan) with a Software MultiGauge V3.0 [22]. These experiments were independently performed at least three times, with similar results.

2.7. Identification of RNA-Binding Proteins in T. vaginalis. The high molecular weight protein bands detected by UV cross-linking assays of the cytoplasmic proteins from trichomonads grown under iron-depleted conditions and the IRE-tvcp4 RNA probe were excised from duplicate CBB-stained gels and submitted to protein identification by MS at the Protein Unit of Columbia University (New York, USA). The protein bands were reduced and alkylated, digested with trypsin, and analyzed by matrix-assisted laser desorption ionization time-of flight mass spectrometry (MALDI-TOF-MS), MS/MS and *de novo* sequencing as previously reported [23, 24]. The specific peptides identified (Table 2) corresponded to the TvACTN3 protein. The score and protein coverage were calculated by the MS-Fit MOWSE and Mascot search algorithms.

2.8. Cloning and Expression of Recombinant TvACTN3r, DIr, DIIr, and DIIIr Proteins. The complete tvactn3 gene (TVAG_239310; 3390 bp) was amplified by PCR using genomic DNA from the *T. vaginalis* CNCD 147 isolate as a template with a sense primer containing a *Bam*HI restriction site (tvactn3-*Bam*HI) and an antisense primer containing a *Not*I restriction site (tvactn3-*Not*I); these primers included the ATG and TAA initiation and stop codons, respectively (Table 1). The corresponding DNA fragments of Domain I (873 bp, 1–291 aa), Domain II (1713 bp, 230–800 aa), and Domain III (1407 bp, 662–1129 aa) were also amplified by PCR using plasmid DNA (containing the complete tvactn3 gene) with specific primers for each fragment (Table 1). The amplicons were cloned into the pCR4-TOPO vector (Invitrogen). The inserts were released by double digestion and subcloned into the pProEX-HTb expression vector according

Table 1: Primers used for PCR, RT-PCR, and qRT-PCR assays to amplify the distinct tvactn gene fragments found in the draft of the *T. vaginalis* genome sequence, mRNA of each tvactn gene and genes used as controls, complete tvactn3 gene and its three domains for expression, and the different amplicons of the IRE sequences used as RNA probes.

Gene	Location[a] (bp)	Primers (5′-3′)	
		Forward	Reverse
Tvactn1[b]	1512–1648	CCGCTTGCCTTACAGCACTCGG	CCCTTGTTGAAGTGGTCGAGCAT
Tvactn2[b]	1551–1676	TACACAGTTCCTCGCCAAGCAG	CCTCTGTTGGGCTGTGGTTGACA
Tvactn3[b]	1540–1698	CAGCGCGCTGCCAACGTTGAC	CCAAGGCAAGCTGTGTACATGGCTG
Tvactn4[b]	1561–1667	CCTTAAAGCAACAGTTAGCAGCAGC	CCTGTTCGTTTGCTCTTGCAATTAC
Tvactn5[b]	1561–1673	CCCCAGGCGAAGAACCAGAAATT	CCGTTTGAGTCCATTGCGACTAACT
β-Tubulin[b]	611–722	CATTGATAACGAAGCTCTTTACGAT	GCATGTTGTGCCGGACATAACCAT [25]
Tvactn3[c]	1–3390	GGCGGGATCCATGTCTAATAATCGTGGACTTCTAGAC	GGCGGCGGCCGCTTAGGCATAGATAGAATTGAC
Tvactn3 DI[d]	1–873	GGCGGGATCCATGTCTAATAATCGTGGACTTCTAGAC	GGCGAAGCTTTCCTGGAACTGTCTGGTCGTAC
Tvactn3 DII[e]	688–2400	GGCGGGATCCCACTTCTTCGCTGGCGAGTCA	GGCGGCGGCCGCGACCTTCTCGGCGATGGCAAGAACC
Tvactn3 DIII[f]	1984–3390	GGCGGGATCCGACATCACATTCGCCTTCTTGACAC	GGCGGCGGCCGCTTAGGCATAGATAGAATTGAC
Tvpfo a[g]	2281–3458	GAAGAGGGCAAGAACTGGGATC	ATCTTCTTGTAGCCCTCGTAA [23]
Tvcp12[h]	8–276	GATTTCAAACTTGCTTCCGGCATT	CTTGACTGTTTGGCCCTTGGAAA [25]
IRE-tvcp4[i]	−3–28	TAATACGACTCACTATAGGGCACATGTTCGTTCAGGCACCAT	CTTTCTGCTCATGTGCCTGAACGAACATGTG [11]
disrupted IRE-tvcp4[j]	12–107	TAATACGACTCACTATAGGGGGCACATGAGCAGAAAGC	GGAGAGCCAAATGCCAAG [11]

[a]Location of the region amplified by PCR, RT-PCR, and qRT-PCR of each tvactn gene. [b]Primers used for RT-PCR and qRT-PCR assays to check Tvactn gene expression under distinct iron concentrations. [c]Restriction sites (underlined) for *Bam*HI and *Not*I enzymes used to subclone the complete tvactn3 gene from the *T. vaginalis* CNCD 147 isolate. [d]Restriction sites (underlined) for *Bam*HI and *Hind*III enzymes used to subclone the Actin-binding domain (DI) of tvactn3 in a bacterial expression system. [e]Restriction sites (underlined) for *Bam*HI and *Not*I enzymes used to subclone the Spectrin Repeats Domain (DII) of tvactn3 in a bacterial expression system. [f]Restriction sites (underlined) for *Bam*HI and *Not*I enzymes used to subclone the EF-hand Domain (DIII) of Tvactn3 in a bacterial expression system. [g]Primers used for RT-PCR assays to check pfo a gene expression under distinct iron concentrations used as an expression control. [h]Primers used for RT-PCR assays to check tvcp12 gene expression under distinct iron concentrations used as an expression control. [i]Primers used for PCR of IRE-tvcp4 sequences. [j]Primers used for PCR of a *deletion mutant* that disrupts the IRE-tvcp4.

to the manufacturer's instructions (Invitrogen). The DNA sequence of tvactn3 was deposited in GenBank with accession number KF280188. His-tagged recombinant TvACTN3r, DIr, DIIr, and DIIIr were expressed in *E. coli* BL-21 (DE3) by induction with 1 mM IPTG for 16 h at 16°C. The recombinant proteins were purified from the soluble fraction by affinity chromatography using Ni-NTA-Sepharose as recommended by the manufacturer (GE Healthcare Bio-Sciences Corp, Piscataway NJ, USA). Purified recombinant proteins were dialyzed three times against PBS at 4°C and quantified by the Bradford method (Bio-Rad).

2.9. Generation of Anti-TvACTN3r, DIr, DIIr, and DIIIr Antibodies. Female New Zealand white rabbits weighing 3.0 kg were intramuscularly immunized twice with 300 μg affinity-purified TvACTN3r, DIr, DIIr, or DIIIr proteins in a 1 : 1 ratio with TiterMax Gold (Sigma) adjuvant, as recommended by the manufacturer. The animals were bled weekly, and their sera were tested by WB assays against each recombinant protein and cytoplasmic extracts from *T. vaginalis* cultured in regular medium. Before rabbit immunization, the preimmune (PI) serum was obtained from each rabbit and used as a negative control for all experiments with antibodies.

2.10. Antibodies. To detect the presence of cross-reacting IRP-1-like proteins in *T. vaginalis*, we used an affinity-purified rabbit polyclonal antibody against rat IRP-1 (rIRP-1, AB15506, Millipore). We also used a rabbit polyclonal antibody against α-chACTN. In addition, rabbit polyclonal antisera were produced against purified recombinant TvACTN3r and its domains (α-TvACTN3r, α-DIr, α-DIIr, and α-DIIIr). To produce control sera for the western blot (WB) assays of different cellular fractions, we used a mouse polyclonal antibody against a trichomonad PFO A protein for the membrane fraction [23] and a rabbit polyclonal antiserum against a trichomonad cytoplasmic HSP70 protein (produced by Torres-Romero et al., manuscript in preparation) for the cytoplasmic fraction. To produce a negative control serum for the supershift assays, we used a rabbit polyclonal antibody against the recombinant TvTIM2r protein [21].

2.11. Western Blotting. After electrophoresis, recombinant TvACTN3r, DIr, DIIr, or DIIIr, or cytoplasmic extracts of *T. vaginalis* grown in 0, 20, or 250 μM iron were transferred onto nitrocellulose (NC) membranes and blocked using 10% fat-free milk in PBS-0.05% Tween 20 (PBS-T) buffer for 18 h at 4°C. The NC membranes were washed five times with PBS-T at 25°C and incubated for 18 h at 4°C with each antibody. The antibodies were diluted in PBS-T as follows: α-TvACTN3r (1 : 150,000), α-DIr (1 : 1,000), α-DIIr (1 : 1,000), and α-DIIIr (1 : 1,000). The NC membranes were washed five times with PBS-T at 25°C, incubated with secondary antibodies (α-rabbit or α-mouse immunoglobulin Gs [IgGs] coupled to peroxidase) (Bio-Rad) at a 1 : 3,000 dilution in 10% fat-free milk in PBS-T for 2 h at 25°C, washed five times with PBS-T, and developed with 4-chloro-1-naphthol (Bio-Rad) or by chemiluminescence using a SuperSignal West Pico Kit (Pierce). The corresponding PI rabbit or mouse serum was used as a negative control. These experiments were independently performed at least three times and yielded similar results.

2.12. Northwestern Blotting (NWB). The Northwestern blot assay was performed by combining previously described methods [17, 24] with a few modifications. In brief, recombinant proteins were resolved by 10% SDS-PAGE, transferred onto NC membranes, blocked with 10% fat-free milk and 20 μg/mL yeast tRNA (Sigma) in EB (EBY) for 18 h at 4°C, and washed three times with EBY at 25°C. The NC membranes were incubated for 18 h at 4°C with EBY containing 10–15 ng/mL radiolabeled RNA; washed twice with EB; washed another two times with B buffer (10 mM Tris-HCl [pH 7.5] and 50 mM NaCl); and blocked again for 1 h at 37°C with STMT buffer (1 M NaCl, 0.1 M Tris-HCl [pH 7.5], 2 mM $MgCl_2$, and 0.05% Triton X-100) containing 3% BSA. After extensive washing with EB, the NC membranes were air-dried and exposed for autoradiography. These experiments were performed independently at least three times, with similar results.

2.13. In Silico Analysis of TvACTN3. Multiple alignments were performed with the ClustalW program. The nucleotide sequences of all tvactn genes were obtained from the *T. vaginalis* genome project database (http://www.trichdb.org/). To identify functional RNA-binding domains, we analyzed the deduced protein sequence of TvACTN3 using the SMART (http://smart.embl-heidelberg.de/) [26, 27], Motif Scan (http://hits.isb-sib.ch/cgi-bin/PFSCAN), and PROSITE programs (http://prosite.expasy.org/prosite.html) [28].

2.14. RNA Isolation, Semiquantitative RT-PCR, and Real-Time qRT-PCR Analyses. The total RNA from parasites (10^7) grown in 0, 20, or 250 μM iron was extracted using TRIzol reagent (Sigma). For semiquantitative RT-PCR, the total RNA (1 μg) was reverse-transcribed using the SuperScript II reverse transcriptase kit (Invitrogen) and an oligo (dT18) primer. A 0.5 μg quantity of cDNA was then used as a PCR template [25]. Gene-specific primers [29] were used for PCR amplification of the *T. vaginalis* α-actinin (tvactn1, tvactn2, tvactn3, tvactn4, and tvactn5) transcripts (Table 1). To produce an internal control, a 112-bp fragment of the β-tubulin gene was amplified by PCR with specific primers [25]. As additional controls, the tvpfo a (iron-upregulated gene) [23] and tvcp12 (iron-downregulated gene) transcripts were also amplified using specific primers [11] (Table 1).

Quantitative RT-PCR was performed for each tvactn gene using an ABIPRISM 7300 Sequence Detector (Applied Biosystems). In brief, the RT-PCR amplification mixtures (25 μL) contained 1 μg cDNA from each condition; 10 pmol specific primers for tvactn1, tvactn2, tvactn3, tvactn4, or tvactn5 (Table 1); and 2× SYBR Green 1 PCR Master Mix (12.5 μL) buffer (Applied Biosystems). The cycling conditions for all tvactn genes and transcripts included 10 min of polymerase activation at 95°C, followed by 25 cycles of 95°C for 20 s, 55°C for 30 s, and 72°C for 30 s. Each assay (in triplicate) included a standard curve of eight 1/10 serial dilutions of

tvactn3 or β-*tub* cDNA (1 μg of each tested cDNA) and a no-template control. All PCR efficiencies were greater than 95%. The results obtained by the Sequence Detection Software (version 1.3; Applied Biosystems) were exported as tab-delimited text and imported into Microsoft Excel for further analysis. To confirm the amplification specificity, PCR products were subjected to standard curve analysis. The levels of tvactn1, tvactn2, tvactn3, tvactn4, or tvactn5 mRNA were quantified by qRT-PCR analysis relative to β-tubulin mRNA as an internal control.

2.15. Statistical Analysis. All data were expressed as the means ± S.D. from three samples, and qRT-PCR experiments were repeated three times. The significance of the difference between means was determined by one-way ANOVA using Sigma-Plot11. The level of significance was also determined by the Bonferroni method comparing all groups versus control ($P < 0.001$) for Figure 4(b). The scores showing statistical significance are indicated in the figures with asterisks.

2.16. Ethical Statement. This study was performed with strict accordance with the recommendations of the Guide for the Use of Laboratory Animals of the Center of Research and Advanced Studies of the National Polytechnic Institute (CINVESTAV-IPN). The protocols and experiments were approved by the Institutional Animal Care "CICUAL" at the CINVESTAV-IPN. Animals were kept in environmentally controlled animal facilities at CINVESTAV-IPN. The final bleeding was performed under sodium pentobarbital anesthesia and efforts were always made to minimize suffering.

3. Results

3.1. Cytoplasmic Proteins from T. vaginalis Grown in Iron-Depleted Concentrations Specifically Interact with IRE-tvcp4 and IRE-fer. We previously demonstrated the specific interaction between an atypical IRE stem-loop structure in the 5′ region of tvcp4 mRNA with human recombinant IRP and HeLa cell cytoplasmic proteins, which suggested the presence of RNA-binding proteins in trichomonad cytoplasmic extracts [11]. To determine if *T. vaginalis* has RNA-binding proteins that specifically interact with IRE structures and may participate in a posttranscriptional regulatory mechanism parallel to the IRE-IRP system described in other organisms, we performed REMSA with cytoplasmic extracts from *T. vaginalis* grown in iron-rich (Tv-H) and iron-depleted (Tv-L) media and radiolabeled RNA probes of trichomonad IRE-tvcp4, and the human IRE-fer that was used as a positive control. Figure 1(a) shows the formation of one RNA-protein complex (RPC) with *T. vaginalis* cytoplasmic extracts under iron-depleted conditions using both probes (lanes 3 and 6); the complexes were sensitive to reducing agents (data not shown). These results suggest that there are RNA-binding proteins in the trichomonad extracts that interact with hairpin RNA structures in iron-depleted conditions and in the absence of reducing agents.

RNA competition assays were also performed to determine the specificity of the RPC formed between the trichomonad cytoplasmic proteins and both tested IREs. The addition of a molar excess of unlabeled homologous or heterologous IRE probe (IRE-fer and IRE-tvcp4) relative to labeled IRE significantly decreased the amount of RPC (Figure 1(b), lanes 3–6 and 11–14, resp.) in a concentration-dependent manner. An excess of unlabeled unrelated transcripts was used as competitor RNA [19], which did not affect RPC formation, as expected (Figure 1(b), lanes 7, 8 and 15, 16, resp.). These data demonstrate that the RNA-protein complexes detected with trichomonad cytoplasmic proteins are specific and imply the existence of RNA-binding proteins in *T. vaginalis*, in spite of the lack of aconitase/IRP proteins in trichomonads.

3.2. IRE-tvcp4 and IRE-fer mRNA Probes Specifically Interact with at Least Four Protein Bands from T. vaginalis Extracts. To determine the size of the proteins in the RPC, UV cross-linking assays were performed using cytoplasmic extracts from *T. vaginalis* grown in iron-depleted conditions and radiolabeled IRE-tvcp4 and IRE-fer mRNA probes. Figure 2(a) shows that both RNA probes interacted with at least four proteins of 135, 110, 70, and 45 kDa (lanes 2 and 7). The 45-kDa protein band was more intense in the presence of IRE-tvcp4 than in the presence of IRE-fer. The presence of reactive bands required the simultaneous occurrence of RNA and protein molecules during UV irradiation. Few or no reactive bands were observed when the cross-linking reaction was treated with proteinase K (lanes 3 and 8) or RNases (lanes 4 and 9) or when unlabeled IREs were used (lanes 5 and 10), indicating that the radioactive bands were formed when cytoplasmic trichomonad proteins and labeled-RNA were present in the reaction and specifically interacted with one another.

3.3. The 135-kDa Protein Band That Binds to IRE-tvcp4 and IRE-fer Is a T. vaginalis α-Actinin (TvACTN3). To identify the 135-kDa protein detected in the UV cross-linking assays (Figure 2(a)), the corresponding protein band was excised from the duplicate CBB-stained gel and prepared for MS analysis by tryptic mapping of the 135-kDa protein band by MALDI-TOF-MS, MS/MS and *de novo* sequencing. The masses of 35 peptides obtained from the 135-kDa protein band corresponded to peptide masses from the TVAG_239310 cytoplasmic TvACTN3 of *T. vaginalis* [29]. Only 1/35 peptides (peptide 33) was common to TvACTN1 and 2/35 peptides (peptides 4 and 34) were common to TvACTN2 (Table 2). None of the identified peptides were found in TvACTN4 and TvACTN5. The protein sequence coverage was 43% with a MS-Fit MOWSE score: $2.64e + 11$; Mascot score: 212, and expected value $5.8e - 15$. To confirm this identification, the 135-kDa protein band was processed by ESI-LC-MS/MS. A single peptide: FMIEEISVEEATAR (peptide 4) was identified. This peptide was common to α-actinin TvACTN2 and TvACTN3 of *T. vaginalis*. Since only one peptide was obtained, a new analysis by *de novo* sequencing was performed and four peptide sequences: EEYNQAAQK,

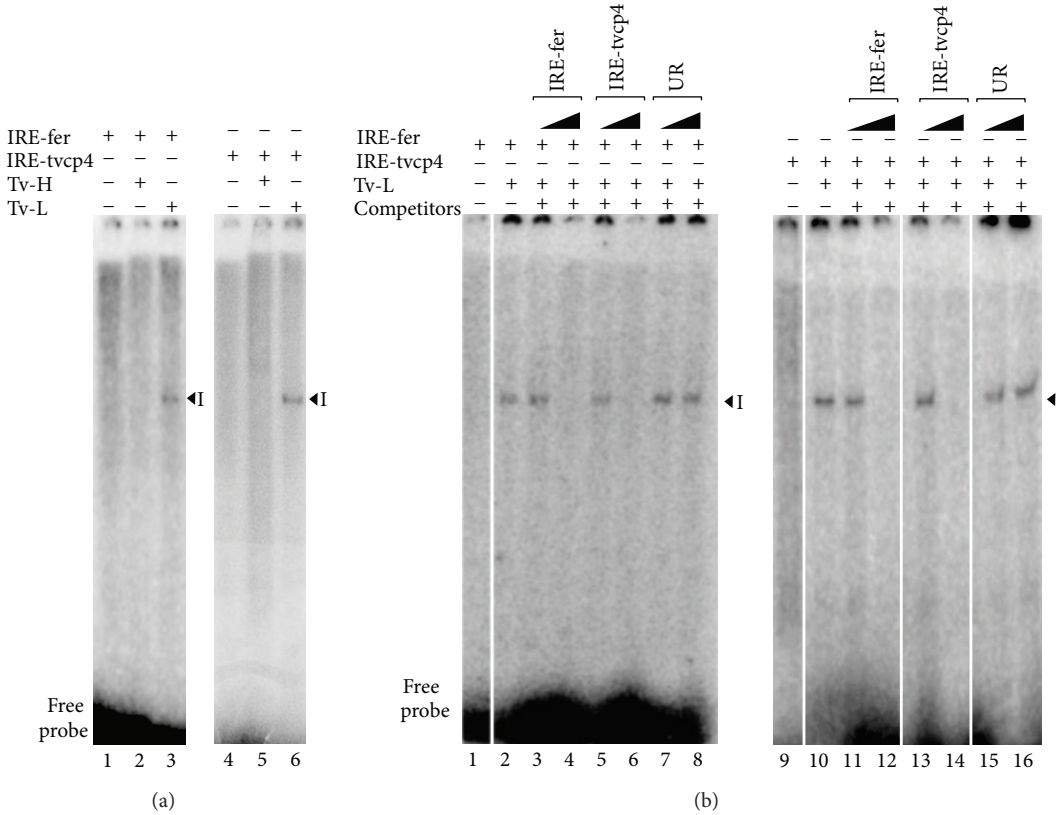

Figure 1: Presence of RNA-binding proteins in iron-depleted *T. vaginalis*. (a) RNA gel-shift assays (REMSA) to detect RNA-protein complex (RPC) formation using IRE-fer (lanes 1–3) and IRE-tvcp4 (lanes 4–6) RNA probes and *T. vaginalis* cytoplasmic extracts from parasites grown in iron-rich (H) (lanes 2 and 3) or iron-depleted (L) (lanes 5 and 6) medium. Experiments with IRE-fer are controls. RNA free probes used as negative controls (lanes 1 and 4). (b) REMSA competition assays performed with the IRE-fer and IRE-tvcp4 RNA probes and *T. vaginalis* cytoplasmic extracts in the absence of competitors (lanes 2 and 10) or in the presence of a 50- or 100-fold molar excess of unlabeled IRE-fer RNA (lanes 3 and 4), IRE-tvcp4 (lanes 13 and 14), or unrelated transcript (lanes 7, 8 and 15, 16). A cross-competition assay in the presence of a 50- or 100-fold molar excess of unlabeled IRE-tvcp4 RNA (lanes 5 and 6) and IRE-fer RNA (lanes 11 and 12). Experiments were performed three times and yielded similar results.

TAIAAEK, QECLDVINTER, and IQPTLEEPYQ that corresponded to TvACTN3 of *T. vaginalis* were obtained. Two of them were part of the sequence of peptides 18 and 23 identified by MALDI TOF (Table 2).

To confirm this identification, we performed a WB assay using a commercial polyclonal antibody against recombinant chicken α-actinin (α-chACTN) with cytoplasmic extracts from iron-depleted *T. vaginalis*. This antibody recognized protein bands of 135, 110, 65, and 40 kDa (Figure 2(b), lane 3). Similar molecular weight protein bands (135, 110, 60, and 50 kDa) were also detected with a commercial polyclonal α-rIRP-1 antibody (Figure 2(b), lane 4). Interestingly, these two antibodies showed cross-reactivity to the 135- and 110-kDa protein bands of *T. vaginalis*.

3.4. Actinin Proteins from T. vaginalis Are Present in the RNA-Protein Complex Formed between Cytoplasmic Extracts and RNA Probes from Humans and Trichomonads. To corroborate the presence of actinin in the RPC formed between trichomonad cytoplasmic proteins and RNA probes (IRE-tvcp4 and IRE-fer), a supershift assay was performed by adding the α-chACTN polyclonal antibody and the α-bACTN monoclonal antibody to the REMSA reaction. Figure 2(c) shows that both heterologous anti-ACTN polyclonal and monoclonal antibodies reduced RPC formation between the cytoplasmic extracts of iron-depleted *T. vaginalis* and both IRE probes (lanes 3–6 and 9–12, resp.) at two antibody concentrations; an unrelated antibody was used as a negative control (lane 13). These results confirm the presence of trichomonad α-actinins in the RPC.

3.5. Only Three of the Five α-Actinin Encoding Genes Are Expressed in T. vaginalis under Different Iron Concentrations. Five annotated sequences in the *T. vaginalis* genome encode α-actinin genes: TVAG_156680, TVAG_190450, TVAG_239310, TVAG_247460, and TVAG_260390; we named these genes tvactn1, tvactn2, tvactn3, tvactn4, and tvactn5, respectively. We performed a multiple alignment analysis of the deduced amino acid sequences [29] (see Supplementary Figure S1 in Supplementary Material available online at http://dx.doi.org/10.1155/2014/424767). The five α-actinin proteins have different sizes (609, 931,

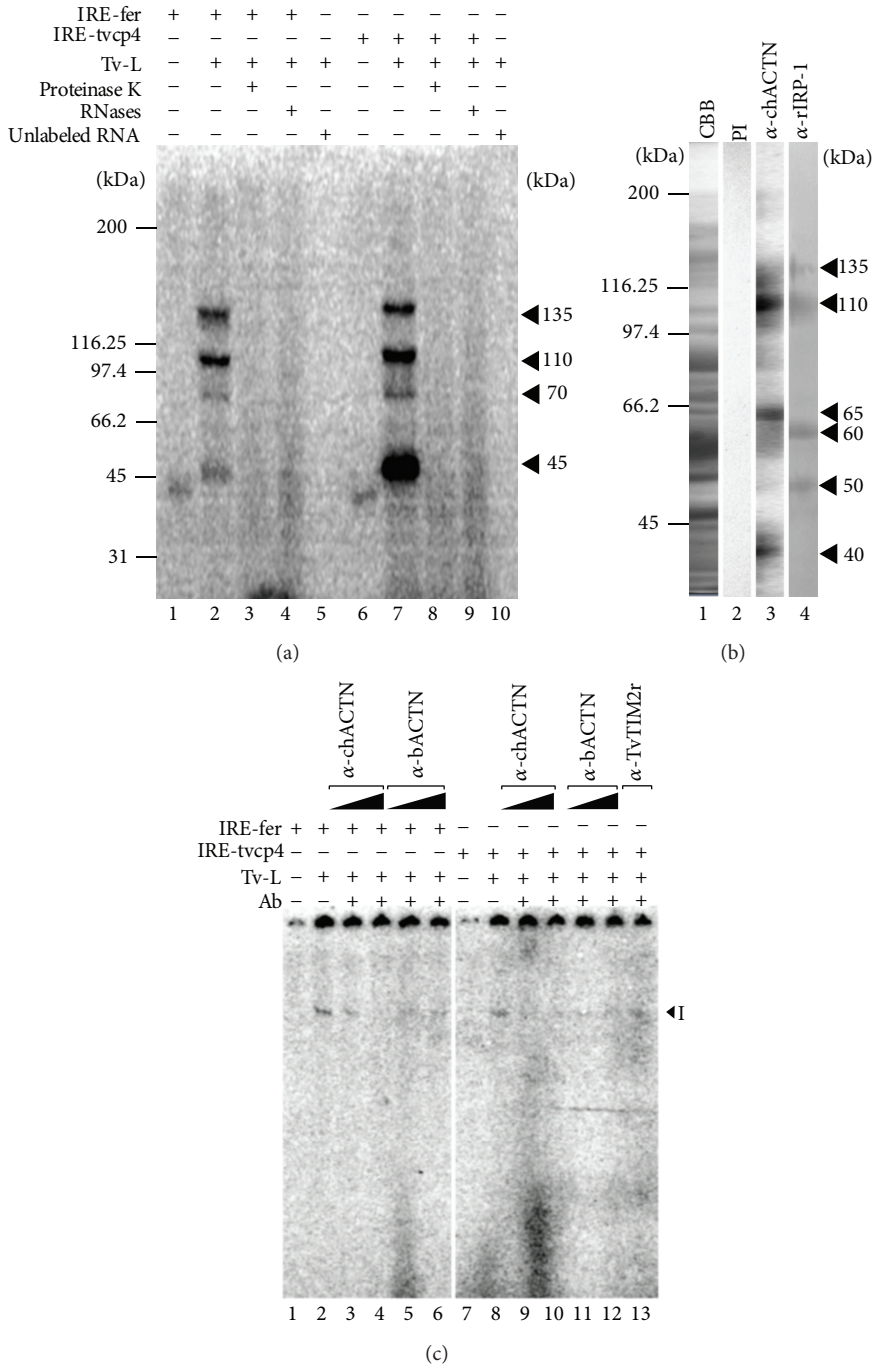

Figure 2: Identification of *T. vaginalis* TvACTN3 by 1-D gel electrophoresis and mass spectrometry. (a) UV Cross-linking assay of ^{32}P-labeled IRE-fer and IRE-tvcp4 transcripts and *T. vaginalis* cytoplasmic extracts grown under iron-depleted conditions (Tv-L) (lanes 2 and 7, resp.). The specificity of the interaction was demonstrated by treatment with proteinase K (10 μg, Promega) (lanes 3 and 8) and RNases (lanes 4 and 9) and a complete binding reaction using unlabeled IRE-fer and IRE-tvcp4 (lanes 5 and 10) or only the labeled probes (lanes 1 and 6). Molecular mass markers are indicated in kilodaltons (kDa). Arrowheads indicate the positions of the RNA-protein complex bands of 135, 110, 70, and 45 kDa. A representative result of three independent experiments with similar results is shown. (b) Cytoplasmic extracts of *T. vaginalis* grown in iron-depleted medium were Coomassie blue-stained (lane 1) or transferred onto NC membranes for Western blot (WB) assays (lanes 2, 3, and 4); and incubated with preimmune (PI) serum (negative control, lane 2), anti-chicken α-actinin (α-chACTN, lane 3), or anti-rat-IRP-1 (α-IRP1, lane 4) antibodies. (c) Representative supershift assays. Radiolabeled IRE-fer and IRE-tvcp4 RNA probes (lanes 1 and 7, resp.) were incubated with cytoplasmic proteins from *T. vaginalis* grown under iron-depleted conditions without (lanes 2 and 8) or with the α-chACTN polyclonal antibody (1 μg) (lanes 3 and 9), (2 μg) (lanes 4 and 10), or with the anti-bACTN monoclonal antibody (1 μg) (lanes 5 and 11), (2 μg) (lanes 6 and 12), or with a nonrelated antibody (α-TvTIM2r; lane 13). The arrowhead indicates RNA-protein complex. A representative result of three independent experiments yielding similar results is shown.

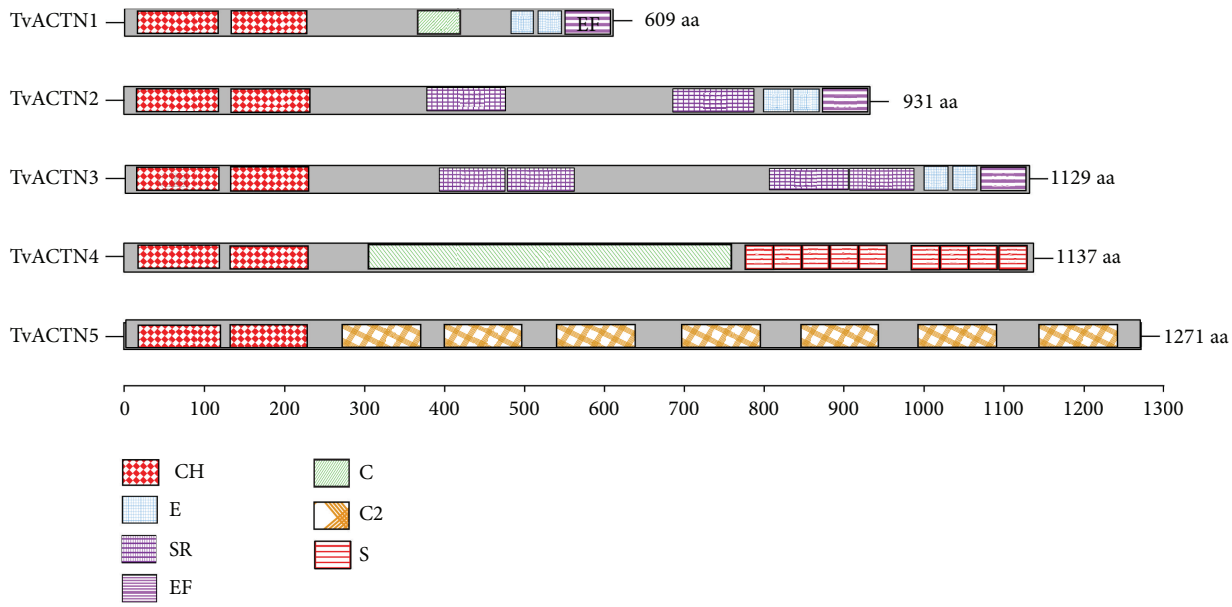

Figure 3: Putative functional domains present in TvACTNs of *T. vaginalis*. Principal motifs of the deduced amino acid sequences of the five tvactn genes reported in the *T. vaginalis* genome sequence [29]. TvACTN1 (609 aa), TvACTN2 (931 aa), TvACTN3 (1129 aa), TvACTN4 (1137 aa), and TvACTN5 (1271 aa). By SMART, MOTIF SCAN, and PROSITE programs, we found the principal motif sequences present in the five TvACTNs proteins, two calponin domains (CH) at the N-terminus followed by variable spectrin repeats (SR) in the central rod domain, and two EF-hands: EF-hand (E) and calcium-insensible EF-hand (EF) at the C-terminus. TvACTN4 and TvACTN5 present more divergent central region and C-terminus. TvACTN4 has one coiled coil (C) and nine SEL domains (S), and TvACTN5 presents seven C2 domains (C2).

1129, 1137, and 1271 amino acid [aa] residues, resp.) and different identities compared with TvACTN3 (55.19, 53.25, 22.1, and 15.56% with TvACTN1, TvACTN2, TvACTN4, and TvACTN5, resp.). All of the proteins have two calponin domains (CH) at the N-terminus that confer the ability to bind actin, followed by spectrin repeats (SR) in the central rod domain and two EF-hands (EF-H) at the C-terminus. The number of spectrin repeats is variable in TvACTN2 and TvACTN3, and the central domain of TvACTN1, TvACTN4, and TvACTN5 has different specific domains compared to the other α-actinins (Figure 3).

We then analyzed which of the *T. vaginalis* actn genes are expressed under different iron concentrations. Semiquantitative RT-PCR and qRT-PCR assays using specific primers for each tvactn gene (Table 1) were performed using RNA isolated from trichomonads grown in 0, 20, or 250 μM iron. Figure 4(a) shows that the *T. vaginalis* tvactn1, tvactn2, and tvactn3 genes were better expressed in the presence of iron (lanes 2 and 3) than under iron-depleted conditions (lane 1). Neither tvactn4 nor tvactn5 was expressed under these experimental conditions (lanes 1–3). The expected control tvactn1–5 gene fragments were amplified from genomic DNA. The level of the β-tubulin transcript in the same RNA samples at each iron concentration was used to normalize the transcript quantities. Two genes differentially regulated by iron were also used as controls (tvpfo a for positiveand tvcp12 for negative iron regulation, resp.), and an RT-PCR without reverse transcriptase was used to exclude genomic contamination (Figure 4(a)). The qRT-PCR analysis confirmed these results and demonstrated that the expression of the tvactn3 gene is greatly reduced in the absence of iron in comparison to tvactn2 and tvactn1 expression, and tvactn4 and tvactn5 were not amplified under any of the tested iron concentrations and used experimental conditions. The differences observed among the tvactn1, tvactn2, and tvactn3 amplicons were significant ($P < 0.0001$), with the exception of tvactn1 ($P < 0.005$), and were dependent on the iron concentration (Figure 4(b)).

3.6. Cloning and Expression of TvACTN3 and Its Three Domains. To demonstrate that the 135-kDa actinin (TvACTN3) is one of the RNA-binding proteins that interacts with the human IRE-fer and the atypical IRE-tvcp4 of *T. vaginalis*, we first performed an *in silico* analysis of the reported tvactn3 gene sequence in the *T. vaginalis* genome (TrichDB Accession no. TVAG_239310). This gene contains a 3390-bp open reading frame (ORF) encoding a complete TvACTN3 protein of 1129 aa residues with a theoretical size ~124.2-kDa and *pI* of 4.9. It has a short 5′-UTR with two putative Inr sequences 3-bp and 10-bp upstream of the ATG initiation codon. The 3′-UTR is 11 bp long and has the typical regulatory regions for polyadenylation [30, 31]. The TvACTN3 protein contains three domains: Domain I (DI), which includes two calponin or actin-binding domains (CH) at the N-terminus; Domain II (DII), which is followed by four spectrin repeats (SR) in the central rod domain; and Domain III (DIII), which includes three EF-hands (EF-H) at the C-terminus (Figure 5(a)).

We cloned, expressed, and purified the complete tvactn3 gene sequence and its three domains to obtain recombinant

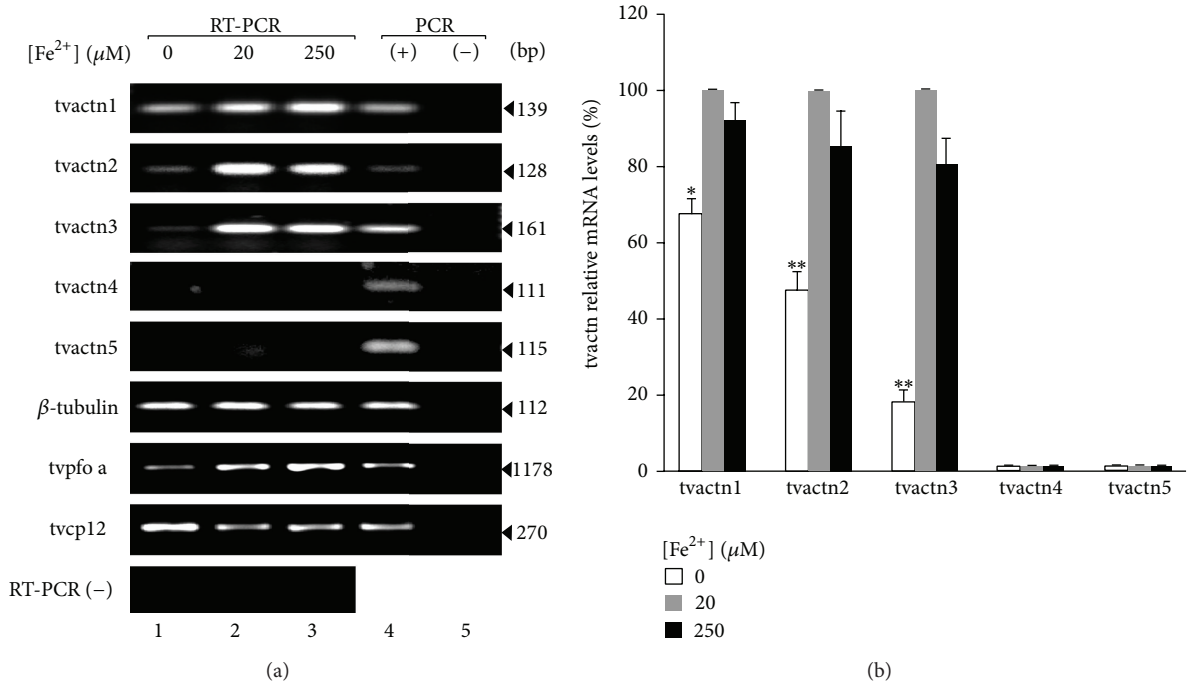

Figure 4: Effects of iron on the transcription of *T. vaginalis* actinin genes. (a) RT-PCR with specific primers for each *T. vaginalis* actinin gene (tvactn1, tvactn2, tvactn3, tvactn4, and tvactn5; Table 1) using cDNA from parasites grown under iron-depleted (0 μM; lane 1), normal (20 μM; lane 2), and iron-rich (250 μM; lane 3) conditions (tvactn1 to tvactn5). RT-PCR with specific primers for the β-tubulin gene using the same cDNA as an internal control. tvpfo a and tvcp12 genes were used as control genes that are overexpressed under iron-rich or iron-depleted conditions, respectively. A reverse transcriptase minus [RT-PCR (−)] reaction was used to verify the lack of gDNA contamination in the cDNA samples using the same pairs of primers for each gene; gDNA was used as a positive control (+), except in RT-PCR (−), in which no DNA was added. PCRs without gDNA were used as negative controls (−). The sizes of the amplicons are given in bp. (b) qRT-PCR was used to quantify the different levels of the five tvactn mRNAs in trichomonads grown under different iron conditions. Bars represent the standard error of triplicated samples. Asterisks (*) $P < 0.005$ or (**) $P < 0.0001$ compared iron-depleted with iron-rich or normal conditions.

proteins for functional assays and to identify the putative RNA-binding domain. The amplicons were obtained by PCR using *T. vaginalis* genomic DNA or plasmid DNA-TvACTN3 and specific primers for each gene fragment (Table 1). These segments were cloned, sequenced, and expressed in a bacterial system after the induction with IPTG (Figures 5 and 6).

The complete TvACTN3 protein was expressed as a recombinant ~135-kDa protein (TvACTN3r) and purified by Ni-affinity chromatography. Polyclonal antibodies against the purified protein were produced in rabbits (α-TvACTN3r) (Figure 5(b)). This antibody reacted with a 135-kDa protein band in the total protein extract of parasites grown in iron-depleted conditions; PI serum was used as a negative control (Figure 5(c)). Following cell fractionation of parasites grown in different iron concentrations, this protein was detected in the total extracts and cytoplasmic fractions as expected. The amount of protein was not affected by the iron concentration (Figure 5(d)) compared to the control proteins (PFO A for the membrane and HSP70 for cytoplasmic fractions).

We also obtained recombinant proteins and polyclonal antibodies corresponding to each TvACTN3r domain as follows: Actin Binding Domain (DI), Spectrin Repeats Domain (DII), and the EF-hand Domain (DIII), which had molecular weights of 35, 64, and 53 kDa, respectively (Figure 6). Each of the antibodies recognized the complete TvACTN3r protein as well as the native TvACTN3 protein in total protein extracts, as expected. In addition, the antibodies against each domain only recognized the corresponding recombinant protein, while the anti-TvACTN3r antibody recognized all three domains as expected (Figure 7).

3.7. The Polyclonal TvACTN3r Antibody Supershifted RNA-Protein Complex I. To test our hypothesis about the participation of TvACTN3 in RNA-protein interactions, we performed a supershift assay using the α-TvACTN3r antibody in an REMSA reaction between trichomonad iron-depleted cytoplasmic extracts and the IRE-tvcp4 RNA probe. Figure 8(a) shows that the RPC I (lane 2) was supershifted by the α-TvACTN3r antiserum in a concentration-dependent manner, and an additional second RPC (II) was also observed (lanes 3–5). Moreover, antibodies against each TvACTN3-specific domain (DIr, DIIr, DIIIr) yielded a similar effect (data not shown). An unrelated negative control antibody at the highest concentration (α-TvTIM2r) had no effect on RPC formation, as expected (lane 6). Similar results were obtained by supershift assays when the IRE-fer RNA probe was used in the presence of α-TvACTN3r antibody (data not shown). These results showed the participation of TvACTN3 in the ribonucleoprotein complex that binds the two IREs.

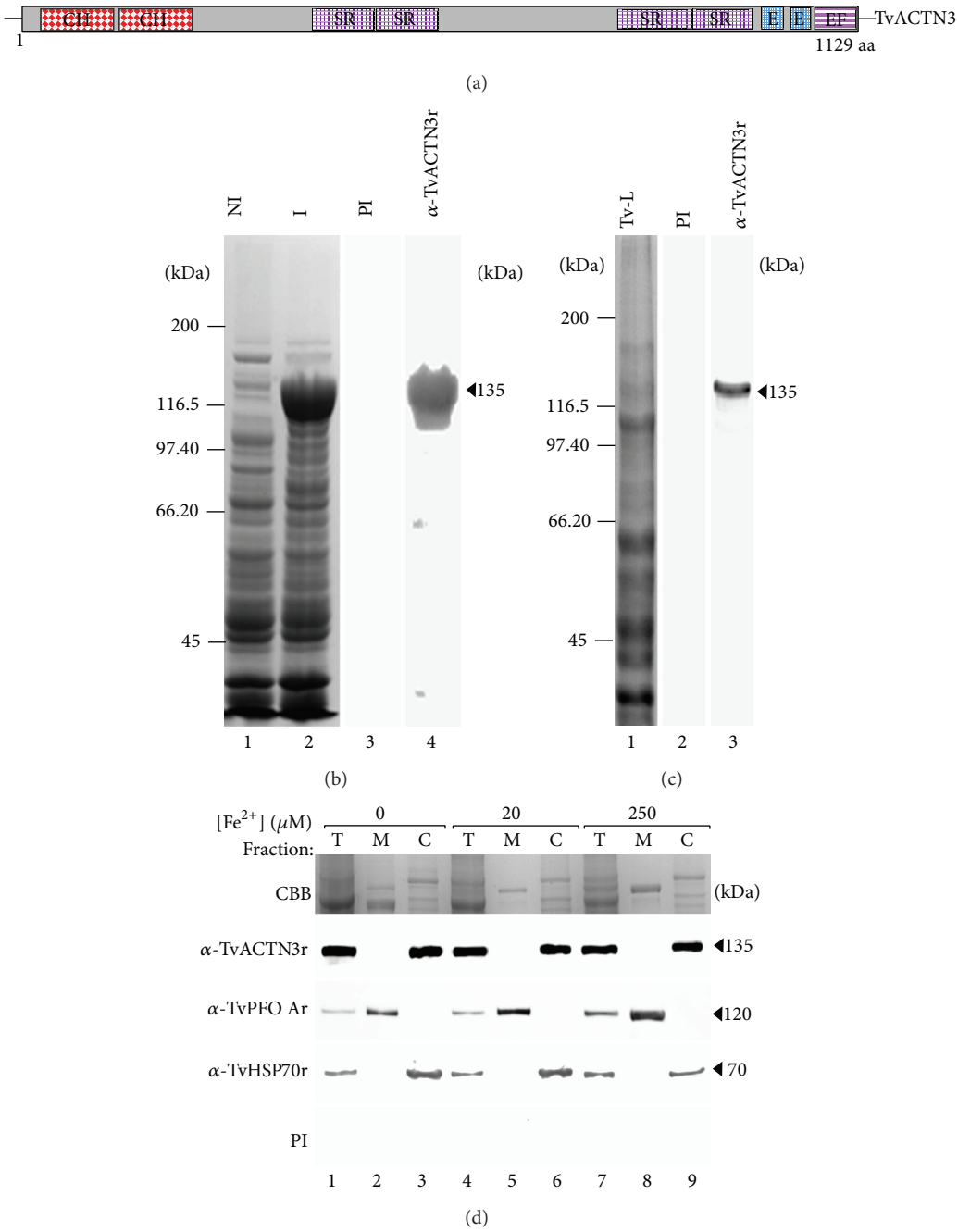

Figure 5: Expression of the native *T. vaginalis* tvactn3 gene and the cloning and expression of recombinant TvACTN3 (TvACTN3r) and its cellular distribution. (a) Principal motifs of the deduced amino acid sequence of the TvACTN3 protein, including Domain I (DI), which contains two calponin-homology domains (CH), followed by four spectrin repeats (SR) in the central rod domain, and three EF-hands (E); one of them is insensitive to calcium (EF) at the C-terminus. (b) Expression of the 6x-His-tagged TvACTN3r protein. Bacteria *E. coli* were transformed with pProEX-HTb-TvACTN3 plasmid and protein expression was induced by the addition of 1 mM IPTG for 16 h at 16°C. Protein extracts were separated through 7.5% SDS-PAGE and gels were stained with Coomassie Brilliant Blue (CBB), noninduced bacterial extract (lane 1), IPTG-induced bacterial extract (lane 2). Immunodetection of TvACTN3r polypeptide by WB assays using specific rabbit antibodies: preimmune (PI) serum used as a negative control (lane 3), α-TvACTN3r serum (lane 4). (c) Detection of the native TvACTN3 expression by WB with an α-TvACTN3r antibody. CBB-stained *T. vaginalis* total extract (lane 1), *T. vaginalis* total extract transferred onto a NC membrane and incubated with the PI serum (lane 2), or with α-TvACTN3r antibody (lane 3). (d) Trichomonad cell fractionation of parasites grown in iron-depleted (0 μM; lanes 1–3), iron-normal (20 μM; lanes 4–6), and iron-rich (250 μM; lanes 7–9) conditions: Total (T), Membrane (M), and Cytoplasmic (C) fractions were analyzed by WB with α-TvACTN3r, α-TvPFO Ar, and α-TvHSP70r polyclonal antibodies. The last two antibodies were used as controls. Arrowheads indicate the size or position of the protein bands detected by antibodies. kDa, molecular weight standards in kilodaltons. A representative result of three independent experiments with similar results.

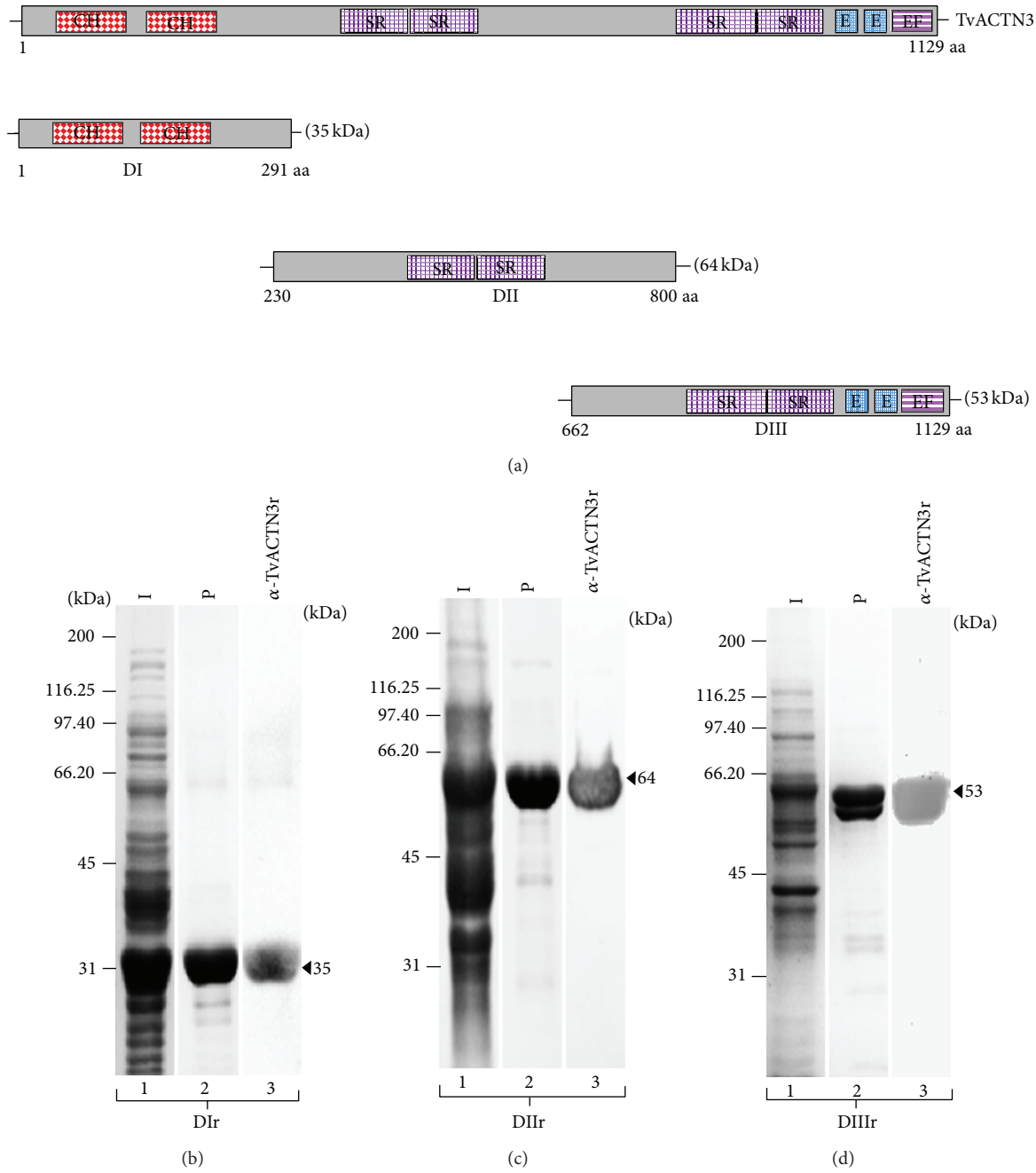

Figure 6: Expression and recognition of TvACTN3 domains DIr, DIIr, and DIIIr by α-TvACTN3r antibody. (a) Map of domains used to generate the recombinant proteins (DIr, DIIr, and DIIIr) of TvACTN3. ((b)–(d)) Induction (I), purification (P), and recognition by WB of DIr, DIIr, and DIIIr proteins. Expression of the 6x-His tagged DIr, DIIr, and DIIIr proteins. Bacteria *E. coli* were transformed with pProEX-HTb- DIr, DIIr, or DIIIr plasmid and protein expression was induced by the addition of 1 mM IPTG for 16 h at 16°C. Protein extracts were separated through 10% SDS-PAGE and gels were CBB-stained, IPTG-induced (I) bacterial extract (lanes 1). Affinity purified recombinant proteins using Ni-NTA-Sepharose (lanes 2; P). Immunodetection of DI, DII, or DIII polypeptide by WB assays using α-TvACTN3r serum (lanes 3). kDa, molecular weight markers in kilodaltons (Bio-Rad).

3.8. Identification of the Putative RNA-Binding Domain(s) of TvACTN3. To identify the putative RNA-binding domain in TvACTN3, we conducted two different functional assays, that is, an NWB assay and a UV cross-linking assay using the purified recombinant proteins (TvACTN3r, DIr, DIIr, and DIIIr). Figure 8(b) shows that the radiolabeled IRE-tvcp4 RNA probe in the NWB assays specifically bound to the complete recombinant protein (TvACTN3r) and its DIr and DIIr domains as well as the recombinant hIRP-1r, which was used as a positive control. The probe did not bind to the negative control protein BSA (panel II). An absence of RNA-protein interactions was observed when an unrelated

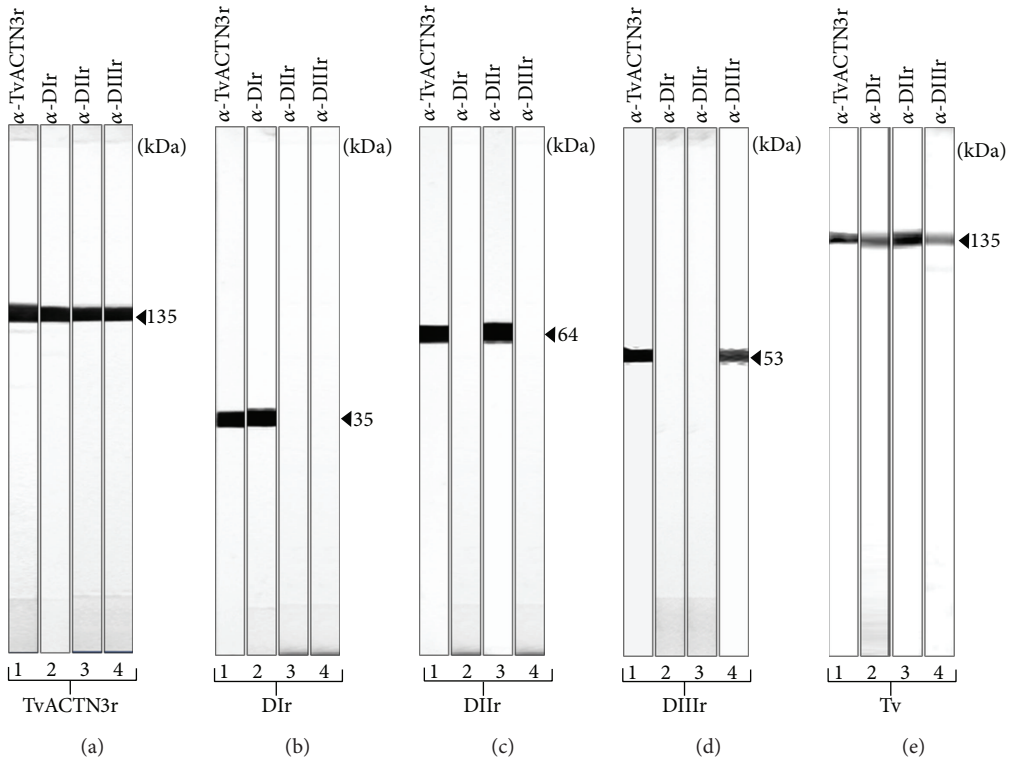

Figure 7: Production of polyclonal antibodies and specific recognition of TvACTN3 domains (DIr, DIIr, and DIIIr) and *T. vaginalis* cytoplasmic proteins by the specific antibodies. WB assays using (a) TvACTN3r; (b) DIr, (c) DIIr, (d) DIIIr purified recombinant proteins; and (e) cytoplasmic proteins from *T. vaginalis* grown in regular iron conditions used as antigens and transferred onto NC membranes and incubated with α-TvACTN3r, α-DIr, α-DIIr, and α-DIIIr polyclonal antibodies (lanes 1–4). kDa, molecular weight markers in kilodaltons (Bio-Rad).

radiolabeled RNA and a tvcp4 *deletion mutant* that disrupts the IRE-tvcp4 RNA [11] were used as negative control probes (panels III and IV, resp.).

To confirm these results, we also performed UV cross-linking assays to analyze the RNA-protein interactions using the same recombinant proteins and radiolabeled RNA probes as described in Figure 8(b). Figure 8(c) shows that a specific interaction was only observed between the IRE-tvcp4 RNA probe and the DIIr domain of TvACTN3 (panel II) and hIRP-1r, compared with the negative controls (panels III and IV). Similar results were observed when the radiolabeled IRE-fer RNA probe was used as a positive control (data not shown). Taken together, these results suggest that in trichomonads grown under iron-depleted conditions TvACTN3r may function as an RNA-binding protein using its central domain to interact with IRE mRNA structures.

3.9. Domain II of TvACTN3r Has Putative RNA-Binding Domains That May Be Used to Interact with RNA. An *in silico* analysis of DI and DII sequences using the SMART, Motif Scan, and PROSITE programs resulted in the identification of different regions of TvACTN3 DII putative motifs that have been reported to be involved in RNA-protein interactions, such as the BRIGHT (292–386 aa) [32], B5 (344–401 aa) [33], LA (392–448 aa) [34], Pumilio-binding (428–464 aa) [35–37], and KH (433–502 aa) [36–38] domains (Figure 8(d), Table 3). Based on the sequences found in the *T. vaginalis* genome and NCBI database, none of these putative RNA-binding motifs were identified in the other TvACTN proteins (Figure 3; Supplementary Figure S1) or in ACTN from other organisms such as *Aedes aegypti* (gi|157115648|), *Gallus gallus* (gi|211083|), *Homo sapiens* (gi|178058|), *Drosophila melanogaster* (gi|22831541|), *Naegleria gruberi* (gi|284087152|), *Paracoccidioides brazilien-sis* (gi|226286950|), *Wuchereria bancrofti* (gi|402588131|), and *Entamoeba dispar* (gi|167384828|) (data not shown).

4. Discussion

Iron plays an important role in host-parasite interactions by stimulating cytoadherence and complement resistance and by reducing cytotoxicity and apoptosis induction in host cells [39]. The mechanisms by which iron modulates virulence gene expression in trichomonads are poorly understood. At the transcriptional level, gene expression is mediated by an iron-responsive promoter [13] and the coordinated interactions of at least three Myb proteins [40–42]. To date, this type of regulation has been described only for

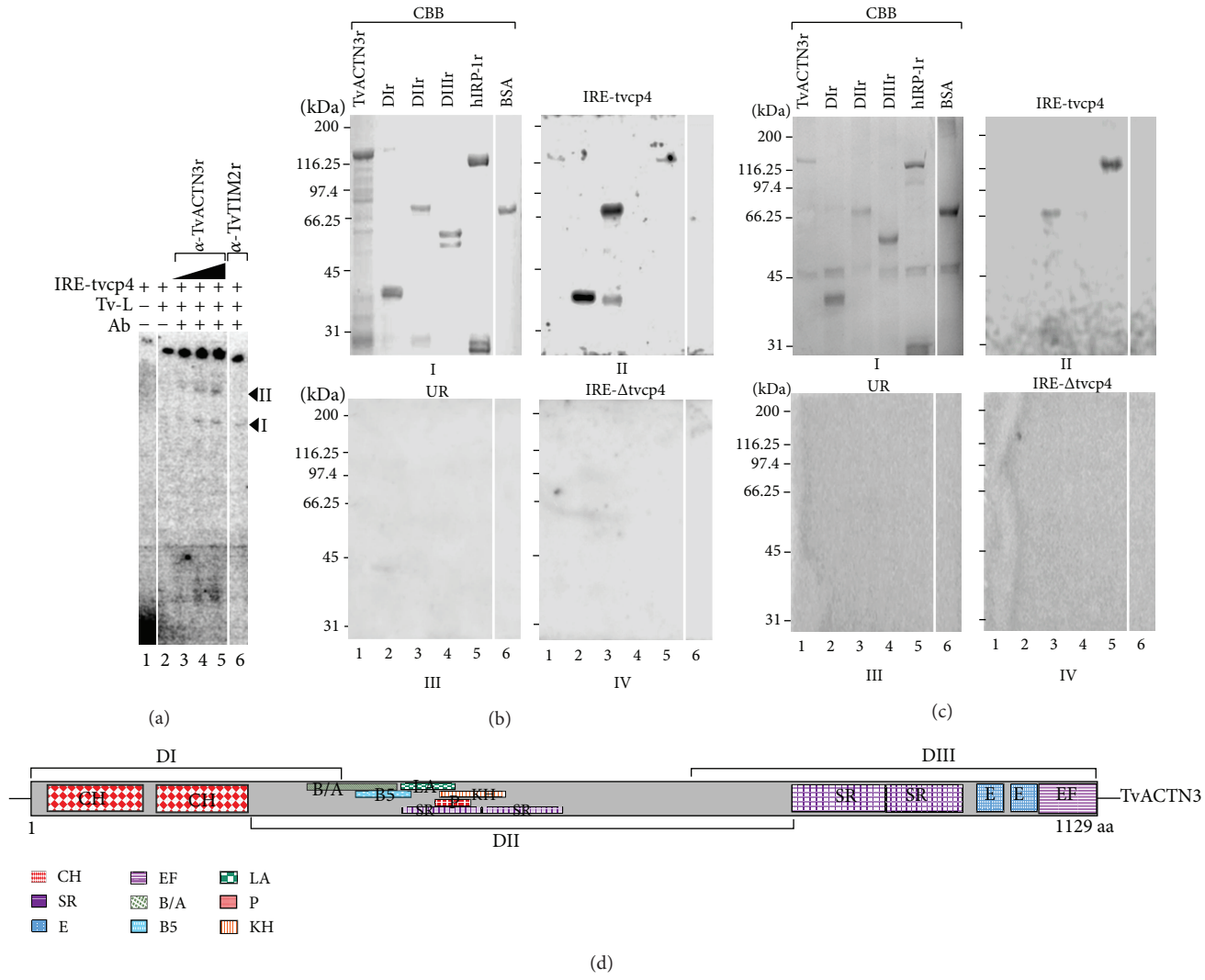

Figure 8: Interaction of TvACTN3r with trichomonad IRE RNA. (a) Representative α-TvACTN3r antibody supershift assays. A radiolabeled IRE-tvcp4 RNA probe (lane 1) was incubated with cytoplasmic proteins from *T. vaginalis* grown under iron-depleted conditions without (lane 2) or with different quantities of α-TvACTN3r antibody (lanes 3–5) or an unrelated antibody (α-TvTIM2r; lane 6). Arrowheads indicate the RNA-protein complexes. A representative result of three independent experiments with similar results is shown. (b) Northwestern blot assay. The recombinant proteins TvACTN3r; DIr, DIIr, and DIIIr and the controls hIRP-1r; and BSA were separated by SDS-PAGE on 10% polyacrylamide gels (panel I) and transferred onto NC membranes, which were incubated with a radiolabeled IRE-tvcp4 RNA probe (panel II). The controls included a radiolabeled nonrelated RNA (panel III) and a radiolabeled *deletion mutant* that disrupts IRE-tvcp4 RNA (panel IV). (c) UV cross-linking assays of the recombinant proteins TvACTN3r, DIr, DIIr, and DIIIr and radiolabeled IRE-tvcp4 RNA probes resolved by SDS-PAGE on 10% polyacrylamide gels (panel II). As controls, TvACTN3r and its domains were incubated with radiolabeled nonrelated RNA (panel III) and a radiolabeled *deletion mutant* that disrupted IRE-tvcp4 RNA (panel IV). In addition, a control from a representative gel of the different recombinant proteins in cross-linking mix was CBB-stained (panel I); kDa, molecular weight standards in kilodaltons. A representative result of three independent experiments with similar results is shown. (d) Identification of putative RNA-protein interaction motifs in TvACTN3 by *in silico* analysis. The complete protein and the different domains of TvACTN3 are illustrated with brackets, and the possible motifs for RNA-protein interactions are indicated. The boxes show the location of the motif described on top of the figure and in Table 3.

the ap65-1 gene, which is upregulated by iron [13]. Recently, the positive expression of TvCP4 by iron was described at the protein level, and predictions of an atypical IRE stem-loop structure located at the 5′ end of the tvcp4 mRNA suggest that an ancestral form of RNA stem-loop structures is involved in a novel iron posttranscriptional regulatory mechanism mediated by RNA-protein interactions parallel to the IRE/IRP system [11, 12].

In this work, we identified and characterized a 135-kDa cytoplasmic protein corresponding to α-actinin, called TvACTN3, as one of the protein components involved in RNA-protein interactions that could mediate posttranscriptional regulation by iron in *T. vaginalis*. Our data suggest that this protein is part of a ribonucleomultiprotein complex capable of interacting with the IRE-tvcp4 and IRE-fer stem-loop structures (Figures 2(a), 2(c), and 8; Table 2).

Table 2: Peptides identified by MALDI-TOF-MS analysis of the 135-kDa protein band of *T. vaginalis* that interacted with RNA IRE-tvcp4 probe by UV cross-linking assay (Figure 2(a))[a].

Peptide number[b]	Measured m/z (av)[c]	Calculated m/z (av)[d]	Error[e]	Position[f]	Peptide sequences (aa)[g]
1	1516.59	1516.65	−0.06	6–18	(R)GLLDDAWEQTQIK(V)
2	1749.93	1749.91	0.02	32–47	(K)GIPFDNVLEEFADGVK(L)
3	1640.95	1641.02	−0.07	48–61	(K)LIQLLEIVSKEPMK(G)
4	1624.73	1624.81	−0.08	119–132	(K)FMIEEISVEEATAR(D)
5	928.98	929.11	−0.13	133–140	(R)DALLLWAK(K)
6	2099.52	2099.28	0.24	171–187	(K)FRPNMLDYDSLDQTQQK(E)
7	2114.98	2115.28	−0.30	171–187	(K)FRPNMLDYDSLDQTQQK(E) + Oxidation (M)
8	2030.39	2030.24	0.15	220–237	(K)SVVTQVAEFFHFFAGESK(T)
9	1308.21	1308.39	−0.18	254–264	(K)AIEEEALNYEK(Q)
10	1369.87	1369.63	0.24	294–304	(K)SKLFNCIKFGR(V)
11	1180.53	1180.44	0.09	305–314	(R)VVRPVIVDKR(G)
12	1279.12	1279.48	−0.36	340–350	(K)EELLPPNLNLK(F)
13	1392.58	1392.51	0.07	398–409	(K)AINLTGDLYEQR(D)
14	1934.50	1934.07	0.43	410–427	(R)DALNNYLQQAQEAAGTVK(E)
15	1599.90	1599.83	0.08	428–440	(K)ELQPQFVELVELR(L)
16	1847.28	1847.11	0.17	448–464	(R)TVIAVDGEFEQLIATIK(R)
17	2003.26	2003.30	−0.04	448–465	(R)TVIAVDGEFEQLIATIKR(L)
18	1321.37	1321.44	−0.06	482–492	(K)KIEEYNQAAQK(Y)
19	1214.35	1214.33	0.03	502–512	(K)QDLEAIAGELR(E)
20	1762.73	1762.98	−0.25	530–544	(R)NGVSDIRPMFQELEK(Q)
21	1779.30	1778.98	0.32	530–544	(R)NGVSDIRPMFQELEK(Q) + Oxidation (M)
22	3063.49	3063.38	0.12	545–572	(K)QSLHLGIENTPDAVTAMYTACLSQAQDK(I)
23	2108.58	2108.35	0.24	628–645	(K)ASIQPTLEEPYQYLQSIK(Y)
24	3199.79	3199.39	0.40	660–687	(R)DSDITFAFLTTLLNQLEEQLQSESNDAR(I)
25	1363.80	1363.47	0.33	698–708	(K)YVDIANEFHQK(V)
26	1732.90	1732.94	−0.04	720–734	(R)RNAYLSAQLELGNKR(E)
27	1576.51	1576.75	−0.24	721–734	(R)NAYLSAQLELGNKR(E)
28	3097.45	3097.48	−0.03	750–777	(R)DTLHIRVNDSPATISKVYANALQIITDK(L)
29	1656.07	1655.93	0.14	802–816	(K)VVQNVELTGTLLELK(D)
30	3332.99	3332.65	0.34	824–851	(K)AQAQEILPELPTLDAPWEDLCDFNLNYR(V)
31	1549.64	1549.68	−0.04	992–1004	(K)GLQISEEQLTEFR(E)
32	2601.90	2601.78	0.12	1005–1024	(R)ETFNHFDKDHTNFLQYFELR(A)
33	1027.15	1027.13	0.03	1054–1061	(K)LNFDEYVK(F)
34	1024.19	1024.19	0.00	1062–1069	(K)FMLDHFSK(A)
35	3225.53	3225.52	0.01	1082–1109	(K)AIANNNPILTDAQLDQYFKGEEAEYLRK(V)

[a]Masses listed represent 43% sequence coverage with 2.64*e* + 11 MS-Fit MOWSE score and 212 Mascot score and 5.8*e* − 15 expect value. [b]Consecutive number assigned to the identified peptides. [c]Measured peptide mass average [m/z (av)] obtained by MALDI-TOF-MS after tryptic digestion of the 135-kDa protein band excised from a duplicate CBB-stained gel used as a control for the UV cross-linking assays (Figure 2(a)). This protein was identified as actinin3 from *T. vaginalis* (tvactn3, TVAG239310). [d]Calculated peptide mass average [m/z (av)] obtained from a theoretical tryptic digestion of the deduced amino acid sequence of the *T. vaginalis* tvactn3 gene (TVAG 239310; tvactn3) reported in the genome of *T. vaginalis* [29]. [e]Error represents the difference after comparing the measured and calculated peptide mass averages [m/z (av)]. [e]Position in amino acid residues of the identified peptides (start-end) in the deduced amino acid sequence of *T. vaginalis* tvactn3 gene, tvactn3. [g]Amino acid sequence of the peptides obtained from a theoretical tryptic digestion of tvactn3 (see Figure S1).

We demonstrated a specific interaction between cytoplasmic proteins in *T. vaginalis* grown under iron-depleted conditions and IRE structures from this parasite as well as human ferritin by REMSA assays (Figure 1). These data support our previous results, suggesting the presence of a posttranscriptional regulatory system in *T. vaginalis* that has been conserved during evolution [11, 12]. However, this parallel mechanism in *T. vaginalis* uses atypical hairpin RNA structures and different RNA-binding proteins (RBPs). This finding is not surprising because this parasite lacks aconitase

Table 3: Putative motifs present in tvactn3 that may be involved in DNA-RNA interactions.

Domain	Sequence[a]	Consensus sequence/60%[b]	Location aa[*]	GO Function	Reference
BRIGHT/ARID	VKSKLFNCIKFGRVVRPVIVDKRGVAMKTWGQ LVTKCNSNGRPIPQVKEELLPPTLNLKFEEIEKT ASDRRDELTKILEELQAKLINAFDEAANA	pppp.FbppLbpFbccptp...b.plPhls .cs..lDLapLa.hVpcbGGbppVsps+p. Wpclsppbsbss.....sssthpL+pbYb+bLbsaEpbbp.	292–386	DNA-binding	[32]
B5	PPTLNLKFEEIEKTASDRRDELTKILEELQAKLI NAFDEAANAKIAVCDDINNKAINL	.pslplphsclscllGhsls.....pclhclLpcLG.... bplp.ps.....s.bpVplPsaR..hDlpbc....hDLlEEltRlaGY	344–401	RNA-binding, Magnesium ion binding, ATP binding	[33]
LA	DDINNKAINLTGDLYEQRDALNNYLQQAQEAA GTVKELQPQFVELVELRLNNRVKRT	pclppplb+QlEaYFScbNLspDbFLpcpbs c..-GaVPlphlssFp+l+ sL∗p-....hpbIspAL.+p S.....sblcls-c...sp+ lRRp..	392–448	RNA-binding	[34]
Pumilio-Binding	ELQPQFVELVELRLNNRVKRTVIAVDGEFEQLIATIK	.bpsplhplsp.cpaGspllQ+hlcbss.p... pppbllp...	428–464	RNA-binding	[35–37]
KH	FVELVELRLNNRVKRTVIAVDGEFEQLIATIKRL IEGNKAAIFEYENKKKIEEYNQAAQKYVDEVAQLKQ	..s.hpbpl..lss....pb htblIG+pG. ..pslcplppps.ssplpl. p.....pphlpl pts....pslpbsbpbl.pblp....	433–502	RNA binding domain	[36–38]

[a]The protein sequence of tvactn3 was used to search in the SMART 7 program to identify the presence of DNA-RNA binding putative domains in the aa sequence. The computational program used for this analysis presented the aa in a single word code. The other codes mean the following: (−) aa negatively charged: D or E; (*) aa S or T; (l) Aliphatic aa: I, L, V; (+) aa positive charged; (t) A, G, S aa; (a) aa with aromatic group: F, H, W, Y; (c) charged aa: D, E, H, K, R; (s) small aa: A, C, D, G, N, P, S, T, V; (p) polar aa: C, D, E, H, K, N, Q, R, S, T; (b) Big aa: E, F, H, I, K, L, M, Q, R, W, Y; (h) Hydrophobic aa: A, C, F, G, H, I, L, M, T, V, W, Y. [b]A PSI-BLAST search using the complete tvactn3 sequence (residues 1–1129) of *T. vaginalis* and $E < 0.01$ enable us to identify each of the DNA-RNA binding domains sequences (BRIGHT/ARID, B5, LA, Pumilio-Binding, and KH domains) present in the DII of tvactn3 shown in Figure 8(d). These aa sequences showed a 60% similitude with the consensus sequences of these motifs by multiple alignments.

activity and IRP-like protein encoding genes [29]. Herein, we showed the presence of four cytoplasmic RBPs that specifically bind to IRE-fer and IRE-tvcp4 with molecular weights ranging from 135-kDa to 45-kDa in iron-depleted trichomonad cytoplasmic extracts (Figure 2(a)). This specific localization suggests that these proteins could be working as RBPs. However, the difference in molecular weight relative to IRP-1 or IRP-2, as well as the negative effect of β-mercaptoethanol on RNA-protein complex formation, suggests the presence of atypical RBPs in this particular mechanism. Similar results have been reported in other protist parasites [43–47].

Why is actinin 3 one of the RNA-binding proteins in this parasite? According to the genome sequence of *T. vaginalis*, this parasite has five different α-actinin-encoding genes [29]. Sequence multiple alignments at the nucleotide and protein levels revealed that the N- and C-terminal domains (Domains I and III) are conserved among the five trichomonad α-actinins. The central region (Domain II) is the most divergent due to differences in the number of spectrin repeats in each isoform (Figure 3). However, only one α-actinin has been studied previously. The 110-kDa α-actinin (dubbed TvACTN2 in here) was found throughout the cytoplasm of pear-shape *T. vaginalis*. In the amoeboid form, high levels of α-actinin were found in the periphery of this cell, mainly in the pseudopodia and adhesion plaques that colocalized with the actin protein [48]. In addition, overexpression of tvactn2 gene has been reported for parasites adhered to vaginal epithelial cells and under low iron conditions [49]. Moreover, in the TrichDB database tvactn2 showed the highest number of ESTs obtained from parasites grown under different environmental conditions as compared to the other four tvactn genes. However, the tvactn2 gene showed the lowest number of ESTs under low iron conditions. Our results are consistent with those observed in the TrichDB ESTs (Figure 4), showing less expression of tvactn genes in parasites grown under iron-depleted than under regular or unsynchronized cultures as well as regarding the absence or very poor expression of tvactn4 and tvactn5 genes under different growth conditions.

The participation of TvACTN3 in the RNA-protein complex formation was evaluated by different functional assays utilizing tools we generated, namely, recombinant proteins (TvACTN3r and its three domains) and specific antibodies against each of the recombinant proteins (Figures 5–7). Supershift, NWB, and UV cross-linking assays revealed that the TvACTN3r protein possible through the DIIr domain can bind RNA hairpin structures (Figure 8). These results suggest the role of TvACTN3 as an RNA-binding protein.

The typical role of α-actinin is to serve as a ubiquitous cytoskeletal conserved protein in eukaryotic cells that cross-links actin filaments and plays an important role in motion and morphological changes [50]. α-Actinin belongs to the spectrin superfamily, which is characterized by the ability to bind actin and by the presence of several spectrin repeats [51]. Its other important roles in the cell are linking the cytoskeleton to different transmembrane proteins, regulating the activity of several receptors and serving as a scaffold to connect the cytoskeleton to diverse signaling pathways. Over the course of evolution, alternative splicing and gene duplication have led to a substantial functional assortment within the α-actinin protein family. This diversity is most marked in mammalian cells, in which four α-actinin-encoding genes produce at least six different products or isoforms. Each isoform has different tissue and subcellular localizations, expression profiles, and biochemical characteristics [52]. Similar relationships are likely to be expected for the five actinin-encoding genes of *T. vaginalis*, which appear to have specific expression levels under different iron concentrations (Figure 4). These results are consistent with recently reported RT-PCR, microarray, and EST data (http://www.trichdb.org/) [49, 53].

Moreover, the *T. vaginalis* genome has undergone multiple gene duplication events; the presence of five α-actinin coding genes likely represents a neofunctionalization process. Although actinin primarily function as an actin-binding protein, gene duplication throughout evolution led to the acquisition of new roles inside the cell, including RNA-binding, depending on the microenvironmental conditions. This is not surprising because cytoskeletal proteins are also involved in RNA-cytoskeletal associations and mRNA localization in most of cell types. The association of RNAs with cytoskeletal proteins is required in cellular processes such as mRNA transport and protein synthesis [54]. Cytoskeletal proteins such as β-actin and annexin A2 also contribute to the posttranscriptional regulation of gene expression of specific genes through interactions between these proteins and *cis*-acting elements, generating a higher-order structure and regulating the localization and translation of these specific transcripts [55–57].

Because RNA-protein interactions were identified only under iron-depleted concentrations, we analyzed the expression of the tvactn3 gene. We observed that this gene is upregulated by iron at the mRNA level (Figure 4); however, protein expression appears to be constitutive (Figure 5(d)). The interaction of actinin TvACTN3 with RNA could occur in the absence of iron through some of the putative RNA-binding motifs found in the central DII domain, particularly in the region between residues 230 and 662, as suggested by *in silico* analysis (Figure 8; Table 3). These data suggest that iron may control the interaction of TvACTN3 with actin or RNA possible by causing conformational changes by switching functions depending on the iron concentration but without modifying the amount of protein. However, we can speculate that (a) under iron-rich concentrations TvACTN3 is an actin-binding protein that promotes polymerization and stabilizes actin filaments and that (b) under iron-depleted concentrations TvACTN3 is an RNA-binding protein that interacts with RNA hairpin structures that may be involved in a parallel posttranscriptional iron regulation mechanism. Work is in progress to analyze these possibilities.

The RNA-TvACTN3 interaction seem to be absent in the other four *T. vaginalis* α-actinins and in α-actinins from other species when using different computational programs. Thus to identify the putative RNA-binding domain in the TvACTN3 central domain DII, additional studies are needed to define the particular region(s) of DII responsible for the RNA-protein interaction, which could include the putative motifs identified previously (Table 3) or a new

uncharacterized motif that might be responsible for the novel RNA-binding property identified in the TvACTN3 of this early evolving protist parasite. It will also be necessary to determine whether TvACTN3 also interacts with other IRE-like structures present in the multiple iron-regulated genes, as recently described [49, 50], in addition to the structure identified in the 3′-UTR region of the iron-downregulated tvcp12 gene, which encodes another CP of *T. vaginalis* and plays a role in cytotoxicity (unpublished results). Thus, this finding could represent a novel posttranscriptional iron regulatory mechanism common to iron-regulated genes in *T. vaginalis*.

5. Conclusion

In summary, our results showed that TvACTN3 is one of the cytoplasmic proteins acting as an RNA-binding protein that could participate in iron regulation at the posttranscriptional level by a mechanism mediated by RNA-protein interactions parallel to the IRE/IRP system.

Conflict of Interests

The authors declare that there is no conflict of interests regarding the publication of this paper.

Acknowledgments

This work was partially supported by CINVESTAV and by Grants 162123 and 153093 (to Rossana Arroyo) from Consejo Nacional de Ciencia y Tecnología (CONACYT), México, and Grants ICYT-299 and ICYT-186 from Instituto de Ciencia y Tecnología del Distrito Federal (ICyTDF), México, (to Rossana Arroyo). Jaeson Santos Calla-Choque was scholarship recipient from Secretaria de Relaciones Exteriores del Gobierno de México (SRE) and ICyTDF. The authors are grateful to Ma. Elizbeth Alvarez-Sánchez, Ph.D. for her great help with the qRT-PCR assays. We are grateful to Mary Ann Gawinowicz, Ph.D., Special Research Scientist, at Herbert Irving Comprehensive Cancer Center for her help in the MS analysis. We are also grateful to Dr. Lucas Kühn from the Swiss Institute for Experimental Cancer Research (ISREC) for his kind donation of the pSPT-fer and pGEX-hIRP-1 plasmids used as controls in this study. M. V. Z. Manuel Flores-Cano and Martha G. Aguilar-Romero are acknowledged for their technical assistance. The authors are grateful to Biol. Rodrigo Moreno-Campos for the art work. A special thank is due to to all the reviewers for their constructive comments.

References

[1] P. Aisen, C. Enns, and M. Wessling-Resnick, "Chemistry and biology of eukaryotic iron metabolism," *International Journal of Biochemistry and Cell Biology*, vol. 33, no. 10, pp. 940–959, 2001.

[2] U. Testa, *Proteins of Iron Metabolism*, CRC Press, Boca Raton, FL, USA, 2000.

[3] K. Pantopoulos, "Iron metabolism and the IRE/IRP regulatory system: an update," *Annals of the New York Academy of Sciences*, vol. 1012, pp. 1–13, 2004.

[4] T. Rouault and R. Klausner, "Regulation of iron metabolism in eukaryotes," *Current Topics in Cellular Regulation*, vol. 35, pp. 1–19, 1997.

[5] A. M. Thomson, J. T. Rogers, and P. J. Leedman, "Iron-regulatory proteins, iron-responsive elements and ferritin mRNA translation," *International Journal of Biochemistry and Cell Biology*, vol. 31, no. 10, pp. 1139–1152, 1999.

[6] J. Wang and K. Pantopoulos, "Regulation of cellular iron metabolism," *Biochemical Journal*, vol. 434, no. 3, pp. 365–381, 2011.

[7] C. P. Anderson, M. Shen, R. S. Eisenstein, and E. A. Leibold, "Mammalian iron metabolism and its control by iron regulatory proteins," *Biochimica et Biophysica Acta*, vol. 1823, pp. 1468–1483, 2012.

[8] M. C. Kennedy, L. Mende-Mueller, G. A. Blondin, and H. Beinert, "Purification and characterization of cytosolic aconitase from beef liver and its relationship to the iron-responsive element binding protein," *Proceedings of the National Academy of Sciences of the United States of America*, vol. 89, pp. 11730–11734, 1992.

[9] T. A. Rouault, "The role of iron regulatory proteins in mammalian iron homeostasis and disease," *Nature Chemical Biology*, vol. 2, no. 8, pp. 406–414, 2006.

[10] D. J. Haile, T. A. Rouault, J. B. Harford et al., "Cellular regulation of the iron-responsive element binding protein: disassembly of the cubane iron-sulfur cluster results in high-affinity RNA binding," *Proceedings of the National Academy of Sciences of the United States of America*, vol. 89, no. 24, pp. 11735–11739, 1992.

[11] E. Solano-González, E. Burrola-Barraza, C. León-Sicairos et al., "The trichomonad cysteine proteinase TVCP4 transcript contains an iron-responsive element," *FEBS Letters*, vol. 581, no. 16, pp. 2919–2928, 2007.

[12] J. C. Torres-Romero and R. Arroyo, "Responsiveness of *Trichomonas vaginalis* to iron concentrations: evidence for a post-transcriptional iron regulation by an IRE/IRP-like system," *Infection, Genetics and Evolution*, vol. 9, no. 6, pp. 1065–1074, 2009.

[13] C.-D. Tsai, H.-W. Liu, and J.-H. Tai, "Characterization of an iron-responsive promoter in the protozoan pathogen *Trichomonas vaginalis*," *The Journal of Biological Chemistry*, vol. 277, no. 7, pp. 5153–5162, 2002.

[14] L. S. Diamond, "The establishment of various trichomonads of animals and man in axenic cultures," *Journal of Parasitology*, vol. 43, pp. 488–490, 1957.

[15] M. E. Alvarez-Sánchez, E. Solano-González, C. Yañez-Gómez, and R. Arroyo, "Negative iron regulation of the CP65 cysteine proteinase cytotoxicity in *Trichomonas vaginalis*," *Microbes and Infection*, vol. 9, no. 14-15, pp. 1597–1605, 2007.

[16] R. Arroyo, J. Engbring, and J. F. Alderete, "Molecular basis of host epithelial cell recognition by *Trichomonas vaginalis*," *Molecular Microbiology*, vol. 6, no. 7, pp. 853–862, 1992.

[17] Z. Popovic and D. M. Templeton, "A Northwestern blotting approach for studying iron regulatory element-binding proteins," *Molecular and Cellular Biochemistry*, vol. 268, no. 1-2, pp. 67–74, 2005.

[18] B. R. Henderson, E. Menotti, C. Bonnard, and L. C. Kuhn, "Optimal sequence and structure of iron-responsive elements. Selection of RNA stem-loops with high affinity for iron regulatory factor," *The Journal of Biological Chemistry*, vol. 269, no. 26, pp. 17481–17489, 1994.

[19] L. T. Timchenko, P. Iakova, A. L. Welm, Z.-J. Cai, and N. A. Timchenko, "Calreticulin interacts with C/EBPα and C/EBPβ

mRNAs and represses translation of C/EBP proteins," *Molecular and Cellular Biology*, vol. 22, no. 20, pp. 7242–7257, 2002.

[20] E. A. Leibold and H. N. Munro, "Cytoplasmic protein binds in vitro to a highly conserved sequence in the 5' untranslated region of ferritin heavy- and light-subunit mRNAs," *Proceedings of the National Academy of Sciences of the United States of America*, vol. 85, no. 7, pp. 2171–2175, 1988.

[21] E. E. Figueroa-Angulo, P. Estrella-Hernandez, H. Salgado-Lugo et al., "Cellular and biochemical characterization of two closely related triosephosphate isomerases from *Trichomonas vaginalis*," *Parasitology*, vol. 139, pp. 1729–1738, 2012.

[22] A. L. Gutiérrez-Escolano, M. Vázquez-Ochoa, J. Escobar-Herrera, and J. Hernández-Acosta, "La, PTB, and PAB proteins bind to the 3′ untranslated region of Norwalk virus genomic RNA," *Biochemical and Biophysical Research Communications*, vol. 311, no. 3, pp. 759–766, 2003.

[23] P. Meza-Cervantez, A. González-Robles, R. E. Cárdenas-Guerra et al., "Pyruvate: Ferredoxin oxidoreductase (PFO) is a surface-associated cell-binding protein in *Trichomonas vaginalis* and is involved in trichomonal adherence to host cells," *Microbiology*, vol. 157, no. 12, pp. 3469–3482, 2011.

[24] S. L. Zhao, C. Y. Liang, W. J. Zhang, X. C. Tang, and H. Y. Peng, "Mapping the RNA-binding domain on the DpCPV VP4," *Archives of Virology*, vol. 151, no. 2, pp. 273–283, 2006.

[25] C. R. León-Sicairos, J. León-Félix, and R. Arroyo, "Tvcp12: a novel *Trichomonas vaginalis* cathepsin L-like cysteine proteinase-encoding gene," *Microbiology*, vol. 150, no. 5, pp. 1131–1138, 2004.

[26] I. Letunic, T. Doerks, and P. Bork, "SMART 6: recent updates and new developments," *Nucleic Acids Research*, vol. 37, no. 1, pp. D229–D232, 2009.

[27] J. Schultz, F. Milpetz, P. Bork, and C. P. Ponting, "SMART, a simple modular architecture research tool: identification of signaling domains," *Proceedings of the National Academy of Sciences of the United States of America*, vol. 95, no. 11, pp. 5857–5864, 1998.

[28] C. J. A. Sigrist, L. Cerutti, E. De Castro et al., "PROSITE, a protein domain database for functional characterization and annotation," *Nucleic Acids Research*, vol. 38, no. 1, Article ID gkp885, pp. D161–D166, 2009.

[29] J. M. Carlton, R. P. Hirt, J. C. Silva et al., "Draft genome sequence of the sexually transmitted pathogen *Trichomonas vaginalis*," *Science*, vol. 315, no. 5809, pp. 207–212, 2007.

[30] D. R. Liston and P. J. Johnson, "Analysis of a ubiquitous promoter element in a primitive eukaryote: early evolution of the initiator element," *Molecular and Cellular Biology*, vol. 19, no. 3, pp. 2380–2388, 1999.

[31] N. Espinosa, R. Hernández, L. López-Griego, and I. López-Villaseñor, "Separable putative polyadenylation and cleavage motifs in *Trichomonas vaginalis* mRNAs," *Gene*, vol. 289, no. 1-2, pp. 81–86, 2002.

[32] P. B. Dallas, S. Pacchione, D. Wilsker, V. Bowrin, R. Kobayashi, and E. Moran, "The human SWI-SNF complex protein p270 is an ARID family member with non-sequence-specific DNA binding activity," *Molecular and Cellular Biology*, vol. 20, no. 9, pp. 3137–3146, 2000.

[33] X. Dou, S. Limmer, and R. Kreutzer, "DNA-binding of phenylalanyl-tRNA synthetase is accompanied by loop formation of the double-stranded DNA," *Journal of Molecular Biology*, vol. 305, no. 3, pp. 451–458, 2001.

[34] D. J. Kenan and J. D. Keene, "La gets its wings," *Nature Structural and Molecular Biology*, vol. 11, no. 4, pp. 303–305, 2004.

[35] T. A. Edwards, S. E. Pyle, R. P. Wharton, and A. K. Aggarwal, "Structure of pumilio reveals similarity between RNA and peptide binding motifs," *Cell*, vol. 105, no. 2, pp. 281–289, 2001.

[36] T. Glisovic, J. L. Bachorik, J. Yong, and G. Dreyfuss, "RNA-binding proteins and post-transcriptional gene regulation," *FEBS Letters*, vol. 582, no. 14, pp. 1977–1986, 2008.

[37] B. M. Lunde, C. Moore, and G. Varani, "RNA-binding proteins: modular design for efficient function," *Nature Reviews Molecular Cell Biology*, vol. 8, no. 6, pp. 479–490, 2007.

[38] M. F. García-Mayoral, D. Hollingworth, L. Masino et al., "The Structure of the C-Terminal KH Domains of KSRP Reveals a Noncanonical Motif Important for mRNA Degradation," *Structure*, vol. 15, no. 4, pp. 485–498, 2007.

[39] E. E. Figueroa-Angulo, F. J. Rendon-Gandarilla, J. Puente-Rivera et al., "The effects of environmental factors on the virulence of *Trichomonas vaginalis*," *Microbes and Infection*, vol. 14, pp. 1411–1427, 2012.

[40] S.-J. Ong, H.-M. Hsu, H.-W. Liu, C.-H. Chu, and J.-H. Tai, "Multifarious transcriptional regulation of adhesion protein gene ap65-1 by a novel Myb1 protein in the protozoan parasite *Trichomonas vaginalis*," *Eukaryotic Cell*, vol. 5, no. 2, pp. 391–399, 2006.

[41] S.-J. Ong, H.-M. Hsu, H.-W. Liu, C.-H. Chu, and J.-H. Tai, "Activation of multifarious transcription of an adhesion protein ap65-1 gene by a novel Myb2 protein in the protozoan parasite *Trichomonas vaginalis*," *The Journal of Biological Chemistry*, vol. 282, no. 9, pp. 6716–6725, 2007.

[42] H.-M. Hsu, S.-J. Ong, M.-C. Lee, and J.-H. Tai, "Transcriptional regulation of an iron-inducible gene by differential and alternate promoter entries of multiple Myb proteins in the protozoan parasite *Trichomonas vaginalis*," *Eukaryotic Cell*, vol. 8, no. 3, pp. 362–372, 2009.

[43] M. Muckenthaler, N. Gunkel, D. Frishman, A. Cyrklaff, P. Tomancak, and M. W. Hentze, "Iron-regulatory protein-1 (IRP-1) is highly conserved in two invertebrate species—characterization of IRP-1 homologues in Drosophila melanogaster and Caenorhabditis elegans," *European Journal of Biochemistry*, vol. 254, no. 2, pp. 230–237, 1998.

[44] D. Zhang, G. Dimopoulos, A. Wolf, B. Miñana, F. C. Kafatos, and J. J. Winzerling, "Cloning and molecular characterization of two mosquito iron regulatory proteins," *Insect Biochemistry and Molecular Biology*, vol. 32, no. 5, pp. 579–589, 2002.

[45] C. Alén and A. L. Sonenshein, "Bacillus subtilis aconitase is an RNA-binding protein," *Proceedings of the National Academy of Sciences of the United States of America*, vol. 96, no. 18, pp. 10412–10417, 1999.

[46] S. Banerjee, A. K. Nandyala, P. Raviprasad, N. Ahmed, and S. E. Hasnain, "Iron-dependent RNA-binding activity of *Mycobacterium tuberculosis* aconitase," *Journal of Bacteriology*, vol. 189, no. 11, pp. 4046–4052, 2007.

[47] Y. Tang and J. R. Guest, "Direct evidence for mRNA binding and post-transcriptional regulation by *Escherichia coli* aconitases," *Microbiology*, vol. 145, no. 11, pp. 3069–3079, 1999.

[48] M. F. Addis, P. Rappelli, G. Delogu, F. Carta, P. Cappuccinelli, and P. L. Fiori, "Cloning and molecular characterization of a cDNA clone coding for *Trichomonas vaginalis* alpha-actinin and intracellular localization of the protein," *Infection and Immunity*, vol. 66, no. 10, pp. 4924–4931, 1998.

[49] A. S. Kucknoor, V. Mundodi, and J. F. Alderete, "Adherence to human vaginal epithelial cells signals for increased expression of *Trichomonas vaginalis* genes," *Infection and Immunity*, vol. 73, no. 10, pp. 6472–6478, 2005.

[50] R. K. Meyer and U. Aebi, "Bundling of actin filaments by α-actinin depends on its molecular length," *Journal of Cell Biology*, vol. 110, no. 6, pp. 2013–2024, 1990.

[51] J. D. Dixson, M. R. J. Forstner, and D. M. Garcia, "The α-actinin gene family: a revised classification," *Journal of Molecular Evolution*, vol. 56, no. 1, pp. 1–10, 2003.

[52] B. Sjöblom, A. Salmazo, and K. Djinović-Carugo, "α-Actinin structure and regulation," *Cellular and Molecular Life Sciences*, vol. 65, no. 17, pp. 2688–2701, 2008.

[53] L. Horvathova, L. Safarikova, M. Basler et al., "Transcriptomic identification of iron-regulated and iron-independent gene copies within the heavily duplicated *Trichomonas vaginalis* genome," *Genome Biology and Evolution*, vol. 4, pp. 1017–1029, 2012.

[54] R.-P. Jansen, "RNA—cytoskeletal associations," *The FASEB Journal*, vol. 13, no. 3, pp. 455–466, 1999.

[55] A. Vedeler, H. Hollas, A. K. Grindheim, and A. M. Raddum, "Multiple roles of annexin A2 in post-transcriptional regulation of gene expression," *Current Protein & Peptide Science*, vol. 13, pp. 401–412, 2012.

[56] P. M. MacDonald, "bicoid mRNA localization signal: phylogenetic conservation of function and RNA secondary structure," *Development*, vol. 110, no. 1, pp. 161–171, 1990.

[57] A. F. Ross, Y. Oleynikov, E. H. Kislauskis, K. L. Taneja, and R. H. Singer, "Characterization of a β-actin mRNA zipcode-binding protein," *Molecular and Cellular Biology*, vol. 17, no. 4, pp. 2158–2165, 1997.

Hindawi Publishing Corporation
BioMed Research International
Volume 2014, Article ID 714749, 9 pages
http://dx.doi.org/10.1155/2014/714749

Research Article

mAb CZP-315.D9: An Antirecombinant Cruzipain Monoclonal Antibody That Specifically Labels the Reservosomes of *Trypanosoma cruzi* Epimastigotes

Cassiano Martin Batista, Lia Carolina Soares Medeiros, Iriane Eger, and Maurilio José Soares

Laboratório de Biologia Celular, Instituto Carlos Chagas/Fiocruz, Rua Professor Algacyr Munhóz Mader 3775, Cidade Industrial, 81350-010 Curitiba, PR, Brazil

Correspondence should be addressed to Cassiano Martin Batista; cassianombatista@gmail.com

Received 26 August 2013; Revised 16 December 2013; Accepted 20 December 2013; Published 23 January 2014

Academic Editor: Wanderley de Souza

Reservosomes are large round vesicles located at the posterior end of epimastigote forms of the protozoan *Trypanosoma cruzi*, the etiological agent of Chagas disease. They are the specific end organelles of the endocytosis pathway of *T. cruzi*, and they play key roles in nutrient uptake and cell differentiation. These lysosome-like organelles accumulate ingested macromolecules and contain large amounts of a major cysteine proteinase (cruzipain or GP57/51 protein). Aim of this study was to produce a monoclonal antibody (mAb) against a recombinant *T. cruzi* cruzipain (TcCruzipain) that specifically labels the reservosomes. BALB/c mice were immunized with purified recombinant TcCruzipain to obtain the mAb. After fusion of isolated splenocytes with myeloma cells and screening, a mAb was obtained by limiting dilution and characterized by capture ELISA. We report here the production of a kappa-positive monoclonal IgG antibody (mAb CZP-315.D9) that recognizes recombinant TcCruzipain. This mAb binds preferentially to a protein with a molecular weight of about 50 kDa on western blots and specifically labels reservosomes by immunofluorescence and transmission electron microscopy. The monoclonal CZP-315.D9 constitutes a potentially powerful marker for use in studies on the function of reservosomes of *T. cruzi*.

1. Introduction

The kinetoplastid protozoan *Trypanosoma cruzi* is the etiological agent of Chagas disease, which affects about eight million people in the 18 countries in which it is endemic, mostly in Latin America [1, 2]. This parasite has a complex life cycle, with two developmental stages in the insect host (replicative epimastigotes and infective metacyclic trypomastigotes) and two stages in mammalian hosts (replicative intracellular amastigotes and infective bloodstream trypomastigotes). Macromolecule endocytosis plays an important role in this flagellate protozoan, allowing survival in the very different environments it colonizes. The endocytosis pathway has been elucidated mainly in epimastigote forms: molecules enter the cells via the flagellar pocket and cytostome, both located in the anterior region of the cell and accumulate in the reservosomes, the end compartments of the endocytosis pathway [3–6].

Reservosomes are large round vesicles located at the posterior end of *T. cruzi* epimastigotes [7]. The lack of molecular markers for cytoplasmic compartments in this parasite makes it difficult to clarify all the functions of reservosomes, which have characteristics typical of prelysosomes, lysosomes, and recycling compartments [8]. Subcellular localization [9] and proteomics [10] experiments have shown reservosomes to contain large amounts of a cysteine proteinase, known as cruzipain [11] or GP57/51 [12]. The native GP57/51 has been isolated from epimastigotes and used to generate a monoclonal antibody (mAb) [13]. Subcellular localization experiments demonstrated the presence of this protein in vesicles of the endosomal/lysosomal system and close to the flagellar pocket [12, 14]. At about the same time, the native

cysteine proteinase (cruzipain) was isolated and characterized [11, 15]. A monospecific rabbit polyclonal antibody against this protein labeled reservosomes, the membrane lining the cell body and flagellum, the inside of the flagellar pocket, and even the cytostome [16]. Thus, no antibody directed against cruzipain has yet been reported to label reservosomes specifically, despite the accumulation of the enzyme in this organelle.

We report here the characterization of a mouse monoclonal antibody (mAb CZP-315.D9) against recombinant *T. cruzi* cruzipain (TcCruzipain) that specifically recognizes reservosomes. This mAb has potential as a powerful molecular marker for studies on the function of this organelle.

2. Materials and Methods

2.1. Ethics Statement. Experiments involving animals were approved by the Ethics Committee of Fiocruz (Protocol P-47/12-3 with license number LW-15/13).

2.2. Reagents. Polyethylene glycol (PEG), phenylmethylsulfonyl fluoride (PMSF), l-*trans*-epoxysuccinyl-l-leucylamido-(4-guanidino)-butane (E-64), alkaline phosphatase (AP)-conjugated goat anti-mouse or goat anti-rabbit antibodies, mouse anti-histidine antibody, rabbit anti-protein A antibody, bromophenol blue, β-mercaptoethanol, bovine serum albumin (BSA), Dulbecco's modified Eagle's medium (DMEM), HT (hypoxanthine and thymidine) medium, HAT (hypoxanthine, aminopterin, and thymidine) medium, and Roswell Park Memorial Institute-1640 (RPMI-1640) medium were purchased from Sigma Co. (St. Louis, MO, USA). Transferrin-Alexa 633, horse-radish peroxidase (HRP-) goat anti-mouse IgG (H+L), Hoechst 33342, goat anti-mouse antibodies coupled to AlexaFluor-488 or AlexaFluor-594, goat anti-rabbit antibody coupled to AlexaFluor 594, Bench Mark prestained Protein Ladder, and Bench Mark Protein Ladder were purchased from Life Technologies-Invitrogen Co. (Carlsbad, CA, USA). Alu-Gel-S adjuvant was purchased from Serva Electrophoresis GmbH Co. (Heidelberg, Germany). Fetal calf serum (FCS) was purchased from Cultilab Ltda (Campinas, SP, Brazil). Isopropylthio-β-galactoside (IPTG) was purchased from Anresco Laboratories Inc. (San Francisco, CA, USA). SureBlue TMB Substrate was purchased from Kirkegaard and Perry Laboratories (KPL, Gaithersburg, MD, USA). Bradford solution was purchased from BIO-RAD (Hercules, CA, USA).

2.3. Parasites. Cultured epimastigotes of *T. cruzi* clone Dm28c [17] were maintained at 28°C by weekly passages in liver infusion tryptose (LIT) medium [18] supplemented with 10% heat-inactivated fetal calf serum (FCS). For TcCruzipain cloning, DNA was isolated by phenol-chloroform extraction [19], from three-day-old cultures of epimastigotes.

2.4. Construction and Purification of Recombinant TcCruzipain Protein. The whole gene encoding *T. cruzi* cruzipain (TcCruzipain, 1404 bp, gene ID Tc00 .1047053507603.260) was used to design primers (Forward: 5′-ATGTCTGGCTGGGCTCGTGCGCTG-3′ and Reverse: 5′-TCAGAGGCGACGATGACGGCTGTGGGTA-3′) with recombination sites (attBs) for use on the Gateway cloning platform (Life Technologies-Invitrogen, USA). *Escherichia coli* strain C43+ was used for recombinant protein production (TcCruzipain + pDEST17 vector expressing a histidine tag), which was induced by incubating the cell culture for 7 h with 1 mM IPTG. The production of the recombinant protein (50 kDa TcCruzipain + 6 kDa histidine tag) was confirmed by western blotting with a probe directed against the histidine tag, and the recombinant protein was purified from the polyacrylamide gel by elution.

2.5. Construction of Recombinant Cruzipain Domains. The whole cruzipain gene was used for domain analysis by pFAM software (Sanger Institute, Cambridge, UK). Cruzipain has three protein domains: pre-pro (aminoacids 38–94), catalytic (aminoacids 123–335), and C-terminal extension (aminoacids 337–417). The nucleotide sequence encoding each protein domain was used to design specific primers, as follows: (a) pre-pro (nucleotides 1 to 368), Forward: 5′-ATGTCTGGCTGGGCTCGTGCG-3′ and Reverse: 5′-CGCGCCCAACTACCTCAACCTTCAC-3′; (b) catalytic (nucleotides 369 to 1005), Forward: 5′-CCCGCGGCAGTGGATTG-3′ and Reverse: 5′-CACCGCAGAGCTCGCCTCCTCC-3′; (c) C-terminal extension (nucleotides 1011 to 1404), Forward: 5′-GGTCCCGGTCCCACTCCTGAGCCA-3′ and Reverse: 5′-TCAGAGGCGGCGATGACGG-3′. Primers had recombination sites (attBs) for use on the Gateway cloning platform (Life Technologies-Invitrogen, USA). *Escherichia coli* strain C43+ was used for recombinant protein production (TcCruzipain protein domains + pDEST17 vector expressing a histidine tag), which was induced by incubating the cell culture for 4 h with 1 mM IPTG. Production of recombinant proteins was confirmed by western blot with a probe directed against the histidine tag.

2.6. Monoclonal Antibody Production. Three male BALB/c mice (30–45-days old) received four intraperitoneal doses of 20 μg TcCruzipain + Alu-Gel-S and a last intravenous (without Alu-Gel-S) injection, separated by intervals of one week. The animals were checked before immunization for antibody cross reactivity with protein extracts of *T. cruzi* epimastigotes (preimmune serum) by western blot assay.

The spleen of a TcCruzipain-reactive mouse was used in a cell fusion protocol [20]. Spleen cells were obtained by filtration, centrifugation, and washing and were fused with Ag8XP3653 myeloma cells (generously supplied by Dr. Carlos R. Zanetti, from Laboratório de Imunologia Aplicada, Universidade Federal de Santa Catarina, Brazil) in the presence of 50% polyethylene glycol (PEG). After fusion, the cells were resuspended at a density of 2.5×10^6 cells/mL in RPMI medium supplemented with 20% FCS and 100 μL of this suspension was added to each well of a 96-well plate. The cells were allowed to grow for 24 h at 37°C, under an atmosphere containing 5% CO_2, and 100 μL of HAT medium was then added to the cell culture. The medium was replaced every 48 h. Hybrid cells were selected

over a period of 14 days, and the medium was then replaced with HT medium for an additional four days. Hybrid cells were selected and propagated in RPMI medium containing 20% FCS. Positive hybridomas were selected by indirect ELISA, western blotting, and indirect immunofluorescence (see below).

The most stable hybridoma in cryosurvival assays [20] was cloned by limiting dilution. The SBA Clonotyping-HRP System (Southern Biotech, Birmingham, USA), based on capture ELISA, was used to identify mAb isotype, in accordance with the manufacturer's instructions. Positive hybridomas and clones were cryopreserved at the Laboratório de Biologia Celular (ICC/FIOCRUZ-PR).

2.7. ELISA. For indirect ELISA, recombinant TcCruzipain (0.15 μg/well) was adsorbed onto 96-well immunoplates (Nunc, Roskilde, Denmark) by incubation overnight at 4°C with sensitizing buffer (0.05 M sodium carbonate and sodium bicarbonate, pH 9.6). The plates were then blocked by incubation for 1 h with 5% nonfat milk powder in PBS supplemented with 0.01% Tween 20 (PBS-T). The hybridoma supernatants were added to the immunoplates and incubated for 1 h at 37°C. The plates were washed five times with PBS-T and incubated for 1 h at 37°C with HRP-conjugated goat anti-mouse IgG (1 : 4,000). The plates were then washed five times with PBS-T and immunoreactivity was visualized with the SureBlue TMB Substrate, with optical density (OD) being read at 450 nm in an EL800 ELISA reader (BioTek, Winooski, VT, USA). Only OD values higher than 0.300 were considered positive.

2.8. Western Blot. For expression analysis of native cruzipain on *T. cruzi* epimastigotes, total protein extracts of the parasites were prepared by resuspending PBS-washed parasites (10^9 cells/mL) in denaturing buffer A (40 mM Tris-HCl pH 6.8; 1% SDS; 360 mM β-mercaptoethanol). PMSF (1 mM) and E-64 (100 μM) were used as protease inhibitors. Protein content was determined in a Bradford assay [21]. The samples were resuspended in denaturing buffer B (40 mM Tris-HCl pH 6.8; 1% SDS; 360 mM β-mercaptoethanol; 6% glycerol; 0.005% bromophenol blue) and boiled at 100°C for 5 min. Protein extracts (15 μg protein/lane) were fractionated by SDS-PAGE in 10% polyacrylamide gels and the resulting bands were transferred onto nitrocellulose membranes (Hybond C, Amersham Biosciences, England), according to standard protocols [19, 22]. Following protein transfer, the membranes were blocked by incubation with 5% nonfat milk powder/0.05% Tween-20 in PBS. The membranes were then incubated for 1 h with blocking buffer containing preimmune serum (diluted 1 : 200), antirecombinant TcCruzipain polyclonal serum (diluted 1 : 500), antirecombinant TcCruzipain hybridoma (CZP-315) supernatant, or antirecombinant TcCruzipain monoclonal antibody (mAb CZP-315.D9, diluted 1 : 100). The membrane was washed three times in 0.05% Tween-20/PBS and then incubated for 1 h with AP-conjugated rabbit anti-mouse IgG (diluted 1 : 10,000). A polyclonal antirecombinant actin (TcActin; diluted at 1 : 200) mouse serum [23] was used for normalization. The membrane was then washed three times with 0.05% Tween-20/PBS and the reactive bands were visualized with BCIP-NBT solution, as described by the manufacturer.

To verify the specificity of mAb CZP-315.D9, whole protein extracts of *E. coli* (15 μg protein/lane) and purified recombinant TcCruzipain (2 μg protein/lane) were fractionated by SDS-PAGE in 10% polyacrylamide gels, transferred onto nitrocellulose membranes, and incubated with either the antirecombinant TcCruzipain polyclonal serum (diluted 1 : 1000 in blocking buffer) or the mAb CZP-315.D9 (diluted 1 : 100 in blocking buffer). The membrane was washed three times in 0.05% Tween-20/PBS and then incubated for 1 h with AP-conjugated rabbit anti-mouse IgG (diluted 1 : 10,000). The membrane was then washed three times with 0.05% Tween-20/PBS and the reactive bands were visualized with BCIP-NBT solution, as described by the manufacturer.

For analysis of cruzipain domain labeling, protein extracts of *E. coli* vector (with cruzipain domains) were fractionated by SDS-PAGE (15 μg protein/lane) in 10% polyacrylamide gels, transferred onto nitrocellulose membranes, and incubated with the antirecombinant TcCruzipain polyclonal serum (diluted 1 : 1000) or with the mAb CZP-315.D9 (diluted 1 : 100). The experiment then continued was described above.

2.9. Fluorescence Microscopy. *T. cruzi* epimastigotes were washed twice in PBS, fixed by incubation for 30 min with 4% paraformaldehyde, permeabilized by incubation for 5 min with PBS/0.5% Triton, and incubated for one hour at 37°C with preimmune serum diluted 1 : 150 in PBS pH 7.4 containing 1.5% BSA (incubation buffer), anti-TcCruzipain polyclonal serum diluted 1 : 500 in incubation buffer, anti-TcCruzipain hybridoma (CZP-315) supernatant, or antirecombinant TcCruzipain mAb (CZP-315.D9) diluted 1 : 40. Samples were washed three times with PBS and then incubated, in the same conditions, with goat anti-mouse secondary antibody coupled to AlexaFluor 488 or 594 diluted 1 : 600 in incubation buffer. The samples were washed three times with PBS, incubated for 5 min with 1.3 nM Hoechst 33342 (DNA marker), and examined under a Leica SP5 confocal laser microscope (Leica Microsystems, Wetzlar, Germany).

We further analyzed colocalization of native cruzipain in the Golgi apparatus in transfected epimastigotes expressing the *T. cruzi* Golgi marker TcHIP/AC [24]. Three-day-old culture transfected epimastigotes were washed twice in PBS, fixed for 30 min with 4% paraformaldehyde, and incubated for one hour at 37°C with anti-TcCruzipain mouse polyclonal serum (1 : 500) and rabbit anti-protein A antibody (1 : 40,000). The samples were washed three times in PBS and incubated, in the same conditions, with the secondary antibodies: goat anti-mouse antibody coupled to AlexaFluor 488 and goat anti-rabbit antibody coupled to AlexaFluor 594 (both diluted 1 : 600). Fluorescence microscopy was then carried out as described above.

2.10. Endocytosis Assay. *T. cruzi* epimastigotes were washed twice in PBS and then subjected to nutritional stress in PBS for 15 min at 25°C. They were then incubated for 30 min at 28°C with transferrin coupled to Alexa 633 (1 mg/mL) diluted 1 : 40. This period was long enough for the ingested

Table 1: Characterization of mAb CZP-315.D9 with the SBA Clonotyping-HRP System. Numbers are the optical density (OD) values read at 450 nm. Only OD values above 0.300 were considered positive. RPMI medium was used as a negative control.

	Ig (H+L)	IgM	IgA	IgG1	IgG2a	IgG2b	IgG3	Kappa	Lambda
Anti-TcCruzipain serum	1.207	0.852	0.585	1.24	0.816	0.996	0.19	1.125	0.33
Hybridoma 315	0.99	0.085	0.077	1.259	0.512	0.078	0.069	0.362	0.058
mAb CZP-315.D9	0.788	0.055	0.056	1.105	0.085	0.164	0.065	0.459	0.133
Medium (RPMI)	0.059	0.056	0.049	0.064	0.068	0.061	0.072	0.108	0.059

transferrin to accumulate in the reservosomes [3]. For the colocalization of transferrin with native cruzipain, the fed parasites were then fixed by incubation for 30 min with 4% paraformaldehyde, permeabilized by incubation for 5 min with 0.5% Triton in PBS, and incubated with the CZP-315.D9 mAb diluted 1 : 40 in incubation buffer. The samples were washed three times in PBS and then incubated, in the same conditions, with a goat anti-mouse secondary antibody coupled to AlexaFluor 488 (1 : 600) in incubation buffer. The samples were washed three times with PBS, incubated for 5 min with 1.3 nM Hoechst 33342, and examined under a Leica SP5 confocal laser microscope.

2.11. Transmission Electron Microscopy. Culture epimastigotes were collected by centrifugation, washed three times in phosphate buffer (pH 7.2), and fixed for 1 h at room temperature with 0.1% glutaraldehyde + 4% paraformaldehyde in 0.1 M phosphate buffer. The cells were then washed in phosphate buffer, dehydrated in graded ethanol series, and infiltrated overnight at low temperature (−20°C) with a 1 : 1 dilution of ethanol 100%: Lowicryl K4M or Lowicryl K4M MonoStep resin (EMS, Hatfield, PA, USA). After embedding for 6 h in pure resin, the samples were polymerized for 48 h at −20°C under UV light. Ultrathin sections (70 nm) were collected on nickel grids, incubated for 30 min with 50 mM ammonium chloride in PBS (pH 7.2), and then incubated for 1 h with mAb CZP-315.D9 diluted 1 : 20 in incubation buffer. After washing in this buffer, the grids were incubated for 1 h with a rabbit anti-mouse antibody coupled to 10 nm gold particles diluted at 1 : 20 in incubation buffer. After washing in buffer and distilled water, the grids were stained for 45 min with 5% uranyl acetate and for 5 min with lead citrate and observed in a JEOL 1200EXII transmission electron microscope operated at 80 kV.

3. Results

3.1. Production, Characterization, and Specificity of the Anti-TcCruzipain Monoclonal Antibody. The *T. cruzi* cruzipain gene was amplified, cloned (as confirmed by sequencing), and expressed in *E. coli*, producing a 56 kDa recombinant protein (50 kDa of TcCruzipain sequence + 6 kDa of his-tag) that was purified and used to immunize BALB/c mice. The mouse with the most responsive and specific anti-TcCruzipain serum (as determined by western blotting and subcellular localization by indirect immunofluorescence) was chosen for fusion of splenocytes with myeloma cells. Seven positive hybridomas were detected by indirect ELISA. The most stable hybridoma (CZP-315) was used to obtain clones by limiting dilution. An IgG1 isotype (OD value: 1.105) and kappa-positive (OD value: 0.459) monoclonal antibody (mAb CZP-315.D9) was obtained after selection by indirect ELISA, western blotting, and indirect immunofluorescence assays (Table 1).

A western blotting assay was performed to compare the reactivity of the anti-TcCruzipain polyclonal serum and the mAb CZP-315.D9 to *E. coli* protein extracts and to purified recombinant TcCruzipain. The anti-TcCruzipain serum recognized three protein bands between 80 and 110 kDa in *E. coli* (Figure 1(a), Ec lane 1) and several protein bands with the recombinant TcCruzipain (Figure 1(a), Czp lane 1), but with higher reactivity to a protein band between 50 and 60 kDa, compatible with TcCruzipain (50 kDa TcCruzipain + 6 kDa histidine tag). On the other hand, the mAb CZP-315.D9 recognized no protein bands in *E. coli* (Figure 1(a), Ec lane 2) but recognized the protein band between 50 and 60 kDa in the purified TcCruzipain fraction (Figure 1(a), Czp lane 2). Furthermore, both polyclonal and monoclonal antibodies recognized three protein bands below 50 kDa in the TcCruzipain fraction.

We further assessed the specificity of the CZP-315.D9 mAb against whole-epimastigote extracts by western blotting. Both anti-TcCruzipain polyclonal serum and CZP-315 hybridoma supernatant recognized two protein bands between 50 and 60 kDa, whereas the CZP-315.D9 mAb recognized mainly the protein band with about 50 kDa. The preimmune serum did not recognize any proteins. Actin (42 kDa), used for normalization, was detected with a polyclonal anti-TcActin mouse serum (Figure 1(b)).

Western blot assay was performed to determine which cruzipain domain (pre-pro domain, catalytic domain or C-terminal extension) was recognized by the polyclonal serum and by mAb CZP-315.D9. While the polyclonal serum recognized all protein domains and crossreacted with *E. coli* (protein bands below 50 kDa, Figure 1(c)), the mAb CZP-315.D9 did not, or weakly, recognize the pre-pro domain (Figure 1(c)).

3.2. Localization of Cruzipain in Reservosomes and Colocalization with Ingested Transferrin. T. cruzi epimastigotes were incubated with preimmune serum, anti-TcCruzipain polyclonal serum, CZP-315 hybridoma supernatant, or mAb CZP-315.D9. As expected, no labeling was observed with the preimmune serum (Figure 2(a)). The anti-TcCruzipain polyclonal serum labeled several round spots at the posterior end of the parasites (reservosomes) and a single spot at the anterior end of the cells, lateral to the kinetoplast (Figure 2(b)), corresponding to the Golgi complex (see below). The CZP-315

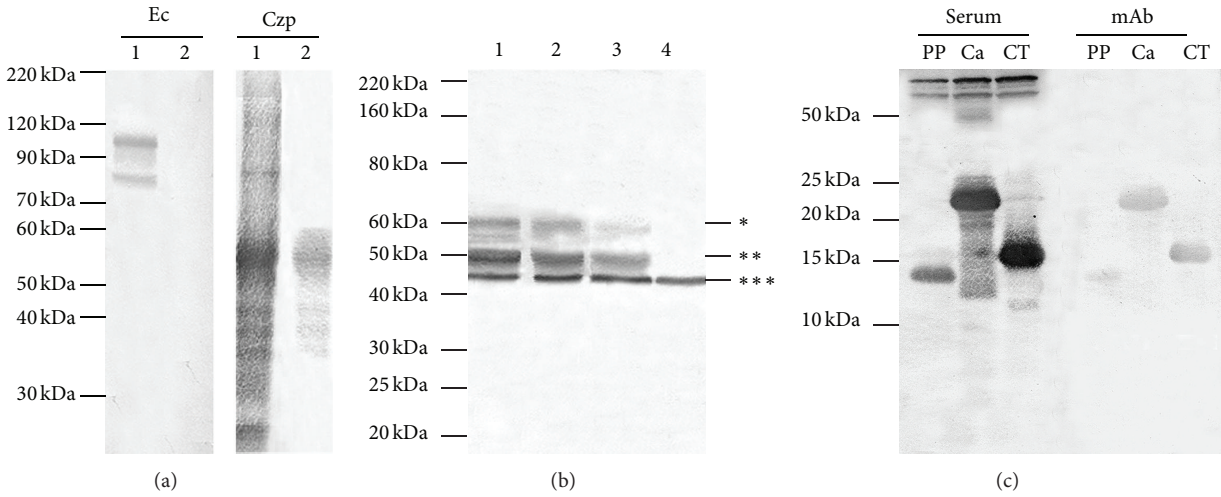

Figure 1: Western blot analysis of antibodies against TcCruzipain. (a) Protein extracts of *E. coli* (Ec) and purified recombinant TcCruzipain (Czp) incubated with anti-TcCruzipain polyclonal serum (lane 1) or CZP-315.D9 monoclonal antibody (lane 2). (b) Total protein extracts of *T. cruzi* epimastigotes incubated with anti-TcCruzipain serum (lane 1), CZP-315 hybridoma supernatant (lane 2), CZP-315.D9 monoclonal antibody (lane 3) or preimmune serum (lane 4). Actin was used for normalization. (c) Protein extracts of vector-bacteria containing recombinant cruzipain domains incubated with polyclonal antibodies (serum) or with mAb CZP-315.D9 (mAb) against TcCruzipain. PP: prepro domain; Ca: catalytic domain; CT: C-terminus domain. The Bench Mark Protein Ladder was used to determine molecular weights. *Immature cruzipain; **mature cruzipain; ***TcActin.

hybridoma supernatant and the mAb CZP-315.D9 recognized only the round spots (reservosomes) at the posterior end of the parasites (Figures 2(c) and 2(d)).

Incubation of TcHIP/AC transfectant epimastigotes with both anti-protein-A tag and anti-TcCruzipain polyclonal sera showed colocalization of the protein A tag and TcCruzipain at a single spot at the anterior end of the cells, lateral to the kinetoplast, corresponding to the single Golgi complex of the parasites (Figures 2(g) and 2(h)). No colocalization was observed at the posterior end of the parasites, which displayed only cruzipain labeling in several round structures (reservosomes).

An endocytosis assay was performed to validate the mAb CZP-315.D9. Alexa 633-conjugated transferrin was internalized and directed to the reservosomes, where it colocalized with cruzipain labeling (Figures 2(i)–2(l)).

We further assessed the immunolocalization of cruzipain by transmission electron microscopy (TEM). After incubating mAb CZP-315.D9 with ultrathin sections of epimastigote forms, gold labeling was found specifically in reservosomes (Figure 3). Weaker labeling was found in reservosomes from cells embedded with Lowicryl resin, which appeared electronlucent (Figures 3(a)–3(c)). More intense labeling was found in reservosomes from cells embedded with Lowicryl MonoStep resin (Figures 3(d) and 3(e)), which appeared more electrondense.

4. Discussion

Reservosomes are large round vesicles at the posterior end of *T. cruzi* epimastigote forms, in which the macromolecules taken up by the parasites accumulate [3]. Reservosomes are thus specific end organelles of the endocytosis pathway of this protozoan and can be used as exclusive markers/targets for these parasites. Proteomics analyses have shown that reservosomes contain several lysosomal enzymes [10], including a major cysteine proteinase known as cruzipain [11] or GP57/51 [12]. However, the antibodies against cruzipain currently available do not specifically target the reservosomes [11, 12]. We, therefore, aimed to produce a monoclonal antibody (mAb) against recombinant cruzipain (TcCruzipain) that specifically labeled reservosomes.

Indirect immunofluorescence assays to detect cruzipain in *T. cruzi* epimastigotes showed that (a) following incubation with a polyclonal serum against TcCruzipain, labeling was restricted to the reservosomes and in a single spot lateral to the kinetoplast and (b) following incubation with hybridoma supernatant and the mAb against TcCruzipain, labeling was restricted to the reservosomes. Immunolocalization of cruzipain by transmission electron microscopy showed gold labeling specifically in reservosomes. More intense labeling in electrondense reservosomes could be due to sample preservation in different resins (Lowicryl K4M and Lowicryl K4M MonoStep). Previous antibodies against cruzipain have labeled reservosomes, the membrane lining the cell body and flagellum, the inside of the flagellar pocket, and even the cytostome [9, 12, 14, 16]. Our monoclonal antibody, therefore, appears to be a suitable tool for the specific labeling of reservosomes.

TcHIP is a marker of the Golgi apparatus of *T. cruzi* [24]. Incubation of TcHIP/AC-transfected epimastigotes with both anti-protein-A tag and anti-TcCruzipain polyclonal sera revealed colocalization of protein A and TcCruzipain in a single spot at the anterior end of the cells, close to the kinetoplast, in a region corresponding to the Golgi complex. Cruzipain is a glycoprotein that is edited in the Golgi complex

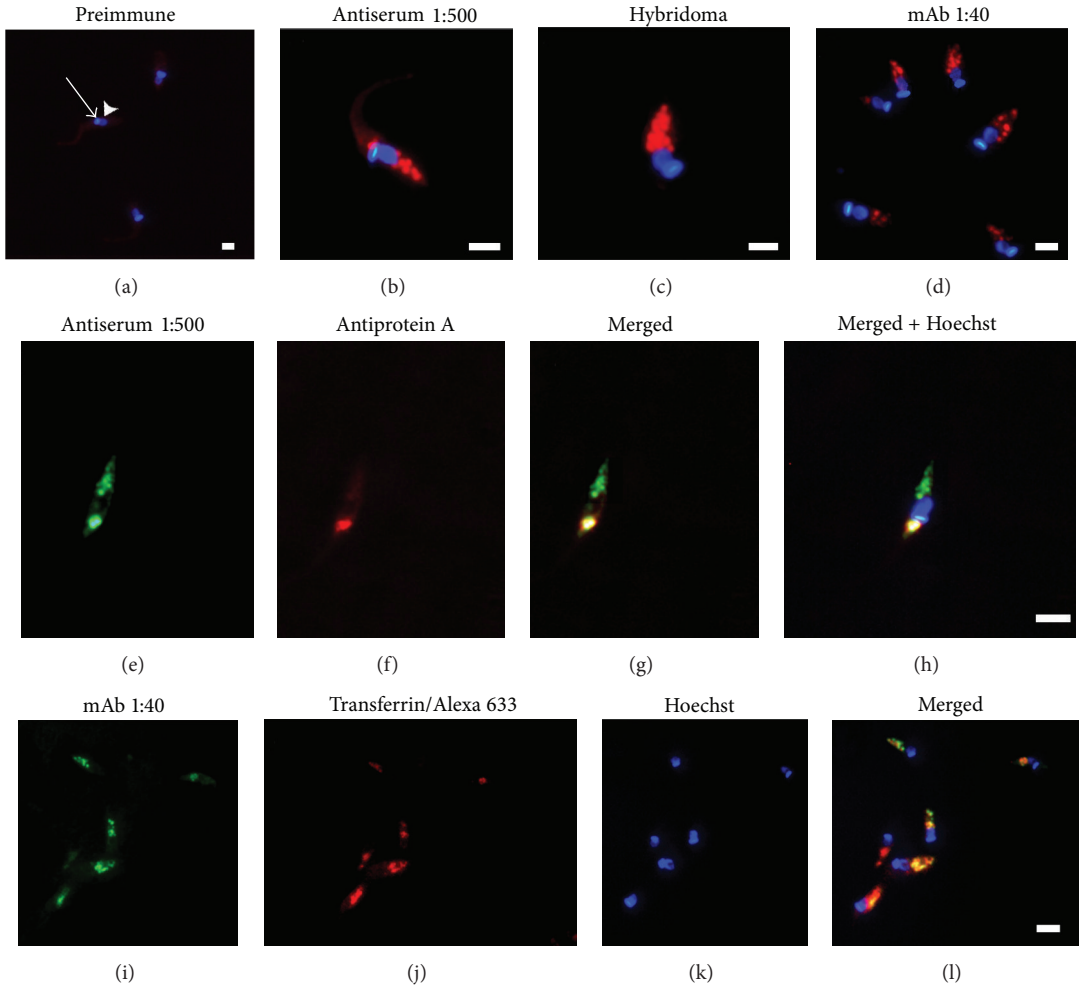

Figure 2: Immunolocalization of cruzipain and its colocalization with TcHIP/AC and ingested transferrin in *Trypanosoma cruzi* epimastigotes. The nucleus (arrowhead) and kinetoplast (arrow) are stained blue with Hoechst 33342. (a) Incubation with preimmune serum. (b) Incubation with anti-TcCruzipain serum. Note labeling of reservosomes and a single spot at the anterior end of the cell. (c) Incubation with CZP-315 hybridoma supernatant. Note that only reservosomes are labeled. (d) Incubation with CZP-315.D9 monoclonal antibody. Labeling is specific for reservosomes. ((e)–(h)) Colocalization of anti-TcCruzipain serum (green staining) with the Golgi marker TcHIP (red staining) in TcHIP/AC-transfected epimastigotes. ((i)-(l)) Endocytosis assay with transferrin coupled to Alexa 633 (red staining), and its colocalization with cruzipain (green staining) in epimastigotes, resulting in yellow staining. Bars = 5 μm.

and then directed to the endosomal/lysosomal system via the *trans*-Golgi network [25, 26]. Our polyclonal serum, therefore, also recognized immature cruzipain in transit through the Golgi complex, whereas the CZP-315 hybridoma and CZP-315.D9 mAb recognized the mature cruzipain in the reservosomes.

In western blot assays with whole extracts of *T. cruzi* epimastigote forms, both the anti-TcCruzipain serum and the CZP-315 hybridoma supernatant recognized two protein bands between 50 and 60 kDa, whereas the CZP-315.D9 mAb reacted strongly with a protein band at about 50 kDa. Cruzipain is produced as a 57 kDa protein, from which 6 kDa is cleaved to generate the mature cysteine protease, which thus has a molecular weight of 51 kDa (GP57/51) [12]. These data thus indicate that our CZP-315.D9 mAb recognizes mainly the mature enzyme in the reservosomes. Western blot assay to compare recognition of the anti-TcCruzipain polyclonal serum and the mAb CZP-315.D9 to purified recombinant TcCruzipain showed that the monoclonal recognized mainly a protein band between 50 and 60 kDa (50 kDa TcCruzipain + 6 kDa histidine tag), thus confirming the higher specificity of this mAb, as compared to a polyclonal antiserum. Both polyclonal and monoclonal antibodies recognized three protein bands below 50 kDa in a TcCruzipain fraction, probably due to proteolysis.

Cruzipain has three protein domains: pre-pro, catalytic, and C-terminal extension [27]. Our polyclonal serum recognized all protein domains by western blot analysis. On the other hand, mAb CZP-315.D9 recognized the catalytic domain and the C-terminal extension but did not, or weakly, recognize the pre-pro domain. This double binding can be dependent on conformational epitopes. No labeling with

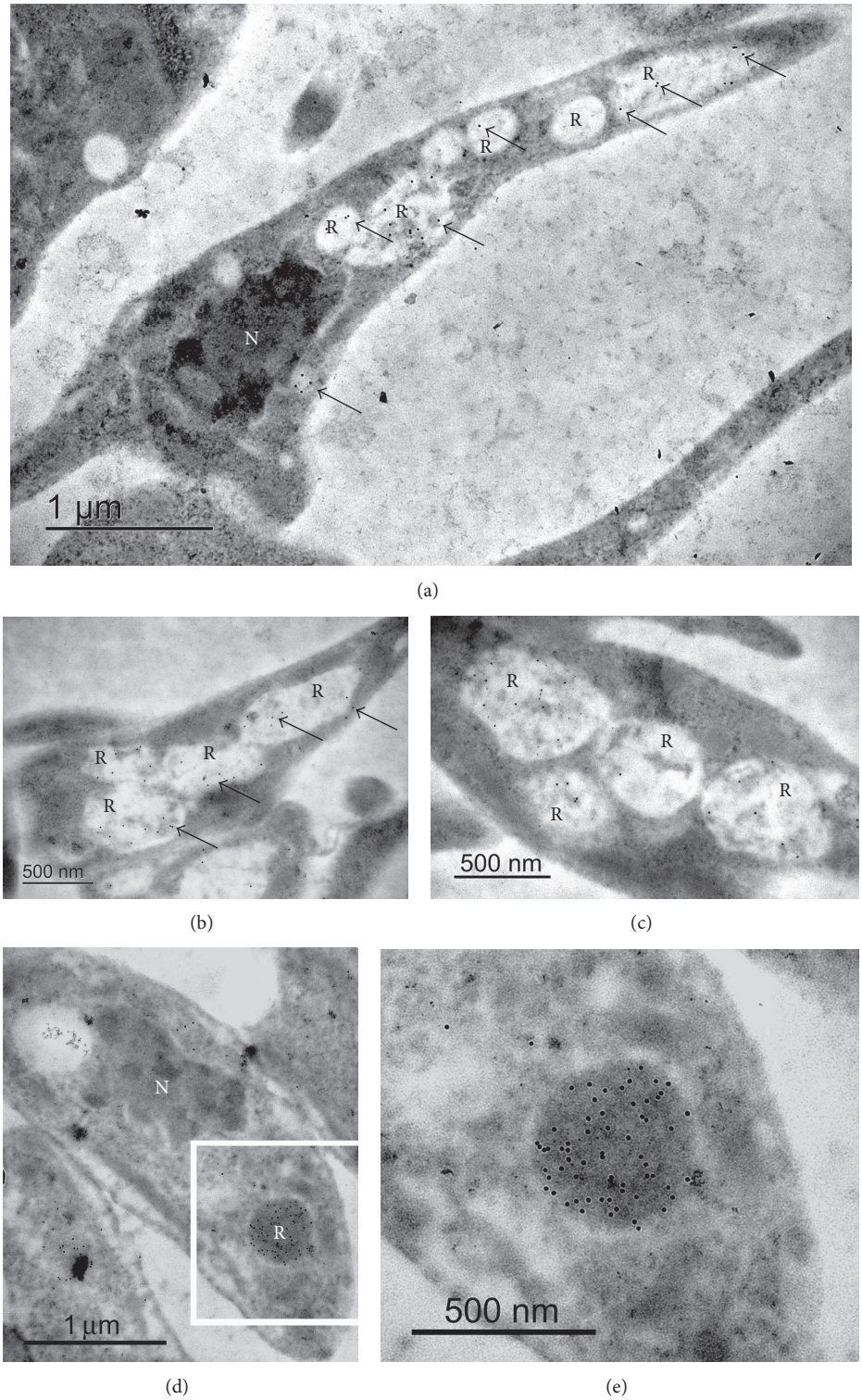

Figure 3: Immunolocalization of cruzipain in *Trypanosoma cruzi* epimastigotes by transmission electron microscopy. Ultrathin sections were incubated with the mAb CZP-315.D9, followed by a secondary antibody coupled to 10 nm gold particles. Note the specific gold labeling (arrows) in the reservosomes. Weaker labeling was found in cells embedded with Lowicryl K4M resin ((a)–(c)), while more intense labeling was found in the electrondense reservosomes of cells embedded with Lowicryl K4M MonoStep resin ((d)-(e)). (e) shows a high magnification of the area delimited in (d). N: nucleus; R: reservosome.

the pre-pro domain indicates why the mAb CZP-315.D9 does not recognize the immature cruzipain present in the Golgi complex.

An endocytosis assay was carried out with epimastigotes to validate the mAb CZP-315.D9. Transferrin ingested by the parasites was clearly colocalized with cruzipain labeling in the reservosomes. Thus, we demonstrate here, for the first time, the production of a specific mAb against reservosomal cruzipain. Monoclonal antibodies present several advantages over polyclonal sera, such as specificity, reproducibility, and ethical advantages [28]. The mAb produced in this study thus appears to be a potentially powerful molecular marker for studies on the function of this species-specific organelle, which plays an important role in the endocytosis of nutrients and cell differentiation (metacyclogenesis) in *T. cruzi* [29, 30].

5. Conclusions

We report here the production of a kappa-positive monoclonal IgG antibody (mAb CZP-315.D9) that recognizes recombinant *T. cruzi* cruzipain (TcCruzipain). This mAb binds mainly to a protein with a molecular weight of about 50 kDa on western blots and specifically labels reservosomes in *T. cruzi* epimastigotes by immunofluorescence and transmission electron microscopy. It thus constitutes a potentially powerful marker for use in studies on the function of these organelles.

Conflict of Interests

The authors declare that there is no conflict of interests regarding the publication of this paper.

Acknowledgments

The authors thank the Centro de Microscopia Eletrônica (CME) at Federal University of Paraná (UFPR) for use of the transmission electron microscope, Haruo Alexandre Inoue for cloning the *T. cruzi* recombinant cruzipain at the Gateway platform of the Carlos Chagas Institute/Fiocruz-PR, and Claudia Maria do Nascimento Moreira for technical assistance.

References

[1] J. R. Coura and P. A. Viñas, "Chagas disease: a new worldwide challenge," *Nature*, vol. 465, pp. 56–57, 2010.

[2] C. J. Salomon, "First century of Chagas' disease: an overview on novel approaches to nifurtimox and benznidazole delivery systems," *Journal of Pharmaceutical Sciences*, vol. 101, no. 3, pp. 888–894, 2012.

[3] M. J. Soares and W. De Souza, "Endocytosis of gold-labeled proteins and LDL by *Trypanosoma cruzi*," *Parasitology Research*, vol. 77, no. 6, pp. 461–468, 1991.

[4] W. De Souza, I. Porto Carreiro, K. Miranda, and N. L. Cunha E Silva, "Two special organelles found in *Trypanosoma cruzi*," *Anais da Academia Brasileira de Ciencias*, vol. 72, no. 3, pp. 421–432, 2000.

[5] W. de Souza, "Special organelles of some pathogenic protozoa," *Parasitology Research*, vol. 88, no. 12, pp. 1013–1025, 2002.

[6] W. de Souza, C. Sant'Anna, and N. L. Cunha-e-Silva, "Electron microscopy and cytochemistry analysis of the endocytic pathway of pathogenic protozoa," *Progress in Histochemistry and Cytochemistry*, vol. 44, no. 2, pp. 67–124, 2009.

[7] M. J. Soares and W. de Souza, "Cytoplasmic organelles of trypanosomatids: a cytochemical and stereological study," *Journal of Submicroscopic Cytology*, vol. 20, no. 2, pp. 349–361, 1988.

[8] N. Cunha-e-Silva, C. Sant'Anna, M. G. Pereira, I. Porto-Carreiro, A. L. Jeovanio, and W. de Souza, "Reservosomes: multipurpose organelles?" *Parasitology Research*, vol. 99, no. 4, pp. 325–327, 2006.

[9] M. J. Soares, T. Souto-Padron, and W. de Souza, "Identification of a large pre-lysosomal compartment in the pathogenic protozoon *Trypanosoma cruzi*," *Journal of Cell Science*, vol. 102, no. 1, pp. 157–167, 1992.

[10] C. Sant'Anna, E. S. Nakayasu, M. G. Pereira et al., "Subcellular proteomics of *Trypanosoma cruzi* reservosomes," *Proteomics*, vol. 9, no. 7, pp. 1782–1794, 2009.

[11] J. J. Cazzulo, M. C. Cazzulo Franke, J. Martinez, and B. M. Franke de Cazzulo, "Some kinetic properties of a cysteine proteinase (cruzipain) from *Trypanosoma cruzi*," *Biochimica et Biophysica Acta*, vol. 1037, no. 2, pp. 186–191, 1990.

[12] A. C. M. Murta, P. M. Persechini, T. de Souto Padron, W. de Souza, J. A. Guimaraes, and J. Scharfstein, "Structural and functional identification of GP57/51 antigen of *Trypanosoma cruzi* as a cysteine proteinase," *Molecular and Biochemical Parasitology*, vol. 43, no. 1, pp. 27–38, 1990.

[13] A. C. Murta, V. C. Leme, S. R. Milani, L. R. Travassos, and J. Scharfstein, "Glycoprotein GP57/51 of *Trypanosoma cruzi*: structural and conformational epitopes defined with monoclonal antibodies," *Memorias do Instituto Oswaldo Cruz*, vol. 83, pp. 419–422, 1988.

[14] M. Vieira, P. Rohloff, S. Luo, N. L. Cunha-E-Silva, W. de Souza, and R. Docampo, "Role for a P-type H+-ATPase in the acidification of the endocytic pathway of *Trypanosoma cruzi*," *Biochemical Journal*, vol. 392, no. 3, pp. 467–474, 2005.

[15] O. Campetella, J. Martínez, and J. J. Cazzulo, "A major cysteine proteinase is developmentally regulated in *Trypanosoma cruzi*," *FEMS Microbiology Letters*, vol. 55, pp. 145–149, 1990.

[16] T. Souto-Padron, O. E. Campetella, J. J. Cazzulo, and W. de Souza, "Cysteine proteinase in *Trypanosoma cruzi*: immunocytochemical localization and involvement in parasite-host cell interaction," *Journal of Cell Science*, vol. 96, no. 3, pp. 485–490, 1990.

[17] V. T. Contreras, T. C. Araujo-Jorge, M. C. Bonaldo et al., "Biological aspects of the Dm 28c clone of *Trypanosoma cruzi* after metacyclogenesis in chemically defined media," *Memorias do Instituto Oswaldo Cruz*, vol. 83, no. 1, pp. 123–133, 1988.

[18] E. P. Camargo, "Growth and differentiation in *Trypanosoma cruzi*. I. Origin of metacyclic trypanosomes in liquid media," *The Revista do Instituto de Medicina Tropical de São Paulo*, vol. 6, pp. 93–100, 1964.

[19] J. Sambrook, E. F. Fritsch, and T. Maniatis, *Molecular Cloning—A Laboratory Manual*, Cold Spring Harbor Laboratory Press, New York, NY, USA, 2nd edition, 1989.

[20] G. A. C. A. Mazzarotto, S. M. Raboni, V. Stella et al., "Production and characterization of monoclonal antibodies against the recombinant nucleoprotein of *Araucaria hantavirus*," *Journal of Virological Methods*, vol. 162, no. 1-2, pp. 96–100, 2009.

[21] M. M. Bradford, "A rapid and sensitive method for the quantitation of microgram quantities of protein utilizing the principle of protein dye binding," *Analytical Biochemistry*, vol. 72, no. 1-2, pp. 248–254, 1976.

[22] U. K. Laemmli, "Cleavage of structural proteins during the assembly of the head of bacteriophage T4," *Nature*, vol. 227, no. 5259, pp. 680–685, 1970.

[23] L. C. Kalb, R. E. G. Pinho, C. V. P. Lima, S. P. Fragoso, and M. J. Soares, "Actin expression in trypanosomatids (Euglenozoa: Kinetoplastea)," *Memórias do Instituto Oswaldo Cruz*, vol. 108, no. 5, pp. 631–636, 2013.

[24] C. M. Batista, L. Kalb, C. M. N. Moreira, G. T. Batista, I. Eger, and M. J. Soares, "Identification and subcellular localization of TcHIP, a putative Golgi zDHHC palmitoyl transferase of *Trypanosoma cruzi*," *Experimental Parasitology*, vol. 134, pp. 52–60, 2013.

[25] M. A. de Matteis and A. Luini, "Exiting the Golgi complex," *Nature Reviews Molecular Cell Biology*, vol. 9, no. 4, pp. 273–284, 2008.

[26] M. Anitei and B. Hoflack, "Exit from the trans-Golgi network: from molecules to mechanisms," *Current Opinion in Cell Biology*, vol. 23, no. 4, pp. 443–451, 2011.

[27] A. E. Eakin, A. A. Mills, G. Harth, J. H. McKerrow, and C. S. Craik, "The sequence, organization, and expression of the major cysteine protease (cruzain) from *Trypanosoma cruzi*," *Journal of Biological Chemistry*, vol. 267, no. 11, pp. 7411–7420, 1992.

[28] M. S. Even, C. B. Sandusky, and N. D. Barnard, "Serum-free hybridoma culture: ethical, scientific and safety considerations," *Trends in Biotechnology*, vol. 24, no. 3, pp. 105–108, 2006.

[29] M. J. Soares, "The Reservosome of *Trypanosoma cruzi* epimastigotes: an organelle of the endocytic pathway with a role on metacyclogenesis," *Memorias do Instituto Oswaldo Cruz*, vol. 94, no. 1, pp. 139–141, 1999.

[30] R. C. B. Q. Figueiredo, D. S. Rosa, Y. M. Gomes, M. Nakasawa, and M. J. Soares, "Reservosome: an endocytic compartment in epimastigote forms of the protozoan *Trypanosoma cruzi* (Kinetoplastida: Trypanosomatidae). Correlation between endocytosis of nutrients and cell differentiation," *Parasitology*, vol. 129, no. 4, pp. 431–438, 2004.